2005 VISUALIZATION CHALLENGE PAGE 1989

23 September 2005

Science

Vol. 309 No. 5743
Pages 1949–2120 $10

Voyager 1
Crosses the Termination Shock

125 YEARS OF GLOBAL Science

AAAS

START AUTOMATING

with the fully automatic, bench-top instrument that purifies plasmid and genomic DNA... all with the push of a button.

The Mini-Prep 96

MacConnell RESEARCH

STOP MANUAL MINI PREPS START AUTOMATING

800.466.7949 www.macconnell.com

Don't just get ahead, leap ahead.

SideStep™ Lysis and Stabilization Products for Quantitative PCR.

Stratagene's new SideStep™ lysis and stabilization product line ensures accurate gene expression data by eliminating sample loss, and allows you to go directly from cells to a real-time quantitative PCR analysis without RNA purification. RNA is stable in SideStep cell lysates for up to 6 months, giving you flexibility to perform future analysis without harming sample integrity.

- **Provides comparable results to purified RNA**
- **Saves time and increases sample throughput**
- **Ideal for QRT-PCR and siRNA knockdown analyses**

Need More Information? Give Us A Call:

Stratagene USA and Canada
Order: (800) 424-5444 x3
Technical Services: (800) 894-1304 x2

Stratagene Japan K.K.
Order: 03-5159-2060
Technical Services: 03-5159-2070

Stratagene Europe
Order: 00800-7000-7000
Technical Services: 00800-7400-7400

www.stratagene.com

Ask Us About These Great Products:

SideStep™ Lysis and Stabilization Buffer (100 rxn)	**400900**
SideStep™ Lysis and Stabilization Buffer (50 rxn)	**400901**
SideStep™ mRNA Enrichment Kit	**400902**
Brilliant® SYBR® Green SideStep™ QPCR Master Mix[a]	**400904**
Brilliant® SideStep™ QRT-PCR Probe Master Mix, 1-step[a,b]	**400907**

a. Purchase of this product is accompanied by a license under the foreign counterparts of U.S. Patents Nos. 4,683,202, 4,683,195 and 4,965,188 for use in the polymerase chain reaction (PCR) process, where such process is covered by patents, in conjunction with a thermal cycler whose use in the automated performance of the PCR process is covered by the up-front license fee, either by payment to Applied Biosystems or as purchased, i.e., an authorized thermal cycler.

b. Use of labeling reagents may require licenses from entities other than Stratagene. For example, use of fluorogenic probes in 5' nuclease assays may require licenses under U.S. Patent Nos. 6,214,979, 5,804,375, 5,210,015 and 5,487,972 owned by Roche Molecular Systems, Inc. and under U.S. Patent No. 5,538,848 owned by Applied Biosystems.

STRATAGENE®

GE Healthcare

Why do 100,000 scientists trust GE Healthcare for all their protein purification needs?

Here's Ä clue.

To 100,000 scientists worldwide, the name ÄKTA™ has always meant outstanding protein purification, and now it's brought to you by GE Healthcare. With the ability to purify virtually 100% of all biomolecules, the ÄKTAdesign™ platform can handle the toughest of challenges. Whatever the scale, from laboratory, to process development and manufacturing, there's an ÄKTAdesign system to meet every need. All systems in the ÄKTAdesign family work with the intelligent UNICORN™ software, which makes it easy to control every stage of your purification processes. Accurate, reproducible results just take a little pure imagination.

Visit www.amershambiosciences.com/aktadesign

imagination at work

GE15-05

Science

Special Issue

Voyager 1

A bow shock around a young star in the Orion nebula, imaged by the Hubble Space Telescope. A similar interstellar shock marks the edge of our solar system. Voyager 1 is heading toward this edge and recently crossed a second inner "termination shock" where the solar wind abruptly slows as it approaches the interstellar medium. Four Reports and a Viewpoint in this issue describe the crossing and data from the heliosheath, the region between the termination shock and interstellar space. [Image: NASA and the Hubble Heritage Team (STScI/AURA)]

Volume 309
23 September 2005
Number 5743

Departments

News of the Week

News Focus

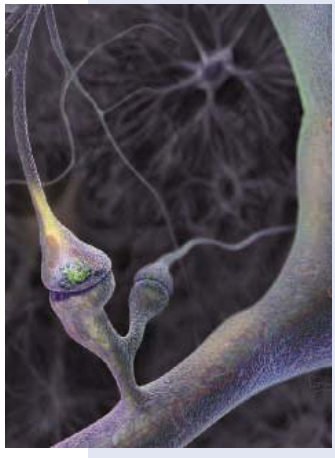

1989

1978

Letters

Books *et al.*

Policy Forum

Contents continued

Systems Biology — Cell-Free Protein Synthesis

EasyXpress — the fast and easy way to produce proteins

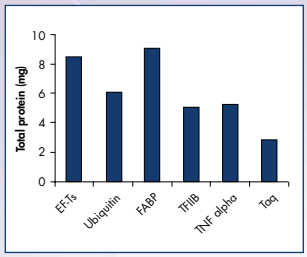

Typical yields from a single large-scale kit

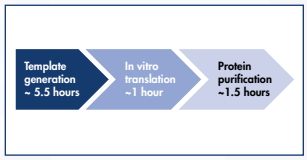

Fast procedures — from gene to protein in a single day

Producing proteins used to be difficult and time-consuming. Not any more. QIAGEN's EasyXpress is the fast and easy way to produce proteins.

By using EasyXpress™ Kits you get:

- **Efficient in vitro synthesis** — of native and posttranslationally modified eukaryotic proteins
- **Application-specific labeling** — for screening, protein interaction, and structural studies
- **Scalable, high yields** — a range of kits offering 3 µg to 5 mg of protein per reaction
- **Fast procedures and easy handling** — pure protein in hours, compared to weeks using conventional methods

To find out how fast and easy producing protein can be, visit www.qiagen.com/EasyXpress !

QIAGEN

Science

Perspectives

Review

2010

Science Express www.sciencexpress.org

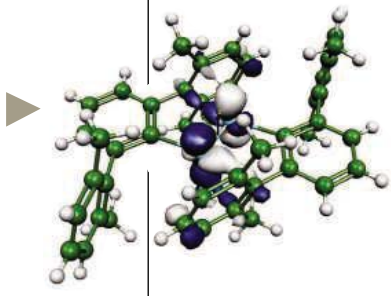

Technical Comment Abstracts

Brevia

Research Article

Reports

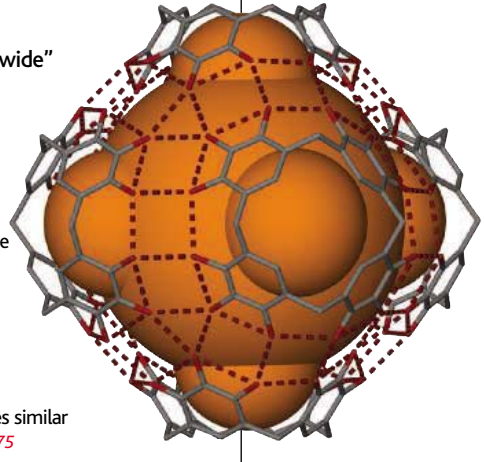

2037

Contents continued

Now The Right Side Knows What The Left Side Is Doing.

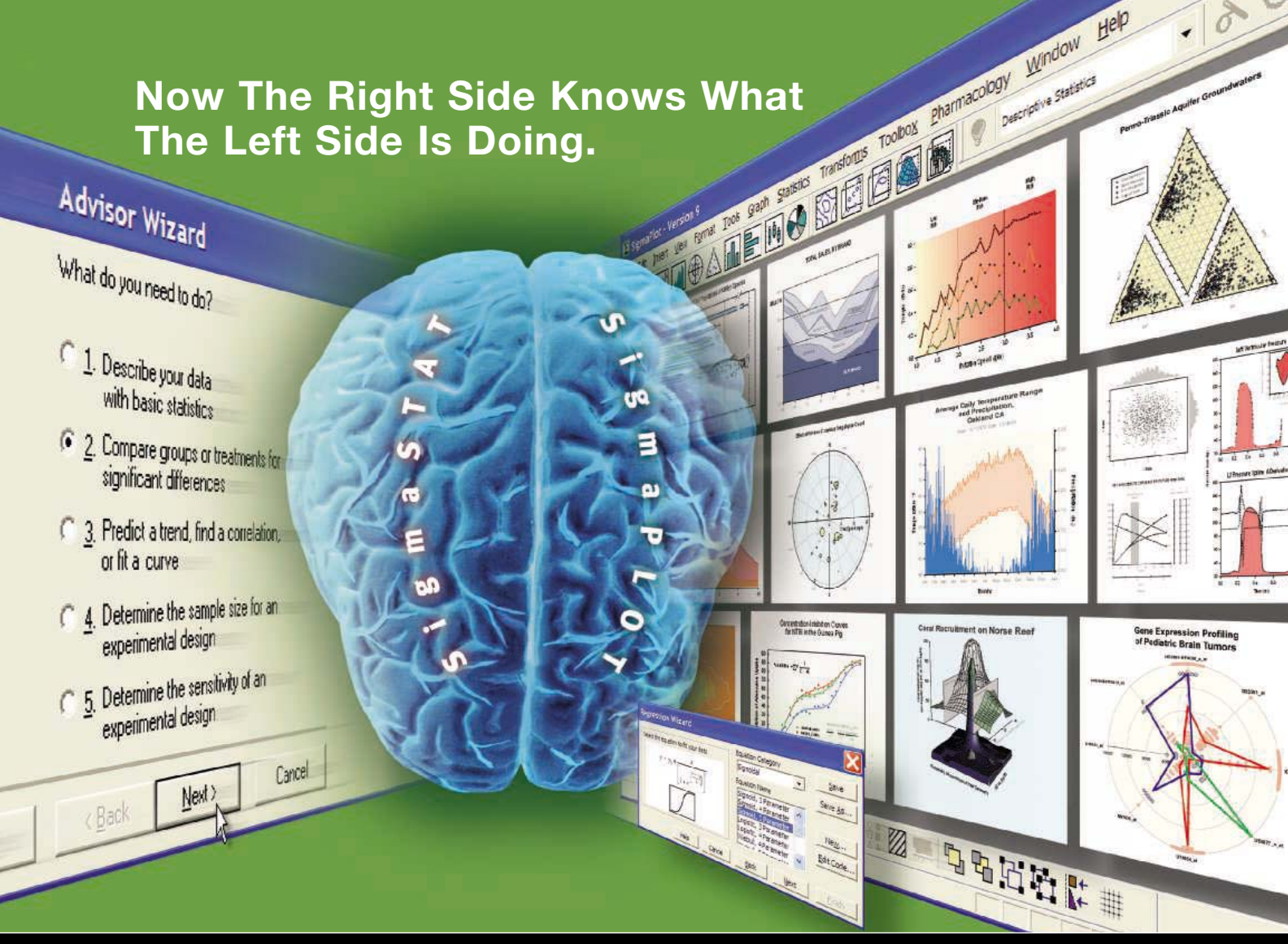

Combine the Powerful Statistical Output of SigmaStat with the Publication-quality Graph Creation of SigmaPlot

SigmaPlot is the award-winning technical graphing and data analysis software package used by more than 100,000 researchers worldwide who need to produce defensible research and create compelling graphs that clearly present their results for technical publications, presentations or the web. SigmaStat 3.1 now seamlessly integrates with SigmaPlot 9.0 for deeper statistical analysis within SigmaPlot's statistics menu.

SigmaPlot allows you to:

> Create graphs easily and publish your work anywhere
> Import, analyze & manage data quickly and easily
> Choose over 80 different 2-D and 3-D graph types
> Customize every element of your graphs
> Instantly access SigmaPlot from Microsoft® Excel
> Streamline your work by automating repetitive tasks

SIGMAPLOT
Exact Graphs for Exact Science

Add SigmaStat 3.1 to get easy-to-use, expert statistical analysis within SigmaPlot!

SigmaStat guides you through your analysis:

> Suggests the appropriate statistical test
> Checks assumptions in the data to avoid statistical error
> If your data violates any of those assumptions, the Advisor Wizard suggests another test
> Generates an intelligent report that explains your results in plain English – not statistical jargon
> Even handles messy data with missing values

SIGMASTAT
Advisory Statistics for Scientists

With SigmaStat you'll have the expertise of a professional statistical consultant at your fingertips!

FREE ONLINE TUTORIALS & 30-DAY TRIAL SOFTWARE AVAILABLE AT WWW.SYSTAT.COM

SigmaScan®
Automated Image Analysis

TABLECurve 2D
Automated Curve Fitting Analysis

TABLECurve 3D
Automated Surface Fitting Analysis

PeakFit
Automated Peak Separation Analysis

SYSTAT
Comprehensive Statistical Analysis

adsci

Reports continued

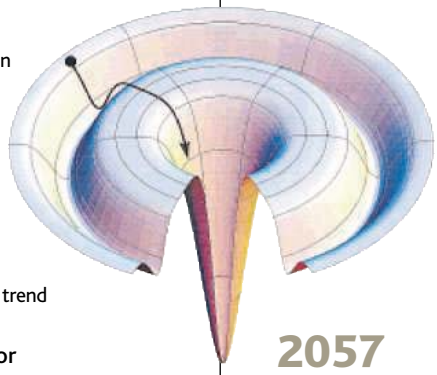

2057

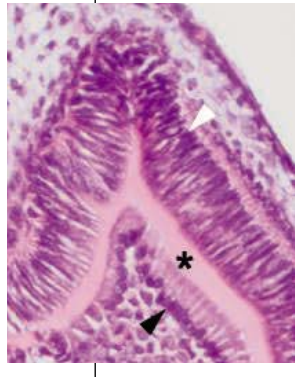

2067

AAAS
ADVANCING SCIENCE, SERVING SOCIETY

SCIENCE (ISSN 0036-8075) is published weekly on Friday, except the last week in December, by the American Association for the Advancement of Science, 1200 New York Avenue, NW, Washington, DC 20005. Periodicals Mail postage (publication No. 484460) paid at Washington, DC, and additional mailing offices.

Domestic individual membership and subscription (51 issues): $135 ($74 allocated to subscription). Domestic institutional subscription (51 issues): $550; Foreign postage extra: Mexico, Caribbean (surface mail) $55; other countries (air assist delivery) $85. First class, airmail, student, and emeritus rates on request. Canadian rates with GST available upon request, GST #1254 88122. Publications Mail Agreement Number 1069624. **Printed in the U.S.A.**

Change of address: allow 4 weeks, giving old and new addresses and 8-digit account number. **Postmaster:** Send change of address to *Science*, P.O. Box 1811, Danbury, CT 06813–1811. **Single copy sales:** $10.00 per issue prepaid includes surface postage; bulk rates on request. **Authorization to photocopy** material for internal or personal use under circumstances not falling within the fair use provisions of the Copyright Act is granted by AAAS to libraries and other users registered with the Copyright Clearance Center (CCC) Transactional Reporting Service, provided that $15.00 per article is paid directly to CCC, 222 Rosewood Drive, Danvers, MA 01923. The identification code for *Science* is 0036-8075/83 $15.00. *Science* is indexed in the *Reader's Guide to Periodical Literature* and in several specialized indexes.

Contents continued ▶

Advancing RNAi Technology.

Dharmacon...the world's most trusted siRNA resource

- The largest and most referenced siRNA supplier
- Target any unique human, mouse or rat gene
- Highest level of guaranteed silencing available
- Innovative technologies to enhance specificity
- Breakthrough siRNA transfection reagents
- Expert technical support

Leading RNAi researchers count on Dharmacon's state-of-the-art *SMART*selection™ and *SMART*pool® technologies for potent and specific gene silencing. Four individual siRNAs and a *SMART*pool siRNA reagent are available for over 66,000 unique human, mouse, and rat genes - each with the industry's best performance guarantee and backed by our expert technical support. Simply use our on-line si*GENOME*™ search tool to identify the siRNA reagents for your target gene.

No wonder Dharmacon is the most frequently referenced siRNA supplier in peer-reviewed journals!

Want to know more about RNAi? Visit our website to request your FREE copy of the RNAi Technical Reference & Application Guide today.

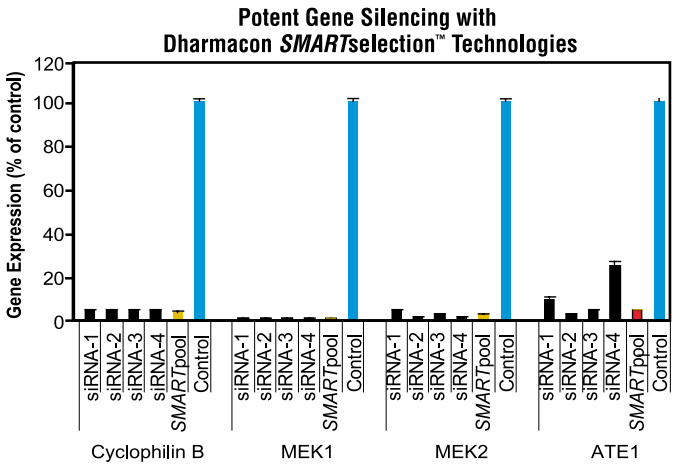

DHARMACON
RNA TECHNOLOGIES

www.dharmacon.com
Tel: 303-604-9499 or 800-235-9880 Fax: 303-604-9680

For European offices and distributors, please visit www.perbio.com
PERBIO

AAAS Responds to Hurricane Katrina

AAAS and its journal *Science* share the deep sense of loss occasioned by the devastation wrought by Hurricane Katrina.

Science
www.scienceonline.org

Related Background and News from Science
As an aid to policy-makers, scientists, and the public in understanding the large-scale forces and smaller scale scientific, social, and political background to the disaster, we are making available, free to all visitors, a selection of past *Science* articles related to hurricanes, coastal disasters, and disaster policy.
www.sciencemag.org/sciext/katrina

Donate and Find Resources
Among the many victims of Hurricane Katrina are scientists, engineers, and teachers who are rebuilding their facilities and classrooms. They need spare and unused resources, such as computers, books, journals, lab equipment, lab space, and teaching materials. If you have resources to share or are in need of resources, please visit our online brokering system.
www.aaas.org/katrina

sciencenow www.sciencenow.org
Daily News Coverage

Listening to Lice
Whale parasites tell the evolutionary story of their hosts.

What a Tooth Reveals
Like modern humans, Neandertals may have had a long childhood.

Beans, Beans, Good for Your… Cancer
Compound found in common foods may slow tumor growth.

Conflict in the lab?

science's next wave www.nextwave.org Career Resources for Young Scientists

Global: Mind Matters—Managing Conflict in the Lab *I. Levine*
Our Mind Matters expert offers tips on how to prevent and deal with inevitable conflicts in the lab.

US: Not Just a Pretty Picture *J. Austin*
Illustrator Graham Johnson is a winner in this year's Science and Engineering Visualization Challenge.
related 2005 Visualization Challenge page 1989

Canada: Modeling a Career—Industrial Internships for Mathematicians *A. Fazekas*
A Canadian math and technology society offers internships for young mathematicians.

UK: Yours Transferredly—A Place in the Sun? *P. Dee*
Phil Dee considers postdoc options while keeping his irons in the domestic and overseas job markets.

MiSciNet: Defending Your Graduate Life *C. Parks*
Jami Valentine shares her graduate school experiences and talks about her defense preparation.

science's sage ke www.sageke.org Science of Aging Knowledge Environment

Perspective: Membrane Permeabilization—A Common Mechanism in Protein-Misfolding Diseases
H. A. Lashuel
If it looks like a pore and acts like a pore, is it a pathogenic pore?

News Focus: Plumbing Problem *M. Leslie*
Lymph system malfunctions might promote obesity.

News Focus: Two Ways About It *R. J. Davenport*
Phosphate-adding proteins send neurons down different roads to death after a stroke.

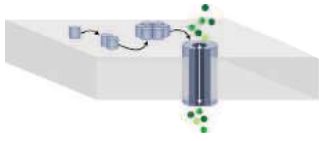

Amyloid proteins make pores in membranes.

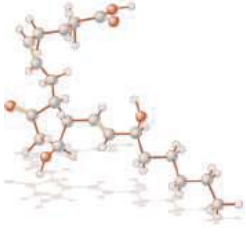

Prostaglandin E_2.

science's stke www.stke.org Signal Transduction Knowledge Environment

Perspective: Evaluation of Selective Prostaglandin E_2 (PGE_2) Receptor Agonists as Therapeutic Agents for the Treatment of Asthma *K. F. Chung*
Multiple prostaglandin receptors complicate the search for new treatments for asthma.

ST on the Web
Check out the new sites added to the Educator Sites and Protein Databases sections.

Separate individual or institutional subscriptions to these products may be required for full-text access.

BIBLIOGRAPHY CENTRAL

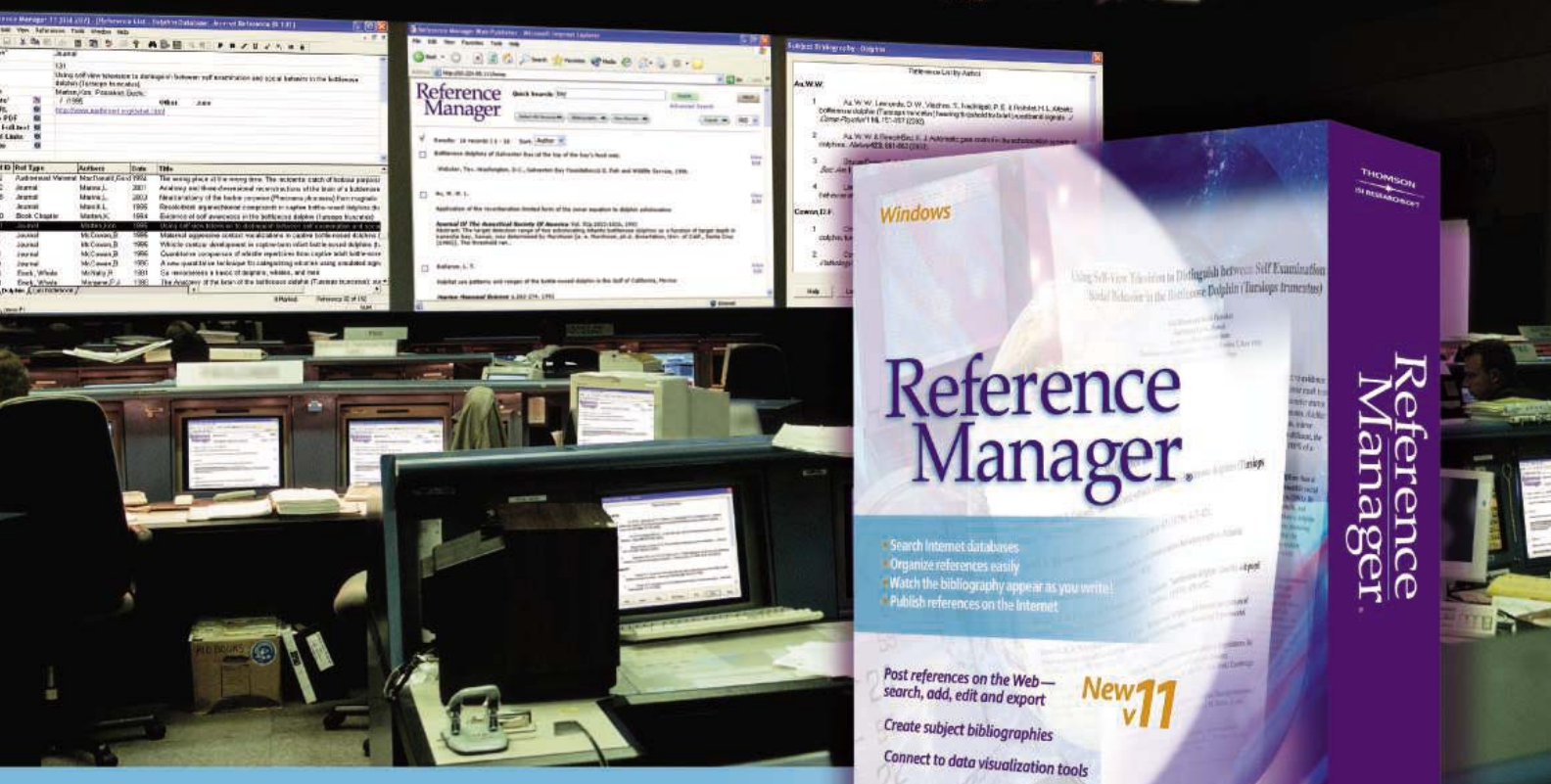

Your High-Tech Command and Control Center for References.

Introducing Reference Manager 11—a powerful upgrade to the bibliographic software that streamlines research, writing and publishing.

Reference Manager has served corporate, government and academic researchers worldwide for over 20 years. And now version 11 delivers new ways to share and view your reference collections: Post your databases to the Web. Collaborate with colleagues over a network. Link to full text pdf files.

These are just some of the powerful features that await you. Reference Manager is your command and control center for all things reference related.

What's new in v11:

- Publish Reference Manager databases to the Web or intranet
- Create subject bibliographies instantly
- Access new and updated content files at www.refman.com
- Share traveling libraries with colleagues
- Connect to data visualization tools

Put innovation into action. Order or upgrade today.
Available for Windows in a single-user and network edition.
Phone: 800-722-1227 • 760-438-5526 • info@isiresearchsoft.com

Download a Free Demo Today
www.refman.com

THOMSON
ISI RESEARCHSOFT

Keeping the Guests Apart

Many proteins form remarkably intricate pocket structures to orient and direct molecular reagents. Simpler nanometer-scale enclosures can also be formed by self-assembly from molecules in solution through hydrogen bonding or coordination to metal centers. **Dalgarno *et al.*** (p. 2037) show that one such structure can encapsulate two polyaromatic dye molecules but keep them rigidly apart, as evidenced by x-ray diffraction in the solid state and fluorescence-quenching studies in solution. The rigidity seems to arise from π-stacking and CH···π interactions between the guest molecules and the capsule walls.

Calling in the Bodyguards

Plants attacked by herbivorous insect pests can bring out their own chemical defenses, but can also call in "bodyguards," predators that prey on the first round of pests. Volatile compounds are important in this signaling triangle. **Kappers *et al.*** (p. 2070; see the news story by **Pennisi**) have now engineered *Arabidopsis* to produce the volatile compounds necessary to call in such bodyguards by targeting terpenoid metabolism.

Roomy Solids

Metal-organic framework compounds, which can have high surface area and useful gas storage capabilities, are normally held together by coordination to single metal centers. Recently, it was shown that hydrothermal synthesis of Cr ions, organic dicarboxylates, and fluorhydric acid produced porous frameworks anchored by inorganic trimers that are linked into large supertetrahedrons. **Férey *et al.*** (p. 2040; see the Perspective by **Hupp and Poeppelmeier**) now report the computational design and synthesis of a related compound based on Cr ions and terephthalate that is stable up to 275°C and adopts a zeotype cubic structure with a giant cell volume (~702,000 cubic angstroms), as determined from an analysis of x-ray powder diffraction data. The network of extra-large pore sizes (diameters of 30 to 34 angstroms) leads to a very high nitrogen sorption capacity of nearly 6000 square meters per gram, and allows even large Keggin polyanions to be incorporated into the cages.

A Very Long Wave

The recent Sumatra tsunami that produced devastation around the Indian Ocean traveled several times around the globe before dissipating. This history is recorded in a global tide-gauge network, and **Titov *et al.*** (p. 2045, published online 25 August 2005) have used an ocean model to understand the global propagation of this tsunami. Large waves were recorded in places such as the coast of Peru, locally in Antarctica, and at Halifax, Nova Scotia, far from the earthquake, and with a very indirect path. The modeling suggests that the waves were in part guided by Earth's mid-ocean ridge system.

Out of a Wetter Africa

Between 3 million and 1 million years ago, the modern human genus *Homo* arose, *Homo erectus* appeared, and our ancestors migrated out of Africa. During this sequence of events, the general trend of African climate has been thought to be one of increasing aridity. **Trauth *et al.*** (p. 2051, published online 18 August 2005) now present a record of lake development and disappearance in rift basins from East Africa, the region from which most of the human fossils from that time comes. Three separate periods, each roughly 200,000 years in duration, were apparently wetter and caused the rift lakes to be deep and extensive.

Carry-on Chromosome

One approach to dissecting human diseases with multiple interacting loci has been to try and express large numbers of genes on human transchromosomal fragments or constructed artificial chromosomes in mice. Down syndrome (DS) depends on trisomy in chromosome 21, and several attempts have been made at recapitulating the disease through a transchromosomal approach. **O'Doherty *et al.*** (p. 2033; see the news story by **Miller**) report the germline transmission of a transchromosomal fragment carrying 91% of chromosome 21 genes. At least 58 of these were transcriptionally active and, although the fragment was not expressed uniformly in all somatic cells, the transchromosomal animals displayed a phenotype sharing similarities with DS, including behavioral and physiological abnormalities. The ability to transmit such a large human chromosomal fragment in mice should also allow the exploration of other complex genetic diseases.

Ready to Jump

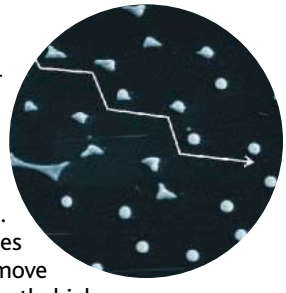

Many studies have followed the rebound of droplets hitting a solid surface, but **Habenicht *et al.*** (p. 2043) have isolated just the second half of this process. They used a laser to melt irregularly shaped gold nanoparticles. Formation of the melted droplet causes the center of mass of the particle to move away from the surface, and for sufficiently high fluences, the process is rapid enough to desorb the droplet with speeds on the order of 10 meters per second.

Carotenoid and Retinal United

Carotenoids provide antenna molecules that increase the spectral range over which light energy can be absorbed and subsequently transferred to chlorophylls for use in photosynthesis. Retinal is the light-absorbing chromophore in a family of proton pumps—the archaeal and bacterial rhodopsins. **Balashov *et al.*** (p. 2061) describe the intermingling of these two phototransduction pathways within the bacterium *Salinibacter ruber*. They find a 1:1 complex of the carotenoid salinixanthin and the retinal-containing

CONTINUED ON PAGE 1963

CREDITS (TOP TO BOTTOM): KOPPERT BIOLOGICAL SYSTEMS; HABENICHT *ET AL.*

Roche Applied Science

FastStart PCR Product Family

Challenge the Performance of Your PCRs

	FastStart Taq DNA Polymerase	FastStart High Fidelity PCR System
Specificity	High	High
Sensitivity and yield	High	High
Amplicon length	0–3 kb	0–5 kb
Fidelity relative to Taq Polymerase	Equal	4X better
Utility in challenging assays	High	High
Amplification of difficult templates	Yes	Yes

Table 1. Characteristics of FastStart products.

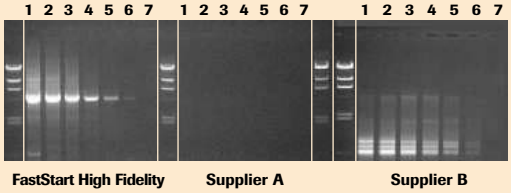

1:100 ng hum. gen. DNA
2: 50 ng hum. gen. DNA
3: 25 ng hum. gen. DNA
4: 10 ng hum. gen. DNA
5: 5 ng hum. gen. DNA
6: 1 ng hum. gen. DNA
7: 0 ng hum. gen. DNA

Figure 1. Amplification of a 4.8 kb tPA fragment from different amounts of human genomic DNA, using conditions recommended by each manufacturer.

For years, our **FastStart Taq DNA Polymerase** has provided superior specificity, sensitivity, yield, and ease of use in hot start PCR.

Now, you can also increase accuracy in hot start PCR and amplify longer fragments with our **new FastStart High Fidelity PCR System**—a blend of FastStart Taq DNA Polymerase and a new thermostable proofreading protein (Table 1).

Improve the overall efficiency of your lab!

Use either enzyme in standard and high-throughput applications to:

- **Produce higher yields of the desired amplicon**—not non-specific fragments (Figure 1)
- **Amplify the most difficult templates** by using the supplied additives (GC-RICH Resolution Solution or DMSO)
- **Perform the most challenging applications** and start assays that were not possible previously.

Upgrade your hot start PCR by visiting **www.roche-applied-science.com/pcr** to learn more about both of these products!

Roche Diagnostics

Roche Diagnostics GmbH
Roche Applied Science
68298 Mannheim
Germany

protein xanthorhodopsin and show that light absorbed via the carotenoid is transferred to the retinal and used as an energy source for pumping protons across the cell membrane.

Understanding Noise in Gene Expression

Extensive variation among populations can be largely attributed to genetic differences. However, even when genetics are the same (as with identical twins or clonal populations of cells), variability still exists. **Raser and O'Shea** (p. 2010) review the level of variation in gene expression among cells measured as "noise" in gene expression and summarize the current understanding of the sources and consequences of noise as well as its regulation.

Polypyrimidine-Tract Binding Protein Structures Revealed

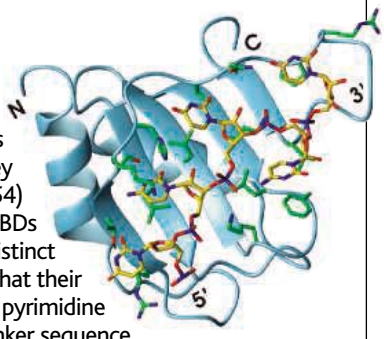

Polypyrimidine-tract binding protein (PTB) is a eukaryotic protein that binds to UC-rich RNA substrates through four RNA binding domains (RBDs) and plays a key role in messenger RNA splicing. **Oberstrass *et al.*** (p. 2054) have determined the solution structures of the four RBDs each bound to a pyrimidine tract. Each domain has a distinct specificity, and the third and fourth domains interact so that their bound RNAs are antiparallel. Thus, RBD34 can bind two pyrimidine tracts in the same RNA only if they are separated by a linker sequence and can induce RNA looping to regulate alternative splicing.

Manipulating Muscle Satellite Cells

Satellite cells of muscle are thought to provide progenitors for muscle repair and regeneration, but are rare and difficult to isolate. **Montarras *et al.*** (p. 2064, published online 1 September 2005) successfully isolated muscle satellite cells from a mouse line that expresses green fluorescent protein using flow cytometry. When satellite cells isolated from the diaphragm were grafted into muscles of the *mdx* mouse, a model for muscular dystrophy, the cells effectively supported repair of the muscle and establishment of resident satellite cells. However, in vitro culture of the satellite cells to expand their numbers did not improve efficiency of engraftment.

A Toothy Problem

In mammalian tooth development, epithelial enamel knots appear where cusps will develop in a species-specific manner, but the question remains whether enamel knots really exert a causal effect on cusp patterns. **Kassai *et al.*** (p. 2067) show how regulation of enamel knots has dramatic effects on cusp patterning. Ectodin, a recently identified bone morphogenic protein antagonist in tooth development, appears to provide a "negative" image of genes expressed in the enamel knots that give rise to cusps and integrates the induction and inhibition of enamel knots. The enamel knots of ectodin null-mutant mice were enlarged and altered cusp patterns so extensively that they resembled the teeth of the black rhinoceros.

Ancient Linguistics

Studying the relationship of languages has traditionally depended on recognizing "cognate sets" of word pairs matched across languages and reconstructing the changes in their sounds and meaning. However, because of linguistic erosion, this method is limited to a time depth of only 8000 to 10,000 years, but much human migration occurred before then. **Dunn *et al.*** (p. 2072; see the Perspective by **Gray**) develop a method that uses the language structure, rather than vocabulary, to construct language phylogenies, and allows a much deeper sampling of linguistic time. Using features such as the ordering of sentence elements or the grammatical elements of gender or tense, they constructed phylogenies of Papuan languages in Island Melanesia that may have been separated since the late Pleistocene.

CREDIT: OBERSTRASS *ET AL.*

Social Security Meets Race

President Bush has appealed to African-American voters by arguing that they would benefit from the replacement of part of the traditional Social Security retirement income system with private retirement accounts. The argument goes like this: The average 50-year-old African American has a life expectancy of 27.3 years, as compared to an average of 30.5 years for Caucasians. This means that African Americans receive retirement benefits for fewer years and are more likely to die before receiving any benefits at all. In a system of private retirement accounts, African Americans could bequeath their accounts to their heirs, thereby closing some of the "black-white" wealth gap and ensuring that blacks no longer get a bad deal from Social Security.

There are good reasons for introducing private retirement accounts, such as increasing national savings and improving labor supply incentives. But achieving racial parity in Social Security benefits is not one of them. Blacks benefit disproportionately from other features of Social Security. Because they have below-average lifetime earnings, they are helped by the Social Security benefit formula that replaces a larger fraction of pre-retirement earnings for low earners than for high earners. For the retirement portion of Social Security, these two effects almost exactly cancel, meaning that blacks receive rates of return on their Social Security payroll tax payments at least equal to those for whites. When benefits for disability and young survivors are included, blacks clearly receive an above-average return from the current Social Security system. Because Social Security benefits are protected from inflation and last as long as you live, they are especially valuable to low-income groups that count on them for a large portion of retirement income. Thus, changing Social Security may in fact harm, rather than help, blacks.

It is hard to judge how different racial and ethnic groups would fare under an approach that has not yet been fully defined, but there are reasons for worry. First, the president proposes to divert payroll tax revenue away from the current system. That raises the chance that disability and survivor benefits will be cut, disproportionately affecting blacks. Second, there might not be any redistribution from high earners to low earners in the privatized portion of the reformed system, meaning that gains to blacks from the bequeathability of accounts will be at least partially offset. Third, any sensible privatization plan will require retirees to convert their account balance into annuities upon retirement; because members of long-lived groups will receive annuity payments for more years, there will continue to be redistribution from groups with low life expectancy to groups with high life expectancy. Fourth, the introduction of market risk into Social Security will be more of a burden for low-income groups such as blacks.

One could design a system with privatized accounts in which blacks do fine: by maintaining disability benefit levels, enhancing redistribution from high earners to low earners, and requiring that annuities provide payments to the retired worker or his or her heirs for a minimum of 10 years. Blacks could indeed be winners from such a reform. But these features are unrelated to privatization; all could be accomplished within the traditional Social Security system. If the real objective is to help demographic groups with short life expectancy, tinkering with Social Security rules may not be the best approach. Instead, investing in the health of low-income populations with early mortality could produce greater benefits in the short run and help to close the longevity gap in the long run. Under the present system, if black and white longevities were equal, blacks would receive about $4 billion of additional Social Security benefits per year. That's less than 2% of spending on Medicaid, the nation's medical assistance program for low-income individuals. Even if that sum were sensibly invested in expanding access to health care, improving community health centers, increasing research expenditures on racial differences in disease, and so on, it is doubtful whether longevity differences could be eliminated. That's because the differences are large, and the things that are likely to have the biggest impact—changing diet and exercise habits—are hard to alter with government policy. Thus, investing in the health of low-income populations may well be the best way to spend money on behalf of groups with short life spans. But we should not kid ourselves into believing that investments of this size will erase racial differences in health outcomes. And the president should not kid African Americans that Social Security privatization will make them richer.

Jeffrey Liebman

Jeffrey Liebman is professor of Public Policy at the John F. Kennedy School of Government, Harvard University, Cambridge, MA.

10.1126/science.1117804

CREDIT: J. SCOTT APPLEWHITE/AP

EDITORS' CHOICE

edited by Gilbert Chin

CELL BIOLOGY

A ROCK, a Tumor Cell, and a Hard Place

Tumors are generally stiffer than surrounding healthy tissue, a characteristic that has been exploited in certain diagnostic procedures such as breast self-examination. Tumor rigidity reflects not only intrinsic properties of the tumor cells but also an increased stiffness of the extracellular matrix (ECM). Whether ECM stiffening plays an active role in tumor cell growth or is an innocent bystander has been unclear.

Paszek *et al.* investigated this question by monitoring the behavior of human mammary epithelial cells cultured with ECM components that had been cross-linked to polyacrylamide gels of varying stiffness. These experiments revealed that even a small increase in matrix rigidity enhanced epithelial cell growth. Mechanistically, this effect was traced to a mechano-regulatory circuit that links physical cues from the matrix to transmembrane ECM receptors (integrins), to intracellular regulators of cell contractility such as ROCK (Rho-associated protein kinase), and to a key signaling pathway for cell growth, the mitogen-activated protein kinase pathway. These results suggest that factors causing a sustained increase in matrix stiffness—for example, a chronic inflammatory response—may promote malignant transformation. — PAK

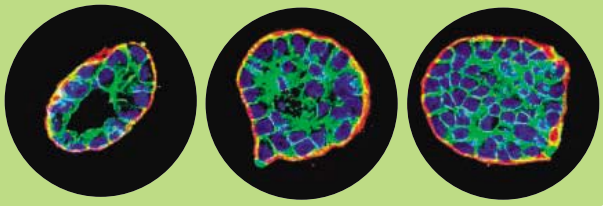

Cell growth with increasing stiffness.

Cancer Cell, in press.

MEDICINE

New Routes to Drugs

Twentieth-century dogma was that drug development for neglected diseases is neglected because there is not enough (or no) profit to be made from the generally impoverished populations who suffer these infections. A recent analysis by Moran reveals a more optimistic turn of events for this century with the burgeoning of public-private partnerships (PPPs), such as the Medicines for Malaria Venture, the Drugs for Neglected Diseases Initiative, and the TB Alliance. PPPs are becoming pivotal in coordinating the efforts of Western multinational pharmaceutical firms, with a range of contacts and clinical experience in academia, with the efforts of smaller biotech and developing-country firms. Moran points out that multinationals are not motivated solely by profit; they also want to burnish their reputations and gain strategic access to developing-country markets and labor skills. By integrating and screening projects and expertise, PPPs synergistically reduce drug development costs from about $1 billion for a Western market to tens of millions for a neglected disease. The good news is that the PPPs will get better and more efficient as their experience grows. — CA

PLoS Med. **2**, e302 (2005).

CHEMISTRY

Fast Vibrational Coupling

Multipulse nuclear magnetic resonance (NMR) spectroscopy is useful for determining the conformations of proteins and other large molecules in solution, but its temporal resolution is limited to microseconds. Recently synthesized nanoscale switches and motors operate on a picosecond time scale, and so require a faster method to gauge their operation. In principle, two-dimensional infrared (2D IR) spectroscopy offers the necessary increase in resolution because it measures coupling between atomic vibrations, rather than nuclear spins.

Larsen *et al.* have taken the preliminary step of showing that a 2D IR pulse sequence effectively reveals the static structure of a rotaxane in solution. This common molecular switch motif consists of a macrocycle that is suspended on an axle via hydrogen bonding; elaborations of this basic structure allow the ring to move when light, current, or chemical reagents are applied. The spectroscopic study quantified coupling between vibrating carbonyl (C=O) groups on the ring and those on the shaft. Analysis of the data through modeling yielded the distance (r = 6.9 Å) and angle (θ = 48°) between these groups, opening the door to a real-time dynamics study of switch and motor operations. — JSY

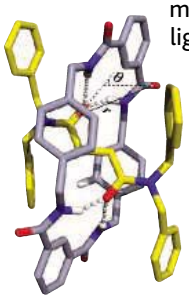

The rotaxane with the carbonyl oxygens in red.

Proc. Natl. Acad. Sci. U.S.A. 10.1073/pnas.0505313102 (2005).

APPLIED PHYSICS

Highly Heat-Sensitive

The most severe tests of calorimetry are surface processes, where the small number of reaction, binding, or adsorption events limits the amount of heat available for measurement. Fon *et al.* have constructed a cryogenic suspended SiN calorimeter that has a heat capacity resolution of 0.5 attojoule per Kelvin, compared with a typical state-of-the-art resolution of 1 femtojoule per Kelvin. The fast response of interdigitated AuGe resistance thermometers allows sampling every few microseconds, so that temperature changes can be followed via the fast relaxation of the calorimeter. The authors measured the enthalpy change associated with adsorbing 0.16 monolayers of ^{4}He on a device area of 1.2×10^{-9} m^2. The measured value at 2 K corresponds to a heat capacity of 1.4 k_B per helium atom, which agrees well with the measured value for He adsorbed on Grafoil. — PDS

Nano Lett. 10.1021/nl051345o (2005).

BIOCHEMISTRY

A Frozen Giant

Mimivirus (so-named because when subjected to Gram staining it, resembles or mimics a microbe) was first identified a decade ago as a virus growing within amoebae during an outbreak of pneumonia. Since then, its genome has been sequenced

CONTINUED ON PAGE 1969

Integrated Solutions for Protein & Peptide Arrays

- **Protein localization**
- **Differential expression**
- **Interaction profiling**
- **Epitope mapping**
- **Phosphorylation profiling**

Sigma-Aldrich recognizes microarray technology as a central proteomic research tool and is committed to enabling accurate identification of your biological sample's interaction or function against a characterized set of proteins, peptides, antibodies, or tissue extracts.

The foundation of our microarray product line lies in novel and innovative technologies that ensures consistent representation and compatibility with a variety of probes such as DNA, protein, or small molecules. Whether you are screening for antibody expression or protein interaction, be confident your profile pattern is accurate. Discover the advantages of Sigma's microarrays today!

Product Description	Product Code
NEW Panorama Human Cancer Array v1 Microarray	**HPFM2**
Panorama Human p53 Protein Function Microarray	**HPFM1**
Panorama Antibody Microarray – Cell Signaling	**CSAA1**
NEW Panorama Antibody Microarray – Gene Regulation	**GRAA2**
NEW Panorama Antibody Microarray – MAPK & PKC Pathways	**MPAA3**
Panorama Mouse/Rat Tissue Extract Protein Array Kit	**MRPA1**
PEPscreen® Custom Peptide Libraries	*Contact Sigma-Genosys at* **www.sigma-genosys.com** *for details*

Learn more about Sigma's arrays and custom services at
sigma-aldrich.com/arrays

sigma-aldrich.com

LEADERSHIP IN LIFE SCIENCE, HIGH TECHNOLOGY AND SERVICE
SIGMA-ALDRICH CORPORATION • BOX 14508 • ST. LOUIS • MISSOURI 63178 • USA

SIGMA®

and, at 1.2 Mb, shown to be larger than the genomes of some bacteria and to contain more than 1000 open reading frames (potential protein-encoding genes).

Using cryoelectron microscopy, Xiao *et al.* report that the outer protein shell of the virus is about 5000 Å in diameter and supports a dense mesh of 1250 Å–long fibers that may be collagen triple helices. Inside the capsid are two lipid membranes that surround the supersized genome. A three-dimensional reconstruction to 75 Å resolution is consistent with icosahedral symmetry and an impressively high triangulation number of 1179, indicative of a remarkably accurate assembly of protein subunits into the capsid. — GJC

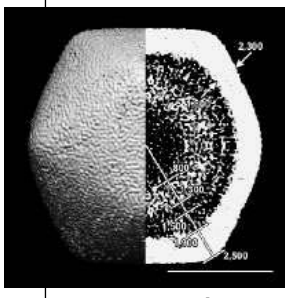

Reconstructed mimivirus showing the surface and a cross section with dimensions in Å; scale bar, 2000 Å.

J. Mol. Biol. 10.1016/j.jmb.2005.08.060 (2005).

CHEMISTRY

Isomer Identification

Although mass spectrometry is among the most sensitive methods used to identify molecules, it is ill-suited for distinguishing structural isomers, which are chemically distinct entities that have the same mass. Gas or liquid chromatography can be used to separate isomers before applying mass spectrometry, but this adds a relatively slow step.

In traditional mass spectrometry, analytes are ionized nonselectively by collisions with electron or atom beams, and the resulting ions are identified as a pattern of fragments on the basis of their mass-to-charge ratios in electric or magnetic fields. Dela Cruz *et al.* instead use phase-modulated ultrashort laser pulses to induce ionization. By first dispersing the pulses through a tunable liquid crystal array, they introduce wavelength-dependent phase shifts that subtly influence the excited state dynamics of the irradiated molecules. Through trial and error, they determine reproducible pulse shapes that induce different fragmentation patterns in different isomers. One well-shaped pulse, for example, causes *p*-xylene to break into methyl and tropylium fragments more than twice as efficiently as *o*-xylene. Once the pulse shape is determined, it can be used to quantify isomer mixtures in less than a second. Similar pulses were achieved for quantifying mixtures of isomers of cresol and nitrotoluene, and of several cis and trans olefin isomers. — JSY

J. Phys. Chem. A 10.1021/jp0539425 (2005).

HIGHLIGHTED IN *SCIENCE*'S SIGNAL TRANSDUCTION KNOWLEDGE ENVIRONMENT

Science's STKE www.stke.org

A Mitochondrial Antivirus Defense

Intracellular viral double-stranded RNA (dsRNA) is detected by the protein RIG-1, which has a C-terminal domain that binds dsRNA. RIG-1 stimulates the coordinated activation of multiple transcription factors, including NF-κB, IRF3, and ATF2, which together act to regulate the expression of type 1 interferons, such as interferon-β (IFN–β), and thus promote the response to viral infection. Seth *et al.* have investigated the role of a protein named MAVS (for mitochondrial antiviral signaling) in mediating the downstream effects of RIG-1. Overexpression of MAVS in HEK293 cells activated IRF-3, NF-κB, and JNK (which activates ATF-2) and increased the abundance of endogenous IFN-β. Silencing MAVS abolished expression of IFN-β in response to Sendai virus. Moreover, MAVS overexpression protected cells from vesicular stomatitis virus–mediated death, whereas MAVS silencing sensitized the cells. Confocal microscopy and subcellular fractionation indicated that MAVS localized to the mitochondria, and localization depended on the transmembrane domain: Replacing this sequence with analogous domains from mitochondrial membrane proteins (Bcl-xL or Bcl-2) preserved MAVS activity, whereas targeting to other membranes reduced it. Thus, MAVS provides an unexpected link between mitochondria and the immune response. Two other groups, Xu *et al.* and Kawai *et al.*, have identified this same protein as an adapter that acts downstream of RIG-1 to stimulate IFN-β expression. — EMA

Cell **122**, 669 (2005); *Mol. Cell.* 10.1016/j.molcel.2005.08.014 (2005); *Nat. Immunol.* 10.1038/ni1243 (2005).

CREDITS: XIAO *ET AL.*, *J. MOL. BIOL.* 10.1016/J.JMB.2005.08.060 (2005)

www.sciencemag.org

Science

1200 New York Avenue, NW
Washington, DC 20005
Editorial: 202-326-6550, FAX 202-289-7562
News: 202-326-6500, FAX 202-371-9227

Bateman House, 82-88 Hills Road
Cambridge, UK CB2 1LQ
+44 (0) 1223 326500, FAX +44 (0) 1223 326501

Subscription Services For change of address, missing issues, new orders and renewals, and payment questions: 800-731-4939 or 202-326-6417, FAX 202-842-1065. Mailing addresses: AAAS, P.O. Box 1811, Danbury, CT 06813 or AAAS Member Services, 1200 New York Avenue, NW, Washington, DC 20005

Institutional Site Licences please call 202-326-6755 for any questions or information

Reprints: Author Inquiries 800-635-7181
Commercial Inquiries 803-359-4578
Corrections 202-326-6501

Permissions 202-326-7074, FAX 202-682-0816

Member Benefits Bookstore: AAAS/BarnesandNoble.com bookstore www.aaas.org/bn; Car purchase discount: Subaru VIP Program 202-326-6417; Credit Card: MBNA 800-847-7378; Car Rentals: Hertz 800-654-2200 CDP#343457, Dollar 800-800-4000 #AA1115; AAAS Travels: Betchart Expeditions 800-252-4910; Life Insurance: Seabury & Smith 800-424-9883; Other Benefits: AAAS Member Services 202-326-6417 or www.aaasmember.org.

science_editors@aaas.org (for general editorial queries)
science_letters@aaas.org (for queries about letters)
science_reviews@aaas.org (for returning manuscript reviews)
science_bookrevs@aaas.org (for book review queries)

Published by the **American Association for the Advancement of Science (AAAS)**, *Science* serves its readers as a forum for the presentation and discussion of important issues related to the advancement of science, including the presentation of minority or conflicting points of view, rather than by publishing only material on which a consensus has been reached. Accordingly, all articles published in *Science*—including editorials, news and comment, and book reviews—are signed and reflect the individual views of the authors and not official points of view adopted by the AAAS or the institutions with which the authors are affiliated.

AAAS was founded in 1848 and incorporated in 1874. Its mission is to advance science and innovation throughout the world for the benefit of all people. The goals of the association are to: foster communication among scientists, engineers and the public; enhance international cooperation in science and its applications; promote the responsible conduct and use of science and technology; foster education in science and technology for everyone; enhance the science and technology workforce and infrastructure; increase public understanding and appreciation of science and technology; and strengthen support for the science and technology enterprise.

Information for Contributors

See pages 135 and 136 of the 7 January 2005 issue or access www.sciencemag.org/feature/contribinfo/home.shtml

EDITOR-IN-CHIEF **Donald Kennedy**
EXECUTIVE EDITOR **Monica M. Bradford**
DEPUTY EDITORS **R. Brooks Hanson, Katrina L. Kelner**
NEWS EDITOR **Colin Norman**

Editorial supervisory senior editors Barbara Jasny, Phillip D. Szuromi; senior editor/perspectives Lisa D. Chong; senior editors Gilbert J. Chin, Pamela J. Hines, Paula A. Kiberstis (Boston), Beverly A. Purnell, L. Bryan Ray, Guy Riddihough (Manila), H. Jesse Smith, Valda Vinson, David Voss; associate editors Marc S. Lavine, Jake S. Yeston; online editor Stewart Wills; contributing editor Ivan Amato; associate online editor Tara S. Marathe; book review editor Sherman J. Suter; associate letters editor Etta Kavanagh; information specialist Janet Kegg; editorial manager Cara Tate; senior copy editors Jeffrey E. Cook, Harry Jach, Barbara P. Ordway; copy editors Cynthia Howe, Alexis Wynne Mogul, Sabrah M. n'haRaven, Jennifer Sills, Trista Wagoner; editorial coordinators Carolyn Kyle, Beverly Shields; publication assistants Chris Filiatreau, Joi S. Granger, Jeffrey Hearn, Lisa Johnson, Scott Miller, Jerry Richardson, Brian White, Anita Wynn; editorial assistants Ramatoulaye Diop, E. Annie Hall, Patricia M. Moore, Brendan Nardozzi, Michael Rodewald; executive assistant Sylvia S. Kihara; administrative support Patricia F. Fisher

News senior correspondent Jean Marx; deputy news editors Robert Coontz, Jeffrey Mervis, Leslie Roberts, John Travis; contributing editors Elizabeth Culotta, Polly Shulman; news writers Yudhijit Bhattacharjee, Adrian Cho, Jennifer Couzin, David Grimm, Constance Holden, Jocelyn Kaiser, Richard A. Kerr, Eli Kintisch, Andrew Lawler (New England), Greg Miller, Elizabeth Pennisi, Robert F. Service (Pacific NW), Erik Stokstad; Carolyn Gramling, Genevra Ornelas, Cathy Tran (interns); contributing correspondents Marcia Barinaga (Berkeley, CA), Barry A. Cipra, Jon Cohen (San Diego, CA), Daniel Ferber, Ann Gibbons, Robert Irion, Mitch Leslie (NetWatch), Charles C. Mann, Evelyn Strauss, Gary Taubes, Ingrid Wickelgren; copy editors Linda B. Felaco, Rachel Curran, Sean Richardson; administrative support Scherraine Mack, Fannie Groom bureaus: Berkeley, CA: 510-652-0302, FAX 510-652-1867, New England: 207-549-7755, San Diego, CA: 760-942-3252, FAX 760-942-4979, Pacific Northwest: 503-963-1940

Production director James Landry; senior manager Wendy K. Shank; assistant manager Rebecca Doshi; senior specialist Jessica K. Moshell; specialist Jay R. Covert; **Preflight** director David M. Tompkins; manager Marcus Spiegler; specialist Jessie Mudjitaba

Art director Joshua Moglia; associate art director Kelly Buckheit; illustrators Chris Bickel, Katharine Sutliff; senior art associates Holly Bishop, Laura Creveling, Preston Huey; associate Nayomi Kevitiyagala; photo researcher Leslie Blizard

***Science* International**

Europe (science@science-int.co.uk) editorial: international managing editor Andrew M. Sugden; senior editor/perspectives Julia Fahrenkamp-Uppenbrink; senior editors Caroline Ash (Geneva: +41 (0) 222 346 3106), Stella M. Hurtley, Ian S. Osborne, Stephen J. Simpson, Peter Stern; associate editor Joanne Baker editorial support Emma Westgate; Deborah Dennison administrative support Janet Clements, Phil Marlow, Jill White; news: international news editor Eliot Marshall deputy news editor Daniel Clery; correspondent Gretchen Vogel (Berlin: +49 (0) 30 2809 3902, FAX +49 (0) 30 2809 8365); contributing correspondents Michael Balter (Paris), Martin Enserink (Amsterdam and Paris); intern Michael Schirber

Asia Japan Office: Asca Corporation, Eiko Ishioka, Fusako Tamura, 1-8-13, Hirano-cho, Chuo-ku, Osaka-shi, Osaka, 541-0046 Japan; +81 (0) 6 6202 6272, FAX +81 (0) 6 6202 6271; asca@os.gulf.or.jp japan news bureau: Dennis Normile (contributing correspondent, +81 (0) 3 3391 0630, FAX 81 (0) 3 5936 3531; dnormile@gol.com); china representative Hao Xin, + 86 (0) 10 6307 4439 or 6307 3676, FAX +86 (0) 10 6307 4358; haoxin@earthlink.net; south asia Pallava Bagla (contributing correspondent +91 (0) 11 2271 2896; pbagla@vsnl.com); asia Richard Stone (rstone@aaas.org)

EXECUTIVE PUBLISHER **Alan I. Leshner**
PUBLISHER **Beth Rosner**

Fulfillment & Membership Services (membership@aaas.org) director Marlene Zendell; manager Waylon Butler; systems specialist Andrew Vargo; specialists Pat Butler, Laurie Baker, Tamara Alfson, Karena Smith, Vicki Linton; circulation associate Christopher Refice

Business Operations and Administration director Deborah Rivera-Wienhold; business manager Randy Yi; senior business analyst Lisa Donovan; business analyst Jessica Tierney; financial analyst Michael LoBue, Farida Yeasmin; rights and permissions: administrator Emilie David; associate Elizabeth Sandler; marketing: director John Meyers; marketing managers Darryl Walter, Allison Pritchard; marketing associates Julianne Wielga, Mary Ellen Crowley, Catherine Featherston; director of international marketing and recruitment advertising Deborah Harris; international marketing manager Wendy Sturley; marketing/member services executive: Linda Rusk; japan sales and marketing manager Jason Hannaford; site license sales: director Tom Ryan; sales and customer service Mehan Dossani, Kiki Forsythe, Catherine Holland, Wendy Wise; electronic media: manager Lizabeth Harman; production associates Sheila Mackall, Amanda K. Skelton, Lisa Stanford, Nichele Johnston; applications developer Carl Saffell

Advertising director worldwide ad sales Bill Moran

Product (science_advertising@aaas.org); midwest Rick Bongiovanni: 330-405-7080, FAX 330-405-7081 • west coast/w. canada B. Neil Boylan (Associate Director): 650-964-2266, FAX 650-964-2267 • east coast/e. canada Christopher Breslin: 443-512-0330, FAX 443-512-0331 • uk/europe/asia Tracey Peers (Associate Director): +44 (0) 1782 752530, FAX +44 (0) 1782 752531 japan Mashy Yoshikawa: +81 (0) 33235 5961, FAX +81 (0) 33235 5852 israel Jessica Nachlas +9723 5449123 • traffic manager Carol Maddox; sales coordinator Deiandra Simms

Classified (advertise@sciencecareers.org); u.s.: sales director Gabrielle Boguslawski: 718-491-1607, FAX 202-289-6742; inside sales manager Daryl Anderson: 202-326-6543; west coast/midwest Kristine von Zedlitz: 415-956-2531; east coast Jill Downing: 631-580-2445; canada, meetings and announcements Kathleen Clark: 510-271-8349; line ad sales Emnet Tesfaye: 202-326-6740; sales coordinators Erika Bryant; Rohan Edmonson Christopher Normile, Joyce Scott, Shirley Young; international: sales manager Tracy Holmes: +44 (0) 1223 326525, FAX +44 (0) 1223 326532; sales Christina Harrison, Svitlana Barnes; sales assistant Helen Moroney; japan: Jason Hannaford: +81 (0) 52 789 1860, FAX +81 (0) 52 789 1861; production: manager Jennifer Rankin; assistant manager Deborah Tompkins; associates Christine Hall; Amy Hardcastle; publications assistants Robert Buck; Natasha Pinol

AAAS Board of Directors retiring president, chair Shirley Ann Jackson; president Gilbert S. Omenn; president-elect John P. Holdren; treasurer David E. Shaw; chief executive officer Alan I. Leshner; board Rosina M. Bierbaum; John E. Burris; John E. Dowling; Lynn W. Enquist; Susan M. Fitzpatrick; Richard A. Meserve; Norine E. Noonan; Peter J. Stang; Kathryn D. Sullivan

AAAS
ADVANCING SCIENCE, SERVING SOCIETY

NetWatch

edited by Mitch Leslie

IMAGES

Island Hopping

Mangrove forests reinforce tropical coastlines, filter runoff, and house throngs of terrestrial and aquatic organisms such as this multicolored crab (right; *Goniopsis cruentata*). Discover more about the intricate ecology of these forests at this snappy virtual tour from the Smithsonian Institution. The excursion circles Mangal Cay in Belize, an island that features a peat bog, mats of cyanobacteria, and tree-climbing shellfish. Twenty-four stops delve into topics such as mangroves' aerial roots, called pneumatophores. These structures pipe oxygen into the soil, promoting the oxidation of toxic compounds. Visitors can also dive into the waters surrounding Mangal Cay, home to everything from delicate anemones to crocodiles, and learn about threats to mangrove forests such as coastal development and shrimp farming.

www.mangroves.si.edu/Trail/VirtualTour.html

TOOLS

A Bigger BLAST

The new site SEQUEROME* supplies a suite of tools for analyzing the results from BLAST searches of DNA and protein sequences. At your fingertips are buttons that allow you to identify where particular DNA-chopping enzymes will cut the sequence or determine what amino acid string it codes for. InstaSeq,† another offering from the same group at Georgetown University in Washington, D.C., scans the Web as well as gene databases for particular DNA, RNA, or protein sequences. The tool can rummage through Microsoft Word files, PDFs, and Web pages.

* sequerome.georgetown.edu/blast/index.jsp

† bioinformatics.georgetown.edu/InstaSeq.htm

EXHIBITS

Secrets of the Phage

After scraping through his chemistry and biology classes, Salvador Luria (1912–1991) only entered medical school in his native Italy because of parental pressure and "my own lack of alternative inclinations." Luria caught the science bug, though, and some 40 years later shared the 1969 Nobel Prize in physiology or medicine for pioneering work on viral genetics. The latest installment in the U.S. National Library of Medicine's Profiles in Science series looks back at his life and career. He was one of the first researchers to harness bacteriophages—viruses that attack bacteria—to probe the mechanics of inheritance. At the site, you can browse photos, letters, selections from Luria's laboratory notebooks, and other documents. For example, you'll find his breakthrough 1943 paper with biophysicist Max Delbrück that solidified the then-controversial idea that bacteria have genes.

profiles.nlm.nih.gov/QL

RESOURCES

Ecology's Early Years

Just about any ecology text will highlight the work of British researcher David Lack (1910–1973), who argued that moderate-sized clutches of bird eggs yield the most surviving offspring. But most books don't supply much information about Lack himself. For brief biographies of Lack and more than 100 other early ecologists, evolutionists, and biogeographers, flip through this reference from Charles Smith, a science librarian at Western Kentucky University in Bowling Green, and colleagues. The site spans the 17th century to 1950 and describes each researcher's significance, provides a chronology, and includes links to any online books or papers. You can dig up details about figures such as the Scottish-born Alexander Wilson (1766–1813), who compiled the first catalog of American birds in between writing poetry.

www.wku.edu/~smithch/chronob/homelist.htm

FUN

Playing Patterns

For an amusing connection between math and music, tune in the new site Wolfram-Tones. Orchestrated by the company Wolfram Research of Champaign, Illinois, the site plays compositions based on cellular automata: complex geometrical patterns that arise from simple rules relating the color of a particular square to the colors of its neighbors. A section from one of these diagrams can serve as a musical score (above), in which the height of each square indicates the pitch of the note. The site lets you cue up songs in genres from hip-hop to country to Latin, or assign different instruments. You can also play around with the underlying math by altering the rule that generated the pattern.

tones.wolfram.com

Send site suggestions to netwatch@aaas.org.
Archive: www.sciencemag.org/netwatch

CREDITS (TOP TO BOTTOM): SMITHSONIAN INSTITUTION, SEA MCKUEN; WOLFRAM RESEARCH; MIT MUSEUM/NLM

This Week

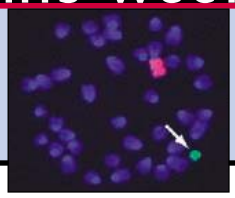

PAGE 1975
Mouse model for Down syndrome

1977
Plants recruit insect defenders

SCIENTIFIC ETHICS

Discovery of Pluto Contender Contested in Planetary Court

When a group of astronomers announced back in July that it had discovered a distant, icy body rivaling Pluto in size, the claim seemed exciting enough. But now it has become entangled in charges of unethical behavior. Planetary astronomers are feeling their way through uncharted territory as they try to sort out conflicting claims to the discovery.

All but one of the facts in the case are uncontested, thanks in part to the crystal-clear memory of the Internet. As first reported by *The New York Times*, astronomers José Ortiz and Pablo Santos-Sanz of the Institute of Astrophysics of Andalucia (IAA) in Granada, Spain, telescopically imaged an object, now temporarily designated 2003 EL_{61}, on 3 nights in March 2003. But they did not analyze the images right away. In the meantime, Michael Brown of the California Institute of Technology in Pasadena and his colleagues independently imaged the same object, analyzed the images, and recognized that it was slowly moving against the field of stars, proving that it is a distant member of the solar system. This was in December 2004. By 20 July this year, after more study, Brown's abstract describing the object in general terms was posted on an open Web site for an upcoming September meeting.

On 25 July, Santos-Sanz pointed out the object in their 2003 images, according to Ortiz writing in a 15 September posting to the Minor Planet Mailing List. The next day, according to electronic archives, the unsecured observing log of the telescope Brown's team used was accessed three times using a computer at the IAA. The log shows exactly when and where Brown and his colleagues had pointed the telescope at EL_{61} at various times during the previous 6 months. In his posting and in a 16 September e-mail to *Science*, Ortiz acknowledges for the first time that he and Santos-Sanz did in fact access the telescope log after Googling Brown's code name for the object mentioned in the meeting abstract.

The day after accessing the observing log, Santos-Sanz used the same computer to report to the Minor Planet Center (MPC) in Cambridge, Massachusetts, that he and Ortiz had discovered what would be designated 2003 EL_{61}. The day after that, 28 July, the telescope Web log was again accessed, this time by a second computer at the IAA. Later the same day, Ortiz used this second computer to notify the MPC of new observations of EL_{61} made by a second group at Ortiz's request. This prompted MPC—a part of the International Astronomical Union (IAU)—to designate the object 2003 EL_{61}, effectively crediting Ortiz and Santos-Sanz with the discovery and thus the privilege of suggesting a name for the object. As yet unaware that the Spanish astronomers had accessed the observing log, Brown e-mailed his congratulations to Ortiz on the 29th.

MPC may have been right to credit the Spanish astronomers at the time, Brown now says, but "I see no reason to believe they made the discovery themselves." Normally, when astronomers hunt for objects in the solar system, they examine their search images within days. That the Spanish researchers happened to find the object more than 2 years after the search but a few days after the observing log became available to them "is just an incredible coincidence," says Brown.

Whose discovery? Michael Brown (*top*) saw the near-Pluto-size body first, José Ortiz (*middle*) reported it first, and Brian Marsden (*bottom*) will decide the winner.

In other fields, such charges of unethical behavior might end up in a formalized adjudication process. In planetary astronomy, there is no such process. Instead, the MPC director chooses winners and losers in astronomical exploration, and the chips fall where they may. MPC Director Brian Marsden "has historically been the czar on these matters," says planetary astronomer Richard Binzel of the Massachusetts Institute of Technology in Cambridge. "It's whoever Brian wants to bestow the discovery on."

Brown concedes that priority in the case of EL_{61} probably cannot be proved one way or the other, but he has no doubt that "they violated one of the central tenets of science, which is that you cite your sources," as he told Marsden in an e-mail message on 15 August. "I request that Ortiz *et al.* be stripped of offial [*sic*] discovery status and that the IAU issue a statement condemning their actions."

After 6 weeks of silence, Ortiz has begun to defend himself. In the mailing list posting, he stands by the order of discovery events. Their analysis had been delayed by technical problems with the images, he says. ▶

CREDITS (TOP TO BOTTOM): CALIFORNIA INSTITUTE OF TECHNOLOGY; INSTITUTO DE ASTROFÍSICA DE ANDALUCÍA; RUTH BAZINET/HARVARD-SMITHSONIAN CENTER FOR ASTROPHYSICS

1978
Venice: That sinking feeling

1980
Salvaging science after Hurricane Katrina

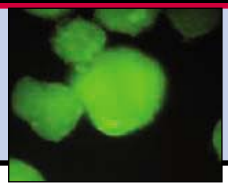

1982
Converting stem cells to germ cells

And in the e-mail to *Science*, he says that their Googling of the code name and accessing the log in the course of a "revision process" is "perfectly legitimate. That is no hacking or spying or anything similar." As to their failure to mention the other group's earlier discovery, he says he had no room for such details, and in the posting, he adds that they weren't even sure the two groups had been looking at the same object.

Marsden doesn't buy that. The failure to mention Brown's observation, he tells *Science*, "just seems ethically improper. The whole story is quite bizarre." But as the judge, jury, and executioner in this case, he awaits a stronger defense from Ortiz. "I haven't done anything," he says. "I'm trying to give Ortiz and his people every chance to prove their case." In the next couple of months, after consulting with members of the IAU committee responsible for naming small solar system bodies, Marsden will decide who the discoverer of 2003 EL_{61} is. And that will probably be that. **–RICHARD A. KERR**

JAPAN

Tokyo Professor Asked to Redo Experiments

TOKYO—Japan's most prestigious university is investigating the basis of several papers published by a faculty member over the past 7 years. Officials at the University of Tokyo say it's the first case of its kind in the institution's history.

The matter involves a group led by Kazunari Taira, a professor of chemistry and biological chemistry in the Graduate School of Engineering. Taira was unable to produce the raw data or experimental notes to support a string of papers from his lab that were published in top-tier journals, according to an interim report by an investigative committee looking into the matter. Taira has promised to redo the experiments, which he says were done by a research associate who entered the data directly into a computer.

The case has caught university officials flat-footed. "We don't have an example of how such a situation would ordinarily be handled," says Yoichiro Matsumoto, a mechanical engineer who led the investigating committee. Both Matsumoto and a university spokesperson say that this is the first time such an allegation has surfaced at the university, known as Todai.

The investigation was triggered by an April letter to the university from the Japan RNA Society. According to a report released last week by the investigating committee, the society questioned the reproducibility of the results reported in 11 papers that appeared between 1998 and 2004 in journals that include *Nature*, *Nature Biotechnology*, and the *Proceedings of the National Academy of Sciences U.S.A.* The committee said the letter, which has not been released, raised questions about whether a gene discovery technique developed by the Todai group works as described. The society also noted that Taira had retracted a 19 June 2003 *Nature* paper because of a misidentification of a key gene and issued a correction to the methodology described in a 9 September 2004 *Nature* paper. Two society officials declined to discuss the letter.

To start its probe, the investigations committee surveyed researchers both in Japan and around the world. Of the nine who replied, none had reproduced the research results, although it's not clear how many had attempted to do so. The committee then selected four papers for a detailed examination and concluded that Taira could not provide raw data or notebooks to support the papers. The committee concluded that the reliability of the research results could not be verified.

Taira told *Science* that the key experiments leading to the questioned results were done by Hiroaki Kawasaki, a research associate. Kawasaki had entered all the raw data and notes directly into a computer, Taira said. However, those files were not properly backed up and now cannot be reconstructed, he added. Taira said that he was unaware Kawasaki was not keeping proper notes. "There is no excuse" for the lax oversight, he said.

Still, Taira is standing behind the results. The gene discovery technique hinges on the use of a synthetic ribozyme, which is a short RNA enzyme, to inactivate genes. Taira says several groups around the world have developed similar approaches and that other groups in Japan have used their ribozyme to identify genes. "This technology has been checked by other professors at other universities, and it has worked," he says.

Shigeo Ohta, a biochemist at Nippon Medical School in Kawasaki, says he used a ribozyme from Taira's group as the basis for a 2003 paper that identifies a gene that may contribute to Alzheimer's disease. "Of course we believe the published results are accurate," he says, adding that his group plans to double-check the results in light of the Todai investigation.

Matsumoto says the committee has not questioned all of the work from Taira's lab. But he says "it's a big mistake" for a group leader to overlook proper recording of experimental details. Taira acknowledges that he will need to reproduce the experiments to put the matter to rest. Kawasaki did not reply to an e-mail message, but Taira says his research associate "feels he can carry out the experiments and prove they are OK."

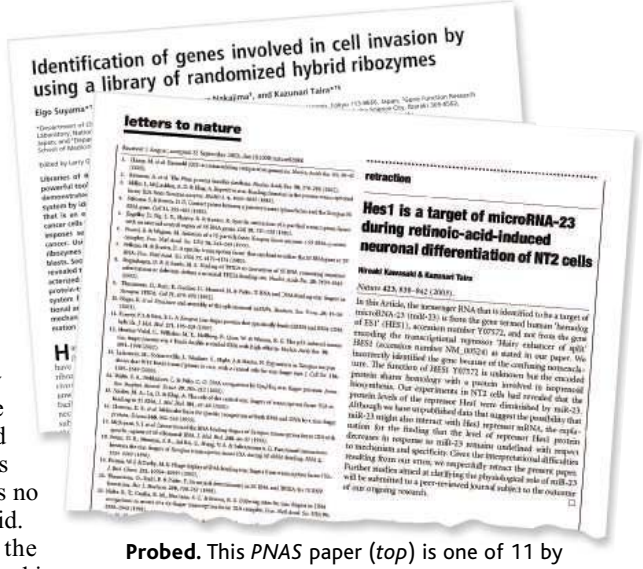
Identification of genes involved in cell invasion by using a library of randomized hybrid ribozymes

letters to nature

retraction

Hes1 is a target of microRNA-23 during retinoic-acid-induced neuronal differentiation of NT2 cells

Probed. This *PNAS* paper (*top*) is one of 11 by Kazunari Taira under scrutiny; one *Nature* paper was retracted 5 months after it appeared.

The university has agreed to give Taira until the end of March to redo the experiments. Matsumoto says the university went public with its investigation—holding a press conference on 13 September—because the committee felt it owed the RNA Society an answer. **–DENNIS NORMILE**

CREDITS (BACK TO FRONT): *PNAS*; *NATURE*

PEER REVIEW

Suggesting or Excluding Reviewers Can Help Get Your Paper Published

CHICAGO, ILLINOIS—It's the closest most scientists will come to picking their own jurors. Amid all the checklists, bibliographic information, and file-attachment instructions, the manuscript submission forms of many journals ask authors a simple question: Are there any individuals you would like to suggest or exclude as potential reviewers?

Having a say over who will review one's work should be a good thing. Authors may be better placed than editors to know who is best qualified to evaluate their findings, and they may have valid reasons for keeping sensitive results out of the hands of a close competitor. Yet many decline to suggest reviewers, and only a small percentage opt to exclude them.

That may change, thanks to the results of three studies presented here last week at the Fifth International Congress on Peer Review and Biomedical Publication, organized by the *Journal of the American Medical Association* and the *British Medical Journal* (*BMJ*) Publishing Group. Either suggesting or excluding reviewers, the studies show, can significantly increase a manuscript's chances of being accepted.

"The studies point out a potential for bias in the peer-review system," says R. Brian Haynes, a clinical epidemiologist at McMaster University in Ontario, Canada, and the editor of two clinical journals. "If that's the case, this is something we should be taking a closer look at."

Journal editors who use author-suggested reviewers tend to disagree about their value, says Sara Schroter, a senior researcher at the *BMJ* Publishing Group. So she and colleagues compared author-suggested reviews to those solicited by editors at 10 journals owned by the company, including *Heart*, *Tobacco Control*, and *BMJ* itself. In a 9-month survey of 788 reviews for 329 manuscripts, the team found no significant difference in the quality (as measured by widely agreed upon criteria judged to be essential for a good review) or timeliness of reviews between the two groups. However, they did find that, compared to editor-suggested reviewers, author-suggested reviewers were more likely to recommend manuscript publication (55.7% versus 49.5%) and less likely to recommend rejection (14.4% versus 24.1%).

"Editors and authors can be confident that either group will do an adequate job at reviewing the manuscript," says Schroter. "But editors should be a bit more cautious about relying on the recommendations of author-suggested reviewers."

Schroter's findings are reinforced by a study conducted by journal consultant Elizabeth Wager and colleagues at BioMed Central, an open-access publisher of online journals. Wager's team compared editor-chosen and author-suggested reviews submitted to 40 of BioMed Central's journals. Using criteria similar to Schroter's, the researchers found little difference in quality between the two groups of reviews. And, like Schroter, they found that author-suggested reviewers were more likely to advocate manuscript acceptance (47% versus 35%) and less likely to recommend rejection (10% versus 23%).

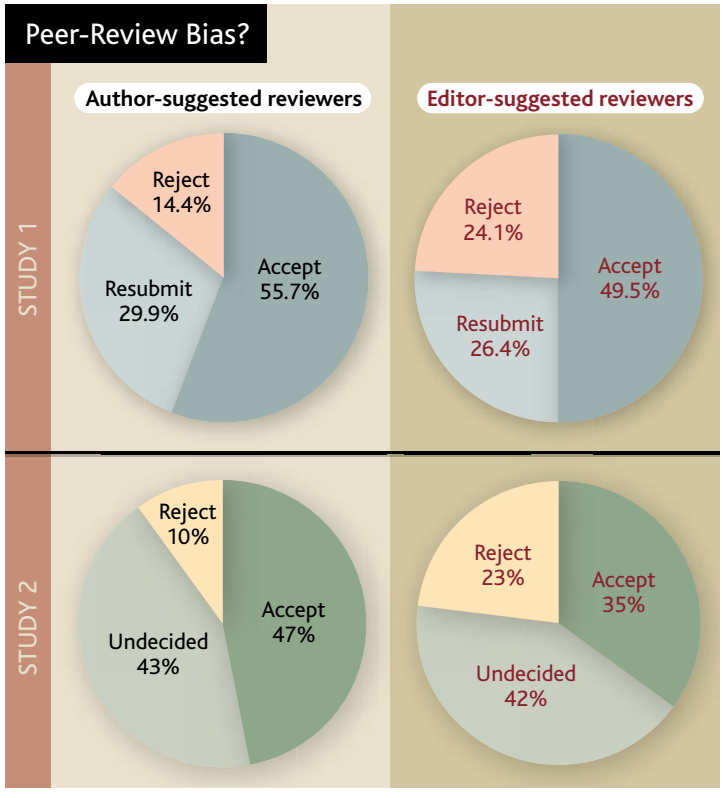

Choose wisely. Author-suggested reviewers are more likely to recommend manuscript acceptance and less likely to advocate rejection than editor-suggested reviewers, according to studies led by Sara Schroter *(above)* and Elizabeth Wager *(below)*.

Opting to exclude reviewers may have an even more dramatic effect on a manuscript's success. Lowell Goldsmith, a dermatological geneticist at the University of North Carolina, Chapel Hill, and the editor of the *Journal of Investigative Dermatology*, and colleagues looked at 228 consecutive manuscript submissions to the journal in 2003. The team found that the odds of acceptance were twice as high for manuscripts for which authors had excluded reviewers compared to those whose authors had not done so. "Excluding reviewers ends up being very, very important," says Goldsmith. "People know their assassins."

What's driving these numbers is not clear. If authors tend to suggest sympathetic reviewers and exclude nitpicky ones, for example, the findings could spotlight biases in the peer-review process. Similarly, bias may be introduced by reviewers in journals at which reviews are not anonymous. Says Wager: "Author-suggested reviewers don't want to be the person that killed their recommender's last study."

But David Nordstrom, an epidemiologist at the University of Minnesota, Twin Cities, and an adviser on grant applications and peer review, isn't as cynical. "I take a fairly benign view," he says: Author-suggested reviewers tend to be familiar with the author's field and may be in a better position to recognize the potential impact of a paper. And Haynes says that more-established researchers, who may have the hubris to exclude reviewers, may also have a better chance of getting manuscripts accepted.

Are such author-tailored reviews likely to increase? Matthias Egger, an epidemiologist at the University of Bern in Switzerland and an associate editor of the *International Journal of Epidemiology*, says it's hard to predict. Many authors are loath to exclude reviewers because it goes against their ideal vision of what science should be about, he says: "Scientists like to believe that personal factors shouldn't play a role in science."

At the same time, he says, there *are* valid reasons to single out reviewers. Some scientists hold grudges, Egger says. Others may have conflicts of interest or are just not qualified to evaluate certain topics. So suggesting or excluding reviewers may help limit bias rather than introduce it. "I've never excluded a reviewer," he says, "but perhaps it isn't such a bad thing to do."

—DAVID GRIMM

CREDITS (TOP ROW) S. SCHROTER *ET AL.*; (BOTTOM ROW) E. WAGER *ET AL.*

GENETICS

Mouse With Human Chromosome Should Boost Down Syndrome Research

After more than a decade of frustrated efforts, researchers have finally pulled off a genetic engineering first, creating a strain of mice with a nearly complete copy of human chromosome 21. The strain's unusual genome mimics the genetic makeup of people with Down syndrome, the most common inherited form of mental retardation.

"This is going to have a huge impact on Down syndrome research," says Roger Reeves, a geneticist at Johns Hopkins University in Baltimore, Maryland. Adds Julie Korenberg of Cedars-Sinai Medical Center and the University of California, Los Angeles: "This mouse not only solves problems, but it raises the next round of questions and creates a way to solve them."

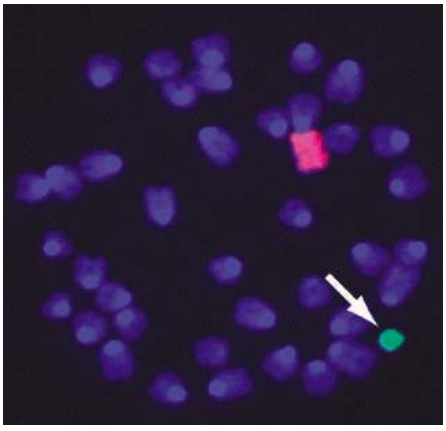

A dash of humanity. A copy of human chromosome 21 (*green*) added to mouse ES cells has yielded mice with symptoms of Down syndrome.

CREDIT: A. O'DOHERTY *ET AL.*, *SCIENCE*

People with Down syndrome have an extra copy of chromosome 21, resulting in mild to moderate mental retardation and abnormal facial features. About 40% of Down syndrome children have heart defects, and many have weakened immune systems. Efforts to model Down syndrome in mice have been complicated by the fact that the mouse versions of the genes on human chromosome 21 are inconveniently scattered across three mouse chromosomes. About two-thirds lie on mouse chromosome 16, the rest on chromosomes 10 and 17. One of the most popular mouse models now in use has an extra bit of mouse chromosome 16 that contains the counterparts of roughly half the genes on human chromosome 21.

To create a more complete mouse model, researchers led by Elizabeth Fisher of the Institute of Neurology in London and Victor Tybulewicz of the National Institute for Medical Research, also in London, took a radically different approach. Rather than trying to duplicate regions of the mouse genome corresponding to human chromosome 21, they tried to put the human chromosome into mice. It wasn't easy.

The team built on a technique pioneered by a Japanese group to add fragments of human chromosomes to mice. They extracted chromosomes from human fibroblast cells and transferred them into mouse embryonic stem (ES) cells. A marker gene indicated which ES cells had picked up chromosome 21—usually just one or two cells out of a batch of tens of millions, Tybulewicz says. The team injected the ES cells into early mouse embryos, which were carried to term by a foster mom. Additional tinkering was needed to create a strain of mice that passed the extra chromosome on to their offspring.

That strain, called Tc1, has about 92% of human chromosome 21, the team reports on page 2033. It also has several characteristics of Down syndrome. Although there's no test for mental retardation in mice, the Tc1 mice have deficits in spatial learning and memory similar to those found in Down syndrome patients; they also have a deficit in "long-term potentiation," a neurophysiological process thought to underlie learning and memory. Perhaps most significant, the mice have heart defects like those seen in Down syndrome patients. "That's a first," says Stylianos Antonarakis, a geneticist at the University of Geneva in Switzerland. "No other mouse so far has the heart defect."

Korenberg says the Tc1 mice are a vast improvement over the existing mouse models because they have not only many more of the genes on human chromosome 21 but also have the human DNA that regulates these genes. "This is a first mouse I would consider a superb model," she says.

But there are some wrinkles, says Charles Epstein of the University of California, San Francisco. He and others suspect that the largest drawback will be that the Tc1 mice don't have an extra copy of human chromosome 21 in every cell. Fisher's team reports, for example, that about a third of brain cells lack the extra chromosome. Mouse-to-mouse variations in which cells have the extra chromosome could complicate future experiments. William Mobley of Stanford University says he's concerned that some of the genes from human chromosome 21 that didn't make it into the Tc1 mice are likely to play an important role in Down syndrome. Even so, he and others says they can't wait to get their hands on these mice. **–GREG MILLER**

ScienceScope

To the Moon, Again

Four astronauts will travel to the moon for a week as early as 2018 using a new rocket system that NASA chief Michael Griffin calls "Apollo on steroids."

This week, Griffin laid out the space agency's plans to spend $104 billion for a return trip to the lunar surface. The plan for the first trip, which the White House recently approved after months of wrangling, includes building a new crew launcher by 2014. The launcher, combining expendable rocket and space shuttle components, would initially carry crew or cargo to the international space station. Then it would be converted to a lunar-bound vehicle, one that Griffin says would be 10 times safer than the current shuttle. A heavy-lift vehicle would follow to provide components for a moon landing and for possible flights to Mars.

At a press conference this week at NASA headquarters, Griffin pledged that "not one thin dime" of science money would be diverted into the space-flight effort. The lunar focus "is a huge opportunity for science," he said, adding, "I believe the global space science community will want to take advantage of that." Lawmakers say they will want far more details on funding; Griffin says savings will come from scaling back the current space-flight program. **–ANDREW LAWLER**

Endangered Species Act Targeted

A powerful critic of the Endangered Species Act (ESA) introduced a bill in Congress this week designed to substantially loosen the act's restrictions on landowners and businesses. Environmentalists say the measure would cripple protections for imperiled organisms.

The proposal, by House Resources Committee chair Richard Pombo (R–CA), would ease regulations by allowing, for example, projects that might harm endangered species to go forward unless federal agencies object. The bill would also set higher scientific standards for listing species under the act and would repeal a section that designates critical habitat, a source of many environmental lawsuits. Pombo, who argues that the act hurts while not effectively protecting species, is also proposing compensation for landowners prohibited from developing by the ESA.

The legislation is expected to face an easier time in the House than in the Senate, which has traditionally been less eager to undo ESA protections.

–ERIK STOKSTAD

INFECTIOUS DISEASE

Old Drugs Losing Effectiveness Against Flu; Could Statins Fill Gap?

ST. JULIAN'S, MALTA—With the threat of a deadly pandemic looming large, flu drugs are coming under increased scrutiny. At a meeting here last week* researchers reported disheartening data showing that the most aggressive of the circulating human flu strains has become resistant to an older class of flu drugs, rendering the drugs all but useless in the yearly battle against seasonal flu and deflating hopes they might be used to fight a pandemic.

But help might come from an unexpected source, according to another study: the cholesterol-lowering drugs called statins. Very preliminary data suggest that these drugs, cheap and widely available, might help prevent serious complications from a flu infection. If that's true, statins would offer a glimmer of hope for countries that, unlike the United States (see ScienceScope, p. 1977) and other wealthy nations, can't afford pandemic vaccines or oseltamivir, the pricey drug of choice for pandemic stockpiles.

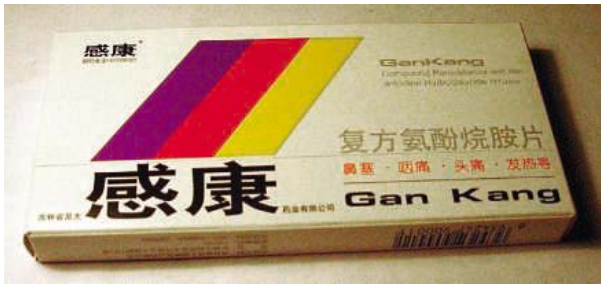

Over the counter. Tens of millions of courses of Gan Kang, a product containing amantadine, were reportedly sold in China last year.

Researchers had long known that amantadine and rimantadine, drugs that block a viral protein called M2, easily trigger resistance in the flu virus and that resistant strains can spread from person to person. But even after decades of use, resistance rates were low, says Rick Bright of the U.S. Centers for Disease Control and Prevention (CDC) in Atlanta, Georgia—until recently. Bright set out to determine when and where the upward trend started, screening more than 7500 flu samples, collected all over the world since 1995, for mutations that confer resistance against both drugs. ▶

* The Second European Influenza Conference, 11–14 September.

PLANT SCIENCE

New Gene Boosts Plant's Defenses Against Pests

With a little help from friends, crop plants may one day be better able to deter herbivores. By tweaking a cellular pathway for producing organic compounds, researchers have, in a proof-of-principle experiment, endowed *Arabidopsis thaliana* with the power to recruit mites as allies against leaf-munching enemies. The insertion of a strawberry gene into the mustard plant leads to two new compounds that attract predatory mites that devour herbivorous spider mites, Iris Kappers, a plant biochemist at Wageningen University in the Netherlands, and her colleagues report on page 2070. "They show it is possible to manipulate the movements of biological control agents through genetic engineering of plants," says Merijn Kant, a plant physiology at the University of Amsterdam.

Through a series of reactions involving multiple enzymes, plants make terpenoids, complex organic compounds that are important to development and growth, as well as to plant-animal interactions, such as pollination and pest deterrence. About 15 years ago, chemical ecologists discovered that lima beans, when infested with spider mites, emit at least one terpenoid that draws spider-mite predators to the scene; strawberries and other plants turned out to use the same defense. Since then, several groups have tried in vain to provide *Arabidopsis* with this capability by adding genes for the various enzymes necessary to make a particular attractant. "It's [been] notoriously difficult," says John Pickett, a biological chemist at Rothamsted Research in Harpenden, United Kingdom.

Whereas the earlier experiments put enzymes into the plant cell's cytoplasm, Kappers and colleagues at Plant Research International in Wageningen targeted the one they had chosen—a sesquiterpene synthase from strawberries—into the cell's mitochondria, which contain farnesyl diphosphate, a key building block for one mite attractant. The researchers attached an extra piece of DNA, one encoding a peptide subunit that directs a protein to mitochondria, to the enzyme's gene. This was "very clever targeting," says Ted Turlings, a chemical ecologist at the University of Neuchatel, Switzerland.

In contrast to the lackluster performance of similar synthases active in the cytoplasm, the mitochondrial-located enzyme exceeded expectations, producing about 25 times more of the expected attractant than had other transgenic *Arabidopsis* plants, the group reports. To their surprise, the researchers found that a second predatory mite attractant, one derived from the first by the removal of four carbon atoms and one alcohol subunit, had also accumulated in their transgenic plants—and sometimes in greater quantities than the intended one.

Help on the way. Transgenic *Arabidopsis* can now recruit predatory mites to cut down spider mite (*inset*) infestations.

Kappers and her colleagues tested the effectiveness of the organic compounds by releasing predatory mites into the center of a circle of *Arabidopsis* potted plants that alternated between wild and transgenic varieties. In the experiment, 388 predatory mites headed for the transgenic plants and 197 headed for the wild-type plants. "This is the first study" to show that the strawberry synthase gene can produce effective attractants in other plants, says Turlings.

Still, Ian Baldwin, a chemical ecologist at the Max Planck Institute for Chemical Ecology in Jena, Germany, is concerned that because such plants would continuously emit attractants, predatory mites won't know when and where prey are available. That uncertainty could cause the plant-mite relationship to break down over time, Kappers agrees. So she's looking for the genes responsible for producing mite attractants only after herbivores attack. Nevertheless, says Kant, the new study "is a major step forward in our ability to manipulate this phenomenon ultimately to our own benefit." —**ELIZABETH PENNISI**

CREDITS (TOP TO BOTTOM): GONG YIDONG; MARCEL DICKE/WAGENINGEN UNIVERSITY

For H3N2, the most virulent of the three strains that return each winter, a dramatic pattern emerged. Until 2002, no country had resistance rates higher than 10%. But in 2003, the rate shot up to 58% in China, then jumped to 74% in 2004. Hong Kong, South Korea, and Singapore followed with similar explosions, and samples taken during the 2005 flu season in Europe and the United States show that resistance has climbed to 14.3% and 11.5%, respectively.

The cause of the upswing is unclear, but Bright says over-the-counter sales of amantadine in China may have played a role. The drug is an ingredient of several anticold and antiflu cocktails sold in China. The leading product, called Gan Kang, is widely available for about $1.50, and a recent report in *China Business* put its 2004 sales at $80 million, or more than 50 million courses. Widespread use may have favored resistant virus strains, says Bright, and the dramatic jump in 2003 may be a result of the SARS panic that year.

Fairly inexpensive, amantadine and rimantadine are primarily used against seasonal flu in the United States and Japan, says Arnold Monto of the University of Michigan, Ann Arbor.

The finding may deal a fatal blow to plans, under way in a few countries, to add amantadine to pandemic stockpiles. That option had already become less appealing after the discovery that H5N1 avian flu strains isolated in Thailand and Vietnam were resistant to the drug—a finding some have linked to veterinary use of the drug in China (*Science*, 24 June, p. 1849). The finding that a human strain now shows widespread resistance—and the fact that pandemic viruses may arise when avian and human strains swap genes—makes it even less appealing.

Instead, most governments are choosing oseltamivir, a drug that blocks a viral protein called neuraminidase. So far, resistance to that drug is rare, and resistant viruses don't seem to grow as well. Still, the CDC study "shows that we should watch and worry," Monto says.

But many countries have other concerns: They don't have the means to buy large stashes of antiviral drugs or, for that matter, pandemic vaccines. That's where the inexpensive statins might come in. Over the past decade, researchers have discovered that these drugs not only lower cholesterol but also reduce levels of immunomodulators called cytokines, dampening inflammation. This is thought to contribute to their protection against cardiovascular disease, but it may also explain why in three studies so far, patients on statins appeared to fare better in bacterial infections in which inflammation plays a major role, such as sepsis and pneumonia.

Because flu viruses trigger cytokine release as well, and complications from flu include heart disease and pneumonia, David Fedson, a retired medical director of Aventis, wondered whether statins might be useful in treating flu. At Fedson's urging, clinical epidemiologist Eelko Hak and colleagues at University Medical Center Utrecht in the Netherlands began looking for evidence in a Dutch database of 60,000 primary-care patients. Such data collections are invariably incomplete; whether a patient was tested for flu or bacterial infections often isn't recorded, for instance. Nonetheless, Hak found tantalizing clues. During flu epidemics between 1996 and 2003, patients who had had at least two statin prescriptions over the previous 12 months had a 26% lower risk of pneumonia and other severe respiratory ailments. In non-flu seasons, statins didn't reduce the risk, suggesting that the drugs offer specific protection against flu complications.

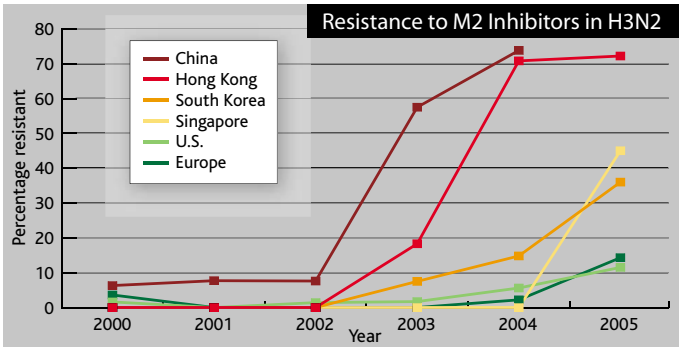

Rising resistance. H3N2 strains around the world are rapidly losing their sensitivity to amantadine and rimantadine, a trend that started in Asia.

SOURCE: R. BRIGHT *ET AL.*, CDC

That doesn't position statins as the next generation of flu drugs yet. The results will need to be confirmed in other patient populations, Hak says; pharmacoepidemiologist Christoph Meier of the University Hospital in Basel, Switzerland, says he will report results from a similar study shortly. Data from old clinical trials with statins should be reexamined, adds Hak, whose colleagues in Utrecht are also planning in vitro studies to determine how statins might have a protective effect. Clinical studies would have to show whether statins should be taken prophylactically—as millions of people do—or once a person is exposed or infected.

Questions aside, the findings generated interest among meeting participants such as Frederick Hayden, an antiviral expert at the University of Virginia, Charlottesville: "It's definitely something that should be explored."

–MARTIN ENSERINK

With reporting by Gong Yidong in Beijing.

ScienceScope

U.S. Tackles Bird Flu

The Bush Administration says it is getting serious about avian influenza. In a 14 September speech to the United Nations, President George W. Bush announced a new International Partnership on Avian and Pandemic Influenza that "requires countries that face an outbreak to immediately share information and provide samples to the World Health Organization [WHO]." The Department of Health and Human Services also promised technical and medical assistance to Southeast Asian nations and has announced a $100 million purchase of vaccine to combat the H5N1 bird flu virus, the leading pandemic candidate.

"We welcome the U.S. initiative," says Peter Cordingley, a spokesperson for WHO's Regional Office for the Western Pacific. He adds, however, that "the devil will be in the details." A key question is whether China will participate.

–DENNIS NORMILE AND JOCELYN KAISER

Japan and Singapore Link Up

Singapore's Agency for Science, Technology, and Research and Japan's RIKEN research agency agreed last week to exchange scientists, share research materials and information, and promote joint research projects. "[W]e need to expand cooperative efforts and relations with Asian nations," says RIKEN President Ryoji Noyori. Although details are still emerging, neuroscience, cancer drug targets, and environmental pathogens relevant to Asia will be three areas of focus for the partnership.

–DENNIS NORMILE

On Tap: HapMap

The comprehensive catalog of human genetic variation, known as HapMap, will be published on schedule in October, officials announced last week. The $135 million public-private effort has identified 3.6 million bases across the human genome that vary from population to population and also from individual to individual. According to the National Human Genome Research Institute, the results should save geneticists a bundle by reducing the multimillion-dollar cost of seeking a disease gene about 30-fold. "In some ways, [HapMap] will have a bigger impact than the sequence did," says Jeffrey Murray, a geneticist at the University of Iowa in Iowa City.

–ELIZABETH PENNISI

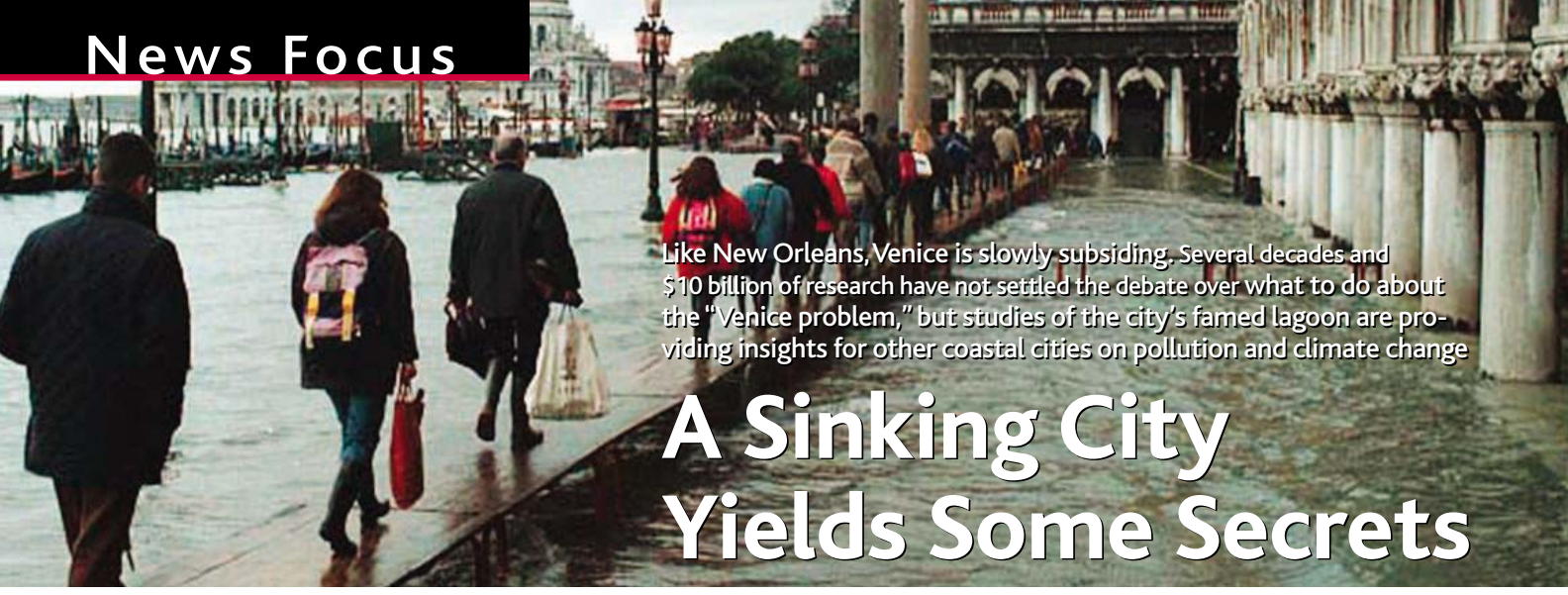

Like New Orleans, Venice is slowly subsiding. Several decades and $10 billion of research have not settled the debate over what to do about the "Venice problem," but studies of the city's famed lagoon are providing insights for other coastal cities on pollution and climate change

A Sinking City Yields Some Secrets

VENICE, ITALY—With a few expert motions of his oar, Fabio Carrera sends the long batèla boat gliding around a corner in this maze of canals. Suddenly, a dim patch of stars is the only light and the gentle swish of water the only sound. The experience evokes a centuries-old past, when Venice was one of the most powerful city-states in the Western world. But times have changed. One clue is the outboard motors protruding from beneath the tarps of moored boats. Another comes in the approach to the tunnel beneath Santo Stefano Church.

Although it is low tide, Carrera has to stoop to clear the moist stone ceiling. "At high tide, this passage is completely inaccessible," says Carrera, an urban information scientist and native Venetian who now divides his time between Worcester Polytechnic Institute in Massachusetts and his watery hometown. Elsewhere in the city, the *acqua alta* overflows the streets, fills the ground floors of buildings, and nibbles away at bricks and plaster.

New Orleans isn't the only coastal city threatened by encroaching waters. Little by little each year, Venice is being swallowed by the sea. Although this has been a problem since the Middle Ages, an accelerating rise in sea levels linked to global warming has turned the sporadic flooding from a nuisance into a looming catastrophe. Crisis already hit once, in 1966, when most of the city's streets were submerged under a meter of water. After 3 decades of debate, construction has now begun on a series of enormous tidal gates to defend the city. The $5 billion plan is controversial, with some critics arguing for different protective measures and others predicting that the coming decades of sea-level rise will render the gates obsolete (see sidebar, p. 1979).

But there's good news as well. The "Venice problem" has made the city a hot spot for scientific research, and there's no shortage of questions to tackle. "Every time we focus on one aspect of the practical problem, we discover another gap in our knowledge," says Pierpaolo Campostrini, an electrical engineer who directs CORILA, the organization that orchestrates Venice's scientific activities. Venice is providing other coastal cities with insights on what global climate change looks like at the local level. The city and its lagoon have also become a model system for studying how physical, biological, and urban processes interact in a marine setting.

Complex interactions. A computer model, overlaid on a satellite image, divides the Venice Lagoon into thousands of interacting triangles to enable study of its processes, such as water flow and sediment transport.

If Italy's Ministry of Education, Universities, and Research has its way, Venice will soon receive 1.5%—$60 million—of the $5 billion allocated for the tidal gates. City officials hope that the fivefold increase in national funding for basic science institutions will attract young people by creating more academic and high-tech jobs in a city whose population is rapidly shrinking. But whether science can revitalize the city or save it from the encroaching sea remains an open question.

At the battlefront of climate change

Zipping across the chalky green water in a motorboat, Campostrini points out a 16th century stone fortress with windows half-submerged. "It's not enough to estimate sea level as a global average," he says. Determining a particular city's risk—and what to do about it—requires an understanding of how climate change plays out locally. Even so, Venice is a "microcosm of the larger changes" taking place, says Trevor Davies, an atmospheric scientist at the University of East Anglia in Norwich, U.K.

For instance, Venice's record of sea-level change is now the most comprehensive in the world. Modern records of watermarks go back to the late 19th century, and researchers are finding ways to push the data farther back in time. A Venetian tradition of painting scenes with the help of *camera obscura* projections, the pinhole predecessor to photography, has left researchers with accurately scaled images of the green algae lines

CREDITS (TOP TO BOTTOM): ASSOCIATED PRESS; NASA/CORILA (SUPERIMPOSED GRID: GEORG UMGIESSER)

on walls that mark the average high-water level. A team led by Dario Camuffo, a climatologist at the University of Padua, Italy, has used them to extend sea-level records back another 300 years. Archaeologists are going back to the Middle Ages by estimating water levels based on the buried remains of former walls and bridges. And geologists are estimating the local sea level 2000 years ago by dating the remains of salt marsh plants that once poked above the water.

To fit these data into the global picture, researchers must also account for Venice's steady sinking due to a combination of moving continental plates and compressing sediments. The effect of a "little Ice Age" that hit Europe in the Middle Ages appears as a spike in sea levels even higher than today, whereas the levels at the time of the Roman Empire were about 1.5 meters lower. The most troubling trend, says geophysicist Alberto Tomasin of the University of Venice, is that sea levels have risen rapidly over the past 50 years.

Rising sea level isn't the only way climate change is affecting the city. Venice is a perfect natural lab for studying these effects, says Davies, because changes in weather patterns are "amplified" as changes in the frequency and severity of flooding events. Davies and Isabel Trigo, a climate scientist at the University of Lisbon, Portugal, have been teasing apart the different factors that cause the flooding.

The first task has been a postmortem of the 1966 disaster. Even without global warming, Venice would be prone to flooding, both because it was built only a couple of meters above the water and because of the city's location at the end of the narrow Adriatic Sea. The mountains to the north create low-pressure systems that suck the water level higher up around the lagoon, and wind tends to blow in from the sea, piling the water higher. And because of the shape of the Adriatic, sometimes swells generated by storms in the Mediterranean fall in phase with the tides, doubling the load of water that rushes into Venice's lagoon. These factors all conspired in 1966, causing the second tide of the day to push into the lagoon before the first could drain out, swamping the city.

With these mechanisms mapped out, Davies and Trigo are finding that climate change can also have a protective effect at the local level, at least in the short term. Venice would be in much deeper trouble by now, says Davies, were it not for a northward drift of the Atlantic storm track over the past 40 years, a trend linked to global warming. As a knock-on effect, storms in the Mediterranean have become less severe, likely saving the city from more 1966-style catastrophes. What happens if climate change nudges the Atlantic circulation farther off track is hard to predict. By studying Venice, says Davies, "you can start to draw out these subtle effects."

CREDIT: MOSE

Holding Back the Sea

Understanding climate impacts is useful. But the goal is to protect Venice. Dams would do the trick, says Campostrini, but the city would lose its income as a port and the lagoon would die without the daily tides. Injecting water into the underground aquifer that was nearly drained 40 years ago would lift the city, but uneven rising could also destroy it.

The compromise solution, called MOSE, is a series of 78 hollow, 300-ton steel gates. The gates will sit flat underwater at the lagoon's three inlets. But in anticipation of a flood, air will be pumped into the structures to make them stand upright and block tides up to a meter higher than those of 1966. Dredging has begun for the massive concrete foundations, but they won't be operational before 2011.

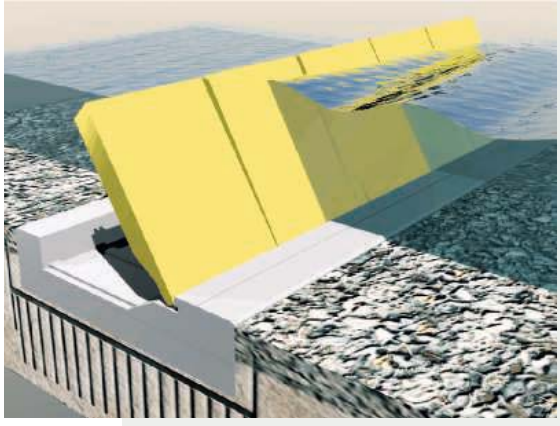

From below. The MOSE gates will rest underwater until floods are predicted and air is forced into their interiors.

The two questions hanging over MOSE are how often they will be used and how high sea levels will rise. By official estimates, the gates will be needed only two or three times a year. But critics say it could be as often as 50, enough to make the lagoon a sewage-contaminated swamp. And if the worst-case scenario of a 1-meter sea-level rise by 2100 comes true, the gates could be useless.

Outsiders' opinions are as mixed as those of Venetians. "Something like the MOSE gates are needed because controlling tidal surges is the only solution," says Caroline Fletcher, a coastal scientist at the University of Cambridge, U.K. But building gates is not enough, according to John Day, an ecologist at Louisiana State University in Baton Rouge who, until 2 years ago, led a long-term study of the Venice lagoon. Day says his study, one of many supported by national funds devoted to Venice, revealed that returning the flow of diverted rivers back into the lagoon would not only deposit sediments to compensate for subsidence but also would support lush wetland vegetation that would act as a buffer to slow the surges. With this natural defense, says Day, the gates would not be needed nearly as often. "Venice's situation is unique, as is New Orleans's," he says, "but they share the long-term problem of subsidence and wetland loss." Day contends that the consortium of industrial partners behind the MOSE project "[doesn't] want to hear about" natural versus engineered solutions.

Meanwhile, some Venetians argue that the entire debate has fallen far from the mark. "The take-home lesson from all this," says Fabio Carrera, an urban information scientist who divides his time between Venice and Worcester Polytechnic Institute in Massachusetts, "is that the cheapest solution is to stop global warming, but no one seems to be talking about that." **–J.B.**

Deep knowledge of a shallow lagoon

In the past 3 decades, Rome has spent more than $10 billion studying and coping with the "Venice problem." In comparison, Italy's national research foundation receives about $1 billion per year. "By the mid-1990s, people began saying that the Venice funding was a *torta*," a giant cake free for the taking, recalls Philippe Pypaert, an environmental scientist at the United Nations Educational, Scientific, and Cultural Organization's European science bureau in Venice. In 2000, the newly established CORILA began reining in the projects by controlling the flow of funds and organizing projects under a few broad goals. "Things are under much better control now," says Pypaert.

Still, Campostrini says that climate change and flooding aren't Venice's only problems. The city's art and architectural treasures require protection and restoration, and there are environmental threats to the surrounding lagoon, which is a bustling seaport and one of Europe's largest protected wetlands.

To help understand the troubles besetting the lagoon, scientists of every stripe are building a model that can not only help them manage the fragile environment but also shed light on the physical and biological aspects of a wetland. "This is our ulti-

mate goal," says Roberto Pastres, a marine scientist at the University of Venice, but it's easier said than done.

Just predicting how the water behaves is mind-boggling. Water flow alters the lagoon's shape by moving sediments, which then changes the flow, and so forth. Add to that feedback loop the many urban and biological influences, and the hopeful modeler faces "an impossibly complex system," says Giampaolo Di Silvio, a hydraulic engineer at the University of Padua.

Fortunately, the researchers already have enormous amounts of information, from the movement of sediments to the distribution of sea life. "The Venice lagoon is the best studied in the world," says Di Silvio. One of the big questions to be answered with the final model, of course, is how the lagoon will react to the new tidal gates. But it will also help scientists around the world study how pollutants are shuttled through marine systems and the factors that lead to oxygen-choking algal blooms. The model may also help answer fundamental questions involving biodiversity and nutrient transport in sea-land systems.

Turning Venice into a science mecca could also save it from a ruinous brain drain. "Venice is in danger of becoming a dead city, like a museum," says Carrera. Driven away by the high waters and high prices, the population has plummeted from 150,000 in the 1950s to 64,000 today. Nearly half of the city's income now comes from the 14 million tourists who flock to Venice each year, with most of the rest coming from port traffic. "We desperately need more young people," says Campostrini, and "one way to attract them is to build up the university and high-tech sectors." Otherwise, Venice may end up being saved from the sea but abandoned by its own people.

–JOHN BOHANNON

John Bohannon is a writer in Berlin, Germany.

After Katrina

Displaced Researchers Scramble To Keep Their Science Going

Despite huge personal losses, New Orleans scientists are hurrying to recreate their labs and lives with some help from the government

Tulane University biochemist Arthur Lustig is still reeling from Hurricane Katrina. He spent 4 days hunkered down in his New Orleans lab before being evacuated by helicopter, then another miserable night in a shelter. His house was likely lost to flooding, and he's not sure whether the 20 years' worth of yeast strains he uses to study telomeres survived the power outage.

But things could be a lot worse. Showered with invitations from colleagues around the country, Lustig is now living with his wife's family in Chicago and working at Northwestern University, with lab space for his four students and one postdoc. "It's a traumatic time. But I think most of us have a positive attitude that we can get over this," Lustig says.

Rescue mission. Staff from Tulane's gene-therapy center bring Dewars of liquid nitrogen to retrieve adult stem cells from flooded research labs.

CREDIT: A. SMOLARZ/TULANE

Thousands of scientists face similar challenges. The flooding that displaced New Orleans residents after Katrina slammed into the Gulf Coast on 29 August exiled faculty members, graduate students, and postdocs from a half-dozen institutions in New Orleans. Thanks to Internet message boards and cell phone calls, many are regrouping in temporary labs and office spaces at other universities. "People have been really wonderful. They realize [Katrina] is a huge impact on careers," says Arthur Haas, chair of biochemistry and molecular biology at the Louisiana State University (LSU) Health Sciences Center in New Orleans. Scientific societies have also rushed to help, posting Web sites for those who haven't yet found spots (www.aaas.org/katrina).

For some, the disruption may be short-lived. Tulane medical school officials hope to get a handle soon on mold in air conditioning ducts, the main obstacle to reopening buildings in their now-dry part of the city. But many researchers have already enrolled their children in schools elsewhere and don't expect to return until January, when university classes resume. Although they are trying to view the forced exile as a minisabbatical, it's hard to be too optimistic about their research. "Will it slow us up competitively? Absolutely," says Lustig.

Against all odds, researchers did what they could to preserve their research materials. In the days after the storm, researchers from Tulane and LSU ventured back by boat, truck, and helicopter with armed guards to top off the liquid nitrogen covering storage containers and retrieve samples hastily ordered by priority. Tulane gene-therapy center director Darwin Prockop organized a convoy from Baton Rouge on 10 September to salvage their National Institutes of Health (NIH)–funded adult human stem cell bank, with staff lugging 36-kg Dewars up four flights of stairs to collect racks of vials.

Tulane scientists saved transgenic mice but had to euthanize most other animals; LSU animal caretakers destroyed or lost to flooding about 8000 animals in four vivariums, says Joseph Moerschbaecher, vice chancellor for academic affairs at LSU's Health Sciences Center. Also lost at Tulane were freezers of blood and urine samples, including those from the Bogalusa (Louisiana) Heart Study, which has followed thousands of children since 1972 to tease out heart disease risk factors. "It's a national tragedy," says Paul Whelton, Tulane senior vice president for health sciences.

Other scientists fear that mold has destroyed animal and plant collections built up over decades. Tulane ecologist Lee Dyer sneaked back and put desiccant and mold killer in drawers containing preserved insects. University of New Orleans (UNO) butterfly expert Phil DeVries and his wife, systematist Carla Penz, fear a severe toll on 30 years' work: preserved butterflies, hundreds of photographs, as well as rare identification books and countless field notebooks. Physical scientists, for their

Katrina Leaves Behind a Pile of Scientific Questions

Amid the cleanup in Katrina's wake, scientists are rushing into the field to gather data before they disappear. It's a sobering exercise. Havidan Rodriguez, who is leading a team from the Disaster Research Center at the University of Delaware, Newark, that is asking evacuees along the Gulf Coast how their basic needs are being met, says the task "is turning out to be more difficult" than similar efforts in Sri Lanka after the 26 December 2004 tsunami. "The breakdown of infrastructure is far greater," he says, "and the poverty is endemic."

One major focus is to reconstruct how the hurricane overcame New Orleans's defenses. The Hurricane Center (HC) at Louisiana State University (LSU), in nearby Baton Rouge, has become the de facto headquarters for that effort. After a whirlwind tour of the region, the center's researchers reported that the storm surge reached a height of 9 meters in some places. They are also updating a model of the floodwater's impact on the city. If the pumps hold out and no new tropical storms hit, says HC coastal scientist Hassan Mashriqui, the city should be fully drained by the end of the month.

Go with the flow. Scientists are monitoring the impact of floodwater being pumped back into Lake Pontchartrain.

Another priority involves tracking the consequences of dumping the city's contaminated floodwater into the surrounding environment. Initial tests by the Environmental Protection Agency and the Louisiana Department of Environmental Quality have allayed the worst fears: Fecal bacteria counts are high, but according to a preliminary analysis, it would take exposure of "a year or longer" to the chemicals at measured concentrations to cause serious health effects. Toxic algal blooms are another fear; the LSU Earth Scan Laboratory has been using an Indian satellite to search Lake Pontchartrain for signs of growth. Colder temperatures next month are expected to make blooms less likely and reduce the risk of further storms.

To help cover the costs of these and other projects, the National Science Foundation (NSF) is providing supplementary funding to existing grants. This week, NSF hoped to award about 30 "exploratory" research grants of between $10,000 and $30,000 chosen from some 120 proposals it received. A second competition closes this week for a larger pot of money. The timing could not have been worse, says NSF's Dennis Wenger, because "Katrina hit right at the end of the fiscal year." But "we're making it work." —JOHN BOHANNON

CREDIT: ASSOCIATED PRESS

part, are worried about damage to sensitive equipment such as electron microscopes.

With their campuses closed until January, many scientists have accepted offers of temporary digs at other institutions. Xavier University microbiologist Shubha Ireland feels especially lucky. She was offered a spot in a molecular biology lab at Oak Ridge National Laboratory in Tennessee. ORNL officials also secured a part-time administrative job for her husband Rick, a lawyer. And a local real estate developer donated a new four-bedroom house for the family to stay in for 6 months. "It's like a dream come true," says Ireland.

Although some scientists expect to use the time mainly to write papers, many others are determined to get back to the bench as quickly as possible. "Nobody is going to miss a beat—at least not in my group," says Zeev Rosenzweig, a chemist from UNO now living in McLean, Virginia, and working at the nearby National Science Foundation (NSF). Rosenzweig moved up by 2 years the start date of a rotating position as officer for NSF's analytical and surface chemistry program and intends to relocate most of his group to the Washington, D.C., area.

Some hope their research will benefit from the unexpected move. UNO physicist Leonard Spinu was invited by a colleague from his native Romania to the National High Magnetic Field Laboratory at Florida State University in Tallahassee, which has some of the best facilities anywhere for his research on magnetic nanomaterials, he says. Tulane neuroscientist Andrei Belousov says his time in the lab of Sacha Nelson at Brandeis University in Waltham, Massachusetts, could spark new collaborations. "I hope it's something we can work together on, not simply charity," says Belousov.

Still others are preparing to rebuild essential research materials. Haas, who lost 20 years' worth of samples for studying the ubiquitin system, expects to spend time re-expressing recombinant proteins at LSU's biomedical research center in Baton Rouge. "We've just got to bang out clones," he says.

Especially hard-hit are graduate students. Tulane's Vincent Shaw, whose adviser is evolutionary biologist Duncan Irschick, found a temporary spot at Brown University in Providence, Rhode Island. But he and his labmates left behind the analyses needed to finish a paper in press, experimental animals now likely to be dead, and freezers full of thawed samples. "Researchwise, I am in a bad place," says Shaw.

Funding agencies are working to smooth these temporary transfers and help displaced researchers get back on track. NSF and NIH are relaxing rules to accommodate those caught in the catastrophe. "We want to protect researchers so that they don't get stuck with the tab" for incurring expenses related to relocation or repair of federally funded projects, says NSF's Jean Feldman, who oversees a hotline that is getting 50 calls and e-mails a day.

In addition to information, the hotlines provide some therapy, says her NIH counterpart, Carol Alderson. "Some PIs [principal investigators] are resilient and just want to know what it'll take to get back to work," says Alderson. "Others sound like the people you hear on television; they've gone through the worst, and they don't think that their institution will ever recover."

Although federal agencies have promised to be as flexible as possible, there's a limit to how far they can bend. NIH, for example, has struck deals with Tulane and LSU allowing faculty to temporarily submit grant applications directly, but NSF says any proposal must still come from the institution. At the same time, both agencies plan to be lenient about enforcing application deadlines, with NSF decreeing a 1-year extension for any scientist in the three-state region whose grant would have expired this month or next.

Although grateful for the outpouring of help, New Orleans administrators worry that some universities are seeing the disaster as a chance to snap up talented faculty. At least a few have already taken permanent positions. "We do not want to see a brain drain. It would be terrible for the region," says Tulane's Whelton. "Our full aspiration is to get back in business and have an even stronger institution than when we left. And we'll need all the help we can to get to that point." —JOCELYN KAISER

With reporting by Adrian Cho, Eli Kintisch, Jeffrey Mervis, and Elizabeth Pennisi.

Scientists Chase After Immortality in a Petri Dish

Efforts to turn embryonic stem cells into sperm and eggs are answering long-standing questions about how the body prepares its genes for the next generation

Sperm and egg cells are the body's best shot at immortality. Although these so-called germ cells play no part in day-to-day survival, in most species they offer the only route for the genome to make it into the next generation. In keeping with that pivotal role, germ cells seem to play by their own rules, developing separately from cells that build all the other parts of the body. Now scientists who study embryonic stem (ES) cells—another type of immortal cell—are attempting to figure out how to coax them to become germ cells in a dish.

If they succeed, the implications would be profound. Such technology would not only provide an unprecedented opportunity to study the development of these crucial cells, but it might also enable scientists to pursue nuclear transfer experiments without needing to harvest egg cells from women donors—a huge obstacle. And in the most futuristic applications, such techniques could someday allow scientists to create sperm and egg in a dish, possibly helping infertile people reproduce or—in a scenario that makes some shudder—leading to designer gametes and made-to-order babies.

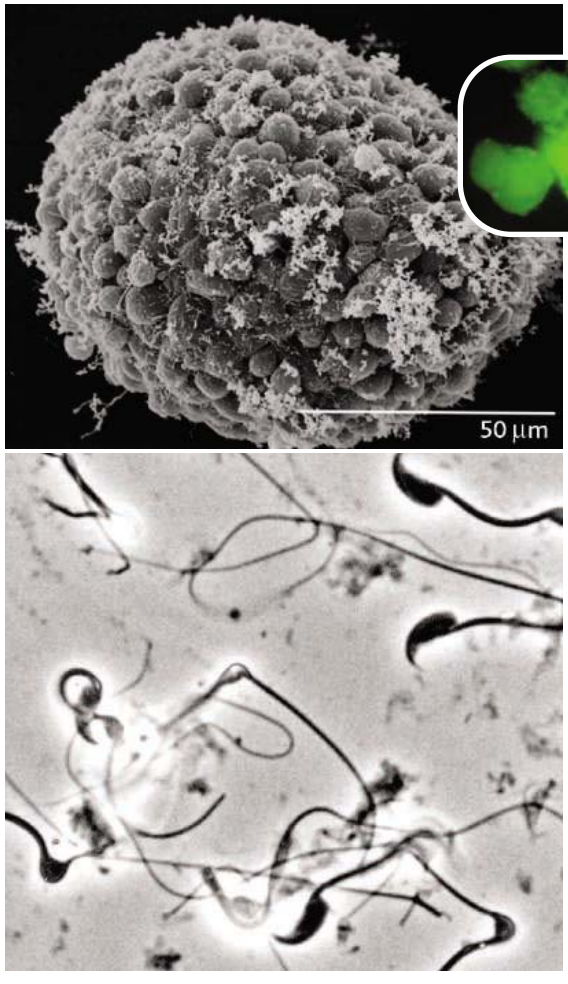

Early success. Differentiating mouse ES cells (*top*) express germ cell proteins (*green*) and form ovarylike structures. Lab-derived germ cells transplanted into mouse testes can produce normal-looking sperm (*bottom*).

Designer gametes may be a distant prospect, but 2 years ago, scientists did seem on the verge of converting ES cells to germ cells. Three different groups reported that sperm- and egglike cells could arise spontaneously in colonies of differentiating mouse ES cells. But the researchers soon tempered their expectations. Although several groups have repeated the earlier results—and new studies suggest even more unexpected sources of germ cells (see sidebar, p. 1983)—mature sperm and egg cells appear only rarely, and no one has managed to show that any of the lab-grown cells can produce a live organism.

Nevertheless, the work is providing insights into how early germ cells determine their fate, how they turn specific genes on and off in a still-mysterious process called imprinting, and how important the environment surrounding differentiating cells—sometimes called the stem cell niche—is for their survival and normal development.

"This is really unique biology that no one has been able to study before," says Renee Reijo Pera of the University of California, San Francisco, whose lab is trying to turn human ES cells into sperm and oocytes. She and her colleagues hope to sort out the genes that control gamete formation in humans—something that has been nearly impossible to study in the lab.

The first hints that such studies might be possible appeared when researchers noticed that ES cells left to grow and differentiate on their own produce a range of cell types: patches of muscle cells that contract in rhythm, groups of neurons, bits of cartilage, and even blood. Several years ago, Hans Schöler and his colleagues, now at the Max Planck Institute of Molecular Medicine in Münster, Germany, set out to see if any of the cells in the random mix might be immature oocytes or sperm.

Because maturing germ cells are difficult to distinguish by their appearance, the scientists developed a mouse ES cell line harboring a gene for green fluorescent protein that lit up only when a key germ-cell gene was expressed. After a few days of unguided differentiation, a few of the clusters sported glowing green cells; after a few more days, these clusters began to look like ovaries. The cells survived in culture for several months, and, perhaps most surprising, seemed to trigger the production in culture of hormones similar to those produced during the female mouse's menstrual cycle (*Science*, 2 May 2003, p. 721).

A few months later, two separate teams published papers in the *Proceedings of the National Academy of Sciences* and *Nature* describing how they had coaxed mouse ES cells to grow into sperm cells (*Science*, 12 December 2003, p. 1875). Toshiaki Noce, Yayoi Toyooka, and their colleagues at the Mitsubishi Kagaku Institute of Life Sciences in Tokyo showed that immature germ cells transplanted into the testes of live mice could become full-fledged sperm, although they didn't manage to fertilize any eggs. Meanwhile, Niels Geijsen and George Daley, both now at Harvard Medical School in Boston, Massachusetts, showed that spermlike cells produced in their lab could fertilize eggs and prompt the formation of early embryos. None of the lab-made germ cells managed to produce a pregnancy, much less a live-born mouse.

That next step has proved difficult. Although several labs can consistently get early germ cells to form, only a tiny percentage enter meiosis—the complicated process of germ-cell division that produces a sperm or egg with a single copy of each chromosome instead of the normal complement of two. "It's still a very rare phenomenon," Daley says.

Nevertheless, a few new ideas are emerging from the studies. For example, Reijo Pera's lab has been focusing on the very first cues that set germ cells aside for separate development. At a June meeting of the International Society for Stem Cell Research, she and her lab described what

CREDITS (TOP TO BOTTOM): HANS SCHÖLER, *PNAS* **100**, 11457–11462 (2003)

Another Route to Oocytes?

Embryonic stem cells may be one path to new eggs, but a scientist at the University of Guelph, Canada, thinks she's found another, unexpected one. At a July meeting of the Society for the Study of Reproduction in Quebec City, Canada, reproductive and molecular biologist Julang Li described to a startled audience how she and her colleagues had transformed skin stem cells drawn from fetal pigs into cells that looked remarkably like oocytes. Since then, her work, now under review at a journal, has sparked discussion among scientists, who consider the results preliminary and agree that more in-depth testing is necessary. But the oocytelike cells are nonetheless "extremely interesting and exciting," says developmental biologist John Eppig of the Jackson Laboratory in Bar Harbor, Maine, who heard her talk. "It seems that it's going to be possible to get germlike cells from a variety of different types of stem cells," he adds.

In her presentation, Li described a series of experiments; in each case, she and her colleagues isolated about 5 million skin stem cells from 40- to 50-day-old fetal pigs. (Full gestation normally takes 114 days.) The scientists put these cells into a solution Li declined to describe. Most stuck to a petri dish and were discarded. Some, however, floated together and formed aggregates. Up to a third of the aggregates appeared to have a large cell in their center. These were transferred to another concoction containing gonadotropin, a hormone that can stimulate oocyte production; Li would not reveal all its ingredients because the culture is detailed in a pending patent application.

Of the aggregates transferred, 1% to 10%, depending on the batch, ballooned into very large cells, 80 to 100 micrometers in diameter. In their shape and other morphology, the cells closely resembled oocytes, although they tended to be slightly smaller. The cells also expressed a half-dozen genetic markers common to eggs. Li reported that some of these cells spontaneously went on to become embryolike structures called parthenotes, which appear when an unfertilized egg begins developing on its own. Parthenotes were also seen by Hans Schöler, now at the Max Planck Institute of Molecular Medicine in Münster, Germany, and his colleagues, who were the first to convert stem cells—in their case, derived from embryos—into cells similar to eggs (see main text).

More than anything, the smooth, circular images Li beamed across a screen were what convinced her audience she was on to something. Eppig noted what looked like a "distinctive" zona pellucida, a transparent membrane that forms around the developing ovum. He also considers the cells superior, in their likeness to oocytes, to those Schöler's team created. Indeed, the images so closely resemble eggs that they may be expressing more oocyte-associated genes than Li tested for, suggests Hugh Clarke, an expert in mammalian oogenesis at McGill University in Montreal, Canada.

But more research is needed to prove that these cells are eggs, say Clarke and others, such as examining their chromosomes and possibly fertilizing them to see if they form a traditional embryo. Eppig notes that despite some hints, it's also far from certain that the cells can enter meiosis and divide. Still, they suggest that when it comes to coaxing germ cells to form, there may be more than one place to start. **–JENNIFER COUZIN**

they call "germ cell particles," clusters of proteins and RNA that seem to distinguish early germ cells from those destined to become somatic cells.

In insects and fish, germ cells develop from a region of the oocyte called the germ plasm, which is particularly rich in RNA and RNA-binding proteins. Mammals, however, seem to set their germ cells aside slightly later in development—and independent of any specific region in the oocyte. Reijo Pera and her colleagues have found human versions of the germ-plasm proteins and RNAs in the human germ cell particles; now they are trying to determine what triggers their formation. The work should turn up new insights into what the proteins and RNAs do, says Geijsen. Even in model animals, he says, "no one really understands what the germ plasm is and does."

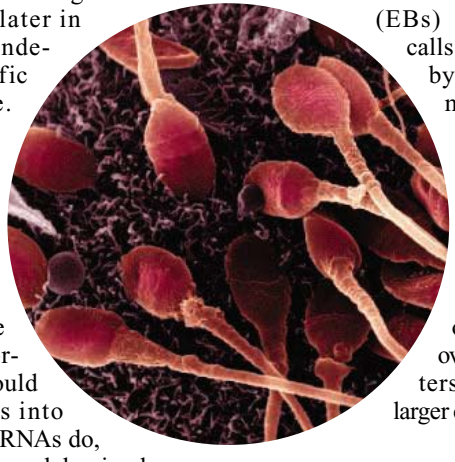

Elusive goal. So far, lab-produced gametes don't measure up to their natural-made counterparts like these human sperm.

CREDIT: GETTY IMAGES

Geijsen and his lab are also focused on the early stages of germ-cell development. When a sperm and egg come together to form a complete genome, many of the genes inherited from the mother or father are specifically turned on or off. This process, known as imprinting, begins in immature germ cells; Geijsen hopes the chance to make unlimited numbers of such cells will enable him to identify some of the molecules that control it.

New results hint at ways to increase the efficiency of producing early germ cells for such studies. Alan Trounson and Orly Lacham-Kaplan of Monash University in Clayton, Australia, reported last month that they can turn clusters of differentiating ES cells called embryoid bodies (EBs) into what Trounson calls "ovarylike" structures by bathing the EBs in media that has first been exposed to newborn mouse testicular cells. In a paper published online in *Stem Cells*, the researchers reported that they coaxed more than 80% of their EBs to form the ovarylike structures: clusters of cells surrounding larger cells that express several oocyte proteins. But Trounson says they have not managed to fertilize any of the oocytelike cells. Nor do they understand what, exactly, the conditioned media contains—much less how it might be influencing the growing cells.

That result could shed light on another mystery: how the gender of germ cells is determined. Why the proteins produced by testicular cells could produce ovarylike structures is not yet clear, Trounson says, but several studies have suggested evidence for germ-cell gender-bending. Schöler and others have found that male ES cells—carrying one X and one Y chromosome—can become oocytes, and Reijo Pera notes that doctors occasionally find so-called testicular eggs in male patients. Female ES cells can't make sperm, however. "The Y chromosome is fundamentally required" for sperm maturation, says Reijo Pera.

Another fundamental requirement for full germ-cell development, apparently, is the so-called niche, the cells and signals that surround the maturing germ cells in the testes and ovaries during development. Studies in fruit flies have shown that developing oocytes interact closely with nurse cells that help guide their movement and maturation. Similar interactions are probably key in mammals as well and may explain why so few of the lab-grown germ cells make it past the earliest stages of development. "Meiosis will not work if you don't have the right cell-cell communication," Schöler says. But he is optimistic that the cell clusters that he and others see in their lab dishes will reveal those signals. "We have the right material" to find the answers, he says—and to move another step toward understanding the germ cell's immortality.

–GRETCHEN VOGEL

Martian Methane: Rocky Birth, Then Gone With the Wind?

CAMBRIDGE, U.K.—In the medieval city where Isaac Newton worked on the gravitational laws, about 850 scientists gathered from 4 to 9 September for the 37th meeting of the American Astronomical Society's Division for Planetary Sciences.

Last year, a spectrometer on board the European Space Agency's Mars Express spacecraft detected methane above areas of the martian surface where there also appears to be subsurface ice (*Science*, 1 October 2004, p. 29). Many researchers hailed the find as possible evidence that bacteria are living in the ice and producing the gas. After all, almost all the methane in Earth's atmosphere is produced by living organisms. Indeed, says planetary scientist Sushil Atreya of the University of Michigan, Ann Arbor, many alternative explanations for the existence of the methane don't work. Volcanic activity would also produce sulfur dioxide, which is not observed. A freak cometary impact in the past few thousand years could have delivered methane to the martian surface, but then the gas wouldn't be concentrated in specific regions.

Methane muddle. Who's found the right concentration, Mars Express or Gemini South (*inset*)?

But, Atreya announced at the meeting, it's too soon to invoke martian microbes as the source. Instead, a little-known geochemical process known as low-temperature serpentinization could be the culprit. In this process, which has been observed on Earth's ocean floor, liquid water chemically alters basalt to produce the gas. Atreya thinks it might produce huge amounts of martian methane, which would then be quickly destroyed by oxidation, ultraviolet sunlight, and possibly also by electrical activity of atmospheric dust.

Atreya says basalt reacts with liquid water to produce minerals known as serpentines, releasing hydrogen in the process. The hydrogen then reacts with carbon dioxide to produce methane. The process operates at temperatures of about 40° to 90° Celsius and is distinct from the high-temperature hydrothermal activity also seen on Earth's ocean floors. At a few kilometers beneath the martian surface, low-temperature serpentinization in reservoirs of liquid water could produce up to 200,000 tons of methane per year, Atreya says—more than enough to explain the concentrations of some 10 parts per billion seen in the atmosphere.

So where does all the methane go? Given that methane concentrations vary widely over the martian surface, it must be destroyed too quickly for the gas to spread out evenly. The explanation may lie in the electrostatic charging of dust particles, says Atreya. In small dust devils and larger dust storms, electric fields as strong as 25 kilovolts per meter could be produced. Such voltages would break up water molecules, and the hydroxyl molecules created would then oxidize methane. If this removal mechanism is indeed operating on Mars, it could mean that the production rate of methane is actually much higher than has been assumed until now.

Indeed, Michael Mumma of NASA's Goddard Space Flight Center in Greenbelt, Maryland, observed Mars with telescopes on Earth and found much higher methane concentrations (up to 250 parts per billion) in some equatorial regions. However, Atreya says "something is weird" about these observations. Such high concentrations would almost blind Mars Express's sensitive spectrometer, a problem that does not occur. Mumma is currently reanalyzing the data using new and better calibrations, but so far there's no indication that the high values will go away, he says.

Snapshots From the Meeting

A rapidly rotating rugby ball. A recently discovered miniplanet in the outer solar system is almost twice as long as it is wide, says David Rabinowitz of Yale University. The object, known as 2003 EL_{61}, has the shape of a squashed rugby ball, measuring 1960 × 1520 × 1000 kilometers. The elongated shape results from the object's rapid rotation; its period of 3.9 hours is the fastest ever measured for a large solar system body. Using the 10-meter Keck Telescope at Mauna Kea, Hawaii, Rabinowitz and his colleagues have also detected a small satellite orbiting the miniplanet at a surprisingly large distance of almost 50,000 kilometers. It's unclear how the system could have formed or whether the rapid rotation and the strange satellite are somehow related. Says Rabinowitz: "2003 EL_{61} may not quite be as big as Pluto, but it's much more interesting dynamically."

Irregular satellites explained? No one really knows how to explain the large number of "irregular" satellites that swing around the giant planets in slow, eccentric, tilted orbits. Most likely they're asteroids, long ago slowed by gas drag and captured by the rotating disks of gas and dust from which each of the planets formed. But computer simulations show that such captured objects quickly spiral into the nascent planet unless something boosts their orbits well outside the cluttered inner parts of the planet-spawning disk.

Now, Brett Gladman and Matija Ćuk of the University of British Columbia in Vancouver think they've found such a mechanism. According to their numerical simulations, an orbital resonance between Jupiter and Saturn that occurred in the distant past would have "pumped up" the orbits of Saturn's irregular satellites to a safe distance from the planet. A similar past resonance between Saturn and Uranus may have preserved the latter planet's irregular satellites, says Ćuk. However, he admits that Jupiter's troop of irregulars is not so easily explained. **–G.S.**

CREDIT: D. DUCROS/ESA; INSET: GEMINI OBSERVATORY/AURA

As for the origin of the gas, Mumma says he's not sure that Atreya's low-temperature serpentinization scenario applies to Mars. "I'd keep the biological option open," he says. A definitive check on the origin of methane will likely have to wait for NASA's Mars Science Laboratory, scheduled for launch in 2009. Says Mumma: "This is going to be a long tale."

Several New Twists for Saturn's Rings

They may appear serene and eternal, but Saturn's rings are changing, and changing fast. Over the past 25 years—the mere blink of an eye in planetary evolution—one particular ringlet in the innermost, tenuous part of the ring system moved 200 kilometers inward and became one-tenth as bright. "That's radical," says Carolyn Porco of the Space Science Institute in Boulder, Colorado, head of the imaging team for NASA's Cassini spacecraft. Porco's team discovered the rapid change by comparing Cassini ring photos with images the Voyager spacecraft sent to Earth in 1980. "This is one of the reasons why we wanted to come back," she says. The dramatic change suggests that this part of the ring system could be young and rapidly developing, although no one yet knows how to interpret the observations.

Other ring results presented at the meeting are equally baffling. For instance, Cassini's temperature measurements of the rings indicate that ring particles are 15° cooler on their night side than on their day side. According to Linda Spilker of NASA's Jet Propulsion Laboratory (JPL) in Pasadena, California, this means that all particles—from a few centimeters to a few tens of meters across—rotate too slowly to bake evenly on all sides. "We always thought that mutual collisions would lead to a wide variety of rotation rates," says Spilker. Maybe the particles are fluffy and porous, she adds, which would dampen the effects of collisions.

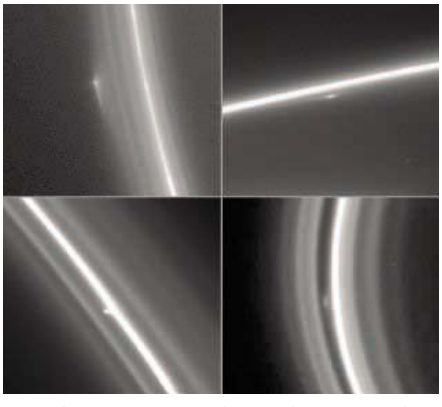

Spiral mystery. Do these objects wind up Saturn's F ring?

CREDITS (TOP TO BOTTOM): ESA/LUNAR AND PLANETARY LABORATORY/UNIVERSITY OF ARIZONA; NASA/JPL

Weirdest of all is Saturn's thin, braided, kinky F ring, which lies just outside the main ring system. Cassini's images show that various strands of the F ring are actually one and the same narrow dust ring, tightly wound into a spiral. This unique structure—unrelated to the spiral density waves that have been seen in other parts of the ring system (*Science*, 9 July 2004, p. 165)—may be caused by a small moonlet discovered by Cassini in an eccentric orbit that appears to cross the F ring. That orbit is a mystery in itself: The F ring is believed to contain many large boulders and moonlets, which would make it hard for a small satellite to survive multiple crossings. Even so, the tiny object (denoted S/2004 S6) has been observed for almost a year.

Cassini has also spotted more bright knots close to the F ring, some of which are very elongated. "We have a hard time deciding which of these objects are real moons and which of them are clumps of dust," says Porco. Even S/2004 S6 may turn out to be a loose clump rather than a solid object. Future observations of Saturn will surely reveal new small satellites. Says Cassini's project scientist Dennis Matson of JPL: "The complexity in the rings is just dumbfounding. We will continue to bring you excitement."

Volcanoes, Monsoons Shape Titan's Surface

Hiking on Titan would be the ultimate extreme sport. Data from the European Huygens lander show that the surface of the large saturnian moon is a jagged landscape of extremely steep valleys, overshadowed by towering ice cliffs. "It's quite dramatic," says planetary scientist Jonathan Lunine of the University of Arizona's Lunar and Planetary Laboratory in Tucson. "You would need an ice ax to scale the 30-degree slopes." It would be tougher than climbing a glacier, he adds: "The ground beneath your feet would feel more like a crumbly rock slope." But at least early travelers to Titan could consult the first three-dimensional maps of parts of the moon's surface, which Lunine presented at the meeting.

The Huygens lander touched down on Titan on 14 January. During its parachuted descent, it took numerous snapshots of the panorama beneath. Lunine's team has now combined these into stereoscopic images of a 1.5-by-3.5-kilometer swath of terrain, showing deep, precipitous valleys carved out by "methane monsoons," as Lunine's colleague Ralph Lorenz calls them after a description in Arthur C. Clarke's 1975 novel *Imperial Earth*. Taking into account Titan's seasons, atmospheric properties, and solar radiation, Lorenz estimates that the "monsoons" happen every few centuries and last for months. They're like the episodic rainstorms in the Arizona desert, but on a different time scale, he says.

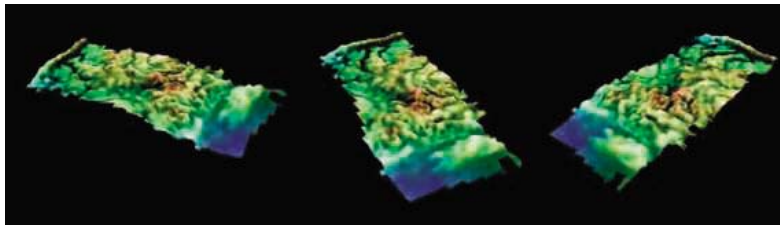

Rough terrain. Stereoscopic images of Titan's surface from the Huygens probe.

The methane in Titan's atmosphere must be continuously replenished because ultraviolet sunlight is constantly breaking down the gas. Researchers do not yet know whether methane has been stored in the mantle since Titan's formation or whether it is being produced by geochemical processes beneath the surface. According to planetologist Gabriel Tobie of the University of Nantes, France, various forms of outgassing—such as cryovolcanism, which brings water-ammonia ice containing trapped methane to the surface—would then release the gas into the atmosphere episodically. Indeed, radar images of Titan's surface obtained by NASA's Cassini spacecraft—Huygens's mother ship—show evidence of volcanic domes, craters, and flows. Some of the latter resemble flows on the slope of Mauna Loa, Hawaii. "There's major resurfacing going on," says volcanologist Rosaly Lopes of NASA's Jet Propulsion Laboratory in Pasadena, California.

Researchers' views about Titan's surface have also changed since Huygens's landing in January. During touchdown, a protruding penetrometer on the bottom of the lander first encountered much resistance and then went through softer material, leading scientists to conclude that Titan was like a crème brûlée with a thin, brittle crust. Now, John Zarnecki of the Open University in Milton Keynes, U.K., head of the Surface Science Package team, thinks it's more likely that the penetrometer hit an ice pebble similar to the ones seen in Huygens's pictures and then pushed it aside.

It will be a while before travel agents offer trips to Titan, but Jean-Pierre Lebreton, Huygens's project scientist at the European Space Agency, hopes to go back soon. "Huygens has paved the way for future missions to the surface of Titan," he says.

–GOVERT SCHILLING

Govert Schilling is an astronomy writer in Amersfoort, the Netherlands.

Random Samples

Edited by Constance Holden

Portrait of Eclipse by famous horse painter George Stubbs.

Genes of a Runner

What makes some racehorses leave others in the dust? Researchers are using the bones of Eclipse, the most celebrated stallion of the 18th century, to look for clues in his DNA.

Analyses of pedigrees and English Derby results have shown that "almost 35% of variation in race performance is due to inherited differences," says Emmeline Hill, a geneticist at University College Dublin, Ireland. But fingering which genes are involved is difficult because the horse genome has not been sequenced, and racehorses stem from 28 horses brought to Europe from the Middle East in the early 1700s. Fewer than a dozen are responsible for 80% of racehorse genes, according to animal geneticist Patrick Cunningham of Trinity College in Dublin.

To boost signal to noise, a team including Matthew Binns, a geneticist at the Royal Veterinary College (RVC) in Hatfield, U.K., is comparing DNA from the greatest racehorses in history. The researchers are starting with DNA from a tooth belonging to Eclipse, whose 216-year-old skeleton now hangs in the RVC museum.

The plan, described at the British Festival of Science last week in Dublin, is to look for differences in genes important for speed and stamina, such as those involved in glucose metabolism or oxygen transport, that correlate with performance. Binns wants to find out how many of Eclipse's genes have carried through to modern thoroughbreds.

Where the Bees Are

Bees are crucial pollinators, second only to wind, but their numbers have been dropping. If electric companies would stop mowing under power lines and allow shrubs and brambles to spread in these right-of-ways, however, they could become bee refuges, scientists say.

Conservation biologist Kimberly Russell of the American Museum of Natural History in New York City compared bees caught in dense scrub with those found in nearby grasslands. The scrub held one-third more species of wild bees and three-quarters of the rarest species, she and her colleagues reported in last month's issue of *Biological Conservation*. They calculate that if the roughly 2 million hectares of power-line strips in the country went unmowed, wild bees could pick up the slack for domesticated honeybees, whose numbers have dropped 50% since 1945 because of parasites, environmental toxins, and loss of habitat.

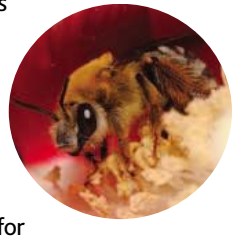

Conservation biologist Gretchen LeBuhn of San Francisco State University in California says this plan could lead to more creative management of biodiversity in the midst of civilization. "Wouldn't it be great to do this at corporate headquarters?" LeBuhn says. "Instead of expanses of grass, you could have ponds for frogs."

Ill-Fated Voyage

An attempt to sail from Oman to India on a replica of a 5000-year-old boat this month (*Science*, 9 September, p. 1670) lasted less than 11 hours. The reed-and-tar construction of the 12.5-meter craft *Magan* proved no match for the Arabian Sea, which swamped it on 7 September a scant 10 kilometers from port. All eight crewmembers were picked up by an escort vessel, according to Oman's Ministry of National Heritage and Culture. No word yet on whether the mariners will try again to recreate this ancient trade route.

World Map of Plant Biodiversity

Biologists rely on maps showing the distribution of wildlife around the world for conservation planning. Now they've got a global chart for plants. Plants have a huge influence on other components of ecosystems, says Taylor Ricketts of the World Wildlife Fund (WWF) in Washington, D.C. Without such data, "we've been flying blind in terms of conservation planning," he says.

The new map, published in the July issue of the *Journal of Biogeography*, plots the number of plant species in each of 867 terrestrial "ecoregions." The most diverse region is the Borneo lowlands, with more than 10,000 species, followed by regions in Central and South America. One of the most impoverished, outside of deserts, was the southern Indian Ocean islands, with some 35 species.

"It's an important benchmark," says Robert Whittaker of the University of Oxford of the map, a joint effort of WWF and botany doctoral student Gerold Kier and colleagues at the University of Bonn, Germany. Whittaker predicts it will have a "powerful impact" on global conservation planning. A novel feature of the map is its assessment of the quality of the data available. The group found them particularly sparse for tropical grasslands submerged most of the year and for the southern Amazon basin.

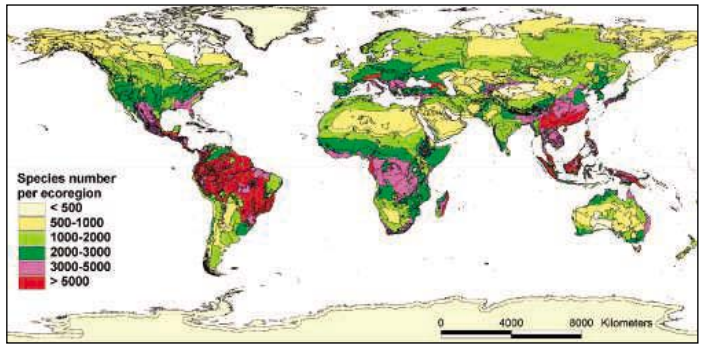

CREDITS (TOP TO BOTTOM): PRIVATE COLLECTION/BRIDGEMAN ART LIBRARY; VALERIE GILES/AMERICAN MUSEUM OF NATURAL HISTORY; KIER *ET AL.*, *JOURNAL OF BIOGEOGRAPHY*, *10.1111/J* **32** (2005)

Edited by Carolyn Gramling

UPDATE

China bound. A federal judge in Seattle, Washington, has ruled that former Microsoft vice president Kai-Fu Lee is free to head Google's new China-based R&D office. Microsoft had sued both Lee and Google, claiming that Lee breached a 1-year, no-competition clause in his contract (*Science*, 29 July, p. 697).

Both sides are claiming victory from the 13 September ruling, which bans Lee from continuing the search and speech technology research he worked on at Microsoft pending a final decision in January. Google has filed a countersuit against Microsoft in California.

In the meantime, Lee is already hard at work, says Michael Kwun, an attorney for Google. "The first steps are getting a facility and hiring engineers," Kwun says. "The court has confirmed he can do that, and he has already started."

JOBS

New line. University of Cambridge has recruited one of the world's foremost experts on stem cells to lead a new institute that it hopes will take it to the top of this hot field.

Next year, developmental biologist Austin Smith will

move from the University of Edinburgh to head up the Institute for Stem Cell Biology. His deputy will be Fiona Watt, now at Cancer Research UK's research institute in London.

The institute will open in August 2006 with room for at least 12 groups. The U.K., unlike the United States, allows researchers to use national government funds to cultivate new lines of human embryonic stem cells. But Smith says that President George W. Bush's restrictive policies have not created an American brain drain. "It's really the reverse," he says. "My goal is to create a place where people can stay in Europe."

DEATHS

A steady contribution. Mathematician and astrophysicist Hermann Bondi, who described the basic theory for how matter falls onto a star or black hole, died in Cambridge, U.K., on 10 September. The Vienna-born Bondi, a lifelong advocate of scientific literacy who taught mathematics at King's College London and later Churchill College in Cambridge, was 85.

With astronomers Thomas Gold and Fred Hoyle, Bondi formulated the once-popular "steady-state" model of cosmology that eventually lost out to the big bang theory. In the 1970s, he was chief of European space research as well as scientific adviser to the British government. Martin Rees, the United Kingdom's Astronomer Royal, says Bondi had tremendous energy and "spoke in a clear and cogent way" that a nonspecialist could understand.

Got any tips for this page?
E-mail people@aaas.org

PIONEERS

Sharing space. With help from astronautics engineer Bob Twiggs of Stanford University in California, Romanian students are building their country's first satellites. But that big news comes in a small package. Sponsored by the Romanian Space Agency, the five students spent a week at Stanford this month learning to build "CubeSats": tiny technological marvels that are 10 cm on a side and weigh less than a kilogram. If all goes well, the first Romanian CubeSat will rocket into space in 2007 via a launcher at California Polytechnic State Institute in San Luis Obispo.

Twiggs has made his CubeSat designs freely available, and some 70 universities around the world now openly share information on design and technology à la Linux. However, the Romanian visit is the first time that students have traveled to Stanford, Twiggs says. The first two satellites were launched in 2003—Stanford's QuakeSat, which can detect pre-earthquake energy emissions, and Japan's remote-sensing CUTE-I—and another 15 await launch next year. But, Twiggs says, "the major purpose is to train budding space scientists."

SOCIETY MATTERS

No talking. Two members of an American Chemical Society (ACS) committee have resigned to protest what they say is the society's tight-lipped handling of its battle against a free federal chemical database.

The flap involves the National Institutes of Health's (NIH's) PubChem, which ACS leaders see as a threat to the fee-based Chemical Abstracts Service (CAS) (*Science*, 2 September, p. 1473). At an ACS meeting in late August in Washington, D.C., member David Spellmeyer distributed fliers announcing that the issue would be discussed at the open meeting of ACS's Joint Board-Council Committee. But CAS president Robert Massie told the crowd there was no time and that those with PubChem questions could talk to an ACS spokesperson.

That was the last straw for Spellmeyer, an IBM researcher, and informatics expert Gary Wiggins (left) of Indiana University, Bloomington, who chose to resign from the committee. "It's mostly because they're not talking about it openly," says Wiggins. ACS spokesperson Nancy Blount says ongoing negotiations with NIH require "confidentiality" and that the council's chair must approve additions to the agenda. But "we do take seriously the request for more communication," she says.

CREDITS (TOP TO BOTTOM): AUSTIN SMITH; LINDA A. CICERO/STANFORD NEWS SERVICE; CHURCHILL COLLEGE/UNIVERSITY OF CAMBRIDGE; INDIANA UNIVERSITY

Spend less time looking for antibodies and more time doing research...

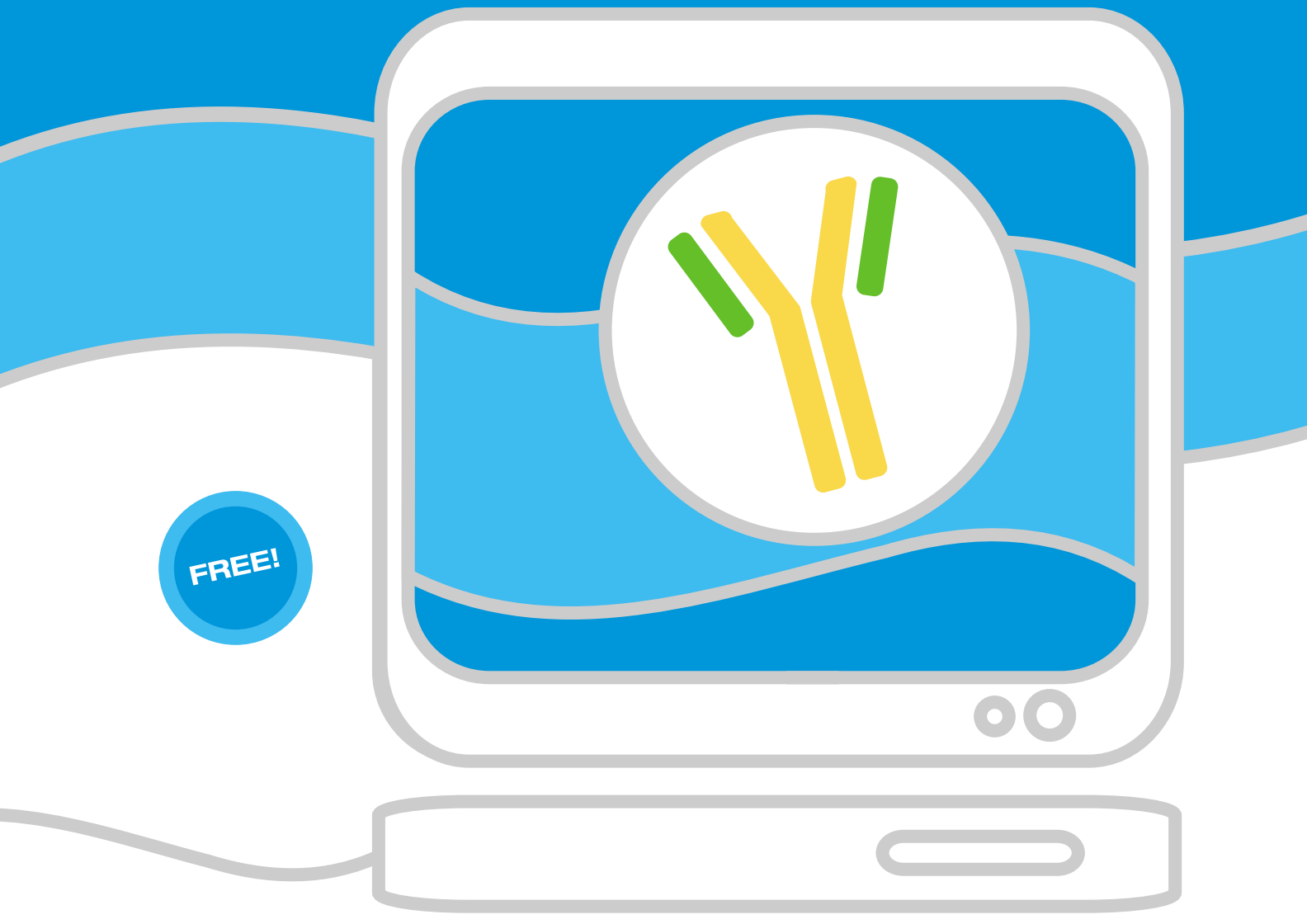

FREE!

Find Antibodies Online

Search over 130,000 antibodies from over 100 companies by antigen, species reactivity, and application... free and online.

- Over 130,000 Antibodies
- Over 100 Antibody Companies
- No Registration Required
- Full Product Specifications
- Over 225,000 Research Products and Instruments
- Direct Access to Product Pages on Company Websites

biocompare®

The Buyer's Guide for Life Scientists™

www.biocompare.com

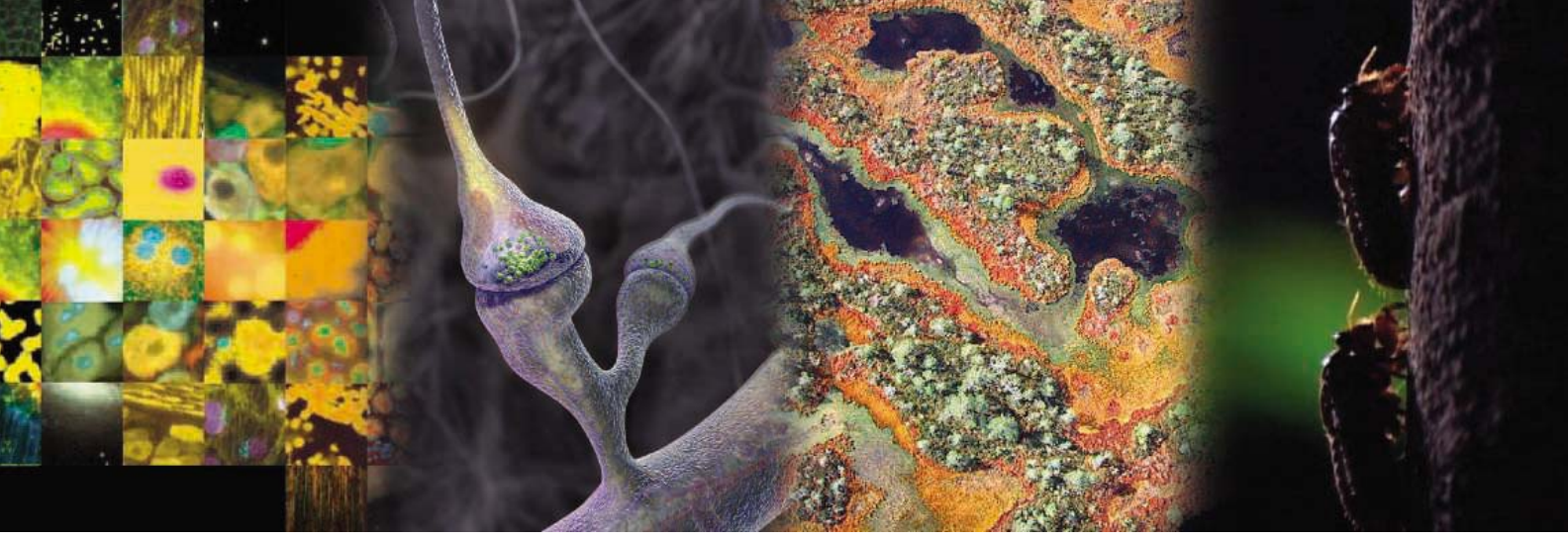

2005 VisualizationChallenge

Some of science's most powerful statements are not made in words. From the diagrams of DaVinci to Hooke's microscopic bestiary, the beaks of Darwin's finches, Rosalind Franklin's x-rays, or the latest photographic marvels retrieved from the remotest galactic outback, visualization of research has a long and literally illustrious history. To illustrate is, etymologically and actually, to enlighten.

You can *do* science without graphics. But it's very difficult to *communicate* it in the absence of pictures. Indeed, some insights can only be made widely comprehensible as images. How many people would have heard of fractal geometry or the double helix or solar flares or synaptic morphology or the cosmic microwave background if they had been described solely in words?

To the general public, whose support sustains the global research enterprise, these and scores of other indispensable concepts exist chiefly as images. They become part of the essential iconic lexicon. And they serve as a source of excitement and motivation for the next generation of researchers.

The National Science Foundation (NSF) and *Science* created the Science and Engineering Visualization Challenge to celebrate that grand tradition—and to encourage its continued growth. In a world where science literacy is dismayingly rare, illustrations provide the most immediate and influential connection between scientists and other citizens, and the best hope for nurturing popular interest. Indeed, they are now a necessity for public understanding of research developments: In an increasingly graphics-oriented culture, where people acquire the majority of their news from TV and the World Wide Web, a story without a vivid and intriguing image is often no story at all.

We urge you and your colleagues to contribute to the next competition, details of which will be available on NSF's Web site (www.nsf.gov), and to join us in congratulating the winners.

Susan Mason of NSF organized this year's challenge; Carolyn Gramling of *Science*'s news staff wrote the text that accompanies the winning images displayed in the following pages; and *Science*'s online editor Stewart Wills put together a special Web presentation at www.sciencemag.org/sciext/vis2005. In addition, Graham Johnson, who won first place in the Illustration category, is profiled on *Science*'s Next Wave (www.nextwave.org).

Curt Suplee, Director, Office of Legislative and Public Affairs, NSF
Monica Bradford, Executive Editor, *Science*

CREDIT: PATRICK OLMERT/NSF

PANEL OF JUDGES
(left to right)

Gary Lees
Chair and Director,
Department of Arts as Applied to Medicine
Johns Hopkins University
Baltimore, Maryland

Thomas Lucas
Thomas Lucas Productions
New York, New York

Felice Frankel
Research Scientist,
Massachusetts Institute of Technology
Cambridge, Massachusetts

Donna J. Cox
Professor, School of Art & Design
University of Illinois, Urbana-Champaign

Michael Keegan
Assistant Managing Editor, News Art
The Washington Post
Washington, D.C.

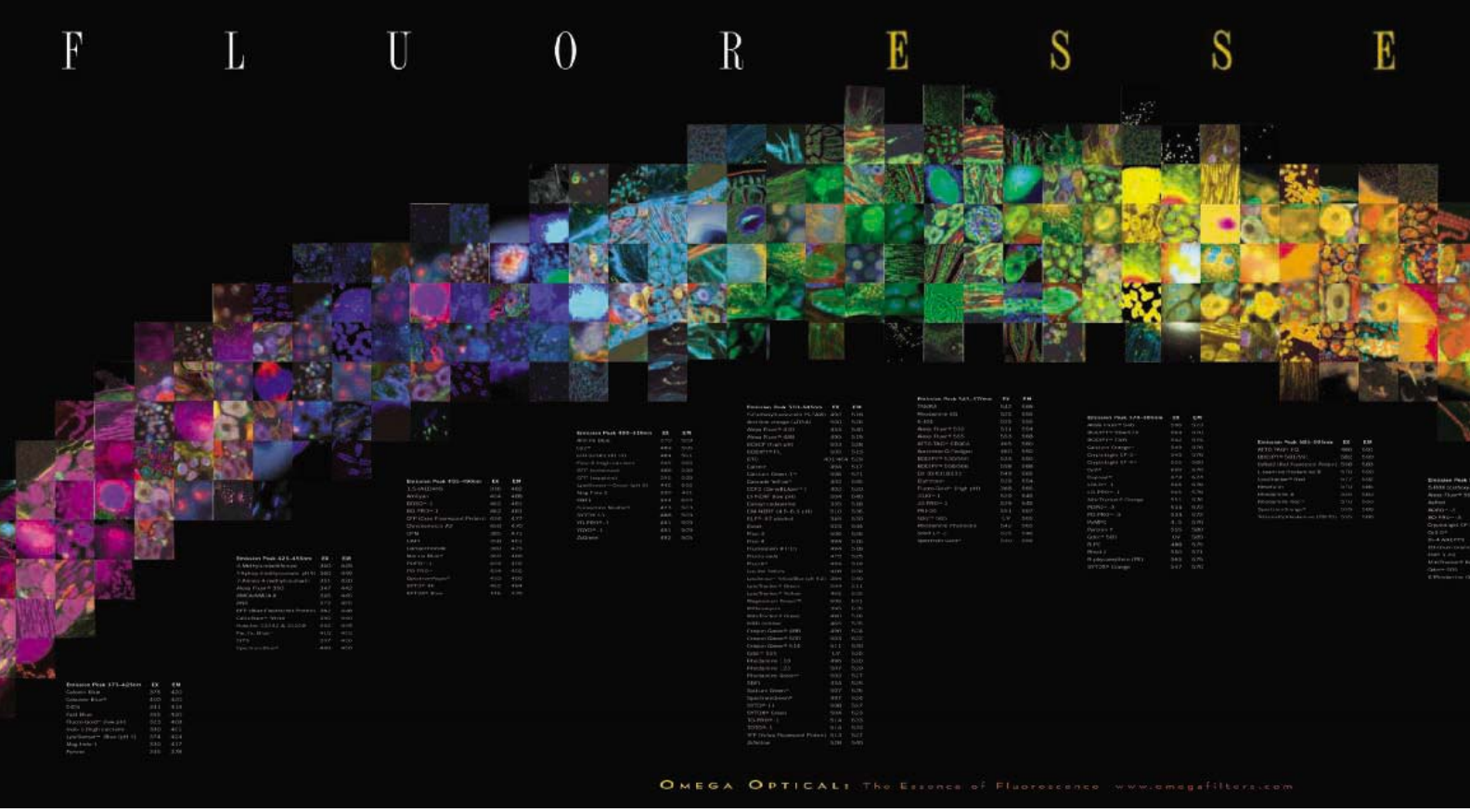

The Synapse Revealed

Graham Johnson, Graham Johnson Medical Media

Deep inside the brain, a neuron prepares to transmit a signal to its target. To capture that expectant, fleeting moment with painstaking detail, science illustrator Graham Johnson based his elegant, highly accurate drawing on ultrathin micrographs of sequential brain slices.

The brain contains billions of neurons, whose network of chemical messages form the basis for all thought, movement, and behavior. Johnson's illustration tells the story of one such signal, a synaptic millisecond that is both eye-catching and accurate in scale and shape. Using the brain slices as references, Johnson sketched the layout of the illustration in pencil, from the convoluted labyrinth of neurons in the background to the clusters of organelles inside the neural cells. After scanning the drawing into three-dimensional modeling software, he colored the image with a palette of dreamy, underwater colors and added the bumpy, realistic texture and glowing lighting reminiscent of a scanning electron micrograph—qualities that help outline the image, pull the central neural interaction forward, and give it a stronger impact, he says.

ILLUSTRATION
First Place

The resulting image is a careful balance between precision and beauty. Because the original data were so complex, Johnson cut the number of neuron interactions depicted to only 30% of the original data—"otherwise, it's just a mass of spaghetti in front of you," he says.

"It gives us the information we need, but at the same time brings an aesthetic, a refinement," says panel of judges member Felice Frankel. "That's really important: to get the viewer to want to look—and then to ask questions."

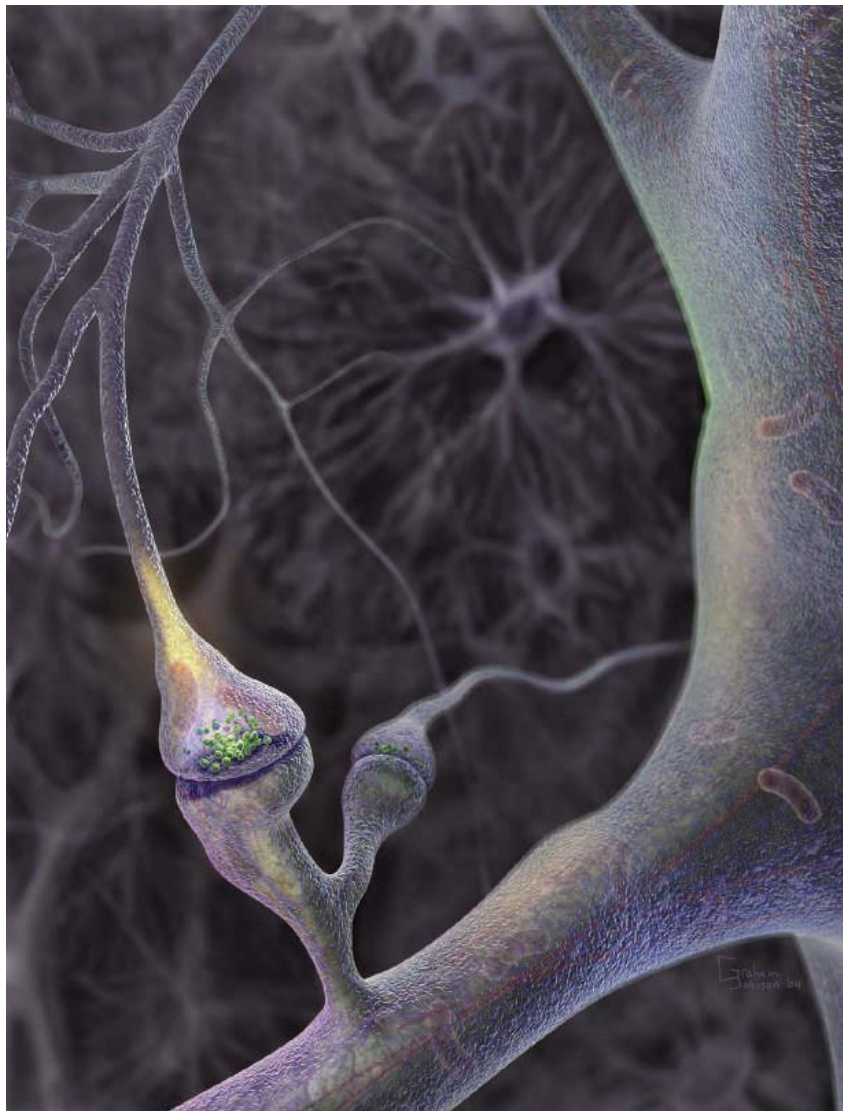

2005 VisualizationChallenge

Fluoressence: The Essence of Fluorescence

Cheryl Aaron, Omega Optical Inc.

A mosaic of colors and flares of light: all this, and emission peaks, too? The winning rainbow of light-sensitive molecules can both spice up a drab laboratory wall and provide a quick-reference guide for fluorescence microscopists.

Fluorescent molecules respond to irradiation by light of a known wavelength, such as ultraviolet, with a colorful glow of their own. As an incoming photon excites the molecule, its electrons vibrate and then relax to their lowest energy level, emitting a longer wavelength of light as the molecule returns to its ground state. Because the excitation and resultant emission wavelengths are highly sensitive and specific to a given fluorophore, scientists can use fluorescent dyes to generate telltale lights that label cells and different biological structures with great accuracy.

INFOGRAPHIC
First Place

The poster was the brainchild of a team of marketing experts at Omega Optical Inc. The company makes optical filters for microscopes, and it wanted to give its customers a useful reference chart, says Omega marketing manager Cheryl Aaron. The design team used a rainbow of photographs of dyes and other fluorophores supplied by both employees and customers, and included critical emission and excitation wavelengths for each fluorophore, to create a graphic they hope will brighten many a university classroom or lab.

"It was a wonderfully intelligent approach to putting all of this information in one place" and also "quite beautiful," says panel of judges member Felice Frankel.

Autumn Color, Estonian Bog

James S. Aber, Emporia State University

PHOTOGRAPHY
First Place

With its intricate patterns within patterns and striking colors, the winning photograph bears a distinct resemblance to a fractal. But scale back—to about 150 meters above the ground—and the sinuous landforms of Estonia's Männikjärve bog begin to reveal themselves.

In the peat bogs of east-central and southwestern Estonia, autumn works a change in the color scheme: Cotton grass turns gold, hardwoods in surrounding forests turn orange and red, and pine trees remain silvery green. The bog water, in sharp contrast, stays an acidic brown. Geologist James Aber of Emporia State University in Kansas recognized the potential beauty of the landscape when he was collaborating with Estonian colleagues to study the glacial geomorphology and geotectonics of the region. But to capture it, he knew he'd need to get off the ground—or at least, his camera would.

Aber used a conventional digital camera in an unconventional setting: He attached it to a kite and operated it from the ground like a radio-controlled model airplane, an early type of remote sensing that has been around since the 19th century. Aber has used the technique for 8 years and has even taught it in courses at Emporia State on aerial photography.

Kite photography "gives us a scale and resolution that are difficult to achieve in other ways," Aber says. The kite flies between 50 and 150 meters above the ground, too low for a conventional airplane and too high for a boom or tower structure.

The photograph was striking, not only because it creates a mood that matches the time of year and the subject of the image but also for its unique technique, says panel of judges member Gary Lees.

NONINTERACTIVE MEDIA
First Place

Return of the 17-Year Cicadas

Roger Hangarter, Indiana University, Bloomington

They're back. Plant biologist Roger Hangarter of Indiana University, Bloomington, knew the cicadas were coming, but he didn't intend to document the event—until they began to emerge, spectacularly, in his own backyard.

Cicadas have a life cycle of 13 to 17 years, most of which is spent underground. Related to aphids, the insects burrow into the ground almost as soon as they're born, living off the sap of trees for the majority of their existence. They surface in the last few weeks of life to transform into full adulthood, mate, lay eggs, and die. Six to 8 weeks later, the young cicadas hatch and head straight for the ground. Southern Indiana's May 2004 round of cicadas, whose lives are detailed in the winning entry, were part of "Brood X," which also surfaced in Maryland and Pennsylvania.

The Indiana cicadas were "absolutely mesmerizing," Hangarter says. They "really took over the community." They also took over his own teeming backyard, motivating him to capture the event on film for friends and family. Collaborating with Indiana University undergraduate and filmmaker Samuel Orr, Hangarter used time-lapse photography and real-time digital video to record the entire life cycle of the cicadas throughout the summer, also adding a soundtrack and descriptive text.

The resulting 5-minute film (whose original length is 17 minutes) was "a discrete, elegant package, beautifully photographed and very detailed," says panel of judges member Thomas Lucas.

& Honorable Mentions

Rip Currents: Nearshore Fundamentals

Steve Deyo, Kevin Fuell, Katharine Olson, Dan Ritter, and Seth Lamos, UCAR/COMET

Is it safe to go in the water? For the answer, weather forecasters can watch this animated guide to rip currents for the right—or wrong—combination of nearshore circulation and wave dynamics. Graphic artist Steve Deyo and colleagues at the University Corporation for Atmospheric Research/Cooperative Program for Operational Meteorology, Education, and Training in Boulder, Colorado, offer a broad range of audiences a three-dimensional peek into current formation processes both above and below the water's surface, amid computer-generated breaking waves and capping sea foam.

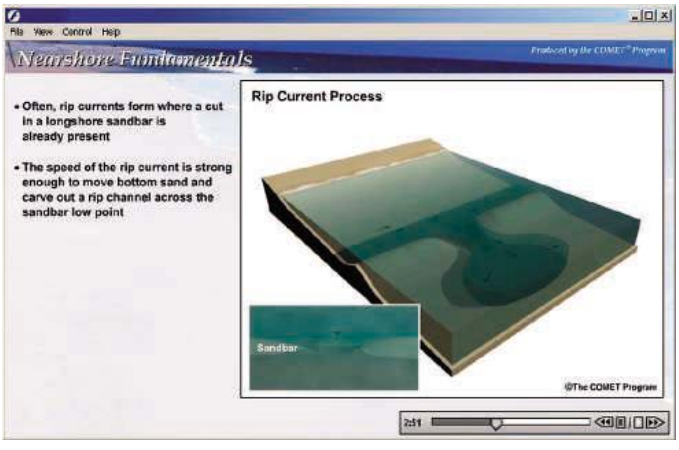

Forces of Nature

Leslie Ann Aldridge, National Geographic TV & Film

Deep under Istanbul, pressure is growing. In the depths of Turkey's North Anatolian fault line, tectonic plates shift and lock, periodically building and releasing stress as destructive energy. In a computer animation based on actual data and models for the fault line, filmmaker Leslie Ann Aldridge of National Geographic TV & Film in Washington, D.C., takes the viewer right down into the fault, recreating the forces behind 60 years of episodic earthquake history—and suggesting where the next earthquake will occur.

INTERACTIVE MEDIA
Honorable Mention

Transpiration: Water Movement Through Plants
Tracey M. Sterling, New Mexico State University

How does a garden grow? Transpiration, the transportation of water through plants from soil to leaves to atmosphere, is an essential part of the hydrologic cycle. From water absorption through a plant's roots to water vapor lost through its leaves, entomologist and plant pathologist Tracy Sterling of New Mexico State University and animator Matt Byrnes created a friendly, interactive activity with a playful design. The animation teaches plant biology basics and offers numerous interactive features, such as changes to environmental conditions that can impact the speed of water movement. And that affects how the garden will grow.

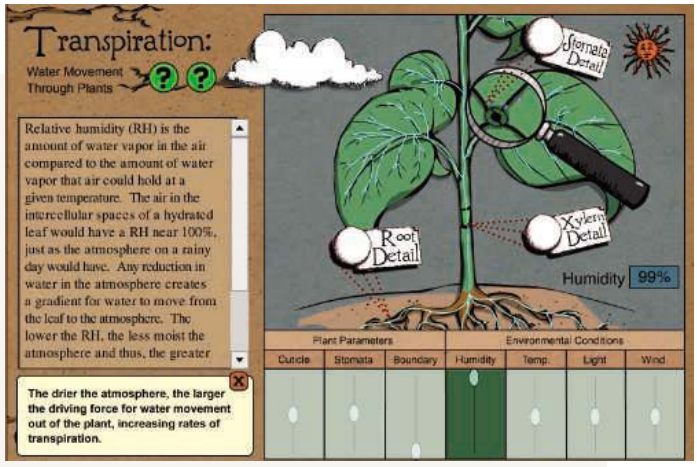

Noninteractive Honorable Mentions *cont.*

Planetary Motion From Eudoxus to Copernicus
Mogi Massimo Vicentini, Civico Planetario di Milano

Although the earliest astronomers took an Earth-centric view of the heavens, Italian graphic designer Mogi Massimo Vicentini puts the viewer at the center of a sweeping story of planetary motion. Planets rotate, oscillate, and appear to move backward as faulty ideas are rejected, until their motion is most satisfactorily explained by Copernicus's (and Kepler's) heliocentric model. Designed for general planetarium audiences at the Civico Planetario di Milano in Italy, the presentation is a twirling visual history of planetary exploration and time.

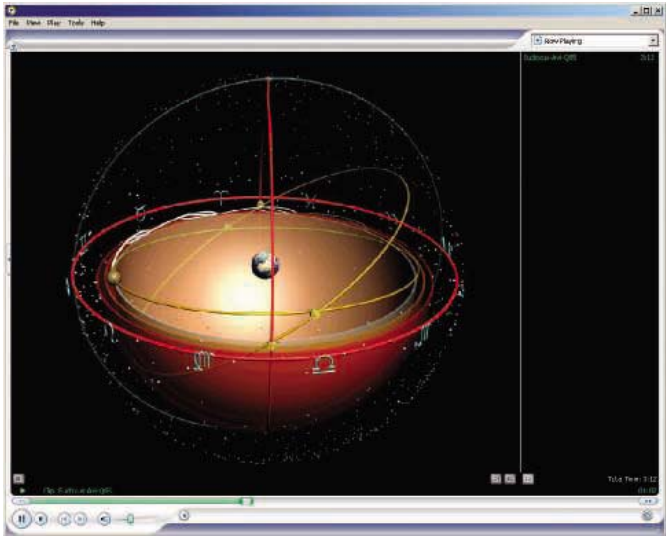

Evolutionary Morphing: Statistical Interpolation of Ancestral Morphology Along an Evolutionary Tree
Nina Amenta, University of California, Davis

Until the right bones are found, computer-visualized virtual fossils can fill in some evolutionary gaps. By precisely relating landmark points on one skull image to similar points on another, computer scientist Nina Amenta of the University of California, Davis, and colleagues calculate hypothetical, three-dimensional ancestors within an evolutionary tree. The resulting video is a transformative, graceful look into monkey morphology, culminating in the evolution of one common ancestor's cranium through five branches of descendents.

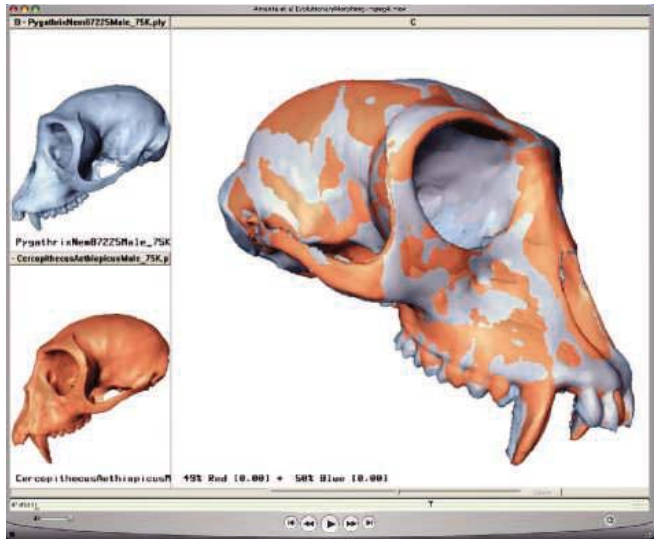

Tracing Modern Human Origins

THE 13 MAY ISSUE CONTAINED THREE PAPERS ("Single, rapid coastal settlement of Asia revealed by analysis of complete mitochondrial genomes," V. Macaulay *et al.*, Reports, p. 1034; "Reconstructing the origin of Andaman Islanders," K. Thangaraj *et al.*, Brevia, p. 996; "Did early humans go north or south?", P. Forster and S. Matsumura, Perspectives, p. 965) that imply that a modern human migration out of Africa with replacement of all non-African archaic humans is an established fact that needs no further argument, and that all that remains now is to ascertain the time(s) and route(s) of the purported migration(s). This presents a profoundly misleading picture about the present state of debate on modern human origins.

Mitochondrial DNA (mtDNA) studies have been used to support ideas about modern human origins, but much information is now known that contradicts the conclusions of the early mtDNA literature. For example, nuclear loci rarely, if ever, show the low coalescence times (~200,000 years) seen in mtDNA, nor do they show strictly African roots. Indeed, there is now growing evidence of strictly non-African polymorphisms that date to before the birth of modern humans (*1*–*5*). Nuclear loci do not always, or even commonly, show the strong signals of expansions that are so strikingly present in human mtDNA (*6*). Why does Macaulay *et al.*'s mtDNA study suggest that a few hundred females migrated out of Africa, whereas the nuclear DNA suggests an effective population of around 10,000 (*7*)? All these data have to be explained before a proper estimation of the place of mtDNA evidence in the overall picture can be made.

> "[These papers] imply that a modern human migration out of Africa with replacement of all non-African archaic humans is an established fact that needs no further argument..."
>
> –HARPENDING AND ESWARAN

Exclusive attention to mtDNA data has led to an extremely one-sided picture of modern human origins. No theory that does not explain all or, at least, most of the facts will survive. Not until the mtDNA data is reconciled with nuclear DNA data and the archaeological and other anthropological evidence will we have an enduring solution to the puzzle of modern human origins.

HENRY HARPENDING[1] AND VINAYAK ESWARAN[2]
[1]Department of Anthropology, University of Utah, Stewart Building, Salt Lake City, UT 84112, USA. [2]Department of Mechanical Engineering, Indian Institute of Technology, Kanpur 208016, India.

References

1. R. M. Harding *et al.*, *Am. J. Hum. Genet.* **60**, 772 (1997).
2. Z. Zhao *et al.*, *Proc. Natl. Acad. Sci. U.S.A.* **97**, 11354 (2000).
3. N. Yu *et al.*, *Mol. Biol. Evol.* **18**, 214 (2001).
4. D. Garrigan *et al.*, *Mol. Biol. Evol.* **22**,189 (2005).
5. J. Hardy *et al.*, *Biochem. Soc. Trans.* **33**, 582 (2005).
6. H. C. Harpending, S. T. Sherry, A. R. Rogers, M. Stoneking, *Curr. Anthropol.* **34**, 483 (1993).
7. N. Takahata, *Mol. Biol. Evol.* **10**, 2 (1993).

Response

BOTH MODERN HUMAN MITOCHONDRIAL DNA (mtDNA) and the male-specific part of the modern human Y chromosome have a recent origin in Africa and were dispersed throughout the rest of the world less than 100,000 years ago (*1*, *2*). This is not to say that there was no (limited) interbreeding of anatomically modern humans with archaic humans, which might be reflected in some autosomal and X-chromosome genes—a possibility that our Report did not address. The current evidence from these loci, however, remains equivocal.

Existing autosomal data do not, in most cases, provide strong evidence for either replacement or hybridization, despite claims to the contrary. The high coalescence time of autosomal loci is not relevant, since in itself this tells us almost nothing about more recent settlement events: A small founder gene pool could well have either a deep or shallow ancestry within a replacement perspective. Given the limited amount of variation in non-recombined stretches of the autosomes, there is typically little power to distinguish different demographic models. This is as true of the autosomal data used by Templeton (*3*) as it is of the data in the papers cited by Harpending and Eswaran. The authors of the most recent of these (*4*) are entirely open about this, but their (frequency-based) suggestion that the root of their tree lies in Asia is mistaken; there is simply insufficient branching structure to fix the geographical location of the root with any confidence. Moreover, supposedly ancient Asian-specific single-nucleotide polymorphisms such as those cited by Harpending and Eswaran are associated with age estimates of enormous uncertainty.

Bold conclusions of ancient Asian ancestry also suffer from limited sampling. Non-African mtDNAs most likely evolved in the Horn of Africa and dispersed from there, but none of the cited papers on autosomal loci include data from this region. Even if such data were available, identifying non-African founder lineages in such low-resolution systems is deeply problematic because of recent back-migration across the Red Sea (*5*). In cases where autosomal loci do have the necessary resolution, they suggest the replacement model (*6*–*8*). The discordant population-size estimates referred to by Harpending and Eswaran are likely more apparent than real, since these long-term values are usually obtained with the multiregional stipulation of random mating and constant population size. The analysis of overly simplistic models with methods that throw away what little information there is in most of these loci throws up straw men, such as the apparent lack of "strong signals of expansion" in some autosomal loci (*9*).

> "Both modern human mitochondrial DNA... and the male-specific part of the modern human Y chromosome have a recent origin in Africa and were dispersed throughout the rest of the world less than 100,000 years ago..."
>
> –MACAULAY ET AL.

VINCENT MACAULAY,[1]* CATHERINE HILL,[2] ALESSANDRO ACHILLI,[3] CHIARA RENGO,[3] DOUGLAS CLARKE,[4] WILLIAM MEEHAN,[4] JAMES BLACKBURN,[4] ORNELLA SEMINO,[3] ROSARIA SCOZZARI,[5] FULVIO CRUCIANI,[5] ADI TAHA,[6] NORAZILA KASSIM SHAARI,[7] JOSEPH MARIPA RAJA,[7] PATIMAH ISMAIL,[7] ZAFARINA ZAINUDDIN,[8] WILLIAM GOODWIN,[9] DAVID BULBECK,[10] HANS-JÜRGEN BANDELT,[11] STEPHEN OPPENHEIMER,[12] ANTONIO TORRONI,[3] MARTIN RICHARDS[2]
[1]Department of Statistics, University of Glasgow, Glasgow G12 8QQ, UK. [2]Institute for Integrative and Comparative Biology, University of Leeds, Leeds LS2 9JT, UK. [3]Dipartimento di Genetica e Microbiologia, Università di Pavia, 27100 Pavia,

LETTERS

Italy. [4]Department of Chemical and Biological Sciences, University of Huddersfield, Huddersfield HD1 3DH, UK. [5]Dipartimento di Genetica e Biologia Molecolare, Università "La Sapienza," 00185 Rome, Italy. [6]National Museum of Kuala Lumpur, 50566 Kuala Lumpur, Malaysia. [7]Universiti Putra Malaysia, 43400 Serdang, Selangor, Malaysia. [8]Department of Forensic Medicine and Science, University of Glasgow, Glasgow G12 8QQ, UK. [9]Department of Forensic and Investigative Science, University of Central Lancashire, Preston PR1 2HE, UK. [10]School of Archaeology and Anthropology, The Australian National University, Canberra ACT 0200, Australia. [11]Department of Mathematics, University of Hamburg, 20146 Hamburg, Germany. [12]Department of Anthropology, University of Oxford, Oxford OX1 2JD, UK.
*To whom correspondence should be addressed. E-mail: vincent@stats.gla.ac.uk

References

1. M. Ingman, H. Kaessmann, S. Pääbo, U. Gyllensten, *Nature* **408**, 708 (2000).
2. Y. Ke *et al.*, *Science* **292**, 1151 (2001).
3. A. R. Templeton, *Nature* **416**, 45 (2002).
4. D. Garrigan, Z. Mobasher, T. Sverson, J. A. Wilder, M. F. Hammer, *Mol. Biol. Evol.* **22**, 189 (2005).
5. T. Kivisild *et al.*, *Am. J. Hum. Genet.* **75**, 752 (2004).
6. S. A. Tishkoff *et al.*, *Science* **271**, 1380 (1996).
7. S. Alonso, J. A. L. Armour, *Proc. Natl. Acad. Sci. U.S.A.* **98**, 864 (2001).
8. W. S. Watkins *et al.*, *Am. J. Hum. Genet.* **68**, 738 (2001).
9. J. Hey, E. Harris, *Mol. Biol. Evol.* **16**, 1423 (1999).

Response

HARPENDING AND ESWARAN QUESTION THE concordance between the phylogenetic signals obtained from mitochondrial versus nuclear DNA markers in relation to modern human origins. It is well known that because of the fourfold higher effective population size (N_e) for diploid autosomal loci, the expected coalescence times of the trees based on them can be four times deeper than a tree drawn from a haploid locus such as mtDNA. It is also statistically more probable than for a locus, with smaller N_e, that the root of the gene tree of a population is not found in all of the fractions arising after population subdivision. Given the stochastic nature of the coalescence process, even the most precise estimate of the time to the most recent common ancestor (MRCA) of all human lineages would not necessarily carry any conclusive information about the patterns of the spread of the genetic variation in this locus. Unlike the nuclear studies cited by Harpending and Eswaran, our mtDNA study and that of Macaulay *et al.* and the commentary on them ("Did early humans go north or south?", P. Forster and S. Matsumura, Perspectives, 13 May, p. 965) are focused on the genetic diversity that has accumulated on top (downstream) of the reconstructed ancestral sequences—founder haplogroups M, N, and R—that are commonly shared among distant non-African populations from West Asia to Australia. The idea behind such a phylogeographic approach is to define the ancestral

nodes in the tree that carry descendants in distinct regions of the world and to study their geographic distribution and time depth through the coalescent method. By this approach, all non-African mtDNA sequences appear to be derived from haplogroups M, N, and R, which in turn coalesce in haplogroup L3, which has a wide distribution in Africa. It is, again, not the overall coalescence time in haplogroup L3 of all the non-African lineages but the averaged coalescence times to founder haplogroups M, N, and R that are considered as the estimators of the time back to the "out of Africa" migration (the outcome could in principle be the same even if the non-African MRCA were equal to the global MRCA). The task of defining such founder haplotypes and estimating their time depth at nuclear loci is, however, complicated because of the lower substitution rate and the reshuffling effect of recombination.

KUMARASAMY THANGARAJ,[1] GYANESHWER CHAUBEY,[1] TOOMAS KIVISILD,[2] ALLA G. REDDY,[1] VIJAY K. SINGH,[1] AVINASH A. RASALKAR,[1] LALJI SINGH[1]

[1]Centre for Cellular and Molecular Biology, Hyderabad-500 007, India. [2]Estonian Biocenter, Riia 23, Tartu-51010, Estonia.

Bacteria and Island Biogeography

IN THEIR BREVIA "LARGER ISLANDS HOUSE more bacterial taxa" (24 June, p. 1884), T. Bell *et al.* show that the bacterial diversity in bark-lined water pans ("treeholes") at the base of beech trees tends to increase with water volume. This result is explained in terms of the theory of island biogeography (*1*).

The result is intriguing, but the interpretation offered would seem most unlikely. The theory of island biogeography implies that in "islands" such as treeholes, species numbers represent a dynamic balance between local extinction of species populations and immigration of species that were not previously present. Absolute population sizes increase with increasing island size, and larger populations are less likely to suffer stochastic extinctions. Larger islands also represent larger targets for immigrating propagules, and so they tend to support more species [although surely the small (~50-ml) treeholes dry out periodically?].

Insofar as there are probably no bacterial species that are exclusively confined to bark-lined holes at the base of beech trees, these habitats can hardly be considered as islands; rather, they are rapidly inoculated by bacteria from the surrounding soil and litter, from rainwater running along branches and down tree trunks, and by atmospheric deposition of ubiquitous bacterial spores. Furthermore, bacterial densities in such water bodies are likely to be at least 10^7 to 10^8 cells ml^{-1}, and although these may comprise many species, such huge population sizes would preclude stochastic extinctions. The assumptions underlying the theory of island biogeography are therefore not met.

Bell *et al.*'s species-area curve does not really fit the predicted power function very well; rather, bacterial diversity seems to increase stepwise at treehole volumes around 1 liter. It is likely that the larger water bodies support additional microhabitats. One possibility is that large treeholes include an anaerobic layer at the bottom that accommodates large populations of other physiological types of bacteria.

TOM FENCHEL[1] AND BLAND J. FINLAY[2]

[1]Marine Biological Laboratory, University of Copenhagen, DK–3000 Helsingør, Denmark. [2]Centre for Ecology and Hydrology Dorset, Winfrith Technology Centre, Dorchester, Dorset, DT2 8ZD, UK.

Reference

1. R. MacArthur, E. O. Wilson, *The Theory of Island Biogeography* (Princeton Univ. Press, Princeton, NJ, 1967).

THE LONG-LASTING DEBATE ABOUT THE ubiquitous distribution of microbes has recently received considerable attention. In the microbial world, is everything potentially everywhere provided that the environmental conditions are adequate? Or do the same rules apply as for macroscopic organisms?

With their Brevia "Larger islands house more bacterial taxa" (24 June, p. 1884), a study on bacterial diversity in water-filled treeholes, T. Bell *et al.* brought an interesting contribution to this debate by showing that, as for larger organisms, a steep microbial taxa-area relationship (i.e., the value of slope z of the regression between diversity and sampling area) is possible. This finding brings support to the proponents of the possible local distribution of microorganisms by contradicting one of the supposed fundamental differences between microbes and larger organisms (*1*).

Although these new results are potentially important, I believe that they are undermined by a methodological limitation of the study. Because Bell *et al.* homogenized the water extracted from the treeholes before analyzing the community composition, they could not provide a measure of within-habitat heterogeneity, an important potential source of overall bacterial diversity in the water-filled treehole. Indeed, the observed increase in bacteria diversity may at least partly be due to one or more of the following confounding factors that may be

associated with a larger body of water: (i) increased potential ecosystem stability (e.g., lower probability of drying out during extended warm and dry periods, lower solute concentration fluctuation resulting from partial evaporation and rain events, and lower temperature fluctuations); (ii) micro-niche diversity (e.g., stratification within the water body and the organic sediments) (*2*); and (iii) food-web complexity (e.g., diversity of metazoa inducing top-down effect) (*3, 4*).

An estimate of possible treehole heterogeneity would allow reassessment of the full value of their results. The lack of this information unfortunately does not allow us to establish if their results indeed are in contradiction with the "everything is everywhere" postulate.

EDWARD A. D. MITCHELL
WSL, Antenne Romande and EPFL-ENAC-ISTE-ECOS, Lausanne 1015, Switzerland.

References

1. B. J. Finlay, G. F. Esteban, T. Fenchel, *Protist* **155**, 15 (2004).
2. M. C. Horner-Devine, K. M. Carney, B. J. M. Bohannan, *Proc. R. Soc. London Ser. B Biol. Sci.* **271**, 113 (2004).
3. L. Jiang, P. J. Morin, *Am. Nat.* **165**, 350 (2005).
4. E. Zollner, B. Santer, M. Boersma, H. G. Hoppe, K. Jurgens, *Freshwater Biol.* **48**, 2174 (2003).

Response

FENCHEL AND FINLAY HAVE ARGUED THAT microbes have a cosmopolitan distribution and that the relationship between species and area is flat (*1*). In the sense that it takes but one black swan to prove that all swans are not white, we have clearly shown that all microbial taxa-area relationships are not flat.

Fenchel and Finlay claim that (i) because no bacterial species are exclusively confined to treeholes, they cannot be considered "islands"; (ii) local extinction and colonization dynamics are unlikely to explain species richness; and (iii) because of their great abundance, bacteria are unlikely to suffer from "stochastic extinction." However, treeholes clearly do follow the standard ecological definition of an island: "a self-contained region whose species originate entirely by immigration from outside the region" (*2*). "Stochastic extinction" refers to individual species; quoting abundances of the whole bacterial community is irrelevant. We do not know the local colonization or extinction rates, so whether species richness within a treehole results in part from a balance of these two rates is a hypothesis that remains to be tested.

Despite Fenchel and Finlay's claims, the fit between the data and a power function is excellent ($R^2 = 0.91$), and the z value (0.26) is within the range of those observed for larger taxa in island habitats (0.2 to 0.35) (*2*), a conclusion that is now supported by other recent studies (*3, 4*). These facts are at

variance with the "everything is everywhere" postulate.

Fenchel and Finlay say that we explain our result in terms of the theory of island biogeography (*5*). In fact our conclusion is that "[t]he result implies that analogous processes structure both microbial communities and communities of larger organisms." This includes many factors beyond those of colonization and extinction, central to MacArthur and Wilson's theory. The challenge is to assay these and their relative importance.

Mitchell's principal criticism is that our results are "undermined by a methodological limitation of the study" because the water was homogenized before describing the communities. To the contrary, it is precisely this technique that makes the results comparable to studies of larger organisms. Nearly every survey of the species-area relationship on islands, including the classic studies that are most often cited (*2*), also homogenized the habitats from each island.

Habitat heterogeneity, ecosystem stability, and food-web complexity are not confounding factors; rather, they are mechanisms that might explain the pattern that we observed. Some form of stratified sampling might have allowed us to assess the degree of correlation between treehole volume and habitat heterogeneity. However, the only appropriate way to establish the mechanisms that underlie the observed pattern is by conducting randomized experiments in which we manipulate the treeholes to directly test these hypotheses. As recent studies have demonstrated (*6*), inferring process from pattern is fraught with difficulty.

We sought to determine if a relationship exists between treehole volume and bacterial genetic diversity. We did not set out to establish the cause of this pattern, nor did we set out to resolve the long-standing debate on the ubiquity of bacterial species. Our conclusion that, as for larger organisms, comparatively steep microbial species-area relationships are possible, is not altered by knowledge of the causal mechanism(s). We agree that the logical next step for research is to uncover the mechanism, but doing so will take more than a stratified sampling procedure.

THOMAS BELL,[1,2] JONATHAN A. NEWMAN,[3] IAN P. THOMPSON,[1] ANDREW K. LILLEY,[1] CHRISTOPHER J. VAN DER GAST[1]*

[1]Natural Environment Research Council (NERC) Centre for Ecology and Hydrology, Mansfield Road, Oxford OX1 3SR, UK. [2]Department of Zoology, University of Oxford, South Parks Road, Oxford OX1 3PS, UK. [3]Department of Environmental Biology, University of Guelph, Guelph, ON N1G 2W1, Canada.

*To whom correspondence should be addressed. E-mail: cjvdg@ceh.ac.uk

References

1. T. Fenchel, B. J. Finlay, *Bioscience* **54**, 777 (2004).
2. M. L. Rosenzweig, *Species Diversity in Space and Time* (Cambridge Univ. Press, Cambridge, 1995).
3. C.J. van der Gast *et al*., *Environ. Microbiol.* **7**, 1220 (2005).
4. I. Reche *et al*., *Ecology* **86**, 1715 (2005).
5. R. H. MacArthur, E. O. Wilson, *The Theory of Island Biogeography* (Princeton Univ. Press, Princeton, NJ, 1967).
6. G. Bell, *Science* **293**, 2413 (2001).

CORRECTIONS AND CLARIFICATIONS

News Focus: "Sky-high experiments" by E. Pennisi (26 Aug., p. 1314). On page 1315, in the first paragraph of the second column, the sentence "Overall, the carbon in the soil increased by 44%" should have read "Overall, the carbon dioxide in the soil increased by 44%."

TECHNICAL COMMENT ABSTRACTS

COMMENT ON "Status and Trends of Amphibian Declines and Extinctions Worldwide"

Bruno V. S. Pimenta, Célio F. B. Haddad, Luciana B. Nascimento, Carlos Alberto Gonçalves Cruz, José P. Pombal Jr.

Stuart *et al*. (Reports, 3 Dec. 2004, p. 1783) reported that 1856 amphibian species are threatened worldwide according to the IUCN Red List criteria. However, a methodic analysis of their results, using Brazilian species as a case study, shows that this number is an overestimate resulting from misuse of the IUCN Criteria and insufficient data.
Full text at www.sciencemag.org/cgi/content/full/309/5743/1999b

RESPONSE TO COMMENT ON "Status and Trends of Amphibian Declines and Extinctions Worldwide"

Simon N. Stuart, Janice S. Chanson, Neil A. Cox, Bruce E. Young, Ana S. L. Rodrigues, Debra L. Fischman, Robert W. Waller

Using information on Brazilian species, Pimenta *et al*. assert that we overestimated the number of threatened amphibians. However, this claim, based on a misunderstanding of the IUCN Red List criteria and a strongly evidentiary attitude to listing species, almost certainly seriously underestimates the number of threatened amphibians in Brazil.
Full text at www.sciencemag.org/cgi/content/full/309/5743/1999c

Letters to the Editor

Letters (~300 words) discuss material published in *Science* in the previous 6 months or issues of general interest. They can be submitted through the Web (www.submit2science.org) or by regular mail (1200 New York Ave., NW, Washington, DC 20005, USA). Letters are not acknowledged upon receipt, nor are authors generally consulted before publication. Whether published in full or in part, letters are subject to editing for clarity and space.

HISTORY OF SCIENCE

Picturing Particle Processes

Gordon Kane

Drawing Theories Apart
The Dispersion of Feynman Diagrams in Postwar Physics
by David Kaiser

University of Chicago Press, Chicago, 2005. 489 pp. $80, £56. ISBN 0-226-42266-6. Paper, $30, £21. ISBN 0-226-42267-4.

Feynman diagrams (representations of elementary particles and their interactions in space and time) are a remarkable intellectual development and tool. Over the past half century, there has been a huge increase in our understanding of the smallest constituents of matter and of their interactions, which build up our world. In the 1940s, we knew of four forces in nature: gravity plus the strong, weak, and electromagnetic forces. Physicists were beginning to develop a quantum theory of the electromagnetic force, but no progress had been made toward describing the weak or strong forces. By 1973, a full relativistic quantum field theory of the weak and strong forces was in place, and the weak and electromagnetic forces had been unified into a simpler force at shorter distances. This progress would probably not have been possible, and certainly not have been as rapid, without the use of Feynman diagrams.

In *Drawing Theories Apart*, David Kaiser describes the evolution of the diagrams from Richard Feynman's original use in 1948 as a means of organizing the extremely long and complicated formulas of the field theory of quantum electrodynamics to the sophisticated and powerful tool used throughout many areas of theoretical physics. The title may capture a number of curious readers, but it will be understood only by science studies specialists. Kaiser (a historian of physics and physicist at the Massachusetts Institute of Technology) recognizes there are really several astonishing aspects to the full success of Feynman diagrams. The first is that they were developed at all. Feynman diagrams are a technology and, like all technologies, might not have been invented. A few theorists, such as Julian Schwinger, could deal with the full quantum field theory formalism of electrodynamics and did not need (nor want) the diagrams. Second, the diagrams can be made to correspond fully to logically separate and calculable pieces of theory, not only for quantum electrodynamics (the calculations for which Feynman created them) but also for any quantum field theory, from condensed matter physics to the theory of the strong interactions. Last, and perhaps most important, in some not-well-understood way that need not have been so, the diagrams also map onto how we physicists think about elementary processes and greatly help us ponder those processes and communicate about them.

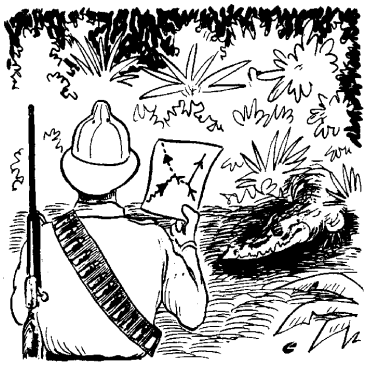

Feynman diagrams in the Amazon jungle.

The initial hundred pages or so of the book will appeal to many readers. Physicists can enjoy a history of the years after World War II from the point of view of the rapid growth of the use of Feynman diagrams. Historians of physics will find a new perspective on several topics. And, especially in the introductory chapter on pedagogy and theory, Kaiser addresses questions of interest to science studies people. (In that chapter, the numbers of footnotes devoted to aspects of science studies and to physics are about equal; further into the book, nearly all the footnotes concern physics.) As Kaiser demonstrates, many older theorists had serious concerns about the validity of Feynman diagrams, whereas a few younger ones—such as Jack Steinberger (who later switched to Nobel Prize–winning experiments) and Cécile DeWitt-Morette—began using the diagrams even before Feynman completed a paper on them. Freeman Dyson's powerful contributions to developing, formalizing, and justifying the diagrams were essential to their acceptance. Kaiser correctly (and repeatedly) emphasizes the basic and crucial role of personal communication among physicists, and he nicely intertwines the changing ways in which theorists were trained during that era with the rapid spread of the use of Feynman diagrams.

Kaiser then turns his focus to the international acceptance of Feynman diagrams, the development of Geoffrey Chew's "S-Matrix theory" of strong interactions, and various technical issues. As is normal in historians' histories of science, the author gives much more space to approaches that failed than would a scientist's history of the same topic. These parts of the book (comprising more than half) will primarily interest physicists who desire a nice tour (with an unusual perspective) of particle theory from the early 1950s to about 1970 and historians of that period's physics. Kaiser ends his account with a short, broad description of the transition to the era of the standard model of particle physics.

The only trap I felt the author did not sufficiently avoid was not fully distinguishing between what I have elsewhere called "research in progress" (RIP) and "completed" subareas of science. As research progresses, the science often changes as understanding improves; that is frequently taken to imply that all science will always change. But in actuality, in many areas of physics (for example, classical optics, classical mechanics, and equilibrium thermodynamics), at some point in time the pieces fell into place and that area stopped changing. Of course research in such areas does not stop (because each will always contain interesting phenomena that remain to be worked out), but the basic theory is in place. It would also be easier for the reader to understand the developments Kaiser describes if he had made a clearer distinction between forces and the rules for deducing their effects. Quantum field theory is a set of rules that applies for any force or interaction. Feynman diagrams, which reflect the structure of quantum field theory, apply for any force.

A major aspect of the importance of Feynman diagrams is their use as calculational tools. To fully understand that importance, it is necessary to understand how theorists work, and Kaiser does. Most of us are familiar with how experimenters function, in the sense that in order to measure something at the frontier they may have to work for months or, now, years, building equipment and analyzing data. It is not so well known that life is basically the same for theorists, who don't just sit around having new ideas. When theorists come up with an idea, they may then have to spend months calculating observable predictions to test whether it is contradicted by existing data, and if the idea is not, whether it implies a feasible new measurement that tests it. Without Feynman diagrams such calculations are hugely more difficult—in many cases, perhaps not doable.

The reviewer is at the Michigan Center for Theoretical Physics, 3444B Randall Laboratory, University of Michigan, 450 Church Street, Ann Arbor, MI 48109–1040, USA. E-mail: gkane@umich.edu

Intellectual tools can have profound impacts. Feynman diagrams have greatly improved how theoretical physicists think and, consequently, our understanding of nature. *Drawing Theories Apart* provides an informative description of how their influence came about.

10.1126/science.1117592

ECOLOGY

Mothers Driving Cycles

Günter Wagner

It is widely known that one needs at least some mathematical knowledge to understand physics at any degree of sophistication above the most elementary. The laws of nature are seemingly written in the language of mathematics. It is less well appreciated that there was a time when this seemed very unlikely. In the 16th century, mathematics was the tool astronomers used to describe and predict the regular motions of heavenly bodies, whereas the realm of terrestrial physics was considered too messy to be amenable to mathematical modeling. But eventually, a mathematical theory covering both celestial and terrestrial physics was developed, and the argument that terrestrial processes are too complex for mathematics was refuted. Ever since I learned about this episode, in Erhard Oeser's history and philosophy of science course at the University of Vienna, I have been skeptical about claims of impossibility, including the claim that life is too messy to yield to mathematical abstraction. We simply cannot tell whether some scientific goal is in fact impossible or we are just admitting our lack of imagination when we declare it to be. *Ecological Orbits* may well turn out to mark such a transition from what was considered unthinkable—namely a rigorous and nontrivial theory of population dynamics akin to a law of nature—to a real scientific achievement.

Ecological Orbits
How Planets Move and Populations Grow
by Lev Ginzburg and Mark Colyvan

Oxford University Press, New York, 2004. 182 pp. $29.95, £17.99. ISBN 0-19-516816-X.

The book is written by Lev Ginzburg, a theoretical ecologist at Stony Brook University, New York, and Mark Colyvan, a philosopher of science at the University of Queensland, Brisbane, Australia. Its title plays on the mathematical analogy between the authors' theory of population dynamics and the Newtonian laws of mechanics that explain the periodic motions of planets around the Sun. Over recent years, Ginzburg and his students have developed a theory of population dynamics that has close mathematical similarities to the Newtonian laws of motion, and in the book the authors use these analogies to explain the existence of population cycles. If the book's substance was merely that—a play on a formal mathematical analogy—the work would not be worth a review here. What makes the book so convincing is that the mathematical analogy derives from an elementary and possibly fundamental change in perspective.

It is fair to say that classical population dynamical theory treats organisms as tokens for bookkeeping, tokens that are endowed with arbitrary probabilistic rules of transformation (death rates, birthrates, etc.). These rules define models that describe population dynamics, models such as the logistic equation or the Lotka-Volterra equation. In contrast, Ginzburg and Colyvan start with the (elementary) observation that the chance of an individual to reproduce or die depends on its ability to acquire its share of the energy available to a population. That is, they treat organisms as the real physical nonequilibrium systems that they actually are. This in itself is not news to biologists, but to make it to the core of a theory of population dynamics is novel.

Somewhat surprisingly, this change in perspective leads to a radically different mathematical shape of the population dynamical equations. As Ginzburg and Colyvan point out, the mathematical difference between their theory and the classical equations is the same as that which separates Newtonian mechanics from Aristotelian physics. The core of this difference is that like Newtonian equations (and, one may add, real bodies), the Ginzburg equations respect a law of inertia. For physical bodies, this means that they continue in motion unless acted upon by a force. But why should something similar hold for populations? What would be the connection between generations that makes what happens to generation N depend on what happened to generation $N-1$? The answer lies in what are called maternal effects: (energetically) well-endowed and healthy mothers give rise to offspring that are themselves better off than the offspring from less well-endowed mothers. Accordingly, their chances in life will differ from those of their less lucky contemporaries. For this reason, the dynamics of populations depend not only on the amount of food available to a generation but also on the conditions under which the parental generation lived.

Why should all this matter? There are both basic scientific and eminently practical reasons. Among the former is that the new form of population dynamics models leads to different explanations of well-known phenomena that do not yet have a good explanation (such as population cycles of lemmings). The new theory also leads to nontrivial predictions—for example, that intrinsic population cycles cannot have a period of less than six generations. In addition, Ginzburg and Colyvan challenge the widely held opinion that there cannot be laws of nature in biology that have a standing comparable to those in physics. Their explanations of these and other points make the short book an exciting read on many levels.

As the authors emphasize, their theory has important implications for the management of endangered populations or, for that matter, any populations we wish to control (such as those of parasites and pathogens). Clearly, controlling a vehicle with strong inertial tendencies (like a boat) requires a different strategy than controlling something that has no inertia (like the cursor on a computer screen). Ginzburg and Colyvan suggest that some difficulties of environmental management stem from the fact that our current tools ignore the inertial aspects of population dynamics. If they are correct, *Ecological Orbits* ought to become an instant classic, one to be read by every professional and aspiring ecologist and environmental biologist. The danger, though, is that not only physical bodies and possibly populations have inertial tendencies—so do habits of mind.

10.1126/science.1119382

The reviewer is in the Department of Ecology and Evolutionary Biology, Yale University, Post Office Box 208106, New Haven, CT 06405–8106, USA. E-mail: gunter.wagner@yale.edu

View from the Bench: Patents and Material Transfers

John P. Walsh,[1,2]* Charlene Cho,[1] Wesley M. Cohen[3]

Scholars have argued that the growing number of patents on research inputs may now impede upstream, noncommercial research by creating an "anticommons" in which rights holders may impose excessive transaction costs or make the acquisition of licenses and other rights too burdensome to permit the pursuit of scientifically and socially worthwhile research (*1*, *2*). Alternatively, owners of the rights over key upstream discoveries may restrict follow-on research through the exercise of exclusivity (*3*, *4*). The prospect of financial gain from upstream research has raised the further concern that academics are becoming more reluctant to share information, findings, or research materials (*5*, *6*). In 2003, a small-sample interview study suggested that, despite numerous patents on upstream discoveries, academic researchers have accessed knowledge without the anticipated frictions (*7*). Receiving material requested from other researchers could, however, prove problematic (*8*, *9*).

The *Madey* v. *Duke* decision of 2002 raised anew the question of the impact of research tool patents on biomedical research by clarifying that there was no general research exemption shielding academic researchers from infringement liability (*10*). This very visible decision and continuing concerns over the impact of research tool patents on academic science prompted our current study.

We report findings from a survey of 414 biomedical researchers in universities, government, and nonprofit institutions (*11*). In this group of academic, biomedical researchers, 19% currently receive industry funding for their research (representing 4% of their research budget); 22% applied for a patent in the past two years, with an average of 0.19 patent applications per year per respondent; 35% have some business activity [i.e., have participated in negotiations over rights to their inventions, have begun developing a business plan, had a startup, had a process or product in the market, or had licensing income].

LOGISTIC REGRESSION PREDICTING RECEIVING REQUESTED MATERIAL

Variable	Estimate
Scientific competition	–0.058 ± 0.029*
Academic supplier	0.007 ± 0.005
MTA	0.012 ± 0.004**
Patented	0.005 ± 0.007
Patent status unknown	–0.004 ± 0.004
Drug	–2.217 ± 0.683**

Values ± SEM. *$P < 0.05$; **$P < 0.01$.

Although common, patents in this field are not typically used to restrict access to the knowledge that biomedical scientists require. To begin with, few academic bench scientists currently pay much attention to others' patents. Only 5% (18 out of 379) regularly check for patents on knowledge inputs related to their research. Only 2% (i.e., 8) have begun checking for patents in the 2 years since *Madey* v. *Duke*, which suggests little impact of the decision. Five percent had been made aware of intellectual property (IP) relevant to their research through a notification letter sent either to them or their institution, which differs little from the 3% who reported having received such notification 5 years ago (prior to the *Madey* v. *Duke* decision). Furthermore, although 22% of respondents report being notified by their institutions to respect patent rights (versus 15%, 5 years ago), such notification did not appreciably affect the likelihood of checking for patents—5.9% of those receiving such instruction checked for patents versus 4.5% of those not receiving instruction.

Only 32 out of 381 respondents (8%) believed they conducted research in the prior 2 years using information or knowledge covered by someone else's patent. However, even for the few who were aware of others' patents, those third-party patents did not have a large impact on their research. Of the 32 respondents who were aware of relevant IP, four reported changing their research approach and five delayed completion of an experiment by more than 1 month. No one reported abandoning a line of research. Thus, of 381 academic scientists, even including the 10% who claimed to be doing drug development or related downstream work, none were stopped by the existence of third-party patents, and even modifications or delays were rare, each affecting around 1% of our sample. In addition, 22 of the 23 respondents to our question about costs reported that there was no fee for the patented technology, and the 23rd respondent said the fee was in the range of $1 to $100. Thus, for the time being, access to patents on knowledge inputs rarely imposes a significant burden on academic biomedical research.

Our research thus suggests that "law on the books" need not be the same as "law in action" if the law on the books contravenes a community's norms and interests (*9*, *12*). Although the new survey did not explicitly ask respondents their opinions about a research exemption, our results suggest that infringement remains of only slight concern. In contrast, research on clinical diagnostic testing (*13*, *14*) suggests that when the research is itself also a commercial activity, patent holders are more likely to assert and clinical researchers more likely to abandon infringing activities.

In addition to examining access to others' intellectual property, we consider the extent to which scientists can access the tangible research materials and data created by other labs, highlighted as another source of friction that may be impeding biomedical innovation (*5*, *8*, *15*). Indeed, concerns about increasing noncompliance with material transfer requests have prompted the National Institutes of Health to issue guidelines designed to encourage the exchange of materials created with federal funding (*16*).

About 75% of our academic respondents made at least one request for a material in the past 2 years. On average, academics made about seven requests for materials to other academics and two requests to industry labs in the past 2 years. However, 19% of our respondents report that their most recent request for a material was denied (*17*). Moreover, noncompliance with such requests appears to be growing (see supporting online text). Campbell and colleagues (*5*) reported that, among genomics researchers, about 10% of requests were denied in the 3 years, 1997–99. For the

[1]Department of Sociology, University of Illinois at Chicago, Chicago, IL 60607 USA. [2]University of Tokyo, Tokyo, Japan. [3]Duke University, Durham, NC 27708, and the National Bureau of Economic Research, Cambridge, MA 02138, USA. *Author for correspondence. E-mail: jwalsh@uic.edu

genomics researchers in our sample, the denial rate for 2003–04 was 18% (95% confidence interval, ±3.7%).

Over a 1-year period, an average of one in six respondents reported that delays in receiving materials from other academics caused at least one project they were working on to suffer a greater than 1-month delay, a substantial delay in a fast-moving research field. Noncompliance by other academics with research input requests resulted in about 1 in 14 scientists abandoning at least one of their projects each year.

We conducted two regression analyses to probe the reasons for noncompliance (see supporting online text). The first examined whether the respondent's most recent request was satisfied (see table, p. 2002). Statistically significant predictors of noncompliance included a measure of scientific competition (i.e., the number of competing labs) and whether the requested material was itself a drug. The patent status of the requested material had no significant effect on noncompliance. A second analysis with other variables—particularly characteristics of the prospective supplier—examined predictors of the number of times the respondent failed to comply with requests (see table, this page). Here, the burden of compliance (i.e., number of requests per dollar of funding); scientific competition; and commercial orientation (i.e., whether the respondent has engaged in any of the business activities listed above) increase the likelihood of noncompliance. Finally, the number of respondent publications, indicative of respondent eminence or the opportunity cost of responding, also increases the likelihood of noncompliance.

In addition to these regressions, we also asked respondents directly why they denied requests. The major self-reported reasons for noncompliance included the cost and/or effort involved and protecting the ability to publish, with commercial incentives much less prominent (*5*, *18*). We find, however, the multivariate regression analysis to be more credible than the self-reported relationships for the following reasons: (i) it uses a more objective measure of commercial orientation, while controlling for the effects of other variables and (ii) it is less likely to be influenced by a "socially desirable response bias" that leads academics to subordinate less socially desirable incentives (e.g., commerce) compared with more desirable ones (e.g., intellectual challenge) (*19*).

We also considered costs and burdens associated with material transfer agreements (MTAs). Only 42% of requests required an MTA, and only 11% of requests for research inputs led to an MTA negotiation lasting more than 1 month. Moreover, in almost all cases, there was no immediate fee for the requested material. However, for 8% of research input requests, negotiating the MTA stopped the research for more than 1 month. Although MTAs do not commonly entail delays or impose fees, they frequently come with conditions. MTAs, especially from industry suppliers, often include demands for reach-through rights of some form. Of executed MTAs, 29% had reach-through claims, and 16% provided for royalties. Twenty-six percent of MTAs imposed publication restrictions. Requests for drugs were the most likely to yield such a restriction, with 70% of such agreements including some restriction on publication of the research results using the transferred drug.

As a case study, we also collected data from an additional 93 academic scientists who are conducting research on one of three signaling proteins (CTLA-4, EGF, and NF-κB) that are patent-intensive research areas with enormous commercial interest, involving large pharmaceutical firms, small biotechnology firms, and universities. These are the very conditions where issues of access to IP should be evident. Although the incidence of adverse consequences due to restricted access to IP was more manifest here than in the random sample, it was still infrequent (only 3% of respondents reported stopping a project in the past 2 years because of a patent). On the other hand, access to materials was even more problematic in these areas than in the random sample (*18*). For example, 30% of researchers in these fields did not receive their last requested material.

Our results offer little empirical basis for claims that restricted access to IP is currently impeding biomedical research, but there is evidence that access to material research inputs is restricted more often, and individual research projects can suffer as a consequence. To the extent that any redirection of a scientist's research effort or reallocation across investigators because of denied access impedes scientific progress, this is cause for concern. In contrast, if such redirection reduces duplicative research or increases the variety of projects pursued, social welfare may even increase (*20*, *21*). In addition, it is not clear whether patent policy contributes to restricted access to materials, although the commercial activities fostered by patent policy do seem to restrict sharing, as do the burden of producing the materials and scientific competition.

Scientific progress in biomedicine may be well served by a study of the welfare impacts of restrictions on material transfers, and, if warranted, greater diligence in the monitoring and enforcement of the applicable NIH guidelines.

NEGATIVE BINOMIAL REGRESSION PREDICTING NUMBER OF REFUSALS TO SEND REQUESTED MATERIAL

Variable	Estimate
Commercial orientation	0.010 ± 0.004*
Scientific competition	0.078 ± 0.040*
Publications	0.075 ± 0.037*
Request burden	0.038 ± 0.019*
Budget	0.008 ± 0.042
Industry funding	0.006 ± 0.005
Drug discovery	0.000 ± 0.007
Male	–0.008 ± 0.004†

Values ± SEM. *$P < 0.05$; †$P < 0.10$.

References and Notes

1. M. A. Heller, R. S. Eisenberg, *Science* **280**, 698 (1998).
2. C. Shapiro, in *Innovation Policy and the Economy*, A. Jaffe, J. Lerner, S. Stern, Eds. (MIT Press, Cambridge, 2000), pp. 119–150.
3. R. P. Merges, R. R. Nelson, *Columbia Law Rev.* **90**, 839 (1990).
4. S. Scotchmer, *J. Econ. Perspect.* **5**, 29 (1991).
5. E. G. Campbell *et al.*, *JAMA* **287**, 473 (2002).
6. J. P. Walsh, W. Hong, *Nature* **422**, 801 (2003).
7. J. P. Walsh, W. M. Cohen, A. Arora, *Science* **299**, 1021 (2003).
8. R. S. Eisenberg, in *Expanding the Boundaries of Intellectual Property*, R. C. Dreyfuss, D. L. Zimmerman, H. First, Eds. (Oxford Univ. Press, Oxford, 2001), pp. 223–250.
9. R. Merges, *Soc. Philos. Policy Found.* **13**, 145 (1996).
10. R. S. Eisenberg, *Science* **299**, 1018 (2003).
11. This sample represents a 40% response rate. Methodological details are available on *Science* Online.
12. R. C. Ellickson, *Order Without Laws* (Harvard Univ. Press, Cambridge, MA, 1991).
13. J. Merz, A. Kriss, D. Leonard, M. Cho, *Nature* **415**, 577. (2002).
14. M. Cho, S. Illangasekare, M. Weaver, D. Leonard, J. Merz, *J. Mol. Diagn.* **5**, 3 (2003).
15. National Research Council, *Sharing Publication-Related Data and Materials* (National Academies Press, Washington, DC, 2003).
16. Department of Health and Human Services, in *Fed. Regist.*, **64**, 72090 (1999).
17. The supplier estimate of noncompliance is much lower—about half of the consumers' estimate. One can assume that the truth lies in between these two numbers.
18. J. P. Walsh, C. Cho, W. M. Cohen, *Patents, Material Transfers, and Access to Research Inputs in Biomedical Research: Report to the National Academy of Sciences* (2005) (www.uic.edu/~jwalsh/NASReport.html).
19. S. Rynes *et al.*, *Hum. Resource Manag.* **43**, 381 (2004).
20. J. R. Cole, S. Cole, *Science* **178**, 368 (1972).
21. P. Dasgupta, E. Maskin, *Econ. J.* **97**, 581 (1987).

22. The authors acknowledge the financial support and guidance of the Committee on Intellectual Property Rights in Genomic and Protein-Related Inventions of the National Academies' Board on Science, Technology, and Economic Policy and Program on Science, Technology and Law. The committee's final report will be published this fall. We thank E. Campbell, R. Cook-Deegan, R. Kneller, S. Merrill, P. Reid, and three referees for their comments; and M. Jiang for research assistance.

Supporting Online Material

www.sciencemag.org/cgi/content/full/309/5743/2002/DC1

10.1126/science.1115813

PHYSICS

Taking the Hall Effect for a Spin

Junichiro Inoue and Hideo Ohno

In 1879, 18 years before the discovery of the electron and long before the discovery of its spin, Edwin Hall observed an effect that now bears his name; he measured a voltage (the Hall voltage) that arises from the deflected motion of charged carriers (electrons and/or holes—the absence of electrons) in solids under an external electric field E and a magnetic field H (*1*). In the late 20th century, the Hall effect, which by then had become a routine and perhaps unexciting characterization technique, unearthed the unexpected nature of two-dimensional charged carriers in semiconductors. It happened twice, first in the discovery of the quantized Hall effect and then when the fractional Hall effect was found (*2*). Because electrons have spin in addition to charge, one may wonder whether spin plays a role in the Hall effect, whether a "spin" Hall effect exists, and then how to observe it and what are the details of its nature (*3*). Recent research has begun to answer all these questions.

In ferromagnets, the Hall voltage consists of two contributions: the ordinary Hall effect (OHE) that leads to the effects originally discovered as mentioned above, and an "anomalous" part that is proportional not to the external field H but to the magnetization of the ferromagnet. This latter phenomenon is called the anomalous Hall effect (AHE) (*4*). Although the mechanism of the AHE has been a subject of controversy, it was known to originate from the spin polarization of carriers (that is, the imbalance in the population of carriers with different spins). The charge current in ferromagnets is dependent on spin (denoted by σ, which can be either "up" or "down"), and assuming Mott's two-carrier approximation (*5*, *6*), one can define spin-dependent resistivity ρ_σ by means of the expression $J_\sigma = (1/\rho_\sigma)E$ (where J_σ is the current density). The spin dependence of ρ_σ may be caused by spin-dependent electronic states or by spin-dependent scattering attributable to imperfections and phonons in crystals. These effects manifest themselves in the Hall voltage via the spin-orbit interaction that couples spin with the orbital motion of carriers. Historically, these effects were thought to result from an intrinsic effective magnetic field in the momentum space due to the phase called the Berry phase acquired by the moving electron (*7*). Two extrinsic mechanisms, skew-scattering (*8*) and side-jump (*9*), were then proposed. Most of the experiments have been analyzed in terms of the extrinsic mechanisms, but the intrinsic AHE was recently revisited (*10*) to give quantitative explanations of AHE in ferromagnetic semiconductors (*11*).

When scattering is spin-dependent, up and down spin electrons are scattered into opposite directions, resulting in spin-up and spin-down charge Hall currents along the direction perpendicular to E. In ferromagnets, the intrinsic spin imbalance makes the two charge Hall currents asymmetric and produces a Hall voltage proportional to the spin polarization (that is, the magnetization). This is the extrinsic AHE. Here, the Hall voltage produced by movement of charge is accompanied by spin; thus, there also exists, along with the charge accumulation that produces the Hall voltage, spin polarization with opposite polarity at the two ends. This accumulation of spins shows that the spin Hall effect (SHE) exists, but in this case it is extrinsic because it originates from spin-dependent scattering. Spin polarization is usually much more difficult to probe locally with high enough sensitivity. For nonmagnets, although the two charge Hall currents cancel and no Hall voltage develops, spin-dependent scattering still produces the up and down spin currents (flow of spins) that flow in the opposite directions, as long as the spin-orbit interaction is nonvanishing, resulting in spin polarization of opposite signs at the edges even in the absence of applied magnetic fields. Thus, SHE may exist with no accompanying Hall voltage (*12*, *13*).

As in the case of AHE, one can conceive of an intrinsic SHE in nonmagnets on which no external magnetic field is applied. Murakami *et al.* (*14*) have predicted for p-type semiconductors that the effective magnetic field originated from the Berry phase makes up and down spin electrons drift toward opposite directions and leads to SHE. The spin-orbit interaction that exists in any material may also produce the intrinsic SHE even for n-type semiconductors. Sinova *et al.* (*15*) have predicted a constant spin Hall conductivity

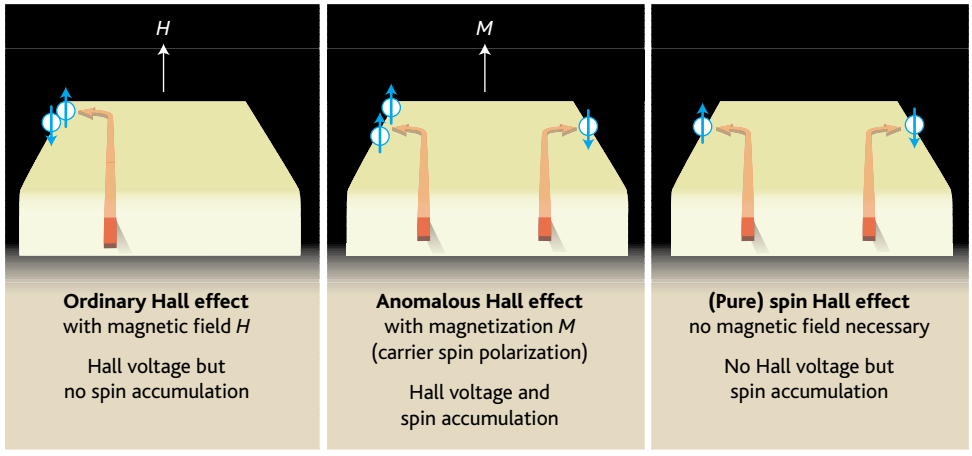

Three Hall effects. **(Left)** The ordinary Hall effect is caused by deflection of carriers moving along an applied electric field (electrons or holes) by an applied magnetic field. Charge accumulation results in a Hall voltage, but there is no net spin accumulation because there are the same number of spin up carriers as spin down ones. **(Middle)** The anomalous Hall effect is the result of spin-dependent deflection of carrier motion, which produces a Hall voltage and spin accumulation at the edges. **(Right)** The pure spin Hall effect is caused by spin-dependent deflection of carriers and produces no Hall voltage when the numbers of deflected spin up and spin down electrons are the same but gives rise to spin accumulation. For simplicity, only the motion of a few carriers is shown in the figure panels.

CREDIT: P. HUEY/*SCIENCE*

J. Inoue is in the Department of Applied Physics, Graduate School of Engineering, Nagoya University, Chikusa-ku, Nagoya 464-8603, Japan. H. Ohno is at the Laboratory for Nanoelectronics and Spintronics, Research Institute of Electrical Communication, Tohoku University, Aoba-ku, Sendai 980-8577, Japan, and the ERATO Semiconductor Spintronics Project, Japan Science and Technology Agency, Kitame-machi 1-18, Aoba-ku, Sendai 980-0023, Japan. E-mail: ohno@riec.tohoku.ac.jp

for two-dimensional electron gas with a Rashba-type spin-orbit interaction produced by the asymmetry of the potential. The intrinsic SHE is a result of the inherent property of the material, as opposed to the extrinsic SHE caused by scattering.

Elucidating the nature of the pure SHE is now an emergent issue for experimentalists as well as theorists. Despite the difficulties associated with the absence of the Hall voltage in the pure SHE, two groups have succeeded in measuring the spin accumulation in nonmagnetic semiconductors by optically detecting the spin accumulation at the sample edge. Kato *et al*. (*16*) spatially resolved the Kerr rotation of the reflected light from n-type bulk GaAs and InGaAs samples and found accumulation of opposite sign at the two edges of the sample. Subsequently, Wunderlich *et al*. (*17*) measured the polarization of light emitted from a p-n junction placed at the edge of a structure. Kato *et al*. suggested that the observed effect may be the extrinsic SHE, as the spin Hall conductivity is low and independent of the crystal orientation, whereas Wunderlich *et al*. concluded that the effect is the intrinsic SHE, because the magnitude of the polarization is consistent with the theoretical prediction. The interpretation of the experimental results is complex, because the current theories predict that the intrinsic SHE is suppressed by disorder effects for two-dimensional electron gas with a Rashba type spin-orbit interaction (*18*), whereas it can remain finite, depending on the type of the spin-orbit interaction (*19*) and the electronic states. The latter prediction may explain the experimental results within the framework of the intrinsic SHE. On the other hand, a recent theory on the extrinsic effect predicts the observed SHE within experimental error with no adjustable parameters (*20*). Nonconservation of spin in the presence of the spin-orbit interaction is also a source of difficulty associated with theoretical analysis.

Very recently, Sih *et al*. have imaged the SHE in a series of two-dimensional electron gases within (110) AlGaAs quantum wells having the crystal orientation in which the Dresselhaus and Rashba spin-orbit interactions are separated (the former out-of-plane, the latter in-plane) (*21*). This information will aid us in establishing the microscopic relation between the spin Hall current and the observed quantities. On the theoretical front, SHE in insulators and its quantized version has been proposed (*22*–*24*); a search for material systems that allow observation of such an effect has been initiated.

The SHE has a practical relevance to the field of spintronics, where spin polarization, manipulation, and detection are essential. Theoretical studies to link SHE with measurable quantities such as spin accumulation and an optical signature are highly desired, because even if spin Hall current itself is intrinsic, the stationary spin accumulation is a result of a balance between spin Hall current and intrinsic/extrinsic effects of the spin relaxation at the edges of the sample. Further systematic experiments that use controllable parameters such as doping or gate voltage certainly will provide us a clear view of SHE. A unified picture of the Hall effect is still being developed 126 years after its discovery.

References and Notes

1. E. H. Hall, *Am. J. Math.* **2**, 287 (1879).
2. Nobel lectures by K. von Klitzing (1985) and by R. B. Laughlin, H. L. Störmer, and D C. Tsui (1998) (http://nobelprize.org/physics).
3. G. E. W. Bauer, *Science* **306**, 1898 (2004).
4. E. H. Hall, *Philos. Mag.* **19**, 301 (1880).
5. N. F. Mott, *Proc. R. Soc. London Ser. A* **153**, 699 (1936).
6. N. F. Mott, *Proc. R. Soc. London Ser. A* **156**, 368 (1936).
7. R. Karplus, J. M. Luttinger, *Phys. Rev.* **95**, 1154 (1954).
8. J. Smit, *Physica* **24**, 39 (1958).
9. L. Berger, *Phys. Rev. B* **2**, 4559 (1970).
10. T. Jungwirth, Q. Niu, A. H. MacDonald, *Phys. Rev. Lett.* **88**, 207208 (2002).
11. H. Ohno, *J. Magn. Magn. Mater.* **200**, 110 (1999).
12. M. I. D'yakonov, V. I. Perel, *Zh. Eksp. Teor. Fiz. Pis. Red.* **13**, 657 (1971).
13. J. Hirsch, *Phys. Rev. Lett.* **83**, 1834 (1999).
14. S. Murakami, N. Nagaosa, S.-C. Zhang, *Science* **301**, 1348 (2003); published online 7 August 2003 (10.1126/science.1087128).
15. J. Sinova *et al*., *Phys. Rev. Lett.* **92**, 126603 (2004).
16. Y. K. Kato, R. C. Myers, A. C. Gossard, D. D. Awschalom, *Science* **306**, 1910 (2004); published online 11 November 2004 (10.1126/science.1105514).
17. J. Wunderlich, B. Kaestner, J. Sinova, T. Jungwirth, *Phys. Rev. Lett.* **94**, 047204 (2005).
18. J. Inoue, G. E. W. Bauer, L. W. Molenkamp, *Phys. Rev. B* **70**, 041303 (2004).
19. B. A. Bernevig, S.-C. Zhang, *Phys. Rev. Lett.* **95**, 16801 (2005).
20. H.-A. Engel, B. I. Halperin, E. I. Rashba, http://arxiv.org/abs/cond-mat/0505535 (2005).
21. V. Sih *et al*., http://arxiv.org/abs/cond-mat/0506704 (2005).
22. S. Murakami, N. Nagaosa, S.-C. Zhang, *Phys. Rev. Lett.* **93**, 156804 (2004).
23. C. L. Kane, E. J. Mele, http://arxiv.org/abs/cond-mat/0411737 (2004).
24. B. A. Bernevig, S.-C Zhang, http://arxiv.org/abs/cond-mat/0504147 (2005).

10.1126/science.1113956

ECOLOGY

Making Sense of Evolution in an Uncertain World

Vincent A. A. Jansen and Michael P. H. Stumpf

Many organisms have adapted to a life with uncertainties. For instance, some pathogenic bacteria have genes that can be switched off to stop disease progression in a host organism or prevent their recognition by an immune system. Such strategies increase an organism's reproductive success and tend to be found in environments in which the conditions are strongly fluctuating. To understand the development of such strategies, evolutionary biologists determine the long-run reproductive success of organisms in fluctuating environments by calculating the Lyapunov exponent, a measure of the average exponential growth rate in an unpredictable environment. Often these calculations are ferociously difficult and rarely lead to simple results. On page 2075 of this issue, Kussell and Leibler (*1*) describe a new method to approximate the long-term reproductive success in fluctuating environments and reveal remarkable insights into evolution in an uncertain world.

Consider again bacteria, which have developed strategies to cope with a sea of potential troubles in their rapidly changing environments, such as the variable natures of their hosts or the changing number of available hosts. Many pathogenic bacteria have evolved phase variation, a process that turns the expression of certain genes on and off (*2*, *3*). This "switch" works through genetic reorganization, mutation, or modification of the regions in the bacterial genome that control gene expression. These genetic changes are heritable, reversible, and stochastic. The effect is that a single bacterium within a population switches independently of others, and the progeny of a bacterial population is phenotypically diverse. This phenotypic diversity serves as a buffer against fluctuations in the environment and allows the population to adapt to unpredictably changing environments.

This strategy of randomization of phenotype is known to ecologists as bet-hedging (*4*). Bet-hedging does more than just produce variation that reduces the chances of population extinction: In a fluctuating environment, bet-hedging evolves and bet-hedgers will in the long run replace equally diverse populations whose members have offspring that are all the same. Even if this

V. A. A. Jansen is at the School of Biological Sciences, Royal Holloway–University of London, Egham, Surrey TW20 0EX, UK. M. P. H. Stumpf is at the Centre for Bioinformatics, Division of Molecular Biosciences, Imperial College London, London SW7 2AZ, UK. E-mail: vincent.jansen@rhul.ac.uk

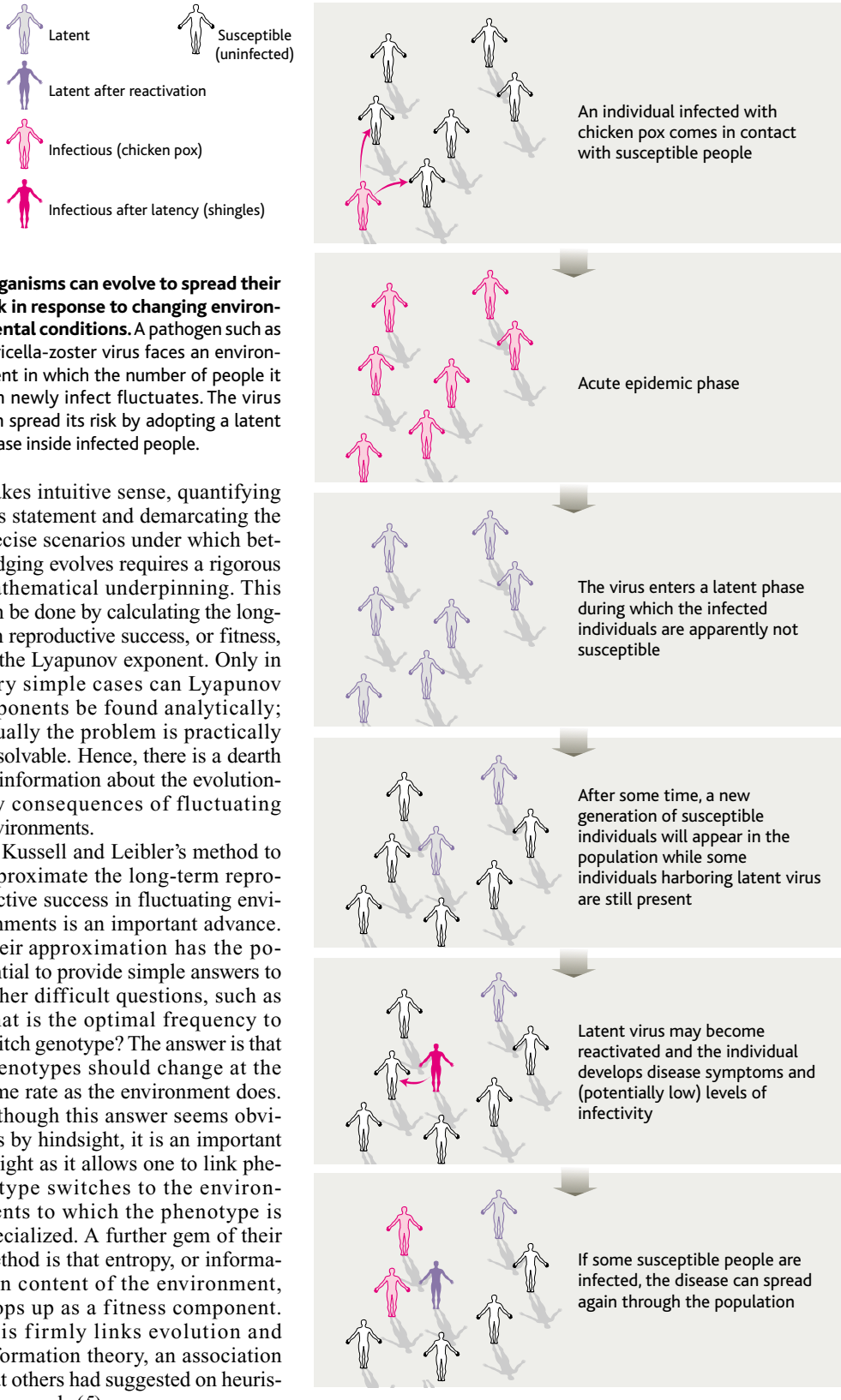

Organisms can evolve to spread their risk in response to changing environmental conditions. A pathogen such as varicella-zoster virus faces an environment in which the number of people it can newly infect fluctuates. The virus can spread its risk by adopting a latent phase inside infected people.

makes intuitive sense, quantifying this statement and demarcating the precise scenarios under which bet-hedging evolves requires a rigorous mathematical underpinning. This can be done by calculating the long-run reproductive success, or fitness, as the Lyapunov exponent. Only in very simple cases can Lyapunov exponents be found analytically; usually the problem is practically unsolvable. Hence, there is a dearth of information about the evolutionary consequences of fluctuating environments.

Kussell and Leibler's method to approximate the long-term reproductive success in fluctuating environments is an important advance. Their approximation has the potential to provide simple answers to rather difficult questions, such as what is the optimal frequency to switch genotype? The answer is that phenotypes should change at the same rate as the environment does. Although this answer seems obvious by hindsight, it is an important insight as it allows one to link phenotype switches to the environments to which the phenotype is specialized. A further gem of their method is that entropy, or information content of the environment, crops up as a fitness component. This firmly links evolution and information theory, an association that others had suggested on heuristic grounds (*5*).

The main question addressed by Kussell and Leibler is whether it is evolutionarily favorable for an organism to monitor the environment to optimize its response. The authors do this by contrasting two different ways of producing variable offspring: either by chance and irrespective of the environmental conditions (stochastic phenotype switching) or by giving rise to offspring with a suitable phenotype after sensing a change in the environment (responsive switching). Which of the two strategies has the highest reproductive success? The real surprise of this paper is that in many cases stochastic switching will be selected over sensing and response. Because the environment has to be monitored, continuous responsive sensing is costly as it requires energy expenditure and the maintenance of suitable molecular machinery, particularly if environmental changes occur infrequently. Stochastic switching also carries a cost, in that it produces individuals that are maladapted to their environment, but this turns into an advantage if the environment changes and these individuals become a standing army from which the most suitable recruits are selected to deal with the new conditions. If this cost is smaller than the cost of continuously sensing the environment, the stochastic switching strategy is selected over responsive switching.

This carries the implication that simple stochastic mechanisms of phase variation abound, not because organisms are constrained in the development of a sensing mechanism, but because this simple stochastic switching mechanism is selectively superior. These insights have some intriguing consequences for the study of the mechanisms of pathogenicity. For instance, the varicella-zoster virus causes chicken pox as a primary infection (see the figure). However, the virus can switch off the expression of many of its genes and "go into hiding" in neuronal cells. After many years, it can reemerge in the form of shingles. Contact with a person with shingles can lead to chicken pox in someone who has never had chicken pox and has not received the varicella vaccine. It is not known why the virus reactivates, and much effort has been devoted to unraveling the reactivation mechanism (*6*). It has been postulated that the latency of varicella-zoster virus is a bet-hedging mechanism in response to the fluctuating number of susceptible individuals in the local population (*7*). Kussell and Leibler's result illustrates why there might not be a refined trigger mechanism: For a virus in a latent state, it must be costly, if not impossible, to continually monitor or sense the number of susceptible individuals surrounding the carrier. If so, a simple stochastic switch is much

CREDIT: P. HUEY/*SCIENCE*

more effective than a sophisticated sensing mechanism.

The ability to analyze long-term outcomes of evolutionary processes in stochastically fluctuating environments is of fundamental importance for understanding evolutionary biology and can, in particular, contribute important insights into the biology of pathogens. As it turns out, randomly creating phenotypic diversity—or not putting all your eggs into one basket—may be all that is necessary, and the work by Kussell and Leibler allows us to assess when this is the case.

References and Notes

1. E. Kussell, S. Leibler, *Science* **309**, 2075 (2005); published online 25 August 2005 (10.1126/science.1114383).
2. E. R. Moxon, P. B. Rainey, M. A. Nowak, R. E. Lenski, *Curr. Biol.* **4**, 24 (1994).
3. D. Metzgar, C. Wills, *Cell* **101**, 581 (2000).
4. J. Seger, H. J. Brockman, in *Oxford Surveys in Evolutionary Biology*, P. H. Harvey, L. Partridge, Eds. (Oxford Univ. Press, Oxford, 1987), vol. 4, pp. 182–211.
5. J. Avery, *Information Theory and Evolution* (World Scientific, Singapore, 2003).
6. R. T. Johnson, *Viral Infections of the Nervous System* (Lippincott, Philadelphia, 1998).
7. M. P. H. Stumpf, Z. Laidlaw, V. A. A. Jansen, *Proc. Natl. Acad. Sci. U.S.A.* **99**, 15234 (2002).

8. Supported by a Welcome Trust Research Fellowship (M.P.H.S.).

10.1126/science.1118711

EVOLUTION

Pushing the Time Barrier in the Quest for Language Roots

Russell Gray

Questions about human origins have an enduring fascination. For centuries, scholars and laypeople have wondered where groups such as Polynesians or Indo-Europeans came from. Linguistic evidence plays a vital role in tracking the movement of people by leaving linguistic trails that are analogous to the genetic signatures that molecular biologists study. Early European explorers in the Pacific, for example, were struck by the remarkable similarities between the far-flung languages of the Pacific (the word for hand in Hawaiian and Samoan is *lima*, in Marquesan it is *'ima*, and in Tahitian *rima*). It might seem a simple matter, therefore, to trace the origin of words used in linguistic and cultural groups and thereby unravel connections between the peoples of the world that extend deep in the past. Perhaps it might even be possible to infer the initial "mother tongue" spoken before our languages diverged. Alas, the task for historical linguists and prehistorians is not this easy. First, superficial similarities in vocabulary must be separated from genuine similarities due to descent. Linguists call these genuine homologies "cognates." The diagnosis of cognates is a challenging task that requires detailed specialist knowledge to detect systematic sound correspondences. Then an even more difficult problem is encountered: The rate of vocabulary evolution is so rapid that it erases distant or "deep" historical connections.

Consider the following thought experiment: Imagine that two languages each diverge in their basic vocabulary from a common ancestor at roughly 20% every thousand years (this is a rough but not entirely arbitrary figure). After 1000 years, 64% of the languages' basic vocabulary would be cognate; after 2000 years, 41%; and after 10,000 years, just over 1%. The problem of rapid lexical decay is exacerbated by chance similarities and recent borrowings that obscure this weak historical link or "signal" (for example, the Maori and Modern Greek words for eye, *mata* and *mati*, superficially appear similar, but no one seriously postulates that this reflects some deep historical link). Instead, most linguists believe that after about 8000 to 10,000 years it is impossible to differentiate between homology and chance resemblances or borrowings. They are therefore highly skeptical of arguments for ancient language relationships, especially when cognacy judgments are made with less than the normal standard of rigor. One highly controversial example is Ruhlen's claim (*1*) that words ostensibly related to a Proto-Amerind term **t'ana* (child, sibling) provide evidence for a putative 12,000-year-old Amerind language family. As Campbell (*2*) has pointed out, the semantic variation that Ruhlen allowed (meanings including small, woman, cousin, son-in-law, old man, friend, and some 15 other terms), coupled with relatively loose phonetic matches (Ruhlen treats *tsuh-ki* and *u-tse-kwa* as related to **t'ana*), make chance resemblance highly likely.

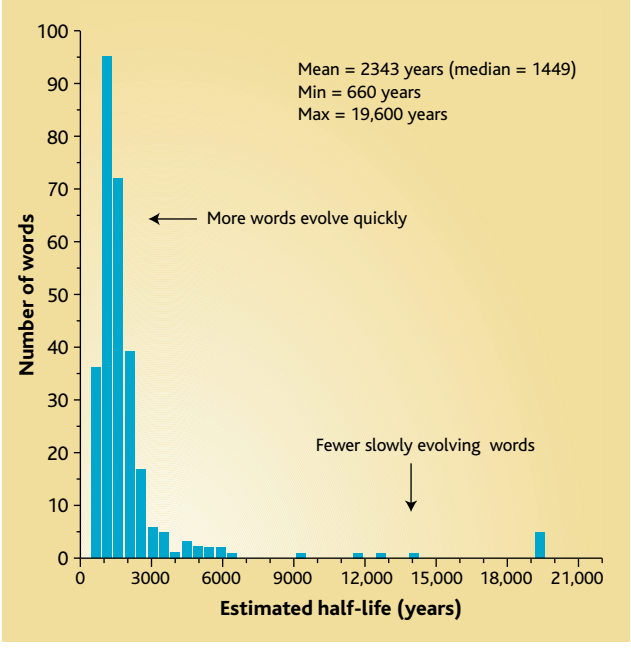

The rate of vocabulary change. A word's half-life is the amount of time required for there to be a 50% chance that it will be replaced by a new word. Most words have a half-life of 2000 years. However, a small number of words have a half-life greater than 10,000 years. This shows that despite the fast average pace of language evolution, some meanings, like highly conserved genes, evolve at a slow rate [adapted from (*3*)]. The *y* axis is the number out of a sample of 200 meanings.

Recent work by Pagel (*3*) suggests that the prospects for discovering deep links between languages may not be quite so bleak. The calculations above assumed that all words change at the same rate. This is not realistic. Pagel adapted stochastic models of genetic evolution to the problem of lexical change. He showed that a distribution of word rates is a much better fit to the data than a single rate. This distribution has a long tail, implying that in principle there are some very slowly evolving words that remain cognate even after 20,000 years (see the figure). It is these very stable words that proponents of long-distance language relationships have focused on. However, the practical task of convincingly separating deep homologies from chance corre-

The author is in the Department of Psychology, University of Auckland, Auckland 92019, New Zealand. E-mail: rd.gray@auckland.ac.nz

spondences and borrowings still remains.

If words hit a time barrier when it comes to detecting linguistic links, must the deep links between languages and cultures remain forever obscured? Linguists such as Nichols (*4*) have argued that language structure holds the key to unlocking our past. By examining structural features such as the position of verbs in clauses and the presence or absence of inclusive/exclusive pronominal contrasts, Nichols claims to recognize linguistic areas and connections that are beyond the reach of the traditional comparative method with its focus on vocabulary. Although this approach appears promising, not all linguists are convinced that the structural features used by Nichols are any more stable than words. Campbell (*5*), for example, cites cases of recently diverged dialects that differ in features that are allegedly stable for periods of more than 10,000 years.

On page 2072 of this issue, Dunn *et al*. (*6*) tackle this debate in a systematic and rigorous manner, using methods derived from evolutionary biology. As Darwin noted (*7*), languages evolve in remarkably similar ways to biological species. They split into new languages, mutate, and sometimes go extinct. There are numerous historical connections between biology and historical linguistics, with linguistics often leading the way in the development of new ideas and methods (*8*). However, despite these connections, linguists have not commonly used the phylogenetic methods that have revolutionized evolutionary biology in the past 20 years [for recent exceptions, see (*9*–*11*)]. To address the problem of detecting deep signal, Dunn *et al*. borrowed two tools from their biological colleagues. First, they constructed a database of 125 structural features for 16 Austronesian and 15 Papuan languages. This enables them to avoid the charge that they merely selected a few features that happened to fit their hypotheses. The number of possible family trees of descent for even quite small numbers of languages is vast. Dunn *et al*.'s second methodological borrowing from biology was the use of a computer program to find the set of optimal trees for the Austronesian and Papuan data sets. To test whether the structural features contain a historical signal, Dunn *et al*. compared the Austronesian structure tree with the traditional classification of these languages. The resulting Austronesian structure tree matched the traditional classification quite well, which suggests that the structural features contained some historical link or signal for at least the 4000-year time depth that the Austronesian of languages studied by Dunn *et al*. are thought to have.

What about time depths beyond the reach of traditional methods? Evolutionary trees show nested patterns of descent, with the most recent divergences toward the branch tips and the most ancient at the tree base or root. The Papuan tree of Dunn *et al.* shows some geographic clustering at its tips. The signal toward the base of the tree is very weak, suggesting that few structural features support these historical links. However, the signal that is present is consistent with a scenario involving a time depth greater than 10,000 years. Dunn *et al*. are careful to emphasize that the signal is weak and discuss alternative hypotheses. Although it does not conclusively demonstrate deep historical signals in structural features, the Dunn *et al*. paper sets new standards for the systematic collection and analysis of structural features. Its approach is likely to be widely emulated by researchers working on languages in other regions. In the future we may see the development of Web-based databases for the languages of the world similar to the GenBank repository for DNA sequences. The task of making accurate inferences about our past is a demanding one that requires the integration and triangulation of inferences from genetic, linguistic, and archaeological data (*12*). The Dunn *et al*. approach is an important step forward in this interdisciplinary endeavor.

References

1. M. Ruhlen, *The Origin of Language: Tracing the Origin of the Mother Tongue* (Wiley, New York, 1994).
2. L. Campbell, in *The Handbook of Historical Linguistics*, B. D. Joseph, R. D. Janda, Eds. (Blackwell, Malden, MA, 2003), pp. 262–282.
3. M. Pagel, in *Time Depth in Historical Linguistics*, C. Renfrew, A. McMahon, L. Trask, Eds. (McDonald Institute for Archaeological Research, Cambridge, 2000), pp. 189–207.
4. J. Nichols, *Linguistic Diversity in Space and Time* (Univ. of Chicago Press, Chicago, 1992).
5. L. Campbell, in *Historical Linguistics 2001*, B. Blake, K. Burridge, Eds. (Benjamins, Amsterdam, 2003), pp. 33–58.
6. M. Dunn *et al*., *Science* **309**, 2072 (2005).
7. C. Darwin, *The Descent of Man* (Murray, London, 1871).
8. Q. Atkinson, R. D. Gray, *Syst. Biol*. **54**, 513 (2005).
9. D. Ringe, T. Warnow, A. Taylor, *Trans. Philol. Soc*. **100**, 59 (2002).
10. R. D. Gray, Q. Atkinson, *Nature* **426**, 435 (2003).
11. A. McMahon, R. McMahon, *Trans. Philol. Soc*. **101**, 7 (2003).
12. P. V. Kirch, R. C. Green, *Hawaiki, Ancestral Polynesia: An Essay in Historical Anthropology* (Cambridge Univ. Press, Cambridge, 2001).

10.1126/science.1119276

CHEMISTRY

Better Living Through Nanopore Chemistry

Joseph T. Hupp and Kenneth R. Poeppelmeier

Tiny holes have huge significance—at least if you're in the business of cracking millions of barrels of crude oil into useful smaller chemical components, converting methanol into gasoline, or transforming toluene into precursors for polymers. Zeolites, the remarkable materials that catalyze these conversions, contain enormous numbers of cavities of roughly nanometer size (*1*). The cavities are uniform in size and shape and are interconnected to form extended channels or pores. The cavities and the portals between them are just the right size to imbibe oil's molecular components and process them into more useful and valuable petrochemicals.

Enhanced online at www.sciencemag.org/cgi/content/full/309/5743/2008

Zeolites are mostly made from the elements of Earth's crust: silicon, aluminum, and oxygen. This makes for strong materials—in essence nanoporous rocks. But this chemical composition constrains the possible applications of these materials. For example, an important problem in chemical catalysis, especially in the area of pharmaceuticals, is the transformation of an achiral reactant selectively into just one of two possible mirror-image products ("enantioselective" catalysis). Yet purely zeolitic schemes for enantioselective catalysis are rarely, if ever, encountered.

What if the most promiscuous of elements—carbon—could be recruited for assembling zeolite-like materials? The versatility and variety of carbon chemistry—the chemistry of life—could, in principle, expand tremendously the range of compositions, architectures, and functional behavior of permanently porous crystalline materials. On page 2040 in this issue, Férey and co-workers report the latest in a series of advances in this area (*2*). The new material, called MIL-101 (where MIL stands for Matériaux de l'Institut Lavoisier), has some remarkable physical attributes. The unit cell volume is ~700,000 cubic angstroms, about 90% of it empty space once volatile solvent

The authors are in the Department of Chemistry, Northwestern University, 2145 Sheridan Road, Evanston, IL 60208, USA. E-mail: j-hupp@northwestern.edu, krp@northwestern.edu

molecules are removed. The estimated internal surface area is ~6000 m^2/g. A tablespoon of MIL-101 has the surface area of a half-dozen football fields, or about seven times the area of the most catalytically effective zeolites.

As elegant as the new material is, the more important questions are "how did they do it?" and "what makes it so difficult?" The notion of enlisting organic chemistry to make new stable and highly ordered porous materials is the focus of scores of research groups around the world. A common approach is to retain some of the inorganic character of zeolites (although not necessarily with the same elements) and build hybrid organic/inorganic materials. The approach works well, at least if the cavities and pores are small. Unfortunately, as the targeted cavities get larger (diameters beyond a nanometer or so), success becomes increasingly rare. Instead, the pores collapse, duplicate frameworks interpenetrate and fill the pores, or, most exasperating of all, some version of the desired porous material is indeed obtained, but the detailed structure is so complex that it cannot be determined from conventional measurements.

To work around these problems, Férey and coworkers make use of three ideas. First, the chances of success increase if discrete multi-atom building units can be designed and generated in the solution phase (see the figures). Powerful examples, most notably from the work of Yaghi *et al*., are framework vertices comprising metal-oxo clusters (*3*). They present the right number of organic ligand attachment sites, in the right orientation, to yield networks defining porous hybrid structures.

Second, if small pores can be obtained, then scaling up the size of the building units may produce large pores. For example, in place of single metal ions or small clusters, the key building unit for MIL-101 is a supercluster consisting of four smaller clusters (stabilized Cr_3O units) linked by difunctional organic components to make a large tetrahedron. Besides increasing the scale, the supercluster presents a larger number of organic ligand attachment points (chelating sites) than does either a small cluster or a single metal ion. Furthermore, the sites are oriented differently on the supercluster surface than on smaller clusters, implying that different framework structures can ultimately be expected.

The third idea has to do with determining the structure of the new hybrid material. Usually this is done by transforming structural data that have been generated in inverse space by diffraction of x-rays by single crystals. However, as unit cells get larger, the chances of growing highly diffracting single crystals get smaller, a problem well known in determining protein structures. Valuable information about structure, again in inverse space, can be obtained from powder x-ray measurements (diffraction by many randomly oriented microcrystals). Owing to the reduced information content of the powder measurement, determining the structure in real space is a demanding problem unless one already has guessed a reasonable model structure as an analysis starting point. This is not so difficult if the possibilities are few. But for complex materials like MIL-101 the number of possibilities is staggering. Férey *et al.* (*2*) reduce the possibilities by using a computational assembly algorithm to find as many candidate structures as possible. They then rank the structures according to energetic stability, again computationally. Finally, they examine the handful of low-energy structures, calculate powder patterns, and look for a match to the experimental pattern. The ranking strategy works because the "solvothermal" conditions used in the synthesis generally produce thermodynamic rather than kinetic structures.

Are hybrid materials with even larger pores and more complex structures on the horizon? Probably, but the more important goal may be to incorporate useful function. Férey *et al*. allude to this, describing briefly the compartmentalized uptake of redox-active guests and the use of MIL-101 as a mold for fabricating nanostructured semiconductors. If unusual optical, magnetic, and electronic behavior can be introduced, interesting applications in chemical sensing and energy conversion will follow. Important for seeing such behavior is the introduction of new kinds of building units—ones where function is on an equal footing with structure. One interesting example is Halper and Cohen's use of large chromophoric coordination complexes as building units, although permanent porosity for the resulting materials has yet to be reported (*4*).

Finally, what about zeolite-like catalysis? Hybrid materials lack the thermal stability to replace inorganic ones in these high-temperature processes. More important will be higher value transformations under milder conditions. Particularly exciting is a new report by Lin and co-workers of enantioselective catalysis (*5*) that tackles just this challenge.

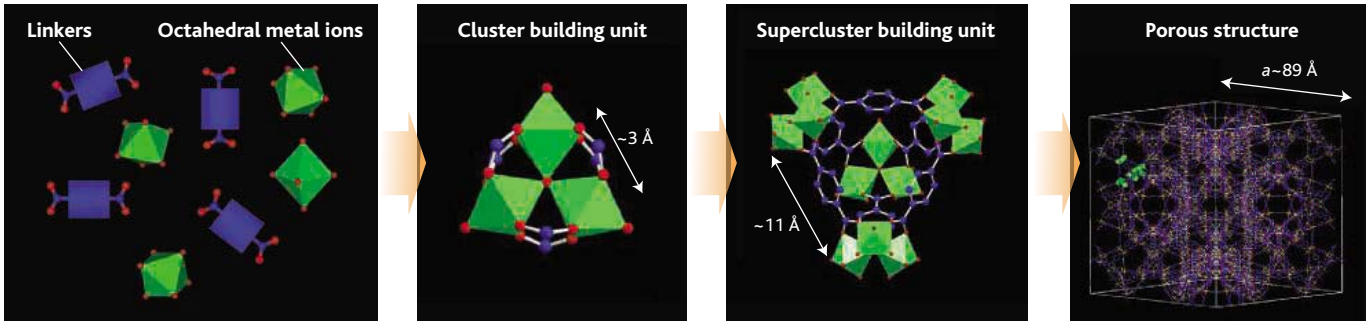

Big results from small holes. Starting from simple assemblies and linking units, larger and larger building blocks combine to form crystalline nanoporous materials with more surface area than zeolites.

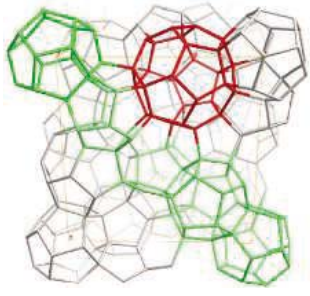

Cagey structures. Zeotype architecture of MIL-101 showing mesoporous cages with diameters of 29 Å (green) and 34 Å (red), featuring 12 Å pentagonal and 15 Å hexagonal openings [adapted from (*2*)].

References

1. P. B. Weisz, *Chemtech*, **3**, 498 (1973).
2. G. Férey *et al*., *Science* **309**, 2040 (2005).
3. O. A. Yaghi *et al*., *Nature* **423**, 705 (2003).
4. S. R. Halper, S. M. Cohen, *Inorg. Chem.* **44**, 486 (2005).
5. C. D. Wu, A. Hu, L. Zhang, W. Lin, *J. Am. Chem. Soc.* **127**, 8940 (2005).

10.1126/science.1117808

Noise in Gene Expression: Origins, Consequences, and Control

Jonathan M. Raser[1,2] and Erin K. O'Shea[2*†]

Genetically identical cells and organisms exhibit remarkable diversity even when they have identical histories of environmental exposure. Noise, or variation, in the process of gene expression may contribute to this phenotypic variability. Recent studies suggest that this noise has multiple sources, including the stochastic or inherently random nature of the biochemical reactions of gene expression. In this review, we summarize noise terminology and comment on recent investigations into the sources, consequences, and control of noise in gene expression.

Any individual in a population of living organisms or cells is unique. Much of population variability is due to genetic differences, but environment and history also contribute to variability in cellular phenotype. Indeed, identical twin humans or cloned cats differ in appearance and behavior (Fig. 1). However, even cells or organisms with the same genes, in the same environment, with the same history, display variations in form and behavior that can be subtle or dramatic. Investigations have focused on the possibility that such variability is inevitable in biological systems because of the random nature of chemical reactions within a cell (*1*). When large numbers of molecules are present, chemical reactions may proceed in a predictable manner. However, when only a few molecules of a specific type exist in a cell, stochastic effects can become prominent.

Gene expression, as defined by the set of reactions that control the abundance of gene products, influences most aspects of cellular behavior, and its variation is often invoked to explain phenotypic differences in a population of cells. Because DNA, RNA, and proteins can be present and active at a few copies per cell, the abundance of gene products is theoretically sensitive to stochastic fluctuations. Four potential sources of variation in gene expression must be considered: (i) as described above, the inherent stochasticity of biochemical processes that are dependent on infrequent molecular events involving small numbers of molecules; (ii) variation in gene expression owing to differences in the internal states of a population of cells, either from predictable processes such as cell cycle progression or from a random process such as partitioning of mitochondria during cell division; (iii) subtle environmental differences, such as morphogen gradients in multicellular development; and (iv) ongoing genetic mutation, either random or directed. We use the term "noise" in gene expression to refer to the measured level of variation in gene expression among cells, regardless of source, within a supposedly identical population.

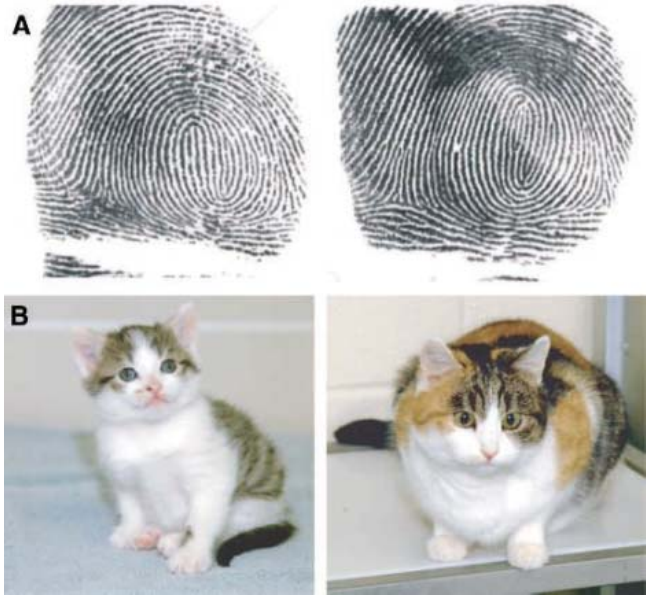

Fig. 1. Examples of possible stochastic influences on phenotype. (**A**) The fingerprints of identical twins are readily distinguished on close examination. Reprinted from (*37*) with permission from Elsevier. (**B**) Cc, the first cloned cat (left) and Rainbow, Cc's genetic mother (right), display different coat patterns and personalities (*38*). Photo credit, College of Veterinary Medicine and Biomedical Sciences, Texas A&M University.

Measurement Techniques and Definitions

Recent investigations have employed green fluorescent protein (GFP) variants, which allow the quantification of protein levels in living cells by flow cytometry or fluorescence microscopy. The coefficient of variation, or noise η, is defined as the ratio of the standard deviation to the mean of the population. Other metrics of variability can be useful as well (SOM Text).

Once genetic mutation and local microenvironments are eliminated as sources of noise, an elegant experimental method can assist in differentiating among the remaining sources (*2*). This method involves quantifying expression of two equivalent, independent gene reporters placed in the same cell, which then allows noise sources to be partitioned into two categories: intrinsic, meaning noise sources that create differences between the two reporters within the same cell (Fig. 2A), and extrinsic, referring to sources that affect the two reporters equally in any given cell but create differences between two cells (Fig. 2B). Stochastic events during the process of gene expression, from the level of promoter-binding to mRNA translation to protein degradation, will manifest as intrinsic noise. Differences between cells, either in local environment or in the concentration or activity of any factor that affects gene expression, will result in extrinsic noise. Extrinsic noise should be further subdivided into two categories (*3*, *4*): global noise, or fluctuations in the rates of the basic reactions that affect expression of all genes (Fig. 2C), and gene- or pathway-specific extrinsic noise (Fig. 2D), such as fluctuations in the abundance of a particular transcription factor or stochastic events in a specific signal transduction pathway. If a factor that causes extrinsic noise is experimentally manipulable, it is possible to eliminate such extrinsic noise by reduction of variability in that factor; for example, cell cycle synchronization will reduce extrinsic

[1]Medical Scientist Training Program, [2]Howard Hughes Medical Institute, University of California–San Francisco, 600 16th Street, GH-S472D, San Francisco, CA 94143–2240, USA.

*Present address: Howard Hughes Medical Institute, Harvard University, 7 Divinity Avenue, Bauer 307, Cambridge, MA 02138, USA.
†To whom correspondence should be addressed. E-mail: erin_oshea@harvard.edu

noise due to differences in cell cycle stage in a population (Fig. 2E).

Experimental Investigation of Noise Sources

The division of noise into "extrinsic" and "intrinsic" categories has proven practical experimentally. Elowitz *et al*. pioneered the two-reporter method in studies of noise in gene expression in *Escherichia coli*, which quantified levels of cyan and yellow fluorescent proteins expressed from identical promoters on the same prokaryotic chromosome (*5*). These studies demonstrated that the stochastic nature of gene expression gives rise to noise in protein levels in a clonal population of *E. coli* and that the relative contributions of extrinsic and intrinsic components to the total noise vary with expression level. Ozbudak *et al*. also quantified noise in gene expression in the prokaryote *Bacillus subtilis* (*6*). By comparing the noise observed in reporters with altered efficiency of transcription and translation, they concluded that prokaryotic transcription is the dominant source of noise in protein levels, as predicted by basic models of stochastic gene expression (*7*–*10*).

We employed the two-reporter system to measure gene expression noise in cells of the diploid eukaryote *Saccharomyces cerevisiae* (*3*). These studies revealed that intrinsic noise in reporter protein levels is detectable and, for one gene, results from slow interconversion between inactive and active promoter states due to stochastic chromatin-remodeling events. However, extrinsic noise is the predominant form of noise for all gene promoters measured in these experiments. Simultaneous measurement of two independent, unrelated gene promoters indicated that much of this extrinsic noise is global in nature, presumably due to fluctuations in some factor that affects expression of all genes and not due to fluctuations in extrinsic factors that affect a particular gene. Blake *et al*. quantified noise in *S. cerevisiae* using a single-reporter method (*11*). Their results for the *GAL1* gene are consistent with the extrinsic noise profile of *GAL1* measured by the two-reporter method, which suggests that this noise is not the result of stochastic chromatin remodeling or transcription. Rather, most of the single-reporter noise is likely due to extrinsic factors such as global noise or noise in *GAL* signaling.

Recent measurements of gene expression in single *E. coli* cells over long time periods have provided insights into the relative amplitude and time scales of intrinsic and extrinsic noise (*12*). Extrinsic noise is the primary source of variability in gene expression, similar to the observation in budding yeast. The authors calculated autocorrelation times for noise, or the time scale over which the protein production rate fluctuates in any given cell (Fig. 2, F to H). The autocorrelation time for intrinsic noise is ≤10 min, consistent with the hypothesis that rapid fluctuations in mRNA numbers are the source of intrinsic noise. The autocorrelation time for global noise factors in protein production rate is ~40 min, similar to the observed cell cycle length, which suggests that whatever factors result in global noise persist on average for about one cell cycle.

In *Drosophila melanogaster*, Ahmad and Henikoff studied the behavior of a GFP reporter subject to position-effect variegation (*13*). The reporter gene displays an expression pattern suggestive of repeated rounds of stochastic activation and inactivation of gene expression, resulting in patches of cells expressing the reporter. Fluctuations in the chromatin state of the reporter gene uncover transcription-factor binding sites, and recruitment of chromatin-modulating activities after transcription-factor binding slows the rate of heterochromatin reformation. In another eukaryotic system, each allele of the gene encoding the cytokine IL-4 is expressed in a probabilistic manner in response to signaling through the T cell receptor (TCR) in mouse T helper 2 lymphocytes (*14*, *15*). The probability of expression for each allele is independent of its parental origin and increased with the strength of TCR stimulation, leading to biallelic expression at higher levels of stimulation. Furthermore, the pattern of allelic expression is different over multiple rounds of activation for some clonal populations, which suggests that the stochastic gene activation observed is a reversible process.

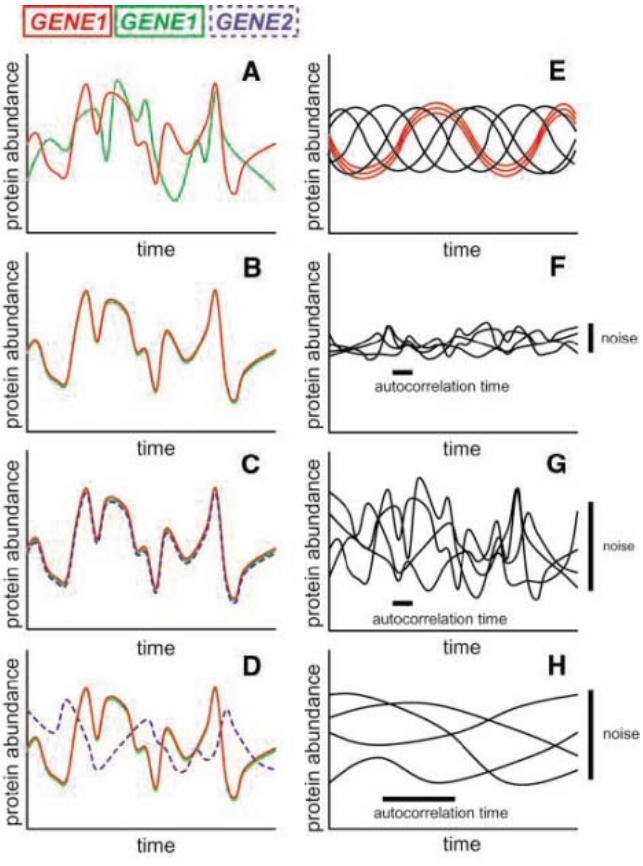

Fig. 2. Noise definitions and characteristics. (**A**) Intrinsic noise results in differences between two reporters of the same gene in a single cell. (**B**) Extrinsic noise affects two reporters of the same gene equally in a single cell but causes differences from cell to cell or in a single cell over time. (**C**) Global noise affects two distinct genes equally but results in differences from cell to cell or in a single cell over time. (**D**) Gene- or pathway-specific extrinsic noise affects two reporters of the same gene equally but causes differences from a reporter of a second distinct gene in a single cell. (**E** to **H**) Noise in a population; each line represents a different cell. (E) Manipulable extrinsic noise: In a synchronized population of cells, cell cycle progression results in predictable changes in protein abundance over time (red lines); when the cells grow asynchronously, the population displays variability (black lines). (F) Noise of low magnitude and short autocorrelation time. (G) Noise of high magnitude and short autocorrelation time. (H) Noise of high magnitude and long autocorrelation time.

Other mammalian genes may show similar patterns of both monoallelic and biallelic ongoing stochastic expression. In a survey of allelic imbalances in gene expression in heterozygous human cells, 18% of the more than 120 genes assayed displayed consistent biases in expression patterns toward one allele (*16*). Such imbalanced expression may be due to slow, reversible stochastic fluctuations in gene expression, or it may be due to stochastic events in processes other than gene expression, nonrandom epigenetic factors, or polymorphism in regulatory sequences.

Consequences of Noise in Gene Expression

Both the magnitude and the frequency of the noise affect the consequence. Small changes in protein abundance may have dramatic effects on fitness if they persist long enough, whereas large fluctuations in abundance may not have any effect if they occur too frequently to affect a cellular process (*12*). The observation that the time scale for intrinsic noise fluctuations is much shorter than that for extrinsic noise suggests that extrinsic noise may affect cellular phenotypes more strongly than intrinsic noise, at least in *E. coli* (*12*).

Small differences in protein abundance may confer a fitness advantage or disadvantage (Fig.

3A). Intrinsic noise can produce fluctuations in the relative expression of two alleles of the same gene in a heterozygote, potentially resulting in cells that express no allele, either individual allele, or both alleles. If the two alleles are functionally divergent, the population of cells could acquire heterogeneity (Fig. 3B). Such fluctuations may contribute to the still-debated phenomenon of hybrid vigor. Alternatively, intrinsic noise in the case of haploinsufficiency may result in increased levels of noise or complete loss of function in a subset of cells. Such a mechanism has been proposed in the case of the human tumor suppressor gene *NF1* (*17*) and prostate neoplasia formation in the mouse (*18*).

A brief period of intrinsic noise followed by feedback may allow for stochastic choice in stable monoallelic expression. This model has been proposed to explain the process of odorant receptor choice in olfactory neurons (*19*, *20*). Each murine olfactory neuron expresses a single allele of one odorant receptor gene out of a choice of ~1500 odorant receptor genes. A functional odorant receptor is required to prevent expression of other odorant receptors, which suggests that receptor choice occurs through stochastic activation of a single promoter followed by inhibitory signaling to the inactive odorant receptor promoters. The resulting heterogeneous population of olfactory neurons enables sensitive differentiation of odorant molecules; the stochastic nature of gene expression may create a functional sense of smell.

Many reports have been made of differentiation of a population of unicellular organisms into two distinct states of gene expression, for example, for the lysis-lysogeny decision in lambda phage-infected *E. coli* (*21*, *22*) as well as the lac operon in *E. coli* (*23*). The stochastic factor that generates the two states of expression has not been experimentally confirmed in any such case, but noise in gene expression remains a plausible culprit (*9*, *10*, *21*, *24*). Noise in gene expression in the context of positive feedback may be sufficient to create switching between the two stable states. The use of stochasticity to populate multiple steady states may play an important role in differentiation in multicellular organisms (Fig. 3C) or in survival in fluctuating environments for unicellular organisms.

Genes are organized into regulatory circuits where the expression of one gene can influence the expression of another. A consequence of this organization is that noise in the expression of one gene may propagate to affect noise in the expression of a downstream gene (Fig. 3D). Recent work in *E. coli* has demonstrated that a synthetic cascade of three transcription factors produces more noise in output than a linear cascade of two transcription factors or than one transcription factor alone (*25*). Such transmission of noise has been analyzed further in other recent work, also in *E. coli*, where the authors examined the sources of noise in a synthetic transcriptional cascade (*4*). Intrinsic noise in the expression of a transcription factor causes extrinsic noise in a downstream target gene.

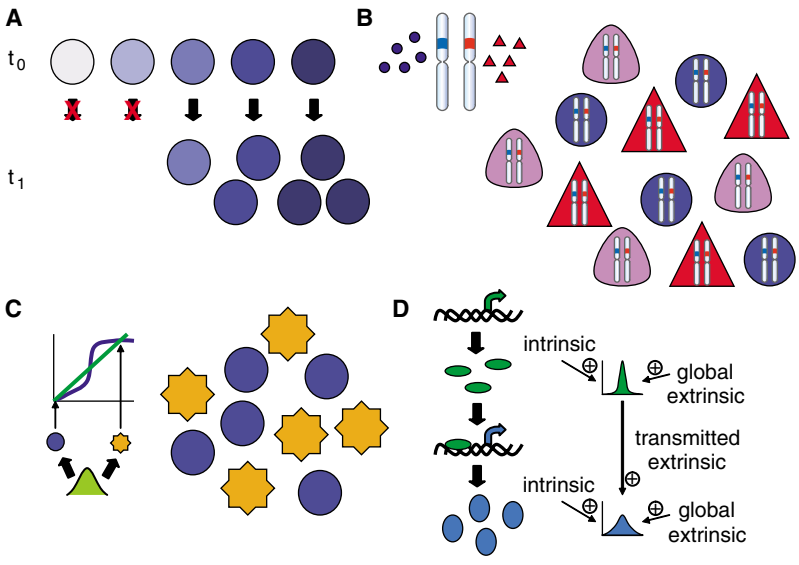

Fig. 3. Consequences of noise. (**A**) Small differences in gene product abundance affect reproductive fitness. (**B**) In a heterozygous diploid population, cells display the phenotypes associated with each homozygote as well as the heterozygote. (**C**) Noise allows simultaneous achievement of multiple steady-state phenotypes in a population. (**D**) Noise can be transmitted from one gene, in this case a transcription factor, to a downstream target. The intrinsic and global extrinsic noise of the transcription factor can cause extrinsic noise in the downstream gene.

Additionally, global noise affecting expression of the transcription factor propagates to the downstream target. Because the factor acts to repress transcription, global fluctuations in the repressor counteract the effects of global fluctuations in the expression of the downstream gene, which suggests that global fluctuations in a transcriptional activator will exacerbate the noise in the target gene.

Control of Noise in Gene Expression

It is expected that control of noise in gene expression is under evolutionary pressure. Several models suggest how such control could generate or suppress the intrinsic noise of gene expression. A theoretical model (*7*–*10*), consistent with experimental evidence from *B. subtilis* (*6*), suggests that frequent transcription followed by inefficient translation results in lower intrinsic noise in protein levels than does infrequent transcription followed by efficient translation (Fig. 4A). Similarly, when promoter fluctuations contribute to intrinsic noise, as in *S. cerevisiae*, frequent promoter activation events followed by inefficient transcription will result in less noise in mRNA levels than infrequent promoter fluctuations followed by efficient transcription (Fig. 4B) (*3*, *11*, *26*). In these models, the control of noise comes at the energetic cost of producing few proteins from numerous mRNA or the cost of repeated rounds of promoter remodeling resulting in a few mRNA. It has been noted that key regulatory proteins in *E. coli* display low translation rates, which could lower noise in protein levels (*6*). Similarly, yeast genes that are essential or encode proteins involved in multisubunit complexes tend to have higher rates of transcription and lower rates of translation (*27*).

The control of gene copy number represents a second way to lower the intrinsic noise in gene expression (Fig. 4C), which is predicted to scale with the inverse square root of the gene copy number. Noise control can therefore be added to the reasons cited for the widespread presence of polyploidy. Also, noise control by increased copy number provides an evolutionary rationalization for exact gene duplications and the maintenance of identical copies of the same gene. For example, two copies of many ribosomal protein genes have been maintained in *S. cerevisiae* after an ancient genome duplication event (*28*).

Becskei and Serrano demonstrated the reduction of noise by means of negative feedback in a simple model in which a transcription factor negatively regulates its own synthesis (Fig. 4D) (*29*). More subtle forms of feedback may exist in which the rates of earlier gene expression steps are affected by later events. For example, the association of histone methylase activity with the elongating RNA polymerase complex during transcription results in the stable methylation of histones, which may affect the subsequent activation of the promoter (*30*).

Noise in gene expression may fundamentally limit the accuracy of cellular processes, such as the circadian oscillator. In a synthetic oscillator based on three transcription factors in *E. coli*, the transmission of noise may have resulted in the loss of coordination among cells (*31*). Mihalcescu *et al.* demonstrated in the unicellular cyanobacterium *Synechococcus elongatus* that circadian oscillations persist for weeks with a stable oscillatory period without extracellular

entraining cues or intercellular communication (*32*), which suggests that the circadian network is strongly resistant to biochemical noise. Recent work has asserted that this oscillator relies on posttranslational molecular events (*33*). Perhaps a core posttranslational oscillator, which can rely on large numbers of molecules and avoid the small-number stochasticity of gene expression, is required for robust oscillations.

Cellular control mechanisms may exist to enable the switch between globally noisy or globally "quiet" states of gene expression. Queitsch *et al*. demonstrated that reduction of heat-shock protein 90 (Hsp90) chaperone activity in *Arabidopsis thaliana* increases morphological diversity in inbred lines, in addition to revealing otherwise silent genetic variation among different lines (*34*). Hsp90 chaperone activity is hypothesized to reduce the effect of stochastic molecular events that might otherwise result in developmental variability.

There may exist buffering agents that reduce either the magnitude of noise in gene expression or the impact of such noise on cellular or organismal phenotype. These buffering agents may be regulated, especially in times of stress, to produce a phenotypically diverse population. Waddington's theories of canalization and genetic assimilation propose that wasteful phenotypic variability in a population is suppressed when the population is well adapted to its environment (*35*). However, if environmental conditions shift, phenotypic noise becomes advantageous because a noisy population will produce some members that are better adapted to the new environment. Recent work supports the idea that it is advantageous to increase variability in times of stress and decrease variability when organisms are well adapted to the environment (*36*). Regulation of global noise factors could provide a molecular basis for such evolutionary flexibility.

Concluding Remarks

Many questions remain concerning the generation of noise in gene expression and its consequences for cellular behavior. The presence of stochasticity in gene expression has been confirmed to result in noise in protein abundance, but other sources of noise may result in phenotypic variability. Beyond the identification of true examples of phenotypic consequence, much work must be done to understand how cellular processes behave robustly in the presence of underlying stochasticity. Such work often requires a nontraditional collaboration between mathematicians, physicists, and in vivo experimentalists. Many biologists are beginning to focus on the limitations and benefits that stochasticity creates for biological systems, and we expect that future investigations will reveal results both unexpected and unpredictable.

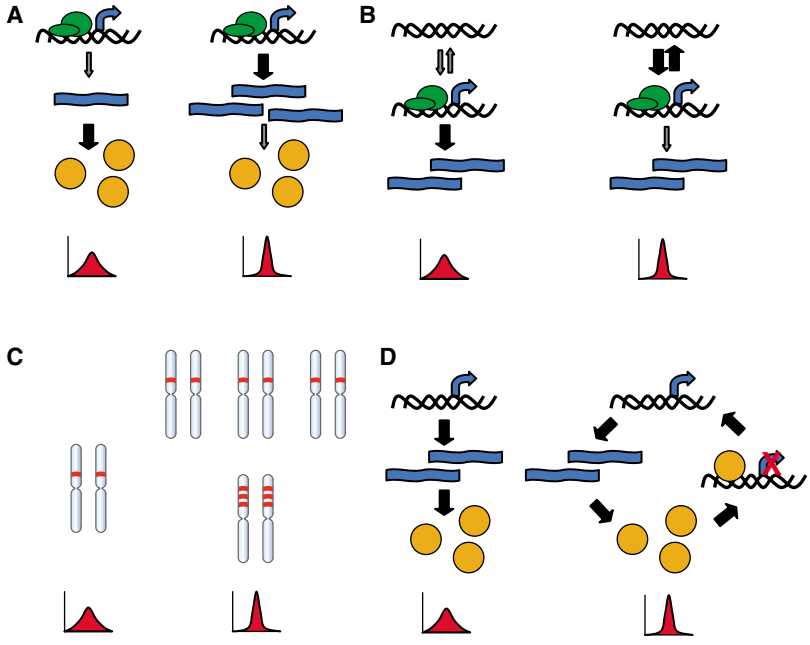

Fig. 4. Control of noise. (**A**) Infrequent transcription followed by efficient translation results in high intrinsic noise in protein levels (left); frequent transcription and inefficient translation results in low intrinsic noise (right). (**B**) Infrequent promoter transitions between inactive and active states followed by efficient transcription result in high intrinsic noise in mRNA levels (left); frequent promoter transitions followed by inefficient transcription result in low intrinsic noise (right). (**C**) Increases in gene copy number through polyploidy (top right) or gene duplication (bottom right) result in decreased intrinsic noise relative to a single gene copy (left). (**D**) Negative feedback, as when a transcription factor represses its own transcription (right), results in decreased noise relative to a linear pathway (left).

References and Notes

1. N. G. van Kampen, *Stochastic Processes in Physics and Chemistry* (North-Holland, Amsterdam, 1992).
2. P. S. Swain, M. B. Elowitz, E. D. Siggia, *Proc. Natl. Acad. Sci. U.S.A.* **99**, 12795 (2002).
3. J. M. Raser, E. K. O'Shea, *Science* **304**, 1811 (2004).
4. J. M. Pedraza, A. van Oudenaarden, *Science* **307**, 1965 (2005).
5. M. B. Elowitz, A. J. Levine, E. D. Siggia, P. S. Swain, *Science* **297**, 1183 (2002).
6. E. M. Ozbudak, M. Thattai, I. Kurtser, A. D. Grossman, A. van Oudenaarden, *Nat. Genet.* **31**, 69 (2002).
7. H. H. McAdams, A. Arkin, *Proc. Natl. Acad. Sci. U.S.A.* **94**, 814 (1997).
8. A. M. Kierzek, J. Zaim, P. Zielenkiewicz, *J. Biol. Chem.* **276**, 8165 (2001).
9. T. B. Kepler, T. C. Elston, *Biophys. J.* **81**, 3116 (2001).
10. M. Thattai, A. van Oudenaarden, *Proc. Natl. Acad. Sci. U.S.A.* **98**, 8614 (2001).
11. W. J. Blake, M. Kaern, C. R. Cantor, J. J. Collins, *Nature* **422**, 633 (2003).
12. N. Rosenfeld, J. W. Young, U. Alon, P. S. Swain, M. B. Elowitz, *Science* **307**, 1962 (2005).
13. K. Ahmad, S. Henikoff, *Cell* **104**, 839 (2001).
14. M. Bix, R. M. Locksley, *Science* **281**, 1352 (1998).
15. I. Riviere, M. J. Sunshine, D. R. Littman, *Immunity* **9**, 217 (1998).
16. T. Pastinen *et al.*, *Physiol. Genomics* **16**, 184 (2004).
17. R. Kemkemer, S. Schrank, W. Vogel, H. Gruler, D. Kaufmann, *Proc. Natl. Acad. Sci. U.S.A.* **99**, 13783 (2002).
18. J. A. Magee, S. A. Abdulkadir, J. Milbrandt, *Cancer Cell* **3**, 273 (2003).
19. A. Chess, I. Simon, H. Cedar, R. Axel, *Cell* **78**, 823 (1994).
20. S. Serizawa, K. Miyamichi, H. Sakano, *Trends Genet.* **20**, 648 (2004).
21. A. Arkin, J. Ross, H. H. McAdams, *Genetics* **149**, 1633 (1998).
22. F. J. Isaacs, J. Hasty, C. R. Cantor, J. J. Collins, *Proc. Natl. Acad. Sci. U.S.A.* **100**, 7714 (2003).
23. E. M. Ozbudak, M. Thattai, H. N. Lim, B. I. Shraiman, A. van Oudenaarden, *Nature* **427**, 737 (2004).
24. J. Hasty, J. Pradines, M. Dolnik, J. J. Collins, *Proc. Natl. Acad. Sci. U.S.A.* **97**, 2075 (2000).
25. S. Hooshangi, S. Thiberge, R. Weiss, *Proc. Natl. Acad. Sci. U.S.A.* **102**, 3581 (2005).
26. M. S. Ko, *J. Theor. Biol.* **153**, 181 (1991).
27. H. B. Fraser, A. E. Hirsh, G. Giaever, J. Kumm, M. B. Eisen, *PLoS Biol.* **2**, e137 (2004).
28. M. Kellis, B. W. Birren, E. S. Lander, *Nature* **428**, 617 (2004).
29. A. Becskei, L. Serrano, *Nature* **405**, 590 (2000).
30. H. H. Ng, F. Robert, R. A. Young, K. Struhl, *Mol. Cell* **11**, 709 (2003).
31. M. B. Elowitz, S. Leibler, *Nature* **403**, 335 (2000).
32. I. Mihalcescu, W. Hsing, S. Leibler, *Nature* **430**, 81 (2004).
33. J. Tomita, M. Nakajima, T. Kondo, H. Iwasaki, *Science* **307**, 251 (2005).
34. C. Queitsch, T. A. Sangster, S. Lindquist, *Nature* **417**, 618 (2002).
35. C. H. Waddington, *Nature* **183**, 1654 (1959).
36. M. Pigliucci, C. J. Murren, *Evolution Int. J. Org. Evolution* **57**, 1455 (2003).
37. A. K. Jain *et al.*, *Pattern Recognition* **35**, 2653 (2002).
38. T. Shin *et al.*, *Nature* **415**, 859 (2002).

39. We regret not acknowledging numerous contributors to this topic. We thank A. Arkin, M. Elowitz, and A. van Oudenaarden for critical commentary. Supported by the Howard Hughes Medical Institute, NIH grant GM51377, the David and Lucile Packard Foundation (E.K.O.), the Burroughs Wellcome/UCSF Interfaces of Science Fellowship program, and the UCSF Medical Scientist Training Program (J.M.R.). E.K.O. is a member of the science board and occasional consultant for Chiron Corporation.

Supporting Online Material

www.sciencemag.org/cgi/content/full/309/5743/2010/DC1
SOM Text
References

10.1126/science.1105891

INTRODUCTION

Voyage of Discovery

Voyager 1 was launched on 5 September 1977. Eighteen months later, when it flew by Jupiter and its moons, it began to change our understanding of our solar system. Now, three decades later, it is still doing so.

Passing Jupiter, Voyager 1 discovered nine active volcanoes on the moon Io: the first evidence of a geologically active body elsewhere in our solar system (eight were still active a few months later, when Voyager 2 passed). It also mapped the fractured icy surface of Europa and other moons, studied a huge storm in Jupiter's atmosphere, found that Jupiter had a ring (changing theories about planetary rings) and a magnetic field (changing planetary radio science), and analyzed a variety of new plasma interactions in Jupiter's atmosphere (*Science*, 1 June 1979*). The next stop, just over 1 year later, was Saturn (*Science*, 10 April 1981). Here, Voyager 1 found gaps and structure in Saturn's rings and several new moons. It discovered lightning in Saturn's atmosphere. It closely observed Titan, showing that it, like Earth, had a nitrogen-rich atmosphere and dynamic clouds. Its close flyby of Saturn flung Voyager on a long, mostly quiet journey heading out of the solar system. Nearly 25 years after passing Saturn, it is now the farthest-traveled human object.

Four Reports and a Viewpoint in this issue describe Voyager 1's next encounter, with the heliosheath. The heliosheath begins where the solar wind, expanding outward at supersonic speeds, meets interstellar material and slows abruptly, forming a shock wave. This shock expands and contracts with the solar cycle; Voyager 1 crossed it at about 95 astronomical units (AU) from the Sun in December 2004 (Pluto orbits about 40 AU from the Sun). Data returned from Voyager 1 provided an in situ view of this shock (called the termination shock) and its effects on cosmic rays and the solar magnetic field, and of particles and plasmas in the heliosheath. As it has in the past, Voyager's observations have changed our view of the solar system, challenging notions about the origin of certain cosmic rays that were thought to be produced in this region. Voyager 1 will continue to collect data while heading toward an even larger shock marking the edge of our solar system (see the cover for an example), perhaps entering interstellar space in 10 to 20 years. Given the past success of Voyager 1, and of its partner, Voyager 2, which is also approaching the heliosheath after exploring all the giant planets, perhaps we should stay tuned.

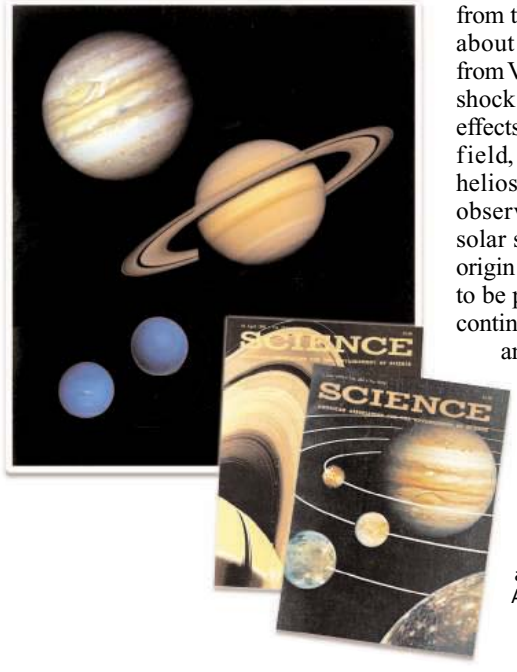

CREDITS (TOP TO BOTTOM): JPL/NASA; *SCIENCE*

–BROOKS HANSON

*These issues of *Science*, and all others going back to the first issue, are available at www.jstor.org and to members of the American Association for the Advancement of Science.

CONTENTS

Science

VIEWPOINT

Journey into the Unknown Beyond

Len A. Fisk

The Voyager 1 spacecraft has passed an important milestone. As is reported in papers in this issue, Voyager 1 has crossed the termination shock of the solar wind, where the wind abruptly decelerates to begin its merger into the local interstellar medium. The termination shock provided surprises; the region beyond is truly uncharted territory.

According to four Reports in this issue (*1*–*4*), the venerable Voyager 1 spacecraft, launched in 1977 and now en route out of the solar system, passed an important milestone on 16 December 2004. By crossing the point where the outward expansion of the atmosphere of the Sun begins the process of merging into the interstellar medium, humankind's most intrepid explorer is now venturing into the unknown beyond.

The outer atmosphere of the Sun continually expands into space in a supersonic flow known as the solar wind. At some point in the outer solar system, the solar wind must decelerate so that it can merge with the local interstellar medium. Supersonic flows perform this deceleration through sharp transitions known as shock waves, where the flow speed abruptly drops. This is the same phenomenon as a supersonic airplane, which is preceded by a shock wave (the sonic boom), the role of which is to decelerate the air ahead so that it can flow smoothly around the aircraft. In the case of the supersonic solar wind, the shock wave that performs the deceleration is known as the termination shock; it terminates the supersonic flow and creates a subsonic flow that can merge with the local interstellar medium. The solar wind flows outward in all directions, and so the termination shock surrounds the solar system (Fig. 1).

The location of the termination shock has been debated for many years. Early in the space age, before we fully appreciated the vastness of even our local solar environment, the termination shock was predicted to be relatively close to the Sun, within the orbits of the planets. Over the years, our knowledge has increased and converged on predictions that the shock would lie between 90 and 100 astronomical units (AU) from the Sun (an astronomical unit is the distance from the Sun to Earth: Pluto averages 40 AU from the Sun). Indeed, Voyager 1 crossed at 94 AU from the Sun.

There have been precursor events that told us that the shock was ahead. There were a series of increases in the intensity of low-energy energetic particles with strong outward anisotropies, which remain a puzzle. Some of the Voyager investigators found evidence that these precursor events were shock crossings (*5*), but others did not (*6*, *7*). For the crossing on 16 December there is a clear consensus: All the observations support a shock crossing. The magnetic field strength increased as a result of the compression at the shock, and there was a change in the properties of the turbulence (*3*); there were plasma waves characteristic of shock crossings (*4*); and the intensity of low-energy particles increased abruptly (*1*, *2*).

Voyager 1 has a disadvantage in that its plasma detector failed some years ago. This instrument would have provided a direct measure of the velocity of the solar wind flow, showing the abrupt decrease in speed across the shock. The energetic particle data, however, can be used to reveal the flow speed, and it is consistent with a shock crossing (*2*). Voyager 2, still tens of astronomical units behind Voyager 1, has a working plasma detector and is estimated to cross the termination shock in 2009 or 2010.

We have had great expectations for the termination shock. In the early 1970s, a new component of the cosmic ray flux was discovered at energies on the order of 10 MeV/nucleon. The new component, labeled anomalous cosmic rays (ACRs), had a most unusual composition: Initially helium, nitrogen, and

Department of Atmospheric, Oceanic, and Space Sciences, University of Michigan, Ann Arbor, MI 48109–2143, USA. E-mail: lafisk@umich.edu

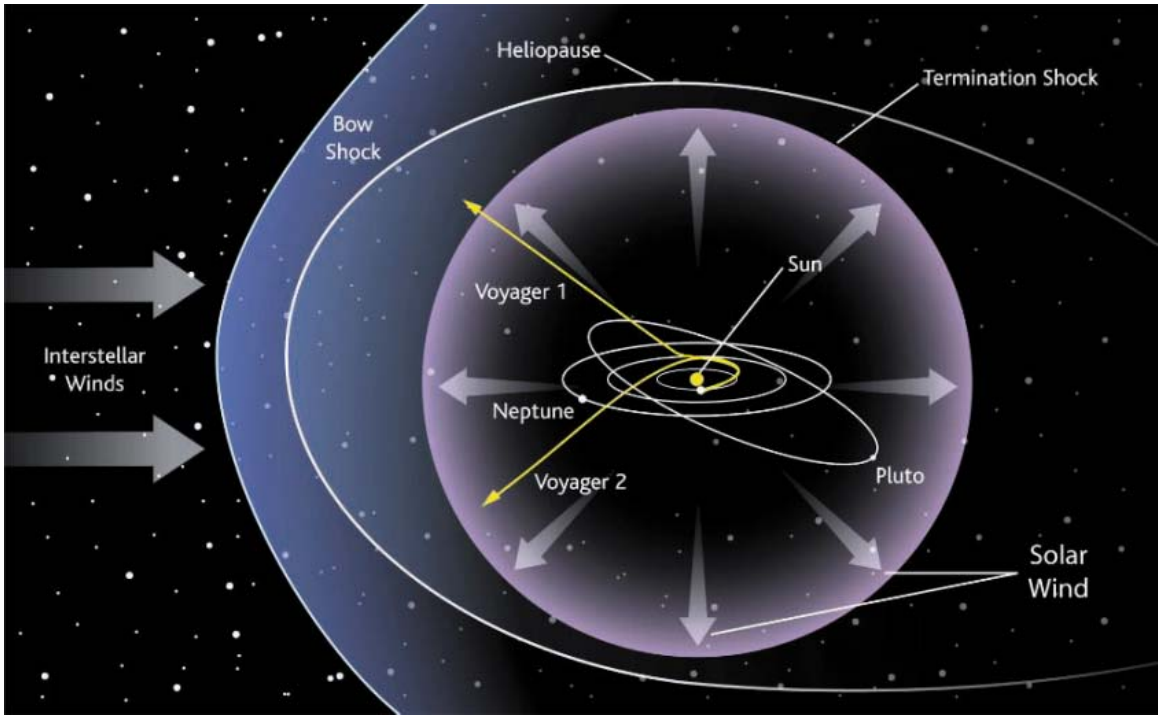

Fig. 1. Voyagers 1 and 2 have flown on different trajectories past the outer planets of the solar system since 1977, and Voyager 1 is reported to have crossed the termination shock of the solar wind at 94 AU from the Sun in December 2004. The solar wind is a supersonic flow, and a shock—the termination shock—is required for the wind to decelerate and merge with the local interstellar medium that bounds the solar system. The solar wind and interstellar gas do not merge easily, so further out beyond the termination shock, there is a true boundary between the solar wind and the interstellar medium: the heliopause. Further out still, if the solar system is itself moving supersonically relative to the interstellar medium, there may be a large bow shock.

oxygen were observed and no other elements, but eventually hydrogen, neon, and argon were also observed. The origin of the ACRs was identified early on (*8*) (although debated for decades). They originate as interstellar neutral gas that flows through the solar system and is ionized and then accelerated in the solar wind. This acceleration is the issue. Immediately upon ionization, the interstellar particles are picked up by the solar wind and acquire energies on the order of 1 keV/nucleon. They must be accelerated by four orders of magnitude to the observed energies of greater than 10 MeV/nucleon. The termination shock has long been considered the likely location for the acceleration (*9*). Indeed, the termination shock should be an accessible example of shock acceleration of energetic particles at work, just like the acceleration at supernovae shocks that is postulated to produce galactic cosmic rays.

However, at the location of the termination shock seen by Voyager 1, there is no evidence of acceleration of the traditional ACRs (*1*). The spectrum of the ACRs does not change at the shock crossing; there is no buildup in intensity. Low-energy ions, below 3 MeV/nucleon, are clearly and indeed abruptly accelerated, but the higher energy ACRs, which we have been observing for decades, are unaffected by the termination shock.

Once again the mantra of space exploration is fulfilled: When we go somewhere that is new, we find the unexpected, and that's what makes it so exciting. The termination shock doesn't perform as we expected; it is clear it is a shock, but not the prodigious accelerator we expected. Indeed, as Voyager 1 flies downstream from the termination shock, the intensity of ACRs continues to grow, as if its source still lies ahead. Voyager is like those intrepid British explorers of the 1800s in search of the source of the Nile; it is off in search of the source of the ACRs.

The last few decades of Voyager, after its last planetary encounter in 1989, have been a little dull. The supersonic flow of the solar wind in the outer solar system ahead of the termination shock is predictable from what we observe in the inner solar system, and we saw pretty much what we expected. Upon crossing the termination shock, the passage of Voyager 1 is into truly uncharted territory, into the subsonic flow of the solar wind and its adjustment to the interstellar medium. Eventually, we could even cross the heliopause into pristine interstellar gas.

We will observe conditions in the subsonic region never seen before. The termination shock creates substantial low-energy energetic ions, which can be a dominant pressure force in the downstream region; interstellar neutral hydrogen is present and readily ionized to affect the dynamics. Energetic particles may be readily accelerated. All this makes for a unique environment. With Voyager 1, then, and with Voyager 2 behind it, the best is yet to come.

References and Notes

1. E. C. Stone *et al.*, *Science* **309**, 2017 (2005).
2. R. B. Decker *et al.*, *Science* **309**, 2020 (2005).
3. L. F. Burlaga *et al.*, *Science* **309**, 2027 (2005).
4. D. A. Gurnett, W. S. Kurth, *Science* **309**, 2025 (2005).
5. S. M. Krimigis *et al.*, *Nature* **426**, 45 (2003).
6. F. B. McDonald *et al.*, *Nature* **426**, 48 (2003).
7. L. F. Burlaga *et al.*, *Geophys. Res. Lett.* **30**, 10.1029/2003GL018291 (2003).
8. L. A. Fisk, B. Kozlovski, R. Ramaty, *Astrophys. J.* **190**, L35 (1974).
9. M. E. Pesses, D. Eicher, J. R. Jokippi, *Astrophys. J.* **246**, L85 (1981).

10.1126/science.1118762

REPORT

Voyager 1 Explores the Termination Shock Region and the Heliosheath Beyond

E. C. Stone,[1]* A. C. Cummings,[1] F. B. McDonald,[2] B. C. Heikkila,[3] N. Lal,[3] W. R. Webber[4]

Voyager 1 crossed the termination shock of the supersonic flow of the solar wind on 16 December 2004 at a distance of 94.01 astronomical units from the Sun, becoming the first spacecraft to begin exploring the heliosheath, the outermost layer of the heliosphere. The shock is a steady source of low-energy protons with an energy spectrum $\sim E^{-1.41 \pm 0.15}$ from 0.5 to ~3.5 megaelectron volts, consistent with a weak termination shock having a solar wind velocity jump ratio $r = 2.6^{+0.4}_{-0.2}$. However, in contradiction to many predictions, the intensity of anomalous cosmic ray (ACR) helium did not peak at the shock, indicating that the ACR source is not in the shock region local to Voyager 1. The intensities of ~10–megaelectron volt electrons, ACRs, and galactic cosmic rays have steadily increased since late 2004 as the effects of solar modulation have decreased.

The termination shock marks the abrupt slowing of the supersonic solar wind as it approaches contact with the interstellar wind. In the heliosheath region beyond the shock, the wind is slower, hotter, and denser as it interacts with the surrounding interstellar matter. A variety of observations over the last 15 years have indicated that the shock was likely at a distance of 90 to 100 astronomical units (AU) from the Sun (*1*), a distance that varies as the solar wind pressure changes over the 11-year solar cycle. A recent estimate (*2*) suggested that the probability that Voyager 1 would cross the shock in 2005 was ~30%, increasing to ~50% by 2008.

The termination shock is also the predicted source of anomalous cosmic rays (ACRs) that originate as interstellar neutral atoms that drift inward close to the Sun where they are ionized and picked up by the solar wind that carries them out to the shock where they are accelerated (*3*). As a result, it was expected that the ACR intensity would reach its maximum at the shock and remain close to that level in the heliosheath.

Voyager 1 (V1) has been in the vicinity of the shock since reaching 85 AU in mid-2002 when it observed enhanced intensities of ions streaming from the shock (*4*, *5*). Two episodes (TSP1 and TSP2) of enhanced intensities of termination shock particles (TSPs) were present upstream of the shock for much of the time since then (Fig. 1). During this period, the dynamic pressure of the solar wind observed by Voyager 2 (V2) beyond 75 AU was gradually increasing, pushing the termination shock outward (*6*) ahead of V1 until mid-2004 when the pressure reached its maximum (*7*) during its 11-year cycle of solar activity. As the solar wind pressure began to decline, the shock started moving inward, crossing V1 at 94 AU on day 351 of 2004 (2004/351). The increased magnetic field observed since that time is the key signature that V1 had entered the heliosheath (*8*).

As shown in Fig. 1, some characteristics of the enhanced intensities of 3.3- to 7.8-MeV protons downstream of the termination shock in the heliosheath differ significantly from the observations of TSPs upstream of the shock [see also (*9*)]. Four low-energy telescopes (LETs) on the Cosmic Ray Subsystem (*10*) provide a measure of the directional intensity of the TSPs. Before crossing the shock, the proton intensity in the LET C telescope was usually lower than that in the A and B telescopes that are sensitive to the azimuthal flow

[1]California Institute of Technology, Pasadena, CA 91125, USA. [2]Institute for Physical Science and Technology, University of Maryland, College Park, MD 20742, USA. [3]NASA/Goddard Space Flight Center, Greenbelt, MD 20771, USA. [4]Department of Physics and Astronomy, New Mexico State University, Las Cruces, NM 88003, USA.

*To whom correspondence should be addressed. E-mail: ecs@srl.caltech.edu

of TSPs outward along the spiral interplanetary magnetic field (the −T direction in the RTN coordinate system). During the upwind period for days 2004/020 to 290, the intensity ratio (A + B)/2C, a measure of the strength of the field-aligned beaming, ranged up to ~10 on individual days and had a mean of 1.7 with a daily root mean square (rms) variation of 1.3. In contrast, in the heliosheath for days 2005/23 to 156 this ratio was 1, with an rms variation of only 0.16. The reduced anisotropy is expected in the heliosheath (*11*) because the TSPs undergo more scattering due to the increased magnetic turbulence (*8*).

Another notable difference is the greatly reduced variability in the intensity evident in the heliosheath. For example, upstream the daily averaged intensities of protons with 0.5 to 0.7 MeV for days 2004/020 to 290 were highly variable, with an rms day-to-day variation of 47%, as compared with an rms variation of 5% in the heliosheath. The latter indicates that the TSP source is relatively steady and the connectivity to the source is stable as expected, because all of the heliosheath magnetic field lines are connected to the shock.

Three distinct energetic particle components are present in the heliosheath spectra of H, He, and O (Fig. 2). The TSP component dominates the lowest energies, with energy spectra that appear to be broken power laws of the form

$$j = j_o(E/E_{norm})^a \qquad E \le E_o$$

$$j = j_o(E_o/E_{norm})^{(a-b)}\ (E/E_{norm})^b \qquad E > E_o$$

where E_o is the break energy. This spectral form has been fit to daily average proton spectra during the periods when TSPs were present. During the upstream TSP events, the spectral slope was quite variable from day to day, typically ranging between −1 and −2 as propagation conditions varied along the magnetic field line connecting V1 to the shock. The break energy, however, was much less variable, with a median value of 3.5 MeV and an rms daily variation of 0.9 MeV for 2002/212 to 2003/030 during the first TSP episode and 3.5 MeV and an rms variation of 0.8 MeV for 2004/026 to 2004/289 during the second episode.

The spectra downstream in the heliosheath are much less variable, with a mean spectral slope $\langle a \rangle$ at low energies of −1.41 and a daily rms of 0.15 with an average spectral break energy of 3.5 ± 0.1 MeV and an rms of 0.3 MeV for the period 2005/090 to 156. The steadiness of the spectrum suggests that the spectral shape is little affected by modulation in the heliosheath, as expected (*12*), and that the spectral slope from 0.5 to 3.5 MeV is characteristic of the source. If the >0.5-MeV TSPs are the result of diffusive shock acceleration, the slope a is determined by the shock strength r according to $r = (2a - 2)/(2a + 1)$. The observed mean and rms values for a would indicate a weak termination shock with $r = 2.6^{+0.4}_{-0.2}$, consistent with that determined from Voyager magnetic field observations (*8*).

The break energy in the TSP proton spectrum has shown little long-term change over the last 3 years, indicating that the upstream and heliosheath TSPs have a common source and that the spectral break is likely a steady-state characteristic of the shock acceleration process in this region of the termination shock. The TSP break energy is much lower than that of ACR H (~100 MeV), which occurs when the acceleration time exceeds the adiabatic cooling time in the expanding solar wind (*13*). Lower energy ions are accelerated more quickly, so the TSP break must be due to other factors. A transient region of the shock with a very small local radius of curvature of <2 AU could limit the maximum local acceleration energy to ~3 MeV (*14*). However, the stability of the cutoff over 3 years requires this to be a stable, not a transient, feature of the shock local to V1, which seems unlikely.

This suggests that the TSP spectral break is due to another property of the acceleration region. As shown in Fig. 1, there is a complex region immediately downstream of the shock in which strong azimuthal streaming persists and the intensity continues to vary, reaching a minimum on day 2005/014. Depending on the inward shock speed, this corresponds to a region ~0.5 to 1 AU in width. Escape from this region near the shock might limit TSP acceleration to <3.5 MeV.

The streaming along the magnetic field upstream of the shock source was expected to

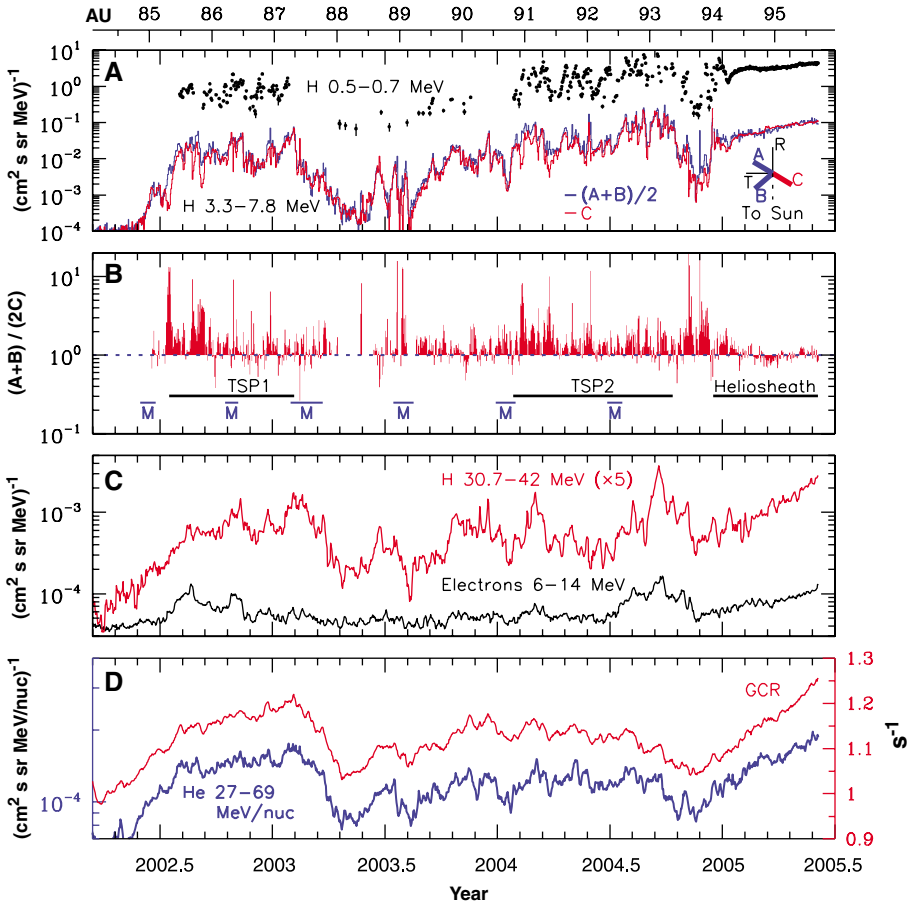

Fig. 1. (**A**) Intensities of energetic termination shock particles (TSPs). The inset illustrates the telescope viewing directions projected into the R-T plane, where −R is toward the Sun and T is azimuthal. The proton intensity (*H*) at 3.3 to 7.8 MeV is observed by particle telescopes A plus B that are sensitive to ions streaming outward along the spiral magnetic field in the –T direction and by telescope C observing in the opposite direction. The intensity of *H* with 0.5 to 0.7 MeV observed by telescope A is shown for times when the background correction was <60%. Voyager 1 crossed the shock and entered the heliosheath on 2004.96 (12/16/05). (**B**) Azimuthal streaming index as indicated by the ratio of the average daily intensity in telescopes A and B to that in C. Upstream of the shock, there were two periods of upstream episodes of enhanced intensities (TSP1 and TSP2) during which streaming anisotropy was usually large and mainly in the −T direction. The streaming anisotropy is much smaller in the heliosheath. Merged interaction regions (labeled M) are indicated (*22*). (**C**) Intensities (5-day moving averages) of ~10-MeV electrons and ~35-MeV H. These increases are strongly correlated and of shorter duration than for lower energy H. (**D**) Intensities (5-day moving averages) of He ions and of galactic cosmic rays (GCR) with $E > 70$ MeV/nucleon. The He intensity is due mainly to anomalous cosmic rays.

be inward along the spiral field if the termination shock is spherical. However, the observed flow was outward along the field, requiring a shock source located inward along the spiral field several AU closer to the Sun than V1. This requires a nonspherical shock, such as could result from an interstellar magnetic field inclined in the right direction (*15*, *16*) if the distortion is large enough in the right location on the shock. Although recent observations of the flow of interstellar neutral H have suggested the plane of inclination of the interstellar field (*17*), the resulting direction and magnitude of the distortion of the termination shock have not yet been modeled. Alternatively, the oblateness of the nose of the shock due to the incident interstellar wind may also provide the needed distortion (*18*). Observations as V2 approaches the shock should further constrain the nature of the shock asymmetry.

The termination shock was expected to be the source of ACRs (*3*), and little modulation of the source spectra (Fig. 2) was expected in the heliosheath (*19*). The ACR component dominates the He spectrum between 10 and 60 MeV/nucleon and is similar to the predicted source spectrum (*20*) above ~30 MeV/nucleon. However, at 20 MeV/nucleon the observed intensity is less than 1/10 of the predicted source intensity, indicating that there is substantial residual modulation of ACRs even in the immediate vicinity of the shock, both upstream and downstream (Fig. 3). A similar modulation of ACR O is apparent in Fig. 2, with only ~5% of the intensity at 4 MeV/nucleon expected for a weak shock source spectrum. Although the ACR source is likely the shock, the source location is remote from the shock region crossed by V1, possibly at lower latitudes where increased turbulence results in a higher rate of diffusive shock acceleration or at polar latitudes. However, it is also possible that a more fundamental change in the model of ACR acceleration is required.

Although the TSP intensity at <1 MeV is evolving slowly in the heliosheath, the level of ACR modulation is changing rapidly, with the intensity at 16 MeV/nucleon increasing by a factor of 4 since first crossing the shock (Fig. 3). This indicates that the ACRs are gaining easier access to the location of V1, possibly as a result of decreasing solar modulation (see below), but it could also indicate a positive radial gradient in the heliosheath and a substantially different ACR source.

The relationship of ACRs and TSPs is unknown. Both are deficient in carbon ions, indicating that they are accelerated pickup ions (*5*) and suggesting the possibility that TSPs undergo a second stage of acceleration to become ACRs [see, e.g., (*21*)]. However, the H/He ratio is >10 for TSPs (Fig. 2), as compared with ~5 for ACRs (*20*), indicating that such a model would require additional fractionation of H in the second stage of acceleration (*21*). Continuing observations of the ACR spectrum by V1 and by V2 as it approaches the shock in the next 2 to 3 years may provide additional insight into the location of the ACR source and the possible role of TSPs in the acceleration of ACRs.

Two other distinctive features of these upstream TSP events (Fig. 1) are the increases of relativistic 6- to 14-MeV electrons and the strong modulation of the ions and electrons by transient disturbances moving out in the interplanetary medium. These large-scale disturbances, known as merged interaction regions (MIRs), originate during episodes of solar activity and evolve in interplanetary space through the coalescence of multiple interplanetary coronal mass ejections (CMEs) and high-speed solar wind. These MIRs are readily identified at V2 through increases in the solar wind speed, the intensity of MeV ions, the strength of the interplanetary magnetic field, and moderate decreases in the galactic cosmic ray (GCR) intensity (*22*). The V2 MIRs, time shifted ~0.2 years to account for the additional convection time to V1, are indicated in Fig. 1. Many of the large-scale changes in the TSPs are associated with the passage of MIRs, including the onset of TSP1 and TSP2 following the passage of MIRs and the termination of TSP1 6 months later by the arrival of an MIR.

The interaction of MIRs with the termination shock may also result in the reacceleration of GCR electrons and higher energy ions. For example, upstream enhancements of MeV electrons and higher energy ions (>10 MeV) observed during the period 2002.54 to 2003.2 were associated with and following the passage of three consecutive MIRs. Enhanced upstream intensities of energetic H and electrons were also associated with an episode of solar activity in late October and early November 2003 (the "Halloween events") that produced some of the largest flares and CMEs observed over the last four solar cycles. The associated MIR produced the largest increase in MeV ions and decrease in GCRs observed at V2 over the current solar cycle. Following the arrival of the Halloween events at V1, a slow decrease in the GCR intensity began at 2004.57 and continued to 2004.88. The GCR decrease at V2 was much faster (0.06 year)

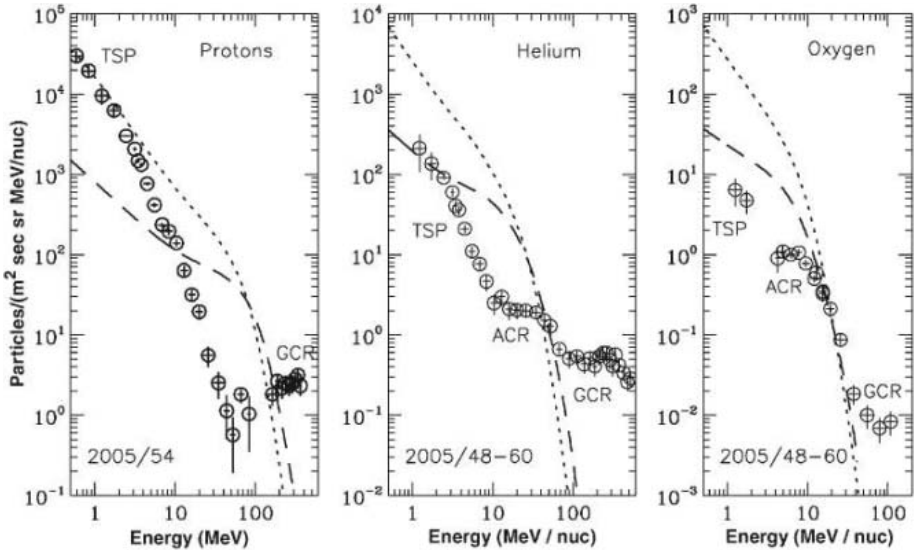

Fig. 2. Typical spectra observed in the heliosheath. The TSP spectra are broken power laws with a break energy of ~3.5 MeV for protons. The He and O spectra are dominated by anomalous cosmic rays (ACRs) at mid-energies and by galactic cosmic rays (GCRs) at higher energies. The predicted ACR spectra at the shock are shown for a strong (r = 4, dashed line) and a weak (r = 2.4, dotted line) shock (*20*).

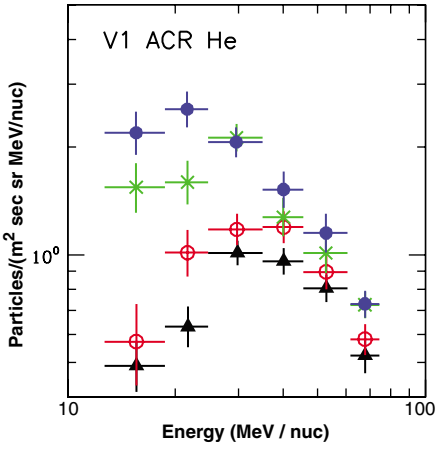

Fig. 3. ACR helium spectra just upstream of the shock (▲) (2004/313 to 350) and in the heliosheath [(○) 2004/352 to 2005/052, (×) 2005/053 to 104, (●) 2005/105 to 156]. The TSP, ACR, and GCR spectra overlap in the observed spectra in Fig. 2. Estimates of the TSP and GCR components have been subtracted in the regions of overlap to determine the ACR He spectra. The ACR He intensity did not reach a maximum at the shock, but continued to rapidly increase at lower energies in the heliosheath, indicating increasingly easy propagation from the ACR source to V1.

because the 2003 Halloween solar activity was in the Southern Hemisphere as is V2 (−25° heliographic latitude), whereas V1 is at +34°. There was also an unusually intense magnetic field at V1 during this period (*8*).

A significant increase in the intensities of ~10-MeV electrons and of 31- to 42-MeV TSP H coincided with the arrival of the Halloween events at V1 (Fig. 1). It is assumed that the electrons are GCRs, suggesting the possibility that the increase in their intensity and that of 31- to 42-MeV TSP H resulted from reacceleration associated with the approach and interaction of the Halloween events with the nearby termination shock.

The GCR intensity at 1 AU was at a low level with limited variation during the period of maximum solar activity from 2000.5 to 2004.0, and a similar pattern was observed at V2 and V1. Following the 2003 Halloween events, the GCR intensity at 1 AU began increasing above the prior levels. At V1 and V2, the steady increase in the GCR intensity began in late 2004, continuing for at least 7 months (Fig. 1). This is due to decreasing solar modulation as solar activity declines. As expected, the lowest rigidity particles such as ~10-MeV electrons and 31- to 42-MeV ACR H are most sensitive to changes in particle transport conditions, contributing to the large intensity increases observed at V1 (Fig. 1). It is interesting that late 2004 also marked the first appearance of TSPs at V2 at 75 AU as it begins to explore the upstream termination shock region while V1 is in the heliosheath.

References and Notes

1. E. C. Stone, *Science* **293**, 55 (2001).
2. G. Gloeckler, J. Geiss, *Adv. Space Res.* **34**, 53 (2004).
3. M. E. Pesses, J. R. Jokipii, D. Eichler, *Astrophys. J.* **246**, L85 (1981).
4. F. B. McDonald *et al.*, *Nature* **426**, 48 (2003).
5. S. M. Krimigis *et al.*, *Nature* **426**, 45 (2003).
6. W. R. Webber, *J. Geophys. Res.*, in press.
7. J. D. Richardson *et al.*, http://web.mit.edu/space/www/voyager/voyager.html.
8. L. F. Burlaga *et al.*, *Science* **309**, 2027 (2005).
9. R. B. Decker *et al.*, *Science* **309**, 2020 (2005).
10. E. C. Stone *et al.*, *Space Sci. Rev.* **21**, 355 (1977).
11. J. Kóta, J. R. Jokipii, *AIP Conf. Proc.* **719**, 272 (2004).
12. J. Giacalone, J. R. Jokipii, *AIP Conf. Proc.* **719**, 266 (2004).
13. V. Florinski, J. R. Jokipii, *Astrophys. J.* **591**, 454 (2003).
14. J. R. Jokipii, J. Giacalone, *Proc. 28th Int. Cosmic Ray Conf.* **7**, 3753 (2003).
15. R. Ratkiewicz *et al.*, *Astron. Astrophys.* **335**, 363 (1998).
16. N. V. Pogorelov, T. Matsuda, *J. Geophys. Res.* **103**, 237 (1998).
17. R. Lallement *et al.*, *Science* **307**, 1447 (2005).
18. J. R. Jokipii, J. Giacalone, J. Kóta, *Astrophys. J.* **611**, L141 (2004).
19. V. Florinski *et al.*, *Astrophys. J.* **610**, 1169 (2004).
20. A. C. Cummings, E. C. Stone, C. D. Steenberg, *Astrophys. J.* **578**, 194 (2002).
21. G. P. Zank *et al.*, *Astrophys. J.* **556**, 494 (2001).
22. F. B. McDonald *et al.*, *Proc. 29th Int. Cosmic Ray Conf.* **SH3.1.06** (2005).

20 July 2005; accepted 16 August 2005
10.1126/science.1117684

REPORT

Voyager 1 in the Foreshock, Termination Shock, and Heliosheath

R. B. Decker,[1]* S. M. Krimigis,[1] E. C. Roelof,[1] M. E. Hill,[1,2] T. P. Armstrong,[3] G. Gloeckler,[2] D. C. Hamilton,[2] L. J. Lanzerotti[4,5]

Voyager 1 (V1) began measuring precursor energetic ions and electrons from the heliospheric termination shock (TS) in July 2002. During the ensuing 2.5 years, average particle intensities rose as V1 penetrated deeper into the energetic particle foreshock of the TS. Throughout 2004, V1 observed even larger, fluctuating intensities of ions from 40 kiloelectron volts (keV) to ≥50 megaelectron volts per nucleon and of electrons from >26 keV to ≥350 keV. On day 350 of 2004 (2004/350), V1 observed an intensity spike of ions and electrons that was followed by a sustained factor of 10 increase at the lowest energies and lesser increases at higher energies, larger than any intensities since V1 was at 15 astronomical units in 1982. The estimated solar wind radial flow speed was positive (outward) at ~ +100 kilometers per second (km s^{-1}) from 2004/352 until 2005/018, when the radial flows became predominantly negative (sunward) and fluctuated between ~ −50 and 0 km s^{-1} until about 2005/110; they then became more positive, with recent values (2005/179) of ~ +50 km s^{-1}. The energetic proton spectrum averaged over the postshock period is apparently dominated by strongly heated interstellar pickup ions. We interpret these observations as evidence that V1 was crossed by the TS on 2004/351 (during a tracking gap) at 94.0 astronomical units, evidently as the shock was moving radially inward in response to decreasing solar wind ram pressure, and that V1 has remained in the heliosheath until at least mid-2005.

We present data suggesting that Voyager 1 (V1) encountered the heliospheric termination shock (TS) as the TS apparently moved radially inward over the spacecraft on 2004/351 (2004.956) at a radial distance from the Sun of 94.0 astronomical units (1 AU = 1.5 × 10^8 km) and at a heliographic latitude of N34.1°. Data obtained from V1 since that time suggest that V1 has remained in the shocked plasma downstream of the TS (the heliosheath, or HS) until at least the middle of 2005 (2005.5). V1 data used herein are from the Low Energy Charged Particle (LECP) instrument that measures intensities of ions 40 keV to ~60 MeV nuc^{-1} and of electrons 26 keV to >10 MeV, determines the composition of ions >200 keV nuc^{-1}, and provides angular information via a mechanically stepped platform (*1*). Ion angular data enable estimates of plasma flow velocities at V1 in the absence of such data from the V1 Plasma Science instrument (which failed in 1980). Data from other instruments on V1 are discussed in accompanying reports (*2*–*4*).

The TS is expected to be a reverse, quasi-perpendicular, collisionless shock across which the solar wind speed decreases from super- to submagnetosonic flow, the solar wind plasma is compressed and heated, and the magnetic field amplitude is increased. Much work has been done to predict the nature and location of the TS, particularly its radial distance from the Sun, in part to prepare for the eventual crossing, or multiple crossings, of the TS by Voyagers 1 and 2 [(*5*, *6*) and references therein]. It is expected that particles are accelerated at and around the TS. Here, we use the term foreshock to describe the region upstream of the TS populated by energetic particles that originate mainly from the TS, HS, and beyond, and that exhibit large and frequent intensity fluctuations or large beaming anisotropies (or both). Because we do not measure ions <40 keV, we have no direct measure of unaccelerated pickup ions or of their influence on the solar wind near the TS or on the TS transition.

LECP observations during the period 2002.0 to 2005.5 (83.4 to 96.0 AU) are shown in Fig. 1. Particle profiles in Fig. 1, A and D,

[1]Applied Physics Laboratory, Johns Hopkins University, Laurel, MD 20723, USA. [2]Department of Physics, University of Maryland, College Park, MD 20742, USA. [3]Fundamental Technologies, 2411 Ponderosa, Suite A, Lawrence, KS 66046, USA. [4]Bell Laboratories, 600 Mountain Avenue, Murray Hill, NJ 07974, USA. [5]Center for Solar Terrestrial Research, New Jersey Institute of Technology, Newark, NJ 07102, USA.

*To whom correspondence should be addressed. E-mail: robert.decker@jhuapl.edu

suggest a division into four periods, A to D, discussed below. Figure 1C shows the first-order anisotropy vector $\mathbf{A}_1/A_0$ of the 3.4- to 17.6-MeV protons (*7*, *8*). Figure 1F shows the estimated radial component of the solar wind flow velocity V_R based on analysis of directional data from low-energy proton channels. The velocity-extraction algorithm permits derivation of plasma flow velocities on a day-by-day basis with the use of concurrent magnetic field vector data (*9*, *10*).

Observations during period A (2002.58 to 2003.10, 85.3 to 87.3 AU) first indicated that V1 was observing new phenomena, including large (factor of ~10 to 50) overall increases in intensities and in the amplitude of superposed intensity variations of ions 40 keV to ≥50 MeV nuc^{-1} and of electrons 26 keV to ≥350 keV (*11*, *12*). Ion angular data showed large beamlike anisotropies, with the beams directed mainly outward away from the Sun along the magnetic field (*13*), that is, nearly in the –T direction (Fig. 1C). These beams imply a source located at a smaller helioradius and at a larger heliolongitude than those of V1. This has led to suggestions of a flaring of the TS away from the stagnation point (*14*) or of an asymmetrical distortion of the TS associated with the interstellar magnetic field orientation (*15*). Period A ended when intensities decreased abruptly, apparently because of passage of a merged interaction region (*16*). Period B (2003.10 to 2004.07, 87.3 to 90.8 AU) was a year-long diminution (but not disappearance) of energetic ion intensities, with smaller, impulsive (~days) increases, reductions in the duration and amplitude of ion beams, and more instances when near-azimuthal beaming anisotropies were directed sunward (i.e., nearly in the +T direction). Period C (2004.07 to 2004.96, 90.8 to 94.0 AU) was a 0.9-year return to high intensities, with superposed ~13- and ~26-day variations (*17*), and to large, mainly outwardly directed ion beams, like those during period A. Elevated intensities continued until ~2004.78, when they decreased abruptly, remained low for ~65 days, then increased rapidly on 2004.96. Period D (2004.96 to 2005.50, 94.0 to 96.0 AU) began on 2004/350 with a short-lived (few hours) intensity spike of ions 40 keV to ~20 MeV and of electrons 0.35 to 1.5 MeV.

Figure 2 shows angular rate data during the period 2004/344 to 2004/359. The 7 hours of data on 2004/350 show a highly anisotropic, short-lived intensity spike. For example, there is a proton anisotropy (S3 – S7)/(S3 + S7) ≈ 0.92 derived from rates counted in sectors 3 and 7 during hour 0900 and an electron anisotropy of ~0.16 during hour 1900. The ions and electrons are streaming sunward along the magnetic field (*18*). Observation of an upstream electron beam coincident with electron plasma oscillations on 2004/350 (*19*) is plausible evidence that the plasma oscillations were being driven by energetic electrons from the TS. This suggests that V1 was very near the TS and traversed a region where the magnetic field was nearly tangent to the TS surface (*19*). V1 Magnetometer (MAG) data show a large jump in field magnitude between 2004/350 and 2004/352 (*20*); this finding suggests that the V1 TS crossing may well have occurred on 2004/351, for which no data exist because of a gap in spacecraft tracking. Plasma oscillations were also observed at four earlier times in 2004, near times of large proton intensity increases (Fig. 1E), which supports our view that LECP particle increases are related to a TS foreshock region.

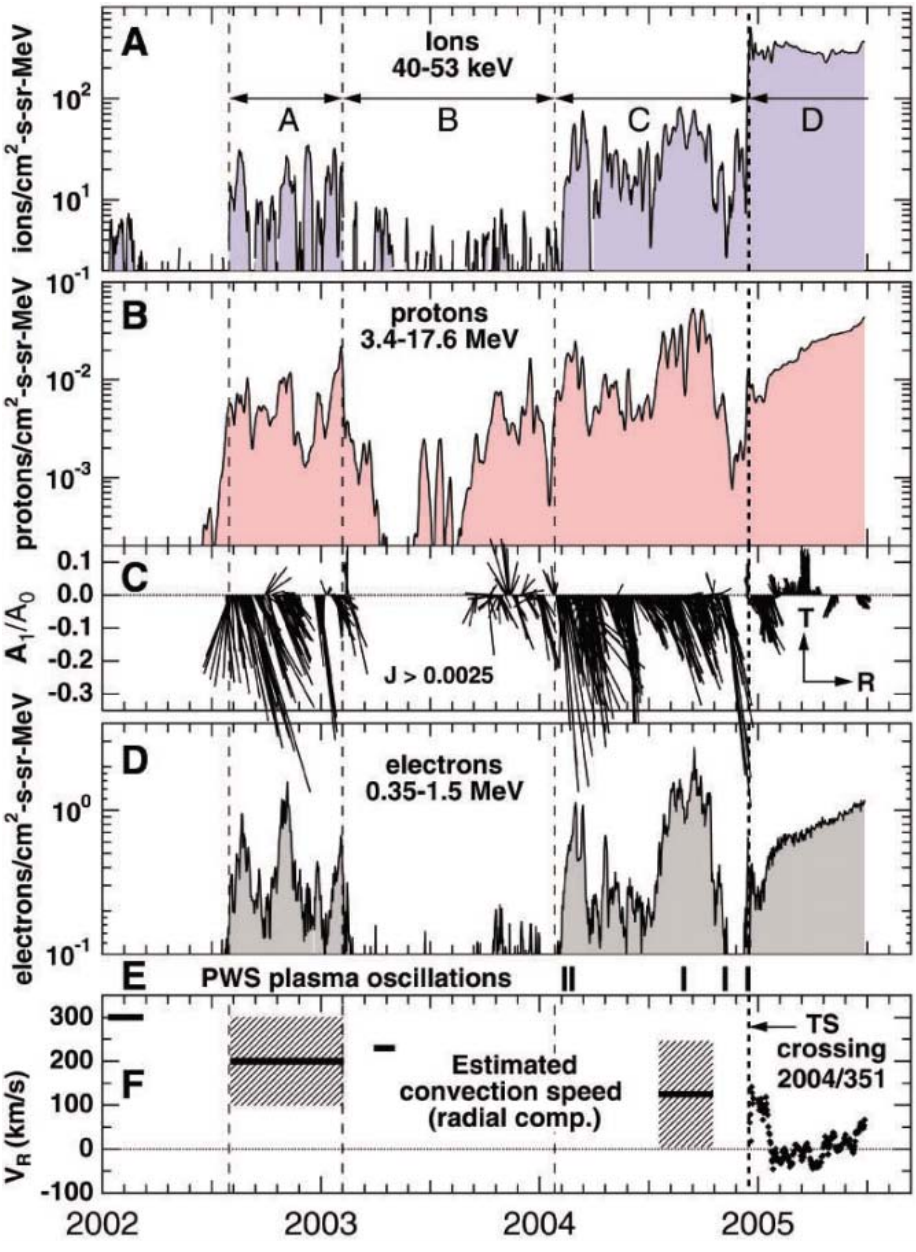

Fig. 1. V1 data during 2002.0 to 2005.5 (83.4 to 96.0 AU). (**A**, **B**, and **D**) Background-corrected, scan-averaged, 5-point smoothed daily-averaged intensities of 40- to 53-keV ions, 3.4- to 17.6-MeV protons, and 0.35- to 1.5-MeV electrons, respectively. (**C**) First-order anisotropy vector $\mathbf{A}_1/A_0$ of proton channel in (B) when its intensity is >0.0025 flux units (inset shows orientation of $\hat{R}$ and $\hat{T}$). Angular data were taken in seven of eight sectors, each of full width 45°, by stepping in the LECP scan plane (Fig. 2A, inset) and accumulating data for 192 s in each sector. Whiskers show the direction that particles are traveling. There are no data from sector 8 because it contains the calibration source. (**E**) Black bars show times when the V1 Plasma Wave (PWS) instrument measured electron plasma oscillations (*4*). (**F**) Estimates of V_R based on 40- to 220-keV ion angular data and velocity extraction algorithm (*9*, *10*). Upper and lower bounds on V_R during period A and the latter half of period C (2004.56 to 2004.78) are indicated by the cross-hatched rectangles and the means by the horizontal bars. V1 Magnetic Field (MAG) daily vector data were used in the velocity extraction algorithm for the period 2004.000 to 2005.164. Horizontal bars during the periods 2002.041 to 2002.172 and 2003.257 to 2003.322 are from Krimigis *et al.* (*11*).

There was a large increase of the 40- to 53-keV ion intensity at the start of period D in Fig. 1A. During period C the intensity varied typically from ~10 to ~40 cm^{-2} s^{-1} sr^{-1} MeV^{-1} (intensity units, iu), reaching occasional peaks of ~80 iu. At the possible TS crossing on 2004/351, the intensity reached a new peak at ~500 iu, dropped, and thereafter was relatively smooth, varying by no more than ±20% about a mean of ~300 iu for the next 6 months. By comparison, the 3.4- to 17.6-MeV proton intensity profile in Fig. 1B has a notably different temporal evolution. The intensity spike on 2004/350 is a factor of ~10 increase relative to the intensity 5 days earlier. On 2005/009 (2005.022) the intensity increased by a factor of 2 within 10 days, and then increased in a relatively smooth exponential manner by a factor of ~4 over the next 0.45 year.

During most of 2004, the normalized anisotropy vector $\mathbf{A}_1/A_0$ had –T and +R components (i.e., streaming outward away from the Sun), with amplitude A_1/A_0 typically ~0.2 to 0.4 (Fig. 1C). From 2004/355 to about 2005/026 (2004.967 to 2005.068), A_1/A_0 decreased from ~0.2 to ~0.1, yet the direction still had –T and +R components. $\mathbf{A}_1/A_0$ changed markedly between 2005/026 and 2005/027; at that time, A_1/A_0 decreased to ~0.03 and the direction reversed (i.e., $\mathbf{A}_1/A_0$ developed a +T component and an R component that fluctuated about zero). This pattern continued until about 2005/105 (2005.285), after which $\mathbf{A}_1/A_0$ varied, starting near zero, then developing small –T and –R components, going to near zero again, and most recently going through a period of small –T and +R components. Qualitatively, such quasi-regular variations of $\mathbf{A}_1/A_0$ are found for all ion channels 40 keV to 20 MeV; quantitatively, there are large energy-dependent differences. Except for the anisotropic shock spike on 2004/350, 0.35- to 1.5-MeV electron intensities remained nearly isotropic, despite frequent, impulsive (~hours) variations in periods A and C, and this isotropy persisted during the exponential recovery after 2005/020 (2005.052) (Fig. 1D).

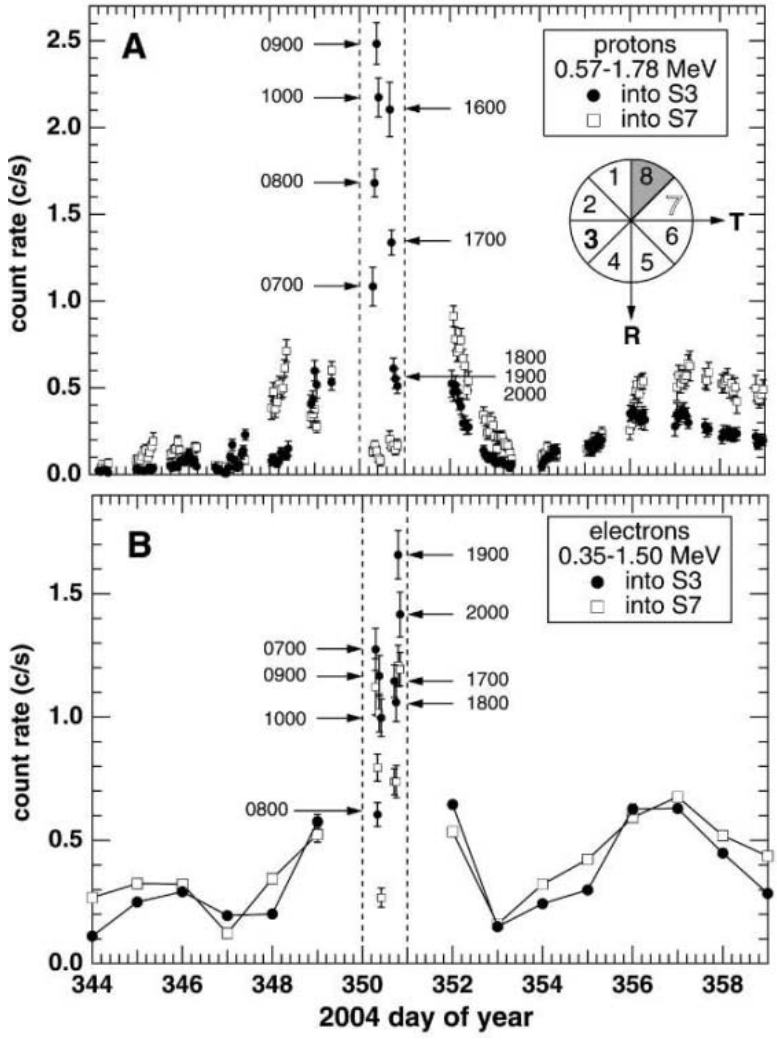

Fig. 2. Angular count rate data during the period 2004/344 to 2004/359 for (**A**) 0.57- to 1.78-MeV protons and (**B**) 0.35- to 1.5-MeV electrons [hourly averaged rates on 2004/350 (dashed vertical lines); daily averages elsewhere]. The inset pie diagram in (A) indicates view directions of the eight 45° sectors in the LECP scan plane, which is nearly parallel to the local R-T plane (*7*). The magnetic field on 2004/350 had a projection onto the LECP scan plane lying nearly on the boundary between sectors 3 and 4 (*18*).

Figure 1F summarizes estimates of V_R from the velocity extraction algorithm (*9*, *10*). In the foreshock region V_R is relatively low, typically within 100 to 300 km s^{-1}. The suggestion of speed reduction with time could be interpreted as a steady slowing of the upstream plasma flow with decreasing distance from the TS, which is consistent with some model predictions (*21*, *22*). There is a large spread in V_R estimates for periods A and C because the radial convective component is very small relative to that of the streaming in the near-azimuthal, antisunward direction during the quasi-recurrent (~26-day) intensity variations that are present in all ion channels. Our original estimate $V_R <$ 50 km s^{-1} during period A was based on a 210-day average and an assumed direction of the average magnetic field (*11*). This value was later revised upward (*23*) to $V_R \approx 200$ km s^{-1}, which agrees well with new estimates based on daily averages (Fig. 1F) (*9*, *10*), when additional background was removed from the lower energy ion channels (*24*) and measured magnetic field azimuths were used. Refinements of the flow-extraction algorithm, including effects such as statistical uncertainties in the magnetic field (*24*), are ongoing.

Estimation of V_R during period D was facilitated by the much higher particle intensities and the weaker anisotropies. Within 5 to 6 days after the possible TS crossing (2004/356–357), V1 began measuring $V_R \approx +100$ km s^{-1}, which continued for 27 to 28 days, until 2005/017 (2005.045), when V_R decreased rapidly (within 5 days), and during 2005/024 to 2005/110 (2005.063 to 2005.300) V_R fluctuated between –50 and 0 km s^{-1}. From about 2005/110 to 2005/163 (2005.300 to 2005.444), $V_R \approx 0$ to +30 km s^{-1}. V_R increased again around 2005/163, and since then $V_R \approx +40$ to +50 km s^{-1} until at least 2005/179. The HS flow velocity has three components, so we may be neglecting flow in the T-N plane by assuming that $V = V_R$ only. Nonetheless, the patterns in the temporal evolution of V_R should be representative of the complete velocity vector. Excursions of V_R from positive to negative and back over a period of ~90 to 140 days could result if V1 were in varying plasma flow downstream of an inwardly moving TS. Then V1 would essentially be sampling the same parcel of plasma for an extended period (*25*).

On the basis of three sets of observations—(i) the sunward ion and electron beams on 2004/350; (ii) markedly reduced particle intensity variations, reduced ion beaming anisotropies, and increased low-energy ion intensities throughout period D; and (iii) the ~120-day stretch in 2005 when V_R fluctuated

about zero—we conclude that V1 was crossed by the TS on 2004/251, evidently as the TS moved radially inward in response to a decrease in solar wind ram pressure (*26*), and that V1 has remained in the HS until at least 2005/179. These conclusions are consistent with those reported by other V1 instrument teams using independent measurements (*2–4*, *19*, *20*, *27*).

Energy spectra in the HS are of interest to studies of acceleration processes. Figure 3 combines ion rate and composition data averaged over a 160-day period in the HS. Anomalous cosmic rays (ACRs) are thought to originate when interstellar neutral atoms, including H, He, and O, are ionized and picked up by the solar wind, convected to the TS, and there accelerated to ~1 to 100 MeV nuc^{-1} (*28–32*). The finite extent of the TS will cause the power-law ACR spectrum to fold over beyond ~100 to 200 MeV (*33*). Ions in the energy range 40 keV to ~20 MeV in Fig. 3, although well fit by a power law with index –1.67, are not ACRs per se, but a separate low-energy population. The high-energy ACRs, which have been extensively modeled (*30–32*), continue to show intensity modulation below 100 MeV (25 MeV nuc^{-1} He, 6.25 MeV nuc^{-1} O). This is puzzling because these data were taken in the near post-TS region, at the expected acceleration site of high-energy ACRs.

The 0.04- to ~20-MeV portion of the spectrum in Fig. 3 may not necessarily be the product of diffusive shock acceleration. Gloeckler *et al*. (*34*) used a simple model in which pickup proton distributions measured at Ulysses (1.6 to 5.4 AU) are extrapolated to 95 AU and heated at the TS. They argue that the postshock LECP protons up to ≥10 MeV are accelerated pickup ions (as presumably would be the He and O), and that up to 80% of the energy available from the solar wind ram pressure can heat and accelerate pickup ions at the TS. The inset of Fig. 3 shows the pickup proton distribution for predicted post-TS pickup proton density N = 0.0008 cm^{-3} and thermal speed V_{th} = 328 km s^{-1}, with the high-energy power-law slope κ = –1.63 and small flow speed V_R = 28 km s^{-1} determined by fitting the 0.04- to 4.0-MeV ion data (*34*). Another implication can be drawn from the low-energy ion energy spectra. Krimigis *et al*. (*35*) found that the plasma beta (ratio of particle pressure to magnetic field pressure) calculated using the pressure in 0.04- to 4.0-MeV ions and the measured magnetic field was >1 from 2002.5 to 2003.1, and also from 2004.0 to 2005.5 based on extrapolated 2002 magnetic field data (*9*).

Figure 4 is a conceptual overview, based on the V1 observations, that synthesizes the TS region and the semi-permanent population of precursor energetic particles that thread its foreshock region and whose propagation, and possibly origin, are controlled by processes in the HS region. The inner boundary (dashed green curve) marks the region ~10 to 15 AU in width that is filled with TS foreshock energetic ions and electrons, extending in energy from a few tens of keV to tens of MeV. Within the inner boundary, large antisunward, unidirectional anisotropies (short black arrows) have large –T components and smaller +R components [as discussed earlier, the origin of the –T streaming may be related to global TS geometry; however, the origin of the +R component (see Fig. 1C) cannot be due entirely to convection, even if the full solar wind velocity of 400 km s^{-1} were assumed (*11*)]. Within the inner boundary, V_R (yellow arrows) slows compared to a typical value of 400 km s^{-1} in the inner heliosphere, and across the TS (thick solid green curve) V_R is reduced further. The shortest radially outward yellow flow vector and the short black arrows within the transition region across the TS denote the roughly 28-day period of ~100 km s^{-1} flow (Fig. 1F) and of ion anisotropy vectors with reduced lengths, but with directions similar to those observed in the foreshock

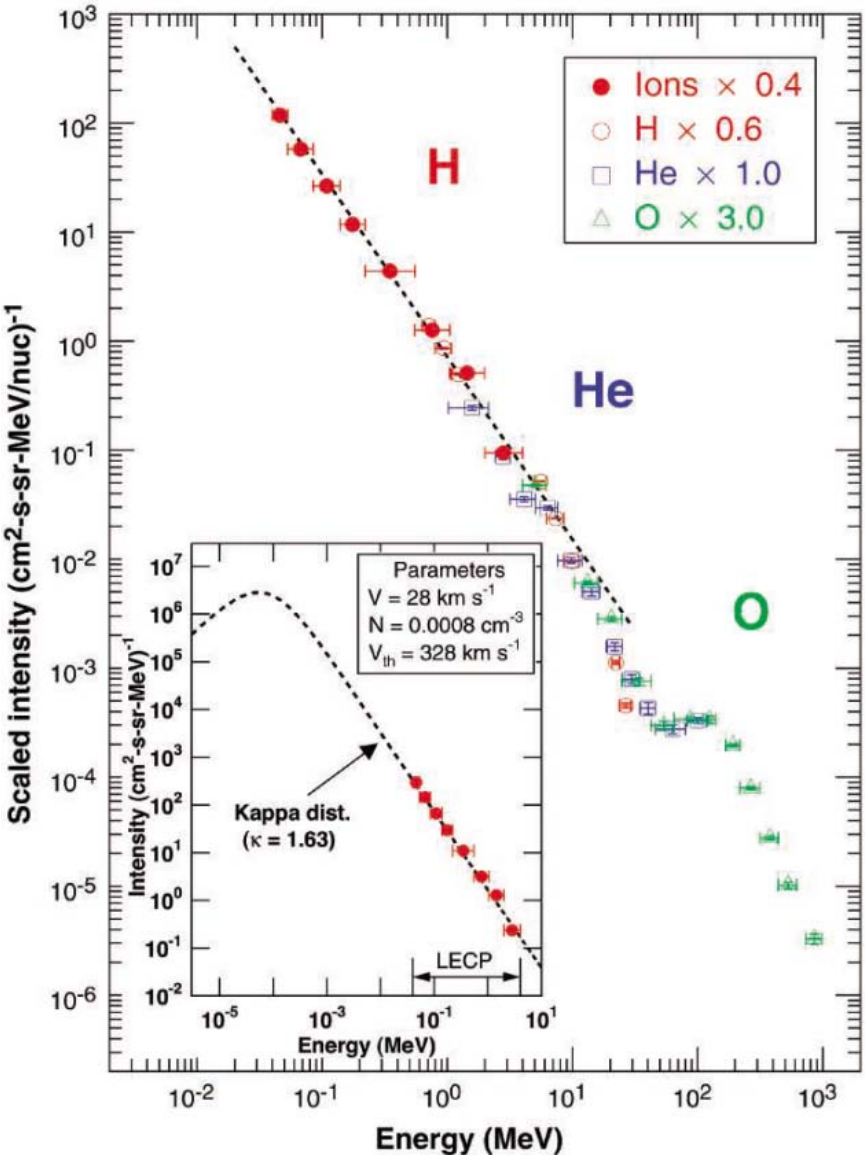

Fig. 3. V1 LECP ion rate channel data and multidetector elemental composition data over the 160-day period 2004/352 to 2005/144. Solid red circles, ion (assumed to be proton) intensities from eight ion channels 0.04 to 4.0 MeV (denoted Ions); open red circles, H; open blue squares, He ions; open green triangles, O ions. The four spectra (Ions, H, He, and O ions) were scaled vertically to construct a single spectrum. Scaling factors are Ions × 0.4, H × 0.6, He × 1.0, and O × 3.0. The dashed line is a power-law of slope –1.67 fit through points 0.04 to 20 MeV. Inset shows convected κ-distribution (dashed curve) that results from a model in which pickup proton distributions observed at Ulysses are extrapolated to 95 AU and heated at the TS (*34*). Fit parameters are the predicted pickup proton density N = 0.0008 cm^{-3} and thermal speed V_{th} = 328 km s^{-1}, and the high-energy power-law slope κ = –1.63 and small flow speed V = 28 km s^{-1} needed to fit the 0.04- to 4.0-MeV ion intensities (solid symbols) that are replotted, unscaled from the main panel (*34*).

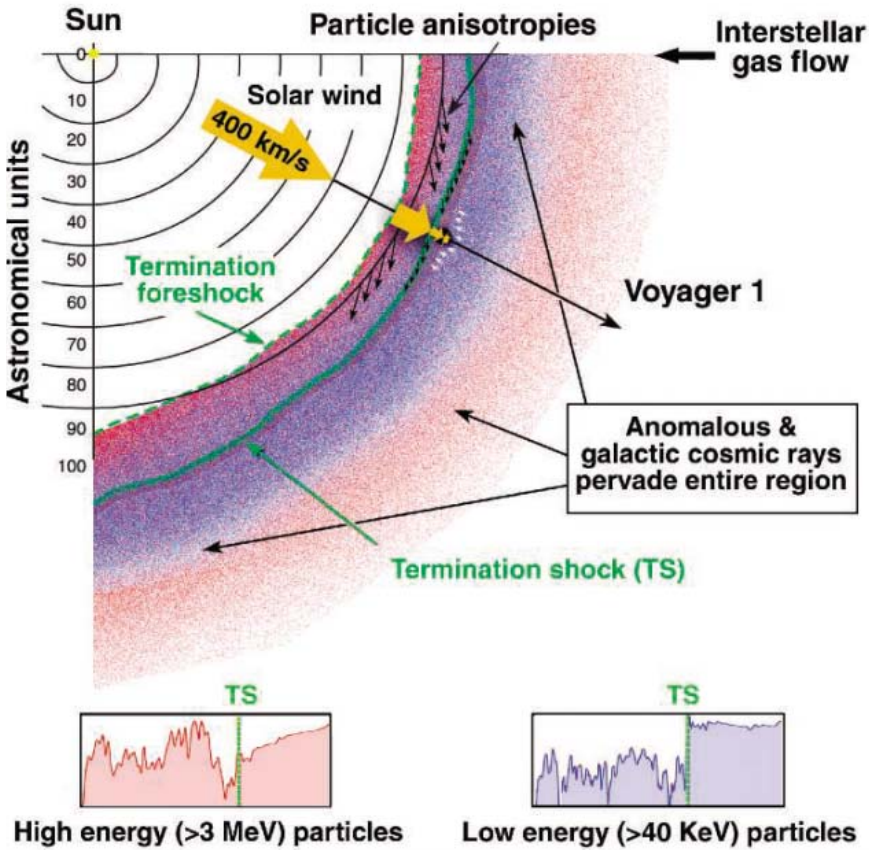

Fig. 4. Conceptual overview of the current picture, based on the V1 data. Viewpoint is that of an observer looking down on the heliosphere from above (solar spin axis vector out of the page), and scales are intended to be illustrative. The Sun is at the origin, the radial path of V1 at N34° is indicated by the long black arrow, and the direction of inflow of the interstellar gas is indicated by the heavy black arrow. Colored shading suggests relative intensities and spatial distributions of high-intensity, low-energy ions (blue); medium-intensity, medium-energy ions (red); and low-intensity, high-energy ions (i.e., anomalous and galactic cosmic rays) (pink). Temporal profiles of the first two populations through the TS foreshock and well into the HS, based on the V1 data (Fig. 1, A and B), are illustrated in the two lower panels.

(Fig. 1C). Then V_R reverses (sunward short yellow arrow) and ion anisotropies develop –R components (small white arrows). The spherical distribution of galactic and anomalous cosmic rays sketched in Fig. 4 can only be regarded, for now, as the simplest possible configuration; given the complexities of the energetic particle precursor and the foreshock region, the cosmic ray distribution may vary along the TS. In fact, the novel properties of this TS observed in a space plasma demand new theoretical explanations, not only for the in situ measurements, but also to provide a theoretical basis for extrapolating from the V1 measurements to the global nature of this vast structure.

References and Notes

1. S. M. Krimigis *et al.*, *Space Sci. Rev.* **21**, 329 (1977).
2. E. C. Stone *et al.*, *Science* **309**, 2017 (2005).
3. L. F. Burlaga *et al.*, *Science* **309**, 2027 (2005).
4. D. A. Gurnett, W. S. Kurth, *Science* **309**, 2025 (2005).
5. G. P. Zank, *Space Sci. Rev.* **89**, 413 (1999).
6. E. C. Stone, *Science* **293**, 55 (2001).
7. The RTN system is a local Cartesian system with unit vectors $\hat{R}$ radially outward from the Sun, $\hat{T}$ in the direction of normal planetary motion, and $\hat{N} = \hat{R} \times \hat{T}$.
8. Spacecraft-frame intensities are represented by a second-order Fourier series in the scan angle $0 \leq \phi < 2\pi$,
$$j(\phi) = A_0 + A_1 \cos(\phi - \phi_1) + A_2 \cos[2(\phi - \phi_2)] \quad (1)$$
Parameter A_0, $\mathbf{A}_1 = (A_1, \phi_1)$, and $\mathbf{A}_2 = (A_2, \phi_2)$ are determined by a least-squares fit to intensities in sectors 1 to 7. In Fig. 1C, the direction of each whisker $\mathbf{A}_1/A_0$ is determined from ϕ_1.
9. S. M. Krimigis *et al.*, in *Proceedings of Solar Wind 11/SOHO 16 Conference: Connecting Sun and Heliosphere*, Whistler, Canada, 12 to 17 June 2005.
10. Estimating convection velocities from angular data taken in the spacecraft frame (K) is complicated by the presence of large, nonconvective anisotropies in all the low-energy ion channels. To allow for such anisotropies, we assume that the directional intensity in the flow frame (K'), which moves with flow velocity $\mathbf{V}$ relative to frame K, is gyrotropic and well represented by the first three terms of the Fourier-Legendre series
$$j'(v', \mu') = a_0(v') + a_1(v')\mu' + a_2(v')(3\mu'^2 - 1)/2 \quad (2)$$
where $v' = |\mathbf{v}'|$ is the particle speed, and $\mu' = (\mathbf{v}' \cdot \mathbf{B})/|\mathbf{v}'||\mathbf{B}|$ is the cosine of the pitch angle between $\mathbf{v}'$ and the magnetic field vector $\mathbf{B}$. Our flow-extraction technique is different from that used by Krimigis *et al.* (*11*). However, our rationale for neglecting a transverse diffusive anisotropy in the region upstream of the TS remains the same (*11*). In the HS, the radial gradients are insufficient to produce a transverse diffusive anisotropy that is comparable to the convective anisotropy, even if the plasma velocity is as little as 50 km s^{-1}. We express $\mathbf{V}$ in terms of its magnitude and direction (in RTN coordinates) as $\mathbf{V} = (V, \theta_V, \phi_V)$, treating V, θ_V, and ϕ_V as parameters. We then obtain an expression for the directional particle intensity in frame K, $j(v, \mu, \varphi)$, in terms of particle speed $v = |\mathbf{v}|$, pitch cosine μ, and gyrophase φ by performing the transformations $j/v^2 = j'/v'^2$, $v' = v'(v, \mu, \varphi)$, and $\mu' = \mu'(v, \mu, \varphi)$. The best-fit flow velocity in the K frame can then be determined by comparing the expression for $j(v, \mu, \varphi)$ with the measured angular intensities of a given ion energy channel, and then applying nonlinear least-squares techniques. When measured vector magnetic field data are folded into the calculation, best-fit values for V, θ_V, and ϕ_V can be determined iteratively. The magnetic field component out of the LECP scan plane is correctly included in the flow extraction procedure when field data are used. Here, we simplified the technique by assuming that only the radial component V_R of the flow velocity is nonzero ($\theta_V = 90°$, $\phi_V = 0°$).
11. S. M. Krimigis *et al.*, *Nature* **426**, 45 (2003).
12. F. B. McDonald *et al.*, *Nature* **426**, 48 (2003).
13. R. B. Decker *et al.*, in *Physics of the Outer Heliosphere, Third International IGPP Conference*, V. Florinski, N. V. Pogorelov, G. P. Zank, Eds. (AIP Conference Proceedings 719, American Institute of Physics, Melville, NY, 2004), pp. 150–155.
14. J. R. Jokipii, J. Giacalone, J. Kota, *Astrophys. J.* **611**, L141 (2004).
15. E. C. Stone, *Eos* **85**, abstract SH41B-01 (2004).
16. N. F. Ness *et al.*, *Eos* **85**, abstract SH41B-02 (2004).
17. R. B. Decker, *Eos* **86**, abstract SH22A-02 (2005).
18. L. F. Burlaga, personal communication, May 2005.
19. D. A. Gurnett, W. S. Kurth, *Eos* **86**, abstract SH22A-05 (2005).
20. L. F. Burlaga *et al.*, *Eos* **86**, abstract SH22A-03 (2005).
21. J. A. le Roux *et al.*, *Geophys. Res. Lett.* **27**, 2873 (2000).
22. G. Gloeckler, J. Geiss, L. A. Fisk, in *Physics of the Outer Heliosphere, Third International IGPP Conference*, V. Florinski, N. V. Pogorelov, G. P. Zank, Eds. (AIP Conference Proceedings 719, American Institute of Physics, Melville, NY, 2004), pp. 201–206.
23. R. B. Decker *et al.*, *Eos* **85**, abstract SH41B-03 (2004).
24. M. Zhang, *Astrophys. J.* **624**, 1038 (2005).
25. J. R. Jokipii, *Astrophys. J.*, in press.
26. J. D. Richardson *et al.*, in *Proceedings of Solar Wind 11/SOHO 16 Conference: Connecting Sun and Heliosphere*, Whistler, Canada, 12 to 17 June 2005.
27. E. C. Stone, *Eos* **86**, abstract SH22A-01 (2005).
28. A. C. Cummings, E. C. Stone, *Space Sci. Rev.* **83**, 51 (1998).
29. A. C. Cummings, E. C. Stone, C. D. Steenberg, *Astrophys. J.* **578**, 194 (2002).
30. J. R. Jokipii, J. Giacalone, *Space Sci. Rev.* **83**, 123 (1998).
31. J. R. Jokipii, in *Acceleration and Transport of Energetic Particles Observed in the Heliosphere: ACE 2000 Symposium*, R. A. Mewaldt *et al.*, Eds. (AIP Conference Proceedings 528, American Institute of Physics, Melville, NY, 2000), pp. 309–316.
32. H. Fichtner, *Space Sci. Rev.* **95**, 639 (2001).
33. V. Florinski, J. R. Jokipii, *Astrophys. J.* **591**, 454 (2003).
34. G. Gloeckler, L. A. Fisk, L. J. Lanzerotti, in *Proceedings of Solar Wind 11/SOHO 16 Conference: Connecting Sun and Heliosphere*, Whistler, Canada, 12 to 17 June 2005.
35. S. M. Krimigis *et al.*, in *Physics of the Outer Heliosphere, Third International IGPP Conference*, V. Florinski, N. V. Pogorelov, G. P. Zank, Eds. (AIP Conference Proceedings 719, American Institute of Physics, Melville, NY, 2004), pp. 133–155.
36. Work at the Johns Hopkins University Applied Physics Laboratory was supported by the Voyager Interstellar Mission under NASA grant NNG04GN62G. We thank L. F. Burlaga and N. F. Ness for providing Voyager 1 MAG data and D. A. Gurnett for providing Voyager 1 PWS data, both before publication.

18 July 2005; accepted 18 August 2005
10.1126/science.1117569

Electron Plasma Oscillations Upstream of the Solar Wind Termination Shock

D. A. Gurnett* and W. S. Kurth

Electron plasma oscillations have been detected upstream of the solar wind termination shock by the plasma wave instrument on the Voyager 1 spacecraft. These waves were first observed on 11 February 2004, at a heliocentric radial distance of 91.0 astronomical units, and continued sporadically with a gradually increasing occurrence rate for nearly a year. The last event occurred on 15 December 2004, at 94.1 astronomical units, just before the spacecraft crossed the termination shock. Since then, no further electron plasma oscillations have been observed, consistent with the spacecraft having crossed the termination shock into the heliosheath.

Electron plasma oscillations, also known as Langmuir waves, are one of the oldest known and most widely studied of all plasma wave phenomena (*1*). For many years it has been known that electron plasma oscillations are generated ahead of planetary bow shocks by energetic electrons escaping into the solar wind upstream of the shock (*2*–*7*). This close relationship led Kurth and Gurnett (*8*) to predict that electron plasma oscillations would be present upstream of the solar wind termination shock. Here, we report the initial observations of these waves.

Electron plasma oscillations are electrostatic oscillations that occur at a characteristic frequency of the plasma known as the electron plasma frequency. The electron plasma frequency is given by $f_p = 8980\sqrt{n_e}$ Hz, where n_e is the electron density in cm^{-3} (*9*). Of the various mechanisms that can excite electron plasma oscillations, an electron beam is one of the most effective. According to the well-known theory of beam-plasma interactions (*10*), electron plasma oscillations are generated whenever the electron velocity distribution has a region of positive slope, $\partial f/\partial v_{\parallel} > 0$. If the region of positive slope occurs at velocities well above the electron thermal velocity, the resulting feature is called a beam. At planetary bow shocks electrons heated at the shock escape upstream into the solar wind along the solar wind magnetic field lines. Although the electron velocity distribution initially may not have a region of positive slope, time-of-flight considerations dictate that only those electrons with velocities greater than a well-defined cutoff velocity can reach a point in the upstream region (*11*). The existence of this velocity cutoff assures that the velocity distribution function has a region of positive slope, thereby establishing the necessary conditions for the growth of electron plasma oscillations (*12*). Because the solar wind magnetic field lines are in contact with a planetary bow shock only over a limited region, beams can only occur in a well-defined region upstream of the shock. This region is known as the electron foreshock. The upstream boundary of the electron foreshock is determined by magnetic field lines tangent to the nose of the shock.

Because the solar wind magnetic field lines are wound into an Archimedes spiral by the rotation of the Sun (*13*), electrons accelerated at the termination shock are expected to escape into the upstream region (Fig. 1). Although electrons can escape into the region upstream of the shock, this idealized configuration does not automatically lead to a region of positive slope in the distribution function of the escaping electrons. For a region of positive slope to develop, the geometry must be such that some of the magnetic field lines are tangent to the shock surface so that the time-of-flight mechanism can operate, similar to the mechanism that occurs at planetary bow shocks. Because the shock surface is unlikely to be smooth and irregularities are almost certainly present in the solar wind magnetic field direction, there are good reasons to believe that such tangent field regions will occur. The main uncertainty is how far beams with regions of positive slope, $\partial f/\partial v_{\parallel} > 0$, can propagate into the upstream region. Because of the complicated physics involved in beam-plasma interactions, it is very difficult to estimated this propagation distance. Kurth and Gurnett (*8*) suggest that it could range anywhere from a small fraction of an astronomical unit (AU) to several AU.

Previous observations (*3*–*6*) have demonstrated that the Voyager plasma wave instrument is easily capable of detecting electron plasma oscillations. The instrument uses an electric dipole antenna to detect the electric field of plasma waves and radio waves (*14*).

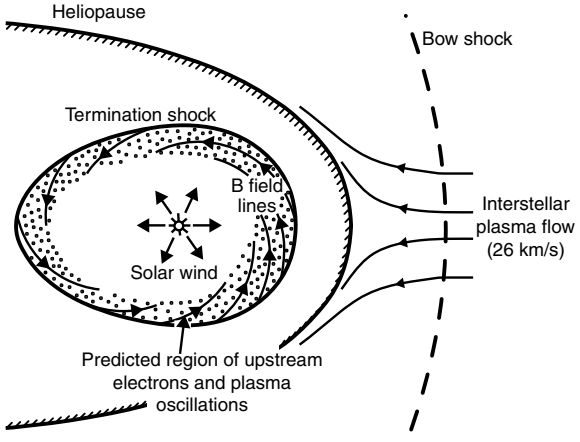

Fig. 1. An idealized conceptual drawing showing the key boundaries that are expected to occur in the outer heliosphere. On the basis of observations of planetary bow shocks, electrons accelerated at the termination shock are expected to form a beam, indicated by the shading, that streams inward along the solar wind magnetic field lines toward the Sun. This beam is expected to excite electrostatic oscillations, called electron plasma oscillations, via a process known as a beam-plasma instability (*8*). The radial thickness of the region where the electron plasma oscillations are expected to occur is greatly exaggerated in this drawing.

Table 1.

Date 2004	Day of year 2004	Radial distance (AU)	Frequency (Hz)	Maximum intensity (μV/m)
11–15 February	042–043	91.0	311	2.0
23–26 February	054–057	91.1	311	1.2
29 August–1 September	242–245	93.0	562	1.1
6–7 November	311–312	93.7	311	1.3
8 December	343	94.0	178	1.3
15 December	350	94.1	178–311	1.7

Department of Physics and Astronomy, University of Iowa, Iowa City, IA 52242, USA.

*To whom correspondence should be addressed. E-mail: donald-gurnett@uiowa.edu

Two types of data are obtained: low-rate electric field spectrum measurements in 16 logarithmically spaced frequency channels from 10 Hz to 56 kHz and high-rate waveform measurements from 50 Hz to 10 kHz. Because only about 1 min of waveform data is obtained per week, whereas the spectrum analyzer data are typically obtained for about 11 to 13 hours per day for Voyager 1 and 7 to 10 hours per day for Voyager 2, the search for electron plasma oscillations associated with the termination shock is best conducted with the use of low-rate spectrum analyzer data. These data provide one electric field spectrum every 16 s. To interpret the data, care must be taken to filter out various types of spacecraft-generated interference that are present, particularly in the lower frequency channels. Once the interference signals are filtered out, electron plasma oscillations can be easily identified by their bursty narrowband characteristics, usually consisting of an emission in a single channel at or near the electron plasma frequency. Occasionally when the electron plasma frequency is between two adjacent filter channels a response is observed in the two adjacent channels. To a good approximation, the electron plasma frequency in the solar wind is given by f_p = 25,000/R Hz, where R is the heliocentric radial distance in AU. Variations of up to a factor of 2 can be expected from this average value.

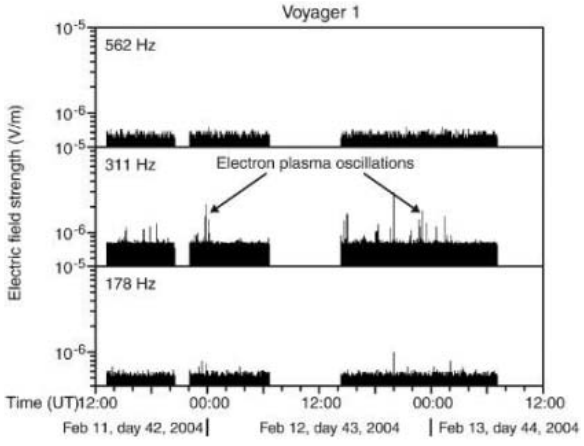

Fig. 2. The electric field intensity observed in the 178, 311, and 562 Hz channels of the Voyager 1 plasma wave instrument on 11 to 15 February 2004, at a radial distance from the Sun of 91.0 AU. The many short impulsive intensity spikes in the 311 Hz channel are plasma oscillations. After many years in which no clear electron plasma oscillation events were observed by Voyager 1 or 2, these are the first observations of plasma oscillations that could possibly be associated with the termination shock. From the equation $f_p = 8980\sqrt{n_e}$, it can be shown that a plasma oscillation frequency of 311 Hz corresponds to an electron density of $n_e = 1.2 \times 10^{-3}$ cm^{-3}. This density is consistent with the nominal electron densities expected in the solar wind at 91 AU.

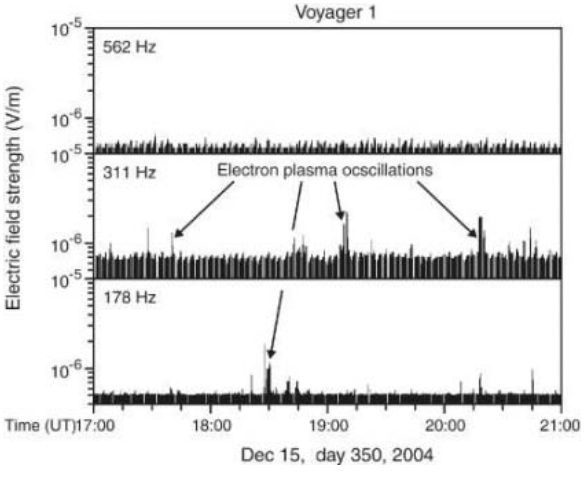

Fig. 3. The electric field intensity of electron plasma oscillations observed late in the day on 15 December 2004, just before crossing of the termination shock at 94.1 AU. This event is coincident with a highly anisotropic 0.35 to 1.5 MeV electron beam detected by the LECP instrument (*17*). The plasma oscillations observed during this event again occur in short bursts, with durations of a few minutes or less, very similar to the 11 to 15 February 2004 event (Fig. 2). Note that the plasma oscillation frequency shifts down to 178 Hz briefly at about 18:30 UT. This frequency shift indicates that the electron density decreased from about 1.2×10^{-3} cm^{-3} to about 3.9×10^{-4} for a short time around 18:30 UT.

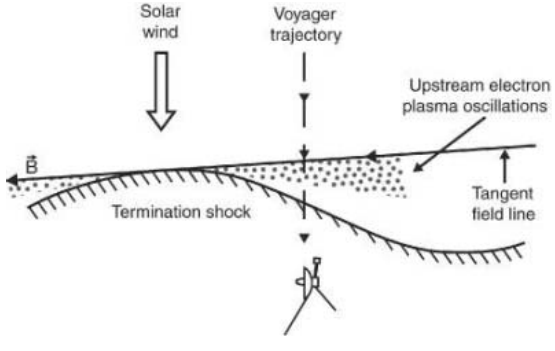

Fig. 4. The detection of a highly anisotropic electron beam by the LECP instrument just ahead of the termination shock that is coincident with the electron plasma oscillations observed on 15 December suggest that the spacecraft passed through a region (shown shaded) where the solar wind magnetic field is nearly tangent to the shock. From time-of-flight considerations it can be shown that very high beam velocities are to be expected in this region, thereby producing conditions favorable for generating electron plasma oscillations (*11*).

In the outer region of the heliosphere, beyond about 10 AU, electron plasma oscillations are almost never observed, except near planetary flybys and occasionally in association with interplanetary shocks (*8*, *15*). The first evidence of electron plasma oscillations possibly associated with the termination shock occurred from 11 to 15 February 2004, when a series of sporadic narrowband emissions was detected in the 311 Hz channel of the Voyager 1 spectrum analyzer at a heliospheric radial distance of 91.0 AU. A plot of the electric field intensities observed during a portion of this event is shown in Fig. 2. The plasma oscillations are spiky and sporadic, as is often the case for such emissions. The frequency of these emissions is almost exactly the frequency expected for electron plasma oscillations at 91 AU, which, by using the formula given above, is 288 Hz. Subsequently, five more events were detected, all by Voyager 1 (Table 1). The last of these events (Fig. 3) occurred on 15 December 2004, at a heliocentric radial distance of 94.1 AU. This event occurred just before the crossing of the termination shock, as identified by the Voyager 1 magnetic field (*16*) and energetic particle (*17*, *18*) instruments. The termination shock crossing is believed to have occurred during a data gap that extended from about 21:05 universal time (UT) on 15 December 2004 to 01:54 UT on 17 December 2004.

Several arguments can be made that the electron plasma oscillations listed in Table 1 are associated with the solar wind termination shock. First, these events are all unusual. No clear examples of electron plasma oscillations comparable to those in Figs. 2 and 3 have been observed in the Voyager 1 data for many years; the last was in association with an interplanetary shock that occurred on 14 September 1991. Also, no comparable events have been detected by Voyager 2, which is closer to the Sun, now at about 77 AU. Second, the frequencies and electric field intensities, typically a few hundred Hz and a few microvolts per meter, are consistent with the predicted plasma frequencies and electric field intensities (*8*). Third, all of the events occurred within about 3 AU of the radial distance at which the termination shock was observed, i.e., from 91.0 to 94.1 AU, and the rate of oc-

currence increased as the distance to the shock decreased. On the basis of these observations one could estimate that the radial thickness of the plasma oscillation region is about 3 AU. However, from Voyager 2 solar wind pressure measurements (*19*) it is known that the solar wind pressure at Voyager 1 was increasing during a substantial portion of the period when the plasma oscillations were being observed, from about mid-2001 to mid-2004. Therefore, it seems likely that the termination shock was moving outward from the Sun, possibly at the same rate as the spacecraft during the early part of this period, so the thickness of the region may be substantially less than 3 AU. Fourth, no further electron plasma oscillation events have been observed by Voyager 1 after 15 December 2004, consistent with a crossing of the termination shock on or about 16 December 2004.

The evidence that the electron plasma oscillations observed by Voyager 1 are associated with the termination shock is particularly compelling for the event that occurred on 15 December 2004. At the time of this plasma oscillation event, the low energy charged particle instrument (LECP) detected an intense highly anisotropic beam of 0.35 to 1.5 MeV electrons streaming away from the termination shock into the upstream region; see figure 2 in Decker *et al*. (*17*). This observation of an upstream electron beam coincident with the electron plasma oscillations provides strong evidence that the plasma oscillations are being driven by an energetic electron beam from the termination shock, exactly as predicted by Kurth and Gurnett (*8*). In analogy with planetary bow shocks, we suggest that just before passing through the termination region the spacecraft passed through a region where the magnetic field is nearly tangent to the surface of the shock, as illustrated in Fig. 4. The tangent field condition could be caused either by waviness of the shock boundary or by irregular variations in the magnetic field geometry. This interpretation is consistent with studies of the Earth's foreshock that show that the highest beam energies are produced near the tangent field line and that the most intense electron plasma oscillations are observed in this region (*11*). The sporadic bursty electric field intensity variations evident in Fig. 3 could be due to either time variations in the tangent field line configuration or nonlinear effects, both of which are known to occur at planetary bow shocks. We also note that the electron plasma oscillations occurred during a period when the LECP was observing large fluxes of anisotropic energetic (3.4 to 17.6 MeV) protons arriving from the shock. Although these protons are unlikely to be responsible for generating the plasma oscillations, they do provide further evidence that the spacecraft was in the region immediately upstream of the shock when the plasma oscillations were observed.

References and Notes

1. L. Tonks, I. Langmuir, *Phys. Rev.* **33**, 195 (1929).
2. F. L. Scarf, R. W. Fredricks, L. A. Frank, M. Neugebauer, *J. Geophys. Res.* **76**, 5162 (1971).
3. F. L. Scarf, W. W. L. Taylor, I. M. Green, *Science* **203**, 748 (1979).
4. F. L. Scarf, D. A. Gurnett, W. S. Kurth, *Science* **204**, 991 (1979).
5. D. A. Gurnett, W. S. Kurth, F. L. Scarf, *Science* **212**, 235 (1981).
6. D. A. Gurnett, W. S. Kurth, F. L. Scarf, R. L. Poynter, *Science* **233**, 106 (1986).
7. D. A. Gurnett *et al.*, *Science* **246**, 1494 (1989).
8. W. S. Kurth, D. A. Gurnett, *J. Geophys. Res.* **98**, 15,129 (1993).
9. T. H. Stix, *The Theory of Plasma Waves* (McGraw-Hill, New York, 1962), p. 10.
10. D. A. Gurnett, A. Bhattacharjee, *Introduction to Plasma Physics* (Cambridge Univ. Press, Cambridge, 2005), pp. 328–330.
11. P. C. Filbert, P. J. Kellogg, *J. Geophys. Res.* **84**, 1369 (1979).
12. I. H. Cairns, *J. Geophys. Res.* **92**, 2329 (1987).
13. A. J. Hundhausen, *Coronal Expansion and Solar Wind* (Spinger-Verlag, Berlin, 1972), pp. 11–14.
14. F. L. Scarf, D. A. Gurnett, *Space Sci. Rev.* **21**, 5162 (1977).
15. M. J. Reiner, R. G. Stone, J. Fainberg, in *Solar Wind Seven*, E. Marsch, R. Schwenn, Eds. (Pergamon, New York, 1992), p. 657.
16. L. F. Burlaga *et al.*, *Science* **309**, 2027 (2005).
17. R. B. Decker *et al.*, *Science* **309**, 2020 (2005).
18. E. C. Stone *et al.*, *Science* **309**, 2017 (2005).
19. J. D. Richardson *et al.*, *J. Geophys. Res.*, in press.

20. We thank E. C. Stone, L. F. Burlaga, N. F. Ness, R. B. Decker, and S. M. Krimigis for discussions and L. J. Granroth for help in developing the computer algorithms necessary to identify and eliminate spacecraft interference from the plasma wave electric field data. The research at the University of Iowa was supported by NASA through contract 959193 with the Jet Propulsion Laboratory, Pasadena, CA.

14 July 2005; accepted 12 August 2005
10.1126/science.1117425

REPORT

Crossing the Termination Shock into the Heliosheath: Magnetic Fields

L. F. Burlaga,[1]* N. F. Ness,[2] M. H. Acuña,[1] R. P. Lepping,[1] J. E. P. Connerney,[1] E. C. Stone,[3] F. B. McDonald[4]

Magnetic fields measured by Voyager 1 show that the spacecraft crossed or was crossed by the termination shock on about 16 December 2004 at 94.0 astronomical units. An estimate of the compression ratio of the magnetic field strength *B* (± standard error of the mean) across the shock is $B_2/B_1 = 3.05 \pm 0.04$, but ratios in the range from 2 to 4 are admissible. The average *B* in the heliosheath from day 1 through day 110 of 2005 was 0.136 ± 0.035 nanoteslas, ~4.2 times that predicted by Parker's model for *B*. The magnetic field in the heliosheath from day 361 of 2004 through day 110 of 2005 was pointing away from the Sun along the Parker spiral. The probability distribution of hourly averages of *B* in the heliosheath is a Gaussian distribution. The cosmic ray intensity increased when *B* was relatively large in the heliosheath.

The existence of a shock at which a stellar wind makes a transition from a relatively cool supersonic flow to a hot subsonic flow was suggested by Weymann (*1*). In the solar wind, this shock is called the termination shock (TS), and the subsonic region between the TS and the boundary with the interstellar medium is called the heliosheath (*2*, *3*). A formula for the position of the TS in the solar wind was given by Parker (*4*). Observations of intense fluxes of energetic particles from 2002 to 2003 (which continued into 2004) suggested that Voyager 1 (V1), at ≈85 astronomical units (AU), was close to the TS (*5*). It was alleged that V1 actually crossed the TS into the heliosheath in mid-2002 (*6*), but this interpretation was not supported by the magnetic field observations (*7*, *8*). This Report and new observations described in this issue (*9*–*11*) indicate that V1 first crossed the TS on about 16 December 2004.

We discuss the V1 magnetic field observations from day 1 of 2004 (2004/001), through 2005/110. During this interval, V1 was at 34°N moving from 90.6 to 95.2 AU radially away from the Sun, and solar activity was decreasing. We believe that the TS was moving toward the Sun and V1 during this interval because the solar wind pressure and speed were decreasing (*12*–*18*). Predictions of the compression ratio B_2/B_1 across the TS (*19*–*21*) varied between ≈2 and ≈3.5. Whang *et al*. (*18*) calculated that this ratio would be ≈3.0 ± 0.2 if the TS were moving inward.

The magnetic field instrument on V1 (*22*) has two identical triaxial sensors mounted on a 13-m boom. The output of each magnetic field

[1]NASA-Goddard Space Flight Center, Greenbelt, MD 20771, USA. [2]The Catholic University of America, Washington, DC 20064, USA. [3]California Institute of Technology, Pasadena, CA 91109, USA. [4]Institute for Physical Science and Technology, University of Maryland, College Park, MD 20742, USA.

*To whom correspondence should be addressed. E-mail: Leonard.F.Burlaga@nasa.gov

sensor has a digitization step size of 0.004 nT, and the primary sensor noise is ≈0.003 nT root mean square. The 1σ uncertainty associated with the measurement of a daily average of B is typically ±0.015 nT. There are data gaps of ≈8 to 16 hours each day depending upon the schedule for tracking by the Jet Propulsion Laboratory's Deep Space Network coverage.

The V1 observations of magnetic field strength B, azimuthal angle λ, and elevation angle δ in heliographic coordinates [figure 1.2 in (*23*)] from 2004/001 through 2005/110 are shown in Fig. 1. Before 2004/351, V1 observed magnetic fields characteristic of the distant solar wind (*7*, *23*). The magnetic field strength increased abruptly between 2004/350 and 2004/352, after which B was unusually large for a period of ≈125 days (Fig. 1A). No V1 data are available for 2004/351. The average B from 2004/357 to 2004/479 relative to the beginning of 2004 is $\langle B_2 \rangle = 0.136 \pm 0.035$ nT, which is 2.4 times as large as the average $\langle B_1 \rangle = 0.056 \pm 0.025$ nT for 2004/001 to 2004/350. The average B from 2005/001 through 2005/110 is 4.2 times as large as that predicted by Parker's model (*4*, *24*) when inferred speeds are used at the latitude 35° (*25*). Such sustained strong magnetic fields have not been observed by either V1 or Voyager 2 since 1985 when V1 was at ≈28 AU. We conclude that V1 crossed the termination shock on 2004/351 (16 December) and that it moved in the heliosheath from 2004/352 through 2005/110.

The magnetic field direction was directed "away" from the Sun (λ ≈ 270°) approximately along the Parker spiral direction from 2004/361 through 2005/110, as indicated by λ(t) in Fig. 1B. The away fields were not expected, since the dominant polarity of the Sun at the latitude of V1 was "toward" the Sun. The cause of the away fields is not fully understood. This observation could be explained if V1 were in a positive sector in the heliosheath moving away from the Sun at approximately the same speed as V1. This explanation has also been proposed by Jokipii (*26*), whose calculations together with our observations suggest an inward shock speed of >90 km/s (*18*) and/or substantial meridional deflection of the heliosheath flow. The magnetic fields in the heliosheath were directed above the solar equatorial plane (Fig. 1C), consistent with meridional flow. Such northward fields were also observed in the solar wind during the latter half of 2004.

Higher resolution magnetic field observations around the crossing of the TS, in the postshock region, and in the heliosheath are shown in Fig. 2. Figure 2A shows 48-s averages of B in the supersonic solar wind from 2004/348 through 2004/350, as indicated by the low values of B and its fluctuations. The average B on 2004/350 was $B_1 \approx 0.031 \pm 0.007$ nT, close to the value predicted by Parker's model (≈0.03 nT). Owing to the lack of tracking, there are no data from 2004/350.878 to 2004/352.081, the interval in which V1 crossed the TS or was crossed by the TS moving toward the Sun. On 2004/352 and 2004/353, V1 was in the heliosheath just behind the TS, and the average, B_2, was 0.093 ± 0.020 nT. The uncertainties in B_1 and B_2 are the standard deviations of the respective distributions. The compression ratio across the TS is $B_2/B_1 = 3.05$; the uncertainty is ±0.04 computed with the error in the mean of B_2 and B_1, and ±1.23 when computed with the standard deviations. To this statistical uncertainty must be added both the uncertainty owing to the lack of data just before and after the shock (which was not observed) and the uncertainty associated with the choice of the averaging interval and other systematic errors. Thus, a compression ratio B_2/B_1 in the range ≈2 to ≈4 is plausible, depending on the time scale.

The fluctuations in B behind the TS from 2004/352 to 2004/366 are large on a scale of several hours to days. The 48-s averages of B between 2004/352 and 2004/366 fluctuate between <0.01 nT (e.g., on 2004/354 and 2004/356) and ≈0.21 nT (on 2004/353, 2004/358, 2004/359, and 2004/360). The hour averages of B between 2004/352 and 2005/110 fluctuate between 0.02 and 0.26 nT. The

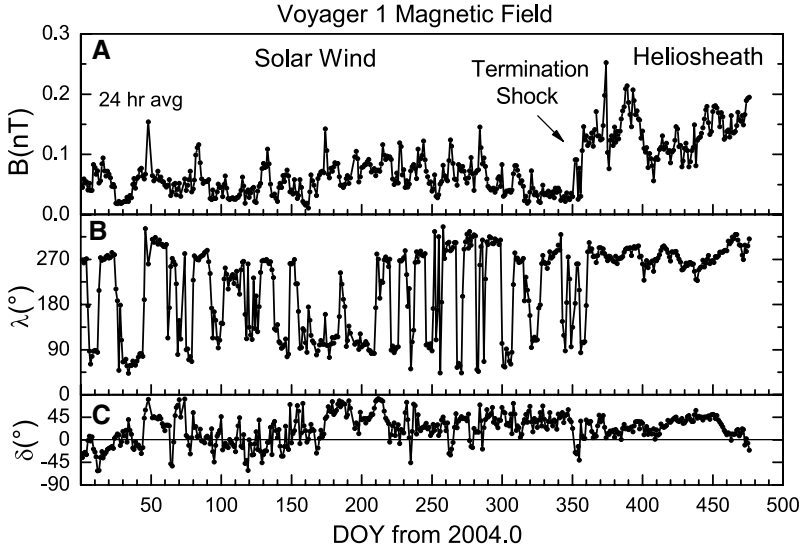

Fig. 1. Daily averages of magnetic field strength B (**A**), azimuthal angle λ (**B**), and elevation angle δ (**C**) as a function of time measured in days from the beginning of 2004. The angles are in heliographic coordinates. DOY, day of year.

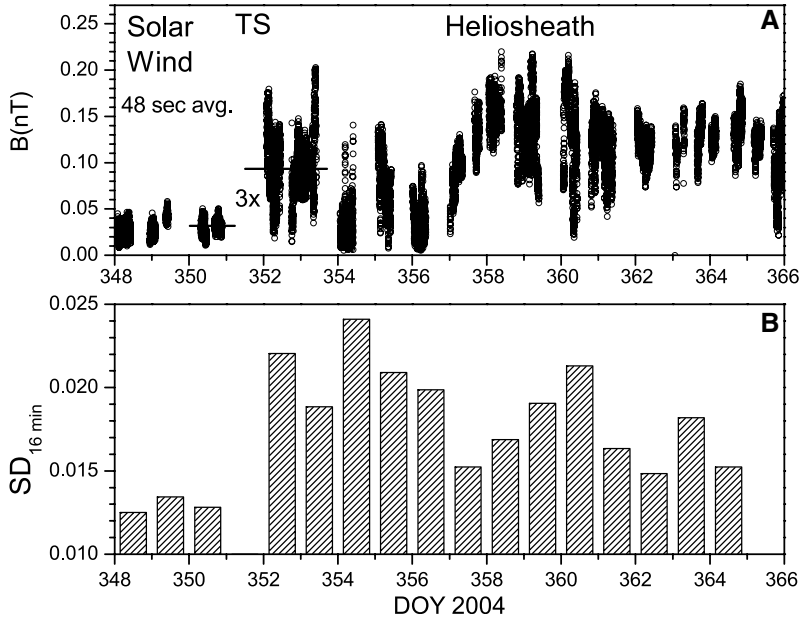

Fig. 2. The magnetic field strength B (48-s averages) (**A**) and the standard deviation of components of the magnetic field (**B**) observed by V1 from 2004/348 to 2004/366. DOY, day of year.

fluctuations in the components of the vector magnetic field **B** are measured by the daily averages of the standard deviations $SD_{16min} \equiv \{[\Sigma\Sigma(B^i_k - \langle B_k \rangle_{16min})^2]/(N-1)\}^{1/2}$, where the inner sum is over the payload components k = 1, 2, 3 (x, y, z) of the 1.92-s data, and the outer sum is over the number of points from i = 1 to N. The fluctuations in SD_{16min} are small, ≈0.012 nT, in the solar wind on 2004/348 through 2004/350 just before the TS crossing (Fig. 2B). The fluctuations in SD_{16min} are large behind the shock (from 2004/352 to 2004/366), even on 2004/354 and 2004/356 when B is close to the supersonic solar wind values. The large fluctuations in B and the components of **B** after the TS crossing together with the relatively large jump in B across the TS suggest that the TS was a quasi-perpendicular, pickup ion–dominated shock (*27*, *19*).

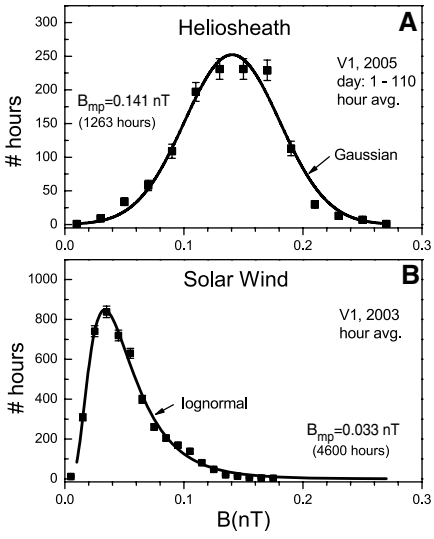

Fig. 3. The distribution of hour averages of B is Gaussian in the heliosheath (**A**), whereas it is lognormal in the solar wind (**B**). Error bars show means ± SD.

The normal to the TS cannot be determined from the available observations owing to the large data gap containing the TS. However, a minimum variance analysis of 48-s magnetic field observations from hour 0156 to hour 1054 UTC on 17 December shows that the magnetic field vectors behind the shock rotated nearly parallel to a plane; the average component of **B** perpendicular to the plane is –0.01 ± 0.02 nT. The normal vector of the rotation plane has azimuthal and elevation angles 11° and –8°, respectively; that is, they are nearly along the radial direction to the Sun. If this rotation plane were parallel to the TS, then the TS would also be nearly normal to the radial direction, but calculations are needed to evaluate the assumption.

The distribution of hour averages of B in the heliosheath from 2005/001 through 2005/110 (Fig. 3A) is well described by a Gaussian distribution, in stark contrast to the lognormal distribution (shown in Fig. 3B with V1 data from 2003) that is characteristic of the supersonic solar wind (*23*, *28*). The Gaussian distribution suggests strongly that V1 entered an unexplored region, the heliosheath. We conjecture that the Gaussian distribution observed in the heliosheath is associated with the thermalization of plasma by the TS and with the plasma's approach to statistical equilibrium.

Finally, consider the observed relationship between daily averages of B (Fig. 4A) and the cosmic ray intensity (CRI) > 70 MeV/nucleon (Fig. 4B). In the supersonic solar wind, characteristic changes in the CRI measured by the Cosmic Ray Subsystem (CRS) experiment on V1 (*29*) and B have been observed by V1 from 1981 (11 AU) to 2003 (≈90 AU) (*7*, *30*). When B is larger than average for a year, the CRI decreases. Thus, if V1 were in the supersonic solar wind from 2004/352, through 2005/110, we would expect to see a large decrease in the CRI as a consequence of the relatively strong magnetic fields observed during that interval. But Fig. 4B shows a large increase in the CRI during this interval. Thus, qualitative change from the previous relationship is further evidence that V1 was in the heliosheath after 2004/351.

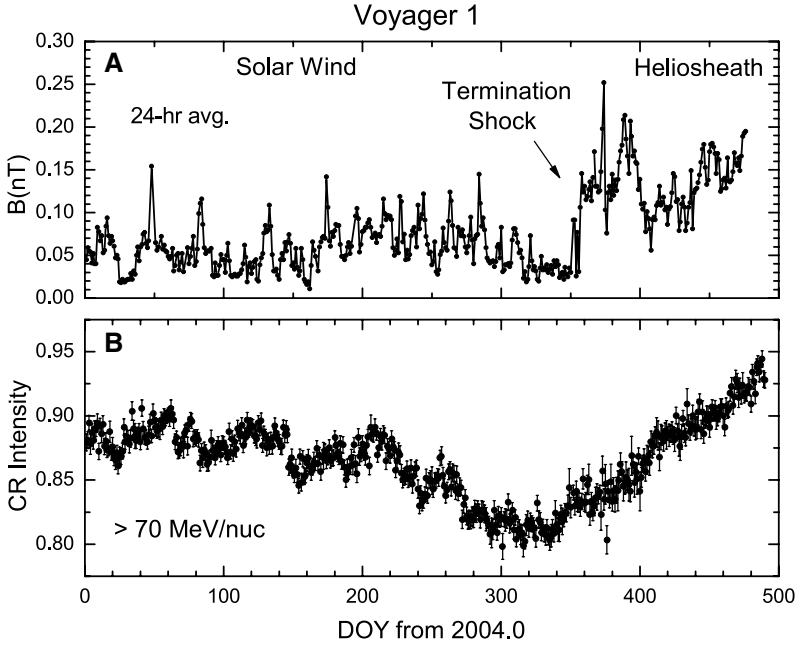

Fig. 4. The relationship between daily averages of the magnetic field strength (**A**) and the intensity of cosmic rays (CR) (**B**) in the heliosheath is different from that in the solar wind. Error bars show means ± SD. DOY, day of year.

References and Notes

1. R. Weymann, *Astrophys. J.* **132**, 380 (1960).
2. T. E. Holzer, *Annu. Rev. Astron. Astrophys.* **27**, 199 (1989).
3. E. C. Stone, *Science* **293**, 55 (2001).
4. E. N. Parker, *Interplanetary Dynamical Processes* (Interscience, New York, 1963).
5. F. B. McDonald *et al.*, *Nature* **426**, 48 (2003).
6. S. M. Krimigis *et al.*, *Nature* **426**, 45 (2003).
7. L. F. Burlaga *et al.*, *Geophys. Res. Lett.* **30**, 2072 (2003).
8. N. F. Ness *et al.*, in *The Outer Heliosphere: IGPP Fourth Annual International Astrophysics Conference*, G. Li, G. P. Zank, C. T. Russell, Eds. (AIP Conference Proceedings 781, Melville, New York, in press).
9. R. B. Decker *et al.*, *Science* **309**, 2020 (2005).
10. E. C. Stone *et al.*, *Science* **309**, 2017 (2005).
11. D. A. Gurnett, W. S. Kurth, *Science* **309**, 2025 (2005).
12. A. J. Barnes, *J. Geophys. Res.* **98**, 15137 (1993).
13. Y. C. Whang, L. F. Burlaga, *J. Geophys. Res.* **98**, 15221 (1993).
14. S. R. Karmesin, P. C. Liewer, J. U. Brackbill, *Geophys. Res. Lett.* **22**, 1153 (1995).
15. C. Wang, J. W. Belcher, *J. Geophys. Res.* **104**, 549 (1999).
16. J. D. Richardson *et al.*, MIT Space Plasma Group Voyager Plasma Science Experiment (available at http://web.mit.edu/space/www/voyager/voyager.html).
17. K. Scherer, H. J. Fahr, *Geophys. Res. Lett.* **30**, 1045 (2003).
18. Y. C. Whang, L. F. Burlaga, Y. M. Wang, N. R. Sheeley Jr., *Geophys. Res. Lett.* **31**, L03805 (2004).
19. G. P. Zank, *Space Sci. Rev.* **89**, 413 (1999).
20. G. P. Zank, H. L. Pauls, *Space Sci. Rev.* **78**, 95 (1996).
21. J. A. LeRoux, H. Fichtner, *J. Geophys. Res.* **102**, 17365 (1997).
22. K. W. Behannon *et al.*, *Space Sci. Rev.* **21**, 235 (1977).
23. L. F. Burlaga, *Interplanetary Magnetohydrodynamics* (Oxford Univ. Press, New York, 1995).
24. L. F. Burlaga, N. F. Ness, Y.-M. Wang, N. R. Sheeley Jr., *J. Geophys. Res.* **107**, 1410 (2002).
25. Y.-M. Wang, N. R. Sheeley Jr., *Astrophys. J.* **355**, 726 (1990).
26. R. Jokipii, *Astrophys. J. Lett.*, in press.
27. P. C. Liewer, B. E. Goldstein, N. Omidi, *J. Geophys. Res.* **98**, 15211 (1993).
28. L. F. Burlaga, *J. Geophys. Res.* **106**, 15917 (2001).
29. E. C. Stone *et al.*, *Space Sci. Rev.* **21**, 355 (1977).
30. L. F. Burlaga, F. B. McDonald, M. L. Goldstein, A. J. Lazarus, *J. Geophys. Res.* **90**, 2027 (1985).

31. T. McClanahan and S. Kramer provided support in the processing of the data. R. Fernandez-Borda computed the zero-level corrections for the instrument. N.F.N. was partially supported by NASA grant NNG04GB71G to The Catholic University of America. N. Sheeley and Yi-Ming Wang provided estimates of the speed at the latitude of V1 for the calculation of the predicted magnetic field strength during 2005, and C. Smith provided the magnetic field strength and D. McComas provided the solar wind speed from the Advanced Composition Explorer spacecraft at 1 AU.

18 July 2005; accepted 15 August 2005
10.1126/science.1117542

Bacterial Immunity Traded for Sperm Viability in Male Crickets

Leigh W. Simmons* and Benjamin Roberts

Pathogen-mediated theories of sexual selection propose that the expression of a male's sexual traits can provide a reliable signal to females of heritable resistance to disease for their offspring. The "immunocompetence handicap hypothesis" relies on the assumption that males trade immunity for reproductive success (*1*, *2*). Phenotypic studies do suggest that activation of the immune system can compromise the expression of secondary sexual traits (*3*). A trade-off between immunity and semen quality has also been suggested, which would hold important implications for understanding postcopulatory selection through sperm competition (*4*) and the longevity costs of reproduction (*2*).

We examined the genetic architecture of immune function and sperm viability in a field cricket (*Teleogryllus oceanicus*), using a standard half-sibling breeding design. Each male (sire) was mated to several females (dams), and the data derived from the offspring were analyzed as a nested analysis of variance with dams nested within sires (*5*). Similarity between paternal half-siblings (sire effects) provide the best estimate of additive genetic variance in a trait, because similarity between full-siblings can arise from common rearing environments or from maternal effects. A total of 485 adult male offspring from 41 sires mated to 105 dams were examined for sperm viability and for three aspects of their immune function: the number of circulating hemocytes, encapsulation ability, and baseline lysozyme activity (*5*).

Sire effects on all measures of immunity and on sperm viability were significant (table S1). Additive genetic variation represented a significant proportion of the total phenotypic variation for these traits (Table 1), indicating that they were heritable. Phenotypic and genetic correlations between the two measures of cellular immunity were positive, whereas correlations between cell-mediated immunity and lysozyme activity were negative (Table 2). Sperm viability was positively correlated, both phenotypically and genetically, with measures of cell-mediated immunity but was negatively correlated with lysozyme activity (Table 2 and fig. S1). There was significant similarity between the phenotypic correlation matrix and the genetic correlation or G matrix (Mantel Test, $r = 0.995$, $P = 0.042$). We excluded the possibility that covariances between immune function traits and sperm viability could reflect an underlying association between each of these traits and body size. Thus, in a subset of 22 sire families (65 dam families), partial correlations between the relevant variables controlling for body weight were similar in sign and magnitude (Table 2).

Our data provide a further example of a genetic trade-off between humoral and cell-mediated components of the insect immune system (*6*). It remains to be seen how these patterns of covariance affect an individual's overall resistance to disease. The trade-off between bacterial immunity and sperm viability could result in a redistribution of resources to cellular components of immunity, explaining the patterns of covariance between immune function traits and sperm viability. However, given that lysozyme activity represents the main form of defense against bacterial infection in crickets (*7*), it seems unlikely that increased cellular immunity could compensate for reductions in lysozyme activity.

Human males treated with antibiotics or immunosuppressive drugs have elevated ejaculate quality and fertility (*8*). Likewise, immune activation by parasitic infection has a negative impact on sperm production in fish (*9*). Although these phenotypic correlations hint at a trade-off between immunity and semen quality, the evolutionary relevance of such associations depends on their underlying genetic architecture (*10*). Our data provide evidence of the genetic trade-off required by the immunocompetence hypothesis (*4*). Sperm viability in this cricket has been shown to be critical in determining a male's fertilization success under sperm competition (*11*), so that males who must activate their lysozyme activity will have decreased paternity, providing a potential avenue by which females could acquire genetic benefits from sperm competition.

Table 1. Coefficients of genetic (CV_A) and residual (CV_R) variation and heritabilities (h^2) for sperm viability and measures of immune function in *T. oceanicus*.

Trait	Mean	SD	CV_A	CV_R	$h^2 \pm$ SE
Sperm viability (%)	83.1	6.40	4.08	6.54	0.28 ± 0.05
Encapsulation (grayscale)	81.9	20.96	17.63	18.19	0.48 ± 0.06
Hemocyte load (per ml)	84447	55777	55.81	32.89	0.74 ± 0.06
Lysozyme (lytic zone mm²)	16.5	3.96	13.51	19.99	0.31 ± 0.05

Table 2. Phenotypic (below the diagonal) and genetic (above the diagonal) correlation matrices. Phenotypic correlations calculated across individuals exceed the critical r_{485} with $P = 0.001$. Partial phenotypic correlations controlling for body size are shown in parentheses.

Trait	Sperm viability	Encapsulation	Hemocyte load	Lysozyme
Sperm viability (%)		0.318 ± 0.120	0.490 ± 0.109	–0.190 ± 0.141
Encapsulation (grayscale)	0.227 (0.271)		0.937 ± 0.024	–0.240 ± 0.064
Hemocyte load (per ml)	0.294 (0.323)	0.724 (0.746)		–0.358 ± 0.067
Lysozyme (lytic zone mm²)	–0.224 (–0.309)	–0.376 (–0.443)	–0.387 (–0.406)	

References and Notes

1. I. Folstad, A. J. Karter, *Am. Nat.* **139**, 603 (1992).
2. B. C. Sheldon, S. Verhulst, *Trends Ecol. Evol.* **11**, 317 (1996).
3. B. Faivre, A. Gregoire, M. Preault, F. Cezilly, G. Sorci, *Science* **300**, 103 (2003).
4. I. Folstad, F. Skarstein, *Behav. Ecol.* **8**, 109 (1997).
5. Materials and methods are available as supporting material on *Science* Online.
6. S. C. Cotter, L. E. B. Kruuk, K. Wilson, *J. Evol. Biol.* **17**, 421 (2004).
7. P. M. Schneider, *Insect Biochem.* **15**, 463 (1985).
8. P. A. Skau, I. Folstad, *Behav. Ecol.* **16**, 109 (2005).
9. S. Liljedal, I. Folstad, F. Skarstein, *Proc. R. Soc. London Ser. B* **266**, 1893 (1999).
10. D. Reznick, *Trends Ecol. Evol.* **7**, 42 (1992).
11. F. García-González, L. W. Simmons, *Curr. Biol.* **15**, 271 (2005).

12. This work was supported by the Australian Research Council.

Supporting Online Material

Materials and Methods
Fig. S1
Table S1
References and Notes

5 May 2005; accepted 17 August 2005
10.1126/science.1114500

Evolutionary Biology Research Group, School of Animal Biology (M092), The University of Western Australia, Crawley, WA 6009, Australia.

*To whom correspondence should be addressed. E-mail: lsimmons@cyllene.uwa.edu.au

An Aneuploid Mouse Strain Carrying Human Chromosome 21 with Down Syndrome Phenotypes

Aideen O'Doherty,[1,3] Sandra Ruf,[1,3] Claire Mulligan,[4] Victoria Hildreth,[5] Mick L. Errington,[3] Sam Cooke,[3] Abdul Sesay,[3] Sonie Modino,[6] Lesley Vanes,[3] Diana Hernandez,[1,3] Jacqueline M. Linehan,[1,2] Paul T. Sharpe,[6] Sebastian Brandner,[1] Timothy V. P. Bliss,[3] Deborah J. Henderson,[5] Dean Nizetic,[4] Victor L. J. Tybulewicz,[3]* Elizabeth M. C. Fisher[1]*

Aneuploidies are common chromosomal defects that result in growth and developmental deficits and high levels of lethality in humans. To gain insight into the biology of aneuploidies, we manipulated mouse embryonic stem cells and generated a trans-species aneuploid mouse line that stably transmits a freely segregating, almost complete human chromosome 21 (Hsa21). This "trans-chromosomic" mouse line, Tc1, is a model of trisomy 21, which manifests as Down syndrome (DS) in humans, and has phenotypic alterations in behavior, synaptic plasticity, cerebellar neuronal number, heart development, and mandible size that relate to human DS. Transchromosomic mouse lines such as Tc1 may represent useful genetic tools for dissecting other human aneuploidies.

Down syndrome (DS) is a complex genetic condition arising from an altered dosage of wild-type genes on human chromosome 21 (Hsa21). One approach to the molecular genetics and pathology of DS has been to model the aberrant gene dosage of trisomy 21 in the mouse by transgenesis with single Hsa21 genes or yeast artificial chromosomes. This approach has highlighted potential loci of interest (*1*, *2*). Alternatively, mouse aneuploidies have been used to model DS. Approximately two thirds of the orthologs of the 243 known Hsa21 genes (current gene estimate, ENSEMBL database) lie on mouse chromosome (Mmu) 16, whereas the remainder are distributed between Mmu10 and Mmu17 (*3*, *4*). Thus, trisomies of Mmu16 have been studied as potential models of DS. Mice with full trisomy Mmu16 are not viable after birth, and because Mmu16 carries genes with orthologs on Hsa21 and at least three other chromosomes, mouse trisomy 16 is equivalent to partial trisomy of four human chromosomes (Hsa3, 16, 21, and 22). Therefore, the most widely used models of DS are the partial, or segmental, trisomy strains Ts65Dn and Tc1Cje, which are trisomic for portions of Mmu16 containing only Hsa21 orthologs (*5*–*7*).

An alternative model is provided by ''trans-chromosomic" (trans-species aneuploid) mouse strains in which mice carry an extra human chromosome and are thus trisomic only for the genes on this chromosome. Such a trans-chromosomic strain for Hsa21 has several advantages for modelling DS. In contrast to transgenic methods to place Hsa21 genes into mice, this approach potentially reflects more closely the 3:2 dosage difference present between trisomic and disomic individuals through the introduction of only one extra copy of each Hsa21 gene. Additionally, the complete genomic sequence can be included, including upstream and downstream regulatory elements of unusually large genes (*8*) or those with complex regulatory elements and multiple transcripts (*9*). Unlike other methods of stable gene transfer, the trans-chromosomic approach should not interrupt endogenous mouse sequences. Furthermore, because individual human chromosomes have orthologs on more than one mouse chromosome, aneuploidy of an individual mouse chromosome is not equivalent to the human situation and only partially represents it, whereas placing an entire human chromosome into mice would model a full human trisomy.

The first transchromosomic mice were created by Oshimura and colleagues, who placed freely segregating portions of Hsa2, 14, or 22 into mouse embryonic stem (ES) cells using microcell-mediated chromosome transfer (MMCT) (*10*, *11*). The ES cells were used to make chimeras, and germline transmission was achieved with a ~2-Mb Hsa2 fragment and a 1.5-Mb Hsa14 fragment (*10*, *11*). Using a similar process, irradiation MMCT (XMMCT), to construct a mouse model for human trisomy 21, we generated a panel of transchromosomic male mouse ES cell lines, each carrying a freely segregating Hsa21 or portions thereof (*12*). When injected into mouse blastocysts, these cell lines gave high percentage contributions in the resultant chimeras; however, they failed to achieve germline transmission of Hsa21. This is consistent with previous findings that an aneuploid chromosome often will not transmit through the male germline (*12*, *13*). Oshimura and colleagues later reported stable germline transmission of an Hsa21 fragment of ~5 Mb that carried an internal deletion and contained genes with homology to Mmu16 only (*14*, *15*). Here, we take this technology forward and report the germline transmission of an almost complete Hsa21 and analysis of the resulting mouse strain, Tc1, which models aspects of human DS.

Generating the Tc1 transchromosomic mouse strains. We took the approach of reproducing the human-mouse transchromosomic cell lines on a female background, through further rounds of XMMCT into the female MPI VI ES cell line (*16*). We analyzed the resultant transchromosomic ES cell lines for human DNA content, using fluorescence in situ hybridization (FISH) to detect Hsa21 and reverse FISH to detect other human chromosomes (*12*). Five MPI VI–derived cell lines were identified, with a single freely segregating Hsa21 as the only human contribution (*17*) (fig. S1A). These cell lines were further assessed for the presence or absence of a panel of Hsa21 markers (Fig. 1A and table S1). Cell line 91-1 contained the most of Hsa21 with two gaps: the first bounded by the markers *CXADR* (at position 17,807,195) and *D21S1922* (at 21,220,691) with a maximum size of 3.4 Mb, and the second was bounded by *IFNAR1* (at 33,649,973) and *RUNX1* (at 35,115,486) with a maximum size of 1.5 Mb (Fig. 1A). Therefore, 91-1 appears to contain at least 42 Mb (90%) of the complete 46.9 Mb of Hsa21, and we estimate that this includes ~92% of all known Hsa21 genes (*17*).

To generate transchromosomic chimeras, ES cells were injected into host blastocysts and the resulting chimeras were mated to mice from the C57BL/6J strain. Germline transmission was achieved from one female chimera, carrying the 91-1 transchromosomic ES cell line. This chimera had only one litter of two pups, a male (Tc1-01) and a female (Tc1-02). These progeny both

[1]Department of Neurodegenerative Disease, [2]Medical Research Council Prion Unit, Institute of Neurology, Queen Square, London WC1N 3BG, UK. [3]National Institute for Medical Research, The Ridgeway, Mill Hill, London NW7 1AA, UK. [4]Centre for Haematology, Institute of Cell and Molecular Science, Barts and The London, Queen Mary's School of Medicine, 4 Newark Street, London E1 2AT, UK. [5]Institute of Human Genetics, University of Newcastle upon Tyne, International Centre for Life, Central Parkway, Newcastle upon Tyne, NE1 3BZ, UK. [6]Department of Craniofacial Development, Kings College London, Guy's Hospital, London SE1 9RT, UK.

*To whom correspondence should be addressed. E-mail: vtybule@nimr.mrc.ac.uk (V.L.J.T); e.fisher@prion.ucl.ac.uk (E.M.C.F.)

retained a freely segregating Hsa21 with the same Hsa21 profile as the parental ES cell line, 91-1 (Fig. 1A and fig. S1B). This transchromosomic mouse strain was designated Tc(Hsa21)1TybEmcf, hereafter referred to as Tc1 (*18*).

In an attempt to establish the Tc1 strain on a number of genetic backgrounds, mouse Tc1-01 was mated either to mice that were an F1 hybrid between C57BL/6J and 129S8 mice [F1(C57BL/6Jx129S8)] or to inbred BALB/c, C3H/He, and C57BL/6J mice. As the inbred line backcrosses progressed and the genetic background became more homogenous, transmission of the human chromosome diminished, to the point where these colonies could no longer be maintained (table S2). Subsequently, only the F1(C57BL/6Jx129S8) colony was retained, with a stable transmission frequency of >40% of progeny inheriting Hsa21 from their mothers, with occasional transmission through the male germline (table S2). We have aged male and female Tc1 mice up to 20 months of age, and at this time they are healthy and mobile with no signs of debilitation. They are thus likely to live well beyond 20 months of age.

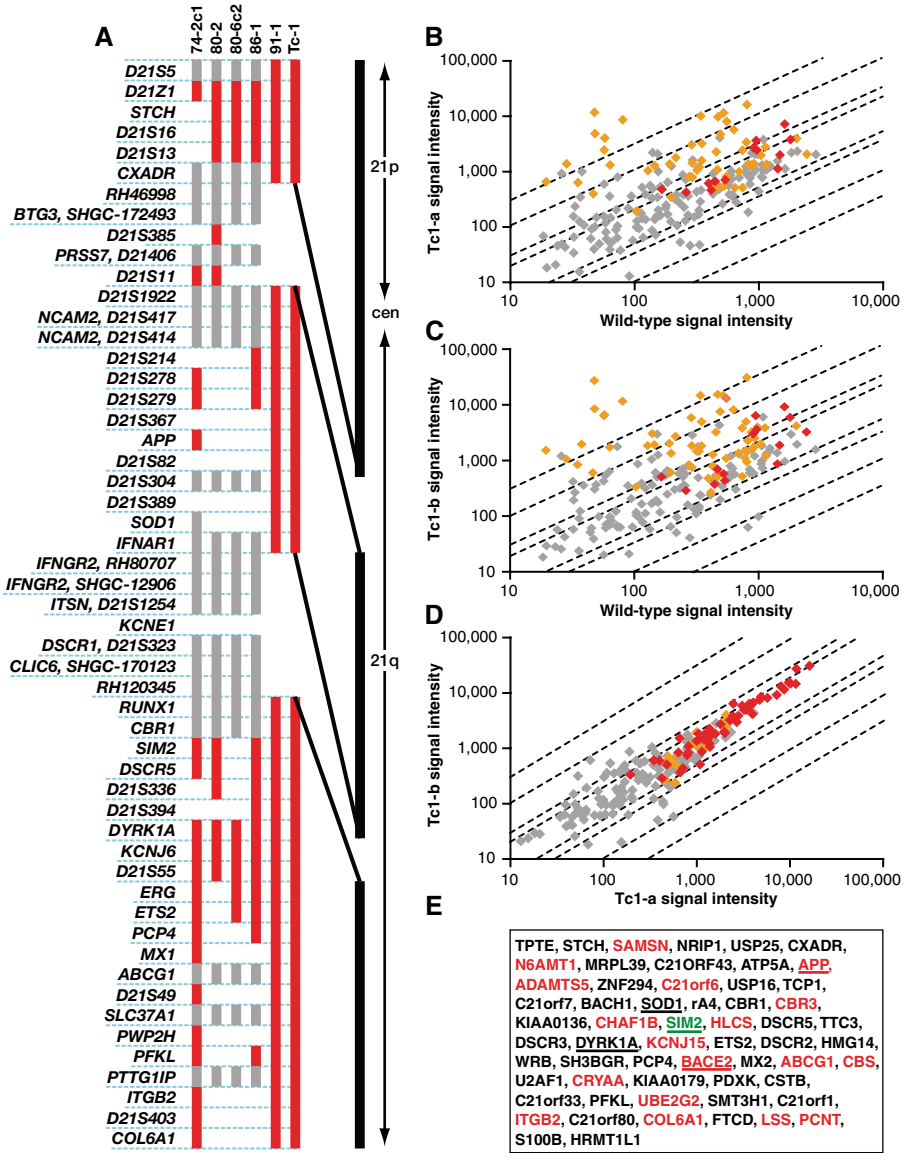

Fig. 1. DNA and expression analysis of transchromosomic cell lines and mice carrying Hsa21. (**A**) Hsa21 content in five transchromosomic ES cell lines (74-2c1, 80-2, 80-6c2, 86-1, and 91-1) and Tc1 mouse DNAs. Cell line and mouse names are shown above the vertical bars that indicate the presence of the Hsa21 markers listed on the left. Markers are shown in order but are not spaced relative to their distance apart on Hsa21 (positions are given in table S1). Red denotes the presence of the marker, gray denotes not scored, and a blank space denotes a negative score, i.e., the marker was not present. *CXADR* was shown to be present by microarray results from Tc1 embryos. The vertical black line on the right is a scaled representation of the physical map of Hsa21, showing the relative spacing and maximum sizes of the two gaps. cen, centromere. (**B** to **E**) RNA samples from two Tc1 whole embryos and one wild-type littermate (E14.5) were hybridized to Affymetrix HG-U133A GeneChips. Array data were scaled to a target intensity of 500 before analysis. (B and C) Scatter plots showing Hsa21 gene signal intensities of embryos (B) Tc1-a and (C) Tc1-b against the wild-type littermate. (D) Scatter plot showing Hsa21 gene signal intensities of embryo Tc1-a against Tc1-b as a hybridization control. In each scatter plot, red points represent genes called present in both embryos, orange points represent genes called present in one of the two embryos, and gray points represent genes below the threshold for detection in both embryos. Diagonal lines indicate the thresholds for twofold, threefold, tenfold, and thirtyfold differences between the two embryos. (E) Genes with increased expression in Tc1 embryos compared to wild-type embryos. Red lettering indicates those found with the reduced stringency search method. Underlined genes were also found by RT-PCR or immunoblot. Expression of one gene, *SIM2* (green), was detected by RT-PCR but not by microarray analysis.

Chromosome retention and gene expression. In previous studies in which chimeric mice have been engineered to carry human chromosome fragments, the human fragment was observed to be differentially retained in different organs and on different genetic backgrounds (*14*, *19*). Thus, we used quantitative polymerase chain reaction (PCR) to determine the level of Hsa21 retention in various tissues from adult Tc1 male mice and observed that retention of Hsa21 ranged from 55 ± 6% in the spinal cord to 24 ± 3% in the spleen (table S3). For two tissues, brain and spleen, we also undertook interphase FISH using an Hsa21 paint and a mouse X chromosome probe as a control to directly count the percentage of nuclei carrying Hsa21 (table S4). Our results showed 66 ± 7% of brain nuclei and 49 ± 5% of spleen nuclei are positive for Hsa21, a higher percentage of positive cells than estimated by quantitative PCR. Mosaicism is also seen in human DS (*20*).

We next undertook a large-scale analysis of gene expression from Hsa21 in Tc1 mice. A comparison of whole embryo RNAs [at embryonic day (E) 14.5] from two Tc1 and one wild-type littermate (Fig. 1, B to D), on Affymetrix human HG-U133A arrays, demonstrated the expression of Hsa21 genes along the entire length of the chromosome, from *TPTE* in the p arm to *HRMT1L1* at the distal end of the q arm (Fig. 1E). A total of 205 Hsa21 probe sets (representing 131 genes) were present on the arrays, of which 51 (representing 39 genes) were classified as increased ($P < 0.01$) in both Tc1 versus littermate comparisons. This method showed an increased signal from only 9 non-Hsa21 probe sets out of a possible total of 22,078. A reduced stringency search (*17*) brought the total number of Hsa21 genes with detectable expression over and above the littermate background to 58 (Fig. 1E). It remains possible that other Hsa21 genes are also expressed in Tc1 mice but were not detected, either because they are not expressed at sufficiently high levels in E14.5 embryos or because cross-reaction between the mouse homolog and the human gene on the microarray may have precluded detection. We also examined the expression of selected human genes previously implicated in various DS neuronal phenotypes

(*APP*, *SOD1, SIM2*, *DYRK1A*, and *BACE2*) in Tc1 tissues by reverse transcription (RT)–PCR and/or immunoblotting (*17*). In all cases, gene expression was detected in Tc1 tissues (fig. S2).

Deficits in synaptic plasticity and learning. Because a primary aspect of DS is mental retardation (*3*), we assessed potential neural deficits in Tc1 mice using behavioral tests of learning and memory. We also examined hippocampal long-term potentiation (LTP), a form of synaptic plasticity that is altered in the Ts65Dn mouse (*21*, *22*) and that provides a putative physiological substrate for hippocampus-dependent learning and memory (*23*). Field recordings of evoked potentials in the dentate gyrus of the hippocampus revealed no differences between wild-type and Tc1 mice in input-output curves (Fig. 2A and fig. S3) or paired-pulse interactions (Fig. 2, B and C), suggesting normal basal synaptic transmission and inhibitory tone. However, Tc1 mice exhibited significantly reduced LTP when compared with wild-type littermates (Fig. 2, D and E). To assess whether this deficit correlated with an effect on hippocampus-dependent memory, we tested Tc1 mutants in a novel-object recognition task (*24*, *25*). Wild-type mice spent significantly more time exploring a novel object than two familiar objects that had been presented in a training session 10 min previously (Fig. 3A). Tc1 mice, however, failed to show significantly greater exploration of the novel object as compared with the familiar objects.

In contrast, a test of hippocampus-dependent short-term memory, the spontaneous alternation T-maze (*26*), did not reveal a significant difference between wild-type and Tc1 littermates (Fig. 3B). This finding suggests that Tc1 mice are able to retain hippocampus-dependent memory for up to a minute but show deficits in retaining memories over longer periods in the novel-object recognition task. To investigate potential behavioral confounds in these learning and memory tests, we subjected wild-type and Tc1 mice to tests of generalized activity, motor coordination, and anxiety. Compared with wild-type littermates, Tc1 mice showed a trend toward hyperactivity, which is a behavioral characteristic of DS, in an open-field test in which the number of boundaries crossed by an animal is scored. However, this trend did not reach significance (Fig. 3C) ($P = 0.07$) and did not manifest itself in abnormal levels of exploration during the novel-object recognition task (fig. S4). There was no indication of a deficit in moving along a static rod, a standard test of motor coordination (Fig. 3D). Hyperactivity may have contributed to a nonsignificant trend toward increased exploration of open arms in the elevated plus maze, a test of anxiety (*27*) (Fig. 3E). These findings suggest that Tc1 mice have deficits in both hippocampal synaptic plasticity and hippocampus-dependent learning and memory.

Cerebellar neuron counts and brain histopathology. As there is a decrease in cell density in the internal granule layer of the cerebellum in the Ts65Dn mouse (*28*–*30*) and total brain volume is reduced in DS, in particular in the cerebellum (*31*–*33*), we counted cerebellar granule neurons in four different cerebellar areas of four wild-type and four Tc1 littermates (table S5). The density of neurons was significantly lower in Tc1 mice (13,189 ± 2198 neurons per mm^2) compared with wild-type mice (15,611 ± 2034 neurons per mm^2) ($P < 0.003$). Comparison of one anatomically corresponding cerebellar lobe (VIII) across four wild-type and four Tc1 littermates showed similarly significant differences [16,515 ± 1516 neurons per mm^2 (wild-type) versus 13,894 ± 1071 neurons per mm^2 (Tc1); $P = 0.03$] (table S5). Preliminary analyses

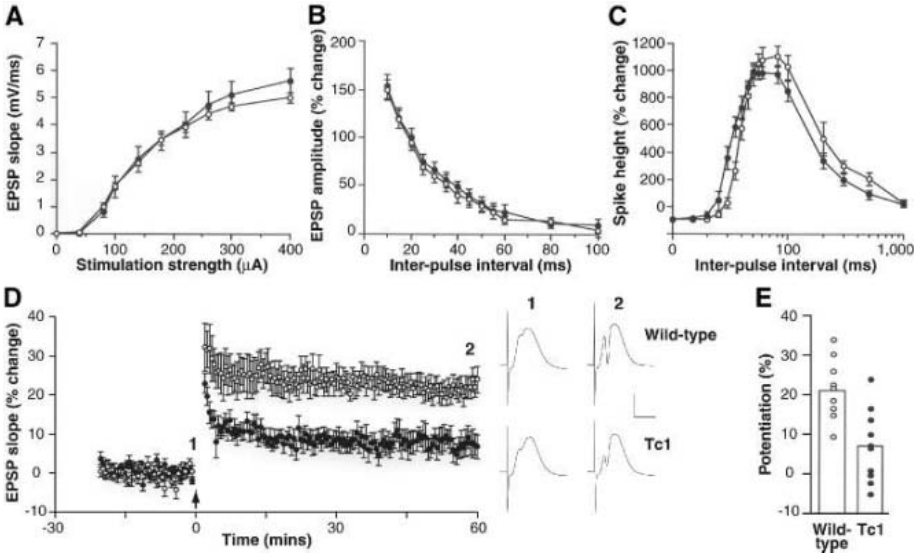

Fig. 2. Short-term plasticity is normal but LTP is impaired in the dentate gyrus of Tc1 mice. (**A**) Input-output curves, (**B**) paired-pulse facilitation of the field excitatory postsynaptic potential (EPSP), and (**C**) paired-pulse modulation of the population spike are similar in wild-type (open circles) and Tc1 (solid circles) littermates. (**D**) LTP averaged for a group of 9 wild-type mice (open circles) and 10 Tc1 littermates (solid circles). The arrow marks the tetanus (six series of six trains of six stimuli at 400 Hz, with 200 ms between trains and 20 s between series). One hour after the tetanus, the magnitude of LTP was 21.9 ± 2.6% in wild-type mice, compared with 7.4 ± 2.9% in Tc1 mutants ($P < 0.001$, 2-tailed t test). Sample potentials from a single wild-type and a single Tc1 mouse, recorded just before (*1*) and 60 min after (*2*) the tetanus, are displayed on the right. Calibration, 5 mV, 5 ms. (**E**) The magnitude of LTP, measured 55 to 60 min after induction, is displayed for each wild-type mouse (open circles) and each Tc1 mutant (solid circles). The open histobars indicate the means for each group. All error bars represent SEM.

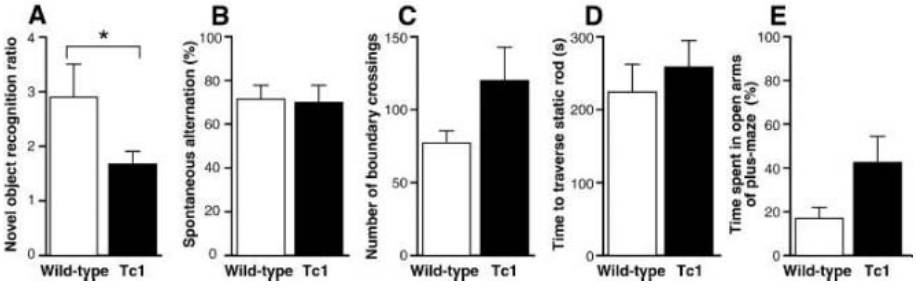

Fig. 3. Tc1 mice have a hippocampus-dependent learning and memory deficit. (**A**) An index of novel-object exploration (the ratio of time spent exploring a novel object to mean time spent exploring a familiar object) in 12 wild-type (open) and 10 Tc1 (solid) littermates reveals a deficit in novel-object recognition in Tc1 mice (*, $P < 0.05$). Wild-type mice took significantly more time exploring a novel object than objects A and B, which had been presented in a training session 10 min previously (object A, 27.7 ± 16.9 s; object B, 31.8 ± 25.0 s; novel object, 69.0 ± 35.2 s; $P < 0.05$ for the novel object compared to either object A or B but not significant for object A compared to object B). (**B**) Five Tc1 mice and seven wild-type littermates performed above chance in the spontaneous alternation T-maze, but levels of alternation are not significantly different across genotypes. (**C**) Ten Tc1 mice displayed a nonsignificant trend toward hyperactivity in an open field compared with 12 wild-type littermates. (**D**) Testing on a static rod task revealed no significant motor deficit in five Tc1 mice as compared with seven wild-type littermates. (**E**) Five Tc1 mice did not spend significantly more time in the open arms of an elevated plus maze than seven wild-type littermates, although a nonsignificant trend may reflect overall increased levels of activity. All error bars represent SEM.

of brain histopathology with standard histological and immunohistochemical techniques, including immunostaining for neural markers (MAP2, neurofilament 200, synaptophysin, and glial fibrillary acidic protein), the microglial marker Iba-1, Tau (AT270 and AT8), and βA4 amyloid showed no anatomical, or cytoarchitectural defects in brain sections of seven wild-type and seven Tc1 littermates aged between 9 and 21 months.

Heart development. Congenital heart defects occur in ~40% of DS individuals (*3*). We therefore compared heart development in E14.5 Tc1 embryos and their wild-type littermates. A perimembranous ventricular septal defect, representing a failure of fusion between the ventricular septum and the proximal outflow tract cushions, was seen in the majority of Tc1 mice studied (7 out of 11); this was associated with an overriding aorta (where the aorta straddles the ventricular septum) in a single case (Fig. 4, A, B, and G). In another fetus, the atrioventricular cushions were unfused, resulting in an atrioventricular septal defect (Fig. 4, C, D and G). A similar condition represents the most common cardiac defect seen in human babies with Down syndrome (*34*). In addition, some of the fetuses with ventricular septal defects also presented with the heart tilted onto its right side, when compared with wild-type littermates (Fig. 4, E and F). A minority of Tc1 fetuses (3 out of 11) showed no obvious cardiac defects (Fig. 4G).

Craniofacial morphology. Craniofacial abnormalities are seen in DS and in the Ts65Dn and Ts1Cje mouse models (*35*, *36*). We were unable to find differences between Tc1 mice and wild-type littermates in analyses of facial bone morphology using light microscopy; all visible cranial and facial bone shapes of the Tc1 heads were found to be normal, with no obvious morphological variation from wild-type littermates. The overall dimensions of the Tc1 skulls were indistinguishable from these wild-type controls. Scanning electron micrographs were prepared of the teeth to accurately compare Tc1 with wild-type dentitions. Tooth shapes, positions, sizes, and cusp patterns were all found to be identical. However, these analyses would not have been able to detect the skull dysmorphology described in Ts65Dn and Ts1Cje mice (*29*, *35*, *36*). We therefore carried out micro–computerized tomography (CT) scans of 10 wild-type and 10 Tc1 littermate heads, comparing distances between anatomical landmarks similar to those used by Richtsmeier, Reeves, and colleagues (fig. S5). All measurements taken of the cranium indicated there were no significant differences between wild-type and Tc1 littermates, although it is possible that there may be differences that could be revealed by complex mathematical modeling approaches, such as Euclidean distance matrix analysis as used by Richtsmeier, Reeves, and colleagues. While the majority of measurements of the mandibles were also similar, Tc1 mandibles were significantly smaller between the coronoid process and the mandibular angle and between the coronoid process and the most superior point on the incisor alveolar rim (fig. S5 and table S6). The mandible is known to be smaller in DS individuals than in the euploid population (*29*, *35*, *36*).

T lymphocyte activation. The T cell receptor (TCR)–induced activation of T lymphocytes has been reported to be defective in DS (*37*), and thus we examined this in Tc1 mice. We consistently found that both $CD4^+$ and $CD8^+$ T cells from both spleen and lymph nodes of Tc1 mice up-regulated CD25 and CD69 to a lesser extent than wild-type cells, in response to stimulation either through the TCR alone with antibodies to CD3ε or in combination with antibodies to the costimulatory receptor CD28 (fig. S6).

The Tc1 mouse as a model of DS. DS manifests with phenotypes common to all affected individuals, such as mental retardation, and phenotypes that are variable between individuals, such as atrioventricular septal defects of the heart (*3*). We have generated a strain of trans-species aneuploid mouse that carries an almost complete human chromosome and recapitulates features seen in humans with DS and in other DS mouse models, including changes in behavior, synaptic plasticity, cerebellar neuronal number, heart development, and mandible size. Altered LTP, for example, has been seen in Ts65Dn mice, whereas DS-like heart defects have not been reported in these or Ts1Cje animals but are seen in Tc1 mice and in chimeric mice carrying a 5-Mb noncontiguous Hsa21 fragment (*3*, *19*, *21*, *22*). Thus, for some aspects of DS, transchromosomic mice may be a better model of the human condition than the mouse chromosome segmental trisomies. Nonetheless, because the wide-scale effects of introducing human proteins into mouse protein complexes in transchromosomic animals are unknown, further work will be required to establish how well transchromosomic mice will model human aneuploidy conditions.

To dissect the molecular genetics of DS, human phenotype-karyotype correlations of the smallest region of overlap have been made for different traits in rare individuals with partial trisomies of Hsa21. Thus, DS critical regions (DSCRs) have been delineated that are described as carrying the gene(s) underlying specific traits, and the major effect gene(s) for several traits have been thought to lie within a few Mb of the marker *D21S55* (*4*, *29*, *38*, *39*). However, in recent studies, Reeves and colleagues studied mice carrying engineered portions of the Ts65Dn chromosome and showed that genes

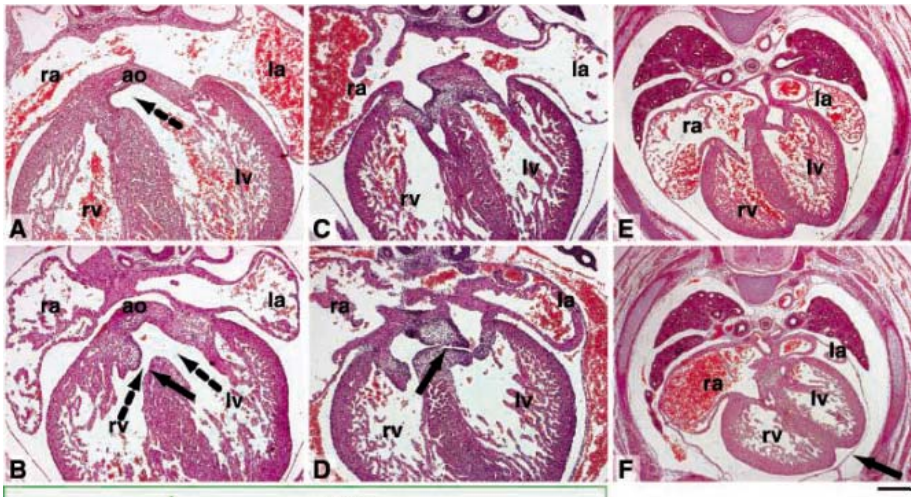

G

Genotype	Ventricular septal defect	Atrio ventricular septal defect	Heart tilted on right side	Normal heart
Wild-type (n=10)	2	0	0	8
Tc1 (n=11)	7	1	3*	3

Fig. 4. Cardiac defects in Tc1 fetuses. Transverse sections of E14.5 Tc1 and wild-type littermates, stained with hematoxylin and eosin. (**A**) Normal ventricular septation in a wild-type fetus, showing fusion of the interventricular septum with the proximal regions of the outflow tract cushions. The dotted arrow shows communication between the aorta and the left ventricle. (**B**) A perimembranous ventricular septal defect (solid arrow) in a Tc1 fetus, allowing the flow of blood between the right and left ventricles. In this case, the aorta is overriding the ventricular septum, allowing blood to enter the aorta from both the right and left ventricles (dotted arrows). (**C**) Normal atrioventricular septation in a wild-type fetus, showing fusion of the inferior and superior atrioventricular cushions and the primary atrial septum with the superior cushion. (**D**) Atrioventricular septal defect in a Tc1 fetus, showing that the inferior and superior atrioventricular cushions remain unfused (black arrow). (**E**) Normal positioning of the heart in a wild-type fetus. (**F**) In a Tc1 fetus the heart is tilted on to its right side, causing the interventricular sulcus to point to the left (black arrow). Scale bar, (A to D) 100 μm; (E and F) 200 μm. ao, aorta; la, left atrium; lv, left ventricle; ra, right atrium; rv, right ventricle. (**G**) Incidence of cardiac defects in Tc1 fetuses and their wild-type littermates. The asterisk indicates mice that also had ventricular septal defects.

lying within the DSCR alone were not sufficient and were largely unnecessary to generate the craniofacial dysmorphologies found in Ts65Dn mice (*29*). We found an intermediate situation in which Tc1 mice have some features of a smaller mandible but not an overall diminution in cranium size; these data support the suggestion of Reeves and colleagues that individual triplicated genes contribute to a particular trisomic phenotype in combination with other genes, and this effect will depend on the function of these genes and the nature of their interactions (*29*).

As the generation of Tc1 mice was based on manipulation of mouse ES cells, we will be able to use chromosome engineering and DNA targeting of Hsa21 (or of endogenous mouse sequences) to examine the dosage effects of individual genes or chromosome regions on the phenotypic abnormalities. Because Tc1 mice are trisomic for genes with orthologs on Mmu16, as well as on Mmu10 and Mmu17, they should contribute both to the analysis of how DS results from trisomy 21 and to the testing of gene dosage effects for individual genes.

Conclusions. We have extended previous approaches to generating transchromosomic mice (*10*, *12*, *14*, *15*) by achieving stable germline transmission of an almost complete human chromosome. This methodology is also relevant for studies of human artificial chromosomes as vectors. Technical issues arise from our studies. Both our analysis and previous studies have found that germline transmission of the human chromosome is dependent on the genetic background and sex of the transmitting parent and that the majority of transchromosomic lines will not give germline transmission, for reasons as yet unknown (*12*, *14*). Finally, trisomy 21, which is found in ~1 out of 43 spontaneous abortions (*40*) and in ~1 in 750 live births (*3*), is just one of many aneuploidy syndromes. Aneuploidies are a common cause of human morbidity and mortality, occurring in at least 5% of all pregnancies (*41*). The Tc1 mouse shows that modelling whole human chromosome aneuploidy syndromes is feasible in the mouse.

References and Notes

1. R. Chrast *et al.*, *Hum. Mol. Genet.* **9**, 1853 (2000).
2. D. J. Smith *et al.*, *Nat. Genet.* **16**, 28 (1997).
3. S. E. Antonarakis, R. Lyle, E. T. Dermitzakis, A. Reymond, S. Deutsch, *Nat. Rev. Genet.* **5**, 725 (2004).
4. D. L. Nelson, R. A. Gibbs, *Science* **306**, 619 (2004).
5. K. Gardiner, A. Fortna, L. Bechtel, M. T. Davisson, *Gene* **318**, 137 (2003).
6. R. H. Reeves *et al.*, *Nat. Genet.* **11**, 177 (1995).
7. H. Sago *et al.*, *Proc. Natl. Acad. Sci. U.S.A* **95**, 6256 (1998).
8. K. Yamakawa *et al.*, *Hum. Mol. Genet.* **7**, 227 (1998).
9. J. Kang *et al.*, *Nature* **325**, 733 (1987).
10. K. Tomizuka *et al.*, *Nat. Genet.* **16**, 133 (1997).
11. K. Tomizuka *et al.*, *Proc. Natl. Acad. Sci. U.S.A* **97**, 722 (2000).
12. D. Hernandez, P. J. Mee, J. E. Martin, V. L. Tybulewicz, E. M. C. Fisher, *Hum. Mol. Genet.* **8**, 923 (1999).
13. D. Hernandez, E. M. C. Fisher, *Trends Genet.* **15**, 241 (1999).
14. Y. Kazuki *et al.*, *J. Hum. Genet.* **46**, 600 (2001).
15. T. Shinohara *et al.*, *Hum. Mol. Genet.* **10**, 1163 (2001).
16. A. K. Voss, T. Thomas, P. Gruss, *Exp. Cell Res.* **230**, 45 (1997).
17. Materials and methods are available as supporting material on *Science* Online.
18. The name Tc(Hsa21)1TybEmcf, which we have shortened to Tc1, is the official name given by the Mouse Nomenclature Committee.
19. T. Shinohara *et al.*, *Chromosome Res.* **8**, 713 (2000).
20. L. Devlin, P. J. Morrison, *Arch. Dis. Child.* **89**, 1177 (2004).
21. A. M. Kleschevnikov *et al.*, *J. Neurosci.* **24**, 8153 (2004).
22. R. J. Siarey, J. Stoll, S. I. Rapoport, Z. Galdzicki, *Neuropharmacology* **36**, 1549 (1997).
23. T. V. Bliss, G. L. Collingridge, *Nature* **361**, 31 (1993).
24. N. J. Broadbent, L. R. Squire, R. E. Clark, *Proc. Natl. Acad. Sci. U.S.A.* **101**, 14515 (2004).
25. R. S. Hammond, L. E. Tull, R. W. Stackman, *Neurobiol. Learn. Mem.* **82**, 26 (2004).
26. R. Lalonde, *Neurosci. Biobehav. Rev.* **26**, 91 (2002).
27. R. G. Lister, *Psychopharmacology* **92**, 180 (1987).
28. L. L. Baxter, T. H. Moran, J. T. Richtsmeier, J. Troncoso, R. H. Reeves, *Hum. Mol. Genet.* **9**, 195 (2000).
29. L. E. Olson, J. T. Richtsmeier, J. Leszl, R. H. Reeves, *Science* **306**, 687 (2004).
30. L. E. Olson *et al.*, *Dev. Dyn.* **230**, 581 (2004).
31. E. H. Aylward *et al.*, *Arch. Neurol.* **54**, 209 (1997).
32. T. L. Jernigan, U. Bellugi, *Arch. Neurol.* **47**, 529 (1990).
33. N. Raz *et al.*, *Neurology* **45**, 356 (1995).
34. C. L. Maslen, *Curr. Opin. Cardiol.* **19**, 205 (2004).
35. J. T. Richtsmeier, L. L. Baxter, R. H. Reeves, *Dev. Dyn.* **217**, 137 (2000).
36. J. T. Richtsmeier, A. Zumwalt, E. J. Carlson, C. J. Epstein, R. H. Reeves, *Am. J. Med. Genet.* **107**, 317 (2002).
37. I. Scotese *et al.*, *Pediatr. Res.* **44**, 252 (1998).
38. J. M. Delabar *et al.*, *Eur. J. Hum. Genet.* **1**, 114 (1993).
39. J. R. Korenberg *et al.*, *Proc. Natl. Acad. Sci. U.S.A.* **91**, 4997 (1994).
40. L. Y. Hsu, in *Genetic Disorders and the Fetus*, A. Milunsky, Ed. (Johns Hopkins Univ. Press, Baltimore, MD, 1998), pp. 179–248.
41. T. Hassold, P. Hunt, *Nat. Rev. Genet.* **2**, 280 (2001).

42. We thank the Wellcome Trust, the Medical Research Council, the Leukaemia Research Fund, the Barts and the London Charitable Foundation, and the British Heart Foundation for support, A. Voss for the MPI VI ES cell line, P. Choquet for help with CT scans, R. Young for graphics, and R. Reeves for helpful comments. Gene array data are deposited at European Molecular Biology Laboratory–European Bioinformatics Institute with accession number E-MEXP-409.

Supporting Online Material

www.sciencemag.org/cgi/content/full/309/5743/2033/DC1
Materials and Methods
Figs. S1 to S6
Tables S1 to S6
References and Notes

6 May 2005; accepted 22 August 2005
10.1126/science.1114535

REPORTS

Fluorescent Guest Molecules Report Ordered Inner Phase of Host Capsules in Solution

Scott J. Dalgarno, Sheryl A. Tucker,* Daniel B. Bassil, Jerry L. Atwood*

Despite recent strides in the synthesis of elaborate nanometer-scale molecular hosts, the internal structure of these self-assembled cages remains ill characterized. We used fluorescent probe molecules, pyrene butyric acid (PBA), as guests in *C*-hexylpyrogallol[4]arene capsules to relay information about the chemical environment on the interior of the assemblies. Spectroscopic and single-crystal x-ray diffraction studies show that, in both solution and the solid state, the host can encapsulate two PBA guests and keep them well separated through specific interactions with the capsule walls.

Proteins form remarkably intricate structures by component self-assembly, such as the icosahedral framework combining 180 subunits in the cowpea chloritic mottle virus (*1*). These frameworks create highly specific pockets of chemical space that can induce selective reactivity (*2*). Recently, chemists have used noncovalent self-assembly strategies to form analogous synthetic nanometer-scale molecular host structures, often resembling the high-symmetry Platonic or Archimedean polyhedra (*3*–*7*). The molecular building blocks are rationally designed to bind one another through complementary interactions, such as hydrogen bonding or coordination to metals.

Our work has focused on cyclic *C*-methylresorcin[4]arene and *C*-alkylpyrogallol[4]arene substrates, which form hexameric hydrogen-bonded capsules in solution that enclose 1200 to 1500 Å^3 of space (*8*–*11*). These capsules are stable in polar and nonpolar solution and can host a variety of ionic and molecular guests (*12*–*17*). However, the interior environment of such synthetic hosts generally remains

Department of Chemistry, University of Missouri–Columbia, 601 South College Avenue, Columbia, MO 65211, USA.

*To whom correspondence should be addressed. E-mail: tuckers@missouri.edu (S.A.T.); atwoodj@missouri.edu (J.L.A)

poorly characterized. Crystallographic evidence of specific host-guest interactions has been scarce, and detailed knowledge of the solution-phase interactions would offer substantial insight toward rational control over guest reactivity.

Here we present the structural characterization and spectrofluorometric studies of a capsule-bound fluorescent probe molecule, pyrene butyric acid (PBA). The supramolecular assembly **1** was synthesized by sonication of a saturated acetonitrile solution containing *C*-hexylpyrogallol[4]arene (PgC_6) and PBA (Fig. 1). Single-crystal x-ray diffraction studies show not only that the PBA molecules interact with the capsule walls in the solid state, but also that the π surfaces of the PBA guest molecules are well separated from one another within the capsule (*18*). The spectroscopic studies corroborate this finding. In solution, the PBA guests also interact with the capsule walls and remain separated from one another within the capsules. The assembly retained structural integrity over four weeks in the solution phase, suggesting that the carboxylic acid groups and the polyaromatic nature of the PBA molecules do not destabilize the overall supramolecular assembly.

Large single orange/brown crystals of **1** grew during slow evaporation of the solution over 2 to 3 weeks after sonication. The single-crystal x-ray diffraction study showed the structure to be a hexameric assembly of PgC_6 containing zero to two PBA molecules (Fig. 2). When crystals of **1** were redissolved in deuterated acetonitrile, integration of the ^1H nuclear magnetic resonance (NMR) spectrum revealed an average of 1.5 molecules of PBA per capsule (*19*). Although there was disorder present on the interior of the capsule, due in part to disparate guest populations, it was possible to model and refine the polyaromatic fragment of a PBA molecule in one position within the structural asymmetric unit. Symmetry expansion of the asymmetric unit around an inversion center generates an entire capsule and shows the polyaromatic sections of the two PBA molecules to be well separated from one another [pyrene centroid···centroid distance of 7.834 Å (Fig. 2)].

The interior volume of the hexameric capsule is approximately 1250 $Å^3$ (*20*, *21*), which easily accommodates two PBA molecules (each 260 $Å^3$) with additional solvent (*22*, *23*). The polyaromatic pyrene fragments of the encapsulated PBA guests interact with the aryl rings of the capsule walls, rather than with one another. The distance between the pyrene planes in a doubly occupied capsule is sufficient for one or more acetonitrile molecules, but it was not possible to model the diffuse electron density in this position as such.

From the crystal structure, it is clear that there is guest-to-wall binding, attributable to π stacking and CH···π interactions between PBA and PgC_6 (*24*). Additional interactions may be present between the butyric acid functionality and the capsule seam hydroxyl groups, but these could not be identified because of the extensive disorder present between the pyrene rings. Evidence of this guest-to-wall binding is also present in solution. The formation of a ground-state complex between PBA and the capsule wall results in expected spectral perturbations (Fig. 3), compared with free PBA in hexane (*25*). The most noticeable difference is the appearance of a new spectral band at 350 nm in the absorption spectrum (Fig. 3A) and a loss of vibronic-band fine structure in the fluorescence emission spectrum (Fig. 3, B to D), as seen in aromatic solvents such as toluene.

We probed the solution-phase behavior of the host-guest assemblies using spectrofluorometry (*26*). On dissolving crystals of **1** in hexane, we observed a significant increase in the fluorescence emission intensity, compared with the spectrum of free PBA in hexane (Fig. 3B). This increased

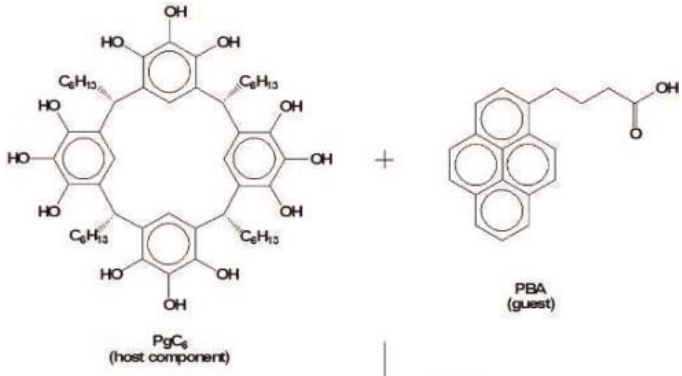

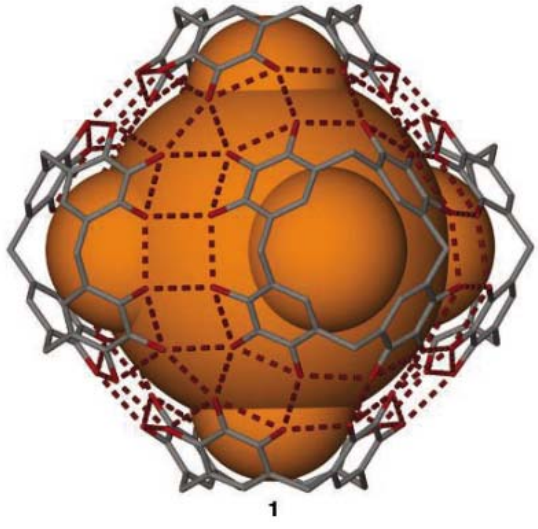

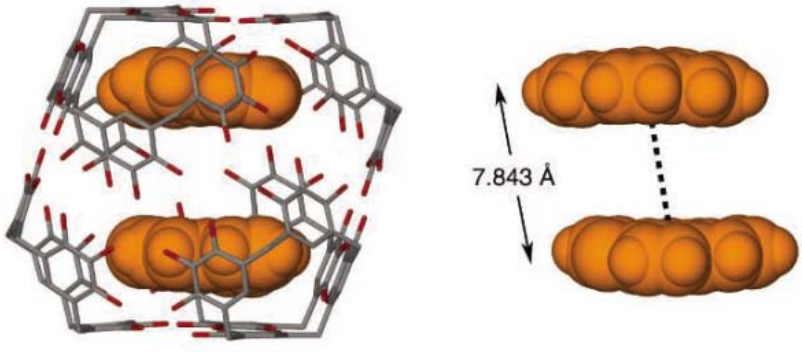

Fig. 1. Schematic for the formation of hexameric assembly **1** containing the fluorophore PBA. The encapsulated space, which is occupied by PBA and acetonitrile, is depicted in orange.

Fig. 2. Diagram of the crystal structure of **1** showing the resolved pyrene fragments (in orange space-filling mode) within the hexameric assembly. The distance between the centroids of the polyaromatic guests is 7.843 Å. The remaining void space is occupied by the butyric acid side chains of the PBA molecules (not shown) and possibly by solvent acetonitrile molecules.

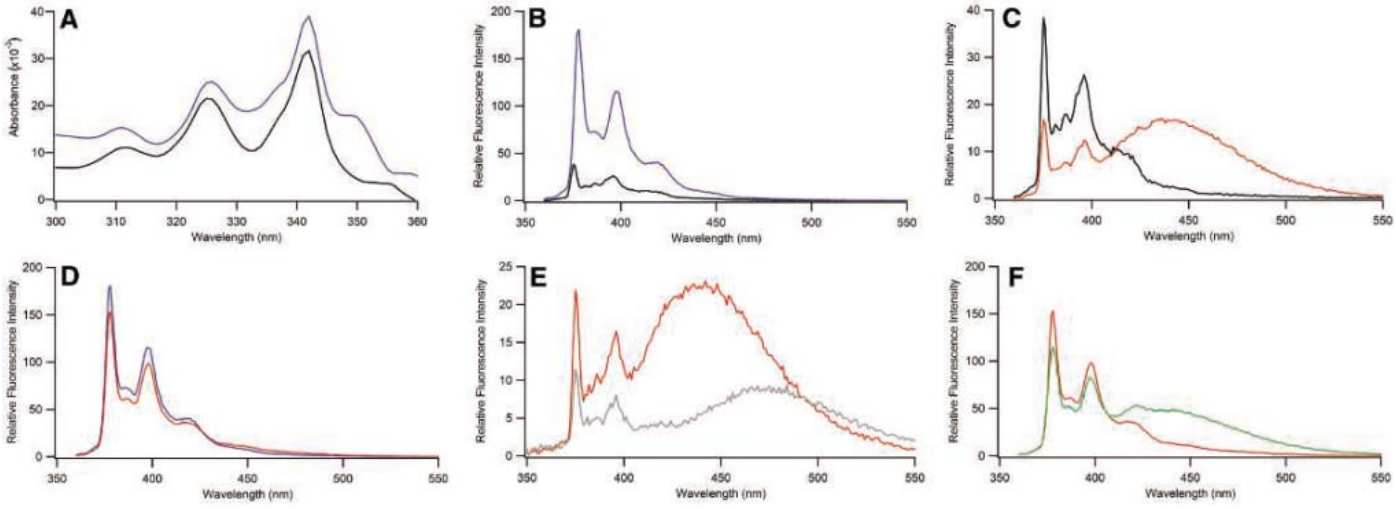

Fig. 3. (**A**) Absorption spectra of PBA in hexane (black) and encapsulated PBA in hexane (blue). Fluorescence emission spectra of (**B**) PBA in hexane (black) and encapsulated PBA in hexane (blue); (**C**) free PBA in hexane (black), with the addition of 10 μl of DMA (red); (**D**) encapsulated PBA (**1**) in hexane (blue), with the addition of 10 μl of DMA (red); (**E**) PBA in hexane and DMA (red), with the addition of 100 μl of acetonitrile (gray); and (**F**) **1** in hexane and DMA (red), with the addition of free PBA (green).

quantum yield appears to result from the structural constraints imposed by the host, which minimize radiationless excited-state decay pathways such as collisional quenching by solvent molecules. Furthermore, there is no emission intensity at 470 nm (*27*) characteristic of an excimer, or excited-state PBA dimer. This result confirms that in solution, as in the solid state, any capsules that enclose two guests keep them rigidly apart.

To further assess the extent to which PBA guests remain encapsulated in solution, we added a known fluorescence quencher, dimethylaniline (DMA). In hexane solution, free PBA forms an excited-state charge-transfer complex, or exciplex, with DMA, leading to a new emission band at 440 nm. This exciplex was not observed in DMA-hexane solutions of **1** (Fig. 3, C and D), suggesting that the PBA guests do not leave the capsule. The DMA is small enough to penetrate the capsules and thereby quench PBA fluorescence (Fig. 3E). This result is most easily explained by the presence of residual acetonitrile within the capsules, because it is known that polar solvents inhibit emission from the exciplex (Fig. 3E) (*25*, *28*). As a final control, we added free PBA to the DMA-hexane solution of **1**, and the exciplex emission emerged as expected (Fig. 3F). It is therefore clear that, at least in nonpolar solvent, the PBA guests in **1** remain tightly enclosed and do not exchange with external PBA.

The assembly was also found to be very robust in polar solution. Acetonitrile stock solutions of **1** were allowed to sit for 30 days and were then transferred to hexane. The amount of PBA that leached from the capsules, as measured by exciplex formation with DMA, was only ~10% (*29*, *30*).

References and Notes

1. T. Douglas, M. Young, *Nature* **393**, 152 (1998).
2. Schumacher *et al.*, *Science* **294**, 2158 (2001).
3. J.-M. Lehn, *Supramolecular Chemistry: Concepts and Perspectives* (VCH, Weinheim, Germany, 1995).
4. J. W. Steed, J. L. Atwood, *Supramolecular Chemistry: A Concise Introduction* (Wiley, Chichester, UK, 2000).
5. R. S. Meissner, J. Rebek Jr., J. de Mendoza, *Science* **270**, 1485 (1995).
6. G. W. Orr, L. J. Barbour, J. L. Atwood, *Science* **285**, 1049 (1999).
7. C. L. Raston *et al.*, *J. Am. Chem. Soc.* **126**, 13170 (2004).
8. L. R. MacGillivray, J. L. Atwood, *Nature* **389**, 469 (1997).
9. J. L. Atwood, L. J. Barbour, A. Jerga, *Chem. Commun.* **22**, 2376 (2001).
10. J. L. Atwood, L. J. Barbour, A. Jerga, *Proc. Natl. Acad. Sci. U.S.A.* **99**, 4837 (2002).
11. G. W. V. Cave, J. Antesberger, L. J. Barbour, R. M. McKinlay, J. L. Atwood, *Angew. Chem. Int. Ed. Engl.* **43**, 5263 (2004).
12. J. Mattay *et al.*, *Eur. J. Org. Chem.* **1999**, 2257 (1999).
13. A. Shivanyuk, J. Rebek Jr., *Chem. Commun.* **22**, 2374 (2001).
14. L. C. Palmer, J. Rebek Jr., *Org. Lett.* **7**, 787 (2005).
15. L. Avram, Y. Cohen, *Org. Lett.* **5**, 3329 (2003).
16. L. Avram, Y. Cohen, *J. Am. Chem. Soc.* **125**, 16180 (2003).
17. A. Shivanyuk, J. C. Friese, S. Döring, J. Rebek Jr., *J. Org. Chem.* **68**, 6489 (2003).
18. Crystal data for **1**: $C_{177.50}H_{237.75}N_{3.25}O_{37.50}$, molecular weight M = 3016.96, triclinic, a = 19.567 [estimated standard deviation (ESD) 3] Å, b = 22.605 (ESD 3) Å, c = 23.309 (ESD 3) Å, α = 69.819 (ESD 3)°, β = 70.133 (ESD 3)°, γ = 72.096 (ESD 2)°, U = 8887 (ESD 2) Å^3, μ = 1.127 mm^{-1}, temperature T = 173 (ESD 2) K, space group $P\bar{1}$, Z = 2, Mo-Kα radiation (wavelength λ = 0.71073 Å), final goodness of fit = 1.624, agreement index R_1 = 0.1810, 60406 reflections measured, 37293 unique (R_{int} = 0.0722) which were used in all calculations. The final weighted agreement index $\omega R(F^2)$ was 0.4443 (all data), where F is a structure factor. X-ray data were collected on a Bruker SMART 1000 charge-coupled device diffractometer (Bruker AXS, Madison, WI).
19. Materials and methods are available as supporting material on *Science* Online.
20. L. J. Barbour, MCAVITY, software program for the determination of the volume of a molecular cavity, University of Missouri–Columbia (http://x-seed.net/cavity.html).
21. M. L. Connolly, *Science* **221**, 709 (1983).
22. T. A. Olszak, F. Willig, W. S. Durfee, W. Dreissig, H. Brodaczek, *Acta Cryst.* **C45**, 803 (1989).
23. The molecular volume of PBA was calculated using the X-Seed program (www.x-seed.net).
24. Three crystallographically unique interactions were evident: two CH···π interactions, with CH···aromatic centroid distances of 2.832 and 2.930 Å; and one π-stacking interaction with an aromatic centroid···centroid distance of 3.847 Å.
25. J. R. Lakowicz, *Principles of Fluorescence Spectroscopy* (Kluwer Academic/Plenum Publishers, New York, ed. 2, 1999).
26. Aggregation of PBA containing capsules appears to be unlikely at 1 × 10^{-6} M (*30*), given that light-scattering studies on PgC_n (where n is a straight-chain alkane) systems, in addition to published ^{13}C NMR studies, were performed at much higher concentrations (3 mM) (*16*).
27. In-house studies of PBA excimer emission (470 nm) are in agreement with the literature for the parent pyrene molecule (*25*).
28. As the exciplex emission is quenched, its spectral maximum is also red shifted with the increase in microenvironmental polarity, in agreement the DMA-quenching literature (*31*).
29. Pyrene butyric acid (Aldrich), dimethylaniline (Aldrich, 99%), acetonitrile (Fisher, high performance liquid chromatography grade), and hexane (Fisher, 95%) were obtained and used as received. PgC_6 was synthesized by literature methods (*7*). Stock solutions of PyBA and the capsules were made by dissolving a known amount of solid in acetonitrile. Spectroscopic samples were prepared by quantitatively transferring known aliquots of the stock solution into volumetric flasks, where the solvent was stripped off under ultrahigh purity nitrogen. Samples containing ~1 × 10^{-6} M PBA were diluted to volume (2.5 ml) with solvent and were analyzed within 30 min of preparation.
30. Absorption and fluorescence emission spectra were collected at ambient temperature in 1 cm^2 Suprasil quartz cuvettes on an HP 8453 (Agilent Technologies, Palo Alto, CA) diode array spectrophotometer and a Cary Eclipse (Varian, Palo Alto, CA) spectrofluorometer, respectively. A slit width of 1 nm was used in the absorption measurements, and the emission settings were as follows: monochromator bandpasses of 2.5 nm, a step size of 2.5 nm, and scan rate of 120 nm/min. All spectra were absorption and/or blank corrected.
31. D. Gupta, S. Basu, *J. Photochem.* **4**, 307 (1975).

32. We acknowledge NSF for financial support of this work. Crystallographic data for **1** [Cambridge Crystallographic Data Centre (CCDC) identification number 276051] can be obtained free of charge at www.ccdc.cam.ac.uk/conts/retrieving.html (or from the CCDC, 12 Union Road, Cambridge CB2 1EZ, UK; international fax: +44-1223/336-033; E-mail: deposit@ccdc.cam.ac.uk).

Supporting Online Material

www.sciencemag.org/cgi/content/full/309/5743/2037/DC1

Materials and Methods

24 June 2005; accepted 23 August 2005

10.1126/science.1116579

A Chromium Terephthalate–Based Solid with Unusually Large Pore Volumes and Surface Area

G. Férey,[1,2*] C. Mellot-Draznieks,[3] C. Serre,[1] F. Millange,[1] J. Dutour,[1] S. Surblé,[1] I. Margiolaki[4]

We combined targeted chemistry and computational design to create a crystal structure for porous chromium terephthalate, MIL-101, with very large pore sizes and surface area. Its zeotype cubic structure has a giant cell volume (~702,000 cubic angstroms), a hierarchy of extra-large pore sizes (~30 to 34 angstroms), and a Langmuir surface area for N_2 of ~5900 ± 300 square meters per gram. Beside the usual properties of porous compounds, this solid has potential as a nanomold for monodisperse nanomaterials, as illustrated here by the incorporation of Keggin polyanions within the cages.

Porous materials with large, regular, accessible cages and tunnels are increasingly in demand for applications in catalysis (*1*), separations (*2*), sensors, electronics, and gas storage (*3*, *4*). Depending on their structure and pore size, these materials allow only molecules of certain shapes and sizes to enter the pores. Furthermore, giant pores may act as nanoreactors, in which the confined volume may generate reactions that do not occur in the bulk material, or as nanomolds for calibrated and monodisperse nanomaterials (*5*). In this respect, the larger the pores, the wider the range of reactants that can be combined or stored.

However, the design of materials with increasingly large pores carries, especially for metal-organic frameworks, the risk of interpenetration of the skeletons within structures. In addition, although the structural characterization of such solids with large cells is usually possible when single crystals are available, the probability of getting the solutions is known to drastically decrease or even to become zero when the cell dimensions increase too much (*6*). These problems have restricted the number of discovered porous solids with extra-large pores, of which cloverite, with a cell volume of ~125,000 Å^3 and pore diameters close to 30 Å (*7*) is the largest.

We recently developed a strategy to overcome these limitations based on the combination of targeted chemistry and computer simulations. Hybrid porous solids result from the three-dimensional (3D) covalent connection of inorganic clusters and organic moieties that act as linkers, and the first step in our "tailor-made" approach is to control the nature of the inorganic cluster and the chemical conditions required for its formation and stability in solution (*8*). In the second step, we use computational strategies, typically our global optimization AASBU (automated assembly of secondary building units) method (*9*–*12*), as recently adapted to hybrids (*13*), or other closely related methods (*14*). The AASBU method explores how an inorganic cluster and an organic linker, or even predefined hybrid building blocks, may connect in 3D space to form periodic lattices. A virtual library of candidate frameworks is produced, along with their crystallographic features (space group, cell parameters, atomic coordinates) and their simulated x-ray diffraction (XRD) patterns. The comparison of the simulated pattern of each candidate structure with the experimental one identifies the targeted experimental structure, giving direct access to the structural solution without any recourse to single crystals. The final structure is refined with the Rietveld method from powder data, the guest species being localized from Fourier difference maps. While tackling the underlying issue of polymorphism of hybrid materials, our computational approach provides a direct-space tool for solving structures that may be highly complex.

To implement our combined method, we first determined (*10*) the adequate chemical conditions leading to the existence of trimeric inorganic building blocks, formed by the assembly of three octahedra sharing a μ_3-O common vertex. Simulations were then performed to combine these inorganic trimers in 3D space with 1,3,5-benzene tricarboxylate (BTC) through the assembly of a computationally designed hybrid building block. Among the various predicted crystal structures, one candidate exhibited the same powder XRD pattern as the powdered chromium trimesate **MIL-100**

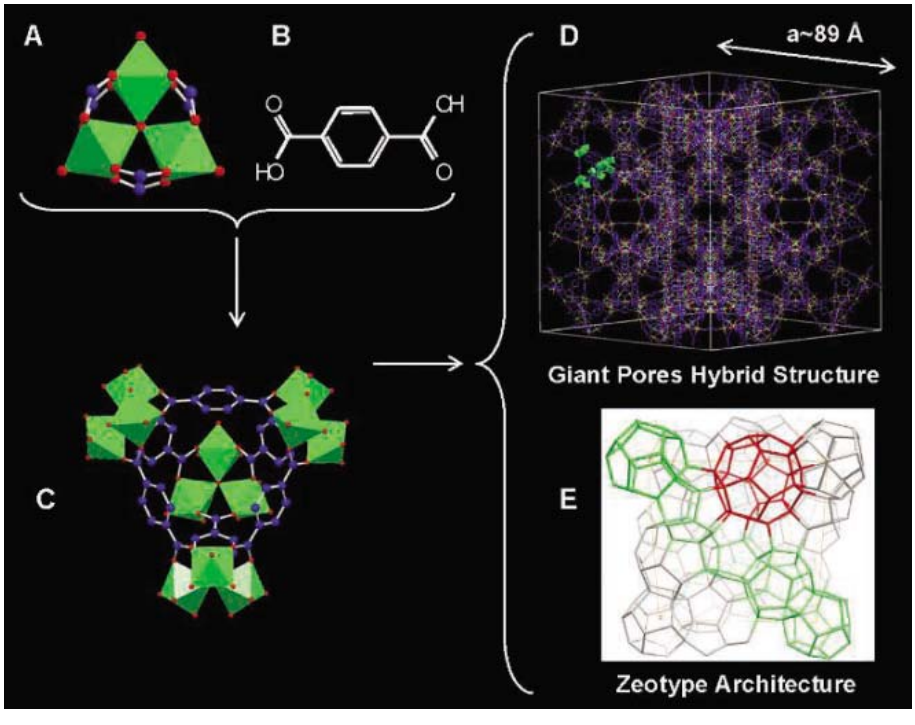

Fig. 1. (**A**) The computationnally designed trimeric building block chelated by three carboxylic functions. The ST was constructed with (**B**) terephthalic acid, which lies (**C**) on the edges of the ST. (**D**) Ball-and-stick representation of one unit cell, highlighting one ST drawn in a polyhedron mode. (**E**) Schematic 3D representation of the MTN zeotype architecture (the vertices represent the centers of each ST) with the medium (in green, with 20 tetrahedra) and large (in red with 28 tetrahedra) cages delimited by the vertex sharing of the ST. Chromium octahedra, oxygen, fluorine and carbon atoms are in green, red, and blue, respectively.

[1]Institut Lavoisier, CNRS Unité Mixte de Recherche 8637, Université de Versailles St-Quentin en Yvelines, 45 Avenue des Etats-Unis, 78035 Versailles Cedex, France. [2]Institut universitaire de France, 103, Boulevard Saint-Michel, 75005 Paris, France. [3]Royal Institution, 21 Albemarle Street, London W1S 4BS, UK. [4]European Radiation Synchotron Facility, 38042 Grenoble, France.

*To whom correspondence should be addressed. E-mail: ferey@chimie.uvsq.fr

(*15*) (MIL, Matérial Institut Lavoisier), revealing a giant cell volume (>380,000 Å^3) and large pore sizes (~25 to 29 Å) consistent with the very high surface area measurement ($S_{Langmuir}$ = 3100 m^2 g^{-1}). This hybrid crystal structure was then refined from synchrotron powder data, allowing the further localization of the guest moities. **MIL-100** showed the feasibility of creating simulation-assisted chemical structures (*16*). With that adressed, we investigated other carboxylates, here terephthalic acid [1,4-benzene dicarboxylate (1,4-BDC)] combined with similar trimers. Compared to other MOFs (metal-organic frameworks), the resulting solid, **MIL-101,** has the best characteristics in terms of cell dimensions (702,000 Å^3), pore sizes (29 to 34 Å), and surface area (5900 m^2 g^{-1}).

The synthesis of **MIL-101** consists in the hydrothermal reaction of H_2BDC (166 mg at 1 mmol) with $Cr(NO_3)_3.9H_2O$ (400 mg at 1 mmol), fluorhydric acid (0.2 ml at 1 mmol), and H_2O (4.8 ml at 265 mmol), for 8 hours at 220°C. This reaction produced a highly crystallized green powder of the chromium terephthalate with formula $Cr_3F(H_2O)_2O[(O_2C)$-C_6H_4-$(CO_2)]_3.nH_2O$ (where n is ~25), based on chemical analysis. The yield based on chromium is ~50%. Analysis of the powder XRD data indicates a cubic cell (a ~ 89 Å) and a close relationship with the augmented Mobil Thirty-Nine (MTN) zeotype structure of MIL-100 (*17*). For the simulation process, a candidate hybrid building block, made on the sole basis of its compatibility with the experimental metal:organic ratio of the targeted **MIL-101,** was computationally designed as a super tetrahedron (hereafter noted ST) (Fig. 1). It was made from the linkage of 1,4-BDC anions and inorganic trimers that consist of three iron atoms in an octahedral environment with four oxygen atoms of the bidendate dicarboxylates, one μ_3O atom, and one oxygen atom from the terminal water or fluorine group. Octahedra are related through the μ_3O oxygen atom to form the trimeric building unit. The four vertices of the ST are occupied by the trimers, and the organic linkers are located at the six edges of the ST. Following our previous strategy (*14*), the ST building blocks were computationally assembled. The size of the ST requires an expansion of the cubic unit cell (space group F *d-3m*) to more than 85 Å before the construction process. The connection between the ST was established through vertices to ensure a 3D network of "corner-sharing" super tetrahedra with an augmented MTN zeotype architecture (*18*) (Fig. 1) and illustrates our concept of scale chemistry (*19*). Once the structure construction of **MIL-101** was computationally completed (74 atoms per asymmetric unit without hydrogen atoms), the model structure of **MIL-101** was directly used for full structural refinement with synchrotron data (table S1 and fig. S1) (*20*). Free water molecules filling the pores were located through successive Fourier differences.

The STs are microporous (with a ~8.6 Å free aperture for the windows), and the resulting framework delimits two types of mesoporous cages filled with guest molecules (Fig. 2). These two cages, which are present in a 2:1 ratio, are delimited by 20 and 28 ST (one by 20 and one by 28) with internal free diameters of ~29 Å and 34 Å, respectively (Fig. 2). These values correspond to accessible pore volumes of ~12,700 Å^3 and ~20,600 Å^3, respectively. The large windows of both cages make the latter accessible to very large molecules. The smaller cages exhibit pentagonal windows with a free opening of ~12 Å, while the larger cages possess both pentagonal and larger hexagonal windows with a ~14.5 Å by 16 Å free aperture (Fig. 2).

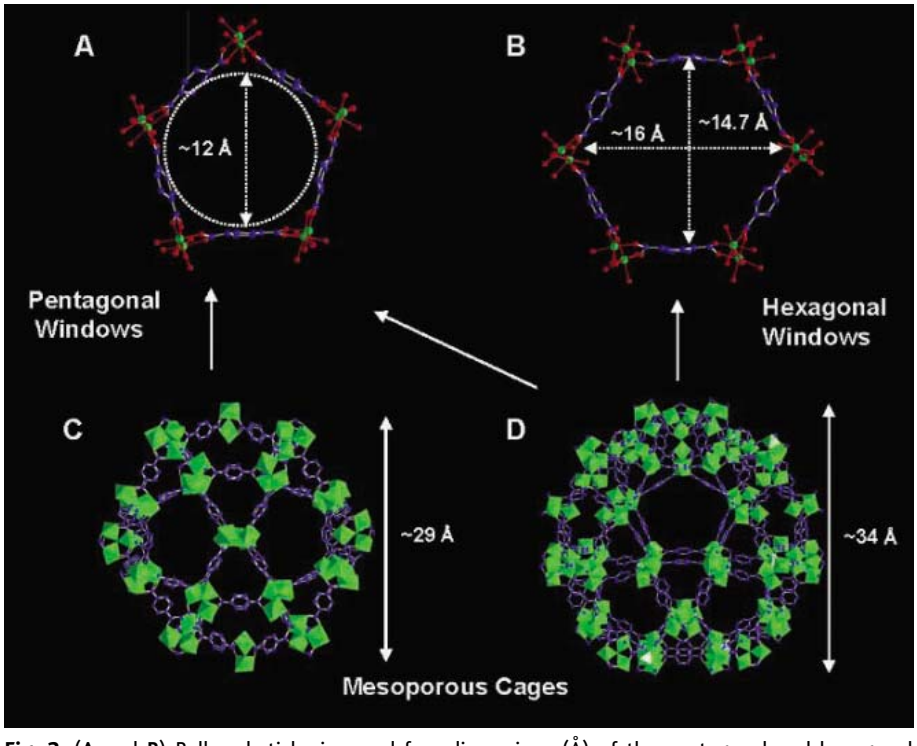

Fig. 2. (**A** and **B**) Ball-and-stick view and free dimensions (Å) of the pentagonal and hexagonal windows. (**C** and **D**) Ball-and-stick view of the two cages. Chromium octahedra, oxygen, fluorine and carbon atoms are in green, red, red and blue, respectively.

Thermogravimetric analysis in air (fig. S2) revealed that **MIL-101** was stable up to 275°C. X-ray thermodiffractometry showed that the evacuation of the guest molecules did not affect the framework. We also found that **MIL-101** exhibited very high uptake of gases. The N_2 sorption isotherm on the dehydrated sample (fig. S3A) is of type I with secondary uptakes at P/P_0 ~ 0.1 and at P/P_0 ~ 0.2, where P is gas pressure and P_0 is saturation pressure, characteristic of the presence of the two kinds of microporous windows. Using the Dubinin-Raduskhvich equation, we found a pore volume near 2.0(1) cm^3 g^{-1} for **MIL-101**. The apparent Brunauer Emmer Teller (BET) and $S_{Langmuir}$ surface area are larger than 4,100(200) and 5,900(300) m^2 g^{-1}, respectively (Fig. 3). The isotherms are probably overestimating the true internal surface area of MIL-101, but comparisons to be made with related materials are possible. To our knowledge, the highest surface area reported for any crystalline or amorphous solid [4500 m^2 g^{-1} (Langmuir)], was obtained with MOF-177, a porous hybrid solid (*20*). The large standard deviations for the surface area of MIL-101 comes both from experimental considerations (such as error on weight measurements and purity of the sample) and from the choice of the points used for the BET or Langmuir calculation (fig. S3B). The as-synthesized **MIL-101** solid exhibits a smaller $S_{Langmuir}$ surface area within the 4500 to 5500 m^2 g^{-1} range because of the presence of variable amounts of free terephthalic acid outside and within the pores. An activation treatment was thus performed to reach the maximal surface area and pore volume (*21*).

MIL-101 is stable over months under air atmosphere and was not altered when treated with various organic solvents at room temperature or under solvothermal conditions. These properties, together with high adsorption capacities, make **MIL-101** an attractive candidate for the adsorption of gas or large molecules. The very large windows easily allow the introduction of new species into the cages and possible enhanced reactions favored by confinement effects (similar to a pressure) in the cages. Moreover, as soon as introduced nanometric species fill the volume, the fixed dimensions of the pores lead

to monodispersed nanomaterials on the scale of 1 to 3 nm. The possibility of their introduction depends on the fit between their size and the accessible dimensions of the windows of each cage. Large species may therefore occupy only the large cages (~20,600 Å^3) while leaving space for other species with different properties in the small cages (~12,700 Å^3). Such a selective placement of guests might lead to hitherto unknown assemblies of monodisperse multifunctional nanomaterials and the possibility of structural characterization of these nano-objects when the host structure is not affected by the introduction of species.

To illustrate this idea, we explored the incorporation of Keggin polyanions in **MIL-101**. Such incorporation has been achieved previously through the encapsulation of a molybdenum Keggin anion in a metal-oxygen system (*22*). The $K_7PW_{11}O_{40}.nH_2O$ salt was selected because of its low acidity, the presence of a ^{31}P nuclear magnetic resonance (NMR) nucleus for NMR characterization, and finally its size (van der Waals radius, ~13.1 Å), which rules out the diffusion of Keggin ions into the small cages. A powdered sample of **MIL-101** was placed in an aqueous solution of the Keggin salt for 2 hours. To probe the presence of the polynanion within the pores, the resulting **MIL-101**–Keggin solid was analyzed by thermal gravimetric analysis (TGA), N_2 sorption measurement, XRD, ^{31}P solid state NMR (Fig. 4), and infrared spectroscopy (fig. S3). All of these techniques confirmed the presence of a large amount of the Keggin ions within the pores: a strong decrease in the weight losses [TGA (fig. S2)] and surface areas [$S_{Langmuir}$ ~ 3,750(250) m^2 g^{-1} instead of 5,900(300) m^2 g^{-1} for **MIL-101** (fig. S3C)] due to the higher density of the Keggan moieties compared to **MIL-101**. We observed significant changes in XRD peak intensities but not of the Bragg peak positions (fig. S4). Infrared spectroscopy confirmed the presence of the polyanions within the pores of MIL-101 (fig. S5). ^{31}P NMR also indicated one single peak at about–12.2(1) parts per million (ppm), confirming that the integrity of the Keggin structure was retained within the pores of **MIL-101** (fig. S6).

Quantitative analysis (*17*) also gave an estimation of ~0.05 Keggin anions per chromium. Considering the size of the $K_7PW_{11}O_{40}$ ion, we assumed that the polyanions could diffuse into the largest cages only, which would allow about five highly charged Keggin moities per large cage (Keggin per cage, ~5.3). Because the volume of a $PW_{11}O_{40}^{7-}$ anion is nearly 2250 A^3, five Keggin ions represent ~10,100 A^3 in volume, which is lower than the ~20,600 A^3 volume of a large cage. The residual volume is probably occupied by cations and water molecules. This successful incorporation of Keggin anions in large amounts strongly suggests that **MIL-101,** a crystallized hybrid solid with a periodical and calibrated porosity, is an excellent candidate for the introduction of gas (*23*) nano-objects in a regular and monodisperse mode with specific physical properties (*24*) or for drug delivery (*25*).

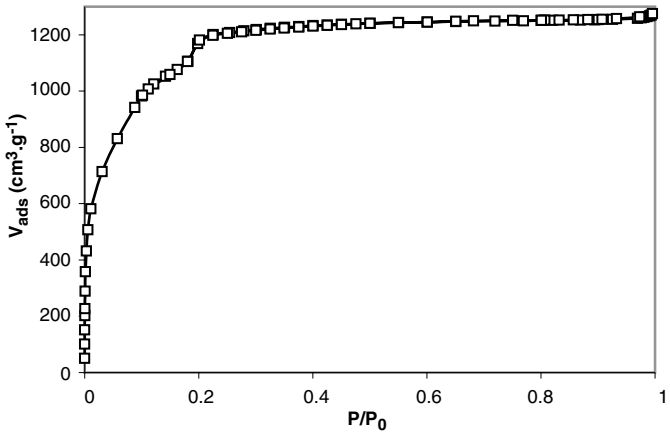

Fig. 3. Nitrogen gas sorption isotherm at 78 K for MIL-101. P/P_O is the ratio of gas pressure (P) to saturation pressure (P_0 = 750 torr).

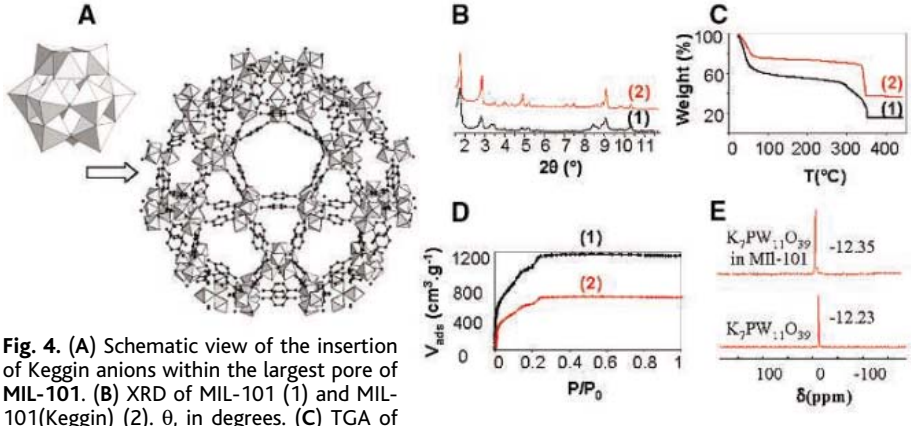

Fig. 4. (**A**) Schematic view of the insertion of Keggin anions within the largest pore of **MIL-101**. (**B**) XRD of MIL-101 (1) and MIL-101(Keggin) (2). θ, in degrees. (**C**) TGA of MIL-101 (1) and MIL-101(Keggin) (2). T, temperature (K). (**D**) Nitrogen sorption-desorption isotherms at 78 K of MIL-101 (1) and MIL-101(Keggin) (2). V_{ads}, volume adsorbed in cm^3 g^{-1}. (**E**) ^{31}P solid-state NMR spectra of the Keggin salt and MIL-101(Keggin). δ, chemical shift in ppm.

References and Notes

1. J. S. Seo *et al.*, *Nature* **404**, 982 (2000).
2. F. Schüth *et al.*, *Handbook of Porous Solids* (Wiley-VCH, Weinheim, Germany, 2002), vol. 3, p. 563.
3. J. L. C. Rosell *et al.*, *J. Am. Chem. Soc.* **126**, 5666 (2004).
4. G. Férey *et al.*, *Chem. Commun.* **2003**, 2276 (2003).
5. B. H. Hong *et al.*, *Science* **294**, 348 (2001).
6. R. S. Batten *et al.*, *Angew. Chem. Int. Ed. Engl.* **37**, 1460 (1998).
7. M. Estermann, L. B. McCusker, C. Baerlocher, A. Merrouche, H. Kessler, *Nature* **352**, 320 (1991).
8. C. Serre *et al.*, *Angew. Chem. Int. Ed. Engl.* **43**, 6286 (2004).
9. S. Girard *et al.*, *Stud. Surf. Sci. Catal.* **135**, 254 (2001).
10. C. Mellot-Draznieks *et al.*, *J. Am. Chem. Soc.* **124**, 15326 (2002).
11. C. Mellot-Draznieks *et al.*, *Chem. Eur. J.* **8**, 4102 (2002).
12. C. Mellot-Draznieks *et al.*, *Angew. Chem. Int. Ed. Engl.* **39**, 2271 (2000).
13. C. Mellot-Draznieks *et al.*, *Angew. Chem. Int. Ed. Engl.* **43**, 6290 (2004).
14. C. Mellot-Draznieks *et al.*, *Z. Anorg. Allg. Chem.* **630**, 2599 (2004).
15. G. Férey *et al.*, *Angew. Chem. Int. Ed. Engl.* **43**, 6296 (2004).
16. G. Férey *et al.*, *Acc. Chem. Res.* **38**, 217 (2005).
17. Materials and methods are available as supporting material on *Science* Online.
18. Available at www.iza-structure.org/databases.
19. G. Férey, *J. Solid State Chem.* **152**, 37 (2000).
20. H. K. Chae *et al.*, *Nature* **427**, 523 (2004).
21. Materials and methods are available as supporting material on *Science* Online.
22. A. Muller *et al.*, *Angew. Chem. Int. Ed. Engl.* **39**, 3414 (2000).
23. Initial hydrogen storage measurements were ~0.45 and 3.75 weight percent at 293 K and 77 K, respectively, at 2 MPa. The values at 77 K seem to be the highest for MOFs after the contestation of previous results (*3*).
24. Initial introduction of semiconducting ZnS nanoparticles in the pores of MIL-101 was successfully achieved with a ZnS/Cr ratio close to 0.5.
25. Incorporation of ibuprofen within MIL-101 has been achieved in large amounts (~1 g of drug per gram of MIL-101) with a total release of the drug within a few days.

26. We thank F. Taulelle and M. Haouas for collecting solid state NMR, M. Latroche for hydrogen sorption measurements, P. Mialane for providing the Keggin salt and for helpful discussions, S. Floquet and E. Cadot for helpful discussion about the introduction of ZnS nanoparticles, and P. Horcajada and M. Vallet-Regi for the drug incorporation study.

Supporting Online Material

www.sciencemag.org/cgi/content/full/309/5743/2040/DC1
Materials and Methods
Figs. S1 to S6
Table S1
References and Notes

17 June 2005; accepted 16 August 2005
10.1126/science.1116275

Jumping Nanodroplets

A. Habenicht,[1] M. Olapinski,[2] F. Burmeister,[3] P. Leiderer,[1] J. Boneberg[1]

Flat gold nanostructures on inert substrates like glass or graphite were illuminated by single intensive laser pulses with fluences above the gold melting threshold. The liquid structures produced in this way are far from their equilibrium shape, and a dewetting process sets in. On a time scale of a few nanoseconds, the liquid contracted toward a sphere. During this contraction, the center of mass moved upward, which could lead to detachment of droplets from the surface due to inertia. The resulting velocities were on the order of 10 meters per second for droplets with radii in the range of 100 nanometers.

When small droplets impinge on a surface, varying degrees of deposition can be observed, ranging from sticking to rebounding. Sticking is essential for ink-jet printing and in agricultural agents that function by sticking to leaves; rebounding is desirable in cases such as self-cleaning surfaces (*1*, *2*).

The physics of impacting droplets has been well studied (*3*–*5*), and various types of (macroscopic) droplet sources have been developed (*6*). The impact-rebound process can be described energetically as the transformation of the impinging drop's kinetic energy (KE) into surface deformation energy, followed by the inverse process, which detaches the drop (*7*).

We examined whether it is possible to begin with deformed droplets on a surface and observe only the transformation from surface deformation energy to KE, as indicated by droplets jumping off the surface. For this purpose, we used droplets in the submicrometer range, which are much smaller than those typically used in impact studies. Such droplets can readily be obtained in an energetically unfavorable pancakelike shape with a large surface-to-volume ratio by preparing nanostructures in the solid state (e.g., by evaporation) on a substrate that in equilibrium is not wetted by the deposited material. Upon melting the nanostructures with a short laser pulse, dewetting sets in, and under appropriate conditions, detachment of the resulting droplets can be observed.

The gold nanostructures we used here were fabricated by colloidal lithography, in which a monolayer of monodisperse spherical particles (with diameters of 1.5 to 3 μm) serves as a deposition mask (*8*, *9*) to produce flat gold triangles with side lengths between 400 and 800 nm (Fig. 1A). The thickness of the evaporated films ranged between 50 and 160 nm. After removal of the colloid mask, these triangular gold structures were irradiated with a frequency-doubled Neodymium Doped Yttrium Aluminum Garnet (Nd:YAG)–laser (wavelength $\lambda = 532$ nm, full-width at half maximum of 10 ns). Because the absorption length of the laser radiation is smaller than the thickness of the nanostructure, we have to consider the temperature distribution inside of the nanostructure. An estimate for the thermal diffusion lengths on the time scale of the laser pulse yields 1600 nm for solid gold and 900 nm for molten gold, which is well above the thickness of the structures used here (*10*). Thus, we can assume that the temperature stays almost homogeneous over the whole volume of each nanostructure.

First, the dewetting of the initially solid triangular gold structures (thickness 50 nm, side length 800 nm; Fig. 1A) on highly orientated pyrolytic graphite (atomically smooth with rare steps) upon melting was studied in ambient conditions. This system exhibits nearly complete nonwetting in equilibrium; the contact angle is 131° (*11*).

After heating with a laser pulse, the metal triangles in Fig. 1A become molten for a certain amount of time (in the nanosecond range) and then solidify again as a result of the heat loss into the substrate. The resulting solids provide insight into the nanostructures at the moment of solidification (Fig. 1B). The laser fluence (energy density) was not constant but increased from the top left toward the bottom right of Fig. 1B. The duration of the molten state is longer along the indicated path, thus providing a sequence of images of the development of the dewetting process from flat triangles toward spherical structures (Fig. 1C).

The dewetting process starts at the corners of the triangles, where the radius of curvature is small and the force due to surface tension is high. The bumps that form there move toward the center, where they converge. In this manner, surface energy is transformed into KE, and the initially horizontal flow is directed upward.

The dewetting dynamics of the nanostructures are comparable to the growth of holes in thin liquid metal films (*12*, *13*), where the low viscosity of these systems allows inertia to play a dominant role, as described by the formula for the retraction velocity given by Brochard-Wyart (*14*), $v = (2|S|\rho_l^{-1}d^{-1})^{0.5}$, in which S is the spreading coefficient (1.904 N/m), ρ_l is the density of liquid gold, and d is the thickness of the metal layer. With these values, we obtained retraction velocities in the range of 65 m/s, implying a time scale on the order of 10 ns for the transition toward a sphere; preliminary time-resolved reflectivity experiments that we used to monitor this transition confirm this estimate.

In the dynamics of our liquid nanostructures, inertia dominates over viscous dissipation. Given this, can the droplets detach from the surface, as they do in the second half of the impact-rebound process observed in macroscopic drops? Such a detachment could happen if the KE of the droplet's center of gravity perpendicular to the surface surmounts the adhesion energy, taking into account dissipative losses. The upper right part of Fig. 2 shows that all of the particles are indeed missing. Apparently, detachment readily takes place if the laser fluence is slightly above the value

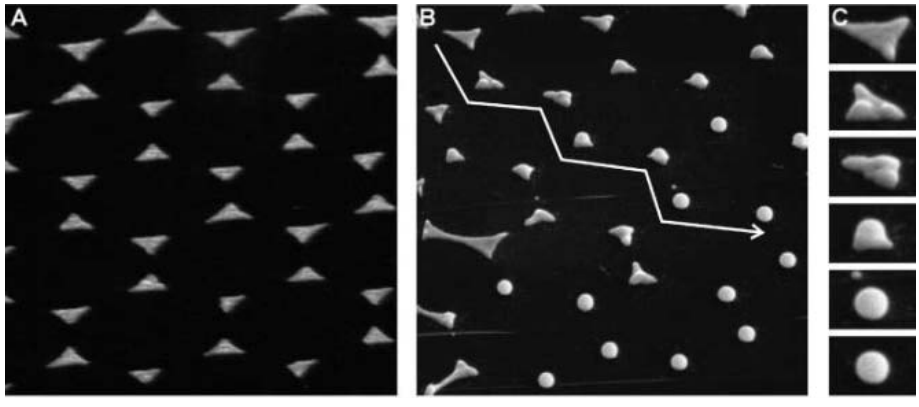

Fig. 1. (**A**) Scanning electron microscope picture of triangular gold nanostructures on highly orientated pyrolytic graphite, as produced by colloidal monolayer lithography, before laser annealing (substrate tilted, image size 8 × 16 μm). (**B**) The same nanostructures after annealing with a nanosecond laser pulse and resolidification. Along the arrow the laser fluence and thus the duration of the molten state increased. The resulting solid nanostructures therefore represent different stages of the dewetting process (**C**).

[1]Department of Physics, University of Konstanz, Universitätsstrasse 10, 78457 Konstanz, Germany. [2]Department of Physics and Center for Nanoscience, Ludwig-Maximilians-Universität München, Geschwister-Scholl-Platz 1, 80539 München, Germany. [3]Fraunhofer Institute for Mechanics of Materials, Woehlerstrasse 11-13, 79108 Freiburg, Germany.

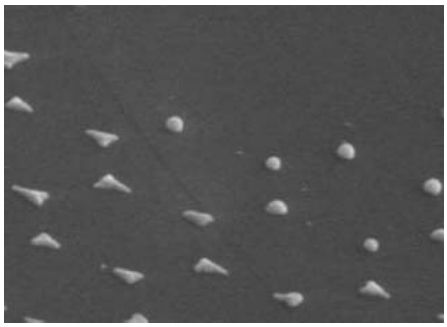

Fig. 2. Laser-molten gold nanostructures on graphite, similar to Fig. 1. In this case, the laser fluence increased from bottom left to top right of the picture. The region where spherical particles formed is quite narrow, and at higher laser fluence the particles have left the surface. Substrate tilted, image size 8 × 12 μm.

necessary for the triangles to stay melted long enough to contract to spheres.

To study the detachment in more detail, we placed our samples in a vacuum chamber and used glass as the substrate (with a root-mean-square roughness of 3 nm) instead of graphite for the gold triangles [contact angle of 140° for SiO_2 (*15*)]. The structures were irradiated with the laser beam from the substrate side. In spite of these changes, the effects described above remained the same. For the determination of the detachment velocity, we used a thin plane of light (provided by an argon laser, wavelength λ = 488 nm, power P = 500 mW) parallel to the substrate at a distance of several millimeters. As particles crossed the light sheet, we monitored scattering with a photomultiplier. From the known distance of the light sheet to the surface, the scattering data can be converted into a velocity distribution.

In Fig. 3A, triangles with a side length of 405 nm and a height of 95 nm were used, which created spheres with a radius R of 120 nm. The particles left the surface with an average velocity (±SD) of 19 ± 2 m/s. When the incident laser fluence was varied (Fig. 3B), a sharp critical value F_C was found, below which the particles did not detach. For fluences greater than F_C, the velocity of the particles remained essentially constant at v = 20 m/s up to about $2F_C$, and then gradually started to increase.

This behavior is in support of the dewetting-induced detachment mechanism outlined above: The velocity is gained from conversion of surface energy to KE, which should be independent of laser fluence. Only at the highest energy densities did the particles pick up considerably more speed, an effect which we attribute to partial evaporation of the particles and thus an additional acceleration created by recoil in front of the substrate. In this higher fluence range, the estimated temperature of the particles reached values above the boiling point of gold (3129 K).

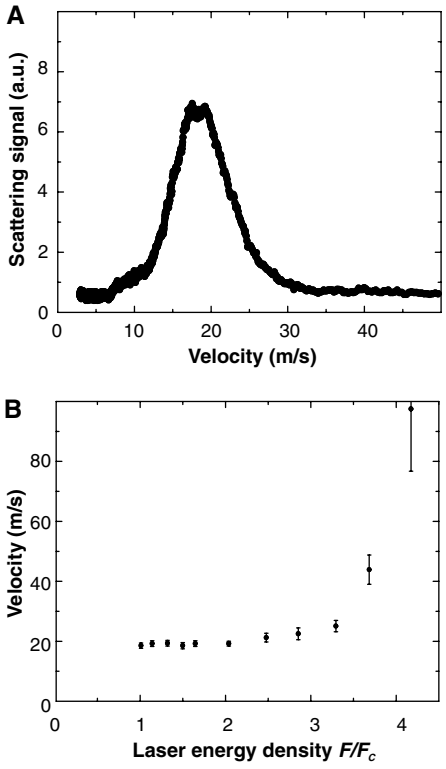

Fig. 3. (**A**) Velocity distribution of particles jumping off the surface, resulting from laser melting of gold triangles with a side length of 405 and 95 nm in height. Here, the laser fluence was a factor of 2 above the threshold value F_C, and the signal was averaged over four time-of-flight measurements on virgin substrate areas. a.u., arbitrary units. (**B**) Velocity of the detached particles versus the reduced laser fluence F/F_C. Error bars show means ± SD.

Also in agreement with the interpretation of dewetting-induced detachment is the dependence of the velocity on the initial structure height (at a fixed lateral size of 405 nm, Fig. 4): Structures with a larger height have a smaller surface-to-volume ratio and thus reach lower velocities.

For an estimate of the conversion from potential to KE, we consider first the change in surface energy ΔE_S of the flat structure in the initial state toward the detached droplet. It is given by

$$\Delta E_S = \gamma_{lv}\left((1-\cos\theta)\frac{\sqrt{3}}{4}k^2 + 3kd - 4\pi R^2\right)$$

where γ_{lv} is the liquid-vapor surface tension of gold [1.15 N/m (*16*)]; θ is the contact angle of liquid gold on glass; k and d are the side length and the thickness, respectively, of the initial triangular structure; and R is the radius of the detached droplet. Here, we have made use of Young's equation, $\gamma_{sl} - \gamma_{sv} = -\gamma_{lv}\cos\theta$, where γ_{sl} is the surface energy density of the solid-liquid interface (*17*). Assuming that evaporation can be neglected (i.e., $\frac{\sqrt{3}}{4}k^2 d = \frac{4}{3}\pi R^3$), the KE of a droplet with velocity v, $E_{kin} = \frac{\sqrt{3}}{8}k^2 d\rho v^2$, where ρ is the density of gold, can be directly compared with ΔE_S. The result as a function of structure height is plotted in Fig. 4, showing that for these particles the conversion ratio from surface energy to translational KE is on the order of 20%. Other channels for energy conversion not considered here are the excitation of droplet oscillations and dissipative friction effects.

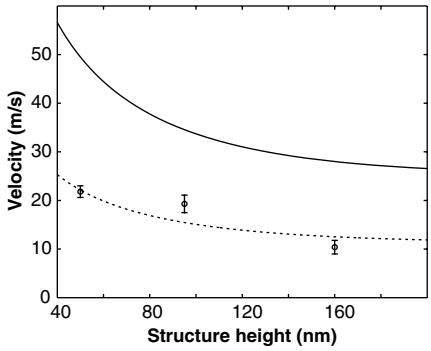

Fig. 4. Droplet velocity obtained upon laser melting of triangular nanostructures with a side length of 405 nm and various heights. The data points show the measured velocity in the low laser fluence regime ($F_C < F < 2.5F_C$). The solid line represents a calculation for 100% conversion of excess surface energy to KE; the dotted line is a fit to the experimental data with an energy conversion of 20%. Error bars show means ± SD.

Because the shape of the nanostructures at the beginning of the dewetting process can be chosen at will (e.g., by preparing the structures by electron beam lithography), one can tailor the flow in these structures for many different geometries. Furthermore, laser annealing allows the freezing of the liquid in different stages of the development and thus the application of scanning microscopy techniques. Therefore, this approach opens a wealth of possibilities for studying the dynamics of liquids on the nanoscale, including droplet impact on surfaces.

References and Notes

1. J. Klein, *Nature* **405**, 745 (2000).
2. H. Sirringhaus *et al.*, *Science* **290**, 2123 (2000).
3. A. M. Worthington, *Proc. R. Soc. London* **25**, 261 (1876).
4. I. V. Roisman, R. Rioboo, C. Tropea, *Proc. R. Soc. Lond. Ser. A* **458**, 1411 (2002).
5. R. Rioboo, M. Marengo, C. Tropea, *Exp. Fluids* **33**, 112 (2001).
6. M. Rein, *Fluid Dyn. Res.* **12**, 61 (1993).
7. R. Richard, D. Quéré, *Europhys. Lett.* **50**, 769 (2000).
8. F. Burmeister *et al.*, *Langmuir* **13**, 2983 (1997).
9. F. Burmeister *et al.*, *Appl. Surf. Sci.* **144-145**, 461 (1999).
10. We calculated the thermal diffusion length as $(2\kappa\tau C^{-1}\rho^{-1})^{1/2}$, where κ is the thermal conductivity (317 W m^{-1} K^{-1} solid and 106 W m^{-1} K^{-1} liquid), τ is the duration of the laser pulse, C is the specific heat (129 J kg^{-1} K^{-1} solid and 149 J kg^{-1} K^{-1} liquid), and ρ is the density of gold (19.3 g cm^{-3} solid and 17.2 g cm^{-3} liquid).
11. U. Gangopadyay, P. Wynblatt, *Mat. Res. Soc. Symp. Proc.* **318**, 393 (1994).
12. J. Bischof, D. Scherer, S. Herminghaus, P. Leiderer, *Phys. Rev. Lett.* **77**, 1536 (1996).
13. S. Herminghaus *et al.*, *Science* **282**, 916 (1998).
14. F. Brochard-Wyart, *J. Phys. II France* **3**, 21 (1993).

15. J. V. Naidich, in *Progress in Surface and Membrane Science*, D. A. Cadenhead, C. F. Danielli, Eds. (Academic Press, New York, 1981), vol. 14, pp. 353–484.
16. I. Egry, G. Lohoefer, G. Jacobs, *Phys. Rev. Lett.* **75**, 4043 (1995).
17. C. Ukiwe, D. Y. Kwok, *Langmuir* **21**, 666 (2005).
18. We are grateful for the experimental contributions by S. Rottmair at the early stages of this work. We acknowledge financial support by the Deutsche Forschungsgemeinschaft within the SFB 513, Project B1 and the Landesstiftung Baden-Württemberg within the Network of Competence "Functional Nanostructures," Project B2.

23 June 2005; accepted 22 August 2005
10.1126/science.1116505

The Global Reach of the 26 December 2004 Sumatra Tsunami

Vasily Titov,[1]* Alexander B. Rabinovich,[2,3] Harold O. Mofjeld,[1] Richard E. Thomson,[2] Frank I. González[1]

Numerical model simulations, combined with tide-gauge and satellite altimetry data, reveal that wave amplitudes, directionality, and global propagation patterns of the 26 December 2004 Sumatra tsunami were primarily determined by the orientation and intensity of the offshore seismic line source and subsequently by the trapping effect of mid-ocean ridge topographic waveguides.

At 07:59 local time (00:59 UTC) on 26 December 2004, a moment magnitude (M_w) 9.3 megathrust earthquake occurred along 1300 km of the oceanic subduction zone located 100 km west of Sumatra and the Nicobar and Andaman Islands in the eastern Indian Ocean (*1*). Highly destructive waves were generated by up to 10-m vertical displacements associated with massive (more than 20 m horizontally), sudden movements of adjacent plates during this event (*2*, *3*). Hundreds of thousands of dead and billions of dollars in damage show the catastrophic regional impact of this tsunami. At the same time, the waves recorded around the world revealed unprecedented, truly global reach of the waves generated on 26 December (Fig. 1). This tsunami is the first for which there are high-quality worldwide tide-gauge measurements and for which there are multiple-satellite altimetry passes of tsunami wave height in the open ocean. In this study, we couple global observations with numerical simulations to determine the principal factors affecting that portion of seismic energy that was transported thousands of kilometers throughout the world ocean in the form of tsunami waves.

We focus on measurements in intermediate and far-field regions (Fig. 2) to characterize the worldwide distribution of magnitudes and general propagation characteristics of the Sumatra tsunami. Although coastal tide-gauge records are available for much of the world ocean, interpretation of this data is complicated because of their varied quality. For example, the sampling rate for Pacific Ocean gauges is generally 15 s to 2 min, but it is only 2 to 30 min for the more sparse observations in the Indian Ocean and 6 to 15 min for the Atlantic Ocean, including the well-instrumented U.S. East Coast.

The first instrumental tsunami measurements were available about 3 hours after the earthquake from the real-time reporting tide gauge at the Cocos Islands (Fig. 1), located approximately 1700 km from the epicenter (*4*). Data from this gauge (Fig. 2A) reveal a 30-cm-high first wave followed by a long train of water-level oscillations with maximum peak-to-trough ranges of 53 cm. Gauge data and run-up measurements from sites in India and Sri Lanka (*5*) at similar distances from the epicenter yielded amplitudes almost 10 times as high as the Cocos Islands values. These substantial wave-height differences are consistent with numerical modeling results that clearly demonstrate the highly directional nature of the Sumatra tsunami (Fig. 1). Data from other tide gauges around the Indian Ocean show amplitudes ranging from about 3 m to less than 0.5 m, with no well-defined attenuation with distance from the source. Similarly, gauge wave heights are not necessarily correlated with the heights of tsunami inland inundation (run-up) in the vicinity of the gauge. The few tide-gauge records available for areas with substantial inundation show recorded water elevations smaller by a factor of 2 to 5 than measured tsunami run-up in the same area. For example, at Chenai, 1.5 m at the gauge translated into a 3- to 4-m run-up, whereas 1.5 m at Phuket gauge was a 3- to 6-m run-up. This well-known discrepancy (*6*) complicates determination of the true tsunami heights from coastal data. Many of the gauges in the Indian Ocean region were either destroyed (e.g., Thailand) or malfunctioned (e.g., Colombo, Sri Lanka), so that the largest amplitudes may not have been recorded.

Data from regions outside the Indian Ocean (Fig. 2) present an even more complex picture of tsunami behavior. The measurements indicate that, contrary to near-field regions, maximum tsunami wave heights were not associated with the leading waves. In the North Atlantic and North Pacific, maximum waves arrived several hours to 1 day after the initial tsunami (*7*). Furthermore, larger tsunami amplitudes were recorded at Callao, Peru, 19,000 km east of the epicenter than at the Cocos Islands 1700 km to the south of the epicenter. Similarly, wave amplitudes at Halifax, Nova Scotia, were also greater than at the Cocos Islands, even though these waves had propagated more than 24,000 km west across the Indian Ocean and then north along the entire length of the South and North Atlantic Ocean.

Satellite altimetry measurements of tsunami amplitude—corrected for quasi-permanent ocean circulation features such as eddies—were obtained from the Jason-1 and Topex/Poseidon satellites as they transited the Indian Ocean ~150 km apart about 2 hours after the quake (*8*, *9*). The tracks crossed the spreading front of the tsunami waves in the Bay of Bengal down to about 1200 km southward from Sri Lanka. The measurements revealed amplitudes of about 50 to 70 cm of the leading tsunami wave at this location of the Indian Ocean.

To interpret and study such a complex data set, we have employed the rigorously tested MOST (method of splitting tsunami) model (*10*) to simulate worldwide tsunami propagation. Figure 1 summarizes simulation results for a model tsunami source constrained by the open-ocean satellite measurements and available seismic analysis. The slip distribution between the subfaults of our source provides the best fit with the open-ocean satellite data and qualitatively agrees with the magnitude of the earthquake source data (Fig. 1, inset). The details of the coseismic deformation that generated these powerful waves still have substantial uncertainties. The ambiguities and difficulties of interpreting the distinctive seismic data for this event are reflected in substantially different source models derived from the seismic data (*4*, *11*). Geodetic field measurements and Global Positioning System data provide another source interpretation (*3*). The tsunami data provide considerable insight into the large-scale source structure, because they reflect extremely low-frequency source characteristics. Inversion studies of the satellite tsunami data offer yet another version of the source (*12*). For our study, however, the small-scale features of the tsunami source may not be criti-

[1]Pacific Marine Environmental Laboratory, National Oceanic and Atmospheric Administration, Sand Point Way NE, Seattle, Washington 98115, USA. [2]Institute of Ocean Sciences, Department of Fisheries and Oceans Canada, 9860 West Saanich Road, Sidney, British Columbia, Canada V8L 4B2. [3]P. P. Shirshov Institute of Oceanology, Russian Academy of Sciences, 36 Nakhimovsky Prospect, Moscow 117997, Russia.

*To whom correspondence should be addressed. E-mail: Vasily.Titov@noaa.gov

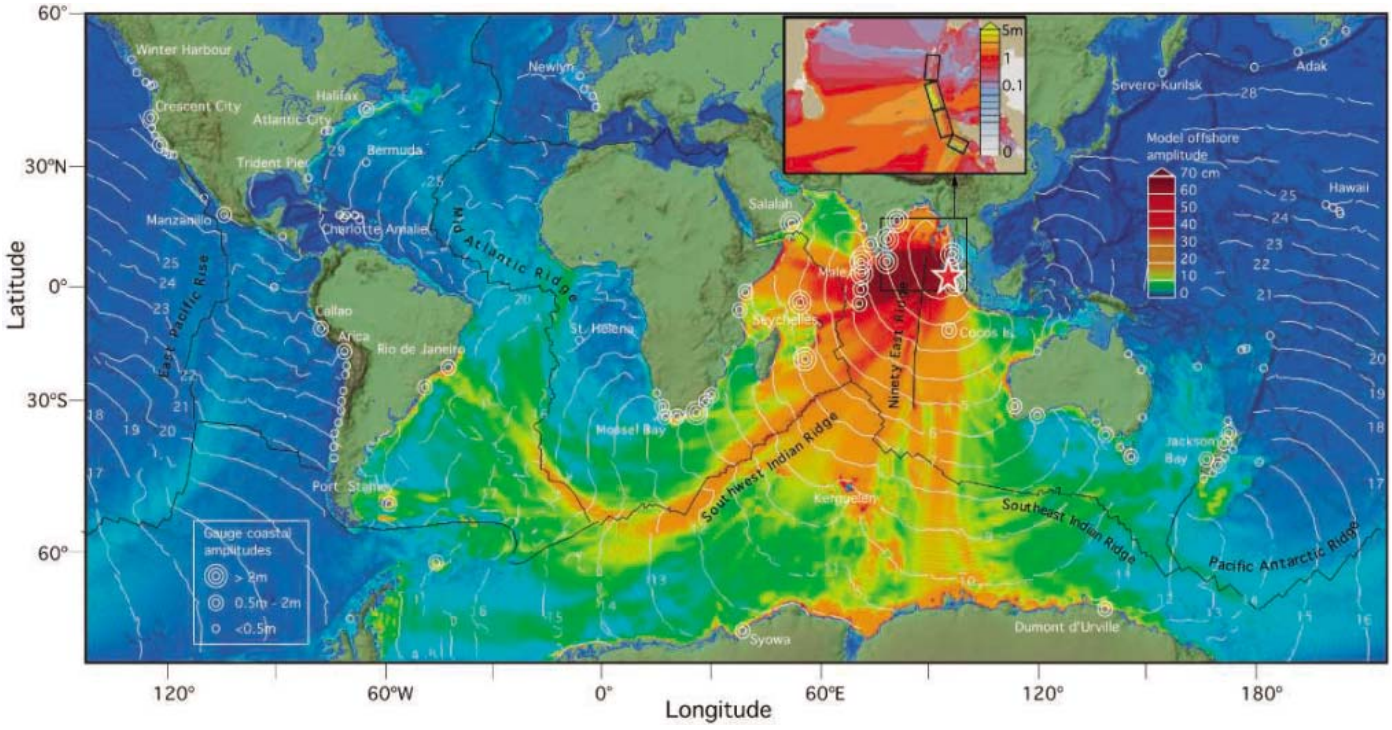

Fig. 1. Global chart showing energy propagation of the 2004 Sumatra tsunami calculated from MOST. Filled colors show maximum computed tsunami heights during 44 hours of wave propagation simulation. Contours show computed arrival time of tsunami waves. Circles denote the locations and amplitudes of tsunami waves in three range categories for selected tide-gauge stations. Inset shows fault geometry of the model source and close-up of the computed wave heights in the Bay of Bengal. Distribution of the slip among four subfaults (from south to north: 21 m, 13 m, 17 m, 2 m) provides best fit for satellite altimetry data and correlates well with seismic and geodetic data inversions.

cal, because tsunami propagation patterns away from the source are not very sensitive to such details. The magnitude of seafloor displacement, aerial extent of displacement, and its location are the most critical source parameters determining characteristics of the far-field tsunami propagation (*13*). Consequently, our model results in Fig. 1 are qualitatively similar to the early MOST model obtained only hours after the earthquake, which used substantially simpler source assumptions not constrained by later data analysis (*14*) (fig. S1 and movie S1). The magnitude (M_w = 9.2) and dimensions of our model source are consistent in general with seismic and geodetic inversions, and it fits well the tsunami altimetry measurements, thus providing a robust model for worldwide propagation.

Model simulations of tsunamis provide insight into open-ocean wave propagation that cannot be determined from tide-gauge recordings alone. This is especially important for open-ocean regions (e.g., the Atlantic coast of Africa and South America) for which there are very few available data. Because tsunami wave dynamics in deep water are linear to first order, the square of the tsunami wave height in the open ocean is directly proportional to the energy of the waves. As a consequence, the distribution of computed maximum open-ocean wave amplitudes are also patterns of tsunami energy propagation (Fig. 1). Although the nearshore wave dynamic is simplified in this model as a result of insufficient resolution, the maximum computed offshore amplitudes provide accurate estimates, because these maximum values are hardly influenced by coastal reflections and, therefore, by model inaccuracies nearshore. The model offshore amplitude distribution matches very well the amplitude variation along coastal tide-gauge records. In particular, we note that the anomalously high coastal amplitudes observed in far-field regions closely correspond to the predominant directions of tsunami energy propagation. Halifax (Canada), Manzanillo (Mexico), Callao (Peru), and Arica (Chile) all recorded wave amplitudes >50 cm, and each site is located at the terminus of a beam of computed tsunami energy that extends more than 20,000 km from the source region.

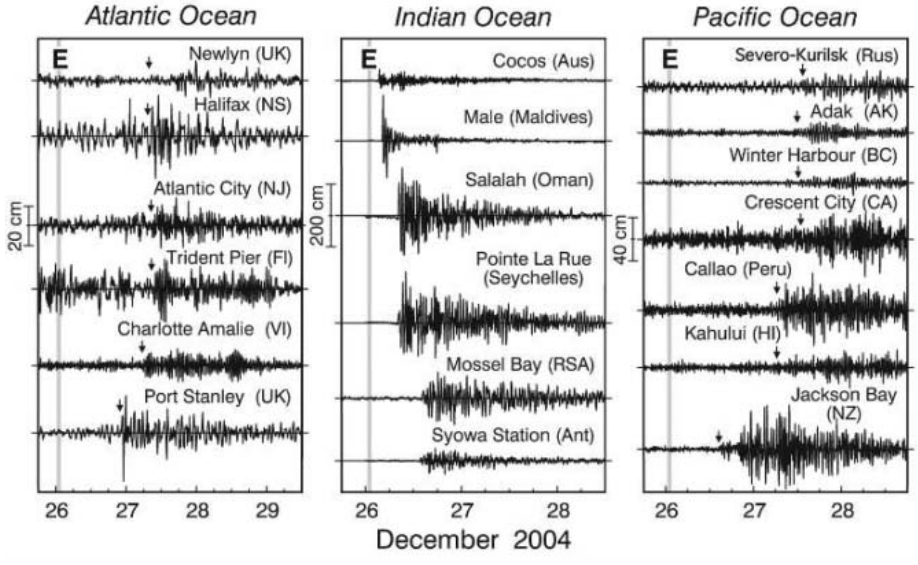

Fig. 2. Time series of tsunami wave heights (cm) as recorded at selected tide-gauge stations in the three major ocean basins. Arrows indicate first arrival of the tsunami.

Our model results support suggestions that there are two main factors affecting tsunami

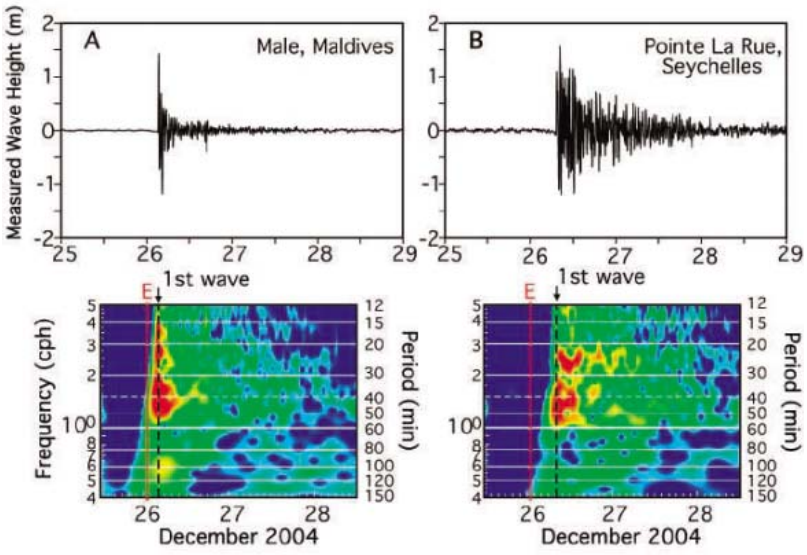

Fig. 3. Wavelet analysis of tsunami wave heights recorded by tide gauges at (**A**) Male, Maldives and (**B**) Pointe La Rue, Seychelles. Each plot shows the first 60 hours of the observed tsunami record and its corresponding wavelet decomposition (frequency/period versus time).

wave directionality: the focusing configuration of the source region (*15*) and the waveguide structure of mid-ocean ridges (*16*). Continental shelves also act as waveguides (*17*) and were apparently responsible for alongshore propagation and persistent "ringing" for the Pacific coasts of South and North America. In the near field, the focusing effect of the large extension of the earthquake source region was the primary factor determining directionality of the 2004 Sumatra tsunami. The long and narrow initial seafloor deformation generated waves with highest amplitudes propagating in the cross-source (here, zonal) direction, with smaller energy waves propagating in the long-source (meridional) direction. This effect is evident in both the model and tide-gauge data.

For far-field waves, seafloor topography is the main factor determining the directionality of energy propagation. Analysis of the Sumatra tsunami model (Fig. 1 and movie S1) illustrates the role of mid-ocean ridges in guiding interocean tsunami propagation. The Southwest Indian Ridge and the Mid-Atlantic Ridge served as waveguides for tsunami energy propagation into the Atlantic Ocean, whereas the Southeast Indian Ridge, Pacific-Antarctic Ridge, and East Pacific Rise served as guides for waves entering the Pacific. Results further show that ridges act as wave guides only until their curvature exceeds critical angles at locations along the tsunami wave paths. For example, the sharp bend of the Mid-Atlantic Ridge in the South Atlantic results in the tsunami ray leaving the waveguide near 40° S and hitting the Atlantic coast of South America with relatively high wave amplitudes. The model predicts the large (~1 m) peak waves observed at Rio de Janeiro (Brazil), but model verification for other locations on the east coast of South America is hampered by lack of instrumentation (Fig. 1). Focusing by the Ninety-East Ridge beamed tsunami energy southward toward the coast of Antarctica. There were no gauge stations on the coast of Antarctica directly in line with the beam of tsunami energy arriving from the Ninety-East Ridge, and only moderate (60 to 70 cm) peak-to-peak waves were recorded at the French Dumont d'Urville station (*18*) and the Japanese station Syowa on the coast of Antarctica. These sites were more than 2000 km to the east and west, respectively, of where our model predicts maximum coastal tsunami waves due to focusing by the Ninety-East Ridge.

For most of the eastern and central Indian Ocean records, the first few waves were the largest (up to 12 hours of anomalously high wave intensity), followed by relatively rapid exponential wave attenuation. Model simulations illustrate that these records are from locations where the largest tsunami waves followed a direct route from the source after initial focusing by the source configuration. This is consistent with source-focusing as the main factor determining evolution of the tsunami in the near field (*19*).

Tide-gauge recordings from the western Indian and other oceans show increased tsunami duration, with maximum waves arriving later in the first wave train. This demonstrates increased input from waves that reached the gauge locations after scattering or refracting from shallow submarine features and reflecting from the coasts. In the case of topographic effects, the multiple refraction and slower propagation of waves constrained by the mid-ocean ridge waveguides led to both the later arrival of the largest amplitude waves and the prolonged duration of tsunami activity associated with distinct bathymetric features. The records for Male in the Maldives and Pointe La Rue in the Seychelles (Fig. 3) serve to illustrate the two different types of tsunami wave patterns. The Male tide gauge recorded a large first wave with rapid amplitude decay thereafter (Fig. 3A), whereas the Pointe La Rue gauge (Fig. 3B) recorded a more complex pattern with substantially slower amplitude decay. Wavelet transforms (*20*) for these data emphasize the more limited duration and higher frequencies of the Male record (~1 day duration, 15- to 50-min periods) compared with the Pointe La Rue record (~3 day duration, 20 to 60 min periods). Male is directly across from the source region with no shallow scatterers in between, whereas Pointe La Rue received both scattered waves (through the Maldives and Chagos Archipelago) and reflected waves (e.g., off the Africa and Madagascar coasts).

The prolonged tsunami records for the Atlantic Ocean (Fig. 2 and fig. S2A) are consistent with substantial tsunami energy propagation along the Mid-Atlantic Ridge waveguide. In the Pacific Ocean, wave trains for the Sumatra tsunami often contained two or more distinct "packets" (Fig. 2 and fig. S2B) with different spectral characteristics. Our model provides a few explanations for this behavior. First, waveguide-driven tsunami dynamics give rise to two packets of waves: one packet of relatively small-amplitude, faster waves that took a direct path across the deeper regions of the ocean and another packet of typically higher amplitude, slower waves that traveled along ridge topographic waveguides.

Because it is so vast, the Pacific Ocean allows for two different propagation paths for most coastal locations. It is also possible that individual wave packets underwent multiple reflections from continental coastlines. Lastly, the packet structure in the Pacific records could be due to leakage of tsunami energy into the Pacific from the Atlantic Ocean. Our model shows (movie S1) tsunami waves propagating through the Drake Passage between South America and Antarctica, with amplitudes comparable with the waves that propagated directly into the Pacific from the west, i.e., from the Indian Ocean. Waves from the Atlantic arrived later at most locations in the Pacific, except for southern Chile, where the waves from the Atlantic arrived first.

Although no direct tsunami damage has been reported for the 2004 event outside the Indian Ocean basin, our study demonstrates the ability for energy from localized earthquakes to be transported throughout the world ocean. Thus, large tsunamis can propagate substantial and damaging wave energy to distant coasts, including different oceans, through a combination of source focusing and topographic waveguides. Local resonant effects may strongly amplify the arriving waves, as occurred during the 1964 Alaska tsunami in Port Alberni, British Columbia, and during the

1960 Chile tsunami in the Magadan region on the northwestern coast of the Sea of Okhotsk.

References and Notes

1. S. Stein, E. A. Okal, *Nature* **434**, 581 (2005).
2. R. Bilham, *Science* **308**, 1126 (2005).
3. C. Subarya *et al.*, *Eos Trans. AGU* **86**, U51A (2005).
4. The Cocos Islands gauge is maintained by the National Tidal Centre of the Australian Bureau of Meteorology.
5. P. Liu *et al.*, *Science* **308**, 1595 (2005).
6. V. V. Titov, C. E. Synolakis, *Geophys. Res. Lett.* **24**, 1315 (1997).
7. Here, we use "amplitude-sensitive" tsunami arrival time estimation because it is more accurate than travel-time algorithms that do not take into account wave amplitude. The tsunami travel times contoured in Fig. 1 are inferred from arrival times for the smallest waves simulated by the MOST tsunami propagation model. The areas without contours delineate regions where arrival times are difficult to estimate because waves of similar small amplitudes arrive at different times from different "packets" and from prolonged wave trains. This creates multivalue arrival times for some locations, reflecting the difficulties in determining tsunami arrival at tide-gauge records with small initial wave amplitudes.
8. J. Gower, *Eos* **86**, 37 (2005).
9. W. Smith, R. Scharroo, V. Titov, D. Arcas, B. Arbic, *Oceanography* **18**, 10 (2005).
10. V. V. Titov, C. E. Synolakis, *J. Waterways Ports Coastal Ocean Eng.* **124**, 57 (1998).
11. C. J. Ammon *et al.*, *Science* **308**, 1133 (2005).
12. K. Hirata, in preparation.
13. V. V. Titov, H. O. Mofjeld, F. I. Gonzalez, J. C. Newman, in *Tsunami Research at the End of a Critical Decade*, G. T. Hebenstreit, Ed. (Kluwer Academic Publishers, Amsterdam, 2001), pp. 75–90.
14. At the time of the initial simulation, the preliminary estimate of the earthquake magnitude was $M_w = 8.5$, representing a release of energy lower by a factor of 16 than the final estimate of $M_w = 9.3$. The only direct tsunami measurement available was for the Cocos Islands. This record provided the initial scaling for the initial specification of the tsunami source, modeled as the instantaneous seafloor deformation of the aftershock area, corresponding to a 1200-km-long rupture along the Sunda Trench. This initial tsunami source length and the resulting magnitude differed substantially from the much shorter rupture length and lower magnitude indicated by the preliminary seismic analysis. However, the resulting model simulations agreed qualitatively with the early tsunami observations. Later seismic analyses (*11*) have confirmed the larger earthquake magnitude and source region.
15. An. G. Marchuk, V. V. Titov, in *Proc. IUGG/IOC International Tsunami Symposium*, Novosibirsk, USSR (1989), pp. 11–17.
16. S. Koshimura, F. Imamura, N. Shuto, *Coastal Eng. J.* **41**, 167 (1999).
17. F. I. González, K. Satake, E. F. Boss, H. O. Mofjeld, *Pure Appl. Geophys.* **144**, 409 (1995).
18. Sea-level records for Dumont d'Urville are available as part of the French ROSAME (Réseau d'Observation Sub-antartique et Antartique du niveau de la Mer) Antarctica and South Indian Ocean Tide Gauge Network. Plots for the tsunami arrival on 26 December 2004, were provided by Laurent Testut (Laurent.Testut@notos.cst.cnes.fr).
19. Here, "near field" for this major tsunami encompasses almost all of the Indian Ocean.
20. Wavelet transforms determine the variation in signal intensity within a hierarchy of frequency bands as a function of time (*21*).
21. W. J. Emery, R. E. Thomson, *Data Analysis Methods in Physical Oceanography* (Elsevier Science, ed. 2, Amsterdam, 2001).

22. We thank the numerous scientists and agencies who contributed the tide-gauge observations reported in this paper and P. Kimber for drafting the figures. We also thank the four reviewers for their constructive suggestions and criticism. This research was partially funded by the Joint Institute for the Study of the Atmosphere and Ocean (JISAO) under NOAA Cooperative Agreement NA17RJ1232 and by the Department of Fisheries and Oceans, Canada. JISAO Contribution 1136; PMEL Contribution 2809.

Supporting Online Material

www.sciencemag.org/cgi/content/full/1114576
Figs. S1 and S2
Movie S1

9 May 2005; accepted 12 August 2005
Published online 25 August 2005;
10.1126/science/1114576
Include this information when citing this paper.

Dating of Multistage Fluid Flow in Sandstones

Darren F. Mark,[1]* John Parnell,[1] Simon P. Kelley,[2] Martin Lee,[3] Sarah C. Sherlock,[2] Andrew Carr[4]

Through ultraviolet laser argon-argon dating of potassium feldspar cements containing fluid inclusions, we determined temperature-composition-time data for paleofluids in a sedimentary basin, including data for an evolving episode of fluid flow recorded in distinct phases of cement. The fluid evolved from mixed aqueous oil 83 million years ago to purely aqueous by 76 million years ago, thus dating the time of oil charge in this reservoir.

The dating of fluid movement (*1*) on continental shelves and in sedimentary basins is critical to the prediction of the distribution of natural resources, including hydrocarbons, water, and metalliferous ore deposits. For example, accurately establishing the direct timing of oil migration within a sedimentary basin could ultimately lead to enhanced oil discovery. However, only indirect dating has been possible by using the age of minerals that predate or postdate oil charge (*2–4*), by using fluid temperatures to predict the timing of entrapment from burial history plots (*5*), and by theoretical prediction of oil generation from heat-flow models (*6*).

Characterization of fluid inclusions within K-feldspar cement (*7*) in sandstones permits the integration of homogenization temperature (*8*) data with high-resolution Ar-Ar ages (*9*), as long as the basin thermal history does not disturb the Ar isotope system. If such temperature-composition-time (*T-X-t*) points can be determined for K-feldspar overgrowths containing oil inclusions, we can directly constrain episodes of oil migration and accumulation. In conjunction with basin modeling, detailed chronologies can be established to relate oil generation and charge into the reservoir. We demonstrate the potential of this approach by using rocks from the Faeroe-Shetland Basin (*10*).

The Victory gas field is 48 km northwest of the Shetland Isles (Fig. 1A, Block 207/1a). Lower Cretaceous reservoir rocks rest unconformably on Lewisian basement. Although now the Victory field is filled with gas, oil migrated into it episodically during the Late Cretaceous period and the Paleocene epoch (*11*). The lower part of the sedimentary succession (well 207/1a-5, 1463 to 1466 m) consists of oil-stained, poorly sorted conglomerate with a sandy matrix. The matrix is cemented by quartz, calcite, kaolinite, pyrite, and K-feldspar. The authigenic K-feldspar (>99% orthoclase, table S1) consists of overgrowths (100 to 500 μm) around detrital grains (cores) of replaced plagioclase and pristine K-feldspar (Fig. 2A), as well as idiomorphic crystals (100 to 200 μm) (Fig. 2B).

K-feldspar overgrowths exhibit a discrete fluid-inclusion zonation pattern, which is delineated by phase and composition variations (Fig. 3). Three distinct fluid inclusion assemblages are seen (*10*).

Primary two-phase oil and aqueous fluid inclusions delineate zone 1. Fluid inclusions are randomly dispersed along the core-overgrowth contact, extending ~25 to 75 μm into the overgrowth, away from the core-overgrowth interface. Aqueous fluid inclusions are 5 to 15 μm across. Oil fluid inclusions are 4 to 10 μm across and fluoresce blue under ultraviolet (UV) light. Fluid entrapment for both compositions occurred between 108° and 125°C [n = 106 homogenization temperature (T_h) measurements]. Zone 2 occupies the midsection of the overgrowth, solely containing primary two-phase aqueous fluid inclusions. The zone is 50 to 200 μm thick; inclusions are 5 to 10 μm in diameter; and the fluids were trapped between 86° to 108°C (n = 78). Zone 3 extends out from zone 2 to the overgrowth edge and is 20 to 100 μm thick, although dissolution at the outer margin suggests it was once larger. Zone 3 inclu-

[1]Department of Geology and Petroleum Geology, Meston Building, Meston Walk, University of Aberdeen, Aberdeen, AB24-3UE, UK. [2]Centre for Earth, Planetary, Space and Astronomical Research (CEPSAR), Department of Earth Sciences, Open University, Walton Hall, Milton Keynes, MK7-6AA, UK. [3]Division of Earth Sciences, Centre for Geosciences, Lilybank Gardens, University of Glasgow, Glasgow, G12-8QQ, UK. [4]Advanced Geochemical Systems Ltd., Towles Fields, Burton on the Wolds, Leicestershire, LE12-5TD, UK.

*To whom correspondence should be addressed. E-mail: d.mark@abdn.ac.uk

sions are monophase, 4 to 5 μm in size, and are assumed to have been trapped at <50°C (*12*). Idiomorphic crystals are not zoned, but their fluid inclusion morphology and microthermometric data indicate precipitation temperatures equivalent to those of zone 2.

Twenty-two individual Ar-Ar analyses (*10*) constrain the age (all Ar-Ar error 2σ) of the detrital plagioclase and K-feldspar grains (Fig. 2C). Replacement of detrital plagioclase by kaolinite and K-feldspar is responsible for a wide range (table S2) of detrital ages [133.2 ± 12.5 to 815.9 ± 6.4 million years ago (Ma)]. Eleven Ar-Ar hybrid ages (Fig. 2C) were determined for optically identified core-overgrowth boundaries. The range of Ar-Ar ages (95 ± 5.4 to 145.2 ± 6.1 Ma) represents variable ratios of ablated core and overgrowth (table S3). Thirty-seven Ar-Ar ages were determined for authigenic K-feldspar: 33 from overgrowths (Fig. 2C) and 4 from idiomorphic crystals. Overgrowth ages exhibit a gradational age profile (table S4), from 83.1 ± 6.2 Ma close to the core-overgrowth interface to 53.5 ± 7.6 Ma at the overgrowth edge. Idiomorphic crystals yielded consistent (weighted mean 73.3 ± 4.7 Ma) ages (table S4).

From the core-overgrowth interface to the overgrowth edge, there is a correlation between age and distance; the closer the ablation pit was to the core-overgrowth contact, the older the Ar-Ar age detected. We can discount Ar loss (*13*), ablation of fluid inclusions containing excess Ar (*14*), or partial ablation of the core in the third dimension as origins for this gradation. For Ar loss to explain the gradational age distribution via partial resetting, subgrains within the K-feldspar overgrowths would have to exhibit size reduction with increased distance from the core-overgrowth contact. Transmission electron microscope (TEM) images show that K-feldspar overgrowths from the Victory well are made up of aggregates of subgrains that have a consistent size of 3 to 5 μm. Individual subgrains have a finely mottled microtexture, which is typical of authigenic K-feldspar (*13*, *15*), and deviate only

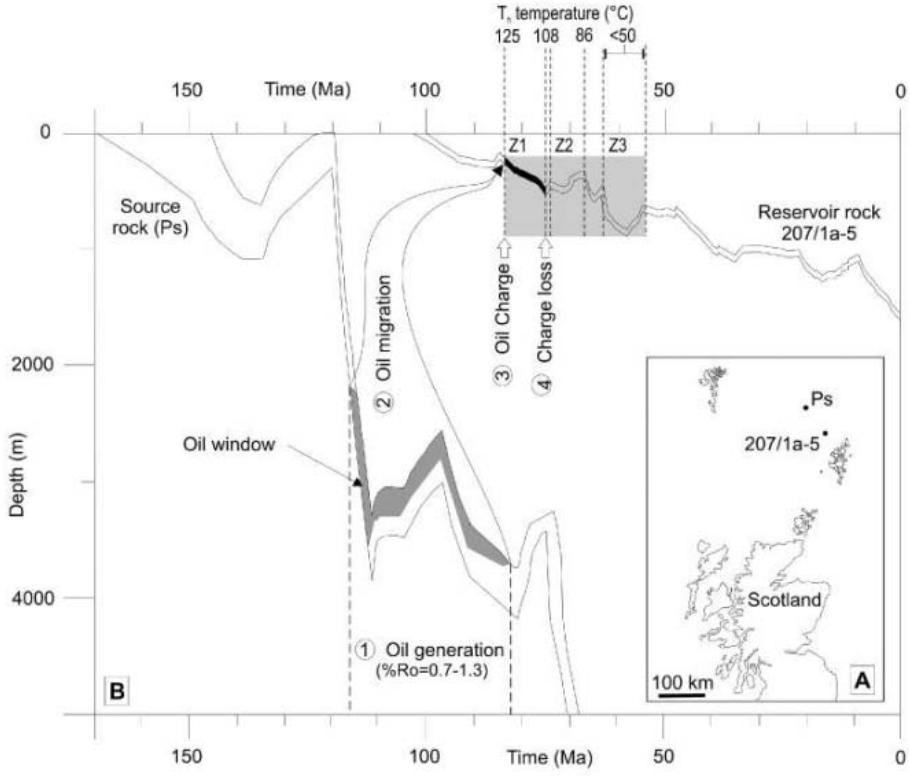

Fig. 1. (**A**) Map showing the location of the Victory reservoir (207/1a-5) relative to the source rock pseudowell (Ps). (**B**) Burial history diagram (the two lines correspond to horizon base and horizon surface) showing both reservoir (207/1a-5) and source rock (Ps) plotted together. Reservoir burial history shows evolution since 103 Ma. *T-X-t* zonation data determined from the study are shown inset against reservoir burial history (gray box: duration of K-feldspar authigenesis). Steps 1, 2, 3, and 4 indicate progressive stages of oil charge model. %R_o is a measure of vitrinite reflectance; 0.7 to 1.3% R_o indicates that the rock has entered the oil window.

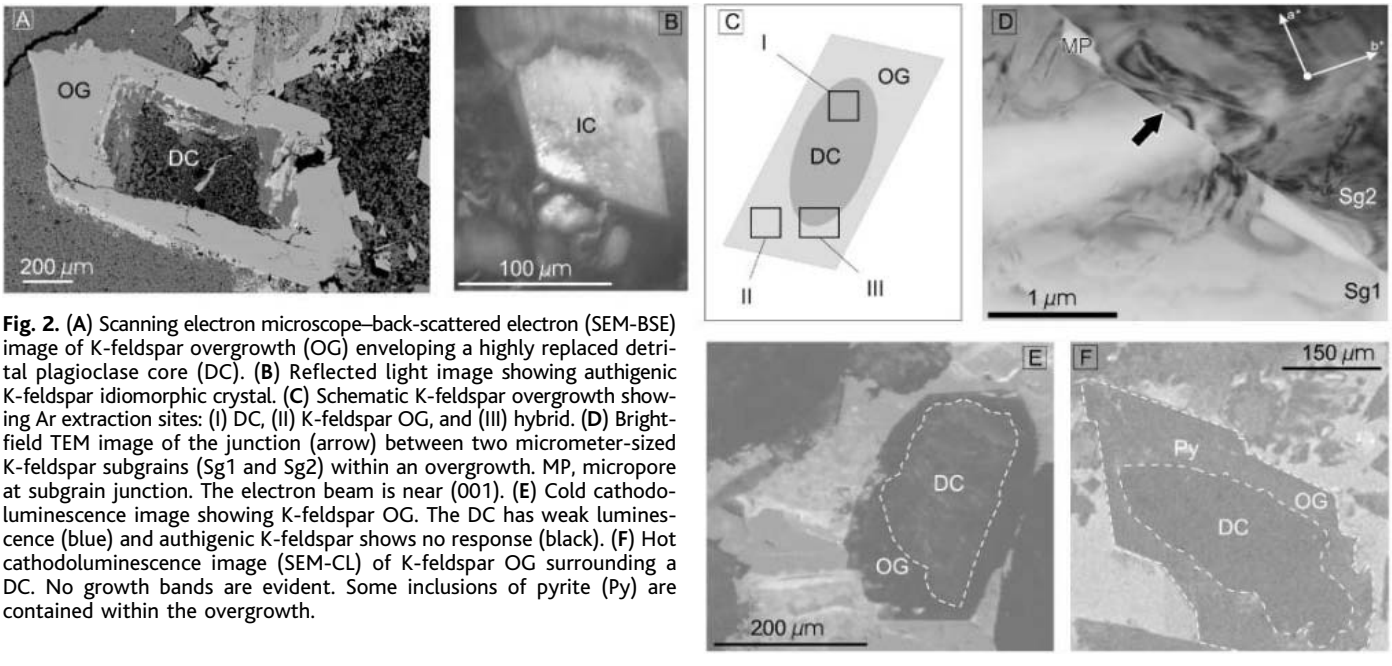

Fig. 2. (**A**) Scanning electron microscope–back-scattered electron (SEM-BSE) image of K-feldspar overgrowth (OG) enveloping a highly replaced detrital plagioclase core (DC). (**B**) Reflected light image showing authigenic K-feldspar idiomorphic crystal. (**C**) Schematic K-feldspar overgrowth showing Ar extraction sites: (I) DC, (II) K-feldspar OG, and (III) hybrid. (**D**) Bright-field TEM image of the junction (arrow) between two micrometer-sized K-feldspar subgrains (Sg1 and Sg2) within an overgrowth. MP, micropore at subgrain junction. The electron beam is near (001). (**E**) Cold cathodoluminescence image showing K-feldspar OG. The DC has weak luminescence (blue) and authigenic K-feldspar shows no response (black). (**F**) Hot cathodoluminescence image (SEM-CL) of K-feldspar OG surrounding a DC. No growth bands are evident. Some inclusions of pyrite (Py) are contained within the overgrowth.

slightly from monoclinic symmetry. The presence of micropores between subgrains outlined by {110} crystal faces (Fig. 2D) is comparable to previously described microtextures (*15*) and indicative of competitive growth between adjacent subgrains. The implications of competitive growth are that subgrain size will increase outward from the detrital grain, not decrease. Ar diffusion-profile models (*10*) show that (fig. S1) 3-μm subgrains that are exposed to the reconstructed (*10*) thermal history for well 207/1a-5 (83 Ma to present) quantitatively retain Ar. Recoil loss of ^{39}Ar (recoil distance ~ 0.1 μm) would not be sufficient in 3- to 5-μm subgrains to explain the observed age profile (*16*, *17*). Basin fluids typically contain excess Ar concentrations in the range of 0.01 to 1 parts per million (*18*). Visual estimation indicates that zones 1, 2, and 3 contain ~0.1%, 0.5%, and 6% (by volume) fluid inclusions, respectively. The production of an apparent Ar age profile (fig. S2), which decreases in age with time from core to rim, is not likely, given that fluid inclusion volumes increase from core to rim (*14*). Ablation of detrital core beneath the overgrowth surface would have produced ages reflecting varying core-overgrowth ablation volumes, although this was minimized by careful targeting of ablation sites and detailed characterization of hybrid Ar-Ar ages.

Accurate mapping of 10 K-feldspar overgrowths allowed direct coupling (table S5) of fluid inclusion data with Ar-Ar data (Figs. 3 and 4). Zone 1 ranges from 83.1 ± 6.2 to 75.6 ± 5 Ma (weighted mean 79.3 ± 2.1 Ma, n = 10), zone 2 extends from 74.6 ± 3.1 to 68 ± 3.6 Ma (weighted mean 71.8 ± 1.8 Ma, n = 12), and zone 3 spans from 63.1 ± 5.4 to 53.5 ± 7.6 Ma (weighted mean 60 ± 3 Ma, n = 11). Statistical analysis confirms zonation and the existence of three different data populations (fig. S3) with distinct changes in fluid composition and temperature at the zone boundaries (Fig. 4). Cold and hot cathodoluminesence did not show any growth-band features within the K-feldspar overgrowths, suggesting that precipitation of each phase occurred from a single episode of evolving fluid flow (Fig. 2, E and F).

The data (Fig. 4) show that K-feldspar precipitation began in the Victory reservoir ~83 Ma as a result of infiltration of hot aqueous fluid (125°C) and oil. By ~63 Ma, the Victory reservoir had cooled to <50°C, and K-feldspar authigenesis ceased ~54 Ma.

The oil charge originated from Late Jurassic–Early Cretaceous shales (Fig. 1, marked Ps) to the northwest of the Victory field (*11*, *19*). The source rock attained oil maturation (*10*) ~115 Ma (thermal maturation modeling, Fig. 1B). Migration from source began 32 Ma before oil charged the Victory reservoir (Fig. 1B), and it is likely that pulses of early expelled oil never reached the Victory reservoir. Oil charged the Victory reservoir ~83 Ma. Uplift at 76 Ma (burial history plot, Fig. 1B) compromised trap and seal integrity, causing the loss of oil charge.

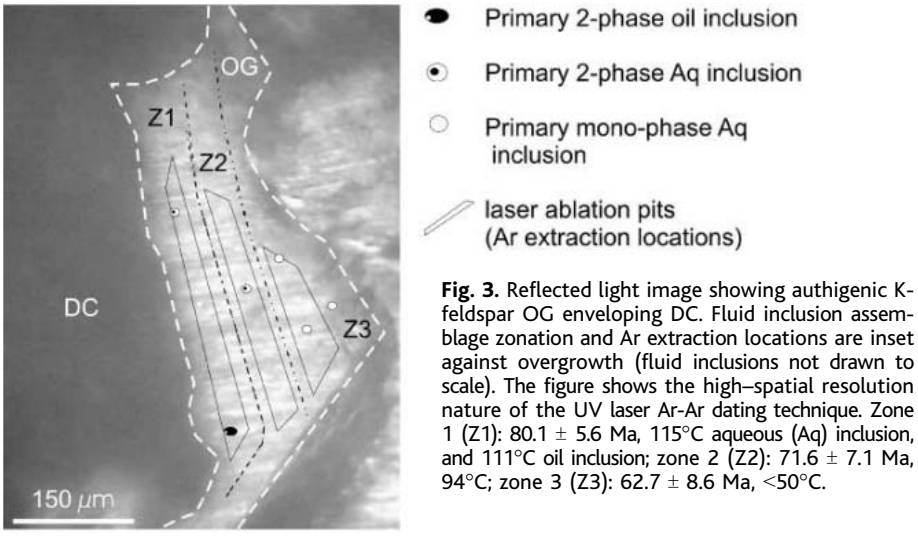

Fig. 3. Reflected light image showing authigenic K-feldspar OG enveloping DC. Fluid inclusion assemblage zonation and Ar extraction locations are inset against overgrowth (fluid inclusions not drawn to scale). The figure shows the high–spatial resolution nature of the UV laser Ar-Ar dating technique. Zone 1 (Z1): 80.1 ± 5.6 Ma, 115°C aqueous (Aq) inclusion, and 111°C oil inclusion; zone 2 (Z2): 71.6 ± 7.1 Ma, 94°C; zone 3 (Z3): 62.7 ± 8.6 Ma, <50°C.

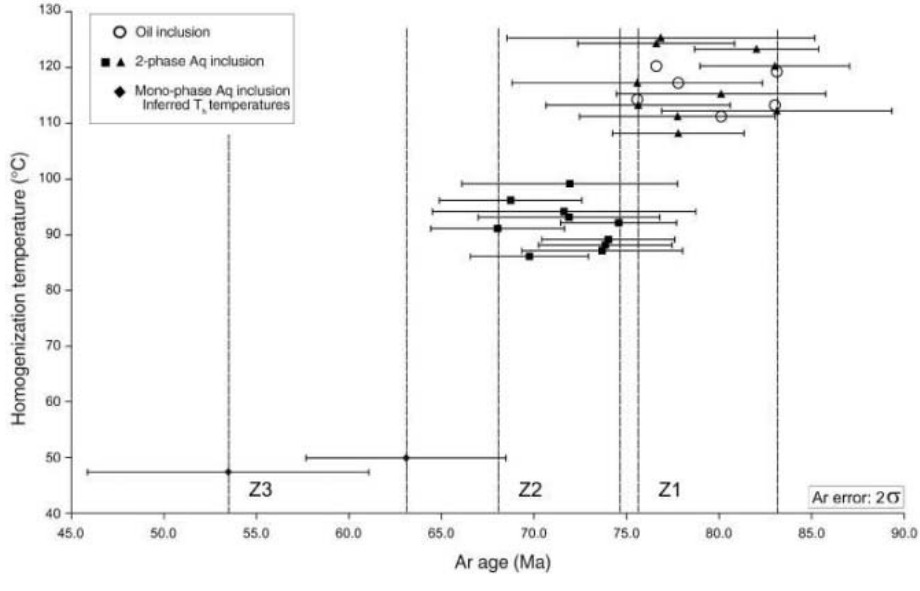

Fig. 4. Cross-plot showing *T-X-t* data obtained from authigenic K-feldspar overgrowths. Data for zone 1 and 2 (Z1 and Z2) were obtained from 10 individual overgrowths (table S4). The error bars shown highlight calculated Ar-Ar error ranges for determined Ar-Ar ages (*10*). Zone 1 oil fluid inclusions (error bar not displayed) possess the same error as does the corresponding aqueous fluid inclusions of matching Ar-Ar age. Zone 3 (Z3) shows inferred homogenization temperature (<50°C) to demonstrate the approximate zone location on cross plot. Two (highest and lowest, n = 11) Ar-Ar ages are shown, in order to highlight maximum and minimum zone age (table S4). No error is displayed for the homogenization temperature (*12*).

References and Notes

1. S. C. Sherlock, T. Lucks, S. P. Kelley, A. Barnicoat, *Earth Planet. Sci. Lett.*, in press.
2. P. J. Hamilton, S. Kelley, A. E. Fallick, *Clay Miner.* **24**, 215 (1989).
3. M. Lee, J. L. Aronson, S. M. Savin, *Am. Assoc. Pet. Geol. Bull.* **69**, 1381 (1985).
4. N. Liewig, N. Clauer, F. Sommer, *Am. Assoc. Pet. Geol. Bull.* **71**, 1467 (1987).
5. D. Karlsen, T. Nedkvitne, S. R. Larter, K. Bjorlyyke, *Geochim. Cosmochim. Acta* **57**, 3641 (1993).
6. A. Carr, I. C. Scotchman, *Pet. Geosci.* **9**, 333 (2003).
7. P. P. Hearn, J. F. Sutter, H. E. Belkin, *Geochim. Cosmochim. Acta* **51**, 1323 (1987).
8. J. Parnell, P. F. Carey, P. Green, W. Duncan, in *Petroleum Geology of Northwest Europe: Proceedings of the 5th Conference*, A. J. Fleet, S. A. R. Boldy, Eds. (Geological Society, London, 1999), p. 613.
9. E. Hagen, S. Kelley, H. Dypvik, O. Nilsen, B. Kjolhamar, *J. Geol. Soc. London* **158**, 801 (2001).
10. Materials and methods are available as supporting material on *Science* Online.
11. M. W. Goodchild, K. L. Henry, R. J. Hinkley, S. W. Imbus, in *Petroleum Geology of Northwest Europe: Proceedings of the 5th Conference*, A. J. Fleet, S. A. R. Boldy, Eds. (Geological Society, London, 1999), p. 713.
12. R. H. Goldstein, *Lithos* **55**, 159 (2001).
13. M. R. Lee, I. Parsons, *Sedimentology* **20**, 597 (2003).
14. S. P. Kelley, *Chem. Geol.* **188**, 1 (2002).
15. R. H. Worden, J. C. Rushton, *J. Sed. Pet.* **62**, 779 (1992).
16. I. M. Villa, *Geochim. Cosmochim. Acta* **61**, 689 (1997).

17. T. C. Onstott, M. L. Miller, R. C. Ewing, G. W. Arnold, D. S. Walsh, *Geochim. Cosmochim. Acta* **59**, 1821 (1995).
18. M. A. Kendrick, R. Burgess, R. A. D. Pattrick, G. Turner, *Econ. Geol.* **97**, 435 (2002).
19. N. J. L. Bailey, P. Walko, M. J. Sauer, in *Petroleum Geology of Northwest Europe*, J. Brooks, K. Glennie, Eds. (Graham and Trotman, London, 1987), p. 711.
20. This work is supported by the Natural Engineering Research Council (NERC) Ocean Margins Project research grant number 3220-GL021-GRA0782. We thank A. Craven for access to the TEM, G. Sherwood for comments, and J. Still for technical assistance.

Supporting Online Material
www.sciencemag.org/cgi/content/full/309/5743/2048/DC1
Materials and Methods
Figs. S1 to S3
Tables S1 to S5
References

13 June 2005; accepted 18 August 2005
10.1126/science.1116034

Late Cenozoic Moisture History of East Africa

Martin H. Trauth,[1] Mark A. Maslin,[2] Alan Deino,[3] Manfred R. Strecker[1]

Lake sediments in 10 Ethiopian, Kenyan, and Tanzanian rift basins suggest that there were three humid periods at 2.7 to 2.5 million years ago (Ma), 1.9 to 1.7 Ma, and 1.1 to 0.9 Ma, superimposed on the longer-term aridification of East Africa. These humid periods correlate with increased aridity in northwest and northeast Africa and with substantial global climate transitions. These episodes could have had important impacts on the speciation and dispersal of mammals and hominins, because a number of key events, such as the origin of the genus *Homo* and the evolution of the species *Homo erectus*, took place in this region during that time.

Recent investigations of both terrestrial and marine paleoclimate archives have led to a concerted debate regarding the nature of Late Cenozoic environmental changes in East Africa and their influence on mammalian and hominin evolution (*1*–*3*). Because terrestrial records of East African environmental change are typically rare, geographically dispersed, and incomplete, Indian and Atlantic Ocean sediment records have been used to reconstruct climatic changes in the region (*3*). However, because of the unique tectonic and magmatic evolution of the East African Rift System (EARS) and resulting changes in topography and drainage patterns, marine sediment records may not reflect contemporaneous environmental changes in East Africa. It is, therefore, important to reach a better understanding of the processes changing the habitat of mammals and hominins before suggesting possible links between climate and faunal changes.

The Rift Valley lakes are excellent recorders of past climate changes in East Africa (*4*, *5*). The western branch of the EARS contains several large and deep lakes that formed during the past 10 million years, and a series of small lakes that are presently partly alkaline has developed in the eastern branch since the Pliocene (*5*). The lake history in the Ethiopian, Kenyan, and Tanzanian rifts is complex and closely tied to the volcanic and tectonic evolution of the area, leading to the formation of internally drained basins with fluctuating river networks and catchment sizes (*5*) (Fig. 1). Although much smaller than the lakes in the western branch and often subaerially exposed, these basins host a rich sedimentary record, with intercalated volcaniclastic deposits that permit high-precision $^{40}Ar/^{39}Ar$ age calibration of lake-level highstands (*5*, *6*) (Fig. 2).

For rift lakes to form, two basic conditions have to be satisfied. First, basins defined by tectonic and magmatic processes have to be present to accommodate the lakes; second, the climate has to sustain a positive precipitation/evaporation balance for a substantial period of time. Here we elucidate East African climate changes in the Late Cenozoic, using detailed sedimentary records from 10 basins of the eastern branch of the EARS. The large geographic dispersion of these basins along a north-south transect helps to separate the effects of volcanic-tectonic and climatic influences on rift sedimentation. Synchronous changes in the hydrological balance inferred from sediment characteristics and silica algae (diatom) assemblages that contrast with the volcanic-tectonic history are attributed to climate change. These relations suggest possible links between climate change and mammalian and hominin evolution during the Late Cenozoic.

The EARS has a great diversity of sedimentary environments. Structurally and magmatically controlled processes have created complex relief and drainage conditions that are highly variable over time, beginning at about 45 million years ago (Ma) and continuing into the present (*7*–*9*). Volcanism and faulting

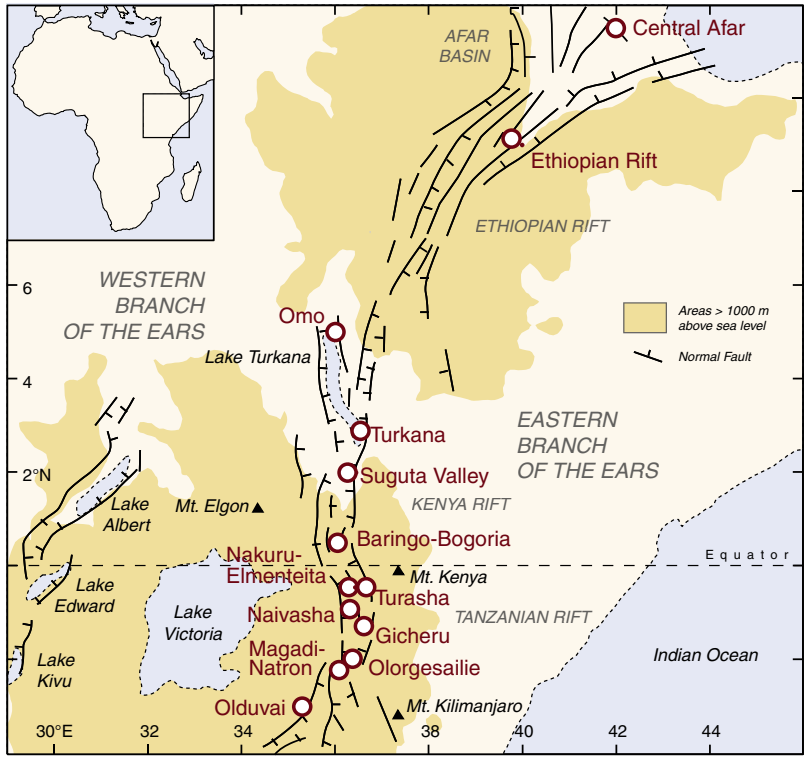

Fig. 1. Map of East Africa, showing topography, rift faults, and sites of lake sediment sequences discussed in the paper.

[1]Institut für Geowissenschaften, Universität Potsdam, Post Office Box 601553, D-14415 Potsdam, Germany. [2]Environmental Change Research Center, Department of Geography, University College London, UK. [3]Berkeley Geochronology Center, 2455 Ridge Road, Berkeley, CA 94709, USA.

were diachronous and progressed from north to south (*7–9*). In the Ethiopian Rift, volcanism started between 45 and 33 Ma; in northern Kenya, it started at about 33 Ma and continued to about 25 Ma; and the magmatic activity of the central and southern segments of the rifts in Kenya and Tanzania started between 15 and 8 Ma (*9*).

Major faulting in Ethiopia from 20 to 14 Ma was followed by the evolution of the Turkana Rift zone in northern Kenya (*9*), whereas east-dipping faults developed between 12 and 6 Ma in the Kenya Rift south of 3°N (*4*, *9*). The early halfgrabens of the Kenya Rift were subsequently faulted antithetically between about 5.5 and 3.7 Ma, generating a full-graben morphology (*4*). Before the full-graben stage, the large Aberdare volcanic complex, with elevation in excess of 4000 m, developed and is now an important topographic barrier on the eastern shoulder of the central Kenya Rift (*10*). By 2.6 Ma, the central sector was further segmented by west-dipping faults, creating the 30-km-wide intrarift Kinangop Plateau and the tectonically active 40-km-wide inner rift (*4*). The inner rift was subsequently covered by trachytic, basaltic, and rhyolitic lavas and tuffs and continues to be affected by normal faulting, leading to further structural segmentation (*4*).

In contrast, sedimentation in the Tanzanian sector of the rift began within isolated basins at ~5 Ma (*11*). Major normal faulting in the Magadi-Natron and Olduvai basins occurred at 1.2 Ma and produced the present-day rift escarpments (*11*). Late Quaternary structural en echelon segmentation during WNW-ESE–oriented extension created numerous sub-basins in the individual rift sectors that commonly hosted smaller lakes (*4*). The southward propagation of rifting, including the formation of faults and magmatic activity, led to the formation of lake basins in the northern part of the rift. The fluvio-lacustrine deposition within the Afar, Omo-Turkana, and Baringo-Bogoria Basins began in the Middle and Upper Miocene, whereas the oldest lacustrine sequences in the central and southern segments of the rift in Kenya and Tanzania are Early Pliocene (*5*). In the following, we provide a compilation of important lake periods in the Ethiopian, Kenyan, and Tanzanian Rifts since the Pliocene (*12*).

Evidence has been found for deep lakes between 2.7 and 2.5 Ma in the western Baringo-Bogoria Basin, where a sequence of five major diatomite beds occurs at precessional intervals, as calibrated by $^{40}Ar/^{39}Ar$ ages on intercalated ash layers (*13*). Contemporaneous lake deposits from adjacent basins have not yet been found (*14–16*). The possibility cannot be excluded, however, that sediments of that age are buried and downfaulted in the central Kenya Rift. In this area, no evidence for lakes exists between a 4.7-to-4.3-million-year-old and ~90-m-thick diatomite sequence at Turasha on the Kinangop Plateau and the ~1-million-year-old lake deposits at Kariandusi. In contrast, diatomites up to 30 m thick on the eastern shoulder of the Ethiopian Rift and the Afar Basin record an important lacustrine period at Gadeb between 2.7 and 2.4 Ma (*17*).

After 2 Ma, the sedimentary record becomes more complete in the eastern branch of the EARS, particularly in the Kenya Rift, and provides strong evidence for several deep lakes between 1.9 and 1.7 Ma. The Plio-Pleistocene Konso-Gardula sedimentary sequence suggests that large lakes existed in the southern sector of the Ethiopian Rift at least temporarily between 1.9 and 1.7 Ma (*18*). Contemporaneously, several large lakes are also documented in the central Afar Basin. Lacustrine deposits are

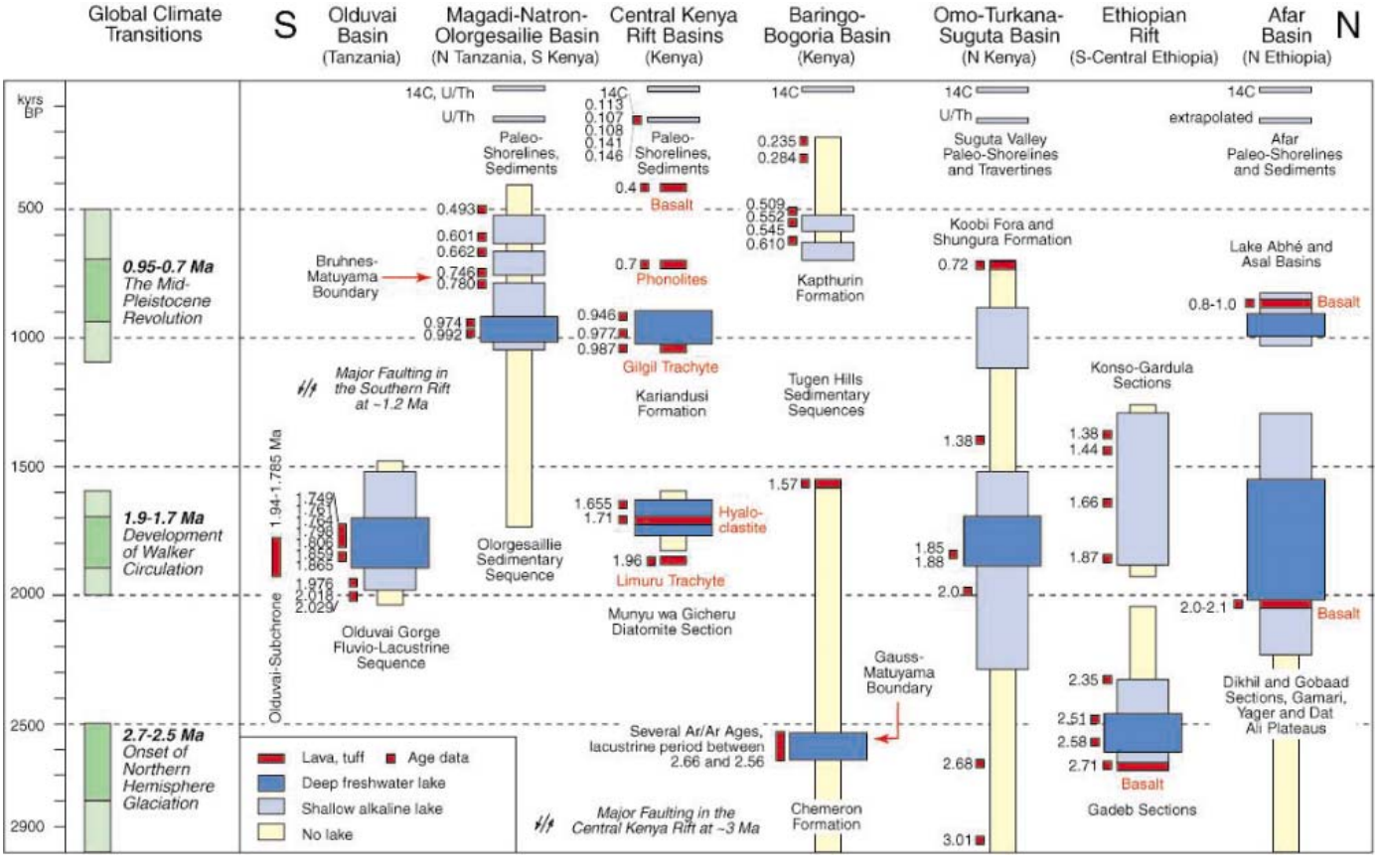

Fig. 2. Compilation of lake and riverine records based on sediment characteristics and diatom assemblages in the Ethiopian, Kenyan, and Tanzanian Rifts. Global climate transitions are from (*29–31*). Paleoenvironmental and radiometric age data are given in millions of years for the Olduvai Basin from (*20*); for the Magadi-Natron and Olorgesailie Basins from (*15*, *16*, *21*); for the Central Kenya Rift Basins, including the Gicheru, Naivasha and Nakuru-Elmenteita Basins, from (*2*, *4*, *32*) and this work; for the Baringo-Bogoria Basin from (*13*, *33*); for the Suguta Basin from (*34–36*); for the Omo-Turkana Basin from (*19*, *22*); for the Ethiopian Rift from (*14*, *17*, *18*); and for the Afar Basin from (*14*). The sedimentary evidence for large lakes is discussed in more detail in (*12*).

exposed on the floors of the Dikhil and Abhé-Gobaad Basins or are interbedded with the latest basaltic lava flows of the present-day plateaus (*14*). Dominated by fluvial conditions for most of its history, the Omo-Turkana Basin provides strong evidence for a large lake fed from the north by the Omo River between 1.9 and 1.7 Ma (*15*, *16*, *19*). At Munyu wa Gicheru, an ~30-m-thick sequence of diatomaceous sediments suggests that a major lake existed between 1.96 and 1.65 Ma in a trough on a platform along the eastern flank of the southern Kenya Rift. In the Tanzanian Rift, the Olduvai Gorge exposes a 2-million-year sedimentary record in an incised river valley draining eastward from the Serengeti Plains (*20*). The ~100-m-thick sequence suggests that a major lake existed between 1.92 and 1.7 Ma (*20*).

Deep lakes also existed between 1.1 and 0.9 Ma in East Africa. The Olorgesailie Formation in the southern Kenya Rift records the formation of a lake shortly before 0.992 Ma, with subsequent alterations between lacustrine and subaerial environments through the next ~500,000 years but no episodes of major erosion (*15*, *16*, *21*). The most important lake period occurs between 0.992 and 0.974 Ma, as documented by the deposition of a 31-m-thick main diatomite bed (*15*, *16*, *21*). An important lake period at about 1 Ma has also been identified in the Turkana Basin (*22*). Comparing the flora contained in lake sediments older than 0.8 million years with Late Pleistocene units (~135,000 years before the present) exposed in the Naivasha and Elmenteita-Nakuru Basins indicating lakes 100 to 150 m deep (*2*), the Early and Mid-Pleistocene lakes were much deeper; that is, several hundreds of meters deep, like the modern lakes in the western branch of the EARS. This prominent lake period recorded in the Olorgesailie and Nakuru-Elmenteita Basins also correlates with a period of deep lakes in the Afar Basin between 1.1 and 0.9 Ma, registered by freshwater diatom species, some of which still live in large temperate lakes today (*14*).

These synchronous changes in the water balance inferred from fluvio-lacustrine deposits contrast with the predominantly southward-propagating and diachronous volcanic-tectonic history of the EARS and can therefore be attributed to regional climate change. It is evident that East Africa experienced three major Late Cenozoic lake periods at 2.7 to 2.5 Ma, 1.9 to 1.7 Ma, and 1.1 to 0.9 Ma. With the exception of the Baringo lacustrine sequence at 2.7 to 2.5 Ma, we cannot conclude at present whether the deep lakes in the eastern rifts were characterized by relatively stable lacustrine conditions for a long period of time (~100,000 years) or if these lakes fluctuated on shorter orbital or suborbital time scales, although preliminary evidence (*13*) supports the latter.

On time scales of more than 100,000 years, rift-related volcanic-tectonic processes shaped the landscape of East Africa and thus profoundly influenced local climates and surface hydrology through the development of relief features. The uplifts of the Kenyan and Ethiopian Plateaus, with attendant changes in topography and rain shadow effects, are believed to be the major driving force for increased variability of surface moisture throughout eastern and southern Africa. Soil carbonate stable-isotope studies provide clear evidence of long-term aridification of the continent (*23*) and perhaps the spread of the savannah mosaic in East Africa (*24*). However, regions with high relief have more complex climates and respond differently to changes in the dominant forcing factors as compared to other African regions, and may result in both decreased and increased water availability. This fact helps to explain the anticorrelation between the East African lake levels and dust records from ocean sediment cores adjacent to West Africa and Arabia (*3*). Obviously, important differences exist in the moisture history of equatorial East Africa, subtropical Africa, Arabia, and Southeast Asia (*1–3*, *25–27*). These differences can best be explained by regional responses to global climate change, combined with the influence of local variations in insolation (*2*, *4*, *28*).

The periods of deep lakes correlate with important global climatic changes. The period between 2.7 and 2.5 Ma corresponds to intensification of the Northern Hemisphere Glaciation (*29*), 1.9 to 1.7 Ma to an important intensification and shift in the east-west zonal atmospheric circulation referred to as the Walker circulation (*30*), and the interval from 1.1 to 0.9 Ma to the initiation of the Mid-Pleistocene Revolution: the shift from glacial/interglacial cycles every 41,000 years to every ~100,000 years (*31*). If these lakes are ephermal features of the landscape forced by precession, that strongly supports the Variability Hypothesis of human evolution (*16*), because the environment inside the East African Rift Valley would have varied rapidly between sustained humid and arid periods, providing the stress required to initiate speciation.

References and Notes

1. S. Clemens, W. Prell, D. Murray, G. Shimmield, G. Weedon, *Nature* **353**, 720 (1991).
2. M. H. Trauth, A. Deino, A. G. N. Bergner, M. R. Strecker, *Earth Planet. Sci. Lett.* **206**, 297 (2003).
3. P. deMenocal, *Earth Planet. Sci. Lett.* **220**, 3 (2004).
4. B. H. Baker, J. G. Mitchell, L. A. J. Williams, *J. Geol. Soc.* (*London*) **145**, 107 (1988).
5. J. J. Tiercelin, K. E. Lezzar, in *The East African Great Lakes: Limnology, Paleolimnology and Biodiversity*, E. O. Odada, D. O. Olago, Eds. (Kluwer, Dordrecht, Netherlands, 2002), pp. 3–60.
6. P. A. Barker *et al.*, in *Past Climate Variability through Europe and Africa, Developments in Palaeoenvironmental Research*, R. W. Batterbee, F. Gasse, C. E. Stickley, Eds. (Springer, Dordrecht, Netherlands), vol. 6, pp. 117–138.
7. KRISP Working Party, *Nature* **354**, 223 (1991).
8. C. J. Ebinger, N. H. Sleep, *Nature* **385**, 788 (1998).
9. C. J. Ebinger *et al.*, *Geol. Soc. Am. Bull.* **112**, 163 (2000).
10. L. A. J. Williams, R. Macdonald, P. T. Leat, in *Proceedings of Regional Seminar on Geothermal Energy in Eastern and Southern Africa* (United Nations Educational, Scientific and Cultural Organization/U.S. Agency for International Development, Nairobi, Kenya, 1983), pp. 61–67.
11. A. Foster, C. Ebinger, E. Mbede, D. Rex, *J. Geol. Soc.* (*London*) **154**, 689 (1997).
12. Supplementary information is available on *Science* Online.
13. A. Hill, A. Deino, J. Kingston, paper presented at the Annual Meeting of the Geological Society of America, Seattle, WA, 2003, session no. 73.
14. F. Gasse, in *Lacustrine Basin Exploration, Case Studies, and Modern Analogs*, B. J. Katz, Ed. [American Association of Petroleum Geologists (AAPG) Memoir, AAPG, Tulsa, OK, 1990], vol. 50, pp. 1-34.
15. R. Potts, *J. Hum. Evol.* **37**, 747 (1999).
16. R. Potts, *Yearb. Phys. Anthropol.* **41**, 93 (1998).
17. M. A. J. Williams, F. M. Williams, F. Gasse, G. H. Curtis, A. D. Adamson, *Nature* **282**, 29 (1979).
18. G. WoldeGabriel, *Geol. Soc. Am. Spec. Pap.* **345**, 83 (2000).
19. F. H. Brown, C. S. Feibel, in *Koobi Fora Research Project*, J. M. Harris, Ed. (Clarendon, Oxford, 1991), vol. 3, pp. 1–30.
20. G. M. Ashley, R. L. Hay, in *Sedimentation in Continental Rifts*, R. W. Renaut, G. M. Ashley, Eds. [Society for Sedimentary Geology (SEPM) Special Publication, 2002], vol. 73, pp.107–122.
21. A. K. Behrensmeyer, R. Potts, A. Deino, P. Ditchfield, in *Sedimentation in Continental Rifts*, R. W. Renaut, G. M. Ashley, Eds. (SEPM Special Publication, 2002), vol. 73, pp. 97-106.
22. C. S. Feibel, J. M. Harris, F. H. Brown, in *Koobi Fora Research Project*, J. M. Harris, Ed. (Clarendon, Oxford, 1991), vol. 3, pp. 321–370.
23. N. E. Levin, J. Quade, S. W. Simpson, S. Semaw, M. Rogers, *Earth Planet. Sci. Lett.* **219**, 93 (2004).
24. L. F. Laporte, A. L. Zihlman, *S. Afr. J. Sci.* **79**, 96 (1983).
25. L. M. Dupont, B. Donner, R. Schneider, G. Wefer, *Geology* **29**, 195 (2001).
26. S. Clemens, W. Prell, D. Murray, G. Shimmield, G. Weedon, *Nature* **353**, 720 (1991).
27. J. E. Kutzbach, F. A. Street-Perrott, *Nature* **317**, 130 (1985).
28. A. C. Clement, A. Hall, A. J. Broccoli, *Clim. Dyn.* **22**, 327 (2004).
29. G. H. Haug, R. Tiedemann, *Nature* **393**, 673 (1998).
30. C. Ravelo, D. Andreasen, M. Lyle, A. O. Lyle, M. W. Wara, *Nature* **429**, 263 (2004).
31. W. H. Berger, E. Jansen, in *The Polar Oceans and Their Role in Shaping the Global Environment*, O. M. Johannessen, R. D. Muench, J. E. Overland, Eds. (Geophysical Monograph Series, American Geophysical Union, Washington, DC, 1994), vol. 85, pp. 295–311.
32. J. G. Evernden, G. H. Curtis, *Curr. Anthropol.* **6**, 177 (1965).
33. A. Deino, S. McBrearty, *J. Hum. Evol.* **42**, 185 (2002).
34. K. W. Butzer, F. W. Brown, D. L. Thruber, *Quaternaria* **11**, 15 (1969).
35. C. Hillarie-Marcel, O. Carro, J. Casanova, *Quat. Res.* **25**, 312 (1986).
36. N. C. Sturchio, P. N. Dunkley, M. Smith, *Nature* **362**, 233 (1993).

37. This project was funded by two grants to M.H.T. and M.R.S. by the German Research Foundation (DFG) and a University College London Graduate School grant to M.A.M. We thank the government of Kenya and the Kenya Wildlife Service for research permits and support; L. Aiello, A. Bergner, P. Blisniuk, M. Collard, P. deMenocal, M. Dühnforth, F. Gasse, F. Grine, and G. Muchemi for inspiring discussions; and S. Higgins, S. Kabingu, T. Schlüter, and M. Ibs-von Seht for logistical support.

Supporting Online Material

www.sciencemag.org/cgi/content/full/1112964/DC1
Methods
SOM Text
Table S1
References and Notes

30 March 2005; accepted 2 August 2005
Published online 18 August 2005;
10.1126/science.1112964
Include this information when citing this paper.

Structure of PTB Bound to RNA: Specific Binding and Implications for Splicing Regulation

Florian C. Oberstrass,[1,4*] Sigrid D. Auweter,[1,4*] Michèle Erat,[1*] Yann Hargous,[1] Anke Henning,[1] Philipp Wenter,[3] Luc Reymond,[3] Batoul Amir-Ahmady,[2] Stefan Pitsch,[3] Douglas L. Black,[2] Frédéric H.-T. Allain[1]†

The polypyrimidine tract binding protein (PTB) is a 58-kilodalton RNA binding protein involved in multiple aspects of messenger RNA metabolism, including the repression of alternative exons. We have determined the solution structures of the four RNA binding domains (RBDs) of PTB, each bound to a CUCUCU oligonucleotide. Each RBD binds RNA with a different binding specificity. RBD3 and RBD4 interact, resulting in an antiparallel orientation of their bound RNAs. Thus, PTB will induce RNA looping when bound to two separated pyrimidine tracts within the same RNA. This leads to structural models for how PTB functions as an alternative-splicing repressor.

The 58-kD polypyrimidine tract binding protein 1 (PTB1) is an abundant eukaryotic RNA binding protein implicated in several aspects of mRNA metabolism, including splicing regulation (*1*), internal ribosomal entry site (IRES)–mediated translation initiation (*2*), 3′ end processing (*3*), and mRNA stability (*4*). The mechanisms of PTB action in these processes are not well understood. For example, in splicing regulation, PTB may simply compete with other splicing factors in binding RNA or it may prevent the splicing machinery from assembling a spliceosome (*5*–*8*). PTB is composed of four RNA binding domains (RBDs) of the RBD/RRM/RNP type (RNA recognition motif/ribonucleoprotein) (*9*). The structures of all four RBDs of PTB in the free state have previously been determined by nuclear magnetic resonance (NMR) spectroscopy and show that all four domains adopt the typical RBD fold with a βαββαβ topology, but RBD2 and RBD3 are extended by an additional fifth β strand (β5) (*10*, *11*). Three linkers of 51, 91, and 23 amino acids separate the RBDs along the polypeptide sequence. PTB binds with an affinity of 1 to 10 nM (K_d) to sequences containing 15 to 25 pyrimidines, with a preference for pyrimidine tracts containing a UCUU sequence element (*12*, *13*). We aim here at elucidating how PTB recognizes RNA so as to understand its different biological functions.

To study the interaction between human PTB and RNA by NMR spectroscopy, we chose the oligonucleotide 5′ CUCUCU 3′ that is found in several intronic regulatory sequences; for example, several copies surround the alternatively spliced c-src N1 exon (*14*, *15*). Titration experiments show that PTB binds to the oligonucleotide in the fast-exchange regime relative to the NMR time scale. Protein saturation is reached at four equivalents of the hexanucleotide, which suggests that each RBD of PTB binds to one RNA molecule. Indeed, isolated RBD1 or RBD2 bind one RNA molecule. Similarly, the C terminus of PTB, containing RBD3, RBD4, and their interdomain linker (protein construct RBD34) binds to two CUCUCU sequences. ^{15}N-TROSY (transverse relaxation-optimized spectroscopy) spectra of the individual domains (RBD1, RBD2, and RBD34) complexed with RNA are identical to the ^{15}N-TROSY spectrum of full-length PTB in complex with four equivalents of CUCUCU in the dispersed regions of the spectra (fig. S1). Thus, RBD1, RBD2, and RBD34 are independent, and the interdomain linkers (except between RBD3 and RBD4) are flexible and do not participate in RNA binding. The difference between PTB1 and its other human isoforms lies in the length of these two linkers; therefore, their functional difference is

[1]Institute for Molecular Biology and Biophysics, Department of Biology, Swiss Federal Institute of Technology, Zürich, ETH-Hönggerberg, CH-8093 Zürich, Switzerland. [2]Department of Microbiology, Immunology, and Molecular Genetics and Howard Hughes Medical Institute, University of California Los Angeles, Los Angeles, CA 90095, USA. [3]Laboratory of Nucleic Acid Chemistry LCAN-EPFL, Lausanne, Switzerland. [4]Molecular Life Science Ph.D. Program, Zürich, Switzerland.

*These authors contributed equally to this work.
†To whom correspondence should be addressed. E-mail: allain@mol.biol.ethz.ch

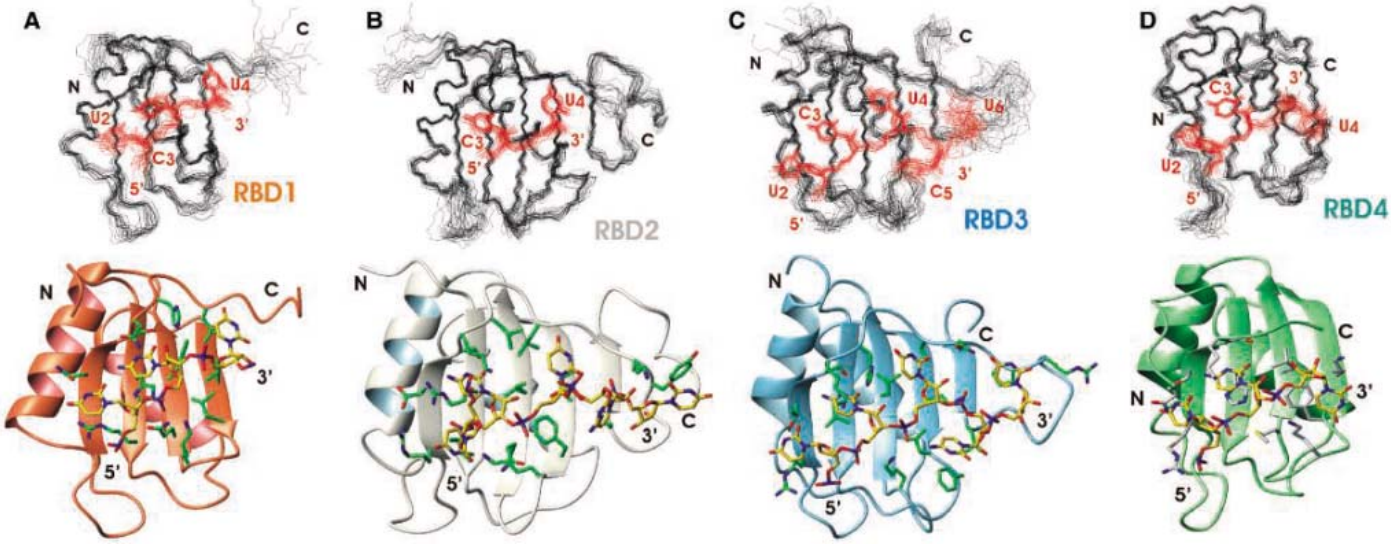

Fig. 1. Overlay of the structural ensemble and view of the most representative structure for each RBD of PTB in complex with RNA. Overlay of the 20 lowest energy structures of PTB RBD1 (**A**, top), RBD2 (**B**, top), RBD3 (**C**, top), and RBD4 (**D**, top) in complex with CUCUCU, the protein backbone, and the RNA heavy atoms of the bound nucleotides are shown. View of the most representative structure of each RBD in complex with CUCUCU: RBD1 (A, bottom), RBD2 (B, bottom), RBD3 (C, bottom) and RBD4 (D, bottom).

likely not to reside in their RNA binding specificity.

To determine the NMR structures of PTB RBD1, RBD2, and RBD34, each in complex with RNA, we used three oligonucleotides: CUCUCU, UCUCU, and CUCU. The structure of the RBDs in complex was initially determined with the hexanucleotide, because the affinity of the RBDs is higher for this RNA. However, each individual domain binds to the hexamer in multiple registers. Therefore, the complex with shorter oligonucleotides helped to identify the intermolecular nuclear Overhauser effects (NOEE) crosspeaks. A total of 1574 interproton distance restraints for RBD1 (including 46 intermolecular), 1950 restraints for RBD2 (including 53 intermolecular), and 4587 restraints for RBD34 (including 64 and 54 intermolecular for RBD3 and RBD4, respectively) were used to obtain precise structures (Fig. 1 and table S1).

In all four RBD-RNA complexes, the nucleotides are spread across the β-sheet surface. Both RBD1 and RBD4 bind the $U_2C_3U_4$ triplet, RBD2 binds the C_3U_4 doublet and U_6, and RBD3 binds the $U_2C_3U_4C_5U_6$ quintet (Fig. 1). When bound, U_2, C_3, and U_4 are each positioned on a separate β strand [β4, β1, and β2, respectively (Fig. 2A)]. The PTB-RNA interactions differ from all other RBD-RNA structures in that the β3 strand of each RBD, which includes part of the RNP1 consensus sequence, participates only weakly in RNA binding (fig. S2). In particular, position 3 and position 5 of the RNP1 motif are usually occupied by aromatic residues that make extensive hydrophobic interactions with the RNA bases and sugars (*9*). Neither of these residues is involved in such interactions in the RBDs of PTB. Instead, this role is fulfilled by the hydrophobic side chains located in β2 (Fig. 2A and fig. S2). PTB RBD2 and RBD3 share an unusual C-terminal extension of the RBD (*10*, *11*) with an additional fifth β strand that has been seen only in these two RBDs. These extensions participate in RNA binding and allow the domain to bind one (RBD2) or two (RBD3) additional nucleotides (Fig. 2, B and C). The overall fold of each PTB RBD is identical in the free (*10*, *11*) and bound state. However, a few loops become more ordered upon RNA binding, such as the β4-β5 loop in RBD2 and RBD3. A detailed description of the protein-RNA interactions can be found in (*16*).

PTB is a sequence-specific RNA binding protein. C_3 is specifically recognized by all four RBDs of PTB, and U_4 by all RBDs except RBD4 (Fig. 2A). U_2 is specifically recognized by RBD1, RBD3, and RBD4. The U_2 O2 is hydrogen-bonded with the C_3 amino group, and its imino group is hydrogen-bonded to Asn, Thr, and Ser side chains in RBDs 1, 3, and 4, respectively (Fig. 2A). These side chains act as hydrogen-bond acceptors but also have the ability to act as donors. Therefore, a cytosine (C_2) could be accommodated instead of U_2. The structure shows that each RBD of PTB recognizes a different RNA sequence that defines its binding register, YCU for RBD1, CU(N)N for RBD2, YCUNN for RBD3, and YCN for RBD4 (Y indicating a pyrimidine and N any nucleotide). These four different RNA recognition consensi for PTB explain the difficulties in finding a clear RNA consensus sequence using SELEX (systematic evolution of ligands by developmental enrichment) (*12*, *13*). However, because 10 of the 14 bound pyrimidines (71%) in our complex are recognized by specific base contacts, the structure reflects the enrichment (72%) of pyrimidines found with SELEX (*12*). PTB sequence specificity is biologically critical, because mutating PTB binding sites to poly(C) or poly(U) alters PTB function in splicing considerably (*12*, *14*, *15*, *17*). This preference of PTB for poly(CU) sequences may explain how PTB can compete effectively with the essential splicing factor U2AF (U2 accessory factor) for 3′ splice sites containing CU sequences, because U2AF prefers a pure poly(U) sequence (*13*). However, this competition mechanism does not fully explain the role of PTB as a splicing repressor (*5*, *8*, *18*).

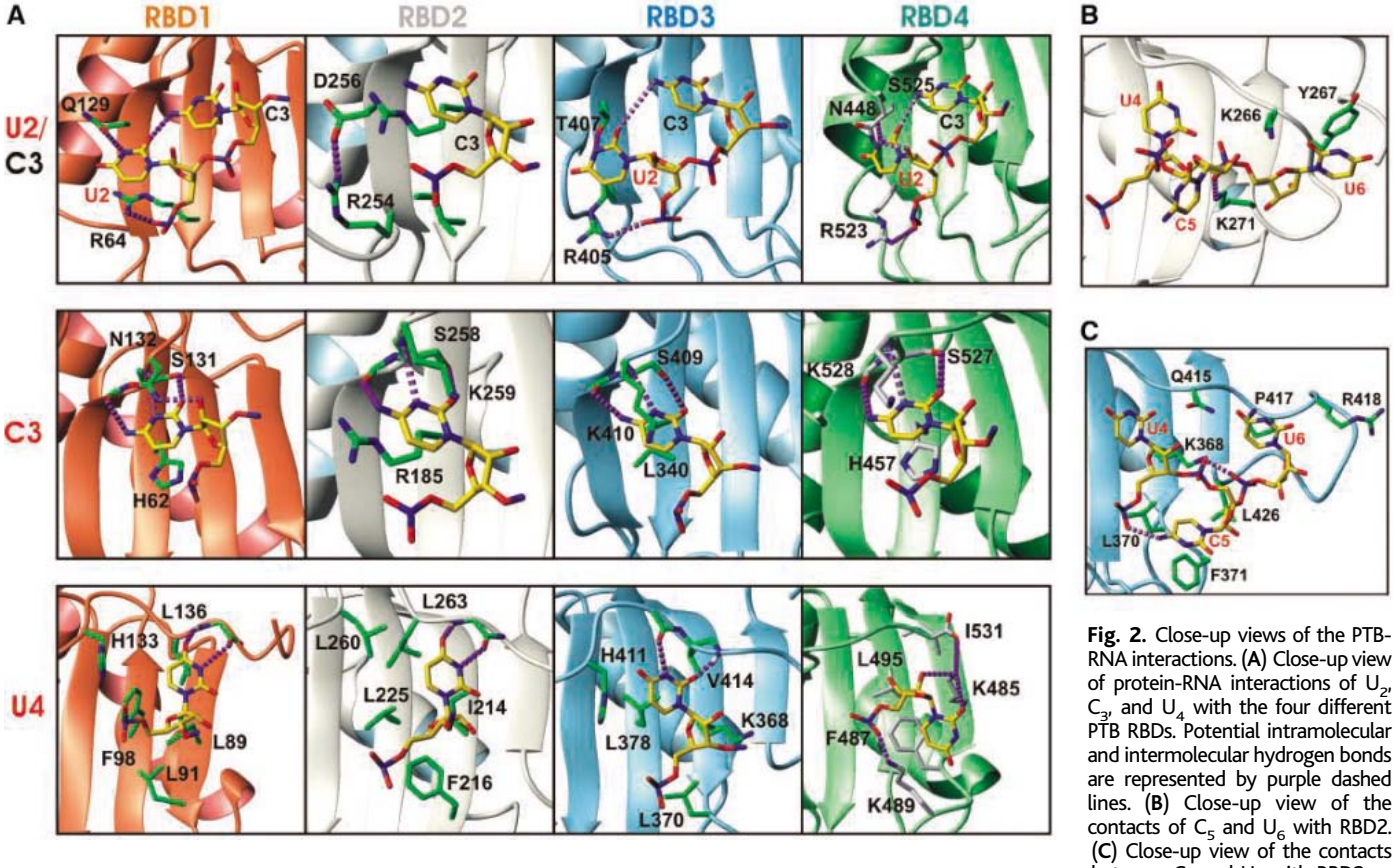

Fig. 2. Close-up views of the PTB-RNA interactions. (**A**) Close-up view of protein-RNA interactions of U_2, C_3, and U_4 with the four different PTB RBDs. Potential intramolecular and intermolecular hydrogen bonds are represented by purple dashed lines. (**B**) Close-up view of the contacts of C_5 and U_6 with RBD2. (**C**) Close-up view of the contacts between C_5 and U_6 with RBD3.

Most interestingly, we found that PTB RBD3 and RBD4 interact extensively and have a fixed orientation relative to one another. More than 20 protein side chains located in helices 1 and 2 of RBD3, in helix 2 of RBD4, and in the interdomain linker form a hydrophobic core between the two domains (Fig. 3). Mutations of only three side chains within helix2 of RBD4 are sufficient to abolish this interdomain interaction (fig. S3). As a result of this orientation, RBD34 can bind two pyrimidine tracts within the same RNA only if they are separated by a linker sequence. We found that an RNA with a spacer of 15 nucleotides between two CUCUCU hexamers is bound with the highest affinity (*16*) (fig. S4). This distinguishes PTB RBD34 from other proteins with two consecutive RBDs, such as poly(A) binding protein (PABP) (*19*), Sex-lethal (*20*), or nucleolin (*21*), in which both domains bind immediately adjacent stretches on a continuous RNA with high affinity. Hence, PTB RBD34 has the capacity to bring two distantly located pyrimidine tracts to a distance as close as 30 Å (the minimum distance that separates the two RNAs across the protein) and induce RNA looping (Fig. 4A).

PTB has been implicated in the splicing repression of several short alternative exons (*1*). RNA binding sites for PTB tend to be clustered in the surrounding intron sequences but can be found within the regulated exon itself. The location and the number of these binding sites differ, but in most cases (*7*, *22*), it is important that multiple PTB binding sites are present. These multiple PTB binding sites can be positioned both upstream and downstream of the alternative exon (*14*, *23*–*27*) or of a branch point (*28*). One model for how PTB represses splicing is that PTB loops out the exon or the branch point by binding several pyrimidine tracts upstream and downstream. This in turn prevents binding of spliceosomal components or their subsequent assembly with later components (*1*). These models usually involve the dimerization of PTB. However, recent studies indicate that PTB may not always dimerize to repress splicing (*7*). It was also shown that PTB is a monomer in solution (*5*, *10*). Our structural work and the footprinting results obtained for PTB on exon 9 of the γ-aminobutyric acid-γ2 (GABA-γ2) premRNA (*6*) let us propose a model in which only a single PTB molecule is necessary to loop out a branch-point adenine (Fig. 4B).

Based on this initial topology, we constructed several other models based on identified PTB binding sites, showing how PTB loops out alternative exons (Fig. 4, C to F). The models with two PTB molecules explain the cooperativity observed in binding studies with such RNAs (*5*). All these structural models highlight the critical role shown for RBD4 in splicing repression (*6*), because removing RBD4 prevents RNA looping around the branch point or the alternative exon.

Our findings suggest that it would be relatively easy for a PTB-repressible exon to emerge during evolution. Because each constitutive intron contains a long uracil-rich pyrimidine tract as part of its 3′ splice-site consensus sequence, spontaneous mutations into cytosines (three U to C mutations would be sufficient) would create strong binding sites for PTB RBD1, 2, and 3, and a weaker one for U2AF that binds preferentially to poly(U) sequences (*13*). This mutated 3′ splice site combined with a short pyrimidine sequence (containing UC or CC dinucleotides that serve as binding sites for RBD4) in the nearby exon or intron would result in an ideal binding site for PTB to form an RNA loop. Such 3′ splice-site mutations could convert a constitutive exon into an alternative exon repressed by PTB (Fig. 4, C and G). It is notable that alternative exons containing PTB binding sites in the 3′ splice site can often be made constitutive by C to U changes in the poly-pyrimidine tract (*15*, *24*, *29*–*31*) .

We found that PTB is both a sequence-specific RNA binding protein with a preference for CU tracts and an RNA remodeler with an ability to bring separated pyrimidine tracts into proximity. This dual capacity could allow PTB to antagonize U2AF binding, as seen in some systems, and also to loop out essential RNA elements, as seen in other systems. These structural findings are also interesting in relation to the role of PTB in IRES-mediated translation, where PTB is thought to have an RNA chaperone activity (*32*, *33*).

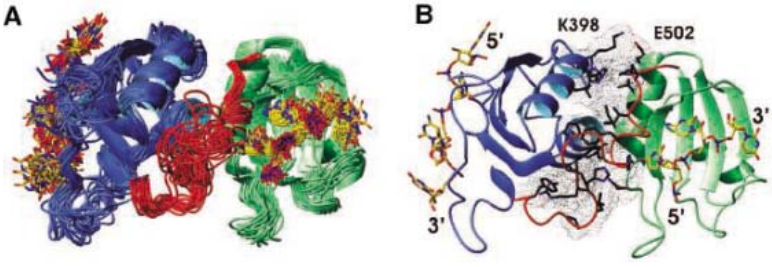

Fig. 3. PTB RBD3 and RBD4 interdomain interactions. (**A**) Overlay of the 20 lowest energy structures of PTB RBD34 in complex with CUCUCU. RBD3 is in blue, RBD4 in green, the interdomain linker in red, and the RNA in yellow. (**B**) View of the most representative structure. The side chains contributing to the interdomain interaction are shown by black sticks and by black dots representing their surfaces.

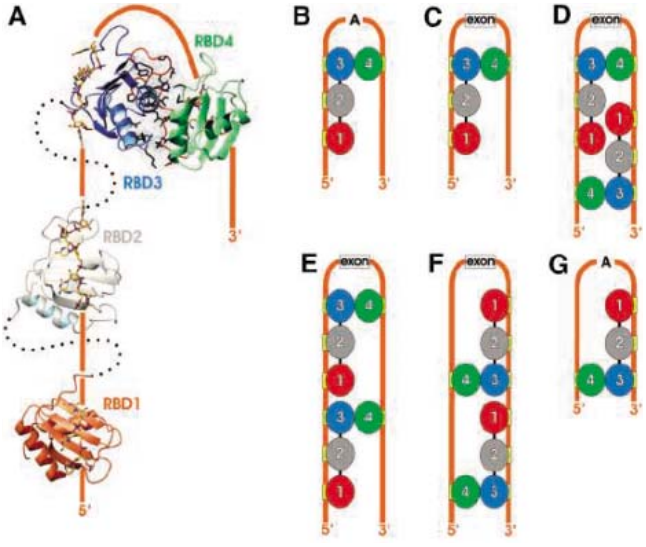

Fig. 4. Structural models representing how PTB loops out RNA (branch point or exon) and in turn represses splicing of alternative exons. (**A**) Model of the structure of PTB with a long RNA containing four pyrimidine tracts based on the structures of the three complexes we have determined. The dotted black line represents the flexible interdomain linkers between RBD1 and RBD2 and between RBD2 and RBD3. The thick orange line represents the long RNA. Note that the orientation of RBD1 and RBD2 along the RNA is not yet determined. (**B**) Model based on the example of GABA-γ2 exon 9 repression (*6*). The branch-point adenine is looped out. (**C**) Model illustrating how one molecule of PTB can repress a short alternative exon (represented by a box). Model based on splicing regulation of the calcitonin and calcitonin gene–related peptide (CT/CGRP) 3′ terminal exon (*26*) and the cTNT exon 5 (*27*). (**D** to **F**) Models involving two or more PTB molecules. The models are based on data obtained for α-tropomyosin exon 3 (*30*), c-src N1 exon (*34*), and FGF-R2 exon IIIb (*25*), respectively. (**G**) Hypothetical model illustrating how PTB loops out a branch point with PTB binding to the 3′ splice site and a short pyrimidine tract upstream of the branch point. The RNA is represented as a thick orange line. Red, gray, blue, and green ovals represent the position of RBD1, RBD2, RBD3, and RBD4 of PTB bound to RNA, respectively.

References and Notes

1. E. J. Wagner, M. A. Garcia-Blanco, *Mol. Cell. Biol.* **21**, 3281 (2001).
2. C. U. Hellen, P. Sarnow, *Genes Dev.* **15**, 1593 (2001).

3. P. Castelo-Branco *et al.*, *Mol. Cell. Biol.* **24**, 4174 (2004).
4. K. P. Knoch *et al.*, *Nat. Cell Biol.* **6**, 207 (2004).
5. B. Amir-Ahmady, P. L. Boutz, V. Markovstov, M. Phillips, D. L. Black, *RNA* **11**, 699 (2005).
6. H. Liu, W. Zhang, R. B. Reed, W. Liu, P. J. Grabowski, *RNA* **8**, 137 (2002).
7. J. M. Izquierdo *et al.*, *Mol. Cell* **19**, 475 (2005).
8. S. Sharma, A. Falick, D. Black, *Mol. Cell* **19**, 485 (2005).
9. C. Maris, C. Dominguez, F. H. T. Allain, *FEBS J.* **272**, 2118 (2005).
10. P. J. Simpson *et al.*, *Structure* **12**, 1631 (2004).
11. M. R. Conte *et al.*, *EMBO J.* **19**, 3132 (2000).
12. I. Perez, C. H. Lin, J. G. McAfee, J. G. Patton, *RNA* **3**, 764 (1997).
13. R. Singh, J. Valcarcel, M. R. Green, *Science* **268**, 1173 (1995).
14. R. C. Chan, D. L. Black, *Mol. Cell. Biol.* **15**, 6377 (1995).
15. R. C. Chan, D. L. Black, *Mol. Cell. Biol.* **17**, 4667 (1997).
16. Additional results, materials, and methods are available as supporting material on *Science* Online.
17. R. F. Roscigno, M. Weiner, M. A. Garcia-Blanco, *J. Biol. Chem.* **268**, 11222 (1993).
18. N. Gromak *et al.*, *EMBO J.* **22**, 6356 (2003).
19. R. C. Deo, J. B. Bonanno, N. Sonenberg, S. K. Burley, *Cell* **98**, 835 (1999).
20. N. Handa *et al.*, *Nature* **398**, 579 (1999).
21. F. H. Allain, P. Bouvet, T. Dieckmann, J. Feigon, *EMBO J.* **19**, 6870 (2000).
22. H. Shen, J. L. Kan, C. Ghigna, G. Biamonti, M. R. Green, *RNA* **10**, 787 (2004).
23. C. Gooding, G. C. Roberts, G. Moreau, B. Nadal-Ginard, C. W. Smith, *EMBO J.* **13**, 3861 (1994).
24. J. Southby, C. Gooding, C. W. Smith, *Mol. Cell. Biol.* **19**, 2699 (1999).
25. E. J. Wagner, M. A. Garcia-Blanco, *Mol. Cell* **10**, 943 (2002).
26. H. Lou, D. M. Helfman, R. F. Gagel, S. M. Berget, *Mol. Cell. Biol.* **19**, 78 (1999).
27. N. Charlet-B., P. Logan, G. Singh, T. A. Cooper, *Mol. Cell* **9**, 649 (2002).
28. M. Ashiya, P. J. Grabowski, *RNA* **3**, 996 (1997).
29. N. Gromak, A. J. Matlin, T. A. Cooper, C. W. Smith, *RNA* **9**, 443 (2003).
30. C. Gooding, G. C. Roberts, C. W. Smith, *RNA* **4**, 85 (1998).
31. R. P. Carstens, E. J. Wagner, M. A. Garcia-Blanco, *Mol. Cell. Biol.* **20**, 7388 (2000).
32. E. V. Pilipenko *et al.*, *Genes Dev.* **14**, 2028 (2000).
33. S. A. Mitchell, K. A. Spriggs, M. J. Coldwell, R. J. Jackson, A. E. Willis, *Mol. Cell* **11**, 757 (2003).
34. M. Y. Chou, J. G. Underwood, J. Nikolic, M. H. Luu, D. L. Black, *Mol. Cell* **5**, 949 (2000).
35. We are grateful to R. Stefl (ETH Zürich) for help with the structure calculation and to L. Skrisovska, C. Maris, and G. Wider (ETH Zürich), S. Curry, and S. Matthews (Imperial College, London) for helpful discussions. We also thank R. Peterson and J. Feigon (UCLA) for sharing recently developed NMR pulse programs. This investigation was supported by grants from the Swiss National Science Foundation, the Structural Biology National Center of Competence in Research to S.P. and F.H.T.A. and by the Roche Research Fund for Biology at ETH Zürich to F.H.T.A. F.H.T.A. is a European Molecular Biology Organization Young Investigator. The coordinates of the structures of PTB RBD1, RBD2, and RBD34 in complex with CUCUCU have been deposited in the Protein Data Bank with accession codes 2AD9, 2ADB, and 2ADC, respectively.

Supporting Online Material
www.sciencemag.org/cgi/content/full/309/5743/2054/DC1
Materials and Methods
SOM Text
Figs. S1 to S4
Table S1
References

26 April 2005; accepted 24 August 2005
10.1126/science.1114066

Direct Observation of the Three-State Folding of a Single Protein Molecule

Ciro Cecconi,[1,2]* Elizabeth A. Shank,[1]* Carlos Bustamante,[1,2,3]† Susan Marqusee[1]†

We used force-measuring optical tweezers to induce complete mechanical unfolding and refolding of individual *Escherichia coli* ribonuclease H (RNase H) molecules. The protein unfolds in a two-state manner and refolds through an intermediate that correlates with the transient molten globule–like intermediate observed in bulk studies. This intermediate displays unusual mechanical compliance and unfolds at substantially lower forces than the native state. In a narrow range of forces, the molecule hops between the unfolded and intermediate states in real time. Occasionally, hopping was observed to stop as the molecule crossed the folding barrier directly from the intermediate, demonstrating that the intermediate is on-pathway. These studies allow us to map the energy landscape of RNase H.

Protein folding remains a major unsolved challenge for modern molecular biology. Theoretical studies emphasize the potential heterogeneous nature of the process; however, traditional bulk biochemical experiments often mask this complexity in their inherent ensemble averaging. For instance, many proteins are observed to populate partially structured conformations early during the folding process (*1*, *2*). These so-called burst-phase intermediates (I) are often formed within the dead time of the measuring instrument (usually milliseconds) and therefore cannot be characterized directly. Thus, controversy remains about whether these intermediates are on-pathway and productive to protein folding, or are off-pathway and do not lead directly to the folded state (*2*, *3*). It is also unclear whether these intermediates constitute distinct thermodynamic states or simply represent a redistribution of the unfolded ensemble when exposed to native conditions (*4*). These issues can be addressed with the use of single-molecule manipulation to follow in real time the trajectories of individual protein molecules during mechanically induced unfolding/refolding processes.

Previous single-molecule manipulation studies have used the atomic force microscope (AFM) to characterize the mechanical unfolding and refolding of tandem repeats of globular protein domains (*5*–*11*). Although informative, this approach has been limited to characterizing the high-force unfolding behavior of proteins. It has been difficult to observe the refolding process directly or to monitor the equilibrium between the folded and unfolded states using this method, in part because of the high spring constants of commercially available cantilevers and the correspondingly high loading rates they exert. In contrast, optical tweezers, with considerably reduced mechanical stiffness and loading rates, can overcome these limitations, as shown in RNA unfolding studies (*12*). Optical tweezers have been used to mechanically unfold the multiglobular protein titin (*5*, *13*); although the resulting data revealed the overall mechanical unfolding response of the molecule, the heterogeneous composition of this protein obscured the unfolding of the individual globular domains and refolding could not be observed directly.

Here, we report the complete force-induced unfolding and refolding trajectory of a single molecule of the *E. coli* protein ribonuclease H* Q4C/V155C (*14*) (referred to herein as RNase H) with the use of force-measuring optical tweezers (*15*). RNase H is a 155-residue, single-domain protein whose structure, stability, and folding mechanism have been extensively characterized using bulk biochemical techniques. The central portion of the polypeptide forms the core of the protein (Fig. 1A), being both the first region to fold (*16*) and the most stable region of the native structure (*17*). This observation and additional kinetic and mutagenesis studies support the hypothesis that RNase H folds via a hierarchical mechanism, in which the most stable regions of the native structure form first during folding (*3*, *18*). It has been impossible, however, to demonstrate this behavior directly with traditional approaches. This wealth of both equilibrium

[1]Department of Molecular and Cell Biology and Institute for Quantitative Biology, [2]Department of Physics, [3]Howard Hughes Medical Institute, University of California, Berkeley, CA 94720, USA.

*These authors contributed equally to this work.
†To whom correspondence should be addressed. E-mail: carlos@alice.berkeley.edu; marqusee@berkeley.edu

and kinetic data makes RNase H an ideal model system to explore single-molecule protein folding trajectories and the nature of protein folding intermediates.

We used two ~500–base pair double-stranded DNA molecules to tether individual RNase H molecules between two polystyrene spheres ~2 μm in diameter (Fig. 1A) (*19*). These "molecular handles," attached to the protein through unique engineered cysteine residues, function as spacers to prevent nonspecific bead-bead interactions and permit manipulation of the ~3 nm diameter protein. RNase H is folded and retains activity when attached to DNA handles (fig. S1). By moving the bead on the pipette relative to the bead in the trap, each RNase H molecule was stretched and relaxed multiple times, generating force-extension curves (Fig. 1B) (*20*). We observed sudden changes in extension of the molecule (transitions) during both stretching and relaxation, corresponding to the unfolding and refolding of the protein. These transitions were not observed during control experiments with DNA handles alone (yellow trace, Fig. 1B). Unfolding transitions occurred at two distinct forces, ~19 pN or ~5.5 pN, whereas the refolding transitions exhibited a single narrow distribution centered at ~5.5 pN, coincident with the lower of the two unfolding transition forces (fig. S2).

The increment in contour length (ΔL_c) corresponding to each transition was estimated by fitting the force-extension curves with the worm-like chain model (*21*). The high-force transitions at ~19 pN were consistent with the complete unfolding of RNase H (ΔL_c of 50 ± 5 nm versus 50.4 nm calculated for the full-length protein). In contrast, the ΔL_c obtained from the low-force unfolding (39 ± 6 nm) and refolding transitions (40 ± 10 nm) imply that the associated conformational changes involve a smaller portion of the polypeptide chain. Indeed, close inspection of the force-extension curves reveals that the refolding transition does not restore the original length of the molecule, leaving a gap between the stretching and relaxation curves at ~5.5 pN (Fig. 1B) and supporting the idea of partial refolding. Together, these data indicate that the native RNase H structure completely unfolds at ~19 pN (N, native → U, unfolded), and then, upon return to ~5.5 pN, partially refolds into an intermediate structure (U → I). The refolding intermediate unfolds again at ~5.5 pN in the next stretching cycle, unless the relaxed protein is incubated for a time sufficient to fully refold (I → N) before being stretched again.

We therefore monitored whether the protein had fully refolded into its native structure by examining subsequent stretching curves for the presence of a high-force unfolding transition. The probability that the intermediate folds into the native state between successive cycles while held at force F for a period of time t is given by

$$P_f(F,t) = 1 - \exp\{-tk_{\mathrm{obs(I\rightarrow N)}}\exp[-(F\Delta x^{\ddagger}_{\mathrm{I\rightarrow N}}/k_{\mathrm{B}}T)]\} \quad (1)$$

(*22*), where $\Delta x^{\ddagger}_{\mathrm{I\rightarrow N}}$ is the distance from the intermediate to the transition state, $k_{\mathrm{obs(I\rightarrow N)}} = k_{\mathrm{m}}k^{\circ}_{\mathrm{I\rightarrow N}}$ [where k_{m} reflects any possible contribution of the instrument to the overall refolding rate (*12*) and $k^{\circ}_{\mathrm{I\rightarrow N}}$ is the rate of the I → N transition at zero force], and $k_{\mathrm{B}}T$ is the product of the Boltzmann constant and absolute temperature. The probability of the I → N transition was determined as a function of force and incubation time, and the data were fit with a linearized form of Eq. 1 (Fig. 2A), yielding $k_{\mathrm{obs(I\rightarrow N)}} = 0.17 \pm 0.03\ \mathrm{s}^{-1}$ and $\Delta x^{\ddagger}_{\mathrm{I\rightarrow N}} = 1.5 \pm 0.3$ nm. Bulk studies on RNase H have also revealed a transient folding intermediate with a similar refolding rate ($k_{\mathrm{I\rightarrow N\langle bulk\rangle}} = 0.74 \pm 0.02\ \mathrm{s}^{-1}$) (*16*).

The hysteresis observed between the unfolding of the native state (N → U) and the refolding transitions suggests that the rate of pulling in these experiments is faster than the rate at which these states can equilibrate under these conditions. By pulling the molecule at different loading rates, the observed unfolding rate of the molecule at zero force is found to yielding the best fit (least squares) values of $k_{\mathrm{obs(I\rightarrow N)}} = 0.17 \pm 0.03\ \mathrm{s}^{-1}$ and $\Delta x^{\ddagger}_{\mathrm{I\rightarrow N}} = 1.5 \pm 0.3$ nm. The error bars are the standard deviations of the data from various refolding times at those forces. (**B**) Force distribution of the native structure unfolding at a loading rate of 13 pN s^{-1} (solid circles) and 53 pN s^{-1} (solid squares), where r is the loading rate and N is the fraction of folded protein (*12*). The best fit (least squares) values are $k_{\mathrm{obs(N\rightarrow U)}} = 3\ (\pm 2) \times 10^{-4}\ \mathrm{s}^{-1}$ and $\Delta x^{\ddagger}_{\mathrm{N\rightarrow U}} = 2.0 \pm 0.1$ nm.

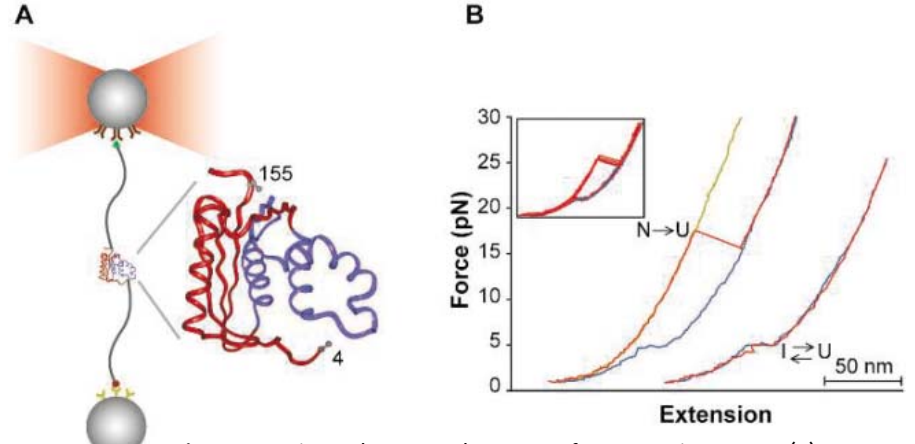

Fig. 1. Experimental setup and RNase H force-extension curves. (**A**) RNase H contains two unique cysteines at positions 4 and 155 (ball-and-stick model) that allow attachment to the DNA handles. The region of RNase H shown in blue comprises the intermediate identified in bulk studies: the core, or most stable region of the protein, as well as the portion formed earliest during folding (*16*, *17*). The sample was tethered to functionalized beads with the use of the digoxigenin and biotin moieties present at the distal ends of the handles. One bead is held in place at the end of a micropipette by suction, the other by the optical trap. (**B**) Stretching (red) and relaxation (blue) force-extension curves from RNase H display high- and low-force unfolding transitions. Refolding transitions were observed at the same forces as the low-force unfolding. A force-extension curve from DNA alone is shown in yellow. Inset shows curves from sequential pulling cycles.

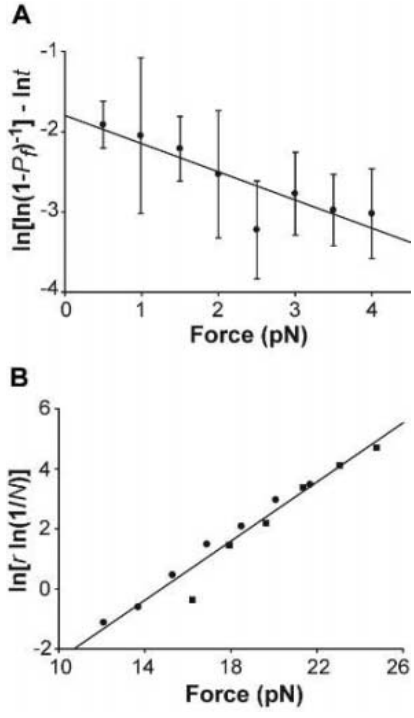

Fig. 2. Refolding probability and unfolding distribution of the native state of RNase H. (**A**) The probability of refolding from I to N (P_f) as a function of force (F) and time (t) was fit to

$$\ln\left[\ln\left(\frac{1}{1-P_f}\right)\right] - \ln t = \ln k_{\mathrm{obs(I\rightarrow N)}} - \frac{F\Delta x^{\ddagger}_{\mathrm{I\rightarrow N}}}{k_{\mathrm{B}}T}$$

be $k_{obs(N\rightarrow U)} = 3\ (\pm 2) \times 10^{-4}\ s^{-1}$, and the distance between the native state and the first transition state is $\Delta x^{\ddagger}_{N\rightarrow U} = 2.0 \pm 0.1$ nm (Fig. 2B) (*23*) when analyzed in a manner analogous to that used in previous AFM studies (*24*). This value of $k_{obs(N\rightarrow U)}$ corresponds well with the $k_{(N\rightarrow U)\langle bulk\rangle}$ value, $1.7\ (\pm 0.04) \times 10^{-5}\ s^{-1}$ (*16*).

In contrast to the hysteresis observed for the N → U transition, the unfolding and refolding transitions of the mechanical refolding intermediate (I → U and U → I) coincide (Fig. 1B), indicating that this process occurs reversibly under the experimental conditions used here (fig. S3). Consistent with this observation, the force-extension curves occasionally displayed rapid fluctuations in extension near 5.5 pN rather than a single sharp transition (fig. S4). We examined this behavior further by relaxing the unfolded protein and holding the polypeptide at a fixed force with the use of the instrument's force-feedback mode (*12*). When held at a force near 5.5 pN, the RNase H molecule displayed bistability: The molecule "hopped" between the intermediate and the denatured form of the protein in real time, with the molecular extension shifting rapidly by 15 ± 4 nm (Fig. 3A). Changing the set point of the force altered this equilibrium between the extended unfolded state and the compact intermediate structure (Fig. 3A). Such hopping has also been seen for a simple RNA hairpin using a similar approach (*12*), and for a chemically destabilized two-state (U ⇆ N) protein monitored for short time periods by fluorescence resonance energy transfer (*25*). We now show the extended real-time equilibrium behavior of a complex globular protein.

The force-dependent rates of unfolding and refolding of the intermediate were determined from the lifetimes of the extended (U) and compact (I) states seen in the hopping experiments. The position of the transition state between I and U was then estimated by fitting the rates to the Arrhenius-like equation

$$k_{I\rightarrow U} = k_m k^{o}_{I\rightarrow U} \exp(F\Delta x^{\ddagger}_{I\rightarrow U}/k_B T) \quad (2)$$

where $k^{o}_{I\rightarrow U}$ is the unfolding rate at zero force, and $\Delta x^{\ddagger}_{I\rightarrow U}$ is the distance from I to the transition state along the reaction coordinate (*12*). A similar analysis holds true for the reverse U → I reaction. The slopes of plots of ln *k* versus force yielded $\Delta x^{\ddagger}_{I\rightarrow U} = 5 \pm 1$ nm and $\Delta x^{\ddagger}_{U\rightarrow I} = 6 \pm 1$ nm. These values are substantially larger than those found for the native-state unfolding ($\Delta x^{\ddagger}_{N\rightarrow U}$) of several other proteins using the AFM (*26*). Our results on RNase H therefore convey a picture of the intermediate as a pliable structure that can deform elastically a great amount before the reaction is committed to unfolding. Such large transition-state distances have been observed in other biomolecules and were interpreted as reflecting the mechanical behavior of structures lacking the nonlocal specific contacts associated with tertiary interactions (*6*, *12*). Thus, the large distance from the intermediate to its transition state and the low forces required to unfold it suggest that this structure is only able to form weak, possibly transient tertiary interactions, and that it therefore resembles a molten globule structure (*27*).

We evaluated the thermodynamics of the U ⇆ I transition ($\Delta G_{(UI)}$) with three independent methods (Fig. 3B). We measured the area under the refolding plateau in the force-extension curves, calculated the force-dependent equilibrium constant between U and I, and analyzed the transitions with the statistics of a two-state system. After correcting for the entropy loss due to tethering and stretching the U state [calculated to be 5.1 ± 0.6 kcal/mol (*19*)], we obtained $\Delta G_{(UI)} = 4 \pm 3$ kcal/mol, 4 ± 2 kcal/mol, and 3.8 ± 0.8 kcal/mol, respectively. The agreement between these free energy values validates the analyses. The remarkable similarity between these values and that observed in ensemble experiments ($\Delta G_{(UI)\langle bulk\rangle} = 3.6 \pm 0.1$ kcal/mol), in conjunction with the similar refolding kinetics ($k_{I\rightarrow N}$), suggests that the intermediate detected in our single-molecule mechanical manipulations correlates with that sampled in solution. To further probe this relationship, we performed similar optical tweezer experiments using a variant of RNase H (I53D) that displays two-state folding in solution (*28*). In this case we saw no evidence of an intermediate (Fig. 3C) (*29*). These results strongly suggest that the intermediate observed in our single-molecule experiments is similar to that detected by ensemble methods, and hence the new features found in this study are relevant to the folding process in solution.

In the ensemble refolding experiments of RNase H, the formation of I occurs very

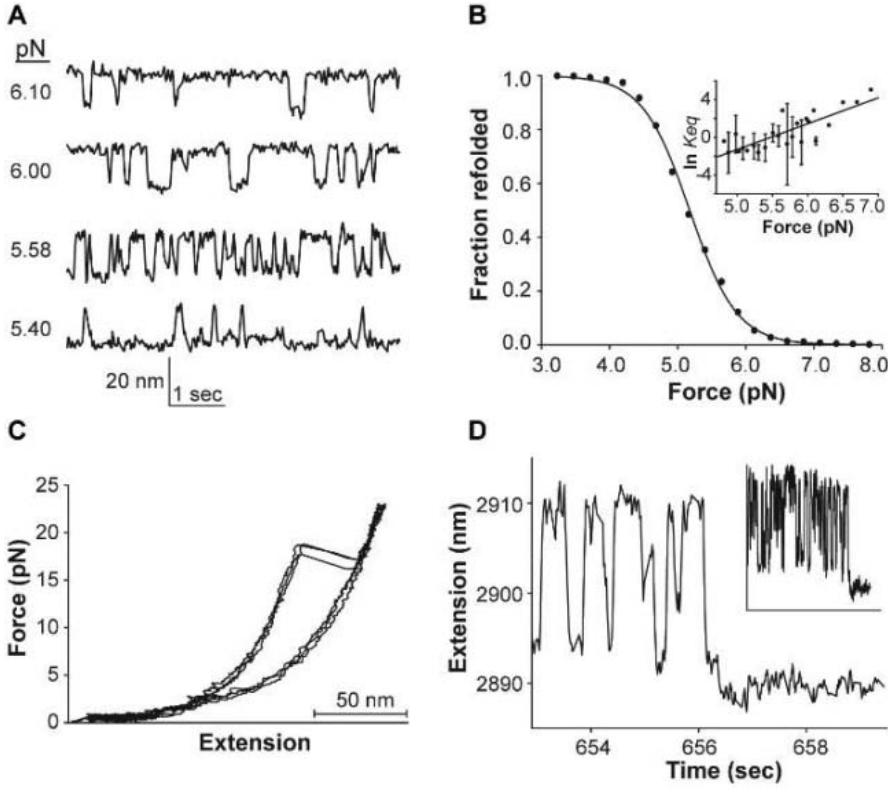

Fig. 3. Characterization of the folding intermediate of RNase H. (**A**) Extension versus time traces for RNase H at various constant forces. (**B**) The probability of U refolding to I as a function of force was obtained from a normalized frequency histogram of refolding forces ($n = 664$). The solid line shows the probability, $P(E)$, of a two-state system (*12*). The best fit (least squares) values are $\Delta G_{(UI)} = 8.9 \pm 0.3$ kcal/mol and $\Delta x_{(UI)} = 11.9 \pm 0.3$ nm. Inset shows the equilibrium constant (K_{eq}) of the U ⇆ I transition at any given force, obtained from the ratio of the lifetimes of the I and U states. Fitting the plot of ln K_{eq} versus force yielded the best fit (least squares) values of $\Delta G_{(UI)} = 9 \pm 2$ kcal/mol and $\Delta x_{(UI)} = 11 \pm 2$ nm (*12*, *19*). Data within 0.024 pN were grouped; error bars are the standard deviations of the data. Measuring the area under the unfolding/refolding plateau (potential of mean force) yielded a $\Delta G_{(UI)}$ of 9 ± 2 kcal/mol and $\Delta x_{(UI)} = 12 \pm 3$ nm (not shown). (**C**) Force-extension curves for the I53D RNase H variant (compare to curves in Fig. 1B). Unlike RNase H, the I53D variant does not show low-force refolding or unfolding transitions. (**D**) Length versus time trace of RNase H. Hopping stops when the protein refolds to the native state. Inset shows a longer time trace.

rapidly (within the 12-ms dead time of the stopped-flow instrument) and is therefore not observed directly (*16*). It has thus been impossible to determine unambiguously whether this kinetic intermediate is a distinct thermodynamic state or simply the result of a shift in the population of a continuum of unfolded states. Both models have been suggested from experimental and theoretical studies (*4*). In our studies, we used force to modulate the equilibrium between the U and I states until the interconversion between these two forms became observable. Our data clearly indicate that the transition between the I and U states is first-order (Fig. 3A) (fig. S5), allowing us to directly characterize the kinetic, thermodynamic, and mechanical properties of this molten globule–like state. The forces holding together the intermediate are small but still substantial (~5.5 pN), amounting to about one-third of the forces that stabilize the fully folded state at the pulling rates used in our experiments. The magnitude of these forces, the sharpness of their distribution, and the first-order nature of the transition from and to the unfolded state clearly indicate that this molten globule–like intermediate is a well-defined, thermodynamically distinct stable molecular form held together by distinct, although not necessarily specific, interactions.

Sometimes during constant force experiments, the hopping corresponding to the U ⇆ I transition spontaneously ceased. An additional compaction always preceded the termination of hopping (Fig. 3D). The size of this compaction, as estimated from the worm-like chain model, corresponds well to that expected for the I → N transition at the given force. Indeed, stretching the molecule after hopping ceased invariably resulted in a high-force unfolding transition (~19 pN), as expected for the unfolding of the native state. Thus, it was possible to observe the I → N transition directly. In 78% of the traces (n = 18) in which hopping stopped, the transition to the native state clearly took place from the folded intermediate structure, as in Fig. 3D. In the rest of the cases, the time spent in I before the transition to N may have been too short to be resolved in our experiments. These data indicate that the refolding intermediate observed in our experiments exists on-pathway to the folded state. Furthermore, the fact that the U → I transition is invariably present in our force-relaxation curves indicates that the same intermediate is also an obligatory step in the folding trajectory of RNase H (Fig. 4A).

The ability to explore the behavior of single protein molecules with the use of optical tweezers has permitted us to map the energy landscape traversed by the small globular protein RNase H in its transitions to and from its unfolded state (Fig. 4B). Our observation of a folding intermediate that corresponds to the intermediate seen in bulk suggests that both methods probe the same fundamental barriers. The new features revealed in this study therefore enhance our understanding of how proteins fold in solution. The intermediate of RNase H forms a distinct thermodynamic state that, although compact and held together by cohesive interactions, is nonetheless highly deformable. This state appears to be both on-pathway and obligatory to the folding trajectory.

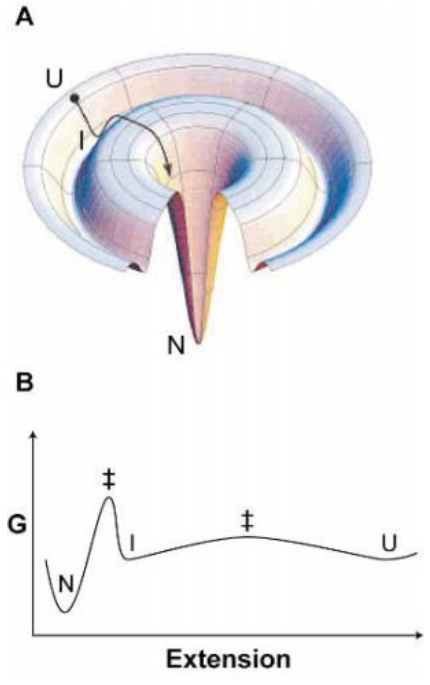

Fig. 4. The energy landscape of RNase H. (**A**) Schematic representation (*31*) of the energy landscape of RNase H depicting a reduction in conformational entropy as the protein folds through an on-pathway, obligatory, and productive intermediate species. (**B**) Free energy reaction profile of RNase H at ~5.5 pN, the force at which $\Delta G_{(UI)} = 0$. Relative distances between states correlate with the values obtained experimentally (Fig. 2, A and B, and Fig. 3A), assuming that $\Delta x^{\ddagger}_{N\rightarrow U}$ obtained at a range of forces between 15 and 20 pN holds for this lower force.

References and Notes

1. P. S. Kim, R. L. Baldwin, *Annu. Rev. Biochem.* **59**, 631 (1990).
2. H. Roder, W. Colon, *Curr. Opin. Struct. Biol.* **7**, 15 (1997).
3. R. L. Baldwin, G. D. Rose, *Trends Biochem. Sci.* **24**, 77 (1999).
4. M. J. Parker, S. Marqusee, *J. Mol. Biol.* **293**, 1195 (1999).
5. M. S. Kellermayer, S. B. Smith, H. L. Granzier, C. Bustamante, *Science* **276**, 1112 (1997).
6. M. Rief, J. Pascual, M. Saraste, H. E. Gaub, *J. Mol. Biol.* **286**, 553 (1999).
7. R. B. Best, B. Li, A. Steward, V. Daggett, J. Clarke, *Biophys. J.* **81**, 2344 (2001).
8. A. F. Oberhauser, C. Badilla-Fernandez, M. Carrion-Vazquez, J. M. Fernandez, *J. Mol. Biol.* **319**, 433 (2002).
9. D. J. Brockwell *et al.*, *Nat. Struct. Biol.* **10**, 731 (2003).
10. M. Carrion-Vazquez *et al.*, *Nat. Struct. Biol.* **10**, 738 (2003).
11. J. M. Fernandez, H. Li, *Science* **303**, 1674 (2004).
12. J. Liphardt, B. Onoa, S. B. Smith, I. J. Tinoco, C. Bustamante, *Science* **292**, 733 (2001).
13. M. S. Kellermayer, S. B. Smith, C. Bustamante, H. L. Granzier, *J. Struct. Biol.* **122**, 197 (1998).
14. J. M. Dabora, S. Marqusee, *Protein Sci.* **3**, 1401 (1994).
15. S. B. Smith, Y. Cui, C. Bustamante, *Methods Enzymol.* **361**, 134 (2003).
16. T. M. Raschke, S. Marqusee, *Nat. Struct. Biol.* **4**, 298 (1997).
17. A. K. Chamberlain, T. M. Handel, S. Marqusee, *Nat. Struct. Biol.* **3**, 782 (1996).
18. T. M. Raschke, J. Kho, S. Marqusee, *Nat. Struct. Biol.* **6**, 825 (1999).
19. See supporting data on *Science* Online.
20. Single-molecule tethers were recognized by identifying the overstretching transition due to the DNA handles. Only those fibers that exhibited an overstretching transition of the expected length (~230 nm) at the correct force (~67 pN) for a single fiber containing 1116–base pair DNA were selected for analysis.
21. J. F. Marko, E. D. Siggia, *Macromolecules* **28**, 8759 (1995).
22. I. Tinoco Jr., C. Bustamante, *Biophys. Chem.* **101-102**, 513 (2002).
23. The $\Delta x^{\ddagger}_{N\rightarrow U}$ and $\Delta x^{\ddagger}_{I\rightarrow N}$ values represent the average width of the potential energy for each state along the mechanical reaction coordinate (*6*, *26*) and thus describe the extent of structural distortion necessary to cross a transition-state barrier. A correlation has been noted between a protein's structure and the position of the unfolding transition state: $\Delta x^{\ddagger}_{N\rightarrow U}$ appears to be large when the stabilizing interactions are predominantly long-range hydrophobic interactions, and small when they consist of clusters of short-range interstrand hydrogen bonds (*6*, *30*). The value of 2 nm measured here for RNase H is on the higher end of the distribution of transition-state distances obtained for other proteins using the AFM (0.25 to 1.7 nm) [(*26*) and references therein].
24. M. Schlierf, H. Li, J. M. Fernandez, *Proc. Natl. Acad. Sci. U.S.A.* **101**, 7299 (2004).
25. E. Rhoades, M. Cohen, B. Schuler, G. Haran, *J. Am. Chem. Soc.* **126**, 14686 (2004).
26. C. Bustamante, Y. R. Chemla, N. R. Forde, D. Izhaky, *Annu. Rev. Biochem.* **73**, 705 (2004).
27. K. Kuwajima, *Proteins* **6**, 87 (1989).
28. G. M. Spudich, E. J. Miller, S. Marqusee, *J. Mol. Biol.* **335**, 609 (2004).
29. The I53D RNase H variant did not exhibit any low-force unfolding transitions; refolding occurred as a gradual compaction rather than as a single sharp transition, and hopping was not observed at any force examined. Refolding to the native state was qualitatively slower for the I53D variant, which suggests that the formation of the molten globule–like intermediate of RNase H speeds up the attainment of its folded state. This is consistent with bulk kinetic studies that suggest that folding can be accelerated if the interactions that stabilize the intermediate stabilize the transition state structure to an even greater extent (*28*).
30. H. Lu, K. Schulten, *Proteins* **35**, 453 (1999).
31. H. S. Chan, K. A. Dill, *Proteins* **30**, 2 (1998).

32. We thank R. Dahlquist for support and experimental advice in the early stages of this work, and the Marqusee and Bustamante labs for helpful discussions. Supported by NIH grants GM50945 (S.M.) and GM32543 (C.B.), U.S. Department of Energy grant AC0376Sf00098 (C.B.), NIH training grant GM008295 (E.A.S.), and a NSF predoctoral fellowship (E.A.S.).

Supporting Online Material

www.sciencemag.org/cgi/content/full/309/5743/2057/DC1
Materials and Methods
SOM Text
Figs. S1 to S6

28 June 2005; accepted 17 August 2005
10.1126/science.1116702

Xanthorhodopsin: A Proton Pump with a Light-Harvesting Carotenoid Antenna

Sergei P. Balashov,[1]* Eleonora S. Imasheva,[1] Vladimir A. Boichenko,[2] Josefa Antón,[3] Jennifer M. Wang,[1] Janos K. Lanyi[1]*

Energy transfer from light-harvesting carotenoids to chlorophyll is common in photosynthesis, but such antenna pigments have not been observed in retinal-based ion pumps and photoreceptors. Here we describe xanthorhodopsin, a proton-pumping retinal protein/carotenoid complex in the eubacterium *Salinibacter ruber*. The wavelength dependence of the rate of pumping and difference absorption spectra measured under a variety of conditions indicate that this protein contains two chromophores, retinal and the carotenoid salinixanthin, in a molar ratio of about 1:1. The two chromophores interact strongly, and light energy absorbed by the carotenoid is transferred to the retinal with a quantum efficiency of ~40%. The antenna carotenoid extends the wavelength range of the collection of light for uphill transmembrane proton transport.

The extreme halophile *Salinibacter ruber* isolated from salt-crystallizer ponds (*1*, *2*) can be grown in aerobic heterotrophic culture in 4 M NaCl. This eubacterium accumulates high concentrations of KCl to adapt to growth in a high–ionic strength environment (*3*), as do haloarchaea. *S. ruber* has a deep red color from salinixanthin, which constitutes nearly 100% of its carotenoid content. The chemical structure of salinixanthin is established, and it was proposed to provide protection from photodamage and stabilize the cell membrane, because both the polyene and the fatty acid parts of this carotenoid acyl glycoside were predicted to be immersed in the lipid bilayer (*4*). We report here that salinixanthin is not the only pigment in the *S. ruber* cell membrane and that heterotrophy is not the only source of energy for this organism. These bacteria contain an unusual retinal protein that uses salinixanthin to harvest light energy in a wider spectral range than is possible with retinal alone and then uses it for transmembrane proton transport. Thus, it is a light-driven proton pump similar to bacteriorhodopsin (*5*) and the archaerhodopsins (*6*) of the archaea, the proteorhodopsins of planktobacteria (*7*), and leptosphaeria rhodopsin of a eukaryote (*8*), but with two chromophores. We term it here xanthorhodopsin. Its carotenoid antenna is a feature shared with chlorophyll-based light-harvesting complexes and reaction centers (*9*, *10*).

Illumination of cell-membrane vesicles prepared from *Salinibacter* produces acidification of the medium (Fig. 1A), which is abolished by the protonophore carbonyl cyanide *m*-chlorophenyl-hydrazone (CCCP). When assayed in 1 M Na_2SO_4, these light-dependent pH changes are unaffected by added chloride ions. Thus, the vesicles contain an outward-directed light-driven proton pump, such as bacteriorhodopsin, and they lack a detectable amount of a chloride pump, such as halorhodopsin, that would produce chloride-dependent light-induced alkalinization in the presence of CCCP (*11*).

The existence of observed light-driven proton transport suggested that *Salinibacter* might contain a bacterial rhodopsin. The wavelength dependence of the transport (action spectrum) was determined by two independent methods: measuring photoinhibition of respiration and measuring light-induced pH changes. The transmembrane electrochemical gradient produced by the light-driven proton pump inhibits respiration of intact *S. ruber* cells and results in a temporary increase of the ambient oxygen concentration (Fig. 1B). As expected, the rise in oxygen level is abolished by the CCCP. This method had been used for demonstrating the physiological function of bacteriorhodopsin in halobacterial cells (*12*, *13*). The action spectrum is more complex than what would be expected for a retinal protein. It exhibits a shoulder at 560 nm, where a retinal chromophore would absorb, and sharp bands at 521 and 486 nm (Fig. 1C) that correspond to the maxima in the structured absorption spectrum of cell membranes (fig. S1) containing

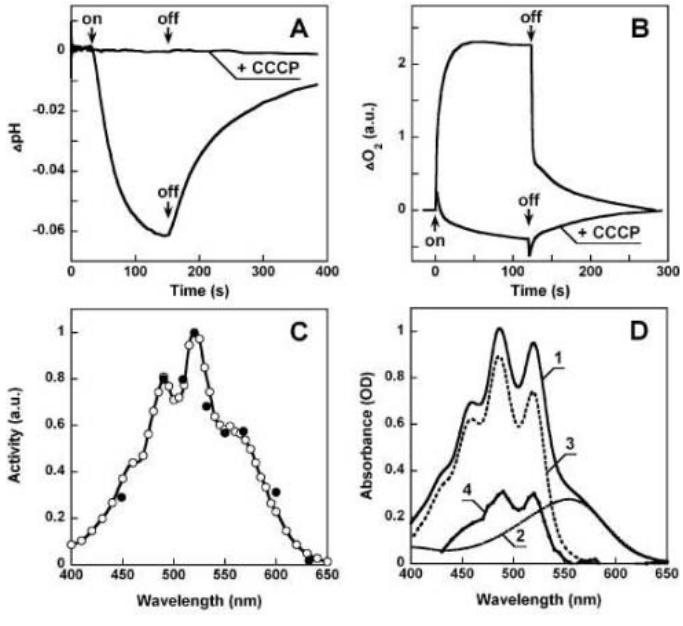

Fig. 1. Light-induced proton transport, inhibition of respiration in *S. ruber*, their action spectra, and an estimation of the efficiency of energy transfer from carotenoid to retinal in xanthorhodopsin. (**A**) pH changes in a membrane vesicle suspension produced by illumination at 550 nm at pH 6.5 are shown in the absence and presence of 20 μM CCCP at a light intensity of 2 mW cm^{-2}. (**B**) Kinetics of light-induced changes in the rate of oxygen uptake caused by photoinhibition of respiration in the cell suspension of *S. ruber* are shown in the absence and presence of 10 μM CCCP, 550 nm, 2 mW cm^{-2}. a.u., arbitrary units. (**C**) Action spectra for photo-inhibition of the respiration by intact cells (open circles) and light-induced proton transport in membrane vesicles (solid circles), measured as in (B) and (A), respectively. (**D**) Estimated absorption spectrum of the complex and the contribution of carotenoid component to it and to the action spectrum are shown, as explained in the text. Spectrum 1: the calculated spectrum of xanthorhodopsin; spectrum 2: bacteriorhodopsin, 10 nm shifted to the blue and appropriately scaled to model the retinal component of xanthorhodopsin; spectra 3 and 4: carotenoid components of the absorption spectrum and the action spectrum, respectively, obtained by subtracting the contribution of the retinal component. The ratios of the integrals of the carotenoid and retinal components are ~2.5 and 1 in the absorption spectrum and the action spectrum, respectively. The increase in the cross sections for light collection and the photoreaction from the carotenoid are thus 3.5-fold and 2-fold. OD, optical density.

[1]University of California, Irvine, CA 92697, USA. [2]Institute of Basic Biological Problems, Russian Academy of Sciences, Pushchino, 142290, Russia. [3]University of Alicante, Alicante, E-03080, Spain.

*To whom correspondence should be addressed. E-mail: balashov@uci.edu (S.P.B.); jlanyi@orion.oac.uci.edu (J.K.L.)

salinixanthin. Figure 1C shows that the action spectrum for light-induced pH changes in membrane vesicle suspensions agrees well with that of the inhibition of respiration. The action spectra indicate that this system depends on a complex of the retinal protein and a carotenoid and that light absorbed by both carotenoid and retinal is effective in proton transport. The contribution of these two components to the action spectrum is shown in Fig. 1D.

The presence of a retinal chromophore was confirmed by bleaching and reconstitution. Incubation of *Salinibacter* cell membranes with hydroxylamine produced a difference absorption spectrum that exhibited the broad minimum at 565 nm expected if retinal were released from a bacteriorhodopsin-like chromophore by this treatment (*14*), as well as the corresponding maximum at 364 nm from the retinal oxime produced (Fig. 2A). Additionally, the difference spectrum contains sharp depletion bands at 521, 487, and 457 nm. The latter three bands are near the absorption maxima of salinixanthin (fig. S1) but show remarkably greater spectral resolution similar to the action spectrum (Fig. 1C). Reconstitution of the membranes, which were washed free of hydroxylamine, with all-trans retinal resulted in the recovery of not only the broad band near 565 nm of the retinal chromophore but also sharp bands (Fig. 2B) that correspond to the negative peaks after bleaching. These sharp bands must originate from one or a few salinixanthin molecules that closely interact with the retinal protein and change their spectrum (mainly narrowing the vibronic bands) when the complex is formed.

The interaction of the two chromophores is modulated in the photocycle. Illumination of the *Salinibacter* membranes with green light at 175 K causes the formation of a photoproduct with a red-shifted retinal band, which is stable at this temperature but reconverts when illuminated by red light (Fig. 3A). This is behavior characteristic of the K photointermediate of bacteriorhodopsin (*15*–*17*). The peculiarity of the difference spectrum of *Salinibacter* retinal protein is that besides the increase of absorbance near 610 nm from the red-shifted retinal chromophore, a set of three additional sharp bands appear at 448, 482, and 518 nm. These peaks originate from a small (~2 nm) blue shift of the three main carotenoid bands. Perturbation of the carotenoid in the K-like photoproduct appears to be electrochromic and suggests close interaction with the retinal. Reversal of the changes of the carotenoid bands with red light (Fig. 3A), which is absorbed by the retinal but not by the carotenoid, is further evidence for interaction between the carotenoid and the retinal in the complex.

The absorption changes during the photocycle at ambient temperature (Fig. 3, B and C) indicate the formation of intermediates similar to the K, L, M, N, and O photoproducts of bacteriorhodopsin (*15*) and proteorhodopsin (*18*). The absorption changes at 410 nm after flash photoexcitation reflect mainly the formation of the M intermediate with a deprotonated retinal Schiff base, as expected in a proton pump. The difference spectra associated with photointermediates also exhibit perturbation of the absorption bands of salinixanthin (Fig. 3C). The changes, arising on the millisecond time scale, involve band-broadening similar to the spectra after bleaching with hydroxylamine (Fig. 2A). Together with the spectrum of the K state (Fig. 3A), they suggest that the carotenoid senses both electrostatic changes and conformational shifts of the retinal and the protein during the photocycle.

Substantial purification of the complex was achieved by repeated incubation of *Salinibacter* membranes with 0.01% dodecyl maltoside, followed by centrifugation to recover the

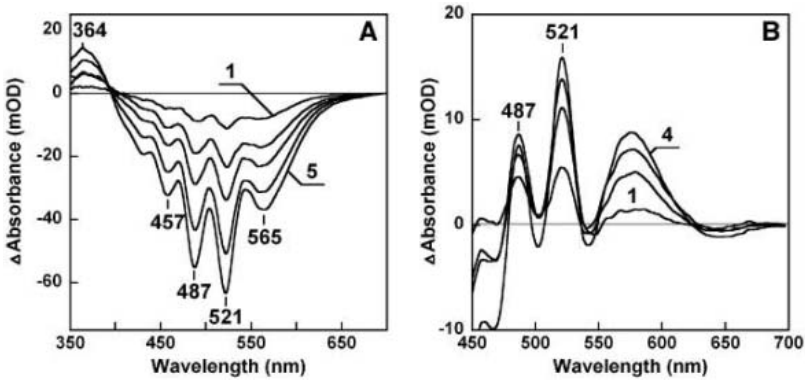

Fig. 2. Spectroscopic detection of the retinal protein of *Salinibacter*. (**A**) Curves 1 through 5 show the difference spectra upon illumination of a cell-membrane suspension at >550 nm in the presence of 0.2 M hydroxylamine, pH 7.2, for 4, 12, 20, 36, and 60 min at 20°C, respectively. The amplitude of the 487-nm difference band is 10 to 15% of the total carotenoid absorbance. (**B**) Curves 1 through 4 show the difference spectra measured 5, 15, 25, and 60 min after addition of all-trans retinal to the *S. ruber* cell membranes, which had been bleached with 0.2 M hydroxylamine.

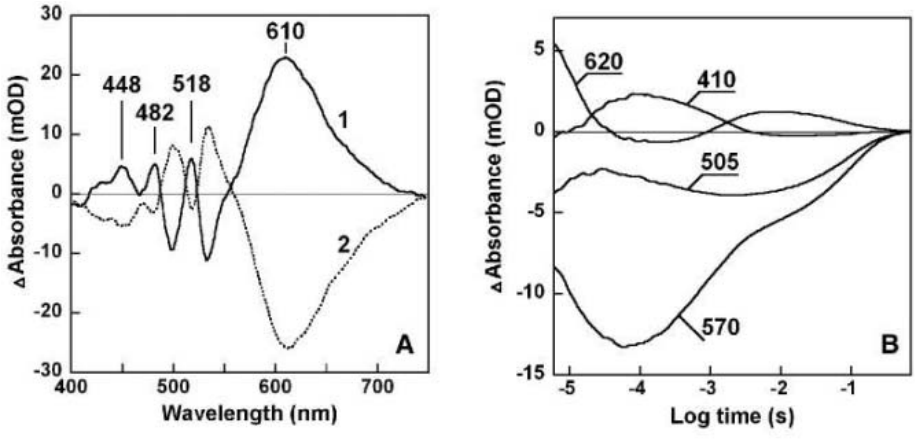

Fig. 3. Absorption changes during the photocycle of xanthorhodopsin. (**A**) Light-induced absorption changes in a water-glycerol suspension of cell membranes at 175 K. Spectrum 1: illumination of membranes with 520-nm light; spectrum 2: subsequent illumination at >650 nm. (**B**) Kinetics of laser flash–induced absorption changes at selected characteristic wavelengths, as indicated, in membranes of *Salinibacter* solubilized with 0.15% dodecyl maltoside in 100 mM NaCl, pH 8.8, 20°C. The global fit indicates that kinetics include at least six components, with time constants of 7.5 μs, 35 μs, 280 μs, 1.3 ms, 11 ms, and 100 ms. (**C**) Transient difference spectra during the photocycle, measured at 10, 30, 60, 100, 160, and 250 ms (curves 1 through 6), after a 532-nm laser flash. Conditions and sample are as in (**B**).

membranes. This procedure extracts most of the excess bulk carotenoids as well as nearly all other proteins (*19*), and the xanthorhodopsin then can be solubilized with 0.15% dodecyl maltoside. The solubilized xanthorhodopsin exhibits a slight blue shift of the retinal chromophore band but retains all the characteristic absorption bands of the membranes, and because of less light scattering, more spectroscopic details are revealed (fig. S2). It appears that after hydrolysis of the Schiff base, salinixanthin loses its rigid environment and acquires a broader, less-structured spectrum, similar to that of the bulk carotenoid (fig. S2). This broadening of the carotenoid absorption bands, which is responsible for the negative peaks in Fig. 2A, is revealed by second-derivative spectra that are better suited for resolving overlapping bands (fig. S3). In such spectra, the narrow carotenoid bands are more pronounced than are the wider band of the retinal chromophore. The overall shape of the carotenoid vibronic bands after bleaching resembles those before bleaching, but the bands shift slightly to the red and become wider (e.g., the width of the 486-nm band increases from ~24 to 36 nm). Further, the shapes and the amplitude ratios of the difference bands after bleaching the sample enriched in xanthorhodopsin are the same as in a sample enriched in bulk salinixanthin. This strongly suggests that salinixanthin is a stoichiometric component of the retinal protein complex.

The spectrum of the xanthorhodopsin complex (Fig. 1D, spectrum 1) was calculated from the spectrum of the partly purified sample (fig. S2) by satisfying the condition that the resolution of the vibronic bands should be the same as are those in the action spectrum (*19*). From the published extinction coefficients of the two chromophores, 240,000 M^{-1} cm^{-1} for salinixanthin (*4*) and 63,000 M^{-1} cm^{-1} for the retinal chromophore of bacteriorhodopsin (*20*), we estimate that the ratio of salinixanthin to retinal is 0.75:1. However, the extinction coefficient for most carotenoids with the same number of conjugated bonds as salinixanthin is lower, ~180,000 M^{-1} cm^{-1} (*19*). With this number, the retinal-to-carotenoid ratio in the purified complex will be 1:1. Only the carotenoid bound in the complex functions as an antenna, because the spectra of bound and free carotenoid are different (fig. S2) and the action spectrum corresponds to the spectrum of the bound state (Fig. 1C). The action spectrum will consist of the retinal chromophore band plus the band of the bound carotenoid, multiplied by the efficiency of energy transfer to the retinal. Because the contribution of the carotenoid bands to the action spectrum is about 40% of their contribution to the absorption spectrum (Fig. 1D), we conclude that the efficiency of energy transfer is ~40%. In photosynthetic organisms, the efficiency of energy transfer between carotenoids and chlorophyll is from 15% to 100% (*9*, *21*, *22*).

Mass spectrometry of the more intense of the two bands on a SDS–polyacrylamide gel from the purified sample (*19*) identified the gene product from a proteorhodopsin- or bacteriorhodopsin-like open reading frame (Fig. 4) in the *Salinibacter* genome (accession number NC_006812), but no other proteins were found in the sample that could bind retinal. Under these conditions, the expression of other retinal proteins, such as halorhodopsin identified in the genome (*23*), must be much less than that of xanthorhodopsin.

For mechanistic reasons that have been thoroughly explored in bacteriorhodopsin (*24*), retinal must be the site of proton translocation in xanthorhodopsin also. The rationale for the carotenoid in the dual light-harvesting system is that it increases the cross section for light absorption and extends it to the spectral region, where the absorption of the retinal chromophore is low. Other functions might be the protection of the retinal protein from photo-oxidation by singlet oxygen, because carotenoids are known to be efficient deactivators of triplet states, and an increase of protein stability. These functions of carotenoids are common in chlorophyll-based photosynthetic systems, where they harvest light energy and transfer it to chlorophyll (*21*), but they have not been shown for retinal-based pumps or receptors (*25*–*27*).

The discovery of a carotenoid antenna in a retinal protein raises an interesting question about energy transfer. The intense absorption bands of carotenoids are caused mainly by transition to the strongly allowed S_2 state (*21*). This state is very short-lived (50 to 200 fs), because through internal conversion, it populates lower-lying excited states, including the S_1 state with a much longer lifetime. S_1 and S_2 both participate in energy transfer to bacteriochlorophyll. However, the energy level of S_1 in spirilloxanthin, a carotenoid with 13 conjugated bonds, similar to salinixanthin, is far below that of the 560-nm absorption band of the retinal chromophore (*21*). If the same is true for salinixanthin, energy transfer cannot be from the lower excited state S_1. Could there be energy transfer from an excited state located between S_2 and S_1, as suggested for carotenoid-chlorophyll complexes (*30*)? If not,

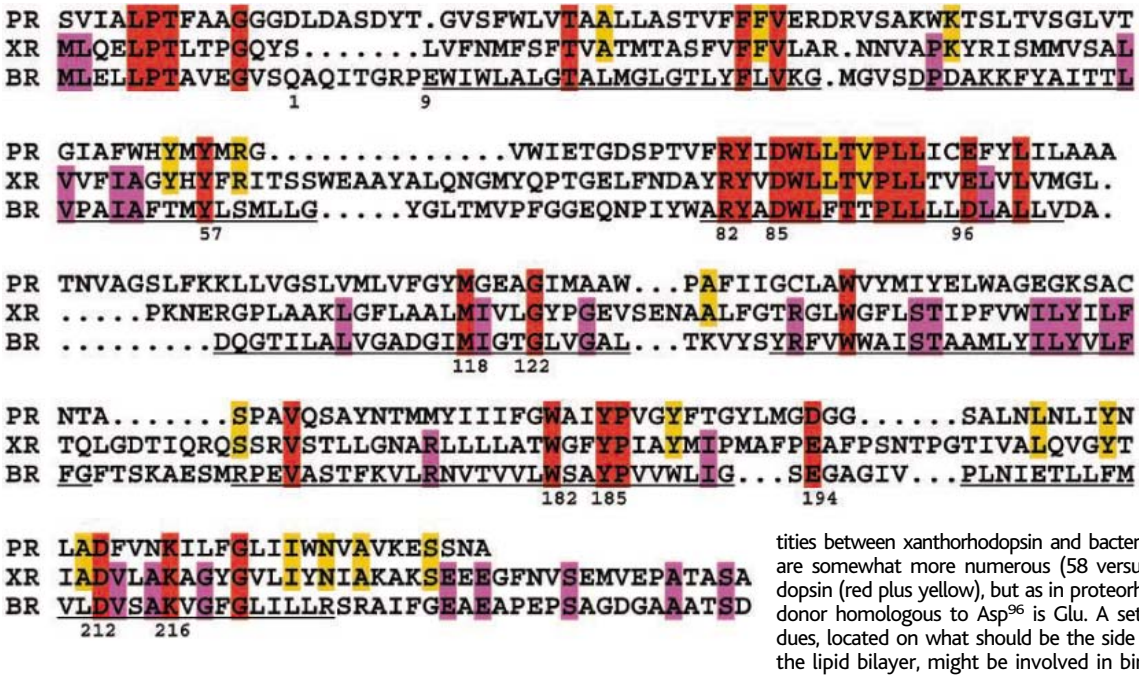

Fig. 4. Alignment of the sequences of xanthorhodopsin (XR), proteorhodopsin (PR), and bacteriorhodopsin (BR). Xanthorhodopsin contains the functionally important residues known for retinal binding and proton transport, including homologs of Tyr^{57}, Arg^{82}, Asp^{85}, Trp^{86}, Asp^{96}, Trp^{182}, Glu^{194}, Tyr^{185}, Asp^{212}, and Lys^{216}, with numbering and helical segments (underlined) for bacteriorhodopsin. There are 30 residues (marked red) common to all three proteins (in two cases, they are Asp/Glu correspondences). The residue identities between xanthorhodopsin and bacteriorhodopsin (red plus purple) are somewhat more numerous (58 versus 46) than with proteorhodopsin (red plus yellow), but as in proteorhodopsin, the internal proton donor homologous to Asp^{96} is Glu. A set of four phenylalanine residues, located on what should be the side of helix E that faces toward the lipid bilayer, might be involved in binding the carotenoid (*31*).

energy transfer will be only from S_2 and rapid, implying close proximity and exact geometry of the donor and acceptor. The substantial changes of the carotenoid spectrum during its retinal-dependent formation of the complex and during the photocycle suggest that the binding site is specially "crafted" to accommodate the carotenoid molecule in a position optimal for energy transfer to the retinal. The xanthorhodopsin complex represents the simplest electrogenic pump with an accessory antenna pigment, and it might be an early evolutionary development in using energy transfer for energy capture.

References and Notes

1. J. Antón, R. Rosselló-Mora, F. Rodríguez-Valera, R. Amann, *Appl. Environ. Microbiol.* **66**, 3052 (2000).
2. J. Antón *et al.*, *Int. J. Syst. Evol. Microbiol.* **52**, 485 (2002).
3. A. Oren, M. Heldal, S. Norland, E. A. Galinski, *Extremophiles* **6**, 491 (2002).
4. B. F. Lutnaes, A. Oren, S. Liaaen-Jensen, *J. Nat. Prod.* **65**, 1340 (2002).
5. D. Oesterhelt, W. Stoeckenius, *Nature* **233**, 149 (1971).
6. Y. Mukohata, K. Ihara, T. Tamura, Y. Sugiyama, *J. Biochem.* **125**, 649 (1999).
7. O. Béjà, E. N. Spudich, J. L. Spudich, M. Leclerc, E. F. DeLong, *Nature* **411**, 786 (2001).
8. S. A. Waschuk, A. G. Bezerra Jr., L. Shi, L. S. Brown, *Proc. Natl. Acad. Sci. U.S.A.* **102**, 6879 (2005).
9. B. Robert, R. J. Cogdell, R. van Grondelle, in *Light-Harvesting Antennas in Photosynthesis*, B. R. Green, W. W. Parson, Eds. *Advances in Photosynthesis and Respiration*, Govindjee, Ed. (Kluwer Academic Publishers, Dordrecht, Netherlands, 2003), vol. 13, pp. 169–194.
10. H. A. Frank, A. J. Young, G. Britton, R. J. Cogdell, Eds., *The Photochemistry of Carotenoids, Advances in Photosynthesis*, Govindjee, Ed. (Kluwer Academic Publishers, Dordrecht, Netherlands, 1999), vol. 8.
11. B. Schobert, J. K. Lanyi, *J. Biol. Chem.* **257**, 10306 (1982).
12. D. Oesterhelt, W. Stoeckenius, *Proc. Natl. Acad. Sci. U.S.A.* **70**, 2853 (1973).
13. F. F. Litvin, V. A. Boichenko, S. P. Balashov, V. T. Dubrovskii, *Biofizika* **22**, 1062 (1977).
14. D. Oesterhelt, L. Schuhman, H. Gruber, *FEBS Lett.* **44**, 257 (1974).
15. R. H. Lozier, R. A. Bogomolni, W. Stoeckenius, *Biophys. J.* **15**, 955 (1975).
16. F. F. Litvin, S. P. Balashov, V. A. Sineshchekov, *Bioorgan. Khim.* **1**, 1767 (1975).
17. S. P. Balashov, T. G. Ebrey, *Photochem. Photobiol.* **73**, 453 (2001).
18. A. K. Dioumaev *et al.*, *Biochemistry* **41**, 5348 (2002).
19. Materials and methods are available as supporting material on *Science* Online.
20. D. Oesterhelt, M. Meentzen, L. Schuhmann, *Eur. J. Biochem.* **40**, 453 (1973).
21. T. Polivka, V. Sundström, *Chem. Rev.* **104**, 2021 (2004).
22. G. A. Montano, Y. Y. Xin, S. Lin, R. E. Blankenship, *J. Phys. Chem. B* **108**, 10607 (2004).
23. A. Peña *et al.*, *Extremophiles* **9**, 151 (2005).
24. J. K. Lanyi, B. Schobert, *J. Mol. Biol.* **328**, 439 (2003).
25. J. L. Spudich, C. S. Yang, K. H. Jung, E. N. Spudich, *Annu. Rev. Cell Dev. Biol.* **16**, 365 (2000).
26. M. Kumauchi, T. Ebrey, in *Handbook of Photosensory Receptors*, W. R. Briggs, J. L. Spudich, Eds. (Wiley VCH, Darmstadt, Germany, 2005), pp. 43–76.
27. Action spectra for bacteriorhodopsin had ruled out an antenna function for bacterioruberin, the main carotenoid in halobacteria (*13*, *28*). No energy transfer was observed for archaerhodopsin either (*29*).
28. A. Danon, W. Stoeckenius, *Proc. Natl. Acad. Sci. U.S.A.* **71**, 1234 (1974).
29. Y. Mukohata, K. Ihara, K. Uegaki, Y. Miyashita, Y. Sugiyama, *Photochem. Photobiol.* **54**, 1039 (1991).
30. G. Cerullo *et al.*, *Science* **298**, 2395 (2002).
31. Single-letter abbreviations for the amino acid residues are as follows: A, Ala; C, Cys; D, Asp; E, Glu; F, Phe; G, Gly; H, His; I, Ile; K, Lys; L, Leu; M, Met; N, Asn; P, Pro; Q, Gln; R, Arg; S, Ser; T, Thr; V, Val; W, Trp; and Y, Tyr.

32. We thank D. T. Ta for sharing his expertise in SDS gel preparation, L. Brown for discussions, and D. Chen for help to optimize culture growth conditions. This work was supported by NIH grant GM29498 and U.S. Department of Energy grant DEFG03-86ER13525 (both to J.K.L.) and by the Spanish Ministry of Science grant BOS2003-05198-CO2 (to J.A.). V.A.B. thanks the Molecular and Cellular Biology program of the Russian Academy of Sciences for support. Sequence data were obtained from the Institute for Genomic Research Web site at www.tigr.org. Sequencing of *S. ruber* (in progress) is with support from NSF.

Supporting Online Materials

www.sciencemag.org/cgi/content/full/309/5743/2061/DC1
Materials and Methods
Figs. S1 to S3
References

27 July 2005; accepted 22 August 2005
10.1126/science.1118046

Direct Isolation of Satellite Cells for Skeletal Muscle Regeneration

Didier Montarras,[1]* Jennifer Morgan,[3,4] Charlotte Collins,[4] Frédéric Relaix,[1] Stéphane Zaffran,[1] Ana Cumano,[2] Terence Partridge,[4] Margaret Buckingham[1]*

Muscle satellite cells contribute to muscle regeneration. We have used a *Pax3*$^{GFP/+}$ mouse line to directly isolate (Pax3)(green fluorescent protein)–expressing muscle satellite cells, by flow cytometry from adult skeletal muscles, as a homogeneous population of small, nongranular, Pax7+, CD34+, CD45–, Sca1– cells. The flow cytometry parameters thus established enabled us to isolate satellite cells from wild-type muscles. Such cells, grafted into muscles of *mdx nu/nu* mice, contributed both to fiber repair and to the muscle satellite cell compartment. Expansion of these cells in culture before engraftment reduced their regenerative capacity.

Satellite cells are skeletal muscle progenitor cells responsible for postnatal growth and repair (*1*). The difficulty of isolating pure populations of satellite cells in sufficient number has precluded their use in cell-based tissue repair assays. These assays have, therefore, employed either muscle precursor cells that correspond to the progeny of muscle satellite cells, obtained after activation and proliferation in culture (*2*–*4*), or mixtures of cells obtained after enzymatic dissociation of skeletal muscles (*5*, *6*). In vivo, quiescent muscle satellite cells are characterized by the expression of surface markers such as M-cadherin (*7*, *8*), syndecan 3 and 4 (*9*), and CD34 (*10*); however, none of these permit unequivocal isolation because of the lack of specificity or availability of suitable reagents. Satellite cells also express transcription factors, notably Pax7, a member of the homeodomain/paired box family of Pax proteins (*11*). Recently, we have shown that, Pax3, the paralog of Pax7, is also expressed in quiescent muscle satellite cells in a subset of muscles (*12*, *13*). The generation of a green fluorescent protein (GFP)–tagged Pax3 mouse line (*Pax3*$^{GFP/+}$) (*14*) permitted us to isolate (Pax3)GFP-expressing cells from adult skeletal muscles by flow cytometry.

Previous observations on *Pax3*$^{nlacz/+}$ mice indicated that satellite cells expressing the transcriptional regulator Pax3 were limited to a subset of adult skeletal muscles, including the diaphragm, most trunk muscles, and some limb muscles (*13*). The *Pax3*$^{GFP/+}$ mouse line shows similar expression. As illustrated in the diaphragm (Fig. 1A), (Pax3)GFP+ cells are found in a typical satellite cell position beneath the layer of laminin that surrounds muscle fibers. Most of these cells also express the transcriptional regulator Pax7 (Fig. 1B), which marks muscle satellite cells (*11*).

Flow cytometric analysis of the cells prepared from diaphragm muscle of adult *Pax3*$^{GFP/+}$ mice (Fig. 1C) indicated that (Pax3)GFP+ cells constitute a population that is negative for CD45 and Sca1 and positive for CD34. These cells were also negative for the endothelial markers CD31 and Flk1 (fig. S1). Forward and side scatter gating (reflecting the size and granularity of the cells, respectively) (Fig. 1C, left) indicated that (Pax3)GFP+ cells constitute a homogeneous population of small, nongranular, mononucleated cells. Immediately after sorting, immunodetection showed the presence of 93% Pax7+ cells and 8% MyoD+

[1]CNRS Unité de Recherche Associée 2578, Department of Developmental Biology, [2]Unité du Développement des Lymphocytes, Unité 668, INSERM, Pasteur Institute, 75724 Paris Cedex 15, France. [3]Department of Paediatrics, Imperial College London, The Dubowitz Neuromuscular Centre, Hammersmith Hospital, Du Cane Road, London W12 ONN, UK. [4]Muscle Cell Biology Group, Medical Research Council Clinical Sciences Centre, Imperial College, Du Cane Road, London W12 ONN, UK.

*To whom correspondence should be addressed. E-mail: dmontarr@pasteur.fr (D.M.); margab@pasteur.fr (M.B.)

cells. Pax7 marks both quiescent and activated satellite cells (*15*), whereas MyoD marks activated satellite cells only (*16*, *17*). This indicates that the majority of the cells did not undergo activation during the few (4 to 6) hours that were required for dissociation and sorting. Colony assays further established the identity of these cells as muscle progenitors, giving rise to 100% Pax7- and MyoD- expressing cells after 3 days in culture (fig. S2). The (Pax3)GFP+ fraction that we isolated thus constitutes a pure population of myogenic cells.

We functionally characterized (Pax3)GFP+ cells, isolated by flow cytometry from adult diaphragm muscle, by grafting them into irradiated tibialis anterior (TA) muscles of immunodeficient *nude mdx* mice (*mdx nu/nu*). These mice lack dystrophin, a structural protein that is mutated in Duchenne muscular dystrophy patients (*18*). Satellite cells of the TA, like those of other lower hindlimb muscles, do not normally express Pax3. The contribution of (Pax3)GFP+ cells to fiber repair was measured by the restoration of dystrophin expression in muscle fibers of host mice, 3 weeks after grafting. Numerous dystrophin-positive fibers were readily detected in the grafted muscles (Fig. 1D, top). Only occasional dystrophin-positive fibers, probably revertant fibers (*19*), were found in the control contralateral, nongrafted TA muscles (Fig. 1D, bottom). Grafting of 2×10^4 cells led to dystrophin expression in an average number of 587 fibers, and grafts of as few as 10^3 cells still resulted in dystrophin expression in an average of 160 fibers (Fig. 1E, left). These yields are comparable to those obtained after grafting 5×10^5 cells isolated by enzymatic dissociation of whole adult muscles (*5*, *6*).

Most grafting experiments have employed muscle precursor cells obtained after a phase of amplification in culture (*2*, *3*). To determine whether such culturing procedures could alter the capacity of cells to contribute to tissue reconstitution, we grafted cultured and noncultured (Pax3)GFP+ cells. Grafting 10^4 noncultured cells led to restoration of dystrophin expression in an average number of 300 fibers, whereas grafting the same number of cultured cells resulted in significantly fewer dystrophin-positive fibers (mean = 88 fibers, $P < 0.02$) (Fig. 1E, right). We also grafted 10^5 cells, corresponding to the progeny after 3 days in culture of 10^4 (Pax3)GFP+ cells. These cells led to restoration of dystrophin expression in an average number of 265 fibers, a figure that is similar to that obtained when grafting 10^4 noncultured cells (Fig. 1E, right). These results show that culturing muscle satellite cells for a few days before grafting reduces their efficiency in fiber repair, suggesting that in vitro expansion is disadvantageous. Clonal assays indicated that cultured cells display a lower proliferation potential than freshly isolated cells and a tendency to differentiate more rapidly (table S1). These features may account for their reduced regenerative capacity.

(Pax3)GFP+ CD34+ donor cells could be recovered by flow cytometry from grafted muscles (Fig. 2A). These cells displayed a myogenic phenotype in culture, expressing MyoD and Pax7 and differentiating into TroponinT-expressing myotubes (Fig. 2B). Single fibers prepared from grafted muscles (Fig. 2C) carried cells of donor origin in a muscle sat-

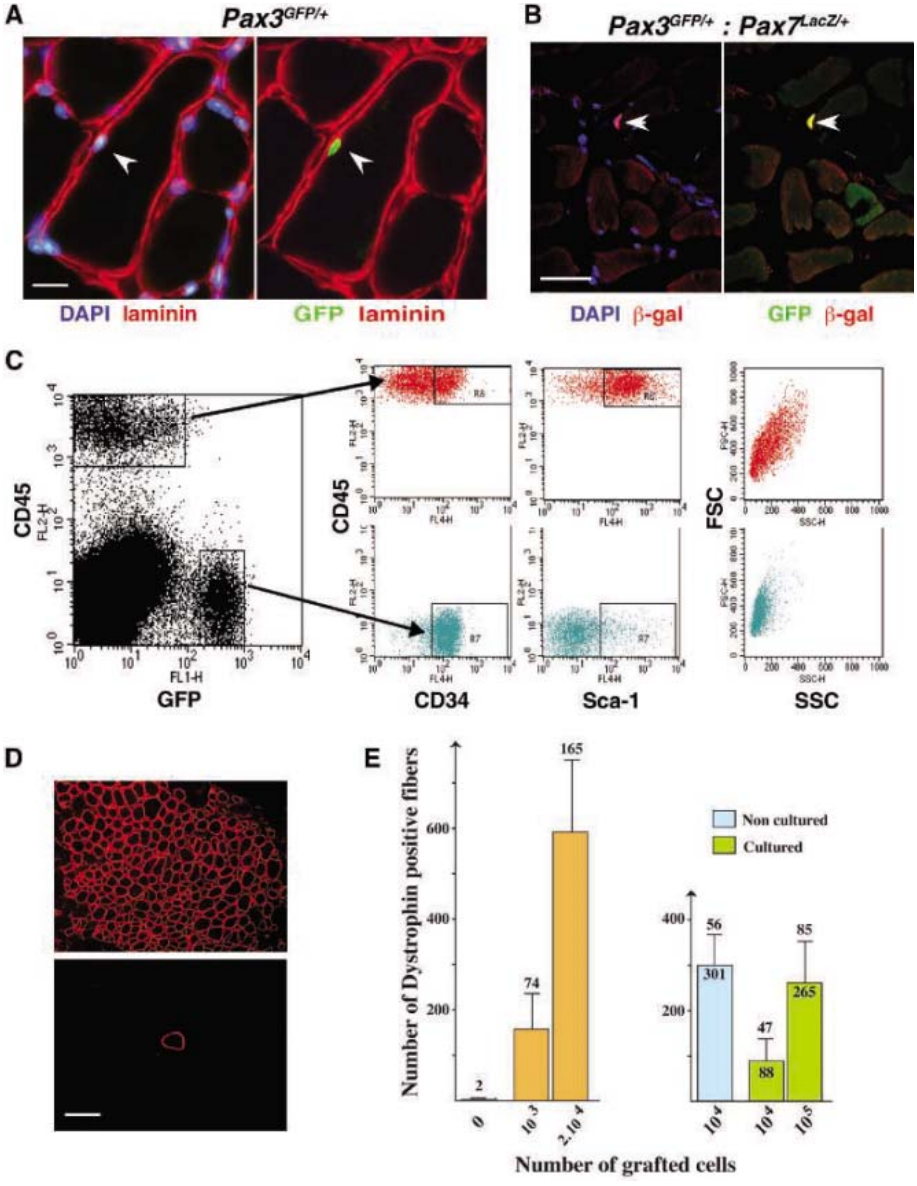

Fig. 1. Characterization of (Pax3)GFP-expressing cells from the diaphragm muscle of adult mice. (**A**) Transverse section of a *Pax3*$^{GFP/+}$ mouse). Left: Immunodetection of laminin (red staining), with 4′,6-diamidino-2-phenylindole (DAPI) coloration. Right: Direct fluorescent detection of GFP+ cells (green staining), together with immunodetection of laminin. Scale bar, 20 μm. (**B**) Transverse section from a *Pax3*$^{GFP/+}$:*Pax7*$^{lacz/+}$ mouse. Left: Immunodetection of β-galactosidase (β-gal, red staining) from the *Pax7* allele, together with DAPI staining. Right: Detection of GFP fluorescence (green staining) from the *Pax3* allele and co-immunodetection of β-galactosidase (red staining) from the *Pax7* allele, resulting in yellow staining. Scale bar, 100 μm. Arrowheads indicate candidate muscle cells. (**C**) Flow cytometry analysis of cells from *Pax3*$^{GFP/+}$ mice. CD34 and Sca1 expression on CD45+ cells (red, top panels) and on GFP+ cells (blue, bottom panels). Top and bottom right panels correspond to forward scatter (FSC) and side scatter (SSC) gating of CD45+ and GFP+ cells, respectively. (**D**) Detection of dystrophin-positive fibers in grafted muscles. Three weeks after grafting with (Pax3)GFP+ cells, TA muscles of *mdx nu/nu* mice were processed for detection of dystrophin. Top: Tranverse section of grafted muscle. Bottom: Control contralateral nongrafted TA. Scale bar, 200 μm. (**E**) Quantitative analysis of experiments as shown in (D). Cells were grafted immediately after sorting (left). The effect of cell culture was examined by injecting cultured or noncultured cells (right). The numbers of injected mice were, from left to right: 4, 5, 4, 6, 5, and 4. Labeled error bars represent SD.

ellite cell position, co-expressing (Pax3)GFP and Pax7. Of 569 cells detected on the surface of 120 single fibers from grafted TA muscles, 17% were satellite cells of donor origin co-expressing Pax7 and (Pax3)GFP. These results show that grafted muscle satellite cells contribute not only to muscle fiber repair but also to the muscle satellite cell compartment. They also show that (Pax3)GFP+ cells retain their Pax3+ identity in the environment of the TA muscle, where endogenous satellite cells do not express Pax3. Injured, as well as intact, TA muscle from *Pax3*$^{GFP/+}$ mice does not normally contain (Pax3)GFP+ cells (fig. S3).

Flow cytometric analysis indicated that (Pax 3)GFP+ cells express the surface marker CD34. We used this surface marker and the parameters defined by forward and side scatter gating for (Pax3)GFP+ cells (Fig. 1C) to determine whether muscle progenitor cells that do not express (Pax3)GFP could also be isolated from adult muscles. The GFP+ CD34+ cells isolated from the diaphragm of adult mice (Fig. 3A) represented 47% of the cells analyzed by flow cytometry. Clonal analysis of the cells from each fraction showed that all of the clones formed (78 out of 192 single cells) were myogenic, as monitored by immunodetection of MyoD and Pax7 and by myotube formation. In contrast, the GFP– CD34+ cells (Fig. 3A) displayed a cloning efficiency of 6% and gave rise to only 2 myogenic clones out of 192 plated cells. The same cell fractions from the lower hind leg muscles (Fig. 3B) gave markedly different results. GFP+ CD34+ cells, representing only 0.25% of the cells, gave rise to 33 clones (out of 96 single cells), all of which were myogenic. The GFP– CD34+ cells, which now represented 52% of the population, gave rise only to myogenic clones, with a cloning efficiency of 39% (76 out of 192 single cells). These results confirm that adult muscle progenitor cells belong to the (Pax3)GFP+ CD34+ cell fraction in the diaphragm, whereas, in lower hind leg muscles, they are in the (Pax3)GFP– CD34+ fraction. Both cell fractions express Pax7 (fig. S4). Thus, the parameters of size and granularity defined for (Pax3)GFP+ cells permit an equally efficient isolation of muscle satellite cells by sorting on the basis of CD34 expression. Skeletal muscle repair assays confirm and extend these observations. Grafting of GFP+ CD34+ cells from the diaphragm of adult mice or GFP– CD34+ cells from lower hind leg muscles of the same mice into TA muscles of *mdx nu/nu* recipients produced comparable restoration of dystrophin expression (Fig. 3, C and D). Thus both preparations participate similarly in muscle fiber repair.

Flow cytometric analysis and characterization of (Pax3)GFP+ cells present in skeletal muscles of adult *Pax3*$^{GFP/+}$ mice have permitted us to define parameters for isolating adult muscle progenitor cells. These cells comprise a population of small, nongranular, CD34+ CD45– Sca1– cells expressing Pax7. In accordance with this, a CD34+ cell fraction from skeletal muscles has been shown to be enriched in myogenic cells (*20*). In a recent study (*21*), adult muscle-associated progenitor cells were also shown to belong to a fraction of CD45– Sca1– CD34+ cells. We have shown recently that the progenitor cells of skeletal muscle during late embryonic and fetal development depend on both Pax3 and Pax7 (*14*). In the adult, not all muscle satellite cells express both genes. As shown here, although those in the diaphragm are Pax3+ Pax7+, satellite cells in lower hindlimb muscles express only Pax7. This distinction is maintained in regenerating muscles as seen in the TA after injury, where satellite cells remain (Pax3)GFP-negative. This is in contrast to a previous report on cells cultured from injured muscle (*22*). When we extended this flow cytometric analysis to a much larger gating window, we still did not detect any (Pax3)GFP+ cells after TA muscle injury (*23*). In muscles such as the diaphragm, Pax3 expression is cell-autonomous because (Pax3)GFP+ cells engrafted into the Pax3-negative TA muscle retain their initial phenotype. The myogenic potential of Pax3-expressing or -nonexpressing satellite cells is indistinguishable in both in vitro and in vivo assays. Distinguishing the potential role of Pax3 in subpopulations of adult muscle satellite cells awaits a conditional mutant, because embryos do not survive in the absence of Pax3.

Assays for muscle repair that have been developed to date are based on the injection of 5×10^5 to 10^6 cells into the muscles of *mdx* mice. Most have been performed with cells either directly obtained by enzymatic dissociation of muscles (*5*, *6*) or after a phase of selection and amplification in culture (*2*, *3*). When 5×10^5 cells from freshly disaggregated

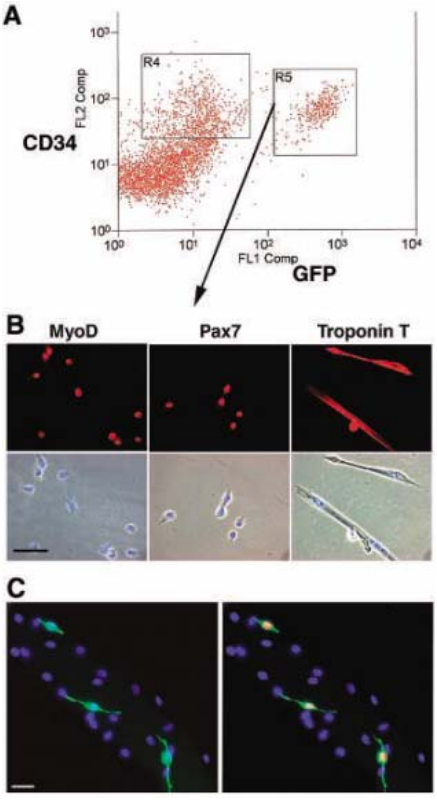

Fig. 2. Recovery of (Pax3)GFP+ cells from grafted TA muscles. (**A**) Three weeks after grafting, TA muscles were enzymatically dissociated and (Pax3)GFP+ CD34+ cells were isolated by flow cytometry. (**B**) Immediately after sorting, cells were plated and their myogenic identity determined by immunodetection of MyoD, Pax7, and Troponin T, after 3, 3, and 5 days of culture, respectively (top panels). Bottom panels show DAPI nuclear stain and phase contrast. Scale bar, 20 μm. (**C**) Detection of (Pax3)GFP+ satellite cells on single fibers of grafted TA muscles. Left: Immunodetection of GFP with DAPI staining. Right: Co-immunodetection of Pax7 and GFP with DAPI staining on the same section. Scale bar, 15 μm. GFP marks both the cytoplasm and the nucleus of satellite cells, whereas Pax7 marks only the nucleus.

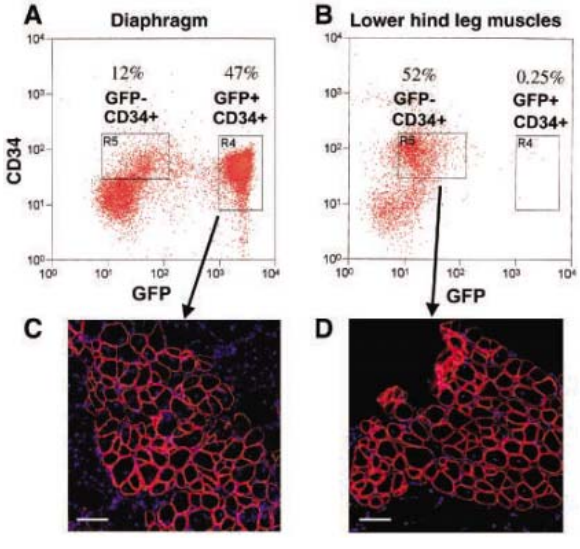

Fig. 3. Isolation of muscle satellite cells in the absence of (Pax3)GFP expression. Flow cytometric analysis of cells from the diaphragm and lower hind leg muscles of adult *Pax3*$^{GFP/+}$ mice. (**A** and **B**) Cells from the diaphragm and from lower hind leg muscles were analyzed for both GFP and CD34 expression as indicated in each panel. The percentages shown correspond to the fraction of positive cells within a FSC/SSC gate as shown in Fig. 1C. (**C** and **D**) Immunodetection of dystrophin in TA muscles of *mdx nu/nu* mice 3 weeks after grafting of 2×10^4 cells from the fractions indicated by the arrows. Scale bar, 50 μm.

muscle were implanted into the TA of irradiated *mdx nu/nu* mice, they formed a mean of 328 dystrophin-positive fibers (*5*). Similar results were obtained after injecting one to two million muscle-derived cultured cells into limb muscle (*2*, *3*). Our results now show that purified satellite cells are much more efficient than these crude or cultured cell populations in contributing to muscle repair.

The culture of muscle progenitor cells before grafting markedly reduces their regenerative efficiency such that the culture expansion itself is an "empty" process, yielding the same amount of muscle as the number of cells from which the culture was initiated. Culture-induced modifications may affect survival or engraftment capacity of the cells (*24*, *25*). However, we did not detect a difference in survival between cultured and freshly isolated cells 1 day after grafting (*23*). The activated state of the grafted cells may diminish their regenerative potential, because freshly isolated progenitor cells are not activated at the time of grafting, unlike their cultured progeny that express MyoD. Clonal assays suggest that the lower regenerative capacity of cultured cells reflects their more rapid differentiation. A similar situation is encountered with hematopoietic stem cells, which begin to differentiate and to lose their tissue reconstitution capacity when cultured (*26*).

Not only do purified muscle satellite cells contribute to muscle repair when engrafted into regenerating *mdx* muscles but some also persist as progenitor cells, adopting a satellite cell position and expressing Pax7. These results, therefore, point to muscle satellite cell self-renewal. The fact that (Pax3)GFP+ cells can be recovered from the muscles into which they were originally transplanted and shown to differentiate into muscle cells in culture also argues in favor of self-renewal. We therefore conclude that the satellite cell selection procedure described here results in cells that can both repair and contribute to the progenitor cell population of damaged muscles. There may be other stem cell types that can be mobilized to contribute to this process (*27*), but the muscle satellite cell population isolated by the flow cytometry parameters that we have defined is clearly a major contributor to muscle regeneration and a potential therapeutic agent.

References and Notes

1. S. B. Charge, M. A. Rudnicki, *Physiol. Rev.* **84**, 209 (2004).
2. Z. Qu-Petersen *et al.*, *J. Cell Biol.* **157**, 851 (2002).
3. G. M. Mueller, T. O'Day, J. F. Watchko, M. Ontell, *Hum. Gene Ther.* **13**, 1081 (2002).
4. D. Skuk, M. Goulet, B. Roy, J. P. Tremblay, *Exp. Neurol.* **175**, 112 (2002).
5. J. E. Morgan, C. N. Pagel, T. Sherratt, T. A. Partridge, *J. Neurol. Sci.* **115**, 191 (1993).
6. J. E. Morgan, R. M. Fletcher, T. A. Partridge, *Muscle Nerve* **19**, 132 (1996).
7. A. Irintchev, M. Zeschnigk, A. Starzinski-Powitz, A. Wernig, *Dev. Dyn.* **199**, 326 (1994).
8. A. Hollnagel, C. Grund, W. W. Franke, H. H. Arnold, *Mol. Cell. Biol.* **22**, 4760 (2002).
9. D. D. Cornelison, M. S. Filla, H. M. Stanley, A. C. Rapraeger, B. B. Olwin, *Dev. Biol.* **239**, 79 (2001).
10. J. R. Beauchamp *et al.*, *J. Cell Biol.* **151**, 1221 (2000).
11. P. Seale *et al.*, *Cell* **102**, 777 (2000).
12. M. Buckingham *et al.*, *J. Anat.* **202**, 59 (2003).
13. F. Relaix, D. Montarras, M. Buckingham, unpublished data.
14. F. Relaix, D. Rocancourt, A. Mansouri, M. Buckingham, *Nature* **435**, 948 (2005).
15. P. S. Zammit *et al.*, *J. Cell Biol.* **166**, 347 (2004).
16. Z. Yablonka-Reuveni, A. J. Rivera, *Dev. Biol.* **164**, 588 (1994).
17. D. D. Cornelison, B. J. Wold, *Dev. Biol.* **191**, 270 (1997).
18. J. C. van Deutekom, G. J. van Ommen, *Nat. Rev. Genet.* **4**, 774 (2003).
19. E. P. Hoffman, J. E. Morgan, S. C. Watkins, T. A. Partridge, *J. Neurol. Sci.* **99**, 9 (1990).
20. R. J. Jankowski, B. M. Deasy, B. Cao, C. Gates, J. Huard, *J. Cell Sci.* **115**, 4361 (2002).
21. R. I. Sherwood *et al.*, *Cell* **119**, 543 (2004).
22. I. M. Conboy, T. A. Rando, *Dev. Cell* **3**, 397 (2002).
23. D. Montarras *et al.*, unpublished data.
24. J. X. DiMario, F. E. Stockdale, *Exp. Cell Res.* **216**, 431 (1995).
25. J. R. Beauchamp, J. E. Morgan, C. N. Pagel, T. A. Partridge, *J. Cell Biol.* **144**, 1113 (1999).
26. J. Antonchuk, G. Sauvageau, R. K. Humphries, *Cell* **109**, 39 (2002).
27. T. Partridge, *Cell* **119**, 447 (2004).

28. We thank D. Rocancourt and C. Cimper for technical assistance. Supported by the Pasteur Institute and the CNRS, with additional grants from the Association Française contre les Myopathies, "the Cellules Souches" Grand Programme Horizontal of the Pasteur Institute, and the EuroStemCell Integrated Project of the European Union 6th Framework Programme. J.M., C.C., and T.P. received support from the Medical Research Council of the UK, the Muscular Dystrophy Campaign, and the Engineering and Physical Sciences Research Council. T.P. occupies a Blaise Pascal chair awarded by the Ecole Normale Supérieure. D.M. dedicates this paper to R. B. Seaver.

Supporting Online Material

www.sciencemag.org/cgi/content/full/1114758/DC1
Materials and Methods
Figs. S1 to S4
Table S1
References and Notes

12 May 2005; accepted 9 August 2005
Published online 1 September 2005;
10.1126/science.1114758
Include this information when citing this paper.

Regulation of Mammalian Tooth Cusp Patterning by Ectodin

Yoshiaki Kassai,[1]* Pauliina Munne,[2]* Yuhei Hotta,[1] Enni Penttilä,[2] Kathryn Kavanagh,[2] Norihiko Ohbayashi,[3] Shinji Takada,[3] Irma Thesleff,[2] Jukka Jernvall,[2,4]† Nobuyuki Itoh[1]†

Mammalian tooth crowns have precise functional requirements but cannot be substantially remodeled after eruption. In developing teeth, epithelial signaling centers, the enamel knots, form at future cusp positions and are the first signs of cusp patterns that distinguish species. We report that *ectodin*, a secreted bone morphogenetic protein (BMP) inhibitor, is expressed as a "negative" image of mouse enamel knots. Furthermore, we show that *ectodin*-deficient mice have enlarged enamel knots, highly altered cusp patterns, and extra teeth. Unlike in normal teeth, excess BMP accelerates patterning in *ectodin*-deficient teeth. We propose that *ectodin* is critical for robust spatial delineation of enamel knots and cusps.

Because cell differentiation and final pattern are directly linked in developing mammalian dentition, it is well suited for dissecting the molecular basis for induction and inhibition. The patterning of teeth involves iterative activation of the nonproliferative epithelial enamel knots at the places of future cusps (*1*, *2*). The surrounding epithelium and the underlying mesenchyme continue to proliferate, which results in folding of the epithelium to produce cusps (*1*, *3*). Spatial arrangements of cusps are typically species-specific and linked to evolution of diverse diets. Because erupted tooth crowns are fully mineralized, events during embryological patterning are critical for correct functional relations between occluding teeth. Consequently, classic studies have shown detailed coordination of development between occluding cusps (*4*), and that developing teeth are capable of self-regulation after external perturbations (*3*, *5*–*7*). This combination of precision and robustness of tooth development presumably extends to the placement of the secondary enamel knots as they are the earliest developmental signs of species-specific cusp patterns (*8*). Mathematical modeling has shown that, like feather patterning, an activator-inhibitor loop of signaling molecules could explain how the enamel knots determine

[1]Department of Genetic Biochemistry, Kyoto University Graduate School of Pharmaceutical Sciences, Kyoto 606-8501, Japan. [2]Developmental Biology Program, Institute of Biotechnology, Viikki Biocenter, Post Office Box 56, University of Helsinki, FIN-00014 Helsinki, Finland. [3]Okazaki Institute for Integrative Biosciences, National Institutes of Natural Sciences, Okazaki 444-8787, Japan. [4]Department of Ecology and Evolution, Stony Brook University, Stony Brook, NY 11794, USA.

*These authors contributed equally to this work
†To whom correspondence should be addressed. E-mail: itohnobu@pharm.kyoto-u.ac.jp (N.I.), jernvall@fastmail.fm (J.J.)

the morphological diversity seen in natural teeth (*9*). However, although not experimentally identified, this model suggested the existence of signaling molecules that inhibit the induction of the enamel knots.

Here we examined the functional role of *ectodin* (ectodermal inhibitor of BMP; GenBank accession number AB059271) in the regulation of mouse enamel knot formation following two lines of inquiry. First, we recently identified *ectodin* [the *Xenopus* ortholog is called *Wise* (*10*)] as a previously unknown protein (*11*) belonging to the Dan/Cerberus family of secreted BMP antagonists (*11–14*). We were interested in the inhibition of BMP signaling during tooth cusp patterning because the earliest differentiation marker of enamel knot cells, a cyclin-dependent kinase inhibitor *p21*, is induced by BMPs (*15*). The second reason for our interest in *ectodin* was that it seemed to be expressed around the primary enamel knot, forming at the onset of tooth crown formation, rather than in it (*11*). This kind of expression pattern, if it was to be repeated around the secondary enamel knots, would be the first of its kind (*16*).

Because histological sections of developing lower molars show complex expression patterns of *ectodin* (Fig. 1A), we analyzed gene expression in three dimensions. The results show that although *ectodin* is expressed in most parts of the forming first molar, the expression is absent in two distinct locations (Fig. 1B). The anterior (the trigonid) and posterior (the talonid) *ectodin*-negative regions contain secondary enamel knots, visible as the epithelial areas expressing *p21* (Fig. 1B). In mouse molar, the buccal and lingual cusps are joined by a transverse crest, and the areas forming these crests also express *p21* but not *ectodin* (Fig. 1B). In contrast, the area forming a valley separating the anterior and posterior cusp pairs expresses *ectodin* (Fig. 1B), suggesting inverse roles for *ectodin* and *p21* in cusp patterning. More distally, an *ectodin* expression domain separates the developing first and second molars, the latter being at the primary enamel knot stage of development (Fig. 1B). As in the first molar (*11*), the primary enamel knot in the second molar has no *ectodin* expression (Fig. 1, A and B).

The inverse expression patterns of *ectodin* and *p21* (Fig. 1B) are intriguing because both are induced by BMPs (*11*, *15*). BMPs are expressed in teeth throughout development (*17*), and mice lacking either type 1a BMP receptor in the epithelium (*18*) or, as a result of *Msx1*-null mutation, *Bmp4* expression in mesenchyme (*19*), have their tooth development arrested before primary enamel knot induction. Thus, although these mutants are indicative of the requirement of BMPs for tooth development, they leave the issue of cusp patterning unresolved. Furthermore, mice lacking functional *p21* have no reported tooth phenotypes (*20*), presumably as a result of redundancy with other cyclin-dependent kinase inhibitors. Ectodin, as an antagonist binding to BMPs (*11*), could be a feedback inhibitor of cusp development by interfering with the induction of *p21*. We first confirmed this by introducing ectodin-soaked beads together with BMP4-soaked beads on dental epithelium (*21*). Whereas BMP4 was sufficient to induce *ectodin* and *p21* in isolated dental epithelium, ectodin inhibited BMP4-induced *p21* expression (fig. S1).

We next investigated regulation of enamel knots by generating *ectodin*-deficient mice (*21*) (fig. S2). Although the overall development of teeth appears fairly normal in *ectodin*-deficient mice, tooth morphologies are highly altered. Changes in cusp patterns become visible as soon as *p21* is up-regulated in the developing secondary knots. The results show enlarged expression domains of *p21* with diminished intercuspal regions in the anterior portion of the first molar (Fig. 1C). Analyses of other enamel knot marker genes confirm that the induction of the enamel knot fate took place at the expense of intercuspal tissue (fig. S3). The distal *p21* expression domain of the first molar extends without interruption to the area normally giving rise to the second molar with no clear morphological separation between these teeth (Fig. 1, B and C). Accordingly, in erupted tooth rows of *ectodin*-deficient mice, the first and the second molars were often fused (21/52 = 40%).

An extra molar forms anterior to the first molar in the *ectodin*-deficient mice (Figs. 1C and 2). This tooth appears to develop slightly faster than the more posterior teeth and, at day 16, the whole crown expresses *p21* (Fig. 1C). To explore its developmental origin, we examined earlier stages using sonic hedgehog (*Shh*) expression as a marker for dental placodes. The results indicate that the extra tooth develops from a separate placode anterior to the first molar (Fig. 2A). Compared to the

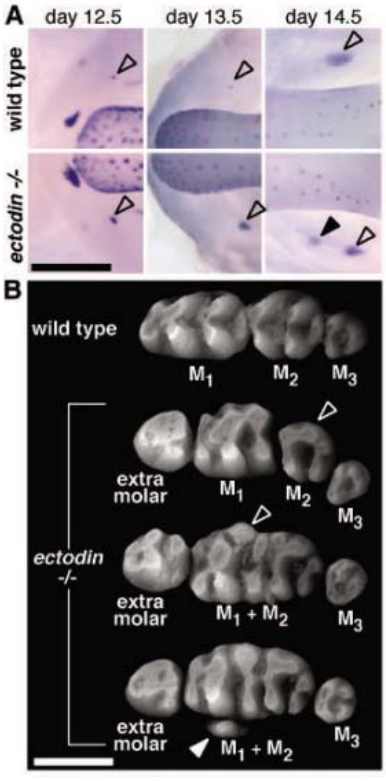

Fig. 2. *Ectodin*-deficient mice have extra teeth, fused molars, and highly altered cusp patterns. (**A**) The molar placodes indicated by *Shh* expression (open arrowhead) were larger in *ectodin*-null mutants than those in wild-type littermates, and at embryonic day 14.5, extra placodes (black arrowhead) appear anteriorly to the forming molars. (**B**) Three-dimensional laser confocal scans revealed that erupted tooth crowns of *ectodin*-deficient mice are broader than wild-type molars, have well-developed transverse crests, and have fused buccal cusps forming an ectoloph (open arrowhead). Extra cusps fused with the ectoloph, a lingual peg-shaped extra tooth (white arrowhead), and fused first and second molars are also observed. Anterior side is toward the left and buccal side is toward the top (B); M_1, first lower molar; M_2, second lower molar; M_3, third lower molar; $M_1 + M_2$, fused molars. Scale bars, 1 mm.

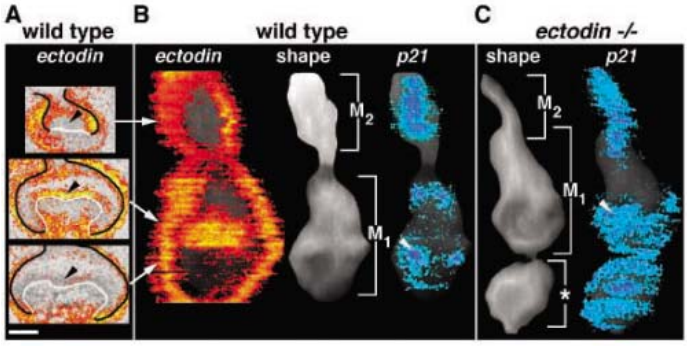

Fig. 1. *Ectodin* is expressed around the enamel knots and *ectodin* deficiency causes expansion of *p21* expression domains. (**A**) Frontal sections of embryonic day 16 mouse lower molars show complex patterns of *ectodin* expression in the forming tooth crown (black arrowheads). (**B**) Three-dimensional reconstructions show that ectodin is expressed around the enamel knots that express *p21* [occlusal views of the inner enamel epithelium marked with a white line in (A)]. (**C**) *Ectodin*-deficient mice show enlarged *p21* expression domains with decreased separation between forming cusps and molars. White arrowhead in (B) and (C) mark the secondary enamel knot forming the protoconid cusp, and asterisk in (C) marks an extra molar anterior to the first molar. Anterior side is toward the bottom (B and C) and buccal side is toward the left; M_1, first lower molar; M_2, second lower molar. Scale bar, 100 μm.

second molar, which develops as an early posterior extension of the first molar, the separate origin of the extra tooth conforms to the lack of fusion with the first molar. Similarities in placodes expressing *Shh* also suggest that the extra molar in *ectodin*-deficient mice is the same as that in mice that overexpress *ectodysplasin* (*22*). It remains to be shown whether ectodin and ectodysplasin function in the same or in parallel pathways regulating placode development.

To study cusp patterns of the *ectodin*-deficient mice, we used high-resolution three-dimensional laser-confocal imaging (*22*). Although most aspects of tooth crowns are affected (Fig. 2B), the most pronounced change was in the buccal side of the crowns. Indicating decreased down-growth of valleys separating cusps, the buccal side had better developed connections or completely fused cusps anterior-posteriorly, forming a longitudinal crest with fused extra cusps (Fig. 2B). This phenotype is reminiscent of the ectoloph, a feature present in, for example, the upper molars of black rhinoceros (resemblance of "*ectodin*" to this classic morphological term is coincidental). This buccal bias is noteworthy because *Bmp4* (*17*), *ectodin*, and *p21* (Fig. 1) are all expressed strongly in the buccal side, and our results may suggest a role for regulation of ectodin in the evolution of lateral bias in teeth. Despite the extensively derived morphology, the *ectodin*-deficient teeth are functional and individual mice do not seem to have occlusal problems with their molar teeth.

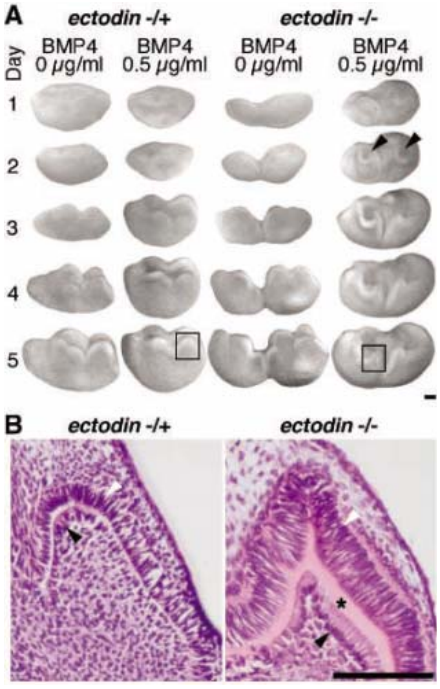

Fig. 3. Ectodin deficiency increases the sensitivity of developing teeth to excess BMP. Cap stage (day 14) teeth of *ectodin* heterozygous and null mutant embryos were cultured with BMP4 in the culture medium for the first 2 days. (**A**) (Left) BMP4 has little effect on tooth development of ectodin heterozygotes, and cusps appear normally during the third day of culture. (Right) In the *ectodin*-null mutants, which develop both the extra and the first molar, cusps are visible by the second day of culture with BMP4 (black arrowheads). The resulting crowns have sharp cusps, and all crowns were covered by dentine after 5 days of culture. (**B**) Histological sections of the regions in the black rectangles in (A) show that ectodin-null mutants cultured with BMP4 have fully polarized ameloblasts (white arrowhead) and odontoblasts (black arrowhead) that have already secreted a layer of dentine (asterisk). In heterozygote teeth cultured with BMP4, ameloblasts and odontoblasts are only starting to elongate. Some teeth cultured without BMP4 have begun to secrete dentine on cusp tips (not shown). All teeth (n = 28) were from the same homozygous-heterozygous crossing. Anterior side is toward the left (A). Scale bars, 100 μm.

Although the phenotype and enlarged enamel knots of the *ectodin*-deficient teeth are strongly suggestive about the role of ectodin in inhibiting enamel knot induction, these results do not directly implicate inhibition of BMP signaling. Next, to test the association of ectodin with BMP signaling in tooth crown development, we exposed *ectodin*-deficient teeth to BMP in culture.

We cultured isolated molars of both *ectodin* null-mutants and heterozygotes, which have wild-type dentition, with BMP4 in the culture medium for the first 2 days (*21*). The results show that in the absence of BMP4, the rates of tooth development of both null mutants and heterozygotes are similar (Fig. 3A). Whereas *ectodin* heterozygous teeth are not particularly sensitive to excess BMP4, the null-mutants show a markedly accelerated crown development, exceeding the rate of normal development in vivo by about 3 days (Fig. 3A). Already after 1 day in culture the null-mutant teeth show cusps and thickening of inner enamel epithelium (Fig. 3A). After 5 days of culture, ameloblasts and odontoblasts are fully differentiated in the null-mutants and the crowns are covered by dentine (Fig. 3B). Compared to both feather and limb patterning, which can be manipulated by BMPs (*23*–*26*), our present results, together with our earlier observations (*27*, *28*), suggest that normal tooth patterning is relatively robust against excess BMP.

Taken together, our results indicate that although the morphology of the *ectodin*-deficient teeth results from shifting the balance of induction toward larger enamel knots (Figs. 1 and 2), the systemic effect of lack of ectodin is the loss of self-regulation (Fig. 3). Thus, excess BMP administered to developing *ectodin*-deficient teeth caused relatively unchecked induction. In contrast, in normal teeth the cusp induction and inhibition cascades cancel each other out under excess BMP. Uniquely in mammals, once erupted, permanent dentition must last the whole lifetime of the animal. This alone suggests that there has been strong selective pressure to make tooth development as "fail-proof" as possible, and we propose that robustness of tooth development to external perturbations requires ectodin to integrate cusp induction and inhibition.

Although *ectodin*-deficient mice have the most extensively modified cusp patterns of mouse mutants studied to date, mice with superfluous production of *ectodysplasin* have some similarities with *ectodin*-deficient mice. Both have extra teeth and longitudinal crests connecting cusps. However, the *ectodin*-deficient mice have buccal crests (Fig. 2B), whereas mice overexpressing *ectodysplasin* have central crests (*22*). This single difference in morphology is enough to alter the mutant phenotypes to resemble rhinoceros and kangaroo teeth, respectively. These morphological alterations, although functional, are obviously larger than evolutionary transitions documented in the fossil record. Hence, it remains to be determined whether fine tuning of enamel knot formation could be sufficient, perhaps by allelic changes as shown for *ectodysplasin* in altering armor plates of sticklebacks (*29*), to account for the evolutionary diversity of teeth.

References and Notes

1. J. Jernvall, P. Kettunen, I. Karavanova, L. B. Martin, I. Thesleff, *Int. J. Dev. Biol.* **38**, 463 (1994).
2. J. Jernvall, I. Thesleff, *Mech. Dev.* **92**, 19 (2000).
3. P. M. Butler, *Biol. Rev.* **31**, 30 (1956).
4. P. M. Marshall, P. M. Butler, *Arch. Oral Biol.* **11**, 949 (1966).
5. S. Glasstone, *Proc. R. Soc. Lond. B. Biol. Sci.* **126**, 315 (1939).
6. S. Glasstone, *J. Dent. Res.* **42**, 1364 (1963).
7. A. R. Fisher, *Arch. Oral Biol.* **16**, 1481 (1971).
8. J. Jernvall, S. V. E. Keränen, I. Thesleff, *Proc. Natl. Acad. Sci. U.S.A.* **97**, 14444 (2000).
9. I. Salazar-Ciudad, J. Jernvall, *Proc. Natl. Acad. Sci. U.S.A.* **99**, 8116 (2002).
10. N. Itasaki *et al.*, *Development* **130**, 4295 (2003).
11. J. Laurikkala, Y. Kassai, L. Pakkasjarvi, I. Thesleff, N. Itoh, *Dev. Biol.* **264**, 91 (2003).
12. W. Balemans, W. Van Hul, *Dev. Biol.* **250**, 231 (2002).
13. N. Kusu *et al.*, *J. Biol. Chem.* **278**, 4113 (2003).
14. O. Avsian-Kretchmer, A. J. Hsueh, *Mol. Endocrinol.* **18**, 1 (2004).
15. J. Jernvall, T. Åberg, P. Kettunen, S. Keränen, I. Thesleff, *Development* **125**, 161 (1998).
16. http://bite-it.helsinki.fi/
17. T. Åberg, J. Wozney, I. Thesleff, *Dev. Dyn.* **210**, 383 (1997).
18. T. Andl *et al.*, *Development* **131**, 2257 (2004).
19. Y. Chen, M. Bei, I. Woo, I. Satokata, I. R. Maas, *Development* **122**, 3035 (1996).
20. C. Deng, P. Zhang, J. W. Harper, S. J. Elledge, P. J. Leder, *Cell* **82**, 675 (1995).
21. Materials and methods are available as supporting material on *Science* Online.
22. A. T. Kangas, A. R. Evans, I. Thesleff, J. Jernvall, *Nature* **432**, 211 (2004).
23. H.-S. Jung *et al.*, *Dev. Biol.* **196**, 11 (1998).
24. S. Noramly, B. A. Morgan, *Development* **125**, 3775 (1998).
25. R. Merino *et al.*, *Development* **126**, 5515 (1999).
26. J. Selever, W. Liu, M. F. Lu, R. R. Behringer, J. F. Martin, *Dev. Biol.* **276**, 268 (2004).
27. J. Jernvall, H.-S. Jung, *Yearb. Phys. Anthropol.* **43**, 171 (2000).
28. Y. Kassai *et al.*, data not shown.
29. P. F. Colosimo *et al.*, *Science* **307**, 1928 (2005).

30. This work was supported by a Grant-in-Aid for

Creative Scientific Research (N.I.) and the 21st Century Centers of Excellence Program (Y.K.) from the Ministry of Education, Culture, Sports, Science and Technology of Japan; a grant from the Mitsubishi Foundation, Japan (N.I.); the Finnish Academy (J.J., I.T.); and the Sigrid Juselius Foundation (I.T.). We thank A. Evans, H. Kettunen, M. Mäkinen, I. Salazar-Ciudad, R. Santalahti, and P. C. Wright for comments or technical help.

Supporting Online Material
www.sciencemag.org/cgi/content/full/309/5743/2067/DC1
Materials and Methods
Figs. S1 to S3

1 July 2005; accepted 23 August 2005
10.1126/science.1116848

Genetic Engineering of Terpenoid Metabolism Attracts Bodyguards to *Arabidopsis*

Iris F. Kappers,[1,2]* Asaph Aharoni,[2,3]* Teun W. J. M. van Herpen,[2] Ludo L. P. Luckerhoff,[1,2] Marcel Dicke,[1] Harro J. Bouwmeester[2]†

Herbivore-damaged plants release complex mixtures of volatiles that attract natural enemies of the herbivore. To study the relevance of individual components of these mixtures for predator attraction, we manipulated herbivory-induced volatiles through genetic engineering. Metabolic engineering of terpenoids, which dominate the composition of many induced plant volatile bouquets, holds particular promise. By switching the subcellular localization of the introduced sesquiterpene synthase to the mitochondria, we obtained transgenic *Arabidopsis thaliana* plants emitting two new isoprenoids. These altered plants attracted carnivorous predatory mites (*Phytoseiulus persimilis*) that aid the plants' defense mechanisms.

The integration of ecology and molecular biology has yielded important progress in understanding complex interactions between organisms and the underlying mechanisms (*1*). In recent years, *Arabidopsis thaliana* L. was shown to be an excellent model plant for investigating ecological interactions such as induced indirect defense. In these tritrophic interactions, plants defend themselves against feeding by herbivorous arthropods by producing volatiles that attract the natural enemies of the herbivores (*2*–*4*). The activities of these natural enemies benefit the plant's fitness, and this defense therefore is evolutionarily advantageous (*5*–*7*). Hence, the term "bodyguard" has been used to describe the function of carnivorous arthropods such as predatory mites (*5*). For example, feeding by caterpillars of the crucifer pest *Pieris rapae* resulted in the emission of volatiles that attracted the parasitoid wasp *Cotesia rubecula* (*8*, *9*). The parasitization of *P. rapae* caterpillars by *C. rubecula* resulted in an increase in plant fitness in terms of seed production and thus benefited the plant (*7*). The individual components of herbivore-induced volatile blends originate from various chemical classes, but isoprenoids dominate the composition of many of these blends (*10*–*13*) and are known to attract carnivorous arthropods (*2*–*14*). One of the herbivore-induced volatiles in *Arabidopsis* is the C16-homoterpene 4,8,12-trimethyl-1,3(*E*),7(*E*),11-tridecatetraene [(*E*,*E*)-TMTT)] (*8*). A related compound, the C11-homoterpene 4,8-dimethyl-1,3(*E*),7-nonatriene [(*E*)-DMNT], has been detected in the headspace of many plant species after herbivory (*12*, *14*, *15*), but not in the (induced or noninduced) volatile mixture of *Arabidopsis* (*8*, *16*).

Our first step in studying the ecological relevance of individual compounds of the complex herbivory-induced volatile mixture was to generate transgenic plants that constitutively emit these chemicals. We chose to engineer the sesquiterpene (3*S*)-(*E*)-nerolidol, a component of the herbivore-induced volatile blend of, for example, maize (*17*) and tomato (*18*) and the first dedicated intermediate en route to (*E*)-DMNT (*15*, *17*) (Fig. 1A). Earlier attempts to produce substantial amounts of sesquiterpenes in transgenic plants failed, most probably because of a lack of sufficient precursors (*19*–*21*). In these experiments, sesquiterpene synthases were targeted either to the cytosol (*19*, *20*)—which is the expected location of farnesyl diphosphate (FPP), the precursor for sesquiterpenes—or to the plastids (*21*). Here, we targeted FaNES1, a strawberry linalool/nerolidol synthase, specifically to the mitochondria. We reasoned that because the mitochondria are the site of ubiquinone biosynthesis and *Arabidopsis* possesses an FPP synthase isoform with a mitochondrial targeting signal (*22*, *23*), FPP should be available in this cell compartment.

The CoxIV (cytochrome oxidase subunit IV) sequence, a bona fide mitochondrial targeting signal (*24*), was used to localize FaNES1 to the mitochondria (*25*). Transgenic *Arabidopsis* plants harboring the CoxIV-FaNES1 construct (Fig. 1B) were generated, and *FaNES1* expression was detected in leaves of primary transformants (Fig. 1C). In earlier work we showed that in protoplasts, CoxIV when fused to green fluorescent protein (GFP) efficiently targeted GFP to the mitochondria (*26*). The headspace of rosette leaves from 4-week-old plants was analyzed using solid-phase microextraction (SPME) as described (*21*), and 9 of

[1]Laboratory of Entomology, Wageningen University, Post Office Box 8031, 6700 EH Wageningen, Netherlands. [2]Plant Research International, Wageningen University and Research Centre, Post Office Box 16, 6700 AA Wageningen, Netherlands. [3]Weizmann Institute of Science, Post Office Box 26, Rehovot 76100, Israel.

*These authors contributed equally to this work.
†To whom correspondence should be addressed. E-mail: harro.bouwmeester@wur.nl

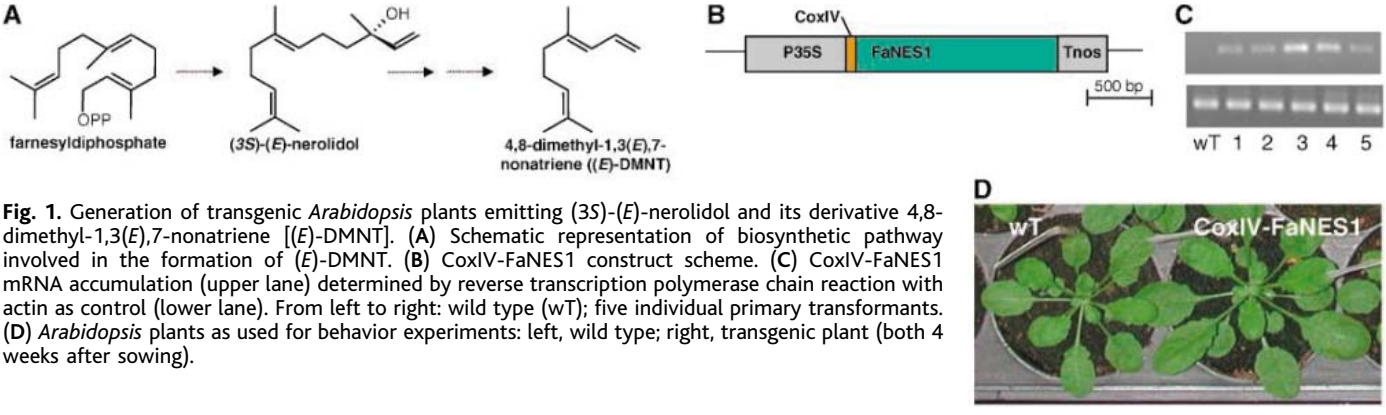

Fig. 1. Generation of transgenic *Arabidopsis* plants emitting (3*S*)-(*E*)-nerolidol and its derivative 4,8-dimethyl-1,3(*E*),7-nonatriene [(*E*)-DMNT]. (**A**) Schematic representation of biosynthetic pathway involved in the formation of (*E*)-DMNT. (**B**) CoxIV-FaNES1 construct scheme. (**C**) CoxIV-FaNES1 mRNA accumulation (upper lane) determined by reverse transcription polymerase chain reaction with actin as control (lower lane). From left to right: wild type (wT); five individual primary transformants. (**D**) *Arabidopsis* plants as used for behavior experiments: left, wild type; right, transgenic plant (both 4 weeks after sowing).

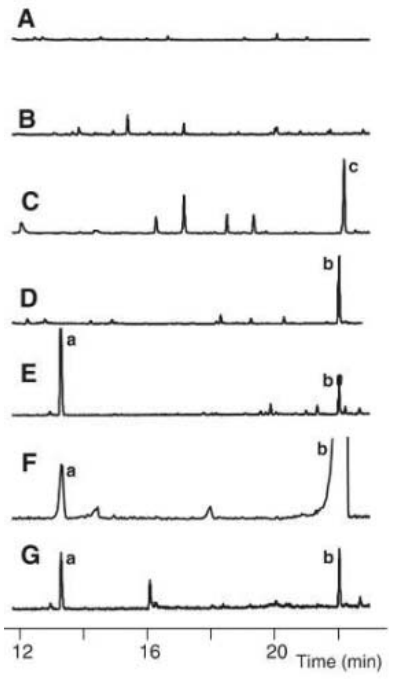

Fig. 2. Gas chromatography–mass spectrometry profile of volatiles emitted by *Arabidopsis* leaves. (**A**) Undamaged wild type; (**B**) wild type, infested by spider mites for 10 days; (**C**) wild type, infested by *P. rapae* for 24 hours; (**D**) undamaged CoxIV-FaNES1, plant 2.2; (**E**) undamaged CoxIV-FaNES1, plant 7.3; (**F**) wild type, detached leaves placed with petiole in (*E*)-nerolidol (10 μg/ml) for 4 hours before headspace sampling; (**G**) CoxIV-FaNES1, plant 2.2 sprayed with 5 μM jasmonic acid 24 hours before headspace sampling. Identified compounds: (a) (*E*)-DMNT; (b) (3*S*)-(*E*)-nerolidol; (c) (*E*)-TMTT. The *y* axis shows peak area of mass/charge ratio 69 + 93.

12 primary transformants emitted (3*S*)-(*E*)-nerolidol (Fig. 2, D and E, peak b). The levels of (3*S*)-(*E*)-nerolidol emitted were 20 to 30 times those from plants with plastid-targeted FaNES1 (*21*). (3*S*)-(*E*)-Nerolidol could not be detected in rosette leaves of wild-type plants (Fig. 2A). Because the heterologous protein was targeted to the mitochondria, these results demonstrate that the sesquiterpene precursor, FPP, is indeed available in this organelle. Interestingly, we also detected (*E*)-DMNT in the headspace of five of the nine (3*S*)-(*E*)-nerolidol–producing plants (Fig. 2E, peak a). (*E*)-DMNT has not been detected before in *Arabidopsis* foliage after herbivory (*8*) nor in the flower headspace (*16*). In our own headspace analyses of rosette leaves derived from wild-type *Arabidopsis* plants, we also did not detect (*E*)-DMNT (Fig. 2A).

Our results show that neither spider mites (*Tetranychus urticae*) nor caterpillars (*P. rapae*) induce (3*S*)-(*E*)-nerolidol or (*E*)-DMNT formation in wild-type *Arabidopsis* (Fig. 2, B and C), although both herbivores are known to induce (*E*)-DMNT in a number of other plant species (*2*, *12*, *14*, *15*). Boland and co-workers have shown that leaves and flowers of several plant species are capable of converting (3*S*)-(*E*)-nerolidol into (*E*)-DMNT constitutively (*27*), and others have shown that the rate-limiting step in the herbivory-induced release of (*E*)-DMNT is the formation of (3*S*)-(*E*)-nerolidol (*15*, *17*). Our results show that the specific introduction of a linalool/nerolidol synthase into the mitochondria of *Arabidopsis* results in the formation of substantial amounts of (3*S*)-(*E*)-nerolidol and that *Arabidopsis* apparently possesses the enzymes that convert (3*S*)-(*E*)-nerolidol into (*E*)-DMNT. This was further confirmed by feeding of (*E*)-nerolidol to leaves of wild-type *Arabidopsis* plants, which resulted in the formation of (*E*)-DMNT (Fig. 2F). We suggest that the enzymes responsible for the conversion of geranyl-linalool into (*E*,*E*)-TMTT (C20 → C16), which is emitted by *Arabidopsis* after herbivory (*8*), are also capable of the C15 → C11 conversion from (3*S*)-(*E*)-nerolidol into (*E*)-DMNT. Jasmonic acid is a known mediator of herbivory-induced signaling (*28*, *29*) and has also been shown to induce (*E*,*E*)-TMTT formation in *Arabidopsis* (*30*). When individual transgenic lines that only emitted (3*S*)-(*E*)-nerolidol were sprayed with jasmonic acid, (*E*)-DMNT was subsequently detected in the headspace (Fig. 2G). Therefore, it is likely that the enzymes en route to (*E*,*E*)-TMTT are upregulated by jasmonic acid, as was previously shown for (*E*)-DMNT formation in maize (*17*).

Both first- and second-generation transgenic plants displayed some growth retardation of the basal rosette (Fig. 1D), but their flowering stems appeared at approximately the same time as in nontransgenic control plants. Mitochondria use FPP for production of ubiquinone and heme A, but apparently the introduction of a sesquiterpene synthase into these organelles does not divert so much of the available FPP that this leads to growth inhibition. This is of importance when considering the impact of our metabolic engineering strategy on plant performance.

Transgenic plants emitting the two new signaling compounds were used to examine the effect on bodyguard attraction. Undamaged transgenic plants (4 weeks old) producing (*E*)-DMNT and (3*S*)-(*E*)-nerolidol in a ratio of

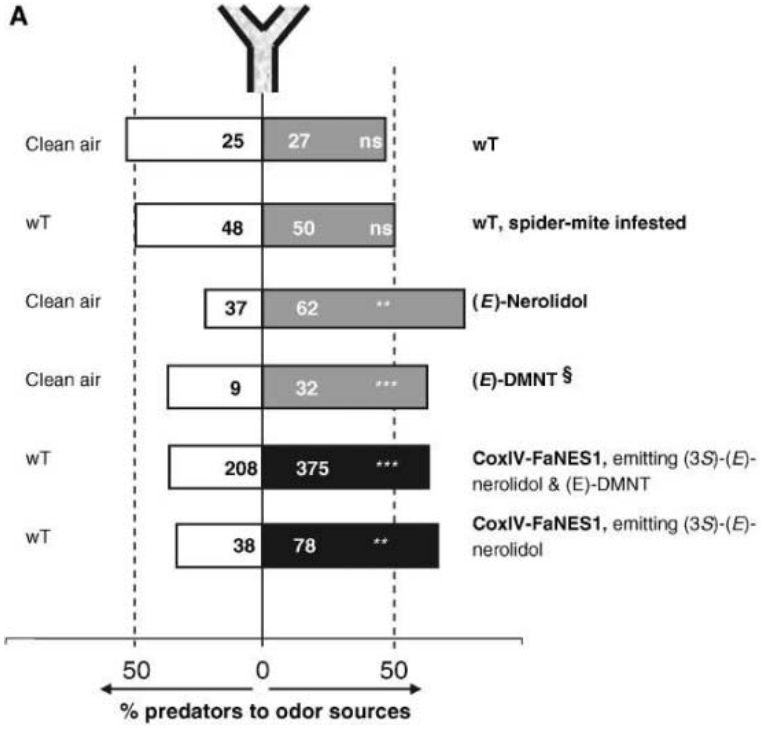

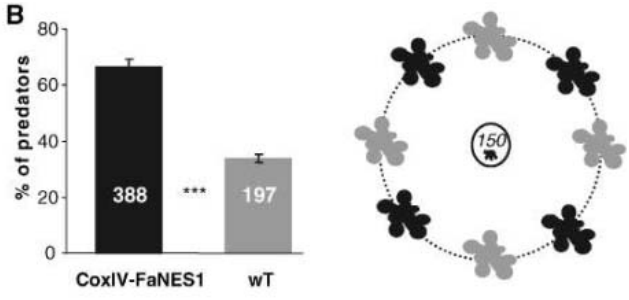

Fig. 3. Responses of *P. persimilis* predatory mites to volatiles released by *Arabidopsis*. (**A**) Response tested in a Y-tube olfactometer. (**B**) Response tested under semi-natural conditions (*22*). Bars represent the overall percentages of predatory mites choosing either of the odor sources; numbers in bars are the total numbers of predators choosing that odor source. Error bars represent SE (n = 10 independent tests). Choices between odor sources were analyzed with a two-sided binominal test on numbers (ns, $P > 0.05$; $^{**}P < 0.01$; $^{***}P < 0.001$). §Data from (*27*).

approximately 2:1 were tested in a closed-system Y-tube olfactometer (*25*) against undamaged wild-type *Arabidopsis* plants of the same age. The predatory mites (*Phytoseiulus persimilis*) highly significantly preferred the volatiles emitted by CoxIV-FaNES1 plants to those of wild-type plants (binomial test, $P < 0.001$; Fig. 3A). An infestation with spider mites (*T. urticae*) that did not result in emission of (3*S*)-(*E*)-nerolidol and (*E*)-DMNT did not make wild-type *Arabidopsis* attractive to predatory mites, the natural enemies of the spider mites (Fig. 3A).

Because CoxIV-FaNES1 plants emitted both (*E*)-DMNT and (3*S*)-(*E*)-nerolidol, we assessed which of the two volatiles attracts the predators. (*E*)-DMNT was previously shown to attract *P. persimilis* (*2*, *31*) (Fig. 3A). However, CoxIV-FaNES1 plants that only emitted (3*S*)-(*E*)-nerolidol and no (*E*)-DMNT were also attractive to *P. persimilis* (Fig. 3A). We then tested the attraction of *P. persimilis* to racemic (*E*)-nerolidol and found that the predators were significantly attracted. Although nerolidol is often reported as a component in the volatile blend induced by herbivory, to our knowledge, attraction of *P. persimilis* or any other carnivorous arthropod to (3*S*)-(*E*)-nerolidol has not been reported previously. Thus, the introduction of a mitochondrially targeted FaNES1 into *Arabidopsis* resulted in the emission of two terpenoids that both attract the predatory mite *P. persimilis*. These signaling molecules, (*E*)-DMNT and (3*S*)-(*E*)-nerolidol, are known to be induced by *P. persimilis*' prey in several plant species (*15*, *17*, *18*), but not in wild-type *Arabidopsis* (Fig. 2B).

Attraction of predators to CoxIV-FaNES1 plants was also tested, using plants in soil under more natural conditions, in an octagon setup (Fig. 3B). In this open setup, the odor spreads through diffusion rather than by directing the odor of enclosed plants through a closed container with an air stream. In 10 independent experiments, we found that the majority of the predatory mites made their first visit to the CoxIV-FaNES1 plants, which demonstrates a clear preference ($P < 0.001$) for the undamaged transgenic plants that emit (*E*)-DMNT and (3*S*)-(*E*)-nerolidol (Fig. 3B).

We have shown that genetic engineering of *Arabidopsis*, resulting in plants that emit one or two novel volatiles, provides a novel tool to investigate the role of signaling compounds in mediating tritrophic interactions. This is especially true for compounds that are not commercially available and not easy to synthesize in enantiomer-pure form, such as sesquiterpenoids [e.g., (3*S*)-(*E*)-nerolidol] and homoterpenes [e.g., (*E*)-DMNT]. The levels of the sesquiterpene alcohol (3*S*)-(*E*)-nerolidol as well as the homoterpene (*E*)-DMNT that were emitted by the transgenic plants are the highest reported so far, indicating that FPP is readily available in the mitochondria for metabolic engineering. Emission of these signaling chemicals from engineered plants demonstrated that these volatiles influence bodyguard behavior in vivo. Our results show that the transgenic approach holds considerable promise for improving crop protection through a transgenic approach (e.g., by exploiting herbivore-inducible promoters coupled to genes responsible for biosynthesis of signaling compounds), so that crop plants can be generated that more effectively recruit biological control agents after infestation with arthropod pests.

References and Notes

1. A. Kessler, R. Halitschke, I. T. Baldwin, *Science* **305**, 665 (2004).
2. M. Dicke *et al.*, *J. Chem. Ecol.* **16**, 381 (1990).
3. T. C. J. Turlings, J. H. Tumlinson, W. J. Lewis, *Science* **250**, 1251 (1990).
4. M. A. Birkett *et al.*, *Proc. Natl. Acad. Sci. U.S.A.* **97**, 9329 (2000).
5. M. Dicke, M. W. Sabelis, in *Causes and Consequences of Variation in Growth Rate and Productivity of Higher Plants*, H. Lambers, M. L. Cambridge, H. Konings, T. L. Pons, Eds. (SPB, the Hague, 1989), pp. 341–358.
6. M. E. Fritzsche-Hoballah, T. C. J. Turlings, *Evol. Ecol. Res.* **3**, 553 (2001).
7. J. J. A. Van Loon, J. G. De Boer, M. Dicke, *Entomol. Exp. Appl.* **97**, 219 (2000).
8. R. M. P. Van Poecke, M. A. Posthumus, M. Dicke, *J. Chem. Ecol.* **27**, 1911 (2001).
9. R. M. P. Van Poecke, M. Dicke, *J. Exp. Bot.* **53**, 1793 (2002).
10. P. W. Paré, J. H. Tumlinson, *Nature* **385**, 30 (1997).
11. N. Dudareva, E. Pichersky, J. Gershenzon, *Plant Physiol.* **135**, 1893 (2004).
12. W. Boland, Z. Feng, J. Donath, A. Gäbler, *Naturwissenschaften* **79**, 368 (1992).
13. G. Arimura, D. P. W. Huber, J. Bohlmann, *Plant J.* **37**, 603 (2004).
14. M. Dicke, *J. Plant Physiol.* **143**, 465 (1994).
15. H. J. Bouwmeester, F. W. A. Verstappen, M. A. Posthumus, M. Dicke, *Plant Physiol.* **121**, 173 (1999).
16. F. Chen *et al.*, *Plant Cell* **15**, 481 (2003).
17. J. Degenhardt, J. Gershenzon, *Planta* **210**, 815 (2000).
18. K. Ament, M. R. Kant, M. W. Sabelis, M. A. Haring, R. C. Schuurink, *Plant Physiol.* **135**, 2025 (2004).
19. T. M. Hohn, J. B. Ohlrogge, *Plant Physiol.* **97**, 460 (1991).
20. T. E. Wallaart, H. J. Bouwmeester, J. Hille, L. Poppinga, N. C. A. Maijers, *Planta* **212**, 460 (2001).
21. A. Aharoni *et al.*, *Plant Cell* **15**, 2866 (2003).
22. N. Cunillera *et al.*, *J. Biol. Chem.* **271**, 7774 (1996).
23. N. Cunillera, A. Boronat, A. Ferrer, *J. Biol. Chem.* **272**, 15381 (1997).
24. R. H. Kohler, W. R. Zipfel, W. W. Web, M. R. Hanson, *Plant J.* **11**, 613 (1997).
25. See supporting data on *Science* Online.
26. A. Aharoni *et al.*, *Plant Cell* **16**, 3110 (2004).
27. J. Donath, W. Boland, *J. Plant Physiol.* **143**, 473 (1994).
28. W. Boland, J. Hopke, J. Donath, J. Nueske, F. Bublitz, *Angew. Chem. Int. Ed. Engl.* **34**, 1600 (1995).
29. R. Karban, I. T. Baldwin, *Induced Responses to Herbivory* (Univ. of Chicago Press, Chicago, 1997).
30. R. M. P. Van Poecke, M. A. Posthumus, M. Dicke, unpublished data.
31. J. G. De Boer, M. A. Posthumus, M. Dicke, *J. Chem. Ecol.* **30**, 2215 (2004).

32. We thank I. Small for the Cox-GFP construct, W. Boland for the synthetic (*E*)-DMNT and (*E,E*)-TMTT, and R. Hall, J. van Loon, and R. Mumm for critically reading the manuscript. Supported by Netherlands Organization for Scientific Research (NWO) Technology Foundation grant WPB 5479 (I.F.K., L.L.P.L.) and VICI grant 865.03.002 (M.D.), by Centre for BioSystems Genomics (CBSG) part of Netherlands Genomics Initiative (NGI) project A-1 (A.A.), and by European Commission contract MC-RTN-CT-2003-504720 "ISONET" (M.D.).

Supporting Online Material

www.sciencemag.org/cgi/content/full/309/5743/2070/DC1
Materials and Methods
References

17 June 2005; accepted 23 August 2005
10.1126/science.1116232

Structural Phylogenetics and the Reconstruction of Ancient Language History

Michael Dunn,[1]* Angela Terrill,[1,2] Ger Reesink,[1,2] Robert A. Foley,[3] Stephen C. Levinson[1,2]

The contribution of language history to the study of the early dispersals of modern humans throughout the Old World has been limited by the shallow time depth (about 8000 ± 2000 years) of current linguistic methods. Here it is shown that the application of biological cladistic methods, not to vocabulary (as has been previously tried) but to language structure (sound systems and grammar), may extend the time depths at which language data can be used. The method was tested against well-understood families of Oceanic Austronesian languages, then applied to the Papuan languages of Island Melanesia, a group of hitherto unrelatable isolates. Papuan languages show an archipelago-based phylogenetic signal that is consistent with the current geographical distribution of languages. The most plausible hypothesis to explain this result is the divergence of the Papuan languages from a common ancestral stock, as part of late Pleistocene dispersals.

The linguistic comparative method used to construct language family trees relies on recognizing "cognate sets": words in different languages that are related in meaning and form because they can be shown to have the same ultimate source in an ancestor language. The

comparative method has helped define the major linguistic family groups that are recognized today. Unfortunately, because of the continual process of linguistic change, the method is limited to a time depth of approximately 8000 ± 2000 years (*1*). However, it is probable that a considerable portion of linguistic diversification occurred at earlier dates, associated with later Pleistocene human dispersals. Alternative attempts to reach further back and link the world's ~300 language families (*2*) into larger taxonomic units are controversial (*3*–*5*).

One example of this older diversification may be found in Island Melanesia. Radiocarbon dating for Island Melanesia has demonstrated Pleistocene occupation more than 35,000 years ago (*6*, *7*) (Fig. 1). Evidence suggests high levels of inter- and intrapopulational genetic variation (*8*, *9*), with no simple relationship with linguistic patterns. The languages spoken in the area are of two groups: (i) over 100 languages belonging to four groups of the well-established Austronesian family, which probably originated in the area close to Taiwan and spread to this region about 4000 years ago (*10*); and (ii) 23 "Papuan" languages, which are not known to have any phylogenetic relation to one another and are of much greater antiquity in the region.

The lexical evidence for relationships between Papuan languages is minimal. Apart from shared Austronesian loans, there are few plausible cognate candidates found in comparisons of pairs of words from Papuan vocabularies (Fig. 2) [see, however, (*11*)]. Assuming that the rate of vocabulary loss in the Papuan languages is similar to rates observed elsewhere, these languages are either unrelated or have been separated at least since the early Holocene or late Pleistocene. These languages do, however, show a high degree of structural similarity, distinguishing them as a group from their Austronesian neighbors, which has led scholars to propose genealogical (or near-genealogical) groupings (*12*, *13*). In the absence of identifiable lexical cognates, we have used computational cladistic analysis of these features of linguistic structure to test whether a phylogenetic signal can be identified beyond the resolution of lexical form-based methods [for other cladistic methods using lexicons, see (*14*–*21*)]. The structural features of a language, like the lexicon, are subject to processes of decay over time and can also be borrowed or exchanged across languages. However, such exchange usually only occurs under special conditions of prolonged and intensive contact, and it is at least plausible that where the lexical signal has been lost, a faint structural signal might still be discernible. Linguistic structure—that is, grammar rather than vocabulary—has previously been used in historical linguistics to show statistical evidence for ancient links between languages from different parts of the world (*1*, *2*, *22*, *23*) but not directly to reconstruct phylogenetic relationships.

A questionnaire-based database was constructed, in which linguistic structural features were coded for their presence or absence in each of the target languages. These characters were abstract (coded without respect to their formal expression) and were selected to provide broad typological coverage, reflecting the known linguistic variation of the region (*24*), as well as to be features that would typically be described in a published sketch grammar. Traits invariant in the region (either entirely absent, such as polysynthesis or proximate/obviative case distinctions; or present in all the languages, such as the existence of a word class of verbs) were not coded. Characters that show strong implicational correlations were excluded, although characters with weaker tendencies to covariance were not excluded where the current state of linguistic typological knowledge does not allow us to systematically distinguish functionally motivated covariance from phylogenetic or areal patterns. The completed data matrix contained 125 binary features coded for 15 Papuan and 16 Austronesian languages spoken in an overlapping region. The Papuan database was mostly compiled by linguists with field experience in the language and was supplemented from published and unpublished sources where available. The Austronesian database was constructed from published sources (*25*). All sets of data were checked by a second coder to ensure consistency.

The binary-coded linguistic features allowed us to treat these as character traits distributed among taxonomic units (languages) and thus to apply cladistic algorithms (maximum parsimony or NeighborNet) to determine potential phylogenetic relationships among them (*26*).

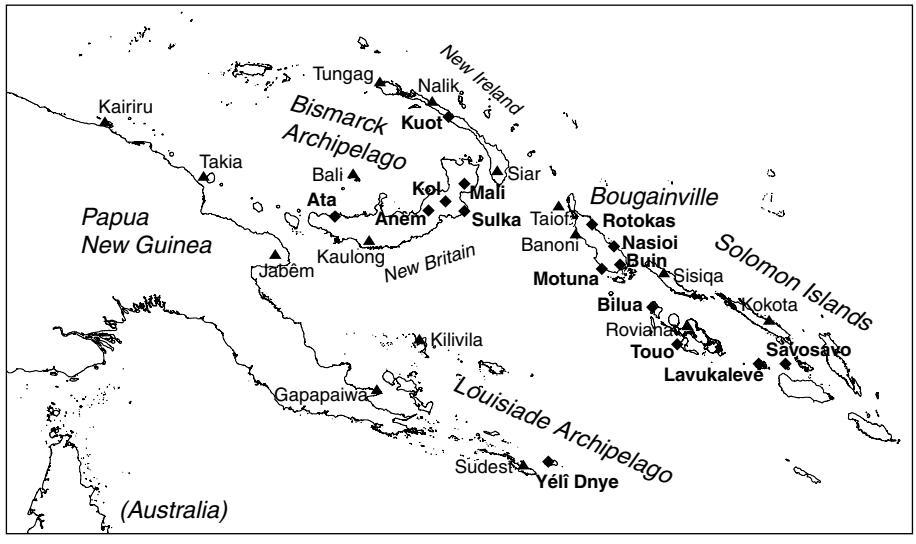

Fig. 1. Island Melanesia, showing the distribution of the Western Oceanic (Austronesian) (triangles) and Papuan (diamonds) languages used in the sample.

	hand/arm	*father*	*eye*
Motu (AN) (mainland PNG)	*ima*	*tama-*	*mata-*
Gela (AN) (central Solomon Islands)	*lima*	*tama-*	*mata-*
Samoan (AN) (Samoa)	*lima*	*tama*	*mata*
Bilua (Pap) (western Solomon Islands)	ngase	*mama*	vilu
Touo (Pap) (western Solomon Islands)	obi	yae	bero
Lavukaleve (Pap) (central Sol. Islands)	tau vegome	kalem	lemi
Savosavo (Pap) (central Sol. Islands)	kakau	mau	nito

Fig. 2. The transparency of cognates in three dispersed Austronesian versus four close Papuan languages (Austronesian cognates/loanwords are shown in italics). The three Papuan languages have an apparent level of 3 to 5% shared vocabulary in a standard 200-word list (*29*). Using a scrambling test, the word list for each language was randomly reordered, and apparent lexeme correspondences were recounted. The level of apparent cognacy on this random list was exactly the same as on the correctly sorted list, demonstrating that the amount of apparently shared lexicon between any pair of Papuan languages is not greater than chance.

[1]Max Planck Institute for Psycholinguistics, Post Office Box 310, 6500 AH Nijmegen, Netherlands. [2]Center for Language Studies, Radboud University, Post Office Box 9102, 6500 HC Nijmegen, Netherlands. [3]Leverhulme Centre for Human Evolutionary Studies, University of Cambridge, Downing Street, Cambridge CB2 3DZ, UK.

*To whom correspondence should be addressed. E-mail: michael.dunn@mpi.nl

The hypothesis that grammatical structure retained a phylogenetic signature was first tested among 16 languages belonging to the Meso-Melanesian, Papuan Tip, and North New Guinea linkages, three sister clades within the Western Oceanic subgroup of Austronesian, the relationship of which has been established by the comparative method (*10*, *27*) {although not completely unambiguously, because there is lexical evidence in particular that the Papuan Tip and the North New Guinea linkages had a period of shared history after their separation from Meso-Melanesian [(*10*), p. 101]}. We carried out a parsimony analysis on the structural data from these languages, from which we obtained a consensus tree [tree length, 224 steps; consistency index (CI) = 0.42; rescaled consistency index (RC) = 0.19; retention index (RI) = 0.46]. When this tree (Fig. 3, right) is compared with the classification based on the comparative method (Fig. 3, left), there is a close match. In the consensus tree, the Meso-Melanesian group forms a major branch. Papuan Tip and North New Guinea together form a clade, with the North New Guinea linkage nested as a subclade within it. This is consistent with uncertainties in the linguistic reconstruction. The internal structure of the Meso-Melanesian group is quite flat, but all except one of the clades posited by the comparative method are congruently represented in the consensus tree. These results show that cladistically analyzed grammatical structure can preserve a signal that is consistent with a known phylogeny derived by traditional lexical techniques.

On the basis of this result, we applied the same method to a set of languages in which lexical similarities are not present. Taking 15 Papuan languages for which we have full structural data and applying the same methods, we obtained a consensus tree of the most parsimonious cladograms for the bootstrapped data set (Fig. 4). This tree has a tree length of 349 steps, CI = 0.35, RC = 0.14, and RI = 0.39. The results show a remarkably geographically consistent pattern: The major clades represent archipelagos, and within each archipelago nearest neighbors tend to form sister clades, despite a nearly complete absence of lexical relatedness.

Interpretation is problematic, because there are no generally accepted independent linguistic criteria for assessing the Papuan trees. One possibility is that these trees reflect contact with local Austronesian neighbors, providing an areal rather than phylogenetic signal. In experiments, combined Austronesian-Papuan consensus trees were in some cases intermeshed, but the result was statistically weak (*28*). Because Papuan and Austronesian are very unlikely to be genuine sister clades, a high degree of homoplasy can be the result of either contact or chance convergence, and combined trees of very remotely related families are likely to be less robust than those where there are good grounds for assuming monophyly. A second possibility is the null hypothesis of no relatedness between the Papuan languages. In that case, we would not expect the orderly and geographically consistent phylogenetic signal that does emerge from the data. This signal is consistent with migration followed by divergence through local isolation. A further possibility is that the geographically consistent tree reflects recent areal contact among Papuan speakers, but most of these languages are not currently spoken in contiguous regions. Because these languages may have been contiguous in the past, regional diffusion also may account for the phylogenetic signal observed, a possibility that we cannot test without more detailed archaeological information.

We therefore suggest that this method reveals evidence of large-scale genealogical clustering of the Island Melanesian languages; the lack of putative lexical cognates dates these relationships considerably before the Austronesian arrival, in line with the radiocarbon dates from the later Pleistocene, when humans entered Island Melanesia from mainland Papua New Guinea.

There remain important issues to resolve. The first is methodological; bootstrap values, especially in the deeper branches, are low by comparison with biological systems, and further work is required to determine whether this reflects rates of convergence, trait covariation, or processes other than phylogenesis alone. Second, the branching sequence does not fit the generally expected dispersal path. A priori, Island Melanesian Papuan languages should show a general west-to-east pattern of diversification, with the center of diversity in the west. The results of our data are more complex. In particular, the position of the Solomons languages is anomalous, located in the tree between the Bismarcks clade and the Bougainville clade, in violation of geographic expectation [because Bougainville is the natural way-station on the route from mainland New Guinea to the Solomons (Fig. 1)]. During the late Pleistocene, Bougainville and the Solomons were

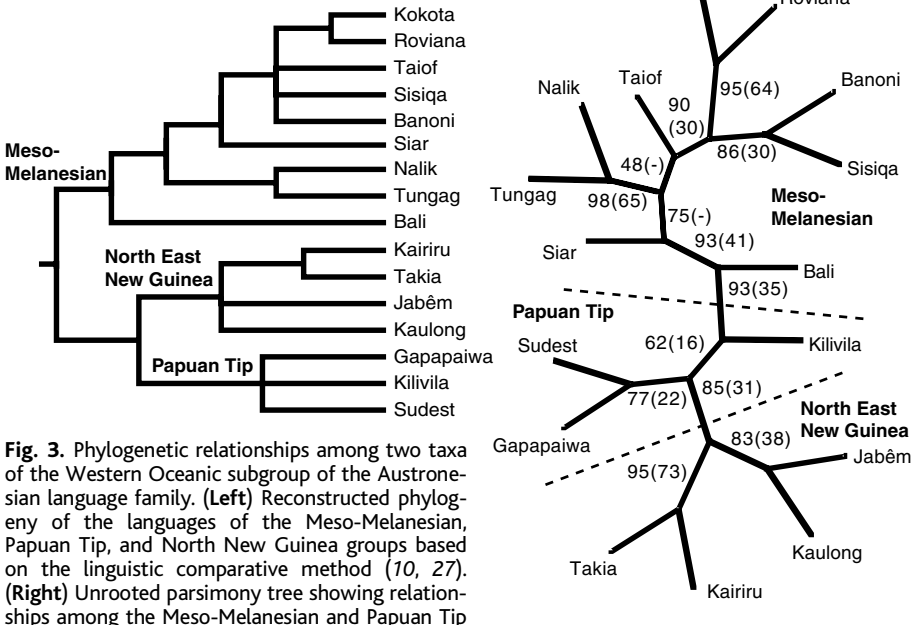

Fig. 3. Phylogenetic relationships among two taxa of the Western Oceanic subgroup of the Austronesian language family. (**Left**) Reconstructed phylogeny of the languages of the Meso-Melanesian, Papuan Tip, and North New Guinea groups based on the linguistic comparative method (*10*, *27*). (**Right**) Unrooted parsimony tree showing relationships among the Meso-Melanesian and Papuan Tip groups based on grammatical traits only (that is, discarding abundant lexical evidence) (the figure shows reweighted and raw bootstrap values). The two trees show a high degree of concordance, with monophyly in both major taxa and the similar geographical structuring of within-taxon diversity.

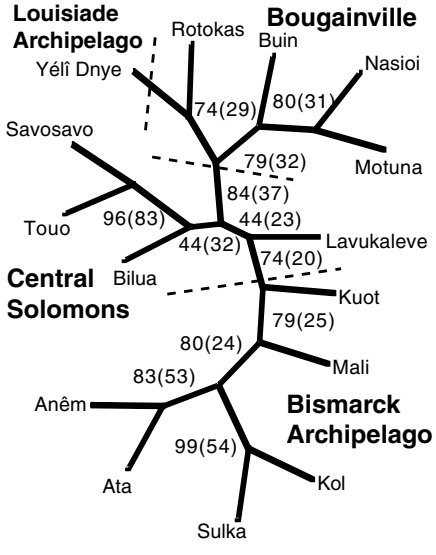

Fig. 4. Maximum parsimony tree of Island Melanesian Papuan languages with reweighted and raw bootstrap values. The tree shows a high level of geographic patterning by island group. Solomon Island languages are intermediate between Bougainville and Bismarck Archipelago languages, which is in violation of geographic progression.

united into a single island, from which the Bismarcks were always separate. A plausible interpretation of the Papuan language tree is thus that the two language groups now located on the Solomons and Bougainville separated from a common ancestor. This could have happened while they could still freely migrate on a common landmass, a time depth (~10,000 years) in accord with that required to erode traces of common vocabulary. This population history hypothesis will require further testing with both linguistic and genetic data.

If grammatical structures can retain a phylogenetic signal beyond the current temporal ceiling on the reconstruction of language history, then the possibility is opened up of finding relationships between others of the world's 300 or so existing language families and isolates.

References and Notes

1. J. Nichols, *Linguistic Diversity in Space and Time* (Univ. of Chicago Press, Chicago, 1992).
2. J. Nichols, in *The Handbook of Historical Linguistics*, B. D. Joseph, R. D. Janda, Eds. (Blackwell, Oxford, 2003), pp. 283–310.
3. J. H. Greenberg, *Language in the Americas* (Stanford Univ. Press, Stanford, CA, 1987).
4. L. L. Cavalli-Sforza, P. Menozzi, A. Piazza, *The History and Geography of Human Genes* (Princeton Univ. Press, Princeton, NJ, 1994).
5. D. Bolnick, B. Shook, L. Campbell, I. Goddard, *Am. J. Hum. Genet.* **75**, 519 (2004).
6. P. Kirch, *The Lapita Peoples* (Blackwell, London, 1997).
7. M. Spriggs, *The Island Melanesians* (Blackwell, London, 1997).
8. D. A. Merriwether *et al.*, in *Genomic Diversity: Applications in Human Population Genetics*, S. S. Papiha, R. Deka, R. Chakraborty, Eds. (Kluwer Academic/Plenum, New York, 1999), p. 153.
9. M. Kayser *et al.*, *Am. J. Hum. Genet.* **72**, 281 (2003).
10. J. Lynch, M. Ross, T. Crowley, *The Oceanic Languages* (Curzon Press, Richmond, UK, 2002).
11. M. Ross, in *The Boy from Bundaberg: Studies in Melanesian Linguistics in Honour of Tom Dutton*, A. Pawley, M. Ross, D. Tryon, Eds. (Pacific Linguistics, Canberra, Australia, 2001), pp. 301–321.
12. S. A. Wurm, *Papuan Languages of Oceania* (Gunter Narr Verlag, Tübingen, Germany, 1982).
13. J. H. Greenberg, in *Current Trends in Linguistics*, vol. 8, *Linguistics in Oceania*, T. A. Sebeok, Ed. (Mouton and Co., the Hague, 1971), pp. 807–871.
14. D. Ringe, T. Warnow, A. Taylor, *Trans. Philol. Soc.* **100**, 59 (2002).
15. P. Forster, A. Toth, *Proc. Natl. Acad. Sci. U.S.A.* **100**, 9079 (2003).
16. R. D. Gray, Q. D. Atkinson, *Nature* **426**, 435 (2003).
17. R. D. Gray, F. M. Jordan, *Nature* **405**, 1052 (2000).
18. C. J. Holden, R. Mace, *Proc. R. Soc. London Ser. B* **270**, 2425 (2003).
19. C. J. Holden, *Proc. R. Soc. London Ser. B* **269**, 793 (2001).
20. K. Rexová, D. Frynta, D. J. Zrzavý, *Cladistics* **19**, 120 (2003).
21. A. McMahon, R. McMahon, *Trans. Philol. Soc.* **101**, 7 (2003).
22. J. Nichols, in *Historical Linguistics 1993. Papers from the Eleventh International Conference on Historical Linguistics*, H. Andersen, Ed. (John Benjamins, Amsterdam, 1995), pp. 337–356.
23. J. Nichols, in *The Origin and Diversification of Language*, N. Jablonski, L. C. Aiello, Eds. (California Academy of Sciences, San Francisco, 1998), pp. 127–170.
24. M. Dunn, G. Reesink, A. Terrill, *Ocean. Linguist.* **41**, 28 (2002).
25. See sources of language data in the supporting online material.
26. Materials and methods and a description of linguistic characters are available as supporting material on *Science* Online.
27. M. Ross, *Proto Oceanic and the Austronesian Languages of Western Melanesia* (Pacific Linguistics C-98, Canberra, Australia, 1988).
28. This intermeshing of trees does reflect long-term contact in New Britain (*26*).
29. D. Tryon, B. Hackman, *Solomon Island Languages: An Internal Classification* (Pacific Linguistics C-72, Canberra, Australia, 1983).

30. This work, as part of the European Science Foundation EUROCORES Programme OMLL, was supported by funds from the Nederlandse Organisatie voor Wetenschappelijk Onderzoek (NWO); the Arts and Humanities Research Council, UK; and the EC Sixth Framework Programme under contract no. ERAS-CT-2003-980409. Additional fieldwork data used in this study were provided by E. Lindström, S. Robinson, T. Stebbins, W. Thurston, and C. Wegener; assistance with coding from published sources was provided by S. Nordhoff and V. Rodrigues. We thank M. Mirazon-Lahr, E. Lindström, and G. Senft for discussion.

Supporting Online Material

www.sciencemag.org/cgi/content/full/309/5743/2072/DC1
Materials and Methods
Figs. S1 and S2
References
Sources of language data
Linguistic characters
Data file

9 May 2005; accepted 15 August 2005
10.1126/science.1114615

Phenotypic Diversity, Population Growth, and Information in Fluctuating Environments

Edo Kussell* and Stanislas Leibler

Organisms in fluctuating environments must constantly adapt their behavior to survive. In clonal populations, this may be achieved through sensing followed by response or through the generation of diversity by stochastic phenotype switching. Here we show that stochastic switching can be favored over sensing when the environment changes infrequently. The optimal switching rates then mimic the statistics of environmental changes. We derive a relation between the long-term growth rate of the organism and the information available about its fluctuating environment.

Organisms adapt readily to regularly varying environments, for instance, by adjusting to the daily light cycles by using internal circadian clocks. Real problems arise when environmental fluctuations are irregular. Organisms can adapt to sudden changes in chemical composition, local temperature, or illumination by sensing the changes and responding appropriately, for example, by switching phenotype or behavior. But there is a cost: each individual must maintain active sensory machinery.

Population diversity offers an alternate way to adapt to randomly fluctuating environments. Different subsets of the total population may be well-adapted to different types of environments. In genetically clonal populations, phenotypic diversity is generated by stochastic phenotype-switching mechanisms (*1–9*). Examples include flagellin phase variation in *Salmonella enterica* (*6*); microsatellite length variation (slipped-strand mispairing), controlling the expression of contingency genes in *Haemophilus influenzae* (*2*, *4*); and swarming motility in *Bacillus subtilis* (*8*). The persistence mechanism in *Escherichia coli*, by which cells switch spontaneously and reversibly to a phenotype exhibiting slower growth and reduced killing by antibiotics (*9*), allows cells to survive prolonged exposure to antibiotics (*10*). Many other switching mechanisms are known in diverse bacteria (*2*, *7*), fungi (*1–3*), and slime molds (*1*).

The idea that randomization of phenotype can be advantageous in fluctuating environments is well established in the ecology and population genetics literature (where it is known as bet-hedging). This idea has found applications in diverse contexts (*11*), and it was previously analyzed in several theoretical and computational studies (*12–18*).

We consider two extreme types of phenotype switching: responsive switching (*R*), occurring as a direct response to an outside cue detected by a sensing mechanism, and spontaneous stochastic switching (*S*), occurring without any direct sensing of the environment. Within a theoretical model, we address several questions. First, under which circumstances should each mechanism be used? For instance, if the detection of a sudden unfavorable environmental change, or the subsequent response, would be too slow, then it could be advantageous to have a subpopulation ready in an appropriate phenotype, before the environmental change.

Second, what determines parameters such as the switching rates? Random environmental

Laboratory of Living Matter and Center for Studies in Physics and Biology, The Rockefeller University, 1230 York Avenue, Box 34, New York, NY 10021–6399, USA.

*To whom correspondence should be addressed. E-mail: kussele@rockefeller.edu

fluctuations experienced by a population over long periods can select among different genetic mechanisms for generating diversity. Organisms whose stochastic switching rates are better adjusted to environmental fluctuations can outgrow organisms that use a different set of switching parameters.

Finally, how does information gathered by organisms about the fluctuating environment affect their survival? The two types of switching differ markedly in this regard. For responsive switching, information about environmental changes is conveyed to the organism directly through the sensing mechanism; whereas for stochastic switching, it is conveyed indirectly by natural selection.

We consider a simple model that encompasses both responsive and stochastic switching and describes a clonal population growing in an environment that fluctuates in time among a finite number (n) of different environment types (Fig. 1). The fluctuating environment is a continuous-time stochastic process, $\mathcal{E}(t)$, designating which environment occurs at time t; the average duration of environment i is τ_i (with the average over all environments equal to τ); the occurrence probability of environment i is p_i; and the probability that environment i follows j is b_{ij} ($b_{ii} = 0$).

Each individual organism is capable of exhibiting one of n different phenotypes. Phenotype i grows with rate $f_i^{(k)}$ in environment k (growth rates may be positive or negative). The phenotype with largest growth rate in environment k is phenotype k (its growth rate is $f_k^{(k)}$), and we refer to it as the fastest-growing phenotype and to all other phenotypes as slower phenotypes. Individuals may switch phenotype at any time, with parameters $H_{ij}^{(k)}$ giving the switching rate from phenotype j to phenotype i in environment k.

Taking the simplest model of growth, the n-dimensional population vector, $\mathbf{x}(t)$, whose ith coordinate is the number of individuals with phenotype i at time t, obeys the following equation

$$\frac{d}{dt}\,\mathbf{x}(t) = A_{\mathcal{E}(t)}\mathbf{x}(t)$$

The matrix $A_{\mathcal{E}(t)}$ may be one of n different matrices, depending on the environment, $\mathcal{E}(t)$. A_k can be written as a sum of a diagonal matrix, whose diagonal entries are the growth rates of each phenotype in environment k ($f_i^{(k)}$), and the matrix of switching rates, $H_{ij}^{(k)}$ (Fig. 1). The sum of all the entries of $\mathbf{x}(t)$ gives the total population size $N(t)$ (*19*).

The two types of phenotype switching correspond to different choices of switching rates. For stochastic switching, these rates are independent of the environment k; therefore, for all values k

$$H_{ij}^{(k)} = H_{ij} \text{ (stochastic switching)}$$

For responsive switching, the sensing mechanism allows switching rates to depend strongly on k. In the extreme case, all phenotypes switch with the same rate H_m to phenotype k in environment k, so

$$H_{kj}^{(k)} = H_m \text{ for all } j \neq k \text{ (responsive switching)}$$

$$H_{ij}^{(k)} = 0 \text{ for all } i \neq k \text{ and } j \neq i$$

The switching rate H_m is physiologically determined but ideally as large as possible, so that individuals spend as little time as possible in slower phenotypes.

To compare the two types of switching, we calculate the so-called Lyapunov exponent Λ (*20*), which is the asymptotic growth rate of total population size (*21*, *22*) given by the large time limit of $(1/t)\log N(t)$. Λ is known to exist under relatively general conditions (*20*) and depends on both the organism (growth rates of its phenotypes and switching rates) and on the temporal sequence of the changing environment $\mathcal{E}(t)$. In general, it is difficult to compute analytically, but we now describe an approximation that allows such computation for our model.

We assume that environmental durations are long enough that the population has time to reach its equilibrium composition before the environment changes. In environment j, this means that $\mathbf{x}(t)$ will eventually point essentially in the direction of the top eigenvector of the matrix A_j. Upon a change of environment from j to i, there will be a delay time, T_{ij}^*, during which the population's composition changes

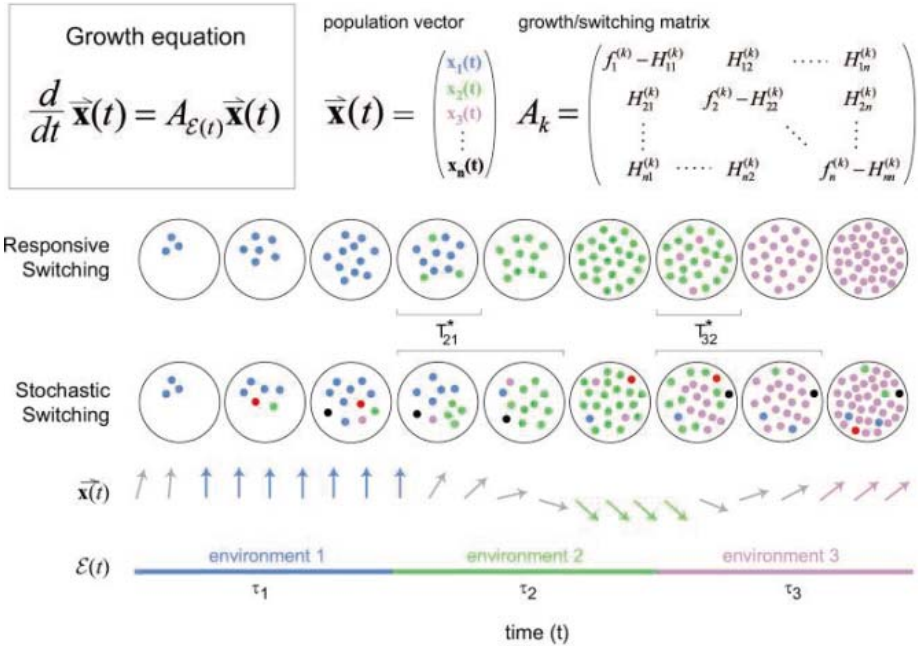

Fig. 1. A population is composed of individuals each capable of exhibiting one of n different phenotypes in n different environments. The growth rate of phenotype i in environment k is $f_i^{(k)}$; among all phenotypes in environment k, phenotype k grows the fastest. Individuals can switch phenotype at any time, responsively or stochastically. $H_{ij}^{(k)}$ is the switching rate from phenotype j to i in environment k, and $H_{jj}^{(k)} = \sum_{i \neq j} H_{ij}^{(k)}$. The boxed growth equation governs the dynamics of the n-dimensional population vector of phenotypes, $\mathbf{x}(t)$. The changing environment is a continuous-time stochastic process, $\mathcal{E}(t)$, taking integer values 1 to n designating the environment at time t. The form of matrices A_k is shown, determining the combined growth and switching rates of all phenotypes when $\mathcal{E}(t) = k$. $\mathcal{E}(t)$ is assumed to be constant on successive time intervals T_l with $l = 1, 2, \ldots$; $\varepsilon(l)$ is the environment occurring at the lth interval, and $L(t)$ denotes the number of intervals T_l elapsed by time t. Environment change probabilities are $b_{ij} \equiv P[\varepsilon(l) = i \mid \varepsilon(l-1) = j]$, so $\varepsilon(l)$ is a Markov chain (assumed ergodic) with n states and transition matrix b, with $b_{ii} = 0$. The equilibrium probability p_i of environment i satisfies $p_i = \sum_j p_j b_{ij}$; the average duration of environment i is τ_i and the average duration of environments is $\tau \equiv \sum_{i=1}^{n} p_i \tau_i$. Total population size is $N(t) \equiv \sum_{i=1}^{n} x_i(t)$. A schematic of the dynamics is shown in which individuals are colored to indicate phenotype, such that the fastest-growing phenotype in each environment matches the environment's color. When environment j changes to i, there is a delay time, T_{ij}^*, in which $\mathbf{x}(t)$ rotates (shown in gray) before the population attains its new composition. In responsive switching, individuals switch directly to the fastest-growing phenotype. In stochastic switching, subpopulations exist in different phenotypes; when the environment changes, the fastest-growing subpopulation brings about a change in population composition. Proportions of slower-growing phenotypes are exaggerated for the purpose of illustration; they may be as small as $\approx 10^{-6}$.

from its old structure (top eigenvector of A_j) to its new one (top eigenvector of A_i) (Fig. 1) (*23*). Thereafter, the population will grow at a rate given by the top eigenvalue of the matrix A_i, $\lambda_1(A_i)$. This simple picture allows for computation of the Lyapunov exponent in the limit of long durations (*24*, *25*).

We find, in this limit, that Λ depends only on mean environmental durations τ_i and transition probabilities b_{ij} and is independent of other characteristics of environmental fluctuations (for example, the variance of environmental durations) (*24*). The biological implication is that a stochastic-switching organism is buffered against changes in the distribution of environmental variations, provided its environment does not fluctuate too quickly. We have verified this observation by simulation (fig. S1).

We now turn to the specific cases of responsive and stochastic switching. Because responsive switching requires a sensing apparatus in addition to the machinery of switching, we introduce the "cost of sensing" c to be the reduction of growth rates due to the presence of sensing machinery. We obtain the long-term growth rate for responsive switching

$$\tau\Lambda_R = \sum_{i=1}^{n} p_i \tau_i f_i^{(i)} - c\tau - \sum_{i,j=1}^{n} p_j b_{ij} \log(1 + \Delta_{ji}^{R}/H_m)$$

$$[\text{long-term growth}] = [\text{fastest growth}] - [\text{sensing cost}] - [\text{delay-time cost}]$$

and for stochastic switching (for small switching rates)

$$\tau\Lambda_S = \sum_{i=1}^{n} p_i \tau_i f_i^{(i)} - \sum_{i=1}^{n} p_i \tau_i H_{ii} - \sum_{i,j=1}^{n} p_j b_{ij} \log(1 + \Delta_{ij}^{S}/H_{ij}) + \ldots$$

$$[\text{long-term growth}] = [\text{fastest growth}] - [\text{diversity cost}] - [\text{delay-time cost}]$$

where $\Delta_{ij} \equiv f_j^{(j)} - f_i^{(j)}$, $\Delta_{ij}^{R} \equiv \Delta_{ij}$, and $1/\Delta_{ij}^{S} \equiv 1/\Delta_{ij} + 1/\Delta_{ji}$.

The general form of the expression for Λ is the same in both cases; only the origin of the second term is different. In stochastic switching, switching to slower phenotypes decreases Λ, incurring a "diversity cost"; in responsive switching, the "sensing cost" appears instead (*26*). The third term in both equations, the "delay-time cost," has a similar form, and is due to the time it takes the population structure to change after a change of environment.

We can now find the switching rates H_{ij} that maximize Λ for a stochastic switching organism, using the above expression for Λ_S

$$H_{ij}(\text{optimal}) = b_{ij}/\tau_j$$

The optimal switching rate from phenotype j to i is proportional to the probability that the environment changes from environment j to i and inversely proportional to the average duration of environment j. Optimal rates are thus precisely tuned to environmental statistics (*14*, *27*).

The long-term growth rate for optimal switching is found to be

$$\tau\,\Lambda_S(\text{optimal}) = \sum_{i=1}^{n} p_i \tau_i f_i^{(i)} - 1 - \sum_{i,j=1}^{n} p_j b_{ij} \log(\Delta_{ij}^{S}\tau_j) - I_{\text{env}}$$

where $I_{\text{env}} = -\sum_{i,j=1}^{n} p_j b_{ij} \log b_{ij}$. The term I_{env} is the entropy, or information content, of the fluctuating environment (*28*). It measures how unpredictable or surprising are the different environmental transitions appearing in the time sequence $\mathscr{E}(t)$. Even for optimal switching rates, the negative term $-I_{\text{env}}$ is present in Λ_S, because stochastic-switching organisms cannot perfectly anticipate the next environment (except when $I_{\text{env}} = 0$). In contrast to responsive switching, which senses a new environment, the stochastic-switching organism cannot overcome the entropy of its environment.

The appearance of I_{env} explicitly in the optimal long-term growth rate of a population points to possibly deeper connections between the fields of population biology and information theory (*29*). For example, consider a stochastic-switching organism with suboptimal rates H'_{ij}. These rates would be optimal in a varying environment with average durations $\tau'_j = 1/\sum_{k\neq j} H'_{kj}$ and transition probabilities $b'_{ij} = H'_{ij}/\sum_{k\neq j} H'_{kj}$. This organism has inaccurate information about its environment, as reflected in its long-term growth rate being lower than Λ_S(optimal) by $\frac{1}{\tau} S_{\text{K-L}} + \frac{1}{\tau}\sum_i p_i[\tau_i/\tau'_i - 1 - \log(\tau_i/\tau'_i)]$. The relative entropy (Kullback-Leibler divergence), $S_{\text{K-L}} \equiv \sum_{i,j} p_j b_{ij} \log(b_{ij}/b'_{ij})$, is the penalty paid for poor information about environmental transitions (*30*).

We may also consider stochastic switching with memory, i.e., when individuals remember the last few phenotypic switches that occurred in their ancestral history. Such memory is advantageous when the fluctuating environment exhibits longer correlations, i.e., when environmental transition probabilities depend on the last m environments. As in the case of sensing, there is a maximal cost for which memory is beneficial, which is related to the amount of information about the environment that such memory can reveal (*25*).

We now compare responsive and stochastic switching using long-term growth rates. If the cost of sensing, c, is small, responsive rather than stochastic switching will be favored. The maximal c for which sensing is advantageous is determined by the inequality $\Lambda_R > \Lambda_S$(optimal). We assume that fastest phenotypes have identical growth rates f, slower phenotypes have growth rates $\tilde{f}$ ($\Delta \equiv f - \tilde{f}$), and all environments have the same duration τ, and we find $c < \frac{1}{\tau}[1 + \log(\Delta\tau/2) - \log(1 + \Delta/H_m) + I_{\text{env}}]$.

The greater the uncertainty of the environment (I_{env}), and the faster the responsive organism responds (H_m), the higher the maximal cost c for which sensing is beneficial. In other words, an organism can afford to pay more for a sensor the more uncertain its environment. The longer environments remain constant, however, the less it pays to have a sensor. Stochastic switching is therefore favored when environments change infrequently (*31*–*34*).

The Lyapunov exponent can be defined even when total population size is bounded, and our main results apply in that case as well, provided that all slower phenotypes are represented in the population (*25*). We have not considered the evolutionary process that adjusts the switching rates. Given enough time, natural selection should change H_{ij} values toward the optimum, effectively extracting information about environmental statistics and translating it into switching rates (*35*).

We presented an analytical calculation of growth rates for structured populations in fluctuating environments and showed explicitly that information about environmental statistics is of central importance in population dynamics.

References and Notes

1. D. R. Soll, B. Kraft, *Dev. Genet.* **9**, 615 (1988).
2. E. R. Moxon, P. B. Rainey, M. A. Nowak, R. E. Lenski, *Curr. Biol.* **4**, 24 (1994).
3. J. Perez-Martin, J. A. Uria, A. D. Johnson, *EMBO J.* **18**, 2580 (1999).
4. C. D. Bayliss, D. Field, E. R. Moxon, *J. Clin. Invest.* **107**, 657 (2001).
5. S. A. Lachke, S. Joly, K. Daniels, D. R. Soll, *Microbiology* **148**, 2661 (2002).
6. H. R. Bonifield, K. T. Hughes, *J. Bacteriol.* **185**, 3567 (2003).
7. M. W. van der Woude, A. J. Baumler, *Clin. Microbiol. Rev.* **17**, 581 (2004).
8. D. B. Kearns, F. Chu, R. Rudner, R. Losick, *Mol. Microbiol.* **52**, 357 (2004).
9. N. Q. Balaban, J. Merrin, R. Chait, L. Kowalik, S. Leibler, *Science* **305**, 1622 (2004).
10. Whereas current experiments have not detected any direct sensing in the case of *E. coli* persistence, further experiments are needed to completely rule out the possibility of more subtle effects, such as the dependence of switching rates on the presence of antibiotics. Direct sensing of the environment might be involved in some of the known mechanisms that are thought to be purely stochastic, and in general, we may expect to find mixtures of stochastic switching and sensing mechanisms.

11. J. Seger, H. J. Brockmann, in *Oxford Surveys in Evolutionary Biology*, P. H. Harvey, L. Partridge, Eds. (Oxford Univ. Press, Oxford, 1987), vol. 4, pp. 182–211.
12. P. Haccou, Y. Iwasa, *Theor. Popul. Biol.* **47**, 212 (1995).
13. A. Sasaki, S. Ellner, *Evolution* **49**, 337 (1995).
14. M. Lachmann, E. Jablonka, *J. Theor. Biol.* **181**, 1 (1996).
15. A. Grafen, *Proc. R. Soc. London Ser. B* **266**, 799 (1999).
16. A. J. Robson, C. T. Bergstrom, J. K. Pritchard, *J. Theor. Biol.* **197**, 541 (1999).
17. M. Thattai, A. van Oudenaarden, *Genetics* **167**, 523 (2004).
18. D. M. Wolf, V. V. Vazirani, A. P. Arkin, *J. Theor. Biol.* **234**, 227 (2005).
19. Here populations are taken to be large enough that deterministic dynamics of $\mathbf{x}(t)$ can be assumed. Stochastic dynamics of small populations are discussed briefly in (*25*).
20. A. Crisanti, G. Paladin, A. Vulpiani, *Products of Random Matrices* (Springer-Verlag, Berlin, 1993).
21. R. C. Lewontin, D. Cohen, *Proc. Natl. Acad. Sci. U.S.A.* **62**, 1056 (1969).
22. J. E. Cohen, *Stochast. Process. Appl.* **9**, 245 (1979).
23. For small switching rates, the delay times can very roughly be thought of as the time for phenotype i to sweep through the population and replace phenotype j as the dominating type. For large switching rates, this is not the case, because the population can be a mixture of multiple phenotypes having comparable numbers of individuals.
24. Following the notation of Fig. 1 and its caption, growth in each environment will, after some delay time T_l^*, be driven solely by the fastest phenotype at a rate $\lambda_1(A_{\varepsilon(l)})$. Provided the environmental duration T_l is long, population growth due to slower phenotypes during the delay time may be ignored with negligible error, yielding $\Lambda = \lim_{t\to\infty} \frac{1}{t}\sum_{l=1}^{L(t)} \lambda_1(A_{\varepsilon(l)})(T_l - T_l^*)$. The delay times T_l^* depend only on environments $\varepsilon(l)$ and $\varepsilon(l-1)$, so $T_l^* = T^*_{\varepsilon(l)\varepsilon(l-1)}$. Because $t \to \tau L(t)$, we find $\Lambda = \frac{1}{\tau}\sum_{i,j=1}^{n} p_j b_{ij} \lambda_1(A_i)(\tau_i - T_{ij}^*)$. Calculation of $\lambda_1(A_i)$ and T_{ij}^* then gives Λ.
25. Details of our calculation, the approximations used, and numerical computations are available as supporting material on *Science* Online.
26. In deriving these expressions, we have assumed that environmental durations are sufficiently long and that switching rates are strictly positive. For Λ_S, we also assumed that switching rates H_{ij} are small (*25*).
27. In certain cases, not switching at all, i.e., remaining in a single phenotype at all times, is better than switching phenotype. This can be the case, for example, when environments change very rapidly. When environments last sufficiently long, the solution given in the text is the optimum.
28. T. M. Cover, J. A. Thomas, *Elements of Information Theory* (Wiley, New York, 1991).
29. The notion of entropy was used previously in population biology as an empirical measure of population diversity, and in the context of age-structured populations as a tool for solving the dynamic equation (*36*, *37*). Demetrius observed that several properties of the stable age distribution are determined by an entropy defined on population genealogies.
30. A similar result is seen in certain types of gambling (*28*), e.g., horse races and stock markets, where the gambler must decide how much money to bet on each possible outcome.
31. R. B. Bourret, A. M. Stock, *J. Biol. Chem.* **277**, 9625 (2002).
32. J. M. G. Vilar, C. C. Guet, S. Leibler, *J. Cell Biol.* **161**, 471 (2003).
33. E. Kussell, R. Kishony, N. Q. Balaban, S. Leibler, *Genetics* **169**, 1807 (2005).
34. Many sensing systems exist in microorganisms such as those involved in chemotaxis (*31*), the *lac* operon (*32*), and onset of stationary phase. In these examples and others, the environmental cue that is sensed occurs often, on the order of tens of generations or less, and our model predicts that sensing is advantageous. For bacterial persistence, experiments suggest that direct sensing might be absent (*9*). The appearance of antibiotic may be a relatively rare event in the natural habitats of *E. coli* (although direct evidence is scarce), in which case our model favors stochastic switching (*33*).
35. By comparing the time to fixation for a mutation that abolishes phenotype switching with environmental durations, we find that natural selection can maintain switching mechanisms. The mechanism may be lost if a very long environmental duration ($\gg\tau_i$) occurs (*25*).
36. L. Demetrius, *J. Stat. Phys.* **30**, 709 (1983).
37. P. Michel, S. Mischler, B. Perthame, *C. R. Acad. Sci. Paris* **338**, 697 (2004).

38. We would like to thank G. Ben Arous, N. Balaban, R. Kishony, C. Bargmann, J. McKinney, L. Keller, R. Losick, A. Murray, A. Grosberg, J. Merrin, and O. Ahmed for discussions. We particularly thank G. Ben Arous and C. Bargmann for their encouragements and many detailed comments about the manuscript. E.K. thanks the Alfred P. Sloan Foundation for financial support.

Supporting Online Material
www.sciencemag.org/cgi/content/full/1114383/DC1
Materials and Methods
Fig. S1
References

3 May 2005; accepted 8 August 2005
Published online 25 August 2005;
10.1126/science.1114383
Include this information when citing this paper.

Small Nucleic Acid Purification

The innovative flashPAGE Fractionator System is a new electrophoresis device for the rapid, streamlined purification of small nucleic acids, such as small interfering-RNAs and microRNAs. Unlike traditional polyacrylamide gel electrophoresis (PAGE), which was optimized for detection only, the new system is designed for the purification of these small molecules. With this system, scientists can save nearly an entire day of labor by purifying small RNA and DNA molecules in about 12 min. The flashPAGE purification system makes use of an electrical current to drive nucleic acids through a proprietary denaturing gel matrix and buffer system and into the lower buffer collection chamber. This chamber is designed for retention of eluted material, isolating highly purified nucleic acids for sensitive downstream investigation.

Ambion For information 800-888-8804 www.ambion.com

Protein Coupling Kits

Two new kits make small-scale affinity purification of antibodies and other proteins easier to perform. The two kits make use of reliable chemistries for covalent attachment of amine- or sulfhydryl-containing molecules. The MicroLink Protein Coupling Kit provides a complete set of reagents for the small-scale coupling of protein via amine groups and spin column purification of target molecules. The kit is suitable for coupling small amounts (25 to 100 μg) of protein. The MicroLink Peptide Coupling Kit provides a complete set of reagents for the small-scale coupling of peptides or other molecules containing sulfhydryl groups and spin column purification of target molecules.

Pierce For information 800-874-3723 www.piercenet.com

Array Designer

Version 4 of Array Designer is software for designing specific and efficient oligonucleotides for microarrays for the challenges of the post-sequencing era. This desktop tool can design hundreds of specific oligonucleotides for complementary DNA microarrays for expression studies or single nucleotide polymorphism (SNP) genotyping. The new version includes the ability to make whole genome arrays and tiling arrays. With Array Designer, the user can start with a list of sequences or a whole genome sequence (for whole genome arrays) to study the entire organism by detecting every gene or exon in the whole genome, characterizing transcriptomes, discovering differentially or alternatively spliced transcript, SNP discovery and genotyping, DNA sequence variation in individuals or populations, splce variant assays, and comparative genome hybridization.

Premier Biosoft International For information 650-856-2703 www.premierbiosoft.com

Fast Filter Wheel

The U_FFWO is a fast observation filter wheel suitable for certain cellular observation techniques on the molecular level, such as fluorescence resonance energy transfer, quantum dot applications, and dual-emission imaging. Designed for use with the Olympus cell^R and cell^M high-end research imaging station for live cell microscopy, the new fast observation filter wheel has a minimal switching time of just 58 ms. This speed is essential for time course investigations of rapid intracellular events that require the acquisition of several images per second with observations made at different wavelengths.

Olympus For information +49 40 2 37 73-5426 www.olympus-europa.com

Chemical Inkjet Printer

The ChIP 1000 Chemical Inkjet Printer is a new tool for proteomics analysis (peptide fingerprint mapping), protein microarray analysis, and nano-western analysis. The ChIP rapidly and reproducibly dispenses picoliter volumes of reagents to defined locations on poly(vinylidine fluoride) (PVDF) membranes, allowing for multiple micro-chemistries on specific western blot spots or bands (from one- or two-dimensional gel electrophoresis), opening new horizons for microscale protein research and repeated analysis. This is accomplished through a piezoelectric reagent delivery system, which includes four independent channels for deposition of multiple chemistries or matrix-assisted laser desorption ionization-time of flight matrices to a stationary support. For the first time, micro-scale on-membrane digestion can be rapidly generated without the time-consuming procedures of in-gel digestion, peptide extraction, and C18 cleanup steps.

Shimadzu For information 800-477-1227 www.shimadzu-biotech.net

Competent Cells

Express BL21(DE3) Competent Cells offer high efficiency cloning and a high level of protein expression in the same cell. With a transformation efficiency of ≥5 x 10^9 cfu/μg, *E. cloni* Electrocompetent Cells eliminate the need to transfer plasmids from a cloning strain into an expression strain. Increased recombinant yields allow fast production of complex expression libraries using any T7 expression vector.

Lucigen For information 608-831-9011 www.lucigen.com

Literature

Cellular Analysis Catalog offers more than 3,200 products, including 1,800 new animal antibodies, a unique menu of major histocompatibility complex tetramers for T-cell research, cell signaling reagents, and multiplex bead assays. These reagents meet the needs of a wide range of research applications using flow cytometry and imaging.

Beckman Coulter For information 800-742-2345 www.beckmancoulter.com

For more information visit GetInfo, *Science*'s new online product index at *http://science.labvelocity.com*

From the pages of GetInfo, you can:
- Quickly find and request free information on products and services found in the pages of *Science*.
- Ask vendors to contact you with more information.
- Link directly to vendors' Web sites.

Newly offered instrumentation, apparatus, and laboratory materials of interest to researchers in all disciplines in academic, industrial, and government organizations are featured in this space. Emphasis is given to purpose, chief characteristics, and availability of products and materials. Endorsement by *Science* or AAAS of any products or materials mentioned is not implied. Additional information may be obtained from the manufacturer or supplier by visiting www.science.labvelocity.com on the Web, where you can request that the information be sent to you by e-mail, fax, mail, or telephone.

Sample Prep

An attractive spin on protein desalting.

Zeba™ Desalt Spin Columns

With our exclusive high-performance, high protein recovery resin and range of volume capacity, you now have the ultimate protein-desalting tool.

The Zeba™ Desalt Spin Columns from Pierce in 0.5, 2, 5 and 10 ml formats complement the Zeba™ Micro Desalt Spin Column† products and allow processing of sample volumes ranging from 2 µl to 4 ml for a full range of desalting options.

- No screening fractions for protein or waiting for protein to emerge by gravity flow
- Minimal sample dilution
- Exceptional protein recovery
- Easy-to-use with no cumbersome column preparation or equilibration

Ordering Information

Description	Product # by Package Size 5/Pack	25/Pack	50/Pack
Zeba™ Micro Desalt Spin Columns	–	89877	89878
Zeba™ Desalt Spin Columns, 0.5 ml	–	89882	89883
Zeba™ Desalt Spin Columns, 2 ml	89889	89890	–
Zeba™ Desalt Spin Columns, 5 ml	89891	89892	–
Zeba™ Desalt Spin Columns, 10 ml	89893	89894	–

Zeba™ Columns are available in various sizes without resin. Visit our web site for more information.

HURRY! Purchase US$250 of Zeba™ Desalting Products direct from Pierce by Dec. 30, 2005, and receive a FREE Pierce Zeba™ Protein Desalting T-shirt. Mention this ad when placing your order. Offer valid in U.S. only. Void where prohibited.

BSA 66,000 M.W.

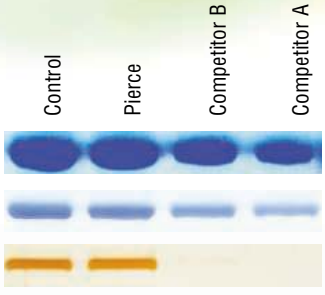

Ubiquitin 8,700 M.W.

Protein recovery after sample processing with commercially available desalting resins in a micro-spin device. Samples of bovine serum albumin (BSA) or ubiquitin at a variety of concentrations were desalted with Pierce high-performance desalting resin (Product # 89877) or the leading competitors' resins in empty Zeba™ Micro Spin Columns from Pierce. In all cases, sample volume was 10 µl plus a 3 µl buffer stacker placed over the sample.

www.piercenet.com/zeba22j

PIERCE

Tel: 815-968-0747 or 800-874-3723 • Fax: 815-968-7316 • Technical Assistance E-mail: TA@piercenet.com • Customer Assistance E-mail: CS@piercenet.com
Outside the United States, visit our web site or call 815-968-0747 to locate your local Perbio Science branch office (below) or distributor

Belgium & Dist.: Tel +32 53 85 7184 euromarketing@perbio.com
China: Tel +86 10 8049 9033 support@perbio.com.cn
France: Tel 0800 50 82 15 euromarketing@perbio.com
Germany: Tel 0228 9125650 de.info@perbio.com
Hong Kong: Tel 852 2753 0686 SalesHK@perbio.com
The Netherlands: Tel 076 50 31 880 euromarketing@perbio.com
United Kingdom: Tel 0800 252185 uk.info@perbio.com
Switzerland: Tel 0800 56 31 40 euromarketing@perbio.com

PERBIO

» advances in:

Proteomics

Protein-Protein Interactions

The emergence of new tools and technologies has led to an exponential increase in studies of interactions among proteins. BY PETER GWYNNE AND GARY HEEBNER

In this issue:

- Tag chemistry
- Equalizer beads
- Chromatography-based separation
- 2-D gel electrophoresis
- Two-hybrid systems
- Mass spectrometry
- Surface plasmon resonance

By studying the ways in which proteins react with each other, researchers hope to achieve two goals: learning more about the ways in which cells function, and developing new drugs to treat disease. But the nature of the entities makes exploration of their interactions a difficult task. "Proteins are vibrating, extremely complex molecules in a constant state of modification, both initiating and driving interactions with many molecules," says Allan Simpson, vice president for research and analysis at **GE Healthcare**. "It requires a large range of technologies to handle and study them."

Nevertheless, several life scientists have taken up the challenge. "The study of protein-protein interactions has probably seen an exponential increase," says Anke Cassing, associate director of corporate strategy at **Qiagen**. "A lot of researchers are focused on protein-protein interactions," adds Frank Montagne, chief scientific officer for **Elchrom Scientific**. "These are key mechanisms for the discovery of new signaling pathways."

To facilitate the study of those mechanisms, increasing numbers of vendors have introduced new tools and technologies. "We've introduced new protein biochip arrays to study protein interactions," says William Rich, CEO of **Ciphergen Biosystems**. "We use SELDI-TOF-MS to detect protein interactions directly from the arrays, which provide advantages over elution-based mass spectrometry methods." Ken Miller, product manager of **Thermo Electron**, points to two other areas of advance. "The sensitivity of analysis capabilities of mass spectrometry has increased," he says. "And a lot of tools have emerged for very selective and effective affinity isolation of proteins and protein complexes." Lothar Germeroth, CEO of German firm **IBA**, outlines other recent improvements in tools. "Methods for stable isotope protein labeling for quantitative proteomics can further the efficiency of mass spectrometry," he explains, "since the technology enables the identification of dynamic changes in the composition of protein complexes in different cellular states."

Improvements in tools for studying protein-protein interactions cover a wide spectrum. "There are approaches now that not only discover or confirm the interaction but allow you to drill deeper and characterize where the interaction contact surfaces reside on the binding partners," says Robert Vigna, technical marketing manager for **Pierce**.

Two Emerging Technologies

To study protein-protein interactions, scientists must first separate and purify the individual proteins. They immediately confront a particular difficulty: Several of the most interesting proteins occur in much smaller concentrations than more mundane entities. To solve this "dynamic range problem," researchers can opt for emerging technologies such as tag chemistry and bead technology. MORE ›››

Inclusion of companies in this article does not indicate endorsement by either AAAS or Science, *nor is it meant to imply that their products or services are superior to those of other companies.*

This is the final special supplement this year on Advances in Proteomics. The first three appeared in the 25 March, 29 April, and 27 May issues of Science.

MOVE YOUR 2D GEL IMAGE ANALYSIS TO A NEW DYMENSION...FAST

FREE* **30 DAY TRIAL**
www.2dymension.com
*subject to status

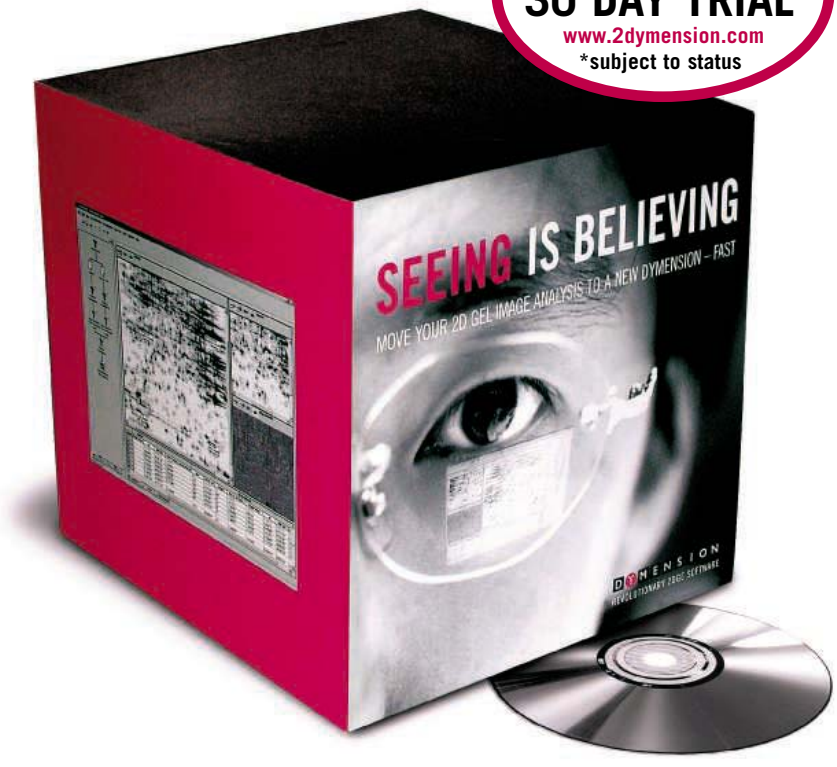

RAPYD

- Instant warping
- Impressively fast spot detection
- Spot matching in seconds

PRECYSE

- Razor sharp warping, spot detection and matching
- Negligible post editing
- Supremely accurate

SYMPLE

- Easy to use interface
- Clear Process Flow chart
- Minimal training required

DYMENSION overturns the accepted conventions of 2D gel electrophoresis analysis. This revolutionary new software will enable you to complete all procedures crucial to comprehensive 2D image analysis, at the touch of a button. Warping, spot detection and spot matching – tasks that once took hours – can now be performed within seconds.

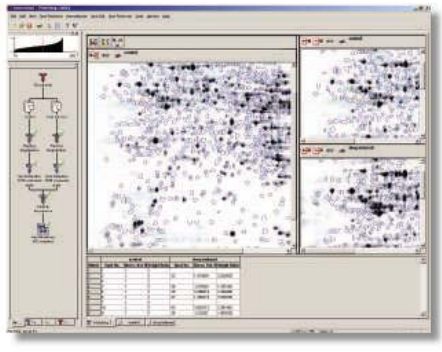

Find out more at: www.2dymension.com

Syngene Europe and International Headquarters
Beacon House Nuffield Road
Cambridge CB4 1TF UK
Tel: +44 (0) 1223 727123
Fax: +44 (0) 1223 727101
Email: sales@2dymension.com

Syngene USA Headquarters
5108 Pegasus Court Suite M
Frederick MD 21704 USA
Tel: 800 686 4407/301 662 2863
Fax: 301 631 3977
Email: ussales@2dymension.com

From research to quality control – base your decisions on the best

For more than 15 years Biacore has been supplying the life science market with a growing range of advanced systems for protein interaction analysis. Unique, high-quality data generated from each instrument supports the many critical decisions that lead to increased productivity in academic and pharmaceutical environments.

Biacore® systems define proteins in terms of their concentration, their specificity of interaction with other molecules, the rates at which they interact, how tightly they bind to another molecule and the thermodynamics involved – all without the use of labels.

Data you can depend on – from the unrivalled global leader in protein interaction analysis.

Protein interaction analysis in:

- **Disease mechanisms**
- **Antibody characterization**
- **Proteomics**
- **Lead selection**
- **Immunogenicity**
- **Biotherapeutic development**

Define · Decide

BIACORE

www.biacore.com

» advances in: Proteomics

As its name implies, tag chemistry pinpoints specific proteins with appropriate chemical tags. "Proteins can be expressed with tags on one or both ends," GE Healthcare's Simpson explains. "Purification is now relatively easy, as the technology is available to capture the tag." IBA's Germeroth extends that point. "Tag-based methods allow you to apply fully processed and modified protein baits to identify the corresponding prey in a native environment," he says. "The advent of tag-based methods such as tandem-affinity purification [TAP] has improved the speed and accuracy of determination of protein-protein interactions."

IBA, which advertises itself as "The TAG Company," markets the One-STrEP protein-protein interaction kit. "Our system is based on the *Strep*-tag technology," Germeroth says. "*Strep*-tag's small size, physicochemical balance, and mild elution conditions allow for a mild and rapid purification of protein complexes in only one step without compromising any protein in these complexes. The technology is ideally suited for automated determination of protein-protein interactions which the pharma industry strongly demands."

QIAGEN has expanded its comprehensive portfolio of Ni-NTA products into the area of bead based assays. In LiquiChip assays, the remarkable selectivity of the Ni-NTA chemistry for His-tagged proteins is used to couple proteins to capture beads, thus enabling multiplex interaction assays.

Ciphergen, has just introduced what it calls Equalizer Beads. "It is basically a bioseparation procedure that uses combinatorial methods to build a chemical library onto beads with a diversity of 1 million to 10 million different affinities," Rich says. "When you put these beads into a very small sample of serum, each bead finds the protein for which it has the most affinity. When you wash away all the excess beads with high abundant proteins, you have concentrated up all the low abundant proteins attached to the beads." Initially, Ciphergen is offering the technology as a service. "But eventually, as its development is improved, we will sell it as a product," Rich says.

Chromatographic Separations

Once scientists have separated out their target proteins, they can use more traditional methods to profile and purify them. High performance liquid chromatography (HPLC) has earned general acceptance as the standard for protein purification because of its exceptional reliability, biocompatibility, and ability to perform a wide variety of chromatographic separations with proteins. Companies that offer the method include **Applied Biosystems** and **Waters**.

GE Healthcare's ÄKTAxpress is a dedicated chromatography system for multidimensional purification of tagged proteins. "We have integrated knowledge into the system so that researchers needing to purify proteins do not need to be skilled chromatographers. It's a protein factory on a lab bench," Simpson says. For chromatographic professionals, the company offers alternative systems, including the ÄKTA Explorer.

Scientific Seminar Series

The 2005 Scientific Seminar Series hosted by **Corning Life Sciences** and cosponsored by *Science* and AAAS (the American Association for the Advancement of Science) gives scientists online advice in the form of novel tips, best practices, and proven techniques that will help them with their research. Remaining seminars in this year's series cover such subjects as scaling up cells, assessing the quality of microarray data, cell based assay performance, permeable supports in drug discovery, cell storage and cryopreservation, and label-free high throughput screening of cell assays. You can find the dates and times of the seminars on the website:

» http://www.corning.com/lifesciences/news_center/web_seminars/

Ciphergen, meanwhile, has developed products that eliminate the need for traditional chromatographic separations. The company's ProteinChip Arrays provide a variety of surface chemistries that allow researchers to optimize protein capture and analysis. "For us, the arrays have always been a miniaturized form of chromatography that scientists can use to rapidly predict optimum chromatographic conditions to scale up protein purification," Rich says. "And if you use it with our Equalizer technology, it works even better."

Separation Via 2-D Gel

The other traditional approach, two-dimensional (2-D) gel electrophoresis was developed specifically to separate protein mixtures. "Where the aim is to catalog the entire protein repertoire of a cell or tissue as comprehensively as possible, 2-D gel electrophoresis and liquid chromatography can be seen as complementary separation methods," Qiagen's Cassing says. "Two-D gel has quality comparable to chromatography," Elchrom's Montagne agrees. "But it's cheaper." Anatoli Tassis, manager of business development and applications development for oligos at Elchrom, points to another advantage of 2-D gels. "You use both the molecular weight and the bioelectric potential to reach your goal," she says. "That gives you better characterization."

Bio-Rad Laboratories, GE Healthcare, and **Invitrogen** have electrophoresis systems with the units, power supplies, and accessories required to perform protein separations. Elchrom recently introduced BlotEX, a new nonacrylamide, high-resolution electrophoresis precast hydrogel specifically designed to increase protein transfer efficiency during Western blotting of proteins. "This is specifically for low expressed proteins," Montagne says. "We aimed it at the pharmaceutical industry searching for new drugs."

At a more general level, Qiagen's Qproteome fractionation tools provide efficient isolation of targeted subsets of proteins. "The kits are easy to use and don't require any special equipment," Cassing says. "And our PhosphoProtein Purification Kit is the only product on the market for complete separation of phosphorylated proteins from unphosphorylated proteins." Another vendor, **Syngene**, has introduced DYMENSION, a software program that can analyze a typical 2-D gel image in seconds. MORE ›››

TaKaRa

Hungry for a new high fidelity PCR polymerase?
Try PrimeSTAR™ HS DNA Polymerase...extreme fidelity.

PrimeSTAR™ HS DNA Polymerase is a novel PCR enzyme that provides maximum fidelity as well as extended product length. Targeted for PCR products intended to be cloned, it offers extremely high accuracy together with high amplification efficiency.

Get a taste of easy, successful, high fidelity PCR with PrimeSTAR™ HS DNA Polymerase!

Extremely Low Error Rate

Sequencing results showed only 12/250,000 mismatched bases in DNA fragments amplified by PrimeSTAR™ HS, demonstrating incredible accuracy!

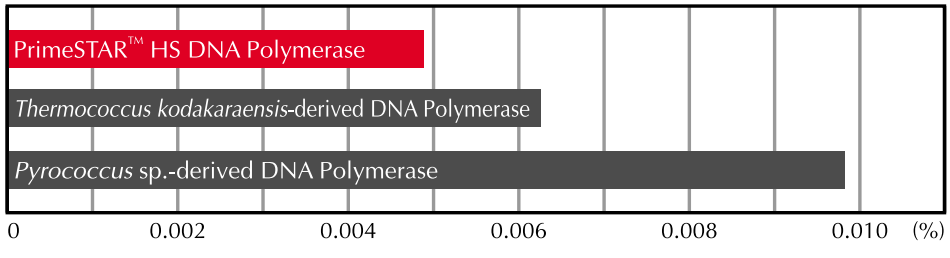

Excellent Amplification Efficiency

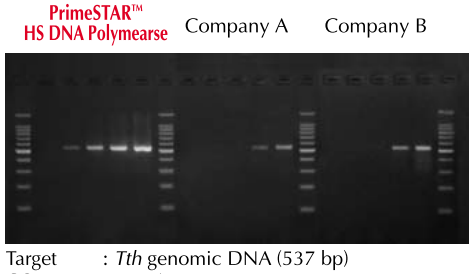

Target : *Tth* genomic DNA (537 bp)
GC-content : ~70%

TaKaRa PCR Related Products are sold under licensing arrangements with F. Hoffmann-La Roche Ltd, Roche Molecular Systems, Inc. and Applied Biosystems.

TAKARA BIO INC.
The Biotechnology Company™

Otsu, Shiga, Japan
Phone: +81 77 543 7247 Fax: +81 77 543 9254

USA: **Takara Mirus Bio Inc.** Toll Free Phone: 888 251 6618 Fax: +1 608 441 2845
Europe: **Takara Bio Europe S.A.S.** Phone: +33 1 41 47 23 70 Fax: +33 1 41 47 23 71
Korea: **Takara Korea Biomedical Inc.** Phone: +82 31 739 3300 Fax: +82 31 739 3311
China: **Takara Biotechnology (Dalian) Co., Ltd.** Phone: +86 411 8764 1681 Fax: +86 411 8761 9946

For more information and a list of Takara distributors worldwide, please visit our website today!

www.takara-bio.com

Science Online

Address: http://www.sciencenow.org

Q **Where can you read breaking science news right now?**

A ***Science*NOW:**
www.sciencenow.org

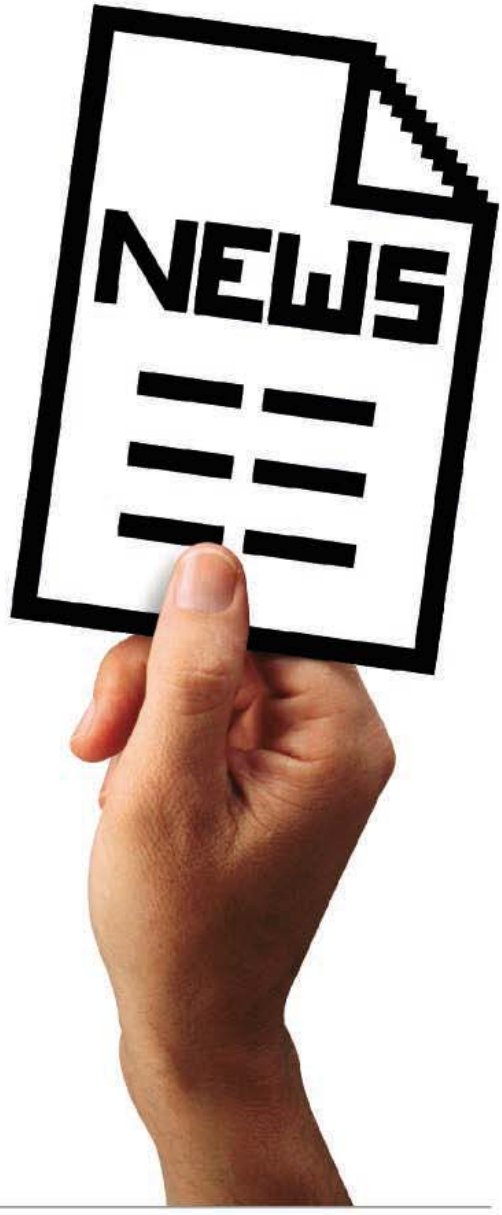

Science's team of tireless reporters works across global time zones to keep you informed—with daily updates of breaking news and current research published in leading science journals. The forefront of exploration and discovery, policy and funding, and science and technology breakthroughs from around the world is at your fingertips. Right now.

As an AAAS member, you have 24/7 access to *Science*NOW. Not a member? Sign up today at www.aaas.org/join

Science, published by AAAS, with over 700,000 readers weekly, is the world's most widely-read general science journal. Scientists around the world submit over 12,000 papers each year for evaluation, with only one in 12 making it into final publication. This rigorous process ensures the quality of material, whether it's research on proteomics, therapeutic cloning, nanotechnology, or dark matter. To find out how to subscribe to *Science*, go to **www.aaas.org/join**

Science
AAAS

PIERCE

Grasp the Proteome®

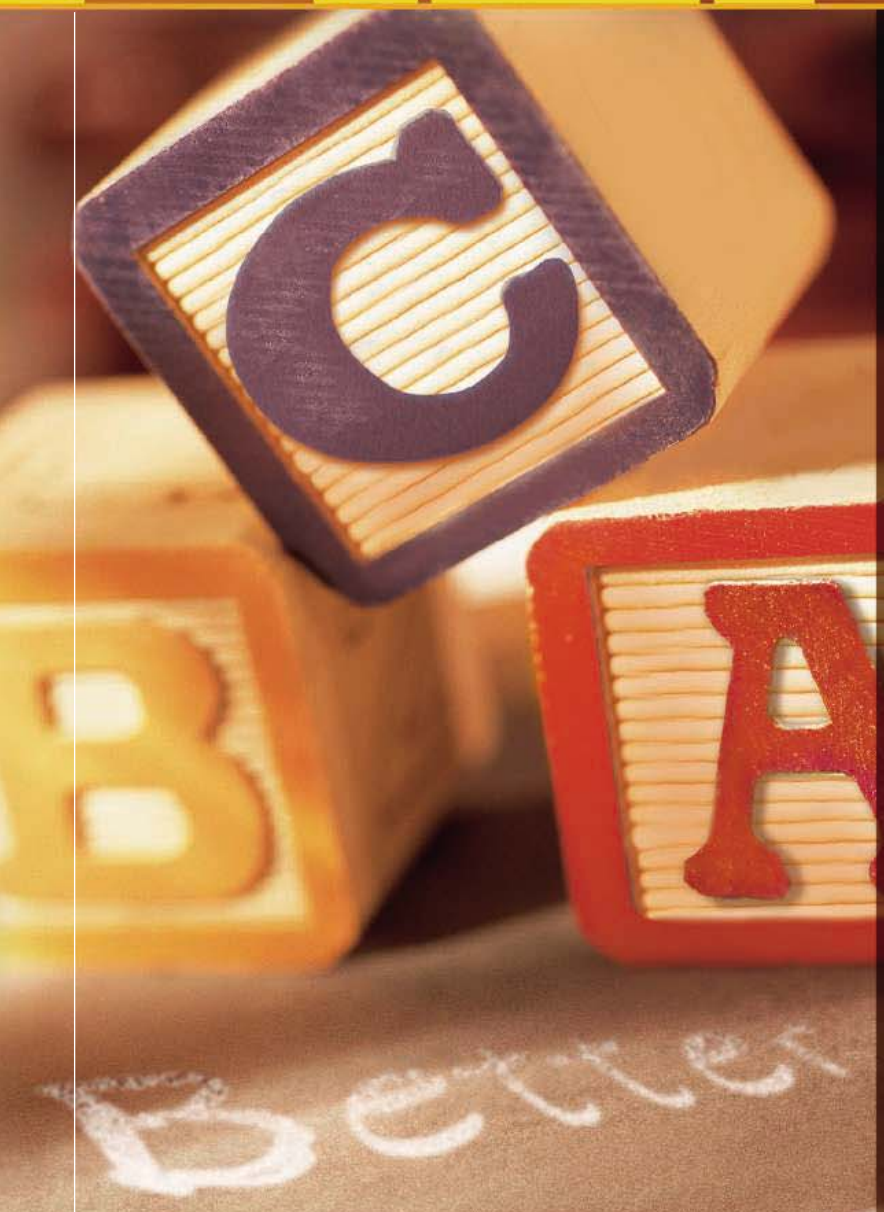

Plays well with others.

IT'S BETTER … THE NEWEST BCA™ PROTEIN ASSAY KIT FROM PIERCE IS NOW COMPATIBLE WITH REDUCING AGENTS

Highlights:

- Compatible with up to 5 mM DTT, 35 mM 2-mercaptoethanol or 10 mM TCEP
- Linear working range: 125-2,000 µg/ml
- Sample volume: 25 µl
- Compatible with most ionic and nonionic detergents
- Significantly less (14-23%) protein:protein variation than coomassie (Bradford)-based methods
- Colorimetric method; measure at 562 nm
- Easy-to-use protocol

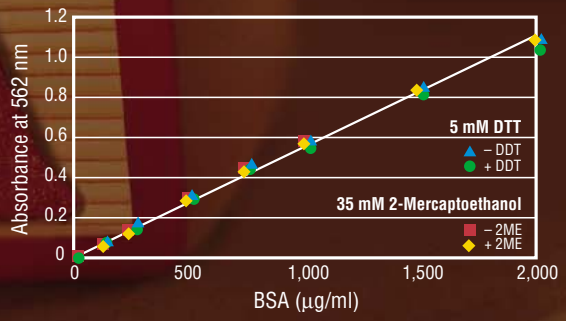

BCA™ Protein Assay – Reducing Agent Compatible produces a linear standard curve in the presence of reducing agents. Color response curves for BSA after treatment with Reducing Agent Compatible Reagent in the presence and absence of 5 mM DTT and 35 mM 2-mercaptoethanol. For data on 10 mM TCEP, visit our web site.

Ordering Information

Product #	Description	Pkg. Size
23250	BCA™ Protein Assay Kit – Reducing Agent Compatible *Sufficient reagents to perform 250 standard tube assays.*	Kit

Please visit our web site www.piercenet.com *for complete kit components.*

HURRY! Purchase the BCA™ Protein Assay Kit – Reducing Agent Compatible (Product # 23250) direct from Pierce by Oct. 31, 2005, and receive a FREE Pierce protein-patterned T-shirt. Mention this ad when placing your order. Offer valid in U.S. only. Void where prohibited.

www.piercenet.com/brac22j

PIERCE

ISO 9001 QUALITY SYSTEM CERTIFIED

Tel: 815-968-0747 or 800-874-3723 • Fax: 815-968-7316 • Technical Assistance E-mail: TA@piercenet.com • Customer Assistance E-mail: CS@piercenet.com

Outside the United States, visit our web site or call 815-968-0747 to locate your local Perbio Science branch office (below) or distributor

Belgium & Dist.:	China:	France:	Germany:	Hong Kong:	The Netherlands:	United Kingdom:	Switzerland:
Tel +32 53 85 7184	Tel +86 10 8049 9033	Tel 0800 50 82 15	Tel 0228 9125650	Tel 852 2753 0686	Tel 076 50 31 880	Tel 0800 252185	Tel 0800 56 31 40
euromarketing@perbio.com	support@perbio.com.cn	euromarketing@perbio.com	de.info@perbio.com	SalesHK@perbio.com	euromarketing@perbio.com	uk.info@perbio.com	euromarketing@perbio.com

PERBIO

FUJIFILM
I&I – Imaging & Information

Life Science

gDNA–The longer, the better !

QuickGene enables you to isolate longer gDNA.

Target: To detect bands of more than 30kb
Result: Target achieved

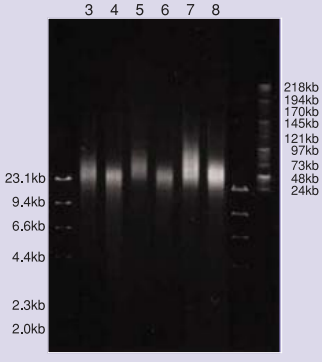

3	Tail	QuickGene-810
4		Spin Column
5	Liver	QuickGene-810
6		Spin Column
7	Lung	QuickGene-810
8		Spin Column

*Sample : Mouse *Processed with RNase

- Isolation of longer DNA made possible with FUJIFILM's innovative hydrophilic membrane technology.
- Rapid isolation with easy operation, isolating DNA in only 6 min.
- Stable RNA isolation
- Isolation with consistent high yield, high purity and high reproducibility, directly usable in PCR or RT-PCR.

Wide variety of protocols with reliable isolation kits

Isolation kits	Processing time
DNA whole blood kit (96 samples)	6 min / 8 samples
DNA tissue kit (96 samples)	13 min / 8 samples
Plasmid kit (96 samples)	6 min / 8 samples
RNA cultured kit (96 samples)	13 min / 8 samples
RNA tissue kit (96 samples)	13 min / 8 samples

QuickGene

Nucleic Acid Isolation System

QuickGene-810

DNA and RNA isolation with a revolutionary membrane

http:// lifescience.fujifilm.com [Download Brochures and Application guides in PDF form]

U.S.A., Canada
Fujifilm Medical Systems U.S.A.,
Tel : +1-203-324-2000 ext.6112
(1-800-431-1850 ext.6112 in the U.S.)
E-mail : SSG@fujimed.com

Europe (excluding UK, Ireland)
Fuji Photo Film (Europe) GmbH
Tel : +49-211-5089-174
E-mail : lifescience@fujifilmeurope.de

UK, Ireland
Fuji Photo Film (U.K) Ltd.
Tel : +44-1234-245291
E-mail : lifesciences@fuji.co.uk

China
Fuji Photo Film (China) Investment Co., Ltd
Tel : +86-21-3302-4655 ext.363
E-mail : wgxiang@fujifilm.com.cn

Japan & Others
Fuji Photo Film CO., Ltd.
Tel : +81-3-3406-2201
E-mail : sginfo@fujifilm.co.jp

» advances in: Proteomics

Three Means of Characterization

Once they have separated and purified their proteins, researchers can turn to a wide range of tools and techniques to characterize them. Two-hybrid systems, surface plasmon resonance (SPR), and mass spectrometry offer slightly different views of protein-protein interactions.

Proteins usually function in families or pathways and interact with related proteins. Researchers often begin their studies by trying to understand how a protein with unknown function relates to other known proteins. The two-hybrid method allows researchers to identify related proteins. The method, available in bacterial, yeast, and mammalian models from such companies as **Promega** and **Stratagene**, can identify protein-protein interactions, protein cascades, and mutations that affect protein-protein binding. "Nothing really compares with the original two-hybrid for screening thousands of potential interactions," says Andrew Farmer, director of cell and molecular biology at **BD Biosciences Clontech**. "But it can produce a lot of false positives."

To overcome that problem, Clontech has developed the BD Matchmaker Two-Hybrid System 3. "The tighter you can make the selection, the less the chance that false positives will come up," says Grigory Tchaga, the company's R&D director for protein and PCR Technologies. "In addition, scientists can use Clontech's pBridge Vector to create a three-hybrid system to screen for interactions that involve three proteins. And the BD Matchmaker One-Hybrid System reveals protein interactions with DNA sequences."

Another way to compensate for yeast two-hybrid's false positives involves pairing the method with SPR, otherwise known as protein interaction analysis, which allows researchers to gather real-time functional data about binding events. "If you use yeast two-hybrid, you need to confirm your data with a more reliable method," says Stephan Löfas, chief scientific officer of Swedish firm Biacore. "Here is where we come in. Our technology permits you to go into the details to confirm whether or not you have seen a real interaction. Also, you don't need to do the type of labeling that would disturb the interactions."

Protein Interaction Analysis and MS

Early this year Biacore introduced a new high performance instrument, the T-100. "Now, in response to demands for even greater productivity, we are introducing a protein interaction array, the Biacore A100," Löfas says. "The unique array-based format of this system enables parallel analysis and multiplexed assays."

Mass spectrometry also works well in collaboration with other separation methods. "2-D gel is a protein purification mechanism that reduces a complex sample to a number of discrete spots," Thermo Electron's Miller explains. "Mass spectrometry allows you to identify what those spots are." To perform the identification, scientists combine electrospray mass spectrometry with matrix-assisted laser desorption ionization-time of flight (MALDI-TOF) techniques. In addition, Miller continues, "Mass spectrometry paired with liquid chromatography seems to identify many more proteins than 2-D gels."

Pierce has paired mass spectrometry with another technology – the use of cross-linking reagents. "After in-gel tryptic digestion of the cross-linked complex, MS analysis of the resulting cross-linked peptides is facilitated," Vigna explains. "Bioinformatic analysis of these peptide masses can give information regarding the contact interface of the binding partners."

Several well-known companies, including Applied Biosystems and **Bruker Daltonics**, manufacture mass spectrometers. Thermo Electron has adapted its Finnigan LTQ family of mass spectrometers by adding additional detectors and a new orbitrap. "These instruments provide a much higher quality of data, accuracy, and resolution," Miller says. "They also create the ability to do top-down proteomics – determining exact protein isoforms. And we have added a MALDI source to the LTQ, giving a very rapid way to introduce samples at the front end. That permits thousands of experiments a month instead of the hundreds or dozens using conventional mass spectrometry."

Challenges remain for scientists who study protein-protein interactions. But the emergence and application of new tools and technologies has given researchers the opportunity to meet them more efficiently and more rapidly.

Peter Gwynne (pgwynne767@aol.com) is a freelance science writer based on Cape Cod, Massachusetts, U.S.A. Gary Heebner (gheebner@cell-associates.com) is a marketing consultant with Cell Associates in St. Louis, Missouri, U.S.A.

ScienceCareers.org

Classified Advertising

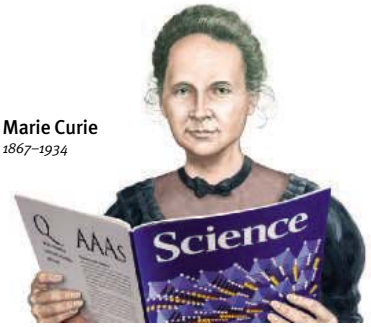

Marie Curie
1867–1934

For full advertising details, go to **www.sciencecareers.org** and click on **How to Advertise,** or call one of our representatives.

United States & Canada

E-mail: advertise@sciencecareers.org
Fax: 202-289-6742

JILL DOWNING
(CT, DE, DC, FL, GA, MD, ME, MA, NH, NJ, NY, NC, PA, RI, SC, VT, VA)
Phone: 631-580-2445

KRISTINE VON ZEDLITZ
(AK, AZ, CA, CO, HI, ID, IA, KS, MT, NE, NV, NM, ND, OR, SD, TX, UT, WA, WY)
Phone: 415-956-2531

KATHLEEN CLARK
Employment: AR, IL, LA, MN, MO, OK, WI, Canada; Graduate Programs; Meetings & Announcements (U.S., Canada, Caribbean, Central and South America)
Phone: 510-271-8349

EMNET TESFAYE
(Display Ads: AL, IN, KY, MI, MS, OH, TN, WV; Line Ads)
Phone: 202-326-6740

GABRIELLE BOGUSLAWSKI
(U.S. Recruitment Advertising Sales Director)
Phone: 718-491-1607

Europe & International

E-mail: ads@science-int.co.uk
Fax: +44 (0) 1223-326-532

TRACY HOLMES
Phone: +44 (0) 1223-326-525

HELEN MORONEY
Phone: +44 (0) 1223-326-528

CHRISTINA HARRISON
Phone: +44 (0) 1223-326-510

SVITLANA BARNES
Phone: +44 (0) 1223-326-527

JASON HANNAFORD
Phone: +81 (0) 52-789-1860

To subscribe to *Science*:
In U.S./Canada call 202-326-6417 or 1-800-731-4939
In the rest of the world call +44 (0) 1223-326-515

Science makes every effort to screen its ads for offensive and/or discriminatory language in accordance with U.S. and non-U.S. law. Since we are an international journal, you may see ads from non-U.S. countries that request applications from specific demographic groups. Since U.S. law does not apply to other countries we try to accommodate recruiting practices of other countries. However, we encourage our readers to alert us to any ads that they feel are discriminatory or offensive.

ScienceCareers.org
We know science AAAS

POSITIONS OPEN

RESEARCH GEOLOGIST
Department of Mineral Sciences
National Museum of Natural History
Smithsonian Institution

The Department of Mineral Sciences invites applications for the position of Research Geologist. Applicants should have a Ph.D. or equivalent experience with a background in one or more of the fields of mineralogy, meteoritics, volcanology, igneous or metamorphic petrology, or geochemistry of solid Earth materials evidenced through publication in the peer-reviewed literature. Preference will be given to those with a continuing commitment to a strong and innovative program of independent and collaborative research. In addition, we seek an individual who will utilize to its fullest capability the existing laboratory instrumentation of the Department of Mineral Sciences, which includes EPMA, FEG SEM, XRD, XRF, FTIR, TOF-SIMS and experimental laboratories. In addition to research, the successful candidate will be expected to participate in museum activities, such as exhibits programs, educational outreach activities, and involvement with professional associations and other organizations within the scientific community. Full-time, four-year term appointment with full government benefits; GS-1350-12; *U.S. citizenship required.* Salary starting is $62,866 per annum. Completed applications must be mailed to: **Smithsonian Institution, Office of Human Resources, ATTN: A. Davis, P.O. Box 50638, Washington, DC 20091-6038**, and must include (1) complete curriculum vitae including list of all peer-reviewed publications, and all extramural grants received with agencies, funding periods and amounts; (2) one set of reprints (no more than three); (3) list of at least five individuals from whom objective letters of professional evaluation may be sought; and (4) cover letter addressing the selective and quality ranking factors which appear in the announcement. Reference additional application procedures in actual announcement – see **website: http://www.sihr.si.edu** or contact **Audrey Davis at telephone: 202-275-1005.** Applications must be received by October 31, 2005, and must reference announcement number 05AD-1234. All applicants will be notified by e-mail or telephone when their application is received. *The Smithsonian Institution is an Equal Opportunity Employer.*

TENURE-TRACK FACULTY POSITION
Developmental Biology Georgetown University
Department of Biology

Applications are invited for a tenure-track position to commence August 2006 at the **ASSISTANT** or (possibly) **ASSOCIATE PROFESSOR** level. This position requires excellence in research and the ability to teach undergraduate and graduate students with innovation and effectiveness. We seek an energetic investigator, actively pursuing fundamental research questions in developmental or evolutionary developmental biology who will complement strengths of present faculty and extend the breadth of our program. The successful applicant will offer two courses per year, including an upper level course that complements his/her area of expertise. Research expectations include establishment of a vigorous, grant-supported research program that involves both graduate and undergraduate students. The successful applicant will have a Ph.D. degree, relevant postdoctoral experience, and demonstrated ability as an instructor. Applications should include: (1) a full curriculum vitae, (2) three letters of reference addressing the applicant's research and teaching accomplishments, (3) a statement of research interests and projected research program, and (4) a statement describing the applicant's teaching philosophy. Review of completed applications will begin November 1, 2005, and continue until the position is filled. Please send application materials to: **Developmental Biology Search Committee, Georgetown University, Box 571229, Washington, DC 20057.** *Georgetown University is an Affirmative Action/Equal Opportunity Employer.*

POSITIONS OPEN

ASSISTANT OR ASSOCIATE PROFESSOR
Plant Evolutionary Biology and Systematics
University of Alberta
Department of Biological Sciences

The Department of Biological Sciences invites applications for a tenure-track position at the Assistant or Associate Professor level in plant evolution and systematics. Excellent applicants will be considered from a range of subdisciplines (systematics, population genetics, evolutionary ecology, etc.), who have expertise in phylogenetic analysis and plant taxonomy. The successful candidate will be expected to serve as the Director of the Department's vascular plant herbarium (ALTA). The candidate must have a strong record of research and demonstrated potential for excellence in teaching.

The University of Alberta offers a competitive salary commensurate with experience and an excellent benefits plan. The Department of Biological Sciences (**website: http://www.biology.ualberta.ca/**) consists of 70 faculty members and 275 graduate students, offering an exciting environment for collaboration with strong research groups in evolution and systematics, ecology, and plant biology. Exceptional infrastructure includes extensive research collections in diverse taxa (**website: http://www.museums.ualberta.ca/**), field stations, plant growth facilities, and service units in molecular biology, plant/soil chemical analysis, microscopy, imaging, and GIS.

Candidates should submit curriculum vitae, a one-page summary of research plans, a statement of teaching interests and reprints of their three most significant publications electronically to: **e-mail: positions@biology.ualberta.ca** or by mail to:

Dr. L. S. Frost, Chair
Department of Biological Sciences
CW 405 Biological Sciences Building
University of Alberta
Edmonton, Alberta, Canada T6G 2E9

Applicants must also arrange for three letters of reference to be sent to the Chair. Closing Date: October 15, 2005. The effective date of employment will be July 1, 2006.

All qualified candidates are encouraged to apply; however, Canadians and permanent residents will be given priority.

The University of Alberta hires on the basis of merit. We are committed to the principle of equity in employment. We welcome diversity and encourage applications from all qualified women and men, including persons with disabilities, members of visible minorities, and Aboriginal persons.

DIRECTOR
Transgenic/Gene Targeting Facility

The Transgenic and Gene Targeting Facility at the University of Kansas Medical Center is looking to hire a **RESEARCH ASSISTANT/ASSOCIATE PROFESSOR** as Director of the transgenic and gene targeting facility. Qualifications include a Ph.D. in biology or related field and at least two years of experience with all phases of transgenic and gene-targeted mouse production, colony maintenance, and animal husbandry. He/she must be proficient in pronuclear and blastocyst injection, embryonic stem cell culture and manipulation for gene targeting, embryo transfer, sperm cryopreservation, and rederivation. The individual is expected to manage facility operations, participate in the design and generation of transgenic and knockout mice, develop technologies to enhance the facility, and oversee two highly motivated technical assistants. Salary will be commensurate with experience. Interested individuals should send their curriculum vitae along with contact information for three references to: **Leslie L. Heckert, Ph.D., Chair, Search Committee, Department of Molecular and Integrative Physiology, University of Kansas Medical Center, 3901 Rainbow Boulevard, Kansas City, KS 66160. Fax: 913-588-7430; e-mail: lheckert@kumc.edu.** *Equal Opportunity Employer.* Paid for by KUMC.

TU/e technische universiteit eindhoven

PhD student Tanya Nimalasuriya is working on a new HID lamp with potential energy savings of up to 50%.

Great opportunities for women in science

www.tue.nl/women-in-science

Career paths leading to Associate Professorships: *Outstanding women candidates with a PhD and relevant post-doctoral experience in research institutes or industry are invited to apply for one of five tenure track research positions at the Eindhoven University of Technology (TU/e). These positions open the way to six-year programs leading to fixed Associate Professorship tenures.*

TU/e is a research-driven, design-oriented university in engineering science & technology with 7000 students and 3000 staff. It offers (pre-)graduate engineering and teacher training programs (BSc and MSc), post-graduate technological design (PDEng) and PhD programs, and post-academic continuing education. TU/e coordinates prominent Dutch research schools and institutes, and has a strong position in international research networks. It is a natural partner for technology-intensive enterprises, and the campus is a fertile breeding ground for new business ventures.

The TU/e is **one of Europe's leading universities** in engineering science & technology. Located in the technological heart of the Netherlands, with a strategic position as one of Europe's leading technology centers, the TU/e has internationally renowned research groups. More than thirty per cent of its researchers come from other countries. The TU/e encourages diversity in its teaching and research programs at all levels.

Five tenure tracks

The TU/e is offering **challenging career paths for talented women** scientists. Five tenure tracks lead to fixed appointments as Associate Professor in some of the university's priority research profiles:

- Polymer Science and Technology
- Biomedical Engineering Sciences
- Nano-engineering of Functional Materials and Devices
- Broadband Telecommunication Technologies
- Catalysis and Process Engineering
- Mechanics and Control
- Science and Engineering of Embedded Systems
- Logistics and Operations Networks

To be a successful candidate, you will have a strong drive to excel in your career as a top innovative scientist. You are an ambitious PhD with relevant post-doctoral experience in research institutes or industry. You have clear potential to ultimately reach a full professorship position, and the ability to combine boundary-breaking, innovative research with teaching and supervising students' research projects. Your academic achievements, recognized by publications in leading international scientific journals, are matched by the ability to successfully compete for external funding.

For more information about these opportunities, the requirements and the procedure for application, as well as about the TU/e in general, please visit our website www.tue.nl/women-in-science or contact Mrs. E. Schmal, HR policy coordinator, e.schmal@tue.nl tel. +31 40 2478314.

The closing date for applications is 20 October 2005.

Staff Scientist in Molecular Regulation of Cytochrome P450s
Research Triangle Park, North Carolina

The Laboratory of Pharmacology and Chemistry at the National Institute of Environmental Health Sciences is recruiting a staff scientist in support of the Human Metabolism Group headed by Dr. Joyce Goldstein. The recruit will be responsible for individual research and collaborative efforts involving some oversight of the molecular biology and genetics efforts by the group. In particular, the incumbent will focus efforts on generating clones of regulatory regions in appropriate vectors for studies in cell culture models and genetically modified mice to investigate the mechanisms through which drugs, hormones, physiological stimuli regulate CYP genes through receptors, regulatory elements and transcription factors. Current major projects include: regulation of human and murine CYP2C genes by drugs, hormones, and physiological changes via elements within promoter regions which bind nuclear receptors and transcription factors such as CAR, PXR, HNF4 and coregulators. The successful candidate is expected to work with minimal guidance, carry the research to publishable stages and work on these and other projects as defined by the group leader.

Minimum qualifications include a doctoral degree, successful completion of postdoctoral training, strong publication record and experience in biochemistry and molecular biology, emphasizing molecular techniques involved in studying gene regulation, such as construction and use of luciferase-promoter constructs for use in cell models and murine models, expression vectors for nuclear receptors, construction of clones containing large complex regulatory regions, and use of multi-component plasmid vectors. Specific familiarity with cytochrome P450 regulation by nuclear receptors, antioxidant elements and background in protein chemistry related to identification of corepressors and coactivators of receptors (e.g. DNA chromatography, ChIP assays, yeast-two hybrid assays, GST pulldown) as evidenced by publication record is desirable.

For additional information, contact **Dr. Joyce Goldstein at 919-541-4495 or goldste1@niehs.nih.gov.** For additional information concerning the research projects and publications of the Human Metabolism Group, visit the following website: **http://dir.niehs.nih.gov/dirlpc/.** Applications from women and minorities are particularly encouraged. **To apply,** submit a curriculum vitae, bibliography, references, brief statement of research interests and arrange for three letters of recommendation to be sent by **November 15, 2005**, to the following address. Applications received after that date will be considered as needed:

Ms. Lisa Rogers (DIR05-09), National Institutes of Health, National Institute of Environmental Health Sciences, P.O. Box 12233, Maildrop, A2-06, 111 Alexander Drive, Room A208, Research Triangle Park, NC 27709, E-mail: dir-appls@niehs.nih.gov

Staff Scientist in Molecular Toxicology
Research Triangle Park, North Carolina

The Laboratory of Molecular Toxicology at the National Institute of Environmental Health Sciences is recruiting a staff scientist in support of the Comparative Genomic Group headed by Dr. Jonathan Freedman. The recruit will be responsible for oversight of the molecular genetics and toxicogenomic efforts by the group. In particular, the successful applicant will be expected to participate in the development of studies using alternative model species (e.g., yeast, C. elegans, Drosophila, Zebrafish) to investigate the molecular mechanisms by which organisms respond to exposure to environmental toxicants. Current major projects include: identification and characterization of intracellular signal transduction pathways affected by transition metal exposure; investigation of mechanisms underlying the detoxification of metals using microarray analysis and comparative genomics; development of heterologous expression systems to examine the mechanism of action of the metal responsive transcription factor (mMTF-1) in order to understand the mechanism of regulation of metal-responsive gene expression in mammals; development of sensitive reporter systems to assess toxicity and mutagenicity of environmental toxicants including metals, drugs and other stressors.

The successful candidate is expected to work with minimal guidance, carry the research to publishable stages and work on these and other projects as defined by the group leader. Minimum qualifications include a doctoral degree, successful completion of postdoctoral training, strong publication record and experience in molecular biology, molecular genetics, toxicogenomics, and high-throughput functional analyses.

For additional information, contact **Dr. Jonathan Freedman** at **freedma1@niehs.nih.gov**. Applications from women and minorities are particularly encouraged. **To apply**, submit a curriculum vitae, bibliography, brief statement of research interests and arrange for three letters of recommendation to be sent by **October 14, 2005** to the following address. Applications received after that date will be considered as needed:

Ms. Cindy Garrard (DIR 05-10), National Institutes of Health, National Institute of Environmental Health Sciences, P.O. Box 12233, Mail drop A2-06, 111 Alexander Drive, Room A206, Research Triangle Park, NC 27709, E-mail: dir-appls@niehs.nih.gov

WWW.NIH.GOV

Health Scientist Administrator

The National Institute on Drug Abuse (NIDA), a major research component of the National Institutes of Health (NIH) and the Department of Health and Human Services (DHHS), is recruiting for a Health Scientist Administrator (HSA). The incumbent serves as HSA in the Science Policy Branch of the Office of Science Policy and Communications. The incumbent: (1) Develops position statements on science and science policy issues related to clinical, behavioral and/or social research, which requires expert knowledge of how these research areas relate to drug abuse and addiction; (2) responds to inquiries from all levels of the Department, other federal agencies, the scientific community, and the general public; (3) works with program staff to develop, direct, and implement the science-based strategic planning and evaluation processes for NIDA's research programs in the areas of clinical, behavioral, or social sciences; and (4) represents the Institute before professional, scientific and public interest groups, as well as interagency task forces.

Successful completion of all requirements for an M.D. or a Ph.D (or equivalent doctoral degree) in an accredited college or university, including (for a Ph.D.) acceptance of the dissertation, in an academic field of the behavioral or health sciences, which has been applied and utilized by the applicant in health or health-related research.
In addition, applicants must have at least one year of specialized experience at the next lower grade level, or equivalent. Specialized experience is experience that is directly related to the position to be filled, and which has equipped the applicant with the particular knowledge, skills, and abilities needed to successfully perform the duties of the position. Annual salary range is $74,782 - $114, 882. A full Civil Service benefits package is available. Physicians may also be eligible for a Physicians' Comparability Allowance of up to $30,000 per year. The position is located in Rockville, Maryland.

APPLICATIONS (RESUME AND APPLICATION QUESTIONS) MUST BE RECEIVED ON-LINE VIA THE HHS CAREERS WEB SITE BEFORE MIDNIGHT EASTERN STANDARD TIME ON THE CLOSING DATE OF THIS ANNOUNCEMENT. PLEASE SEE BELOW FOR DETAILS ON USING THE HHS CAREERS SYSTEM.
For additional information on this position, and for instructions on submitting your application, please see our website, at: **http://www.nida.nih.gov/ or https://jobs.quickhire.com**. Detailed information is provided under vacancy announcement number: **NIDA-05-. 96176DE** Supplemental documentation must be submitted to: **Nancy Delgais, National Institutes of Health, 111 Alexander Drive, Maildrop NH-01, Research Triangle Park, NC 27709 or faxed to 919-541-3659.**

Deputy Director
Division of Intramural Research
National Eye Institute

The Division of Intramural Research, NEI, is searching for a Deputy Scientific Director to work with the Scientific Director in leading and managing the NEI intramural research program and in monitoring, coordinating, and evaluating all aspects of the program's progress in achieving its goals and objectives. The mission of the DIR is twofold: (1) to advance knowledge of how the visual system functions in health and disease using a combination of basic, translational, and clinical science; (2) to develop effective means of prevention, treatment, and rehabilitation for diseases of the eye and visual system. The DIR consists of 32 Principal Investigators and more than 250 scientific support personnel. The laboratory and clinical scientists carry out interdisciplinary studies in genetics, cell and developmental biology, immunology, systems neuroscience, and conduct phase I, II and III clinical trials. In-house core support services include histology, imaging, and knock out and transgenic rodent facilities, and an extensive veterinary research and resources unit.

Applicants for this position must have significant research and administrative experience, an M.D., Ph.D., or equivalent degree in the biomedical sciences, and experience and understanding of administrative policies, procedures, operations, and technology development in a large biomedical research institution. The incumbent's primary responsibilities would be administrative but the possibility exists for some limited individual research activity. The applicant must be a highly collaborative person able to work with diverse groups of individuals, in and out of NIH/NEI. He or she should have skills in science leadership and communication and be innovative in maximizing the impact of available resources. Applicants should submit a curriculum vitae and bibliography to the following address: **Sheila Ayala, Staff Assistant, Office of the Scientific Director, National Eye Institute, Building 31, Room 6A22, 31 Center Drive, Bethesda, MD 20892, Tel: 301-451-6763, EM: sayala@nih.gov**

Tenure-Track Positions
National Institute of Dental and Craniofacial Research

The National Institute of Dental and Craniofacial Research recently established a new Laboratory of Oral Sensory Biology to investigate fundamental mechanisms of sensory perception. The Institute now seeks to recruit Tenure Track Investigators who will establish independent programs within this general area of biology. It is anticipated that successful applicants will use a combination of modern molecular, genetic, cellular, physiological and/or imaging approaches to answer questions about how oral sensory information is detected, encoded and ultimately interpreted by the brain. Candidates must hold a Ph.D, D.D.M, D.V.M, D.D.S., M.D. or equivalent degree and have at least 2 years relevant postdoctoral research experience; salary will be commensurate with experience and qualifications. Additional information on the position may be obtained from **Dr. Nicholas Ryba (nick.ryba@nih.gov)**. Applicants must be US citizens, resident aliens, or non-resident aliens with or eligible to obtain a valid employment authorized visa. A letter of intent, curriculum vitae, bibliography, statement of past accomplishments and future plans, and three letters of reference should be sent to: **LOSB Search Committee, 10 Center Drive, MSC 1188, Building 10 Room 1N106, Bethesda, MD, 20892-1188, USA.** Review of applications will begin **November 18, 2005**, but the NIDCR will continue to accept applications received after that date until the positions are filled.

United States
National Institute of Diabetes & Digestive & Kidney Diseases
of the National Institutes of Health

Research Opportunity at the NIH, DHHS
DIRECTOR, OBESITY CLINICAL RESEARCH CENTER AND CHIEF, DIABETES BRANCH, NIDDK

The Intramural Research Program (IRP) of NIDDK invites applications for the combined position of Chief of the Diabetes Branch and Director of a newly established, NIH-wide initiative in patient-oriented research in obesity ("Obesity Clinical Research Center" – OCRC). The Diabetes Branch, NIDDK conducts basic, translational and clinical research in the areas of diabetes mellitus and obesity. The Chief is responsible for all activities of the Branch, in particular, for integrating the research programs of the several senior investigators and the career development of junior investigators. The goal of the OCRC, which will involve researchers from all Institutes and Centers within the NIH IRP, is to generate knowledge of the pathophysiology, prevention and treatment of obesity and its multisystem co-morbidities, especially type 2 diabetes mellitus. The approach is: 1) to create a center in which to conduct state-of-the-art, patient-oriented obesity research, including metabolic analysis and imaging capabilities, that would support IRP scientists and serve as a magnet facility to foster collaborations with extramural researchers; and 2) to foster multidisciplinary approaches to obesity research, including metabolism, endocrinology, nutrition, gastroenterology, hepatology, imaging, genetics and behavioral sciences.

Priority will be given to applicants at the Professor or Associate Professor level in clinical departments of traditional academic medical centers, or in equivalent positions. The applicant must have a proven record of accomplishments, including evidence of significant, competitively obtained funding for extramural investigators. The appointment will be as a tenured Principal Investigator within NIDDK. The successful candidate will be expected to coordinate the multidisciplinary research proposed for the OCRC and the Diabetes Branch. The position offers unparalleled opportunity to lead a state of the art program in diabetes/obesity research. Salary and benefits are commensurate with the experience of the applicant.

The Diabetes Branch laboratories are in the Warren G. Magnuson Clinical Center and the OCRC Patient Care Unit is a self-contained, metabolic unit located in the new Mark O. Hatfield Clinical Research Center, which are contiguous on the main intramural campus of the NIH in Bethesda, Maryland, a suburb of Washington, D.C.

Interested applicants should send a Curriculum Vitae and list of publications, copies of three major publications, a summary of research accomplishments, a plan for future research and three letters of recommendation to **Dr. James E. Balow, Chair, Search Committee, c/o Ms. Giulia Verzariu, Office of the Scientific Director, NIDDK, Building 10, Room 9N222, NIH, Bethesda, MD 20892.**

Closing Date: October 1, 2005

Department of Health and Human Services
National Institutes of Health
National Institute of Diabetes and Digestive and Kidney Diseases
Equal Opportunity Employers

DuPont Central Research and Development

New Positions at DuPont

DuPont, a science-based company leading the introduction of biotechnology for industrial applications, is seeking Principal Investigators in several areas to join its Central Research and Development organization.

Enzymologist/Protein Engineer
The successful candidate will use their knowledge of enzyme function to develop biocatalytic routes for making chemicals and materials. The work will include identification, expression, and characterization of potential enzyme catalysts, carrying out directed evolution, and designing automated screens to detect enzymatic improvement. The candidate must have advanced knowledge of biochemistry with emphasis in enzyme function, consistent with a PhD in biochemistry or chemistry, and 2+ years of postdoctoral training. Code: RES00333

Microbial Physiologist
This position requires a Ph.D. in Microbiology with a minimum of two years of postdoctoral training and demonstrated strong experience in microbial physiology, molecular genetics, and biochemistry. The successful candidate will have broad understanding of microbial metabolism, including, for example, interactions in complex communities, anaerobic metabolism, and biofilms, and will have a demonstrated track record of patents and /or publications in microbial physiology. Code: RES00331

Organic Chemist/Polymer Chemist
The successful candidate will develop new specialty polymeric materials and formulations as part of a multidisciplinary team focused on medical devices and will be expected to translate customer requirements into concepts for new materials. The position is open to candidates with a Ph.D. in Organic Chemistry or Polymer Chemistry. Demonstrated knowledge of synthetic and mechanistic organic chemistry and/or polymer chemistry is expected. Experience with polymeric materials in medical applications is a plus. Code: RES00329

Chemical Engineer - Polymers
The successful candidate will develop formulations and scale-up for new specialty polymers as part of a multidisciplinary team focused on medical devices. The successful candidate will evaluate process options and conduct experiments to develop commercial processes that meet customer needs. The position is open to candidates with a Ph.D. in Chemical Engineering - Polymers. Demonstrated knowledge of polymer chemistry and chemical engineering principles of polymers is expected. Experience with polymeric materials in medical applications is a plus. Code: RES00330

Environmental Microbiologist
This position requires a Ph.D. in Microbiology with a minimum of two years of postdoctoral training and demonstrated strong experience in microbial ecology, molecular biology, genetics, adaptive mutagenesis, and environmental chemistry. The ability to work with environmental samples from aerobic and anaerobic environments, an understanding of microbial metabolism, and a demonstrated track record of patents and/or publications in environmental microbiology are desired. Code: RES00332

Fermentation Scientist
The successful candidate will possess a strong background in microbial physiology and will be directly responsible for strain evaluation and the development of scaleable fermentation processes in the context of a larger multidisciplinary metabolic engineering effort. To accomplish these goals this individual will have a demonstrated ability to derive quantitative understanding of physiological responses to changes in process conditions and genetic manipulations as derived from the design, execution, and analyses of fed-batch and continuous fermentation experiments. Code: RES00334

DuPont offers an attractive salary and comprehensive benefits. Qualified candidates should apply through DuPont's career web page: http://careers.dupont.com
Click on: Jobs by Region/United States/View US Job Listings
Enter the code in the keyword field (use the new search button for successive searches)

DuPont is an Equal Opportunity Employer.

West Virginia University
Robert C. Byrd Health Sciences Center
School of Medicine
Chair, Department of Biochemistry and Molecular Pharmacology

West Virginia University (WVU) is seeking an accomplished investigator and academic leader to serve as Professor and Chair, Department of Biochemistry and Molecular Pharmacology, School of Medicine. The successful candidate will have strong leadership skills and a creative vision of how to achieve the research, education and service missions of a basic science department in today's multidisciplinary research environment. Research in the Department encompasses diverse areas of investigation, and the educational mission includes graduate and professional training. The WVU Health Sciences Center recently implemented a new institutional Strategic Research Plan (SRP) designed to promote biomedical, behavioral and translational research in a multidisciplinary environment. The SRP established six core Research Centers (Cancer, Respiratory, Cardiovascular, Immunology/Microbial Pathogenesis, Neuroscience, and Obesity/Diabetes). Directors for five of the Centers have already been appointed. The Director of the Obesity/Diabetes Center is yet to be filled and could be coupled with the Biochemistry and Molecular Pharmacology Chair position for applicants with appropriate scientific backgrounds. An important responsibility of the new Chair will be to integrate the traditional Departmental missions of research, education, and service with the broader institutional goal of developing multidisciplinary research initiatives such as NIH Program Project or Center Grants through collaboration with faculty in other departments and the Centers.

Successful candidates will have a distinguished record of research and scholarly accomplishments, outstanding leadership ability, and a record of extramural funding. Skills and the desire to lead and administer diverse educational initiatives of the Department are essential. The position includes a salary competitive at the National level, laboratory space with a generous start-up package, administrative support and resources to recruit faculty.

As part of the commitment to research expansion in the Health Sciences Center, a new research building is planned as well as continued support for and strengthening of core research facilities for proteomics and protein sequencing, cell imaging, and transgenics. These facilities will complement the current expansion of the library and teaching facilities and the Blanchette Rockefeller Neurosciences Institute. West Virginia University is a comprehensive, land grant, and Carnegie-designated Doctoral/Research - Extensive institution, with approximately 26,000 undergraduate and 5,500 graduate students. The WVU Health Sciences Center includes the Schools of Medicine, Pharmacy, Dentistry and Nursing. Each school has both health professional and graduate training programs. The School of Medicine has well-established PhD programs in the biomedical sciences and a joint MD/PhD Scholar program. A Graduate training program in public health is also administered in the School of Medicine. Morgantown has 55,000 residents and is rated as one of the best small towns in the U.S., with affordable housing, excellent schools, a picturesque countryside and many outdoor activities.

Qualifications: PhD or MD degree with a solid record of excellence in research, the ability to attract and sustain NIH funding, and experience in graduate and professional student education. It is very important that the candidate be able to bridge the boundaries of traditional disciplines, including the promotion of collaborative, translational research efforts between basic and clinical faculty. The position will remain open until filled. Submit curriculum vitae, cover letter and three references (in confidence) to: **Dr. Richard Dey, Chair, Neurobiology and Anatomy, Chair, Search Committee, West Virginia University Health Sciences Center, PO Box 9128, Morgantown, WV 26506-9128**. CV's submitted by e-mail should be forwarded to the Administrative Assistant (**cbsmith@hsc.wvu.edu**).

West Virginia University is an Affirmative Action/Equal Opportunity Employer.

Assistant Professor
Tenure Track

The Medical Biotechnology Center (MBC) of the University of Maryland Biotechnology Institute (UMBI) seeks applications for a tenure track faculty position at the Assistant Professor level (position **#300437**). The MBC is one of five research centers of the UMBI (**http://www.umbi.umd.edu**). The MBC is located on the campus of the University of Maryland, Baltimore, in a newly constructed state-of-the-art research facility.

We seek outstanding candidates with expertise in one or more of the following disciplines: molecular and cell biology, cellular physiology and biophysics, transgenics, or functional genomics/proteomics. The current faculty share a common interest in the examination of cellular signals at the molecular level. The ideal candidate will focus on research that broadly complements our current areas of expertise and that harmonizes with the theme of "molecular signaling". The primary criteria for evaluation of candidates will be a record of excellence, originality and productivity in research. We offer an outstanding collaborative environment with a highly competitive salary and start-up package.

Applicants should send (preferably via CD) a letter of application (reference position **#300437**), a complete and current curriculum vitae, a description of research accomplishments, a two-page statement of research interests and objectives. In addition, arrange to have 3 letters of reference sent, preferably from two or three institutions. All materials (including letters of reference) must be received for the application to be considered. Review of applications will begin **September 30, 2005** and continue until a suitable candidate is selected. Please send applications and letters of reference to: **Mr. T. Hughes, Coordinator, Faculty Search Committee, MBC, University of Maryland Biotechnology Institute, 725 W. Lombard Street, Baltimore, MD 21201, USA**.

MBC/UMBI is an Affirmative Action/Equal Opportunity Employer. Women, minorities, veterans, and candidates with disabilities are encouraged to apply.

Senior Associate Dean for Research
University of Illinois at Chicago (UIC)

The University of Illinois at Chicago is seeking candidates for the position of Senior Associate Dean for Research. This is a senior leadership position with direct reporting to the Dean of the College of Medicine. UIC College of Medicine currently has greater than 220 grants, 110 million dollars in expenditures and had 21% growth in RO1s last year. The total campus grant support is 240 million dollars. The Senior Associate Dean for Research is responsible for advising the Dean on major research decisions for the medical school, recruitment of department heads and center directors, management and allotment of research space, administration of research programs, oversight of training of graduate and postdoctoral students, and working with department heads to develop cross departmental thematic research programs. A key requirement is facilitation of new research programs between clinical and basic science departments. The ideal candidate will have a history of an established extramurally funded research program, experience in administration of both basic and clinical science research programs, be a nationally known respected academician in their specialty, and have had successful experience with a collaborative work environment.

Candidates should be eligible for appointment in a basic science or clinical department at senior rank with tenure.

For fullest consideration, nominations and/or letters of application, along with CV and three references, should be submitted by **November 1, 2005** to: **Sarah J. Kilpatrick, MD, PhD, Professor and Head, Department of Obstetrics and Gynecology, Interim Associate Dean for Research, Chair of the Senior Associate Dean for Research Search Committee, M/C 808, 820 South Wood St., Chicago, IL 60612. phone: (312) 996-7006, fax: (312) 413-1857, e-mail: sarahk@uic.edu**.

UIC is an Affirmative Action/Equal Opportunity Employer. Women and minorities are encouraged to apply.

DEAN
The College of Earth and Energy
and
Lester A. Day Family Chair and Director of the Sarkeys Energy Center
The University of Oklahoma

The University of Oklahoma invites nominations and applications for the joint positions of inaugural Dean of the College of Earth and Energy and the Lester A. Day Family Chair and Director of the Sarkeys Energy Center. This new College, which will begin operation in January 2006, brings together the University's world-renowned academic programs in Petroleum and Geological Engineering, and Geology and Geophysics, with the Oklahoma Geological Survey and the Sarkeys Energy Center. The Dean and Director will be a visionary, dynamic and energetic leader who will chart a bold course for the future to engage multiple disciplines and industries in the study of the Earth and energy.

The New College: The College of Earth and Energy is being formed as a response to new challenges in energy and Earth sciences that require a coordinated, multi-disciplinary approach involving academic programs, research centers and institutes, and policy- and service-related organizations. The new College emphasizes science and engineering in all forms of energy; Earth science; and energy management and policy to address the human, business and societal dimensions that are essential to the future. The College also recognizes the importance of linkages with industry and the development of innovative programs that link academia with practice. The units composing the College currently enroll 235 undergraduate and 187 graduate students and employ 50 faculty and 79 administrative and technical staff. The combined research expenditures of these units in 2004-05 (FY05) were $4,440,424.

Responsibilities: The Dean and Director provides overall academic, intellectual and administrative leadership for the College of Earth and Energy and reports to the Senior Vice President and Provost. The successful candidate will be awarded the endowed Lester A. Day Family Chair as Director of the Sarkeys Energy Center. The Dean and Director is responsible for the quality and effectiveness of instructional, research and service programs and serves as the chief spokesperson with external constituencies including advisory boards, donors and the private sector. Further, the Dean and Director has overall responsibility for decision-making in the areas of faculty and staff recruitment, development and retention; resource allocation; and facilities and equipment management, and also actively promotes diversity.

Qualifications: Candidates must have an earned doctorate or equivalent experience and be eligible for appointment as a faculty member in a school of the College at the rank of Professor with tenure. Preference will be given to candidates with a strong commitment to education as demonstrated by success as an instructor in higher education, in industry or government training or outreach programs, etc.; a distinguished record of scholarly research nationally and internationally; outstanding administrative leadership and management skills, fund-raising capabilities, and a working knowledge of higher education. The candidate also must possess effective communication and interpersonal relation skills for establishing wide contacts within the University and beyond, including those with leaders in business, industry and government, and for working effectively with the diverse disciplines within the College. Candidates with executive experience in business, industry and government are encouraged to apply.

The University: Established in 1890, the University of Oklahoma is a public research university that enrolls over 23,000 students at its main campus in Norman and an additional 7,000 students at the Health Sciences Center in Oklahoma City, the Schusterman Center in Tulsa and in continuing education programs. The University ranks first nationally among public institutions in the number of National Merit Scholars per capita and is developing a new Research Campus, contiguous to its main campus, that collocates University, government and private sector components to promote synergy for mutual benefit. Located 20 miles south of Oklahoma City, Norman is rich in culture and the arts with outstanding public schools and a variety of recreational resources.

Applications and Nominations: The search committee will begin screening applications on **1 October 2005** and the search will continue until the position is filled. The preferred start date is 1 January 2006. Applications should include a letter of interest demonstrating how the candidate fulfills the qualifications for this position, a complete curriculum vitae or resume, and the names and addresses of at least six references. Nominations and applications should be directed to:

Paul B. Bell, Jr., Search Committee Chair
Dean, College of Arts and Sciences
Vice Provost for Instruction
Ellison Hall, Room 323
Norman, OK 73019
pbell@ou.edu
Phone: (405) 325-2077 FAX: (405) 325-7709

For more information: **http://www.ou.edu/cee**

The University of Oklahoma is an Equal Opportunity/Affirmative Action Employer and has a policy of being responsive to the needs of dual career couples. Applications from women and minorities are specifically encouraged.

Faculty Position
in Molecular Imaging

Memorial Sloan-Kettering Cancer Center is seeking an innovative individual for a tenure-track position with strong research accomplishments in molecular imaging and biomolecular probes with expertise in nuclear, magnetic, or optical imaging, or nanotechnology. MSKCC offers a unique and exciting research environment with programs in Immunology, Pharmacology, Chemistry, Molecular Biology, Informatics, Cancer Biology and Genetics, Developmental Biology, Cell Biology and Structural Biology as well as world-renowned clinical programs in cancer research, imaging, treatment and prevention. Opportunities for creative collaboration abound and additional new research facilities and resources will be available in about one year.

We have a graduate school in Cancer Biology, a training grant in molecular imaging, and a joint graduate program with Weill Medical College of Cornell University (WMC). We also participate in a Tri-Institutional graduate training program in Chemical Biology with Cornell-Ithaca, WMC and the Rockefeller University (RU) and a Tri-Institutional MD/PHD Training Program with WMC and RU.

Applicants should have an M.D. or Ph.D. degree, a track record of productive investigation, and dedication to translational problems at the interface of imaging with biology, biochemistry or chemistry. Academic rank and an appointment in Memorial Hospital will be made according to the qualifications of the applicant. Candidates should send by December 31, 2005 their curriculum vitae, research objectives and the names of three scientists who can evaluate their accomplishments and potential to **molimg@mskcc.org.** Application materials can also be submitted to **Drs. Hedvig Hricak and David Scheinberg, c/o M. Aiello/Box 428, Department of Radiology and Molecular Pharmacology and Chemistry Program, Memorial Sloan-Kettering Cancer Center, 1275 York Avenue, New York, NY 10021.** Memorial Sloan-Kettering Cancer Center is an affirmative action, equal opportunity employer.

Memorial Sloan-Kettering Cancer Center
The Best Cancer Care. Anywhere.
www.mskcc.org

Position Available at the University of Vermont Department of Biology Molecular Systematics/Evolution

Applications are invited for a tenure-track Assistant Professor position in molecular systematics/evolution, to augment the strength of the Department of Biology in this discipline. Candidates should use modern molecular techniques to investigate the phylogeny, systematics, and evolution of invertebrate taxa.

All applicants are expected to (1) hold a Ph.D. degree in biology or related field and have two or more years of postdoctoral experience; (2) develop a competitively funded program; and (3) teach undergraduate and graduate level courses. Candidates must apply online at **www.uvmjobs.com** and must attach to that application a curriculum vitae, representative publications, and a statement of research and teaching interests. In addition, three (3) hardcopy letters of recommendation should be sent to:

Dr. Joseph Schall
Department of Biology
University of Vermont
120A Marsh Life Science Building
Burlington, VT 05405-0086

Review of applicants will begin on **December 1, 2005**.

The University of Vermont is an Affirmative Action/Equal Opportunity Employer. The Department is committed to increasing faculty diversity and welcomes applications from women and underrepresented ethnic, racial and cultural groups and from people with disabilities.

FELLOWSHIPS

Australian Government
Australian Research Council

FEDERATION FELLOWSHIPS

The Australian Research Council's *Federation Fellowships* are highly prestigious awards designed to attract outstanding researchers to Australia and to build and strengthen world-class research capacity in Australia. The ARC has been offering *Federation Fellowships* since 2002 and currently funds 94 Federation Fellows.

Up to 25 *Federation Fellowships* are available for funding commencing in 2006. The ARC offers a salary of around $A246,000 per year (plus on-costs which include superannuation, leave, etc) with a standard tenure of five years. In addition to salary support, the ARC may provide some eligible successful applicants with a start-up project grant of up to $A400,000. This start-up support is to assist researchers who may not have had access to ARC grants in the past.

Open to outstanding international researchers, *Federation Fellowships* encourage applications from Australian and non-Australian researchers currently working overseas, especially from early- to mid-career researchers who will play a leadership role in building Australia's internationally competitive research capacity.

The Fellowships are available for tenure at Australian higher education institutions and Australian research organisations that are funded primarily for research from Commonwealth, State or Territory Government sources. The next closing date for applications is 14 October 2005.

A Commonwealth Government
***Backing Australia's Ability* Initiative**

For further information and documentation visit the Australian Research Council website at **www.arc.gov.au**; or email **june.mckendry@arc.gov.au**

hma0034012

RESEARCH *in the national interest – enabling the future*

THE UNIVERSITY OF SOUTH DAKOTA SCHOOL OF MEDICINE

PSYCHIATRY VICE-CHAIR OF RESEARCH

Department of Psychiatry
Sioux Falls, South Dakota

Responsibilities will include increasing the Department's research portfolio, developing translational research opportunities and involvement in the School's new MD/Ph.D. program. The Department of Psychiatry, located in Sioux Falls, South Dakota, will be moving into a 110 bed, newly-constructed state of the art academic/psychiatric facility in April, 2006. M.D./Ph.D. or M.D. with R01 funding or equivalent required. Salary commensurate with education and experience. To apply for this position, submit a letter of application, vita, and names, addresses and phone numbers of three professional references to: **The University of South Dakota, Lisa Sorensen, Human Resources, Vice Chair of Research Psychiatry Search, 414 E. Clark Street, Vermillion, SD 57069, Email: hr@usd.edu, Phone: 605-677-5671, Fax: 605-677-6330.** The Disabilities Services (TDD) number for USD is 605-677-6389.

Screening of applications will begin on October 15, 2005 and continue until a suitable candidate is hired.

The University of South Dakota is an Equal Opportunity/Affirmative Action Employer committed to increasing the diversity of its faculty, staff and students.

The University of South Dakota.
SCHOOL OF MEDICINE & HEALTH SCIENCES

WANT TO ELECTRIFY YOUR CAREER?

Become a AAAS Congressional Science & Engineering Fellow.

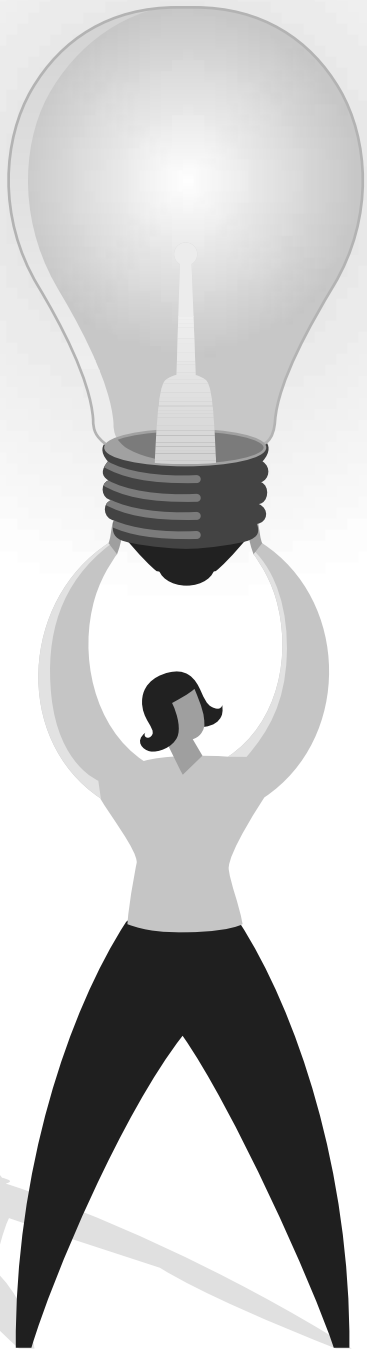

The Program: Scientists and engineers spend one year as special assistants on the staffs of Members of Congress or congressional committees, working in legislative areas requiring scientific and technical expertise. Fellows receive stipends from their sponsoring societies.

Purpose: To provide a unique public policy learning experience, to demonstrate the value of science-government interaction and to make practical contributions to the more effective use of scientific and technical knowledge in government.

Criteria: A prospective Fellow must be a postdoctoral to mid-career scientist or engineer; demonstrate exceptional competence in some area of science or engineering; be cognizant of and demonstrate sensitivity toward political and social issues; and perhaps most importantly, have a strong interest and some experience in applying personal knowledge toward the solution of societal problems.

Sponsors: Approximately 30 national science and engineering societies sponsor or cosponsor Congressional Fellows. Applicants should apply directly to the appropriate professional society. Applicants may apply to more than one society. Stipends, application procedures, timetables and deadlines vary by society. Persons from underrepresented minority groups and persons with disabilities are encouraged to apply.

Apply for 2006–07 Fellowships:
For more information and application instructions, contact AAAS:
Phone 202-326-6700
E-mail fellowships@aaas.org
Website www.fellowships.aaas.org

Eureka! You've found the perfect connection between science and policy.

American Association for the Advancement of Science (AAAS)
American Association of Colleges of Pharmacy (AACP)
American Academy of Neurology (AAN)
American Chemical Society (ACS)
American Dental Association (ADA)
American Geological Institute (AGI)
American Geophysical Union (AGU)
American Mathematical Association (AMS)
American Meteorological Society (AMS)
American Neurological Association (ANA)
American Nuclear Society (ANS)
American Psychological Association (APA)
American Physical Society (APS)
American Society of Agronomy (ASA)
American Society for Microbiology (ASM)
American Society of Civil Engineers (ASCE)
American Society of Mechanical Engineers (ASME)
American Veterinary Medical Association (AVMA)
Child Neurology Society (CNS)
Crop Science Society of America (CSSA)
Federation of Animal Science Societies (FASS)
Geological Society of America (GSA)
Institute of Electrical and Electronics Engineers – United States of America (IEEE-USA)
Institute of Food Technologists (IFT)
Institute of Navigation (ION)
Materials Research Society (MRS)
Optical Society of America (OSA)
International Society for Optical Engineering (SPIE)
Society for Research in Child Development (SRCD)
Soil Science Society of America (SSSA)

Enhancing Public Policy, Advancing Science Careers

www.fellowships.aaas.org

AAAS
ADVANCING SCIENCE, SERVING SOCIETY

POSITIONS OPEN

JOHNS HOPKINS
UNIVERSITY

Department of Molecular Biology & Genetics
School of Medicine

The Department invites applications from outstanding candidates for a tenure-track faculty position at the level of **ASSISTANT PROFESSOR.** The faculty includes molecular and developmental biologists, geneticists, and biochemists working on fundamental problems in biology. Applicants should send curriculum vitae along with a statement of current research interests and long-range goals and should arrange for four letters of recommendation to be sent. All items should be submitted to **e-mail: mgbfacultysearch@bs.jhmi.edu.** Please submit all materials by December 15, 2005. For further information about our Department, please visit the **website: http://www.mbg.jhmi.edu.**

The Johns Hopkins University is an Equal Opportunity/ Affirmative Action Employer.

TENURE-TRACK FACULTY POSITION
Landscape Ecology
University of Toronto at Mississauga

The University of Toronto at Mississauga (UTM), Department of Biology, invites applications for a tenure-track faculty position in landscape ecology at the level of **ASSISTANT PROFESSOR**, effective July 1, 2006. The area of specialization is open and includes all landscape applications of population biology, community and ecosystem ecology, and biogeography. Teaching responsibilities could involve ecology courses in the Biology programs as well as in the interdisciplinary Environment program. Details are at **website: http://link.library.utoronto.ca/academicjobs/display_job_detail_public.cfm?JOBID=1802.**

The successful applicant will have a Ph.D. and preferably postdoctoral experience, an outstanding academic record, and evidence of potential for excellence in teaching. Salary will be commensurate with qualifications and experience. The appointee will be located in the Department of Biology at UTM and, depending on the area of expertise, will also be a member of the appropriate graduate department.

Applications will be accepted until 30 November, 2005. Applicants should provide curriculum vitae, statement of teaching philosophy and interests, an outline of their proposed research, and should arrange to have three confidential letters of recommendation sent on their behalf to: **Professor Angela Lange, Interim Chair, Department of Biology, University of Toronto at Mississauga, Mississauga, Ontario, Canada L5L 1C6. Website: http://www.utm.utoronto.ca/~w3bio/homepage/.** *The University of Toronto is strongly committed to diversity within its community and especially welcomes applications from visible minority group members, women, Aboriginal persons, persons with disabilities, members of sexual minority groups, and others who may contribute to the further diversification of ideas. All qualified candidates are encouraged to apply; however, Canadians and permanent residents will be given priority.*

Ph.D. Fellowships in Food Microbiology. The University of Nebraska–Lincoln is seeking students interested in pursuing a Ph.D. in comparative genome analysis of intestinal microorganisms. Fellow stipends are $22,000 per year (tuition remission included). *Candidates must be U.S. citizens* with B.S. or M.S. in microbiology, biochemistry, immunology, or related field. Experience in molecular biology required. For application information, visit **website: http://www.foodsci.unl.edu** or contact **Dr. Benson** (**e-mail: abenson1@unl.edu**). Other graduate assistantships in molecular food microbiology are also available. *UNL is committed to a pluralistic campus community through Affirmative Action/Equal Opportunity. We assure reasonable accommodation under the ADA; contact Teresa Garcia at 402-472-5778 or e-mail:* tgarcia2@unl.edu *for assistance.*

POSITIONS OPEN

TENURE-TRACK FACULTY POSITIONS
in Environmental, Ecological,
or Toxicological Science
Indiana University, Bloomington

Indiana University invites applications for two tenure-track positions in environmental, ecological, or toxicological science as part of an Interdisciplinary Environmental Science program. The focus of this program is on forest ecology, biogeochemical cycling, or toxic contaminant effects. It is anticipated that one position will be in the School of Public and Environmental Affairs and one in the Biology Department.

Successful candidates will help develop this Environmental Science program, maintain an extramurally funded research program, and participate in undergraduate and graduate teaching.

The applicant's expertise is expected to complement existing faculty in ecology, the atmospheric sciences, biogeochemistry, or toxicology in the School of Public and Environmental Affairs or in the Biology Department. Appointments are expected to be at the **ASSISTANT PROFESSOR** level, but a senior appointment is possible for an exceptional candidate.

Review of applications will begin on November 1, 2005, and continue until the position is filled. Applications should include curriculum vitae and a statement of research and teaching interests. Submit application materials to:

Dr. Clinton V. Oster, Jr.
Associate Dean of Bloomington Programs
SPEA, Room 300
1315 E. 10th Street
Indiana University
Bloomington, IN 47405-1701

For more information see **website: http://www.iu.edu/~speaweb/faculty/open.html.** *Indiana University is an Equal Opportunity, Affirmative Action Employer, Educator and Contractor, M/F/D and strongly committed to achieving excellence through cultural diversity. The university actively encourages applications and nominations of women, persons of color, applicants with disabilities, and members of other underrepresented groups.*

ASSISTANT PROFESSOR
ECOSYSTEM MANAGEMENT

The Department of Biology (**website: http://www.bio.uni.edu**) at the University of Northern Iowa invites applications for a tenure-track Assistant Professor position in ecosystem management effective August 2006. The successful candidate will be expected to teach courses in support of the newly initiated Professional Science Master's Program in Ecosystem Management, contribute to other needs of the Department by teaching major and nonmajor courses as required, and develop a research program in ecosystems services, landscape ecology, or animal ecology that will involve undergraduate and graduate students. Faculty members are also expected to seek extramural funding.

Ph.D. in a biological science and teaching experience required. All-but-dissertations will be considered with evidence of completion by August 1, 2006; postdoctoral research experience desired. Submit evidence of teaching excellence (which might include videotaped demonstrations of teaching, teaching assessments, or other such evidence), curriculum vitae, undergraduate and graduate transcripts, a statement of research interests and goals, a statement of teaching interests and approaches, and three letters of reference to (e-mail applications and letters of recommendation will not be accepted):

Dr. Laura Jackson, Chair of Search Committee
Department of Biology
University of Northern Iowa
Cedar Falls, IA 50614-0421
E-mail: laura.l.jackson@uni.edu
Telephone: 319-273-2705
Fax: 319-273-7125

Application received by October 14, 2005, will be given full consideration. *The Department encourages applications from minority persons, women, Vietnam era veterans, and persons with disabilities.*

POSITIONS OPEN

The BURNHAM INSTITUTE
From research, the power to cure.

ASSOCIATE PROFESSORS, PROFESSORS

Positions are available at the level of Associate or full Professors at The Burnham Institute's Infectious and Inflammatory Disease Center, in the areas of inflammatory disease and infectious disease. Send curriculum vitae, list of publications, and any supporting material to **Professor Robert Liddington, Ph.D., e-mail: rlidding@burnham.org,** or to **Professor Tomas Mustelin, M.D., Ph.D., e-mail: tmustelin@burnham.org, The Burnham Institute, 10901 North Torrey Pines Road, La Jolla, CA 92037.**

ASSISTANT PROFESSOR, Cell Biology. Applications are invited for a tenure-track appointment in the Department of Biological Sciences at Towson University starting fall 2006. Candidates must have a strong commitment to excellence in teaching and research. Teaching responsibilities will include immunology, cell biology, and a graduate course in candidate's area of specialization. The successful candidate will be expected to actively pursue extramural funding to support his/her research program and shall involve undergraduate and graduate students. In addition, the successful candidate will be eligible to compete with other junior faculty for a three-year appointment as the newly established Jess Fisher Endowed Chair in the Biological and Physical Sciences that will entitle the holder of the Chair to receive additional funds to support her/his research program. A Ph.D. is required, postdoctoral experience preferred. A completed application should include curriculum vitae, transcripts from all institutions attended, a one-page statement on teaching philosophy, a one-page statement on research interests, and three letters of professional reference. Review of applications will begin October 28, 2005, and continue until the position is filled. Submit application material to: **Dr. Gail Gasparich, Chair Cell Biology Search Committee, Department of Biological Sciences, Towson University, Towson, MD 21252-0001.** Additional information about the Department is available at **website: http://www.towson.edu/biology/.** *Towson University is an Equal Opportunity, Affirmative Action Employer and has strong institutional commitment to diversity. Women, minorities, persons with disabilities, and veterans are encourage to apply.*

FACULTY POSITION

The Department of Physiology and Cell Biology at the University of Nevada, School of Medicine, in Reno (**website: http://www.unr.edu/physio**) is seeking applicants for a full-time, tenure-track position at the **ASSISTANT PROFESSOR/ASSOCIATE PROFESSOR** level. The Department is seeking an individual with expertise in excitability mechanisms, cellular signaling, development or cellular remodeling. The successful candidate should be experienced with molecular biology techniques such as expression of proteins in heterologous expression systems, transgenic/knockout technologies, functional genomics and proteomics and microarray/ bioinformatics. Candidates must have a strong record of peer-reviewed publications and the ability to develop an independent research program. Candidates must have a strong potential for obtaining extramural funding. Faculty member will be required to participate in the teaching of medical and graduate students. The position will be highly competitive with regard to startup funds, laboratory space, and salary.

To view complete position announcement and requirements, see **website: http://jobs.unr.edu** or contact: **Debbie Chase, search coordinator, e-mail: dchase@unr.edu.** Review of applications will begin October 31, 2005. *Equal Opportunity/Affirmative Action Employer. Women and under represented groups are encouraged to apply.*

VCU

ASSISTANT PROFESSOR

The Department of Medicinal Chemistry, School of Pharmacy (**website: http://phc.vcu.edu**) at Virginia Commonwealth University invites outstanding candidates for a 12-month, tenure-track Assistant Professor position starting fall 2006. Applicants must have a Ph.D. in medicinal chemistry, chemistry, biochemistry, or relevant sciences. The position offers a competitive startup package and salary with expectation of establishing an independent, extramurally funded, vigorous research program, teaching in the graduate and professional programs, and taking on selected administrative responsibilities. Applicants with research interests in medicinal chemistry, e.g., structure-activity relationships, metabolism, natural products, drug design, synthesis and mechanism, receptor pharmacology, chemical biology, enzymology, structural biology, and bioinformatics, are encouraged to apply. Applicants should submit a current curriculum vitae, a description of their proposed research, selected published papers, and a list of areas interested in teaching and should have three letters of reference sent to: **Dr. Umesh R. Desai, 800 East Leigh Street, Suite 212, Richmond, VA 23219. E-mail: urdesai@vcu.edu.** *Virginia Commonwealth University is an Equal Opportunity/Affirmative Action Employer. Women and minorities are encouraged to apply.*

ASSISTANT/ASSOCIATE PROFESSOR
Section of Endocrinology, Diabetes and Metabolism
Chicago, Illinois

The University of Illinois at Chicago (UIC) is recruiting an Assistant/Associate Professor of medicine (rank/tenure commensurate w/ qualifications) in the Section of Endocrinology, Diabetes and Metabolism. The successful candidate will participate in Section clinical and teaching activities and will have 75% of time for research along with startup support. Interest in areas broadly related to insulin resistance, diabetes or obesity preferred. M.D. required. UIC College of Medicine is located one mile west of downtown Chicago on a campus encompassing six health science colleges, the UIC Hospital, and the Jesse Brown VA Medical Center. UIC is among the top 50 universities nationally in federal research funding. Letters of interest, curriculum vitae and the names of three references should be sent by December 31, 2005, to: **Theodore Mazzone, M.D., Chief, Section of Endocrinology, Diabetes and Metabolism, University of Illinois at Chicago, 1819 W. Polk Street (M/C 797), Chicago, IL 60612** or **e-mail: sat@uic.edu.** *UIC is an Affirmative Action/Equal Opportunity Employer.*

The Department of Zoology at the University of Hawaii invites animal physiologists whose research interests integrate with existing departmental strengths in ecology, evolution, and developmental biology to apply for a tenure-track **ASSISTANT PROFESSOR** position. Teaching responsibilities will include an advanced undergraduate course in animal physiology and a graduate course in the individual's specialty. Applicants must have a Ph.D. in a relevant area of biological sciences, evidence of significant research accomplishments, and a commitment to teaching. To apply, send letter of application, curriculum vitae, statement of research accomplishments and goals, and the names, addresses, and e-mail contact of three references to: **Search Committee, Department of Zoology, 2538 McCarthy Mall, University of Hawaii, Honolulu, HI 96822.** Inquiries should be directed to **e-mail: zoology@hawaii.edu.** Closing date: To receive full consideration, applications must be received by November 1, 2005. However, review of applications will continue until position is filled. *Women and Minorities are especially encouraged to apply. Equal Opportunity/Affirmative Action Employer.*

POSITIONS OPEN

Department of Plant Biology at Southern Illinois University Carbondale (SIUC) invites applications for a tenure-track **ASSISTANT PROFESSOR** with expertise in plant bioinformatics or modeling of plant or ecological systems. Future research focus must be nonagricultural. Ph.D. in a relevant discipline is required. Applicants must have a record of peer-reviewed publications. Postdoctoral experience or evidence of externally funded research is desirable. Teaching at the undergraduate and graduate levels will be expected along with the development of an externally funded research program. Applications should include: a statement of research and teaching interests, curriculum vitae, representative publications, and three letters of references, and sent to: **Dale Vitt, Chair, Department of Plant Biology, Mail Code 6509, Southern Illinois University Carbondale, 1125 Lincoln Drive, Carbondale, IL 62901.** Departmental information is available at **website: http://www.science.siu.edu/plant-biology/.** This position is part of a newly formed cluster in mathematical biology at SIUC. Review of applications begins November 1, 2005 and will continue until the position is filled. *SIUC is an Affirmative Action/Equal Opportunity Employer that strives to enhance its ability to develop a diverse faculty and staff, and to increase its potential to serve a diverse student population. All applications are welcomed and encouraged and will receive consideration.*

FACULTY POSITION
BIOLOGY

The Department of Biology at Westminster College seeks a tenure-track **ASSISTANT PROFESSOR** to begin in August 2006. Teaching responsibilities will include physiology, introductory biology, and upper level courses in the candidate's area of expertise. Opportunity exists for participation in interdisciplinary programs, including a neuroscience major. The successful candidate will have broad training, versatility, dedication to quality teaching and advising in a liberal arts environment, and a strong commitment to research with undergraduates. A Ph.D. in the appropriate field is required at the time of hiring.

Westminster College is a coeducational, liberal arts institution with historic ties to the Presbyterian Church (USA). The College enrolls about 1,500 full-time students and employs about 105 full-time faculty. It is located in a beautiful rural setting in close proximity to both Pittsburgh and Cleveland.

Review of applications will begin October 21, 2005, and will continue until the position is filled. Applications, including a statement of teaching philosophy and research goals, and three letters of recommendation, should be submitted to: **Joseph M. Balczon, Chair, Department of Biology, Westminster College, New Wilmington, PA 16172-0001.** *Equal Opportunity Employer.*

VERTEBRATE PHYSIOLOGICAL ECOLOGIST

Penn State Berks invites applications for a tenure-track biology position in the Division of Science beginning in August 2006. A 36-week appointment will be at the level of **ASSISTANT PROFESSOR** and requires a Ph.D. Responsibilities include teaching introductory and upper level undergraduate courses as well as development of a research program that actively involves undergraduates in publishable projects. Preference will be given to candidates with expertise in the following areas: mammalian physiology, evolutionary biology, and field ecology. Teaching and postdoctorate experience is highly desirable. Details of the college can be found at **webstite: http://www.bk.psu.edu/faculty/openpos.html.**

Send via e-mail a letter of application, curriculum vitae, statement of teaching philosophy, description of research program involving undergraduates, and the names and addresses of three references with telephone numbers and e-mails to: **e-mail: dcm9@psu.edu.** Closing date for this position is December 1, 2005. Applications will be accepted until the position is filled. *Penn State is committed to Affirmative Action, Equal Opportunity, and the diversity of its workforce.*

POSITIONS OPEN

RESEARCH ASSISTANT PROFESSOR. Nontenure-track position at the University of Illinois at Chicago, Department of Anesthesiology, for research in molecular biology and/or mitochondrial metabolism. Ability to work independently and establish needed procedures. Able to draft own publications from research studies. Salary commensurate with experience. For fullest consideration, submit applications by October 7, 2005, to: **Dr. June Palmer, University of Illinois at Chicago, Department of Anesthesiology, m/c 515, 1740 W. Taylor, Chicago, IL 60612.** *Affirmative Action/Equal Opportunity Employer.*

TENURE-TRACK FACULTY POSITIONS
Department of Cellular & Integrative Physiology
Indiana University
School of Medicine

The Department seeks applicants for two tenure-track positions. Academic rank will be commensurate with qualifications. Applicants must have an M.D. or Ph.D. degree, at least three years of postdoctoral experience, high quality peer-reviewed publications, evidence of independent research, and competitive funding potential. We seek innovative scientists with expertise in an array of imaging and electrophysiological techniques using integrated molecular, cellular, and whole animal approaches to study cardiovascular-related physiological questions. Although preference will be given to the above, other areas of research will be considered, including membrane biology, cytoskeleton, mechanotransduction, diabetes, exercise, and renal physiology. Successful applicants will be expected to maintain an extramurally funded research program and participate in the teaching of medical and graduate students. Significant resources available include competitive startup packages, newly renovated laboratory space, and long-term research and salary incentives. This is an important phase of growth in the Department, which is expected to add four to six new positions in the next four years. Further information can be found at **website: http://iupui.edu/~medphys.** The first review of applications will be October 1, 2005, and the review will continue until positions are filled.

Applicants should send (in electronic format) their curriculum vitae, brief statement of research interests and goals, and the names of three references to: **Dr. Michael Sturek, Chair, Department of Cellular & Integrative Physiology, c/o Marlene Brown (e-mail: pbio@iupui.edu), 635 Barnhill Drive, M.S. 385, Indianapolis, IN 46202-5120.** *Indiana University is an Equal Employment Opportunity/Affirmative Action Employer.*

FACULTY POSITION IN CHEMISTRY
University of California, Berkeley
Department of Chemistry
(Position #1018)

The Department of Chemistry at the University of California (UC), Berkeley solicits applications for a junior faculty position beginning in the fall of 2006. Creative and energetic candidates who show extraordinary promise or accomplishment in research and teaching are specifically sought in any area of materials chemistry. Exceptional candidates in any area of chemistry will also be considered. Applicants should send curriculum vitae and a proposed research program and arrange to have three letters of recommendation sent to: Chair, Faculty Recruitment Committee, Department of Chemistry, 419 Latimer Hall, University of California, Berkeley, CA 94720-1460. Please refer references to the UC statement on confidentiality at **website: http://www.chance.berkeley.edu/apo/evalltr.htm.** The deadline for receipt of applications is November 15, 2005. Application review will begin with receipt of applications. *The University of California is an Equal Opportunity/Affirmative Action Employer.*

POSITIONS OPEN

ASSISTANT OR ASSOCIATE PROFESSOR
Neurobiology
University of Alberta
Department of Biological Sciences

We invite applications for a tenure-track position at the Assistant or Associate Professor level in research areas related to neurobiology. The successful candidate will be expected to interact with a strong comparative physiology group which has expertise in developmental, molecular, and evolutionary neurobiology and cellular and neuroendocrinology. The candidate should have a strong record of research and demonstrated potential for excellence in teaching. The University of Alberta offers a competitive salary commensurate with experience and an excellent benefits plan. The Department of Biological Sciences (**website: http://www.biology.ualberta.ca/**), with 70 faculty members and 275 graduate students, offers an exciting environment for collaborative research. Exceptional infrastructure includes molecular biology and microscopy/imaging services, animal care facilities and access to Bamfield Marine Sciences Centre. Candidates should submit curriculum vitae, a one-page summary of research plans, a statement of teaching interests, and reprints of their three most significant publications electronically to **e-mail: positions@biology.ualberta.ca** or by mail to:

Dr. L. S. Frost, Chair
Department of Biological Sciences
CW 405 Biological Sciences Building
University of Alberta
Edmonton, Alberta, Canada T6G 2E9

Applicants must also arrange for three letters of reference to be sent to the Chair. Closing date: October 15, 2005. The effective date of employment will be July 1, 2006.

All qualified candidates are encouraged to apply; however, Canadians and permanent residents will be given priority. The University of Alberta hires on the basis of merit. We are committed to the principle of equity in employment. We welcome diversity and encourage applications from all qualified women and men, including persons with disabilities, members of visible minorities, and Aboriginal persons.

ASSISTANT PROFESSOR, Department of Biochemistry and Molecular Biology, SUNY Upstate Medical University. We seek applications to fill a tenure-track Assistant Professor position in the area of nuclear structure and function. The successful applicant will be expected to develop a well-funded research program and to contribute to medical and graduate teaching. We offer a highly competitive startup package. Further information about the Department can be found at **website: www.upstate.edu/biochem.** Candidates should have a Ph.D. and/or an M.D. degree, postdoctoral experience, and a strong publication record. Applicants should submit curriculum vitae along with a summary of their research accomplishments and future research plans and should arrange to have three letters of reference sent to: **David Gilbert, Ph.D., Search Committee Chair, Department of Biochemistry and Molecular Biology, SUNY Upstate Medical University, 750 E. Adams Street, Syracuse, NY 13210.** Or send to **e-mail: biochem@upstate.edu.** Review of applications will begin or November 15, 2005, and continue until the position is filled. *Women and minorities are encouraged to apply. Upstate Medical University is an Equal Opportunity/Affirmative Action Employer.*

POSTDOCTORAL POSITION in Prebiotic RNA Chemistry. University of Colorado at Boulder Postdoctoral position available immediately to study the role of dinucleotide catalysts in prebiotic synthetic reactions and the emergence of the genetic code. (See "A Mechanism for the Association of Amino Acids with Their Codons and the Origin of the Genetic Code," *PNAS* **102:**4442, 2005.) Skills in nucleotide chemistry and reaction kinetics required. Send curriculum vitae and names of three references to: Dr. S. Copley at **e-mail: copley@cires.colorado.edu.** *The University of Colorado at Boulder is committed to diversity and Equality in Education and Employment.*

POSITIONS OPEN

BIOINORGANIC CHEMISTRY

The Department of Chemistry and Biochemistry at Arizona State University has a tenure-track position at the rank of **ASSISTANT** or **ASSOCIATE PROFESSOR** in bioinorganic chemistry. Duties include establishing a vigorous, externally funded research program of national/international recognition, teaching chemistry or biochemistry courses at the graduate and undergraduate levels, and participating on assigned governance and service committees. The successful candidate should have research interests that may include bioinorganic chemistry, metalloproteins, or metal-catalyzed biological processes. Postdoctoral experience is desired. The successful candidate must have a doctoral degree in chemistry/biochemistry or a related field at the time of appointment and demonstrated potential for excellence in both research appropriate to rank and teaching at the undergraduate and graduate levels appropriate to rank.

Applicants must mail curriculum vitae, list of publications, outline of research plans, and statement of teaching philosophy and arrange to have three letters of reference mailed to:

Professor Thomas A. Moore, Chair
Bioinorganic Chemistry Search Committee
Department of Chemistry and Biochemistry
Arizona State University,
P.O. Box 871604
Tempe, AZ 85287-1604

Review of applications begins November 2, 2005; if not filled, every two weeks thereafter until search is closed. Background check is required for employment. *ASU is an Equal Opportunity/Affirmative Action Employer and is committed to increasing diversity.*

TENURE-TRACK FACULTY POSITION

Molecular oncology, Departments of Medicine and Cell Biology, Washington University, St. Louis. The Division of Oncology invites applications for full-time, tenure-track appointment at the rank of **ASSISTANT PROFESSOR**. Candidates must have a Ph.D., M.D., or equivalent degree, relevant postdoctoral experience, and a strong record of research accomplishment. We are seeking candidates with an interest in basic molecular oncology using innovative approaches in developmental, molecular, or cell biology, biochemistry, or biophysics. The successful candidate will be expected to establish and maintain a vigorous, independently funded research program. Competitive salary, ample startup packages, and first-class laboratory space will be provided.

Please provide (1) current curriculum vitae, list of publications, and grant support, (2) a brief statement of research interests, and (3) letters of references from three scientists. Send applications to: **Dr. Lee Ratner, Chair of the Search Committee, Division of Oncology, Campus Box 8069, 660 S. Euclid Avenue, Washington University, St. Louis, MO 63110,** or to **e-mail: lratner@im.wustl.edu.**

The Massachusetts Institute of Technology Department of Chemistry invites applications for tenure-track appointments beginning July 2006.

Applicants with teaching and research interests in inorganic, organic, and physical chemistry, broadly defined are encouraged to apply. The appointments will be the rank of **ASSISTANT PROFESSOR,** but outstanding senior applicants could be considered. Applicants should arrange to have curriculum vitae, a brief description of research plans, and three letters of recommendation sent to:

Professor Timothy M. Swager, Head
Department of Chemistry
Massachusetts Institute of Technology
77 Massachusetts Avenue, 18-398
Cambridge, MA 02139-4307

Application deadline: October 15, 2005. *MIT is an Equal Opportunity/Affirmative Action Employer and encourages applications from minorities and women.*

POSITIONS OPEN

One **RESEARCH ASSISTANT PROFESSOR,** one **INSTRUCTOR,** and two **POSTDOCTORAL** positions are available in the laboratories of **Drs. Feng Liu** and **Lily Dong** at the University of Texas Health Science Center at San Antonio (UTHSCSA). The research projects in Dr. Liu's laboratory focusing on insulin receptor signal transduction and regulation, metabolic syndrome, and aging. The main areas of research in Dr. Lily Dong's laboratory focus on adiponectin receptor signal transduction, obesity, and diabetes. A wide range of approaches from molecular biology, biochemistry, cell biology, to mouse genetic strategies is employed to tackle these problems important for human health. This Ph.D. or M.D. scientist should have strong background in biochemistry and cell/molecular biology and a strong interest in research, good communication skills, and the ability to work independently. Prior experience working with animals is a plus. Interested applicants should arrange to send their resume and letters of reference addressed to Drs. Feng Liu (**e-mail: liuf@uthscsa.edu**) or Lily Dong (**e-mail: dongq@uthscsa.edu**). All faculty and postdoctoral appointments at the UTHSCSA are designated as security sensitive positions. *The University of Texas Health Science Center at San Antonio is an Equal Employment Opportunity/Affirmative Action Employer.*

SOUTHERN ILLINOIS UNIVERSITY EDWARDSVILLE (SIUE)

The School of Pharmacy invites applications for a 12-month tenure-track position at the rank of **ASSISTANT, ASSOCIATE,** or **FULL PROFESSOR.** A Ph.D. in pharmacology, medicinal chemistry, or a closely related area is required. Individuals having previous teaching experience in integrated therapeutics courses and postdoctoral training are preferred. The successful candidate will be expected to demonstrate excellence in teaching in the professional (Pharm.D.) program and to establish an independent and/or collaborative research program. Opportunities for research collaborations exist on the SIUE campus and with the SIU Schools of Dental Medicine and Medicine. Additionally, the proximity of the SIUE School of Pharmacy to numerous educational institutions and pharmaceutical and biotechnology firms in the St. Louis metropolitan area provides for a stimulating intellectual environment. The review of applications will begin immediately and continue until the position is filled. Starting dates are negotiable. To be considered for this position, applicants should submit a letter of application, curriculum vitae, and the names and addresses of three references to: **Michael Crider, Chair, Department of Pharmaceutical Sciences, Southern Illinois University Edwardsville, Edwardsville, IL 62026-2000. E-mail: mcrider@siue.edu; Telephone: 618-650-5162.** SIUE is a state university – benefits to state sponsored plans will not be available to holders of F1 or J1 visas. *SIUE is an Affirmative Action/Equal Opportunity Employer.*

ASSOCIATE/FULL PROFESSOR
Translational Vision Research
College of Physicians and Surgeons
Columbia University

Tenure-track position with endowed professorship and programmatic support now available for established vision scientist, with primary appointment in Department of Ophthalmology and joint appointment in basic science department. Candidate should be active in vision research and have documented strong record in research programs with direct application to treatment of eye diseases. Applicants should submit curriculum vitae, description of research plans, copies of two key publications, and names and addresses of three references to: **Rando Allikmets, Ph.D., Research Director, c/o Elaine Bluberg, Administrative Assistant, Department of Ophthalmology, Columbia University, 630 West 168th Street, New York, NY 10032.** For express mail delivery: **160 Fort Washington Avenue, 5th Floor, Room 509.** Responses should be received no later than November 1, 2005.

Columbia University takes affirmative action to ensure equal opportunity.

Faculty Position in Mammalian Neurogenetics

McLaughlin Research Institute for Biomedical Sciences

McLaughlin Research Institute has opened a search for an innovative scientist applying mammalian genetics to biological problems in the neurosciences. Candidates for this Assistant Professor level position should possess a doctoral degree and a record of research excellence as a postdoctoral fellow or newly independent investigator. The applicant should be capable of developing a productive independent research program that can compete successfully for grant funding. Applicants with interests in neurodegenerative diseases, stem cell biology, protein or organelle trafficking, or hearing are particularly encouraged to apply.

McLaughlin Research Institute (**www.montana.edu/wwwmri/**) offers a unique opportunity for mouse genetic research. The Institute is a small non-profit organization and offers a non-bureaucratic, interactive research environment. The Institute is housed in a spacious modern research building with an excellent mouse facility that includes a transgenic and gene-targeting core. The successful candidate also will become a member of the University of Montana's NIH-funded Center of Biomedical Research Excellence (COBRE) in Structural and Functional Neuroscience (**http://www.umt.edu/csfn/**) offering additional technologies and opportunities for multidisciplinary collaborations.

For specific questions about the Institute contact George Carlson, Pin-Xian Xu, John Mercer, or John Bermingham at MRI, or any of the following members of our Scientific Advisory Committee: Irv Weissman, David Baltimore, David Cameron, Neal Copeland, Jeff Frelinger, Leroy Hood, Nancy Jenkins, or James Spudich.

Applications, including names of individuals we may contact for references, should be sent to:

George A. Carlson, Ph.D.
Director, McLaughlin Research Institute
1520 23rd Street South
Great Falls, MT 59405

An Equal Opportunity/Affirmative Action Employer.

DEPARTMENT OF HEALTH AND HUMAN SERVICES
National Institutes of Health
National Heart, Lung, and Blood Institute

Scientific Review Administrator

The National Heart, Lung, and Blood Institute (NHLBI), a major research component of the National Institutes of Health (NIH), Department of Health and Human Services (DHHS), is seeking four Scientific Review Administrators for the Review Branch, Division of Extramural Affairs. Scientific Review Administrators organize and manage the comprehensive scientific and technical merit review of grant applications and contract proposals through interaction with established scientists in a variety of fields. Scientific Review Administrators are responsible for assuring the fairness and consistency of the review process, and for providing technical guidance to applicants, reviewers, and Institute staff.

Qualifications: Individuals with a Ph.D. or doctoral degree equivalent, and a scientific background in disciplines relevant to heart, lung, blood, or sleep disease research, are encouraged to apply. Experience in grant preparation and in the peer review process is desirable. For the basic qualification requirements, please refer to the NIH guidance for Health Scientist Administrators at **http://www.nhlbi.nih.gov/about/jobs/hsaguide.htm**. U.S. citizenship is required..

Salary: The current salary range is $62,886 to $114,882. In addition, a recruitment bonus may also be considered. Position requirements and detailed application procedures are provided on vacancy announcement NHLBI-05-94008, which can be obtained by accessing **WWW.USAJOBS.GOV**.

How to Apply: You may apply online at the above website or submit a Standard Form 171, Application for Federal Employment; OF-612, Optional Application for Federal Employment; current curriculum vitae/bibliography or other format to: **National Heart, Lung, and Blood Institute, Human Resources Branch G, Two Democracy Plaza, 6707 Democracy Blvd., Suite 700N, Bethesda, MD 20892**. All applications must be received by the October 7, 2005 closing date. For additional information contact **Chris Duggan** at **(301) 402-8028**.

DHHS and NIH are Equal Opportunity Employers. Applications from women, minorities and persons with disabilities is strongly encouraged. The NIH/NHLBI is a smoke free workplace.

USDA Agricultural Research Service
www.ars.usda.gov

National Program Leaders for Horticulture, Crops Entomology, and Bioinformatics (Biological Scientist, GS-0401-14/15)

The USDA, Agricultural Research Service, National Programs, Crop Production and Protection in Beltsville, MD is seeking four National Program Leaders for: (1) Horticulture (two vacancies); (2) Field and Horticultural Crops Entomology; and (3) Bioinformatics. These senior-level positions direct research policies and programs for USDA's chief in-house science agency. The National Program Leaders manage, plan, lead, coordinate and implement comprehensive research program conducted at sites nationwide.

Candidates need an extensive scientific background and must have advanced research experience in one or more of the specialty areas. Recruitment is at the GS-14/15 levels. Salary commensurate with experience (GS-14, $88K - $114K; GS-15, $103K -$135K per year plus benefits). Pre-employment check and a full background investigation may be required. These are permanent, full-time positions.

Candidates must be U.S. Citizens. Application must address specific education and experience requirements. To request copy of vacancy announcement, call **(301) 504-1482** or go to **http://www.usajobs.opm.gov** and search for **#ARS-X5E-0350 (Horticulture); #ARS-X5E-0351 (Crops Entomology)**; and **#ARS-X5E-0349 (Bioinformatics)**. Announcements open on September 19, 2005. Applications must be postmarked by **November 14, 2005**.

USDA/ARS is an Equal Opportunity Employer and Provider.

SCOTT & WHITE

College of Medicine
The Texas A&M University System Health Science Center

Pediatric Hematology-Oncologist

The Section of Pediatric Hematology/Oncology at **Scott and White Clinic** and the **Texas A&M University System Health Science Center College of Medicine** (TAMUS HSC-COM) are seeking a clinician scientist with current research grants for a faculty position in a rapidly growing program. The candidate should be BE/BC in pediatric oncology and committed to an academic career. The successful candidates will join and enhance ongoing efforts in basic and translational research, with an institutional commitment to building a world-class experimental therapeutics program. An outstanding start-up package includes high quality laboratory space, excellent benefits and competitive salaries commensurate with academic qualifications. The position guarantees 75% protected time for research activities.

Scott & White Clinic is a 500+ physician directed multi-specialty group practice that is the leading provider of cancer care in Central Texas. Scott and White Clinic and the 486 bed tertiary Scott & White Memorial Hospital is the main clinical teaching facility for TAMUS HSC-COM. Outstanding clinical practice and laboratory facilities on campus that perform state of the art molecular and cellular biology research, flow cytometry, genomics and biostatistics are in place to support the research effort.

Please contact: **Don Wilson, M.D. Professor and Chairman, Department of Pediatrics, Scott & White, 2401 S. 31st, Temple, TX 76508. (800)725-3627 dwilson@swmail.sw.org Fax (254) 724-4974.**

For more information about Scott & White, please visit www.sw.org For Texas A&M www.tamhsc.edu. Scott & White is an equal opportunity employer.

POSITIONS OPEN

NEUROETHOLOGY
Harvard University
Department of Organismic and Evolutionary Biology

The Department of Organismic and Evolutionary Biology at Harvard University seeks to make one or more appointments in the field of neuroethology. Candidates will be considered for appointment at either tenure-track or tenured levels. We seek an outstanding scientist who will establish an empirical research program and teach both undergraduate and graduate students. The candidate would also be a member of the newly formed Center for Brain Science at Harvard with the opportunity to interact with faculty from other departments in the Faculty for Arts and Sciences and Harvard Medical School. We are especially interested in individuals who conduct rigorous, field and/or laboratory-based tests of general problems in neuroethology, and who employ genomic, neurobiological, endocrinological and/or behavioral approaches. We encourage applications from or information about women and minority candidates.

Applicants should submit curriculum vitae, statements of research and teaching interests and representative publications, and should arrange for three letters of reference to be sent to: **Professor Naomi Pierce, Department of Organismic and Evolutionary Biology, 26 Oxford Street, Cambridge, MA 02138, U.S.A.** Nominations from third parties are also welcome. Review of applications and nominations will begin November 15, 2005.

Further information about the Department is available at its **website: http://www.oeb.harvard.edu.**

Harvard University is an Affirmative Action/Equal Opportunity Employer.

The Biology Department of Gonzaga University invites applications for a tenure-track **ASSISTANT PROFESSOR** position beginning fall 2006. We seek to hire an animal physiologist who will complement the existing faculty. Teaching assignments will include diversity of life (BIOL101), as well as upper division courses in area of specialization and eventually courses for nonscience majors. To receive full consideration, applications and letters (three) of recommendation should be received by 1 November 2005. Application should consist of: cover letter, curriculum vitae, statement of research interests and plans for undergraduate participation, and statement of teaching philosophy and interests. Applications and letters should be sent to: **Biology Search Committee, AD Box 6, Gonzaga University 502 E. Boone Avenue, Spokane, WA 99258.** For further information about applying for this position see **website: http://gonzology.gonzaga.edu/faculty-staff/jobs/.** Gonzaga University is a Jesuit, Catholic, humanistic university looking for candidates who can contribute to its educational needs and missions. *Gonzaga is an Affirmative Action/Equal Opportunity Employer seeking to increase its diversity.*

TENURE-TRACK FACULTY POSITION
UCLA
Department of Molecular, Cell, and Developmental Biology

The Department of Molecular, Cell and Developmental Biology is searching for one faculty appointment; either senior or junior levels will be considered. Research in any area of modern plant biology will be considered, especially those using molecular genetics, genomics, or proteomics approaches to study basic biological process in *Arabidopsis* or other model plants.

Curriculum vitae, summary of research plans, and at least three letters of reference should be sent to: **MCDB Faculty Search (Plant Biology), c/o Grace Angus, Molecular, Cell and Developmental Biology, UCLA, 621 Charles E. Young Drive, South Los Angeles, CA 90095-1606. Telephone: 310-825-4373.** We will begin reviewing applications on November 1, 2005. Visit us at **website: http://www.mcdb.ucla.edu;** also see **website: http://www.uclaaccess.ucla.edu/UCLAACCESS/Web/Default.aspx.** *UCLA is an Equal Opportunity/Affirmative Action Employer. Women and minorities are encouraged to apply.*

ASSISTANT PROFESSOR
BIOTECHNOLOGY

The Department of Biology (**website: http://www.bio.uni.edu**) at the University of Northern Iowa invites applications for a tenure-track Assistant Professor position in biotechnology effective August 2006. The successful candidate will be expected to teach courses contributing to the newly initiated Professional Science Master's Program in Biotechnology, be able to contribute to other needs of the Department by teaching major and nonmajor courses as required, and develop a research program in the area of biotechnology and/or nanobiotechnology that will involve undergraduate and graduate students. Faculty members are also expected to seek extramural funding.

Ph.D. in a biological science and teaching experience required. All-but-dissertations will be considered with evidence of completion by August 1, 2006; postdoctoral research experience desired. Submit evidence of teaching excellence (which might include videotaped demonstrations of teaching, teaching assessments, or other such evidence), curriculum vitae, undergraduate and graduate transcripts, a statement of research interests and goals, a statement of teaching interests and approaches, and three letters of reference to (e-mail application and letters of recommendation will not be accepted):

Dr. Theresa Spradling,
Chair of Search Committee
Department of Biology
University of Northern Iowa
Cedar Falls, IA 50614-0421
E-mail: theresa.spradling@uni.edu
Telephone: 319-273-6214
Fax: 319-273-7125

Applications received by October 4, 2005, will be given full consideration. *The Department encourages applications from minority persons, women, Vietnam era veterans, and persons with disabilities.*

CHAIR DEPARTMENT OF MICROBIOLOGY AND IMMUNOLOGY
University of South Alabama
College of Medicine

The University of South Alabama College of Medicine invites applications and nominations for the position of Professor and Chair of the Department of Microbiology and Immunology. The University is seeking an outstanding scientist and academician with a strong record in research and graduate education to complement and expand the current research and educational programs in the Department and institution. The successful candidate may be a leader in the field of microbiology, immunology, biochemistry, or cell biology, but those individuals having strength in areas involving immnology are especially encouraged to apply. The successful candidate will be expected to support and contribute to the educational programs and missions of the Department and institution, and should possess administrative and leadership skills in mentoring faculty and students. Excellent opportunities exist for strong collaboration with other basic science and clinical departments.

The Chair will lead the Department of 10 full-time faculty who have research interests in prokaryotic genetics and physiology, virology, and immunology. The Department offers Ph.D. and M.D./Ph.D. degrees and provides instruction to medical students. Additonal information about the Department is available at **website: http://www.usouthal.edu/microbiology.**

Review of applicants will begin immediately and will continue until the position is filled. An applicant should submit curriculum vitae and the names of three or more references, a statement of research interests and goals, and a summary of administrative experience to: **Dr. Samuel J. Strada, Senior Associate Dean, College of Medicine, CSAB-170, University of South Alabama, Mobile, Alabama 36688-0002.**

University of British Columbia
Tenure-Track Faculty Positions
Department of Electrical and Computer Engineering

The Department of Electrical and Computer Engineering at the University of British Columbia (UBC) invites applications for tenure-track positions. Positions are offered primarily at the **ASSISTANT PROFESSOR** level, but exceptional candidates will be considered at all ranks. The main area of interest is biomedical/bioengineering (including nanoscale engineering of biological systems; bio-electronics; bio-information processing; instrumentation; diagnostics; devices and sensors; molecular, cell and tissue engineering).

Applicants must demonstrate excellent research potential and teaching ability. The successful applicants will preferably have relevant industrial experience and be active in enhancing educational and research links within the technical community. All faculty members are expected to teach at both undergraduate and graduate levels, and to supervise graduate students. A Ph.D. or equivalent in an appropriate area is required and eligibility for registration as a Professional Engineer in the Province of British Columbia is preferred. Appointments normally start July 1, 2006; however, the starting date is flexible. Salary will be commensurate with experience.

The Department offers a full range of undergraduate and graduate degree programs in electrical engineering and computer engineering. A number of new initiatives – from new Professorships and Chairs with significant support from local companies to new project-based undergraduate teaching – have created an exciting work environment. A new Institute for Computing, Information and Cognitive Systems, partly funded by the Canada Foundation for Innovation (CFI) will provide state-of-the-art laboratories for interdisciplinary research in a number of areas. Significant startup funding to new faculty could be offered through CFI, the Canada Research Chairs Program and other sources. The Department currently has approximately 50 faculty members and 375 graduate students; it is undergoing a major expansion which will allow critical masses of researchers in selected areas to develop. Additional information about the Department is available at **website: http://www.ece.ubc.ca/.**

Applications will be considered on a continual basis until the positions are filled. Applicants should send hard copies of their resumes, statements of research, and teaching interests, and the names of at least three references to:

Chair, Recruiting Committee
Department of Electrical and Computer Engineering
Kaiser Building, Room 5500
University of British Columbia
2332 Main Mall
Vancouver, BC, V6T 1Z4

UBC hires on the basis of merit and is committed to employment equity. We encourage all qualified persons to apply; however, Canadian citizens and permanent residents will be given priority.

POSTDOCTORAL RESEARCHER

Postdoctoral position available at the Blood Systems Research Institute (BSRI), in San Francisco. Research projects include the discovery of new human viruses using shotgun sequencing and the genetic analyses of HCV, HIV, HBV, and WNV. Experience with nucleic acid manipulations and DNA sequence analyses required. BSRI is a newly formed basic research institute dedicated to the science of transfusion medicine (**website: http://www.bsrisf.org**). Send curriculum vitae by September 30, 2005 to **e-mail: delwarte@medicine.ucsf.edu** with copies to: **e-mail: bsricareers@bloodsystems.org** or to **Dr. Eric Delwart, BSRI, 270 Masonic Avenue, San Francisco, CA 94118. Fax: 415-775-3859.** *Preemployment drug screen required. Equal Opportunity Employer Minorities/Females/Persons with Disabilities/Veterans.*

HEAD AND DIRECTOR RESEARCH PROGRAM IN INFECTIOUS DISEASE

Applications and nominations are invited for the Head of Veterinary Molecular Biology (VMB) at Montana State University, Bozeman, MT. MSU is a land-grant university located in a community of 35,000 people with a high quality of life, excellent public schools, and minutes from outstanding recreational opportunities. VMB is a dynamic research and teaching environment with state-of-art facilities for biochemistry, genomics, immunology, and cell biology. The Department is housed in a new 40,000 ft^2 facility, and currently has 21 tenure track and research faculty, 66 professional staff, and 40 graduate and undergraduate students involved in independent research. Current VMB research programs are supported by >$10,000,000/yr in extramural funding expenditures, predominantly from the NIH, and emphasize the study of pathogen biology, host defense, host/pathogen interactions, cell biology, and tissue/animal development. Each tenure track position within the department is 80-90% research. The Head will be responsible for directing the research, teaching and service activities of the Department, and for developing new programs that complement and enhance current thrusts. A competitive salary, new research laboratory, and research funding support the position. The successful candidate will be an outstanding investigator as well as an effective teacher, mentor and manager.

To apply: *No Fax or Electronic Applications*. To complete the application please consult the complete job description at **http://www.montana.edu/level2/jobs.html** and submit applications to: **VMB Department Head Search, c/o Diane Heck, Secretary, VMB Search Committee, PO Box 172860, Montana State University, Bozeman, MT 59717-2860**. Screening will begin **November 7, 2005** and continue until a suitable candidate is identified. For questions contact **Mark Jutila (E-mail:uvsmj@montana.edu) (phone 406-994-4706).**

ADA/EO/AA/Veteran's Preference.

The University of Texas at Austin

Eukaryotic Molecular Biology Positions

The Institute for Cellular and Molecular Biology

The Institute for Cellular and Molecular Biology invites applications for tenure-track/tenured positions in eukaryotic molecular biology. Academic appointments at the level of Assistant, Associate, or Full Professor will be in an appropriate academic unit in the College of Natural Sciences. Candidates should have an outstanding record of research productivity and a research plan that utilizes molecular and biochemical approaches to address important problems in eukaryotic molecular biology. Areas of particular interest include but are not limited to chromatin structure, regulation of gene expression, RNA interference, DNA damage responses, and cell cycle control.

Building on a strong existing faculty, the Institute has recruited more than 30 new faculty members over the past seven years (see www.icmb.utexas.edu). In addition to an interactive and interdisciplinary research environment, the Institute provides administrative and financial support for the Graduate Program in Cell and Molecular Biology and state-of-the-art core facilities including mass spectrometry, electron and confocal microscopy, DNA microarrays, robotics, and mouse genetic engineering.

Austin is located in the Texas hill country and is widely recognized as one of America's most beautiful and livable cities.

Please send a single PDF file containing your curriculum vitae, summary of research interests, and names of three references before November 1, 2005 to **icmbfacultysearch@biosci.utexas.edu**. In addition, send a hard copy of the same addressed to the co-chairs of the search committee:

Dr. Tanya Paull and Dr. Jon Huibregtse
Eukaryotic Molecular Biology Search
Institute for Cellular and Molecular Biology
The University of Texas at Austin
1 University Station A4800
Austin, TX 78712-0159

Homepage • http://www.icmb.utexas.edu

The University of Texas at Austin is an Equal Opportunity Employer. Qualified women and minorities are encouraged to apply; a background check will be conducted on applicant selected.

FACULTY POSITIONS
Department of Cell & Developmental Biology

Applications are invited for tenure-track positions at the Assistant or Associate Professor level in the Department of Cell and Development Biology at SUNY Upstate Medical University in Syracuse. The Department, under the new chairman, Dr. Joseph W. Sanger, is beginning a major expansion of its faculty. To complement and enhance the existing research interests, we will be recruiting into the general areas of cellular function and development. At this time we are particularly interested in outstanding candidates with expertise in cardiovascular development and cell signaling, but welcome applications from individuals with research programs in areas of cell motility and the cytoskeleton, cell differentiation, stem cell biology, and organogenesis. Substantial renovation and expansion of departmental research space and core facilities has begun in order to support the department's growth.

Candidates should have a Ph.D. and/or M.D. degree, and postdoctoral experience. Assistant Professors will be expected to develop an independent research program, while applicants at the Associate Professor level should have an established track record of research productivity and funding. Substantial startup packages and competitive salaries will be provided to all successful candidates. All faculty will participate in the training and teaching of graduate and medical students.

Please submit CV, descriptions of research accomplishments, future plans for research and teaching interests as a single PDF file to **fontanek@upstate.edu**. Please have three letters of recommendation sent to **Dr. Christopher Turner, Chair Search Committee, Department of Cell and Developmental Biology, SUNY Upstate Medical University, 750 East Adams Street, Syracuse, NY 13210.** For additional information, visit the departmental website **www.upstate.edu/cdb.**

State University of New York
Upstate Medical University
Formerly known as SUNY Health Science Center

An AA/EEO/ADA employer, committed to excellence through diversity.

UNIVERSITY OF TEXAS SOUTHWESTERN MEDICAL CENTER

Faculty Positions in Infectious Diseases

The Division of Infectious Diseases in the Department of Medicine at the University of Texas Southwestern (UTSW) Medical Center at Dallas is seeking new faculty members at the Assistant Professor, Associate Professor, or Professor levels. Faculty will be expected to develop independent and externally funded independent research programs that focus on understanding the molecular pathogenesis of infectious diseases and/or host defense mechanisms. Preference will be given to applicants performing "cutting-edge" research on medically important pathogens, emerging pathogens, and/or agents of potential biothreat. Excellent opportunities exist for collaborations with faculty members in Infectious Diseases, the Department of Microbiology, and the Center for Immunology at UTSW and with the Regional Center of Excellence (RCE) for Biodefense and Emerging Infectious Diseases. UTSW is an outstanding scientific environment with established strengths in structural biology, biochemistry, molecular biology, genetics, and numerous other areas. Candidates will be expected to contribute to the teaching and research training of Infectious Diseases fellows. The position offers an attractive startup package and laboratory space. Candidates should have an M.D. and/or a Ph.D. degree with at least two years of postdoctoral experience and an outstanding publication record.

To apply, submit a C.V., three letters of reference, and a description of research interests to: **Dr. Beth Levine, Chief, Division of Infectious Diseases, c/o Renee Talley, UT Southwestern Medical Center, 5323 Harry Hines Blvd., Dallas, TX 75390-9113. E-mail: renee.talley@utsouthwestern.edu.**

UT Southwestern is an Equal Opportunity/ Affirmative Action Employer.

POSITIONS OPEN

ASSISTANT/ASSOCIATE/FULL PROFESSOR (Toxicogenomics/Tenure-track)

The Departments of Biological Sciences and Chemistry at Louisiana State University (LSU) jointly invite applications for a tenure-track (tenured) open rank position in toxicogenomics, available August 2006. The incumbent will employ molecular approaches (e.g., genomics, proteomics, metabolomics) to address questions in environmental toxicology. We seek an individual whose research complements our existing strengths in aquatic and/or airborne contaminants, and those with an interest in complex mixtures of contaminants, but will consider all qualified applicants. The successful candidate may be appointed in the Department of Biological Sciences or the Department of Chemistry; joint appointments are also possible. The startup package will be highly competitive. The position has been made possible through the Governor's Biotechnology Initiative, with the goal of enhancing biotechnology research in Louisiana. Required qualifications: Ph.D. or equivalent degree in a biology/chemistry science or related field, postdoctoral experience. The successful candidate will be expected to develop a strong, extramurally funded research program, and contribute to teaching at the graduate and undergraduate levels. An offer of employment is contingent on a satisfactory preemployment background check. Review of applications will begin October 31, 2005, and will continue until candidate is selected. Send curriculum vitae (including e-mail address), a two to three page statement of research and teaching interests, three letters of recommendation, and no more than three representative publications to:

Toxicogenomics Faculty Search
c/o Dr. Mark A. Batzer
Department of Biological Sciences
202 Life Sciences Building
Louisiana State University
Ref: Log #0458
Baton Rouge, LA 70803

Additional information about the Departments of Biological Sciences and Chemistry are available at **websites: http://www.biology.lsu.edu** and **http://chemistry.lsu.edu** respectively. *LSU is an Equal Opportunity/Equal Access Employer.*

Bridging the Rift Foundation (BTR) and Sun Microsystems announce two **POSTDOCTORAL FELLOWSHIPS** in computational biology, for two years at Cornell University. BTR was created to promote peace in the Middle East through scientific collaboration. For more information see **website: http://www.news.cornell.edu/features/BTR/.** The fellowships are for positions in the Database Group in the Department of Computer Science, Cornell University, Ithaca, NY. Applicants must have Jordanian or Israeli passports.

We seek outstanding Ph.D.-level applicants to build a novel scalable database infrastructure for the computational biology community in general and for the Library of the Desert project in particular. Two openings are available for system architects who will contribute to the research and development of the system. Applicants should have earned a Ph.D. degree in database systems or a related area. Experience in leading, architecting, and developing large projects is a requirement. Please send resumes to **e-mail: btr-sun_search-l@cs.cornell.edu.**

RESEARCH ASSOCIATE position is available to study the functional role of aberrant fusion proteins in human cancers (**website: http://www.msm.edu/micro_immuno/reddyl.htm**). Successful, motivated applicants should have a Ph.D./M.D. degree and a background in molecular biology. Please send curriculum vitae and two reference names and addresses to: **Dr. E. Shyam Reddy, Professor and Co-Director (e-mail: ereddy@msm.edu), Cancer Biology Program, Morehouse School of Medicine, Department of Obstetrics/Gynecology, Atlanta, GA 30303.**

POSITIONS OPEN

School of Medicine
TEMPLE UNIVERSITY

STEM CELL, CYTOSKELETON RESEARCHER

Temple University School of Medicine is currently seeking a researcher (Ph.D. or M.D.) at the **ASSISTANT** or **ASSOCIATE PROFESSOR** level who is trained in cell or molecular biology (preferably with a history of grant funding) and whose research interests lie in the area of stem cell research (as related to cancer, including ovarian and breast cancer) and research into the cell cytoskeleton (including the effect of antimitotic drugs) as related to cancer and its treatment.

Please send curriculum vitae and bibliography to: **Henry Simpkins, M.D., Ph.D., Professor and Chairperson, Department of Pathology and Laboratory Medicine, Temple University Hospital, 3401 North Broad Street, Philadelphia, PA 19140.** *Temple University is an Equal Opportunity/Affirmative Action Employer and strongly encourages applications from women and minorities.*

MOLECULAR BIOLOGISTS AND BIOCHEMISTS

POSTDOCTORAL and **RESEARCH ASSOCIATE** positions are available to study neuronal gene regulatory mechanisms and signaling pathways. We are using multi-disciplinary approaches, including transgenic, biochemical, molecular, cellular, imaging and biophysical methods to address a wide range of biological and pharmacological questions related to opioid receptors as well as hormone nuclear receptors and their coregulators in gene regulation. We are focused on the regulatory mechanisms that control the expression of opioid receptors and other neuronal genes, signaling pathways of opioid receptors, and the mechanism of action of nuclear receptors and their coregulators in gene transcription. Ph.D. in various biological sciences or biophysics is required. Previous training in molecular biology, biochemistry, neuroscience or biophysics is preferred.

Interested applicants should send curriculum vitae, statement of research interests, and names of three references to: **Dr. Horace H. Loh, Professor and Head,** either by **e-mail: lohxx001@umn.edu** or to the following address: **Department of Pharmacology, University of Minnesota, 6-120 Jackson Hall, 321 Church Street S.E., Minneapolis, MN 55455. Fax: 612-625-8408.**

The University of Minnesota is an equal opportunity educator and employer.

FACULTY POSITION
Colorado State University

The Department of Biochemistry and Molecular Biology seeks applications for an **ASSISTANT PROFESSOR** with expertise in structural, cellular, or molecular biology. Candidates with research interests complementary to existing departmental strengths, such as chromatin structure, gene expression, infectious diseases, or cytoskeleton dynamics, are strongly encouraged to apply. Further information is available at **website: http://www.bmb.colostate.edu.** Candidates must have a Ph.D., postdoctoral experience, the ability to sustain an independent research program, and the desire to participate effectively in undergraduate and graduate teaching. Please submit curriculum vitae and statements of research and teaching interests online at **website: http://www.bmb.colostate.edu/jobs.cfm.** Three reference letters must be requested by the applicant and sent directly to **e-mail: bmbsearch@colostate.edu.** For full consideration, a complete application must be received by November 11, 2005. Files of finalists will be available to the full faculty for review. *Colorado State University is an Equal Opportunity/Affirmative Action Employer; Equal Opportunity Office: 101 Student Services.*

POSITIONS OPEN

ASSOCIATE CHIEF OF STAFF

The Department of Veterans Affairs (VA) Northern California Health Care System is currently recruiting for a full-time Associate Chief of Staff for Research and Development (ACOS/R&D), to head its research program. VA Northern California is an integrated health care system, which provides a full range of health care services to veterans in Northern California. VA Northern California has two major campuses and nine locations in the Northern California area. Clinical and nonclinical research is conducted at our two main campuses located at Sacramento and Martinez, California. The Sacramento campus is the site of our new medical center, which includes 16,000 square feet of basic research laboratory space and a nine-bed, 8,000 square foot NIH-funded General Clinical Research Center in collaboration with University of California, Davis (UCD). Applicants for the ACOS/R&D position must have an M.D. and/or Ph.D. degree. The successful candidate is expected to maintain an outstanding research program and facilitate the growth of new and existing intramural research programs as well as building interdisciplinary collaborations with researchers at our affiliate, UCD. The selected applicant will be provided research space at the VA Sacramento campus. Candidates should possess previous experience in administrative or leadership positions, preferably in the VA, a record of research excellence, and be eligible for academic appointment at the level of Associate Professor or Professor at our university affiliate, UCD. Candidates should forward a letter of interest describing their research and teaching background and current interests, curriculum vitae, reprints of three publications, and names and addresses of at least three references to: **VA Research Office, Attn: ACOS Search Committee, 10535 Hospital Way, Mather, CA 95655.** For full consideration applications must be received by October 11, 2005. *VA is an Equal Opportunity Employer.*

The U.S. Department of Labor, Office of Workers' Compensation Program, Division of Energy Employees Occupational Illness Compensation seeks a **HEALTH SCIENTIST** (Toxicologist) in Washington, D.C. The Energy Employees Occupational Illness Compensation Program Act (EEOICPA) provides compensation and medical benefits for Department of Energy workers who sustain employment-related illnesses as a result of exposure to beryllium, ionizing radiation, and other toxic substances unique to nuclear weapons production and testing. The program was recently expanded to cover a wider range of illnesses. The agency is looking for a candidate who is an expert in employee chemical/toxicological exposures, with experience in formulating policy. The Department of Labor offers a variety of workplace benefits. Salary ranges from $88,369 to $114,882 per annum, with potential for other bonuses.

To apply or obtain additional information, go to **website: http://www.usajobs.opm.gov** and review announcement number ESA-OWLS-05-136-DEU, or **telephone: 202-693-0004.** All online applications/resumes must be received by October 11, 2005. *USDOL is an Equal Opportunity Employer.*

FORMULATION DEVELOPMENT CHEMIST with Bachelor's or foreign equivalent in chemistry or pharmaceutical science and two years experience to develop specialty oral solid dosage formulations such as delayed release tablets. Handle sifter, fluid bed coater, granulator and compression machine for development. Provide in-process, finished product and stability testing support using HPLC, dissolution apparatus and Karl Fisher titrator. Perform facility and HVAC system qualification of the pharmaceuticals using particle counter, anemometer, decibometer, air sampler and hygrometer. Support scale up operations based on SUPAC guidance. Write protocols and reports. Two years experience as Chemist, Quality Assurance is acceptable. Mail resume to: **Accumed Inc., 2572 Brunswick Pike, Lawrenceville, NJ 08648.** Job Location: **Lawrenceville, NJ Human Resources Department.** *Equal Opportunity Employer.*

Audubon

Vice President and Chief Scientist
National Audubon Society

Audubon, one of the hemisphere's premier conservation organizations, seeks a seasoned leader who is recognized internationally in the field of ornithology to shape Audubon's strategic approach to conservation and guide the organization's science programs. This is a high-paced, exciting, leadership position, requiring superior interpersonal skills and at least 10 years of progressively responsible senior level management experience in the non-profit sector. The Chief Scientist will promote the expansion of citizen science and citizen stewardship initiatives to engage local, national and international stakeholders in strategic conservation activities. The ability to integrate and align Science activities and programs with those of Audubon's public policy and education efforts is highly desired.

Advanced degree in Ornithology, Conservation Biology, or Natural Resource Management with an emphasis on birds is required. Nationwide field experience and an understanding of both the practical and theoretical realms of conservation planning throughout the hemisphere are strongly desired. The ability to effectively articulate the significance of data and other scientific and technical information for Audubon's membership and the general public is essential.

Position will be based in Washington DC. Frequent travel required. For complete job description, see our website at **www.Audubon.org**. Send resume, cover letter, and salary history to: **Seniorpositions@audubon.org**. The review process will begin **September 30, 2005** but applications will be accepted until the position is filled.

CBSE Othmer Department of Chemical & Biological Sciences & Engineering

Polytechnic University

The Polytechnic University Announces the Opening of Two Endowed Chairs in Chemical and Biological Engineering

Polytechnic University, the second oldest technological university in the United States, is delighted to issue a call for nominations and direct applications for two endowed Distinguished Chairs of Chemical Engineering for senior or junior faculty. Both chairs, endowed with $2.5 million each, are available starting on July 1, 2006 in the newly established Othmer Department of Chemical and Biological Engineering.

We aim to attract to the two chairs individuals with internationally recognized records of research accomplishments in chemical engineering, particularly those with a significant overlap with biology and/or energy issues. The desired candidates should have at least one degree in Chemical Engineering, a strong commitment to undergraduate and graduate education and the ability and energy to further first class research activities at Polytechnic. The recruitment of distinguished colleagues to occupy these chairs is part of an effort to strengthen the undergraduate and graduate programs in chemical and biological engineering, and to assure that Polytechnic University remains one of the premier technological institutions in the world.

We are also interested in receiving applications from junior faculty for an Early Career Endowed Chair of Chemical Engineering. Those candidates must show a clear promise to be inspiring teachers and establish successful internationally recognized research programs.

Applications and/or nominations should be sent electronically to **Professor Walter Zurawsky (zurawsky@poly.edu)** or **Professor Edward Ziegler (eziegler@poly.edu)**. All applications and nominations related to these outstanding opportunities will be handled with the utmost discretion and confidentiality.

Polytechnic University is located in Brooklyn, New York, inside the MetroTech Center, a 16-acre academic/research/commercial complex, just across the Brooklyn Bridge, minutes from Manhattan. For additional information about the department or Polytechnic University visit **www.poly.edu**.

EOE/AA

The Cleveland Clinic Foundation
Lerner Research Institute

Alzheimer's Disease Research Faculty Position
Department of Neurosciences

The Department of Neurosciences seeks additional faculty for its Alzheimer's Disease Research Program. Targeted areas of interest include molecular mechanisms of neurodegeneration in transgenic mice, in vitro models and/or postmortem tissue from AD patients. Applicants must have a Ph.D. and /or M.D. and a strong desire to secure independent funding. Successful candidates will be offered attractive start-up packages and are expected to integrate with clinical and basic science programs within The Cleveland Clinic Foundation and Case Western Reserve University.

The Department of Neurosciences and the Lerner Research Institute (www.lerner.ccf.org) are undergoing rapid growth. The Department of Neurosciences has strong programs in developmental neurobiology, excitable membranes, and cell signaling.

Candidates should submit curriculum vitae, a list of publications, a brief statement of research interests, and three letters of reference to:

Bruce D. Trapp, Ph.D
Department of Neurosciences NC30
The Cleveland Clinic Foundation
9500 Euclid Ave
Cleveland, OH 44195

AA/EOE

Director Nanoscale Facility at Cornell University - 04456

Located in Ithaca, N.Y., Cornell University is a bold, innovative, inclusive and dynamic teaching and research university where staff, faculty, and students alike are challenged to make an enduring contribution to the betterment of humanity.

Cornell University seeks a prominent scientist/engineer and research administrator as a faculty member, serving half-time as the chief officer of Cornell's Nanoscale Facility (CNF; **www.cnf.cornell.edu**); this position reports to Cornell's Vice Provost for Research. This individual will also hold a tenured appointment in an academic department suited to the candidate. CNF's skilled staff of 25+ provides leading-edge fabrication and characterization tools for nanoscale R&D to 750+ users annually. Last fall CNF relocated into a $100M state-of-the-art building and was awarded an NSF grant through 2009, with an additional five years possible. The Director is responsible for formulation of facility policies, selection of scientific and technical personnel, overall management of financial support, and development of outreach and educational activities. The Director will represent Cornell to the NSF and within the National Nanotechnology Infrastructure Network, a 13-member consortium. Selection will be based upon outstanding research accomplishments and demonstrated leadership experience. The appointment, for 5 years, may be renewed; the post is available as soon as a suitable candidate is found.

Send nominations or applications, including a resume and suggested references, to: **Joseph A. Burns, Chair of CNF Search, Vice Provost for Physical Sciences and Engineering, 222 Day Hall, Cornell University, Ithaca NY 14853 (jab16@cornell.edu; 607-255-7200).**

Cornell University

Cornell University is an Affirmative Action/ Equal Opportunity, Employer and Educator

http://chronicle.com/jobs/profiles/2377.htm

POSITIONS OPEN

OLD DOMINION UNIVERSITY
Computational Biology
FACULTY IN MODELING, SIMULATION, AND VISUALIZATION

Old Dominion University (ODU) is recruiting five tenure-track faculty members (**ASSISTANT/ASSOCIATE PROFESSOR** level) five endowed chairs in targeted areas of modeling, simulation, and visualization (MS&V). These positions along will form the core of MS&V academic and research program at ODU. University's Virginia Modeling, Analysis and Simulation Center (VMASC) is one of the world's leading university research centers for computer modeling, simulation, and visualization. The mission of the Center is to conduct collaborative MS&V research and development, provide expertise to industry and governmental agencies, and to promote ODU, Hampton Roads, and Virginia as a center of MS&V activities. The Center has over 50 research and administrative staff and works closely with faculty researchers from across the University. In 2004, the Center conducted approximately $10.5M in funded research. ODU offers master's and doctoral degrees in modeling and simulation supported by faculty from all six academic colleges and research faculty from VMASC. The program has an enrollment of approximately 55 master's and 45 doctoral students.

ODU is located in the Hampton Roads, the nation's center for the military application of MS&V. The region is home to the Joint War Fighting Center, the Joint Battle Center, the U.S. Army's Training and Doctrine Command, the Military Transportation Management Command, the Armed Forces Staff College, U.S. Navy's Commander Operational Test and Evaluation Force, the Naval Sea Systems Command, and the Space and Naval Warfare Center. In addition, Newport News Shipbuilding, Jefferson Lab, and NASA – Langley Research Centers are important users of MS&V technology. The economic value of MS&V related business activity in Hampton Roads is estimated to be over $500M. Leveraging the strength that has been brought about by VMASC, Virginia's Governor Mark R. Warner recently announced a $1.45M state initiative to market and promote the region and establish a national Institute for Homeland Security and Crisis Management.

One of these available Assistant/Associate Professor positions is in the area of computational biology (in Department of Biological Sciences). This faculty member will be expected to pursue vigorous funded research program, and have significant involvement with VMASC as well as with the interdisciplinary graduate program in modeling and simulation. This individual will benefit from our existing areas of strength in bioengineering, ecology and evolutionary biology, infectious disease biology, and medical imaging, as well as emerging strengths in bioinformatics. The successful candidate must have an earned Ph.D. Preference will be given to candidates with a strong background in MS&V research. Consideration for appointment at the Associate Professor rank requires a solid record of external funding.

Screening will begin on November 15, 2005. A letter of application and a current resume with names, addresses, telephone numbers, and e-mail addresses for at least three references should be sent to: **Dr. Christopher Osgood, Department of Biological Sciences, Norfolk, VA 23529. Telephone: 757-683-3605, e-mail: cosgood@odu.edu.** *Old Dominion University is an Affirmative Action, Equal Opportunity Institution and requires compliance with the Immigration Reform and Control Act of 1986.*

POSTDOCTORAL POSITION
Human Cancer Gene Therapy

Federally funded laboratory program conducting human clinical trials and basic research in T cell gene therapy for prostate, melanoma, breast, colon cancers. Advanced retroviral vector development and engineering T cell effector responses. Contact: **Dr. R.P. Junghans, Roger Williams Medical Center/Boston University School of Medicine** via **e-mail: mjamison@rwmc.org** with resume, research summary, names of three references.

POSITIONS OPEN

FACULTY POSITIONS

The Children's Memorial Research Center/Children's Memorial Hospital and the Feinberg School of Medicine at Northwestern University seek outstanding candidates for full-time up to three tenure-track faculty positions in the Mary Ann and J. Milburn Smith Child Health Research Program, an interdisciplinary program designed to integrate laboratory, clinical and population research (for details, please refer to its **website: http://www.childrensmrc.org/childhealthresearch/**). The positions offer outstanding scholarly and scientific resources in a collegial and collaborative clinical and research environment (**websites: http://www.childrensmrc.org; http://thepoint.childrensmemorial.org/**). High quality office and laboratory space and excellent start-up support will be provided. The rank of academic appointment and salary is negotiable. Applicants who are physician-scientists should expect to spend at least 70% of their time on research.

Candidates should have a Ph.D. and/or M.D. degree and exceptional research potential in the areas of reproductive/perinatal epidemiology; obesity and metabolic syndrome; allergy; genetic epidemiology; pharmacogenomics; and bioinformatics. Major responsibilities of the positions are to develop innovative and independent research programs and to participate in ongoing funded research projects.

Applications responding to this announcement can be submitted until January 15, 2006. Start date is negotiable. Applicants should send curriculum vitae, a two to three page statement of proposed research plan and long-term goals, and three letters of recommendation to:

Xiaobin Wang, MD, MPH, ScD
Director, Mary Ann and J. Milburn Smith Child Health Research Program
Children's Memorial Research Center (CMRC)
Feinberg School of Medicine
Northwestern University
2300 Children's Plaza, Box 157
Chicago, IL 60614

Northwestern University is an Affirmative Action, equal Opportunity Employer. Hiring is contingent upon eligibility to work in the USA. Women and minorities are especially encouraged to apply.

FACULTY POSITION
PLANT BIOCHEMISTRY
Department of Biochemistry and Molecular Biology
Penn State University

Applications are invited for a tenure-track position as **ASSISTANT PROFESSOR** of plant biochemistry. Candidates should have a strong record of research accomplishment and have the potential for developing an extramurally funded program of research that complements and builds on Penn State's current strengths in plant biology. The successful candidate will benefit from opportunities to collaborate with scientists in the departments of Biochemistry and Molecular Biology, Biology, and Chemistry and in the College of Agricultural Sciences, as well as within an interdisciplinary graduate program in plant biology with a large number of highly interactive plant scientists (see **website: http://plantphys.psu.edu** for faculty listing). We are particularly interested in candidates using biochemical approaches to solve interdisciplinary problems at the cell and molecular levels, particularly in the areas of plant growth, development, and signal transduction.

Please submit curriculum vitae, a summary of past, current, and future research, and a statement of teaching interests and philosophy, and arrange to have three references sent to: **Chair, Plant Biochemistry Search, Department of Biochemistry and Molecular Biology, 108 Althouse Laboratory, The Pennsylvania State University, University Park, PA 16802.** Review of applications will begin November 28, 2005. *Penn State is committed to Affirmative Action, Equal Opportunity and the diversity of its work force.*

POSITIONS OPEN

DRAKE UNIVERSITY
Biology Department

Pending final budgetary approval, full-time tenure-track **ASSISTANT PROFESSOR** in vertebrate biology, beginning fall semester 2006. Ph.D. required, with postdoctoral experience desirable. Geographic information system training and ability to curate a vertebrate collection is desirable.

Teaching responsibilities include an evolution-oriented capstone course, a vertebrate specialty course, and participation in the general/preprofessional introductory biology course. A commitment to inquiry-based teaching in an interdisciplinary setting is expected, along with externally funded research that can engage undergraduates.

Send curriculum vitae, e-mail addresses of three references, philosophical statement on teaching and research, publication sample, and transcripts to:

Dr. Wayne Merkley
Professor of Biology
Drake University
2507 University Avenue
Des Moines, IA 50311

For full consideration, all application materials should be received by December 1. Position open until filled. *Drake University is an Equal-Opportunity Employer, and actively seeks applicants who reflect the diversity of the nation. No applicant shall be discriminated against on the basis of race, color, national origin, creed, religion, age, disability, sex, gender identity, sexual orientation or veteran status.*

TENURE-TRACK POSITIONS IN PHARMACOLOGY
Mercer University
Southern School of Pharmacy

The Department of Pharmaceutical Sciences at Mercer University Southern School of Pharmacy in Atlanta, GA, invites applications for two 12-month tenure-track faculty positions in pharmacology at the **ASSISTANT** OR **ASSOCIATE PROFESSOR** level. Applicant must have a Ph.D. A degree in pharmacy or a strong background in pharmacy education is highly recommended. Rank is commensurate with qualifications and experience. Qualified candidates will be expected to teach in both the professional (pharmacology and medicinal chemistry or physiology) and graduate programs and establish an independent, extramurally funded research program and mentor graduate students. Research interests in the area of pharmacology are not limited to a specific area.

The Department of comprised of 14 full time tenure-track faculty, two full time research faculty, and more than 30 Ph.D. students. The school is located on the Atlanta campus of the University. The campus' 335 wooded acres create a serene and secluded atmosphere despite its close proximity to downtown Atlanta. For complete announcement and to apply online, please access **website: http://www.mercerjobs.com.**

Affirmative Action/Equal Opportunity/Americans with Disabilities Act Employer.

POSTDOCTORAL FELLOW

A Postdoctoral position is available to study cytoskeletal and transcriptional signaling pathways in neurofibromatosis (NF); specially, the role of small GTPases and their effectors in the pathogenesis of NF1 and NF2. Projects include, but are not limited to, discovery of new targets for p21-activated protein kinases, development of genetic models for such kinases and their substrates, and the role of small GTPases and their effectors in cell division. The successful candidate should have a Ph.D. and/or M.D. with less than two years of postdoctoral experience. A strong background in molecular biology, cell imaging, and/or transgenic mouse technology is required. To apply, please send curriculum vitae and the names of three references to: **Dr. Jonathan Chernoff, Fox Chase Cancer Center, Room W451, 333 Cottman Avenue, Philadelphia, PA 19111-2497. E-mail: j_chernoff@fccc.edu.** *Equal Opportunity Employer.*

POSITIONS OPEN

FACULTY POSITION IN GENETICS

The College of William and Mary's Department of Biology invites applications for a tenure-track position at the **ASSISTANT PROFESSOR** level in genetics. Research areas of particular interest include viral, archaeal, and yeast genetics, but outstanding candidates in other areas of molecular genetics are encouraged to apply. The successful candidate will be expected to establish and maintain an extramurally funded research program involving both undergraduate and Master's degree students. Teaching responsibilities include an upper division course in transmission genetics and another course in the candidate's area of expertise. Candidates must demonstrate the potential and motivation to achieve excellence in teaching. Previous experience teaching undergraduate courses would be viewed favorably, and postdoctoral research experience is expected. A competitive startup package is available.

Review begins November 15, 2005, and will continue until an appointment is made. Submit a letter of application, curriculum vitae, and statements of research plans and teaching philosophy, and arrange to have three letters of reference mailed directly to: **Genetics Search Committee, Department of Biology, The College of William and Mary, P.O. Box 8795, Williamsburg, VA 23187-8795.** Further information on the Department of Biology and this position may be obtained at **website: http://www.wm.edu/biology/.** Information on the College may be obtained at **website: http://www.wm.edu/.** *The College is an Equal Employment Opportunity/Affirmative Action Employer.*

UNDERGRADUATE TEACHING POSITION
Brandeis University

The Biology Department seeks a full-time faculty member to teach biology laboratory and lecture classes to begin Fall, 2006. Candidate should have a Ph.D. in the area of molecular/cell/genetics, postdoctoral and/or teaching experience, and be committed to undergraduate education. This will be a one-year, renewable appointment and salary and rank will be commensurate with experience.

Applicants should submit curriculum vitae, statement on teaching philosophy, and names of three references to:

Judith E. Tsipis, Biology Search
Biology Department, M.S. Number 008
Brandeis University,
Waltham, MA 02454-9110
Website: http://www.bio.brandeis.edu

First consideration will be given to applications received by November 1, 2005. *Brandeis University is an equal opportunity employer, committed to building a culturally diverse intellectual community and strongly encourages applications from women and minorities.*

TENURE-TRACK POSITION in Mammalian Development
Brandeis University

Brandeis University has an opening for a tenure-track appointment in the Department of Biology beginning Fall, 2006. We seek individuals studying mammalian development using transgenic approaches in mice. Candidates interested in studying the development of the nervous system are especially encouraged to apply, although all areas of mammalian developmental biology will be considered. Candidates should have a Ph.D., M.D. or both as well as postdoctoral experience. Applicants should submit curriculum vitae, research plan, and arrange for three letters of recommendation to be sent to: **Developmental Biology Search Committee, M.S. 008, Department of Biology, Brandeis University, 415 South Street, Waltham, MA 02454-9110.**

First consideration will be given to applications received by December 1, 2005. *Brandeis University is an equal opportunity employer, committed to building a culturally diverse intellectual community and strongly encourages applications from women and minorities.*

POSITIONS OPEN

PURDUE UNIVERSITY

Purdue University Calumet invites applications for the position of **HEAD OF THE DEPARTMENT OF BIOLOGICAL SCIENCES**, to begin in July 2006. The successful candidate must have a Ph.D. in a biological science and have the rank of full professor. A strong record of teaching, externally funded research, administrative experience, and community and professional engagement is expected. Purdue University Calumet, the Chicago-area campus of the Purdue University system, is a M.S. Comprehensive University with a current enrollment of 9,200 students. The Department consists of nine full-time faculty and has approximately 350 undergraduate majors and 30 graduate students. In addition to courses for majors, the department provides service courses for many core programs of the University. The new Head will be expected to foster development of a Departmental vision and strategic plan that will lead to a new level of accomplishment and recognition. Opportunities for collaborative initiatives exist with new institutes and centers at Purdue Calumet as well as with corporations in the new Purdue Technology Center in Merrillville, IN. Interested applicants should submit curriculum vitae, statements of philosophy on teaching, research/scholarship and administration, and contact information for three references to: **Biological Sciences Head Search, Department of Biological Sciences, Purdue University Calumet, 2200 169th Street, Hammond, IN 46323** or **e-mail: biosearch@calumet.purdue.edu.** Application review will start January 5, 2006. *Purdue University Calumet is an Equal Access/Equal Opportunity/Affirmative Action Employer.*

YORK UNIVERSITY
DEPARTMENT OF BIOLOGY

Applications are invited for two tenure-track positions, one in animal physiology and one in molecular and/or cell biology, both at the **ASSISTANT PROFESSOR** level.

For the animal physiology position, preference will be given to candidates using integrative approaches to address principles of regulatory mechanisms. For the molecular and/or cell biology position, preference will be given to candidates using molecular approaches to understand fundamental questions in any area of biology with the emphasis being on research excellence.

Further information about the Department of Biology can be found at **website: http://www.biol.yorku.ca/dept/.**

The successful candidates will have a Ph.D., postdoctoral experience and an outstanding research record, and will be expected to develop a strong, externally funded research program and contribute to teaching biology-related courses at undergraduate and graduate levels. The start date for both positions is July 1, 2006. All positions at York University are subject to budgetary approval.

Applicants should send curriculum vitae, an outline of their research plans, single copies of three publications, and three signed letters of reference by November 1, 2005 to: **Chair (designate area) Search Committee, Biology Department, Farquharson Life Science Building, 4700 Keele Street, Toronto ON, Canada M3J 1P3.**

York University is an affirmative action employer. The affirmative action program can be found on York's website at www.yorku.ca/acadjobs or a copy can be obtained by calling the affirmative action office at 416-736-5713. All qualified candidates are encouraged to apply; however, Canadian citizens and permanent residents will be given priority.

POSITIONS OPEN

FACULTY POSITION
NEUROSCIENCE

The California State University, Long Beach (CSULB) Department of Biological Sciences invites applications for a tenure-track position, beginning fall 2006. **ASSISTANT PROFESSOR** level preferred, exceptionally experienced candidates considered for **ASSOCIATE PROFESSOR.**

Ph.D. in biological sciences with training and research in neuroscience required. Teaching duties: undergraduate neurophysiology and contributions to the physiology core, graduate, and general education courses in an ethnically diverse campus community. Must have published research and show strong potential for developing an externally funded research program involving students. Two years of postdoctoral research experience in sensory physiology, neuroendocrinology, or synaptic physiology and signal transduction preferred. CSULB actively encourages applications from all qualified individuals, particularly scholars from underrepresented groups. Submit application letter, curriculum vitae, detailed statements of research and teaching interests, reprints of two publications, and three letters of recommendation to: **Dr. Editte Gharakhanian, Chair, ATTN: Neuroscience Search, Department of Biological Sciences, California State University, Long Beach, CA 90840-3702. Telephone: 562-985-4807. E-mail: ssuetsug@csulb.edu**. Screening starts November 1, 2005. Additional information at **website: http://www.csulb.edu/depts/biology/.** *CSULB is an Equal Opportunity Employer.*

ANIMAL DEVELOPMENT
Carleton College

The Department of Biology invites applications for a **TENURE-TRACK POSITION** starting September 1, 2006. We seek candidates whose teaching and research interests are in the field of animal development. In addition, we are especially interested in candidates whose expertise includes one of the following: evolutionary developmental biology, comparative genomics, developmental genetics, or bioinformatics. Teaching responsibilities include an upper-level course in animal development with a laboratory, a course in an area of specialty with a laboratory, and team-teaching in the introductory biology sequence. Candidates should be committed to excellence in undergraduate teaching in a liberal arts environment, and dedicated to developing an active research program that engages students. Candidates must have a Ph.D. in developmental biology or a related field, and postdoctoral experience is preferred. Please send letter of application, curriculum vitae, a statement of teaching philosophy and research plans, and three letters of reference to: **Professor Stephan Zweifel, Department of Biology, Carleton College, Northfield, MN 55057-4025.** Application deadline is October 14, 2005. *Carleton is an affirmative action/equal opportunity employer. We are committed to developing our faculty to better reflect the diversity of our student body and American society. Women and members of minority groups are strongly encouraged to apply.*

Science AAAS

Additional job postings not featured in this issue can be viewed online at **website: http://www.sciencecareers.org.** New jobs are added daily!

Manage your job search more effectively by creating an account at **website: http://www.sciencecareers.org.** You can post your resume (open or confidentially) in our database and use it to apply to multiple jobs simultaneously. Track the jobs you have applied to in special tracking folders. Plus, you can create Job Alerts that will e-mail you notification of jobs that match your search criteria.

CONFERENCE

International Society for Cell and Gene Therapy of Cancer
December 9th-11th, 2005
SHENZHEN, CHINA

"GENE THERAPY IN THE 21st CENTURY"

Sponsored by:
SiBiono GeneTech
Introgen Therapeutics
Center for Gene and Vaccine Therapy, Medical University of South Carolina
International Society for Cell and Gene Therapy of Cancer

The International Society for Cell and Gene Therapy of Cancer is focused on developing and integrating practioners of gene therapy throughout the world. This meeting in China is incredibly exciting because China is the first Country to have approved a gene medicine, Gendicine, an adenovirus for treatment of cancer, which is produced and marketed by Shenzhen SiBiono GeneTech, Co., Ltd.

Abstract Deadline:
October 17, 2005
Please visit
www.iscgtchina2005.com
to download abstract submission and conference registration forms.

Registration Deadline:
November 31, 2005

Organized by:
International Society for Cell and Gene Therapy of Cancer

Conference Organizers:
Zhao Hui Peng
Jian-ren Gu
James S. Norris
Yuhong Xu
Jian-yun Dong

WWW.ISCGTCHINA2005.COM

FACULTY POSITION
Assistant/Associate Professor – Molecular Virology

The Department of Molecular Microbiology and Immunology (MMI) **http://www.missouri.edu/~mmiwww** at the University of Missouri-Columbia, School of Medicine, invites applications for new faculty at the Assistant or Associate Professor level. The targeted research area encompasses all areas of molecular virology, including, but not limited to, mechanisms of pathogenesis, virus life cycle and replication strategies, host responses to infection, molecular evolution, tumor virology, gene transfer, and virus assembly and maturation. The successful candidate will be expected to develop and maintain a vigorous research program that will attract continued extramural funding and offers synergism with existing programs. The candidate will also contribute to the teaching and training of graduate and medical students. Candidates with interdisciplinary interests may be considered for joint appointments with other departments. Salary and start-up packages are highly competitive.

The new hire will join a diverse group of virologists (including two faculty hired last year) in the pathogenesis wing of the new Life Sciences Center (LSC) (**http://lifesciences.missouri.edu**), a state-of-the-art, multi-disciplinary facility opened in September, 2004. The LSC is designed to provide a highly interactive scientific environment. It will eventually house approximately 35 investigators (nearly half being new hires), and will serve as the hub of Life Sciences research on the MU campus. Facilities are available within the LSC for BSL2 and BSL3 work, as well as core facilities for proteomics, imaging and DNA services. Additional facilities for flow cytometry, electron microscopy, mouse transgenics, ES cell manipulations, hybridoma production and state-of-the-art NMR structural analysis are in close proximity on the MU campus.

Applicants must possess a Ph.D., M.D., or equivalent degree, and have appropriate post-doctoral training. Interested candidates should submit a curriculum vitae, a statement of research interests and future research goals, and letters from at least three referees to the address below (e-submission preferred). Review of applications will begin **October 15, 2005** and will continue until the position is filled.

Molecular Virology Search Committee
Attn: Ms. Shelly Crawford, Office Supervisor
M616 Medical Sciences Building
Department of Molecular Microbiology and Immunology
University of Missouri-Columbia, School of Medicine
Columbia, MO 65211
(573) 882-8989
crawfords@health.missouri.edu

The University of Missouri is an AA/EOE. To request ADA accommodations, please contact (573) 884-7278 (V/TTY). Women and minorities under-represented in biomedical research are encouraged to apply.

Assistant Professor
Structural Biology and Molecular Electron Microscopy
Harvard Medical School

The Department of Biological Chemistry and Molecular Pharmacology at Harvard Medical School announces a search for an Assistant Professor whose research interests concern the structural biology of macromolecular complexes and subcellular assemblies, especially as studied by molecular electron microscopy and related methods. The appointment is in conjunction with the Center for Molecular and Cellular Dynamics, which provides infrastructure for laboratories at Harvard Medical School and its affiliated hospitals, as well as for groups at the Harvard campus in Cambridge.

Interested candidates should submit a CV, a 3-5 page statement of research interests, and four letters of recommendation to: **Stephen C. Harrison, Harvard Medical School, 250 Longwood Ave., Boston, MA 02115 (attn: Faculty Search).**

Harvard University is an Equal Opportunity Employer. Women and minorities are encouraged to apply.

JOHNS HOPKINS UNIVERSITY

The Johns Hopkins University seeks candidates for two or more tenure-track faculty positions in the related fields of bioinformatics, computational biology and biostatistics to develop and apply novel quantitative methods for molecular biology and genetics. Candidates will be part of a collaborative group involving the Departments of Biostatistics and Molecular Microbiology & Immunology in the School of Public Health and the Department of Oncology in the School of Medicine, with opportunity for appointment in any of the three departments. Ranks will be commensurate with prior experience and achievements. Recent PhDs/MDs and persons with research interests in the creation of novel databases and analytic methods for the study of biological sequences, biological networks, evolution, and gene and protein expression are encouraged to apply.

The Johns Hopkins Schools of Medicine and Public Health are among the world's premier health research institutions. These new faculty positions will expand a highly successful group of quantitative scientists working collaboratively across multiple departments. Please email a CV and letter of research interests to **Giovanni Parmigiani, Chair, Search Committee, in care of margo@jhsph.edu.**

We strongly encourage qualified women and under-represented minorities to apply. Johns Hopkins University is an Equal Opportunity/ Affirmative Action Employer.

POSITIONS OPEN

LOGGING SCIENTIST POSTDOCTORAL/ASSOCIATE RESEARCH SCIENTIST (OPEN RANK)

Borehole Research Group of Lamont-Doherty Earth Observatory of Columbia University, as logging services operator for U.S. component of integrated Ocean Drilling Program (IODP), seeks to fill position of logging scientist at postdoctoral or associate research scientist level.

Successful candidate will contribute to scientific, operational, and technical program associated with development of logging capabilities on IODP's nonriser drilling vessel, acquisition and analysis of log data, use of log database for scientific applications, and communication of logging technologies to scientific community. Position will involve research and development of logging applications for IODP.

Requirements: Ph.D. in marine geology or related field, superior oral and written communication skills. Demonstrated experience in research, broad interest in scientific problems related to marine geology and geophysics, and familiarity with scientific applications of log data desirable. Successful applicant will participate on IODP cruises as logging staff scientist and/or expedition project manager. Appointment level and salary commensurate with experience.

Interested applicants should send current curriculum vitae, statement of research interests, and names of three references to: **Ms. M. Mokhtari, Manager of Human Resources, Lamont-Doherty Earth Observatory of Columbia University, P.O. Box 1000, Palisades, NY 10964** or **e-mail: personnel@admin.ldeo.columbia.edu** with Search # LDO 670 05 020 in subject line. Screening of applicants will start after ad appears for 30 days. *Columbia University is an equal opportunity and affirmative action employer. Minorities and women are encouraged to apply.*

ASSISTANT, ASSOCIATE, OR FULL PROFESSOR IN BEHAVIORAL/ STATISTICAL GENETICS

The Institute for Behavioral Genetics at the University of Colorado, Boulder, seeks to recruit an expert in behavioral/statistical genetics. We invite applications for a tenured or tenure-track position with a joint appointment in an appropriate academic department. Preference will be given to candidates with an active research program involving the development of statistical genetics methods for the study of complex behavioral traits. The appointee will participate in the research and teaching missions of both the Institute and his or her academic department. Minimum requirements are a Ph.D., M.D., or equivalent terminal degree. Applicants should submit curriculum vitae, a statement of research and teaching interests, sample research papers, and at least three letters of recommendation to: **Search Committee (Faculty), Institute for Behavioral Genetics, University of Colorado, 447 UCB, Boulder, CO 80309-0447.** Inquiries should be addressed to: **John K. Hewitt, Search Committee Chair, telephone: 303-492-0742,** or **e-mail: John.Hewitt@Colorado.edu.** Application review will begin immediately and the position may remain open until filled. The appointment is expected to begin August 2006. *The University of Colorado at Boulder is committed to diversity and equality in education and employment.*

MEDICAL WRITER

Physicians' Education Resource (PER) is seeking a medical writer/editor to join its team. PER is a medical education company, located in Dallas, Texas, specializing in the field of oncology. Successful candidates will be responsible for writing manuscripts from original data, reporting highlights from cancer meetings, creating slide sets for pharmaceutical companies, and editing and rewriting author-submitted manuscripts. This full-time position requires a Ph.D. in a biomedical science. Send resume and salary requirements to: **Barb Schmaedeke, Human Resources Director, 3535 Worth Street #185, Dallas, Texas 75246. E-mail: hr@perlp.com.**

POSITIONS OPEN

POSTDOCTORAL, RESEARCH, AND CLINICAL FELLOWSHIPS at the National Institutes of Health U.S. Department of Health and Human Services

Website: http://www.training.nih.gov

NIH is dedicated to building a diverse community in its training and employment programs.

POSTDOCTORAL FELLOWSHIPS Anticancer Drug Development

Several positions open for highly trained postdoctoral fellows to work on anticancer drug development from microbial sources (*PNAS* **99**:14098-14103, 2002; *Cell Cycle* **3**:752-755, 2004; *ONAS* **101**:6427-6432, 2004; *Oncogene* **3**:2367-2378, 2004; *PNAS* **101**:4770-4775, 2004; *Cell Cycle* **3**:1182-1187, 2004; *Cell Microbiol*, September 2005). Must have experience in protein purification, characterization and protein-protein interaction studies as well as studies on cancer therapy and prevention. Must be residents of North America. If interested, please write to: **Professor T.K. Das Gupta, Head, Department of Surgical Oncology, University of Illinois at Chicago (e-mail: tkdg@uic.edu)** or **Professor A.M. Chakrabarty, Department of Microbiology and Immunology at UIC (e-mail: pseudomo@uic.edu).** *UIC is an Equal Opportunity/ Affirmative Action Employer.*

Two **POSTDOCTORAL FELLOWS** to study environmental and nutritional conditions on viral infection of plants (**website: http://humanresources.utoledo.edu/JobOpportunities/**). Applicants with experience in virology, plant nutrition, growth of floriculture crops, and genomics are invited to study nutrient effects on virus infection in bedding plants. Submit resume and three references to:

Dr. Scott Leisner
The University of Toledo
Human Resources Department
Toledo, OH 43606-3390
Telephone: 419-530-1550
E-mail: recruit@utoledo.edu (reference job #1067 and/or 1075 in subject line)

The University of Toledo is an Equal Opportunity, Equal Access, Affirmative Action Employer and Educator.

POSTDOCTORAL POSITIONS M.D. Anderson Cancer Center Science Park – Research Division Smithville, Texas

Postdoctoral positions are available to study the role of chromatin remodeling in DNA repair (*Cell* **119**:767-775) and the functions of nuclear actin and related proteins (*Molecular Cell* **12**:147-155). Additional information is available at **website: http://sciencepark.mdanderson.org/Documents/shen/shen.html.**

To apply, contact: **Dr. Zuetong Shen, e-mail: snowshen@mac.com.**

POSTDOCTORAL POSITIONS are available for (1) developing adenoviral vector–based influenza vaccine and for (2) designing adenoviral vectors for breast cancer gene theraphy. Experience in tissue culture, virology, immunology, molecular techniques, cell biology, and mouse model desirable. Send cirriculum vitae and names of three references to: **Suresh Mittal, Ph.D., Department of Veterinary Pathobiology, Purdue University, West Lafayette, IN 47907 U.S.A. Telephone: 765-496-2894; e-mail: mittal@purdue.edu.** *Affirmative Action/Equal Opportunity Employer.*

POSITIONS OPEN

CHAIR, DEPARTMENT OF CHEMISTRY AND BIOCHEMISTRY. The College of Sciences and Mathematics at Auburn University invites applications and nominations for Chair of the Department of Chemistry and Biochemistry. The College seeks an individual with an earned doctorate in chemistry or biochemistry who is eligible for tenure at the rank of **FULL PROFESSOR** based on a distinguished record of research and teaching that shall continue at Auburn. The individual must demonstrate outstanding leadership and interpersonal skills and should provide a vision to carry the Chemistry and Biochemistry Department forward in the areas of research, scholarship, and outreach. The initial chair appointment will be for four years and may be extended for a second four-year term.

The Chemistry and Biochemistry Department currently has 24 faculty members and anticipates future hires to both fill new positions and to replace upcoming retirements. The Department offers B.S., M.S., and Ph.D. degrees in chemistry and biochemistry; it also offers a B.A. degree in chemistry. The Department's research laboratories, major classrooms, and offices are housed in a modern building, while the undergraduate teaching laboratories are housed in a newly constructed Science Center. Additional departmental information can be accessed at **website: http://www.auburn.edu/chemistry.** *The selected candidate must be eligible for employment in the U.S. at the date of appointment* and must be able to communicate effectively in English.

Applications should be mailed to: **Professor Marie W. Wooten, Chemistry Search Committee Chair, College of Sciences and Mathematics, SCC 248, 315 Roosevelt Concourse, Auburn University, AL 36849.** The application should consist of a detailed curriculum vitae, a letter of intent that describes research, teaching, and administrative interests, a visionary statement for Auburn's Chemistry and Biochemistry Department, a current e-mail address, and the addresses and telephone numbers of at least three references. Nominations only may be sent by to **e-mail: wootemw@auburn.edu.** Review of applications will begin on October 15, 2005, and continue until a candidate is recommended for appointment.

Auburn University is an Affirmative Action/Equal Opportunity Employer. Auburn University encourages women and minorities to apply.

STAFF SCIENTIST POSITION VIRAL EPIDEMIOLOGY Blood Systems Research Institute/ University of California San Francisco (UCSF)

An active research group in the epidemiology of human retroviral (HTLV-I, HTLV-II, HIV) and hepatitis virus infections and in blood transfusion safety research seeks a Staff Scientist in an epidemiology research position. M.D./M.P.H. or Ph.D. in epidemiology or other doctoral degree with equivalent epidemiology or clinical research training is preferred. Preference will be given to candidates with previous experience in conducting epidemiological or clinical research, data analysis with SAS or STATA, prior publication, and excellent English writing skills. Candidates seeking a career in viral epidemiology or blood safety research will have the opportunity to develop their own research program and collaborations with other scientists. The position is with Blood Systems Research Institute, a dynamic blood research institute with historical ties to UCSF, and could lead to a joint appointment at UCSF.

Send curriculum vitae to:

Edward L. Murphy, M.D., M.P.H.
Professor, Laboratory Medicine, Medicine and Epidemiology/Biostatistics
Senior Scientist,
Blood Systems Research Institute
270 Masonic Avenue
San Francisco, CA 94118
Telephone: 415-749-6668
Fax: 415-901-0733
E-mail: syuen@itsa.ucsf.edu

Preemployment drug screen required. Equal Opportunity Employer, Minorities/Females/Persons with Disabilities/Veterans.

Director
Center for Developmental Biology Research
University of Arkansas for Medical Sciences
College of Medicine

The University of Arkansas for Medical Sciences (UAMS) is seeking a dynamic and visionary scientist to develop and lead the multidisciplinary Center for Developmental Biology Research for the College of Medicine. The Director will have a tenure track faculty appointment in the Department of Pediatrics and will be expected to recruit additional scientists in Pediatrics, Neurobiology and Developmental Sciences, and Obstetrics and Gynecology for the Center. The Director will provide strategic and scientific leadership for all aspects of the program.

Essential qualifications include a distinguished record as a senior academic scientist and superior interpersonal and mentoring skills. Suitable candidates will possess a record of established research funding with expertise in developmental biology. Candidates may have a Ph.D., M.D., M.D./Ph.D., or equivalent degrees. Academic rank will be commensurate with experience.

For more information regarding UAMS, link to all sites at: **http://uams.edu**. Interested parties should submit a letter of interest and curriculum vitae to:

Thomas G. Wells, M.D., M.B.A.
Vice Chair for Research
Department of Pediatrics
800 Marshall Street
Little Rock, AR 72202-3591
Email: WellsThomasG@uams.edu

UAMS is an Equal Opportunity Employer.

Indiana University
Schools of Informatics
and Medicine

Senior Faculty Position, Bioinformatics

The School of Informatics and the Center for Computational Biology and Bioinformatics in the School of Medicine at Indiana University seek a senior-level (associate professor or professor) faculty member. The schools have embarked on a major initiative to enhance computational and bioinformatics research. Candidates will be evaluated on the following criteria: (1) strong record of extramural funding for research related to bioinformatics; (2) strong record of publication in bioinformatics research, (3) ability to develop and direct an internationally recognized, and externally funded research program in computational biology and bioinformatics, (4) ability to train graduate students and postdoctoral fellows. (5) MD or PhD in a related field. Outstanding candidates will be considered for tenure at senior rank. Competitive salary, space, and start-up funds are available.

To apply online see: **http://informatics.iupui.edu/c/201**, and include a statement of teaching and research interests, curriculum vita, along with six references by **November 31, 2005** or mail to:

Dr. Douglas Perry, Associate Dean
Indiana University School of Informatics
535 W. Michigan Street
IT 477
Indianapolis, IN 46202-3103

Indiana University is an Equal Opportunity/Affirmative Action Employer, Educator, and Contractor, M/F/D.

ANNOUNCEMENTS

Call for Proposals
BMBF Competition "ExistGo-Bio"

The German Federal Ministry of Education and Research (BMBF) intends to give younger scientists from Germany and abroad, with experience in heading a research group, the opportunity to work on new, applied research oriented approaches in the biosciences in Germany, independently and in their own team in order to translate their inventive research activities into new entrepreneurial initiatives (e.g. formation of a company, spin off).

The teams (staff: 1 group leader, 2 postdoctoral research fellows, 2 Ph.D. students, 2 FTE physicians and/or engineers, 2 technical assistants and, for the second half of the project, additional management expertise e.g. a business economist) are to work for a period of up to 6 years on topics on the frontiers of biology and neighbouring disciplines in order to improve the application (proof of concept) and commercialization (proof of technology) potential of the selected subjects.

The projects will be selected by a jury. Project funding will be in the form of non-repayable grants.

Deadline: February 28, 2006 (first call)

Further information:

http://www.fz-juelich.de/ptj/ExistGo-Bio
Forschungszentrum Jülich GmbH,
Projektträger Jülich PtJ,
D-52425 Jülich
e-mail: ptj-existgobio@fz-juelich.de

Dr. R. Jossek
Tel: +49 (0) 2461 61-3720 **Fax:** +49 (0) 2461 61-2690
e-mail: r.jossek@fz-juelich.de

COSAT
Corporate Office of Science & Technology

Johnson & Johnson

Request for Research Proposals

The Johnson & Johnson Focused Funding Program has provided funding to support basic biomedical research in universities, colleges and research institutions around the world since 1980. It is a key component of the corporation's philanthropy philosophy. The Program provides grants across a broad range of biomedical research disciplines.

This year, the Selection Committee has reserved a portion of the available funds for proposals addressing basic research in the following areas:

- Renal Repair: the use of cells, bioactives, biomaterials and/or devices to repair, regenerate and/or assist the function of damaged kidneys.
- Hearing Loss: prevention or therapy directed towards age-related hearing loss. Pharmaceutical, cell-based, and electronic device innovations are appropriate areas of research.

A one-page preliminary proposal should be submitted electronically as indicated below. Key points to address are the novelty of the research and potential therapeutic benefits. A brief preliminary budget should be included, as well as an indication of the duration of the project.

Submission deadline is October 8, 2005. Rejection or full proposal submission request information will be communicated to all applicants by October 31, 2005. The proposal should be submitted using the instructions at www.jnjcosat.com/rfa.aspx.

Johnson & Johnson does not provide critiques of individual proposals submitted.

Although no proprietary claim is made on the research carried out through a Focused Funding Grant, the relationship built between Johnson & Johnson and the grant recipient may lead to future research agreements or business arrangements when appropriate.

Focused Funding Program
25 Years of Innovation